BULLETIN OF THE EARTHQUAKE RESEARCH INSTITUTE,
UNIVERSITY OF TOKYO. Vol. 39, Part 4. December, 1961.

東京大学
地震研究所彙報

第 39 号　第 4 冊

昭和 36 年 12 月

目　次

論文及報告

			頁
21.	伊豆大島における火山活動と地磁気変化についての一解釈（英文）	上田誠也	579
22.	岩石の熱衝撃破壊について（英文）	上田誠也 藪武夫	593
23.	西南太平洋海域を，夫々の内部でレーリー波が同一の群速度を示す様ないくつかの地区に分けること（英文）	三東哲夫	603
24.	日本周辺を伝わるラブ波の分散について（英文）	三東哲夫	631
25.	表面波と層構造 (1) 低速層の影響および Lg と Rg について（英文）	山口林造	653
26.	表面波と層構造 (2) 海洋構造を伝わる表面波の理論的分散曲線（英文）	山口林造 木沢綏	669
27.	均質な表面層のある不均質な半平面における Love 波の分散（英文）	高橋健人	811
28.	不均質な媒質における表面波の Higher Modes の分散曲線（英文）	高橋健人	823
29.	台湾の地震活動（英文）	徐明同	831

北美濃地震調査報告

30.	昭和 36 年 8 月 19 日白山国定公園附近に発生した地震の調査概報（邦文）	吉山良一	849
31.	1961 年 8 月 19 日北美濃地震踏査概報（英文）	岸上冬彦 音田功	857
32.	北美濃地震における家屋の被害について（邦文）	大沢胖	869
33.	1961 年 8 月 19 日北美濃地震とその余震観測概説（邦文）	萩原尊礼 茅野一郎	873
34.	北美濃地震余震観測——勝原および蛭ヶ野における観測——（邦文）	表俊一郎 唐鎌郁夫 中島直吉 斎藤貞夫 茅野一郎	881
35.	北美濃地震余震観測——岐阜県八幡町における観測——（邦文）	宮村摂三 堀実 安芸敬一 松本英照 安藤誠一	895
36.	北美濃地方の地質構造に関する 2, 3 の問題（邦文）	村井勇 津屋弘逵	909
37.	北美濃地震被害地の地質　第 1 報　福井県打波川上流～岐阜県石徹白川上流地域（邦文）	森本良平 松田時彦	935
38.	山地地盤の振動性状（北美濃地震の余震観測）（英文）	金井清 長田甲斐男	943
	北美濃地震調査報告あとがき	河角広	953

(The titles in occidental languages are given on the back cover.)

地震研究所彙報は，年4回定期に（ただし，第1号より第6号までは不定期に，第7号は3冊として刊行された），彙報別冊は不定期に刊行される．

この彙報に載せられた論文及び報告についての責任は，すべてその著者のみにある．

この彙報についての照会通信は，すべて東京大学地震研究所長にあてられたい．

The Bulletin is published quarterly. (Vols. 1-6 were published at irregular intervals and Vol. 7 consisted of three parts.)
Supplementary Volume is published at irregular interval.

The authors of the papers alone are responsible for the statements and opinions contained in their respective papers.

All communications relating to this Bulletin should be addressed to the Director of the Earthquake Research Institute, University of Tokyo, Japan.

Earthquake Research Institute, University of Tokyo
Address:
No. 1, Motofuji-cho, Bunkyo-ku,
Tokyo Metropolis, Japan.
Telephone: 812-2111-Extension 2145
Cable address: ZISINKEN, TOKYO.

東京大学地震研究所
所在地
東京都文京区本富士町一番地
電話 小石川 812—2111 (代) 構内 2145
電略 ブンケウ トウダイ ヂシン

BULLETIN OF THE EARTHQUAKE
RESEARCH INSTITUTE
Vol. 39 (1961). pp. 579-591

21. An Interpretation of the Transient Geomagnetic Variations Accompanying the Volcanic Activities at Volcano Mihara, Oshima Island, Japan.

By Seiya UYEDA,

Earthquake Research Institute.

(Read May 23, 1961.—Received September 30, 1961.)

Summary

The reversible change in the geomagnetic declination accompanying the major activities of Volcano Mihara, Oshima Island, has been interpreted as being due to heating and cooling, or demagnetization and remagnetization of a subterranean mass at a depth of a few km. In the present paper, an alternative way of interpreting the observation is proposed. In the new model, the heated region is assumed to be a cylinder ($r \cong 430\,m$) extending from the depths to the surface crater. It is shown that the gradual heating of the cylinder from beneath would produce the apparently reversible change in the declination, without requiring any rapid cooling which has been the difficulty in the classical model. Even in the new model, the transfer of heat both in the heating and cooling of the cylinder would need some process such as convective transfer, which is much more effective than the ordinary conductive one.

1. Introduction

A number of investigations have been carried out on the geomagnetic anomaly associated with volcanoes and its variations accompanying the eruptive activity.[1)~11)] In particular, T. Rikitake and I. Yokoyama, with

1) T. NAGATA, *Bull. Earthq. Res. Inst.*, **16** (1938), 288.
2) T. NAGATA, *Bull. Earthq. Res. Inst.*, **19** (1941), 402.
3) T. RIKITAKE, *Bull. Earthq. Res. Inst.*, **29** (1951), 161.
4) T. RIKITAKE, *Bull. Earthq. Res. Inst.*, **29** (1951), 499.
5) T. RIKITAKE, I. YOKOYAMA, A. OKADA and Y. HISHIYAMA, *Bull. Earthq. Res. Inst.*, **29** (1951), 583.
6) I. YOKOYAMA, *Bull. Earthq. Res. Inst.*, **32** (1954), 17, 169.
7) I. YOKOYAMA, *Bull. Earthq. Res. Inst.*, **33** (1955), 251.
8) I. YOKOYAMA, *Bull. Earthq. Res. Inst.*, **34** (1956), 21.
9) I. YOKOYAMA, *Bull. Earthq. Res. Inst.*, **35** (1957), 327, 567.
10) T. NAGATA and S. SAKUMA, *Handbuch der Physik*, XLVIII, (1957), Springer.
11) T. RIKITAKE and I. YOKOYAMA, *J. Geophys. Res.*, **60** (1955), 165.

Fig. 1. Topographical map of Oshima Island. Underlined are the locations of magnetic observatories. Square dots 1, 2, 3 and 4 are the bore-holes. The temperature distributions in the holes are shown in Figs. 8, 9, 10 and 11 respectively.

others, showed by serial observation for more than ten years that the geomagnetic declination around Volcano Mihara, Oshima Island, Japan, changes on occasions of major activity. Continuous measurement of the declination has been conducted at two stations in Oshima Island as indicated in Fig. 1: at Nomashi since 1951 and at the Oshima Zoo since 1956. The results obtained at Nomashi Observatory are reproduced in Fig. 2. In Fig. 2, the difference curve is the difference in the semi-monthly mean values of the declination at Nomashi Observatory and at the Kakioka Geomagnetic Observatory on the Main Island of Japan. The difference has been taken in order to eliminate the effect of the non-local temporary variations such

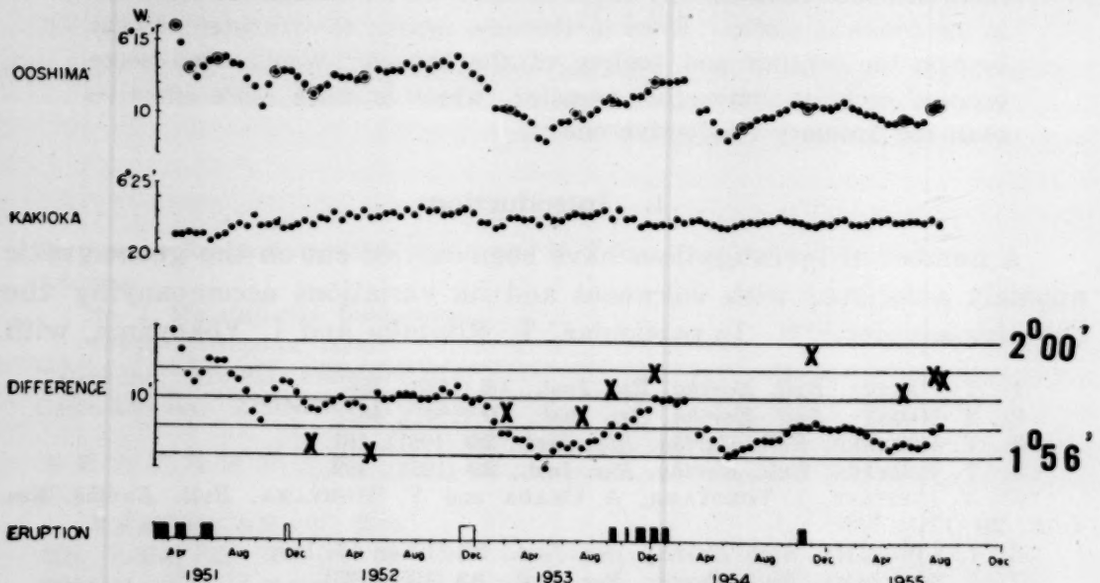

Fig. 2. The semi-monthly means of the westerly declination at Nomashi, Oshima. Eruption of Volcano Mihara is shown in an arbitrary scale. Crosses represent the dip difference between Oshima and Kakioka, referring to the scale on the right hand side. (after Yokoyama and Rikitake)

as magnetic storms. It may be closely observed in this figure that on the occasion of the 1953–1954 activity (the total amount of lava erupted in this period is estimated as 1.9×10^{6} *tons*), the geomagnetic declination at Nomashi Observatory experienced an almost reversible change of some 3~4 minutes of arc: the increase in the westerly declination started a few months prior to the surface activity and apparently disappeared within a few months after the ceasing of the eruptions. Yokoyama[12),13)] suggested that this anomalous variation may be interpreted as being caused by the thermal demagnetization and re-magnetization of a subterranean basaltic mass during the above specified period of time: more precisely, the observed change may be accounted for by the disappearance and re-appearance of a magnetic dipole situated at a depth of 1.6 *km* below sea level right below the volcano. The dipole has a magnetic moment ($|\mathbf{M}|\cong1.2\times10^{13}$ *emu*) oriented parallel to the local geomagnetic force. Supposing the temperature change to be from 100°*C* to 350°*C*, and the accompanying variation of the magnetic moment $J=0.03$ *emu/cc*[14)]*, the radius r of the equivalent sphere centred at $d=1.6$ *km* was obtained as $r=440$ *m* as shown in Fig. 3. This view, as it bears a close relevance

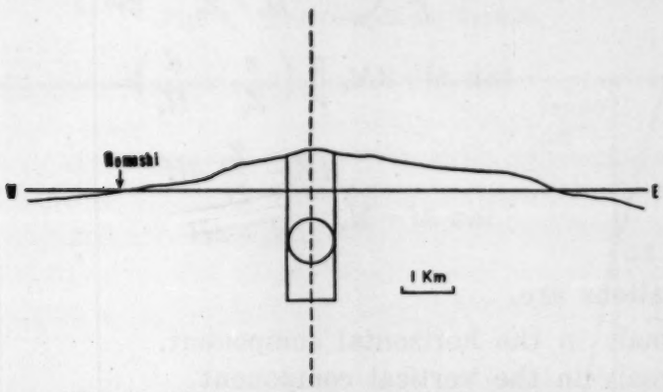

Fig. 3. East-west section of Oshima Island.

to the detail of the processes beneath the volcanoes in action, is of great importance in volcanic studies. The cause of the demagnetization, *i. e.* the heating of the mass may be taken as being the intrusion of hot magma from the depths. It seems, however, as was shown by Yokoyama[15)] that the alleged re-magnetization, *i. e.* the cooling of the above

12) I. YOKOYAMA, *Bull. Earthq. Res. Inst.*, **34** (1956), 185.
13) I. YOKOYAMA, *Bull. Earthq. Res. Inst.*, **35** (1957), 75, 99.
14) T. NAGATA, *Rock-magnetism*, (1953), Maruzen, Tokyo.
* Figures quoted here are the measured values for actual Oshima basalts.
15) *loc. cit.*, 12), 13).

specified spherical mass in such a short period as a few months must be achieved with difficulty unless some very effective cooling process is assumed. The model outlined above will be referred to as the classical model in the present paper.

It is intended in this paper to suggest that there may be an alternative way of interpreting the observed mode of change in the geomagnetic declination without requiring such a rapid cooling of the subterranean mass.

2. A Cylindrical Model

The geomagnetic anomaly at a point P caused by a magnetic dipole of the moment $\mathbf{M}(M_x, M_y, M_z)$ oriented parallel to the geomagnetic force $\mathbf{H}(H_0, 0, Z_0)$ can be expressed by,

$$\Delta H = M_x\left[\frac{-1}{r^3}+\frac{3x}{r^5}\left(x-d\frac{Z_0}{H_0}\right)\right\} \tag{1}$$

$$\Delta Z = 3M_z\left[\frac{-d}{r^5}\left(x-d\frac{Z_0}{H_0}\right)\frac{H_0}{Z_0}-\frac{1}{3r^3}\right] \tag{2}$$

$$\tan\Delta\delta = 3M_z\frac{y}{r^5}\left(\frac{x}{Z_0}-\frac{d}{H_0}\right) \tag{3}$$

$$\tan\Delta I = M_z\frac{\Delta Z-\dfrac{Z_0}{H_0}\Delta H}{H_0+\Delta H} \tag{4}$$

where the notations are,

ΔH: anomaly in the horizontal component,
ΔZ: anomaly in the vertical component,
$\Delta\delta$: anomaly in the declination,
ΔI: anomaly in the inclination,

and r, x, and d are taken as shown in Fig. 4.

Now, let us suppose that in the period preceding the outbreak of the surface activity, the rising magma heats up a cylindrical part of the mountain during its way up and thermally demagnetizes it. In such a case, the state of affairs may be represented magnetically by the intrusion of a cylinder magnetized in the opposite direction to the geomagnetic force. In evaluating the change, in such a case, of the magnetic field at a place fairly apart from the cylinder, it may be

allowable to approximate the gradual intrusion of the cylinder by a piling up of the magnetic dipoles with negative polarity. This is equivalent to approximating the magnetic field around a magnetic disc by means of a magnetic sphere.

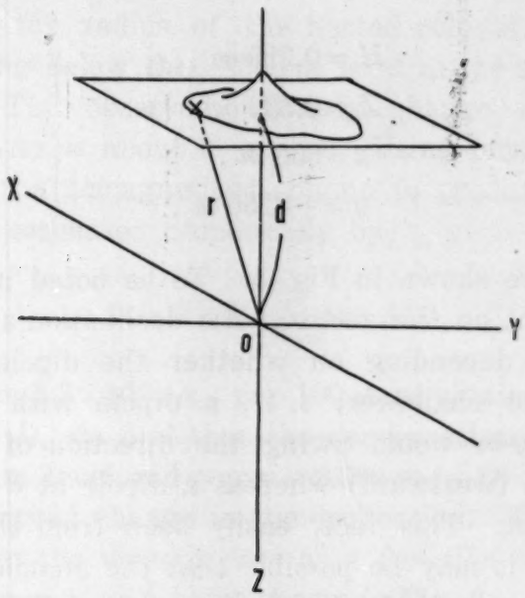

Fig. 4. The co-ordinate system.

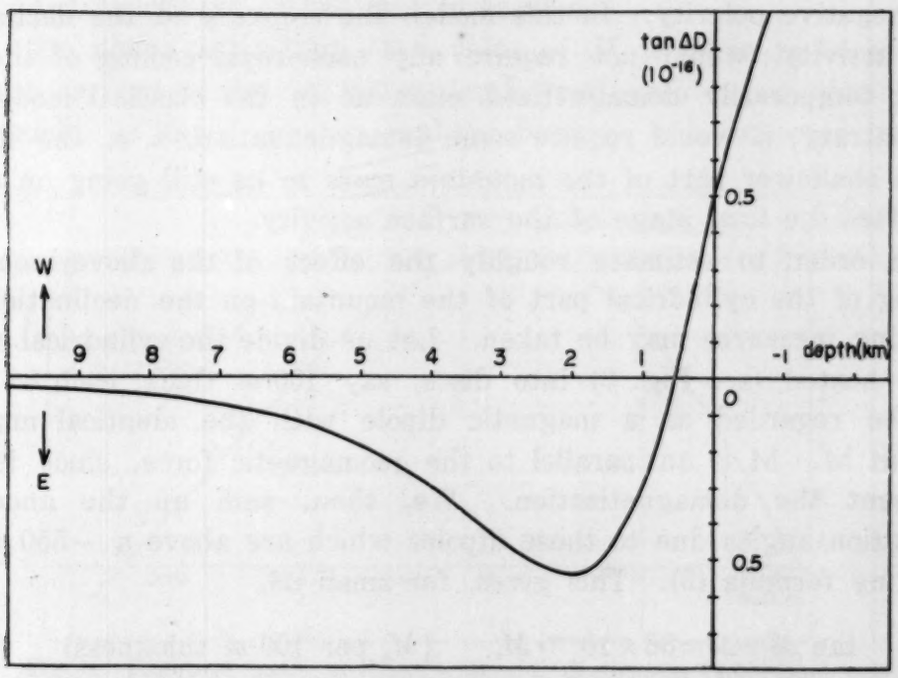

Fig. 5. The anomalous values of declination at Nomashi caused by a unit magnetic dipole with positive polarity at various depths right below the crater.

In the first place, we examine, by the formula (3), the expected anomalous values of the declination at Nomashi Observatory, caused by a unit magnetic dipole with positive polarity, placed at various depths right below the crater. We put,

$$\left.\begin{aligned} H_0 &= 0.295\ oe\ , \\ Z_0 &= 0.330\ oe\ , \\ x &= 650\ m\ , \\ y &= -3250\ m\ . \end{aligned}\right\} \qquad (5)$$

The results are shown in Fig. 5. To be noted in this figure is the fact that the effect on the geomagnetic declination at Nomashi Observatory is contrary, depending on whether the dipole is situated deeper than say 580 m or shallower, *i. e.*, a dipole with positive (negative) polarity at $d>580\ m$ would swing the direction of the local magnetic meridian eastward (westward) whereas a dipole at $d<580\ m$ would have the contrary effect. This fact, easily seen from the form of formula (3), suggests that it may be possible that the anomalous change in the geomagnetic declination before and after the surface eruptive activity (Fig. 2) is explained by the gradual upward growth of a pile of dipoles with negative polarity. In this model, the recovery of the declination, after activity, would not require any such rapid cooling of the deep buried temporarily demagnetized mass as in the classical model. On the contrary, it would require some demagnetization, *i. e.* the heating of the shallower part of the mountain mass to be still going on during and after the final stage of the surface activity.

In order to estimate roughly the effect of the above mentioned heating of the cylindrical part of the mountain on the declination, the following measures may be taken. Let us divide the cylindrical column to be heated (see Fig. 3) into discs, say 100 m thick, each of which may be regarded as a magnetic dipole with the identical magnetic moment **M**. **M** is antiparallel to the geomagnetic force, since it is to represent the demagnetization. We, then, sum up the anomalous declination angles due to those dipoles which are above a $-550\ m$ level following formula (3). This gives, for small $\Delta\delta$,

$$\tan \Delta\delta \fallingdotseq \Delta\delta = 66 \times 10^{-19} \cdot M_z \qquad (M_z \text{ per } 100\ m \text{ thickness}) \qquad (6)$$

Taking the observed amount of the recovery in the declination (Fig. 2) as 3′ of arc, M_z per 100 m thick disc turns out to be $1.3 \times 10^{12}\ emu$.

giving $|\mathbf{M}|=1.8\times10^{12}\ emu$. Since the intensity of the natural magnetization of the basaltic rocks forming the volcano is about $3\times10^{-2}\ emu/cc$[15], the above value of $|\mathbf{M}|$ would lead to the radius of the demagnetized column being about 430 m.

Thus defining the radius of the heated column, we next examine the effect of heating below the $-550\ m$ level at the stage preceding the surface activity. The observed westerly change in the declination preceding the activity is about 3′ of arc. Using formula (3) again, the effective depth of the demagnetized column to produce a 3′ anomaly in declination will be estimated numerically by,

$$\tan\Delta\delta \fallingdotseq M_z \sum_{d=550\mathrm{m}}^{d=D} \tan\Delta\delta\ , \qquad (7)$$

where M_z is taken as $1.3\times10^{12}\ emu$ per 100 m as obtained above. Solving (7) numerically for D, we find that the demagnetization of the column between the $-550\ m$ level and some $-2{,}200\ m$ $(-D)$ would be sufficient to produce the observed change in the declination. The mode of change in the declination in the present case as a function of the depth of the top of the heated region will be as shown in Fig. 6. This mode roughly resembles the observed one shown in Fig. 2, if a constant speed for the upward movement of the lava is assumed.

In the above estimation, the value of M_z is taken to be constant from the surface to the $-2{,}200\ m$ depth, and zero below that depth. This should be far from the reality, because it is expected that the

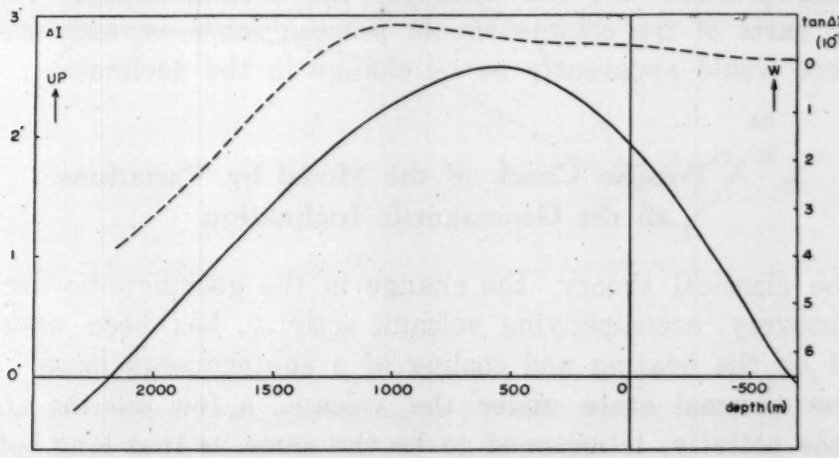

Fig. 6. Expected mode of change in the declination (solid line) and inclination (broken line) at Nomashi.

15) *loc. cit.*, 14).

general temperature beneath the active volcano increases with the depth and consequently the intensity of the natural magnetization would diminish continuously with the increase in depth. Without any definite information as to the actual temperature distribution, the argument here should be taken only to point out that the westward change in declination may be explained by the heating of the columner part deeper than say the $-550\,m$ level. In principle, the lower limit of the effective column should be the depth at which the general temperature reaches the Curie point of the ferromagnetic ingredients of the rocks.

Based on the consideration outlined above, the model to be presented here may be stated as follows. Preceding the period of major activity, the magma gradually rises from beneath, finding its way up through filling existing fissures and creating new ones. This process will heat up the columner part surrounding its major path and demagnetize it. As long as the demagnetized region is below some critical depth ($-550\,m$), the anomalous change in the geomagnetic declination at Nomashi Observatory is westward. But, after it passes this depth, the anomalous change tends eastward. When the heating near the surface of the summit is completed (this is assumed to be a few months later than the time when the lava reaches the surface, owing to slowness in the transfer of heat), the anomalous change in the declination is apparently cancelled out giving an appearance of recovery. Cooling after the end of activity would proceed more slowly, and the change in the declination accompanying this slow process would be much less pronounced than in the heating process. If, for instance, the cooling of both the upper and lower parts of the column should proceed more or less simultaneously, there would apparently be no change in the declination.

3. A Possible Check of the Model by Variations in the Geomagnetic Inclination

In the classical theory, the change in the geomagnetic declination and its recovery, accompanying volcanic activity, has been assumed to be caused by the heating and cooling of a subterranean mass. In that model, the thermal state under the volcano, a few months after the peak of the activity, is assumed to be the same as that long before the activity. It is, therefore, necessary that all of other elements of the geomagnetic field should also resume their original values. On the other hand, in the model presented in this paper, the thermal state a

few months after the peak activity is quite different from the original: the former state is throught to be the most heated state and the recovery in the declination is only apparent.

Let us take the magnetic inclination or the dip angle as the example of other geomagnetic elements. As stated above, the change expected from the classical theory should be reversible with time, just as in the case of the declination. In order to estimate the possible change in the dip angle anticipated from the new model, a measure similar to that taken in estimating the declination change has been taken: *i. e.*, first calculate the anomalies in the H and Z components (ΔH and ΔZ) due to a dipole with a positive unit magnetic moment at various depths from the formulas (1) and (2) as illustrated in Fig. 7. From these results, the expected change in the dip angle accompanying the change in the declination specified in Fig. 6 can be obtained as the dotted curve in Fig. 6 shows. It may be clearly observed in the figure that the dip angle does not recover in the present model.

In Oshima Island, continuous measurement was carried out only for the declination during the active periods concerned. Data on the dip angle at Nomashi are available only for the times when occasional absolute

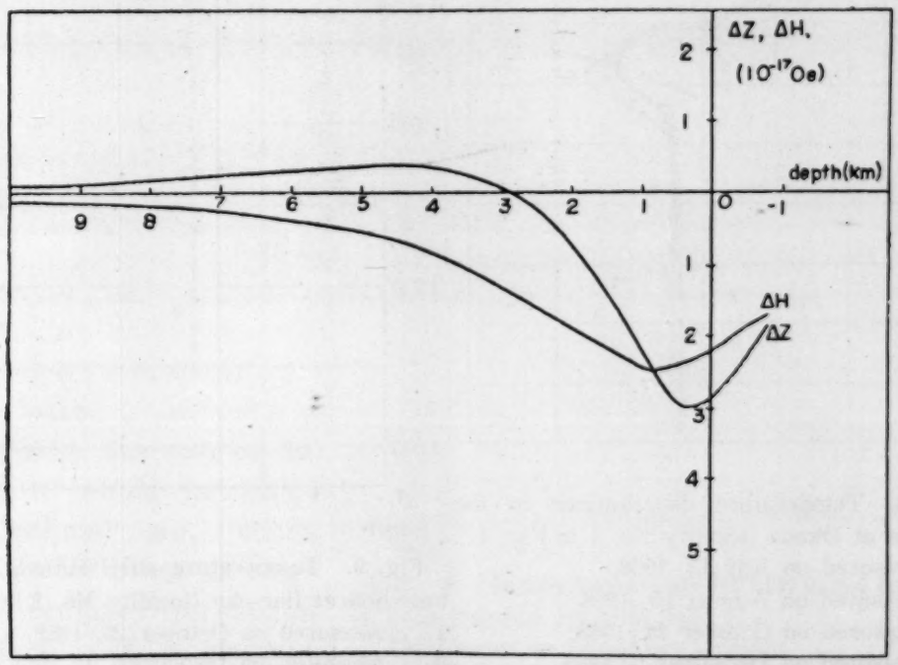

Fig. 7. The anomalous values of horizontal and vertical components at Nomashi caused by a unit magnetic dipole with positive polarity at various depths right below the crater.

measurements were conducted.* These data, though scanty, are plotted in Fig. 2 by crosses. Unfortunately the data are missing for the most critical period, *i. e.* for the middle part of 1954, so that it is not possible to say definitely if the recovery in the dip angle did or did not take place. It seems, however, that the general trend seems to fit the "non-recovery" hypothesis better, giving support to the new model. The continuous recording of the three geomagnetic components, which is now carried on at Nomashi Observatory, will provide a more definite check concerning this point in the future active periods of the volcano.

4. Discussion

The model described in the preceding sections has been devised in order to avoid the rapid cooling of the subterranean mass that was

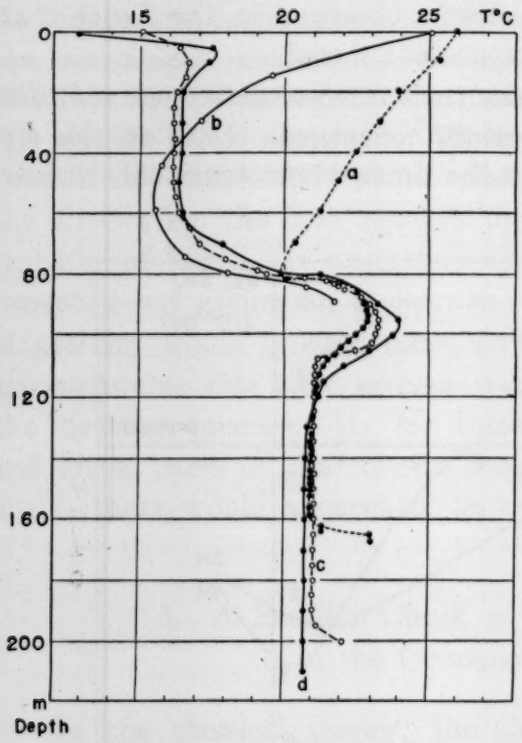

Fig. 8. Temperature distributions in the bore-hole at Okada (locality No. 1 in Fig. 1.).
a....measured on July 13, 1958.
b....measured on August 10, 1958.
c....measured on October 24, 1958.
d....measured on December 5, 1959.
(after Hôrai and Uyeda)

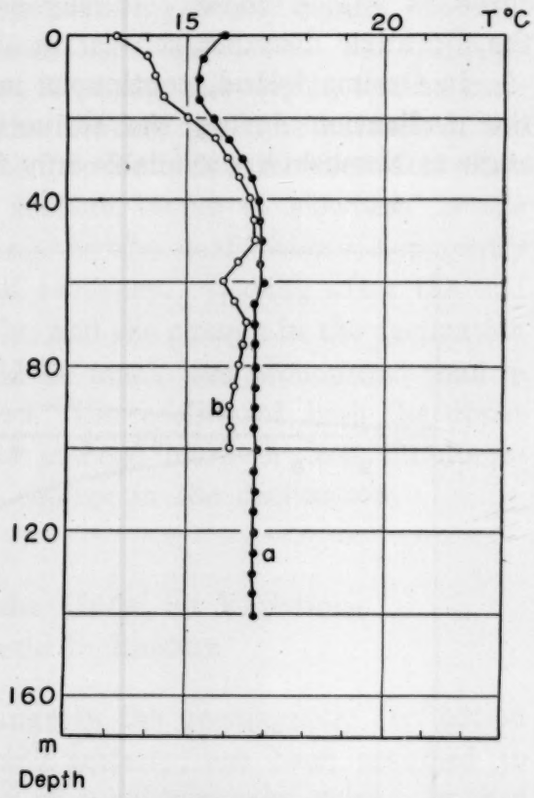

Fig. 9. Temperature distributions in the bore-hole at Jino-oka (locality No. 2 in Fig.1.).
a....measured on October 25, 1958.
b....measured on December 10, 1958.
(after Hôrai).

* By the courtesy of Dr. I. Yokoyama.

required in the classical model. In the new model no such cooling is necessary to explain the observed mode of the change in the geomagnetic field accompanying a *single* period of activity. It was reported, however, that the changes were detected for the two active periods which were in 1950–1951 and in 1953–1954 (see Fig. 2). This fact may indicate that the thermal state, disturbed in the 1950–1951 activity had substantially recovered before the 1953–1954 activity started.

The volume of the cylindrical column (430 m in radius and 3 km in height) to be heated in the present model is about $1.74\times10^{15}\,cc$ and its mass would be about $4.35\times10^{15}\,gr$. The heating necessary to cause sufficient change in the declination is taken to be from 100°C to 350°C throughout the cylinder, for the sake of simplicity. Taking the specific heat of the rock $0.2\,cal/gr$ °C, the total heat required would be some 2×10^{17} *calories*. This value is about five times as large as that in the classical model. The removing of this amount of thermal energy out of the volcano in three years seems to be a rather unusual matter. If this energy is assumed to emanate uniformly from the whole area of the Island ($\sim10^{12}\,cm^2$) in three years, the rate of the heat flow would be about $2\times10^{-3}cal/cm^2\ sec$, which is almost 10^3 times as large as the ordinary terrestrial heat flow. It is evident that the ordinary thermal conduction process cannot

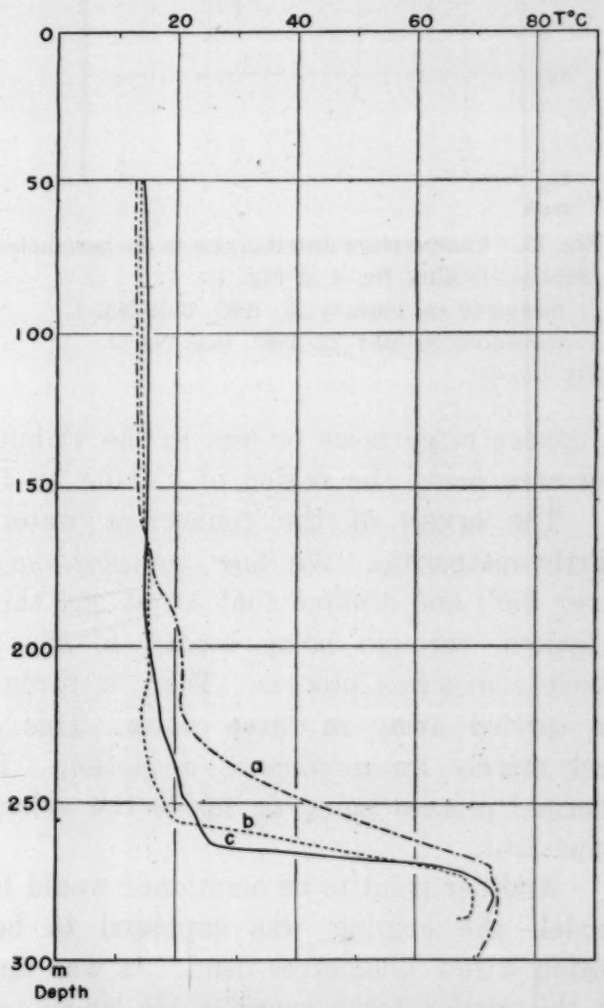

Fig. 10. Temperature distributions in the bore-hole at Yose (locality No. 3 in Fig. 1).
a....measured on December 4, 1959.
b....measured on July 27, 1960.
c....measured on December 3, 1960.
(after the Dowa Mining Company, Hôrai and Uyeda)

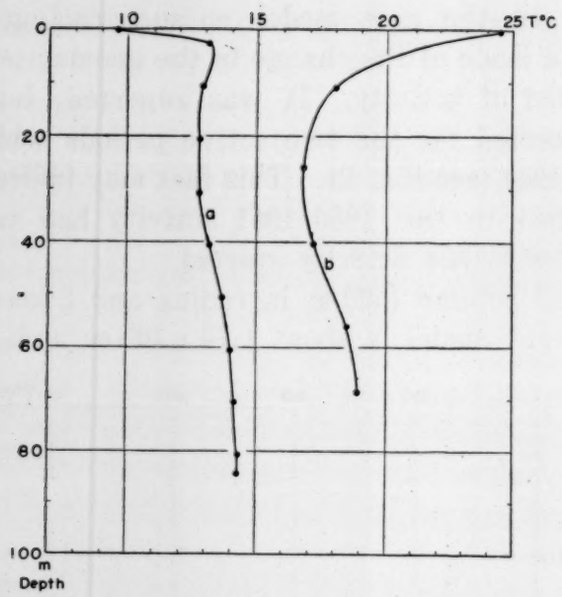

Fig. 11. Temperature distributions in the bore-holes at Sabaku (locality No. 4 in Fig. 1).
a....measured on January 22, 1960, hole No. 1.
b....measured on May 22, 1960, hole No. 2.
(after Uyeda)

bring out such an amount of heat. In fact, the near-surface geothermal gradients at several localities in the Island are known to be even less than the normal value as shown in Figs. 8, 9, 10 and 11. Such lack in the geothermal gradient indicates that the heat output through conduction may be even smaller than in ordinary non-volcanic areas. It may be considered that the heat is transferred, in such a volcanic island, by some sort of convection process and the area of upwelling of the convecting material, probably water and vapour, is concentrated more or less in the vicinity of the crater, the surrounding area being the region of sinking as J. Elder[16] points out.

The origin of the convective water may be partly jevenile and partly meteoritic. We now consider only the meteoritic water ($\sim$300 $cc/yr\ cm^2$) and assume that about one third of the total rain fall participates, through being heated to say $70°C$ and evaporating, in the above convection process. Then, it turns out that the $2\times10^{17}\ cal.$ may be carried away in three years. This estimation is extremely crude and merely an arithmetic deduction. Physical investigation of the thermal process going on inside the volcano should undoubtedly be very important.

Another point to be mentioned would be as follows. In the classical model, the heating was supposed to be concentrated in a spherical region a few kilometres deep. It was implied there that magma stays at this region for a considerable length of time and rises from there to the surface quickly. Clearly the heated region is related to the "magma reservoir". In the present model, on the contrary, no such particular place is assumed at such depth and the magma is assumed

16) J. ELDER, private communication.

to rise more or less with a constant speed all the way through. Filling all the existing cracks and fissures and creating some new ones in all directions, the magma will heat up the cylindrical volume up to the surface. In this respect, the present model does not seem to support the concept of the magma reservoir. If such a reservoir should exist at all it may be at some greater depth.

5. Acknowledgement

The author wishes to thank Drs. T. Rikitake, I. Yokoyama and John Elder, and Mr. T. Yukutake for their interest and criticism. He also acknowledges the courtesy of Mr. K. Hôrai and the Dowa Mining Company who allowed him to refer to their unpublished data on the temperature in bore holes in Oshima Island. Miss E. Nakagawa and Mr. I. Tanaoka assisted the author in drawing the diagrams.

---

21. 伊豆大島における火山活動と地磁気変化についての一解釈

地震研究所　上　田　誠　也

伊豆大島三原山の火山活動に伴なつて，同島野増地磁気観測所では偏角に可逆的変化があることは，力武，横山らによつて確かめられている．この現象は地下数粁の深さに仮定された球状部分が，火山活動の消長に伴なつて加熱，冷却され，その磁性を失なつたり，再獲得したりするとして解釈されている．本論文では多少異なつた解釈法が提出される．新らしいモデルでは加熱される部分は半径約 430m の円筒状の部分であつて，地下深所より火口に達するとされる．このような円筒が下部から徐々に加熱されるとすると，野増観測所における偏角は見掛け上，可逆的な変化を起すことが示される．この場合には，従来のモデルで必要とされたような急速な地下球体の冷却は要求されない．ただし，新らしいモデルにおいても，数年おきに火山活動が起り，これに伴って磁場変動もあるという観測事実を説明するためには，対流現象のような効果的な熱伝達機構を山体内に仮定する必要がある．

BULLETIN OF THE EARTHQUAKE
RESEARCH INSTITUTE
Vol. 39 (1961), pp. 593-601

22. *Some Experiments on Thermal Shock Fracture of Rocks.*

By Seiya UYEDA and Takeo YABU,

Earthquake Research Institute.

(Read May 23, 1961.—Received September 30, 1961.)

Summary

Thermal shock resistance and thermal strain are examined experimentally on basaltic rocks: thermal strain was created in the sample, cylindrical in shape having a coaxially drilled inner hole, by suddenly pouring hot molten metal into its inner hole. It was observed that the thermal strain (tensile) measured on the outer surface of the sample increases with the increase in the temperature of the poured metal. When the thermal strain reached the critical strain, fracture was observed. The temperature of the poured metal when it causes a fracture was in the present case about 800°C onwards.

1. Introduction

Brittle materials fracture when they are subject to quick changes in temperature. Fracture in such cases is called thermal shock fracture. This phenomenon is most commonly experienced when one pours hot water into a glass, and has been much studied on ceramic materials[1),2)] for its technological importance. Evidently the fracture takes place when the magnitude of the thermal stress[3),4)], developed in the material by the non-uniformity in temperature, surpasses the critical breaking strength σ_c. The magnitude of the thermal stress may generally be expressed as,

$$\sigma=\frac{E\alpha T_1}{1-\nu}\times S \qquad (1)$$

1) *J. Amer. Ceram. Soc.*, **38**, No. 1 (1955).

2) W. D. KINGERY, *Property Measurements at High Temperatures* (1959), John Wiley.

3) S. TIMOSHENKO and J. N. GOODIER, *Theory of Elasticity*, Maple Press, York, PA., (1951).

4) *loc. cit.*, 2).

where the notations are;

σ...thermal stress,
E...Young's modulus,
α...coefficient of thermal expansion,
T_1...change in the surface temperature,
ν...Poisson's ratio,
S...function of the time t after the first change in the temperature, the space variables in the material, the size and shape and the thermal properties of both the material and surroundings.

The lowest value of T_1 to cause a fracture in the above formula may be called the thermal shock resistance factor of the test material. Putting $E=5\times10^{11}$, $\alpha=1\times10^{-5}$, $\nu=0.3$ and $\sigma_c=1\times10^{8}$ (all in c. g. s.)[5),6)], the thermal shock resistance of rocks would be,

$$T_1=(1/S)\times12°\text{C} . \qquad (2)$$

S being dependent on various factors in a complicated manner, the thermal shock resistance factor is not a material constant. It may be expected that, if the temperature change at the surface is ideally instantaneous and the contact thermal resistance is ideally small, the thermal shock resistance factor of rocks would be fairly small. It appears however that not much has been published, to the authors' knowledge, on this aspect of rocks.

Some geophysical interest may be found in the thermal shock resistance of rocks, as it would be related to the problems such as the possibilities of fracture of the crustal rocks due to magma intrusion, the formation of cracks and joints in an igneous mass when it cools or the weathering of surface rocks due to solar radiation and so forth.

2. Experiment

The experimental procedures are simple and illustrated in Fig. 1. The test samples are the cylinders, 4 *inches* in diameter of compact basalt, taken from the bore-hole near the outer somma of volcano Mihara, Oshima Island. They were supplied by the Dowa Mining Company which owns the hole. A coaxial inner hole one inch in diameter was drilled by a diammond drill in each sample. The thermal shock was given by suddenly pouring in molten metal of known tempera-

5) F. BIRCH, ed., *Handbook of Physical Constants* (1954), *Geol. Soc. Amer.*
6) K. MOGI, to be published in this Bulletin.

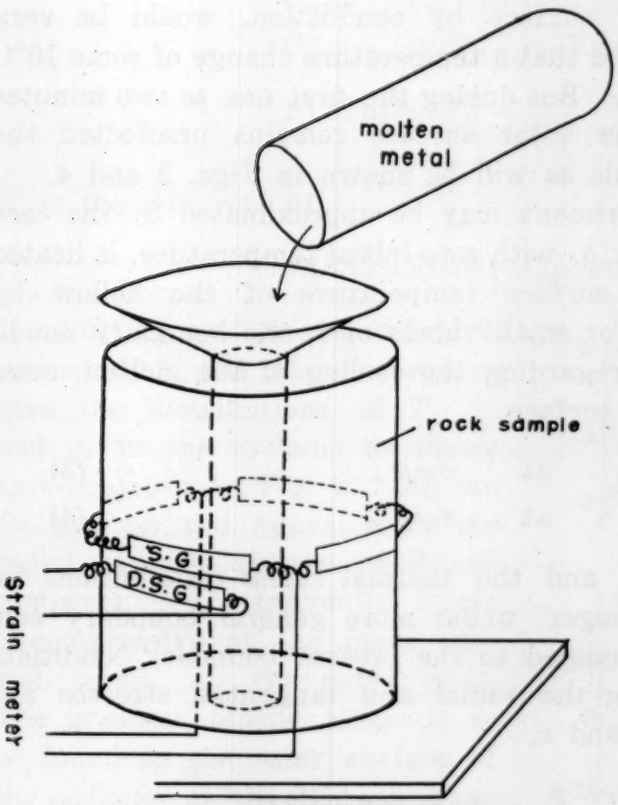

Fig. 1. Experimental procedures.
S. G.....metal wire strain gauge,
D. S. G.....dummy strain gauge.

ture to fill the inner hole. The melting of the metals was conducted by heating the pieces of metal in an alumina crucible. Metals such as tin, lead, zinc, aluminium and copper were tried and among these non-noble metals, aluminium and lead were found to be convenient for the purpose. The temperature of the molten metals was measured just before the pouring either by a Pt-PtRd thermocouple or an opitical pyrometer: the accuracy of the measurements seems to be no better than ~20°C.

The strains caused by the thermal stresses were measured on the outer surface of the sample by means of an ordinary metal wire strain gauge apparatus. Four metal strain sensitives were attached to the outer surface of the samples following the ordinary techniques and the readings were taken mannually with a commercial apparatus, or recorded by a penwriting oscillograph. It is obvious that the type of strain measurement employed here is not the best, since the electrical resistance of the metal wires is essentially dependent on temperature. Although a dummy gauge was always used to eliminate the effect of change in the ambient temperature, the rapid and non-uniform variations in the temperature which were unavoidable in the present experiments caused spurious readings a few minutes after the pouring in of hot metal. When the temperature in that part of the specimen, where the wire-gauges are attached, changes, the apparent reading will be the superposition of the various effects such as, the thermal change in the electrical resistance of the wire-gauges, the thermal expansion of both the specimen and the genuin thermal strains. Therefore, the readings after the time when the temperature change at the inner hole surface

has propagated to the outer surface by conduction, would be very complex. In fact, it was found that a temperature change of some 10°C would upset the measurement. But during the first one to two minutes when the temperature of the outer surface remains unaffected the results seemed fairly reasonable as will be shown in Figs. 3 and 4.

Mathematically, the experiment may be approximated by the case where a hollow cylinder $a<r<b$, with zero initial temperature, is heated internally by changing the surface temperature of the hollow by $T_1(T_1>0)$ stepwise at $t=0$. For small values of t, the boundary conditions may be simplified as, disregarding the cooling of the molten metal and the heating of the outer surface,

$$T=T_1 \quad \text{at} \quad r=a\,, \tag{3}$$

$$T=0 \quad \text{at} \quad r=b\,, \tag{4}$$

The temperature distribution and the thermal stress distributions for such a case were given by Jaeger[7] under more general boundary conditions. Jaeger's solution simplified to the present boundary conditions may be shown to be, denoting the radial and tangential stresses and thermal diffusivity by σ_r, σ_θ and κ,

$$T(r,\ t)=T_1\frac{\log b/r}{\log b/a}-\sum_{s=1}^{\infty} e^{-\kappa(S_s/a)^2t}\,F(S_s/a)C_0(S_sr/a) \tag{5}$$

$$\begin{aligned}\frac{(1-\nu)\,\sigma_r(r,\ t)}{E\alpha}=&\frac{-T_1}{2\log b/a}\left\{\frac{b^2(r^2-a^2)}{r^2(b^2-a^2)}\log b/a-\log r/a\right\}\\&-\sum_{s=1}^{\infty}e^{\kappa(S_s/a)^2t}F(S_s/a)\left\{\frac{b(r^2-a^2)C_1(S_sb/a)}{r^2(b^2-a^2)S_s/a}\right.\\&\left.-\frac{C_1(S_sb/a)}{(r/a)S_s}+\frac{2(b^2-r^2)}{\pi(b^2-a^2)S_s^2(r/a)^2}\right\}\end{aligned} \tag{6}$$

$$\begin{aligned}\frac{(1-\nu)\sigma_\theta(r,\ t)}{E\alpha}=&\frac{-T_1}{2\log b/a}\left\{\frac{b^2(r^2+a^2)}{r^2(b^2-a^2)}\log b/a-1-\log r/a\right\}\\&-\sum_{s=1}^{\infty}e^{\kappa(S_s/a)^2t}\,F(S_s/a)\left\{\frac{b(r^2+a^2)C_1(S_sb/a)}{r^2(b^2-a^2)S_s/a}+\frac{C_1(S_sr/a)}{S_sr/a}\right.\\&\left.-C_0(S_sr/a)-\frac{2(b^2+r^2)}{\pi(b^2-a^2)S_s^2(r/a)^2}\right\}\end{aligned} \tag{7}$$

where

7) J. C. JAEGER, *Phil. Mag.*, **36** (1945), 418.

$$C_0(x)=J_0(x)Y_0(S_s)-Y_0(x)J_0(S_s)\ ,$$
$$C_1(x)=J_1(x)Y_0(S_s)-Y_1(x)J_0(S_s)\ ,$$
$$F(S_s/a)=\pi T_1\left[\frac{J_0^2(S_sb/a)}{J_0^2(S_sb/a)-J_0^2(S_s)}\right], \tag{8}$$

S_s is the s-th root of

$$J_0(S_s)Y_0(S_sb/a)-J_0(S_sb/a)Y_0(S_s)=0\ . \tag{9}$$

Putting $a=1/2\ inch$, $a/b=1/4$, and $\kappa=10^{-2}$, the above formulas give the distributions of T, σ_r, and σ_θ in the cylinder as shown approximately in Fig. 2. As can be seen in the figure, while the radial stress is always small and compressive, the tangential stress is compressive at the inner part and tensile at the outer part. The greatest tensile stress is to be found on the outer surface of the cylinder at the instant when the heating in the inner hollow starts: the maximum of

$$\sigma_\theta(1-\nu/E\alpha T_1),$$

which is the value of S in (1), amounts to 1 on the inner surface and 0.6 on the outer surface. From these results it is expected that the fracture, in such an ideal case, would start from the outer surface inwards at the instant when the hot liquid is poured in.

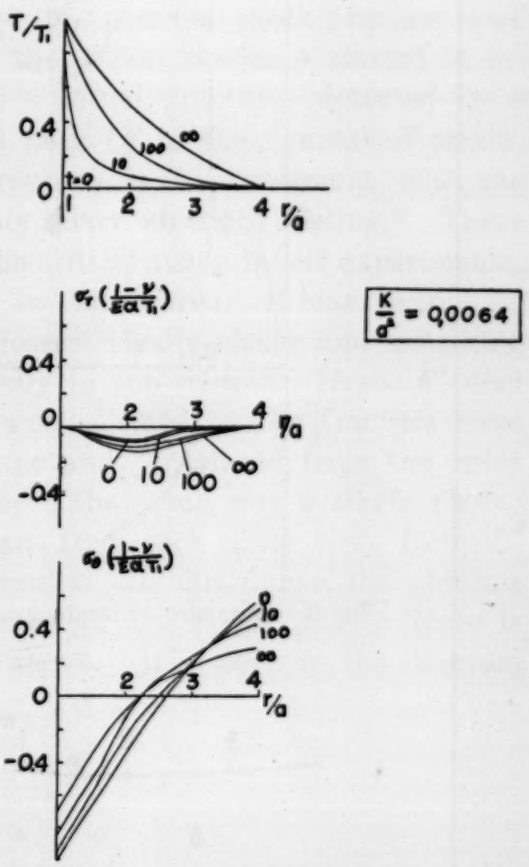

Fig. 2. Temperature and stress distributions in a hollow cylinder.

Figs. 3 and 4 are the examples of the strain (apparent) measurements. The ordinate is the reading of the strain-meter (Fig. 3) and the output signal of the strain-meter recorded by a pen-writing oscillograph (Fig. 4), and the abscissa is the time after the pouring of the metal. In all cases, the stress was found to be tensile, as expected. But, unlike the above expectation, the maximum of the tangential tensile stress took place one or two minutes after the pouring. This is considered as

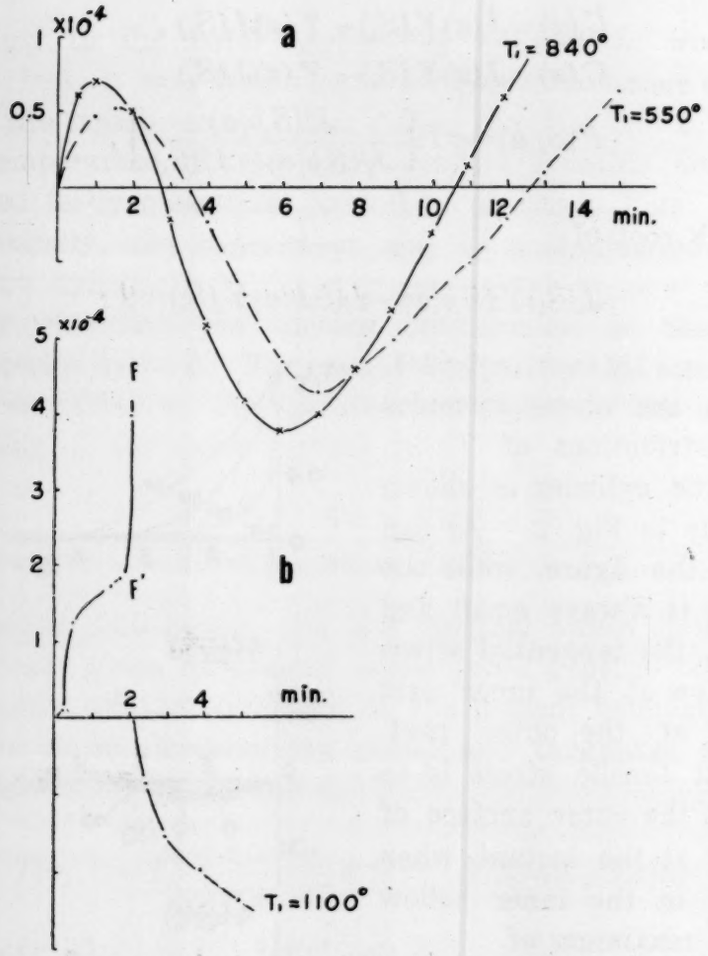

Fig. 3. Examples of strain gauge readings as dependent on time.

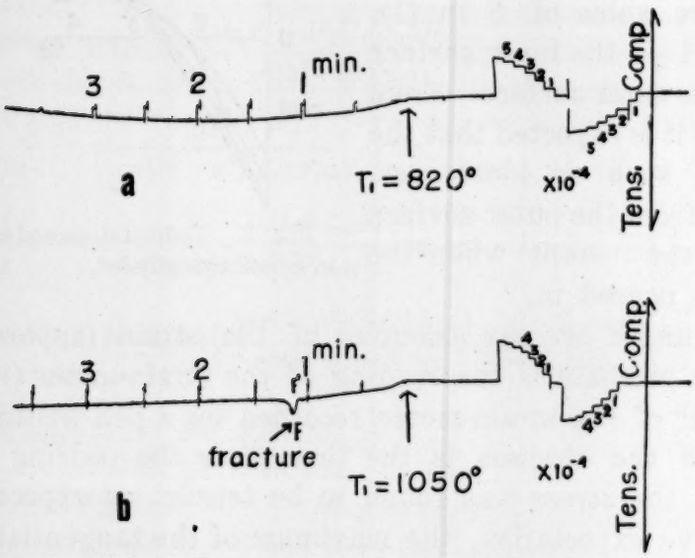

Fig. 4. Examples of strain-meter records.

being due to the fact that the temperature at the inner hole surface in actual cases did not change exactly stepwise so that the simplified boundary conditions (3) could not be met. After a few minutes, the strain decreased and became even compressive. It seemed, however, that this was only apparent because of the temperature disturbance in the strain gauge. Considering these, it may be appropriate to take the maximum value of the tensile strain (M in Figs. 3 and 4) as the thermal strain in our experiments.

In the cases of Figs. 3 (b) and 4 (b), thermal shock fracture took place. As shown in these figures, the strain suddenly started to increase just before the fracture. The actual fracture, detected by a sharp click, occurred at the pointed peak (F in the figures) of strain. The magnitude of the strain at fracture is in agreement with the critical tensile strain of rocks under ordinary strength testing.[8] There seems to be two ways of assigning the critical strain in our experiments, *i. e.* whether to take either F or F' in the figures. It may be possible that after F' the deformation is no longer ideally elastic and some kind of yield is taking place perhaps locally in the sample. If so, F' may be the true critical strain. The cracks formed by the fracture were more or less parallel to the radial plane and penetrated from the outer surface to the inner one. In most cases the crack was a single plane: occasionally three planes *ca.* 120° apart from each other were formed.

Fig. 5 summarizes the general results. In this figure, the abscissa is the temperature of the poured metal or the T_1 and the ordinate is the maximum thermal strain defined above. It is seen in the diagram

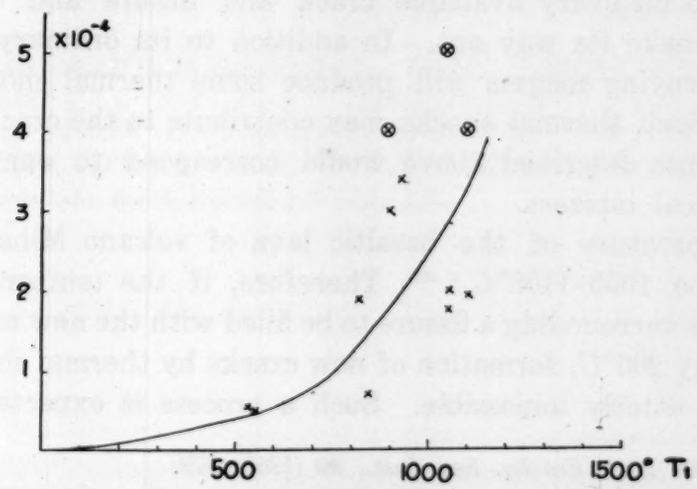

Fig. 5. Maximum observed thermal strain as dependent on the temperature of the poured metal.

that the thermal strain increases regularly with the increase in T_1. The increase however is not quite linear with T_1. The reason for this is not known. The circles with a cross correspond to the strains at F in Figs. 3 and 4 and the crosses right below each of them correspond to the strains at F'. As can be seen in the diagram, thermal shock resistance of the basalt under the present conditions seems to be about 800°C. This value is considerably higher than that expected from the simple ideal calculation described above.

3. Discussion

One of the authors (U. S.)[8] put forward a hypothesis, in order to explain the mode of temporary change in the local geomagnetic field on an occasion of major activity at volcano Mihara, that in the volcanic activity, the molten magma would rise rather slowly all through its journey from the depths to the surface. In the more orthodox view, the magma is believed to be stored in a "magma reservoir" several kilometres deep and to come out from there very quickly, through a more or less open vent. In the new hypothesis, it was postulated that the heat transfer in an active volcano would be very effective perhaps by virtue of some convective machanism, so that at the very beginning of each active period the hot magma wonld somehow have to make its way up through already cooled and solid mountain mass, which had provided a vent for the magma and had been heated during preceding activity some years before. If such is the case, the new fluidal magma would have to fill every available crack and fissure and create some new ones to make its way out. In addition to its ordinary mechanical force, the intruding magma will produce some thermal shock upon the wall rocks. Such thermal shocks may contribute to the crack-formation. The experiments described above would correspond to our own sphere of volcanological interest.

The temperature of the basaltic lava of volcano Mihara has been reported to be 1050–1100°C.[9),10)] Therefore, if the temperature of the mountain mass surrounding a fissure to be filled with the new magma should be less than say 200°C, formation of new cracks by thermal shock fracture would not be utterly impossible. Such a process is expected to proceed

8) S. UYEDA, *Bull. Earthq. Res. Inst.*, **39** (1961), 579.
9) R. TAKAHASHI and T. NAGATA, *Bull. Earthq. Res. Inst.*, **15** (1937), 1047.
10) T. MINAKAMI, *Bull. Earthq. Res. Inst.*, **29** (1951), 487.

almost instantaneously as compared with any process of heat transfer. Hence, the magma intruded into new cracks will meet practically non-heated wall rocks so that some further thermal shock fracture may be formed. This process would continue until the magma reaches the surface and by that time a fairly large portion of the mountain may have been penetrated with a resulting number of cracks and heated up to above 200–300°C. In the hypothesis referred to as 8), the heated portion is assumed to be a cylinder having a radius of 430 *m*.

In the experiment, however, the sample was of a very particular form. It is by no means guaranteed that the thermal shock resistance *in situ* would be the same as that obtained here. To make sure whether or not such thermal shock fracture would in fact play any significant rôle in volcanism, more realistic experiments as well as more exact knowledge regarding the state under the volcano would be required.

4. Acknowledgement

The authors would like to thank Dr. K. Mogi who allowed them to use his strain meter and to the Dowa Mining Company who put numerous pieces of rock-specimens at the authors' disposal.

---

22. 岩石の熱衝撃破壊について

地震研究所 {上田誠也 / 藪武夫}

玄武岩の熱衝撃抵抗および熱歪を実験的に調べた．熱歪は，円筒状内孔を有する玄武岩柱に，種々の温度の熔融金属を注入して生ぜしめられた．標本表面に発生する引つ張り歪みは，ストレーンゲージによつて測定されたが，注入金属の温度とともに増大することが観られた．また破壊を起す場合の金属温度はほぼ 800°C 以上であつた．800°C 以上の温度差を有する高温岩漿が，地層岩石内に突然注入した場合には，熱衝撃破壊の発生が予想される．

Bulletin of the Earthquake Research Institute
Vol. 39, (1961), pp. 603-630

23. *Division of the South-western Pacific Area into Several Regions in each of which Rayleigh Waves Have the Same Dispersion Characters.*

By Tetsuo A. Santô,

Earthquake Research Institute.

(Read July 28, 1961.—Received September 30, 1961.)

Abstract

In the previous papers, the writer classified the dispersion curves of Rayleigh waves into seven kinds, and gave them the characteristic numbers from "1" to "7". These curves were revealed to be not independent of each other. For example, when Rayleigh waves pass across three differing regions with dispersion characteristic numbers "1", "3" and "7" with a pass length ratio of 3:3:4, the resultant dispersion character along the total path shows the character "5". Similar relations could be found also with the other curves (Fig. 3).

Using these relations, a trial was made to divide the complicated oceanic area in the western side of the "Andesite line" into four regions "1" (purely oceanic type), "3" (sub-oceanic type), "5" (sub-continental type) and "7" (purely continental type).

At first, the present oceanic area was divided into four regions by using the dispersion data obtained along thirty-two paths for Tsukuba Station (Fig. 4). Secondly, the same work was done by adding other dispersion data along thirteen paths for three stations, Hongkong, Honolulu and Suva (Fig. 11).

In order to check the results, the group velocities of Rayleigh waves across these divided regions were calculated by least square method (Figs. 6, 12). The result showed that our division map was quite satisfactory.

Judging from the division map obtained, it was recognized that the crustal structure in the western side of the "Andesite line" was certainly more continental than in the eastern side of it. In the sea region deeper than 4 km, for instance, Rayleigh waves show the characteristic number "1" in the eastern side, while they show the sub-oceanic one "3" in the western side. The region in which Rayleigh waves show the dispersion characterized by type "1" is, in the western side of the "Andesite line", limitted to regions with a much greater ocean depth, the depth being greater than 6 km.

Rayleigh waves through the East China Sea or the Borneo Sea show the purely continental dispersion character "7". Only in the central part of the South China Sea or in small parts of the Celebes Sea, does the dispersion of Rayleigh waves show the sub-oceanic character "3".

Four kinds of dispersion curves in the divided regions were compared with the theoretical ones, and it was found that the shift of the dispersion character from "1" to "7" could be explained by decreasing the compressional waves velocity in the crust from 6.9 km/sec to 5.0 km/sec and by increasing the thickness of the crust from 5 km to 20 km. (Fig. 13).

1. Introduction

Four kinds of seismological methods have often been used to determine the crustal structure of the earth. The first two are the "reflected or refracted wave method" that is, the method by observing the reflected or refracted body waves which are generated at some discontinuity near the surface of the earth. The other two are based upon the observation of surface wave dispersions, which is classified into two. The first one is the "phase velocity method", that is, the method by observing the dispersive character of phase velocity and the other the "group velocity method" by observing that of group velocity.

Among these, the last method has very often been used by many seismologists on account of its simplicity. This method, however, has its own weakness, *i.e.*, what it gives us is an information only about the average crustal structure along a path between an epicenter and an observation station. For this reason, when the path covers various regions with different crustal structures, this method gives us no information about these local crustal structures.

The present writer has made investigations into the dispersion of Rayleigh waves along the various oceanic paths to Japan by using the records of the Columbia-type seismograph at Tsukuba Station[1),2),3)]. The most interesting fact which attracted our attention was that the

1) T. A. SANTÔ, "Observation of Surface Waves by Columbia-type Seismograph Installed at Tsukuba Station, Japan (Part I).—Rayleigh Wave Dispersions across the Oceanic Basin—." *Bull. Earthq. Res. Inst.*, **38** (1960), 219.

2) T. A. SANTÔ, "Rayleigh Wave Dispersions across the Oceanic Basin around Japan (Part II)." *Bull. Earthq. Res. Inst.*, **38** (1960), 385.

3) T. A. SANTÔ, "Rayleigh Wave Dispersions across the Ocean Basin around Japan (Part III)—On the Crust of the South-western Pacific Ocean—." *Bull. Earthq. Res. Inst.*, **39** (1961), 1.

dispersive character of Rayleigh waves changed remarkably in the south western Pacific Ocean. The result is shown in Figs. 1 and 2, in which the number beside each curve and travelling path means the characteristic number which the writer gave to each individual dispersion curve, from the typical oceanic one ("1") to the typical continental one ("7") in this order.

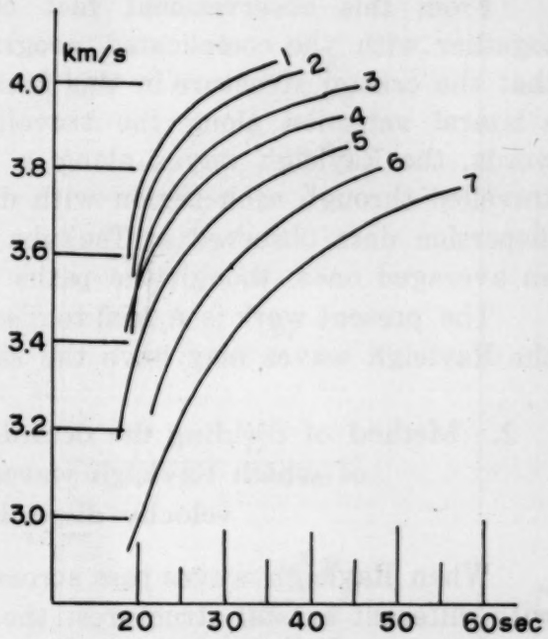

Fig. 1. Seven kinds of dispersion curves.

As is known, there runs a line, called the "Andesite line", in the south-western Pacific region (see the chain line in Fig. 2) which separates the region of predominantly andesitic volcanism from the region of the oceanic basin of predominantly basaltic volcanism. However, it has not been surveyed to ascertain whether or not the continental crustal condition just at the western side of the line continues over the whole area in this side. For this reason, it becomes very interesting that the

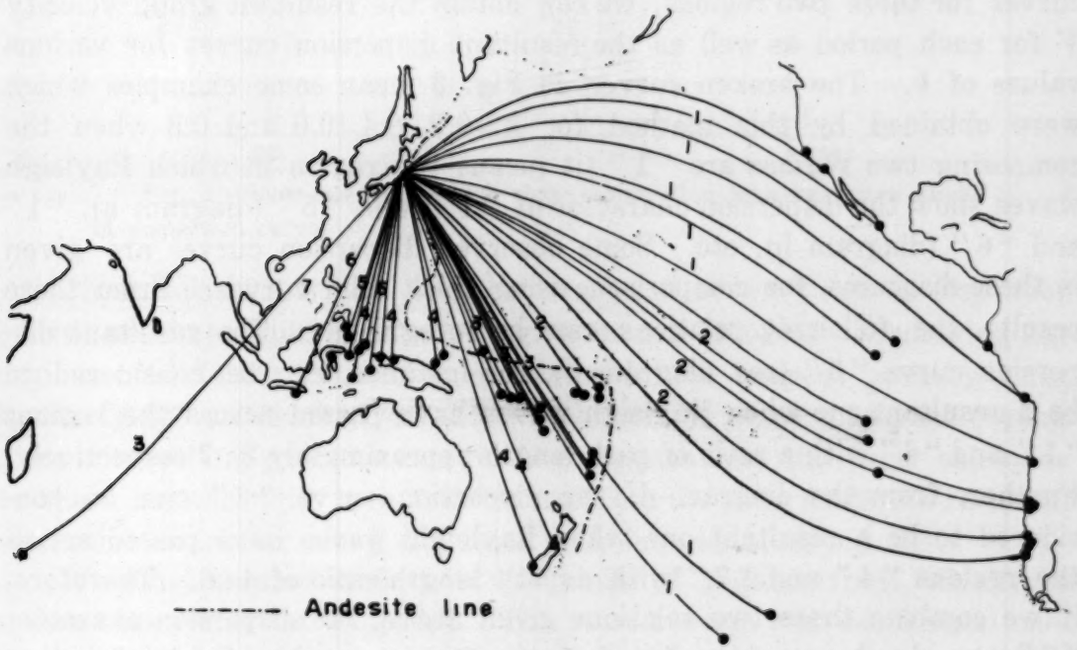

Fig. 2. Main travelling paths of Rayleigh waves across various oceanic paths.

dispersion character of Rayleigh waves on this side changes gradually from "2" to "7" with the shift of the travelling path westward.

From this observational fact concerning the dispersion character together with the complicated geographical conditions, we can suggest that the crustal structure in this area will be very complicated and has a lateral variation along the travelling paths to Tsukuba. In other words, the Rayleigh waves along a path across this area must have travelled through each region with different velocities. Therefore, the dispersion data observed at Tsukuba along these paths are nothing but an averaged ones, though the paths are all ocanic ones.

The present work is a trial to discover some regions in each of which the Rayleigh waves may have the same dispersive character.

2. Method of dividing the oceanic area into some regions in each of which Rayleigh waves have the same group velocity dispersion character.

When Rayleigh waves pass across two regions A and B, for instance, with different crustal structures, the resultant group velocity V can be found by the following simple relation, $k\Delta/V_A+(1-k)\Delta/V_B=\Delta/V$, in which, V_A and V_B are the group velocities of Rayleigh waves across A and B regions respectively and k is the ratio of the path length over the region A to the total one Δ. Therefore, if we know two kinds of dispersion curves for these two regions, we can obtain the resultant group velocity V for each period as well as the resultant dispersion curves for various values of k. The broken curves in Fig. 3 mean some examples which were obtained by this method for $k=0.2$, 0.4, 0.6 and 0.8 when the composing two regions are "1" (it means the region in which Rayleigh waves show the dispersion character of "1") and "5" (diagram a), "1" and "6" (diagram b), etc. Some observed dispersion curves are given in these diagrams, for comparison, using thick solid curves. From these results, the following relations can be recognized: The resultant dispersion curve "5" (see diagram b), for instance, can be considered to be a resultant one when Rayleigh waves have passed across the regions "1" and "6" with a ratio of path length approximately 3 : 7 respectively. Further, from the diagram d, the dispersion curve "6" can be considered to be a resultant one when Rayleigh waves have passed across the regions "4" and "7" with a path length ratio of 4 : 6. Therefore, if we combine these two relations given above, the dispersion character "5" can also be considered to be a resultant one when Rayleigh waves

have passed across three regions "1", "4" and "7" with a path length ratio of approximately 3 : 3 : 4. Similar relations can be found for any other curve.

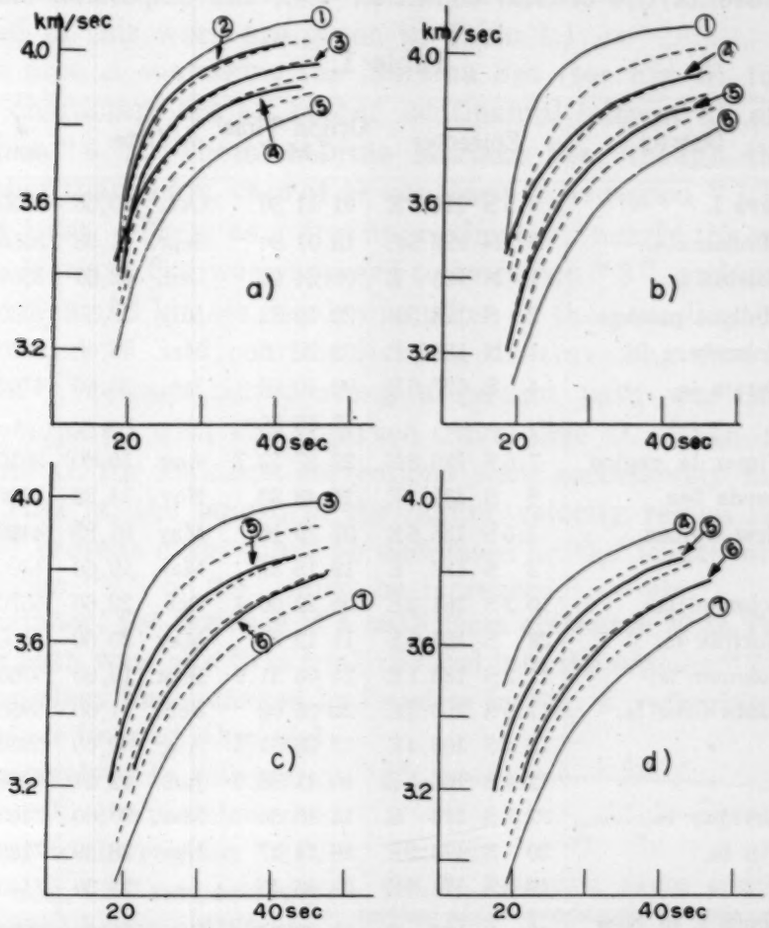

Fig. 3. Some examples which show the relation between seven kinds of dispersion curves.

These relations which hold between the seven kinds of dispersion curves are important ones, which give us a method for discovering the regions of differing dispersive character in the present area by using inversely the relations given above. Namely, if we assume some regions along a travelling path, we can divide each path into the parts belonging to these regions with such suitable path lengths as to make the resultant dispersion character along the total path into an observed one.

We must assume at first, a few kinds of regions from which the present area may be composed. The most oceanic and continental ones "1" and "7" must of course be selected. As has been reported in the

previous paper, the dispersion curve through the Indian Ocean shows "3", differing from that in the central Pacific Ocean ("1"). Therefore, the region, *i.e.*, the curve "3", was selected as a "sub-oceanic" one which represents the crustal condition *i.e.*, the dispersion character, in

Table 1.

No.	N	District	Epicenter	Origin Time (G.M.T.)	Date	Δ (km)	h (km)	M
29	6	Java I.	9.5S 112.5E	01h 11m 30s	Oct. 20,58	5850		
77	3	Mindanao I.	7 N 126.5E	18 01 30	Sept. 11,58	3550		
101	5	Celebes I.	1 N 123 E	09 34 00	Dec. 02,59	3500		6.5
56	5	Molluca passage.	2 S 126.5E	20 15 33	July 22,59	4060		
125	3	Helmahera Is.	1 N 129 E	02 22 06	Mar. 06,60	4080		
114	4	Ceram Is.	4 S 127.5E	04 40 56	Jan. 23,60	4700		6.5
115	4	〃	〃	17 56 30	〃	〃		
217	5	Timor Is. region	7.6S 128.8E	22 27 52.7	Aug. 16,60	5010	63	
34	5	Banda Sea	6 S 131 E	13 48 20	Nov. 14,58	4780		
21	4	New Guinea	3.5S 135.5E	07 19 16	May 01,59	4480		
126	4	〃	3 S 138 E	19 15 37	Mar. 19,60	4390		
221	4	Solomon Is.	10.3S 161.2E	08 22 00.7	Oct. 22,60	5570		6.5
138	4	Norfolk Is.	28 S 167.5E	11 12 31	May 20,60	7650		6.5
207	3	Solomon Is.	11.2S 163.1E	14 04 31.9	Sept. 10,60	5750	48	
116	3	Santa Cruz Is.	11.5S 166.5E	20 56 08	Feb. 11,60	5950		
216	3	〃	12.4S 166.4E	23 36 51.5	Aug. 09,60	5980	80	
238	3	〃	12.4S 166.3E	10 11 56.9	Jan. 02,61	6060	161	6.8
127	3	Loyality Is.	22.5S 174 E	15 19 30	Mar. 30,60	7400		
119	3	Fiji Is.	20 S 174.5E	16 14 47	Nov. 28,59	7180		
123	3	〃	19.5S 174.5E	02 45 45	〃 28,59	7140		
111	4	South I. of New Zealand	42 S 173 E	00 46 56	Feb. 21,60	9270		
12	3	〃	29.5S 176.5W	14 19 51	Oct. 29,59	8550		6.5
9	3	Kermadec Is.	29 S 177 W	22 23 53	Sept. 14,59	8500		6.5
10	3	〃	〃 176.5W	15 31 57	〃 29.59	8510		6.5
206	3	Tonga Is.	27.6S 176.9W	07 35 22	〃 01,60	8480	500	
13	3	〃	24 S 176.5W	13 15 49	〃 14,59	8100		
227	3	South of Tonga Is.	24.2S 176.1W	14 12 21.1	Nov. 23,60	8125	28	7
205	2	Fiji Is.	16.1S 179.6W	20 02 12.8	Sept. 01,60	7160	183	
203	2	Tonga Is.	15.1S 176.1W	14 16 52.4	〃 24,60	7290	92	
17	2	Samoa Is.	15 S 174.5W	20 14 27	Apr. 22,58	7400		6.5
14	3	Tonga Is.	17 S 173 W	21 09 09	Aug. 06,58	7670		6.5
45	2	Samoa Is.	16 S 172 W	17 44 48	Nov. 16,58	7660		6.3

N: Characteristic number of Rayleigh wave dispersion.

the India Ocean. Corresponding to this, the region, *i.e.*, the curve "5" was selected as a "sub-continental" one.

Then, our purpose is to discover these four parts in each travelling path. The actual procedure taken is as follows. (The data of the shocks used in this work are given in Table 1.)

In the area *A* containing the Mariana Sea (see Fig. 5), the observed dispersion characters are all rather continental (almost all of them are from "4" to "6"). Therefore, the Mariana Sea, though the depth is mostly deeper than 4 km, cannot be supposed to be region "1", but must be "3" at least. Then, as a first approximation, nearly the whole of the area in the Mariana Sea was supposed to be region "3", and outside of it, the contour line of 1 km sea depth was taken as the boundary between the regions "5" and "7". Upon this division, the travelling-time of Rayleigh waves with a certain period along a certain path was calculated *C*. This was compared with the observed travel-time *O*. Then if *C* is much greater than *O*, for instance, corrections were successively made on the division. That is, the length of the higher velocity region in the path, "3" in the present case, must be decreased or the length of the lower velocity region "7" or "5" must be increased, ...etc.

For instance, for the case of a path from epicenter 29 to Tsukuba (see Fig. 4), the path was, as a first trial, divided into the regions "7", "5" and "3", by boundary lines marked by *l* and *m* in Fig. 4, referring to the sea depth countour lines of 1 km and 4 km respectively. In this case, X_1, X_3, X_5 and X_7 (the path lengths which belong to the regions "1", "3", "5" and "7" respectively along the path) become 3160 km, 280 km, 2410 km and 0 km respectively. As the group velocities of Rayleigh waves for the period of 30 seconds in the regions "7", "5", "3" and "1" have been observed to be 3.40 km/sec, 3.70 km/sec, 3.88 km/sec and 4.00 km/sec respectively, the travel-time *C* became 930+76+720+0=1628 seconds, which is too much smaller than the observed one *O*, 1648 seconds. Then the value of X_3 was successively so decreased as to become the $O-C$ much smaller.

Fig. 4. Schematic figure which shows the method of discovering the boundaries of different regions. Along the path from 77 to the observed station *O*, the boundaries *m* and *n* which divide the regions (7, 5) and (5, 3) respectively were so moved as $m \rightarrow m'$ and $n \rightarrow n'$ in order to make the values of $O-C$ sufficiently small.

Next, in the case of the path from 77 to the observation station *O*, the boundaries which had been determined along the previous path were prolonged approximately parallel to the contour lines of sea depth.

In this case, however, the resultant dispersion characteristic number for this path is "3" which is remarkably more oceanic than the previous one ("6"). In order to explain this, the purely oceanic portion "1" was inserted along the path at a position in the deep sea region, deeper than 6 km. In this case also, the lengths belonging to each region were so chosen by the trial and error method as to make the value of $O\sim C$ sufficiently small.

These procedures were successively taken one by one for every path. Of course, the individual division itself along each path is not a unique one. But, if these boundaries being obtained on every path are reasonably connected to each other, we may say that the boundaries thus obtained are suitable as a first stage at least.

By connecting the corresponding division points on every travelling path, a map of the divided regions can be made, which is given in Fig. 5. For comparison, a chart is also given in the left, in which, in order to avoid complexity, the travelling paths are omitted. The path

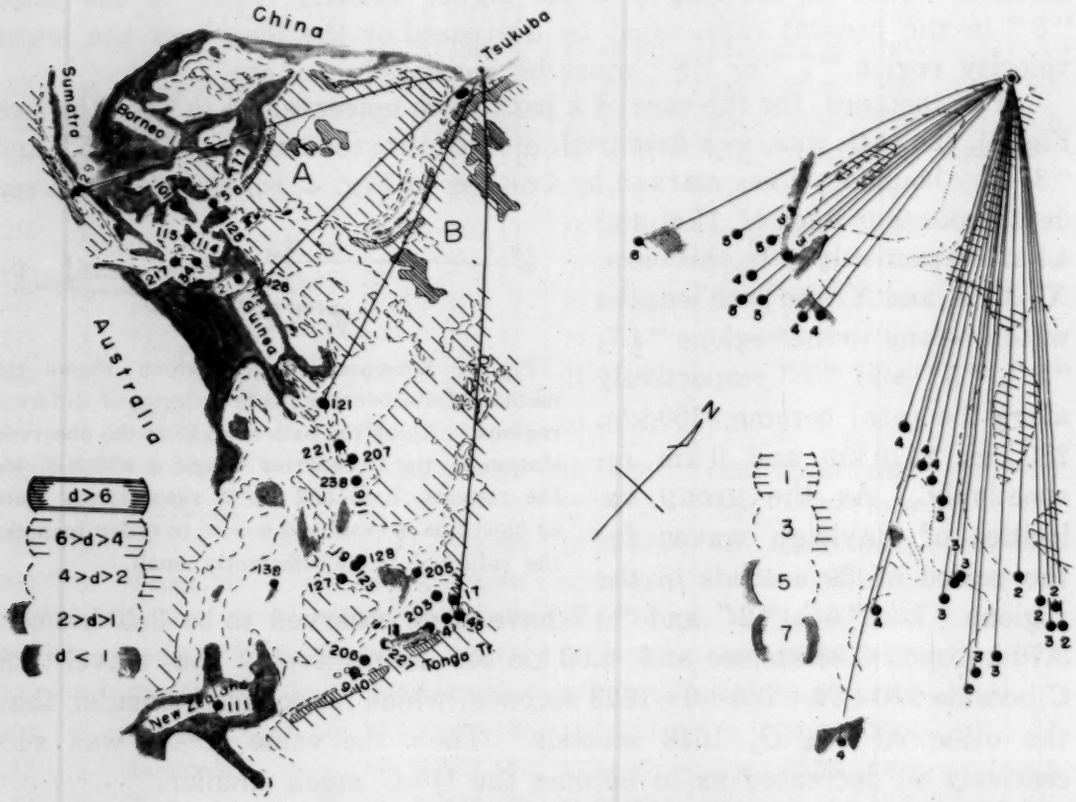

Fig. 5. A chart (left) and the map of the divided four regions in each of which Rayleigh waves have the same dispersion character. The number beside each epicenter in the chart means the shock number. d: sea depth in km.

lengths X_1, X_3, X_5 and X_7 belonging to each region, the observed travel-time C and the calculated one O along each path are given in Table 2.

As a check on this result, on the other hand, we can calculate the group velocities of Rayleigh waves in these four regions by the least square method as follows.

If the divisions were correct and thus, the dispersion characters were the same along every path in each region, we can write down the following k linear equations for every path for a given period T_0.

$$\left.\begin{array}{l} \dfrac{X_{11}}{V_1}+\dfrac{X_{31}}{V_3}+\dfrac{X_{51}}{V_5}+\dfrac{X_{71}}{V_7}=t_1(T_0) \\ \vdots \\ \dfrac{X_{1j}}{V_1}+\dfrac{X_{3j}}{V_3}+\dfrac{X_{5j}}{V_5}+\dfrac{X_{7j}}{V_7}=t_j(T_0) \\ \vdots \\ \dfrac{X_{1k}}{V_1}+\dfrac{X_{3k}}{V_3}+\dfrac{X_{5k}}{V_5}+\dfrac{X_{7k}}{V_7}=t_k(T_0) \end{array}\right\} \quad \cdots\cdots\cdots\cdots\cdots(1),$$

where X_{3j}, for instance, is the travelling path length belonging to the

Table 2.

"A" Group

No.	N	Δ (km)	X_1 (km)	X_3 (km)	X_5 (km)	X_7 (km)	t_{20} (sec)	t_{25} (sec)	t_{30} (sec)	t_{35} (sec)
29	(6)	5850	0	0	2890	2960	1880 (1848)	1720 (1715)	1640 (1648)	1590 (1609)
66	(3)	3550	1000	1140	1160	300	1040 (1037)	950 (958)	915 (932)	890 (918)
101	(5)	4500	400	1660	760	1680	1410 (1380)	1275 (1274)	1220 (1228)	1195 (1202)
56	(5)	4060	300	1560	1600	600	1230 (1214)	1120 (1121)	1080 (1085)	1060 (1065)
125	(3)	4080	850	2300	710	220	1180 (1184)	1070 (1091)	1050 (1059)	1030 (1046)
114	(4)	4700	850	1330	1710	810	1360 (1398)	1280 (1293)	1260 (1254)	1235 (1230)
115	(4)	4700	850	1330	1710	810	1360 (1398)	1280 (1293)	1260 (1254)	1235 (1230)
217	(5)	5010	0	1820	2020	1170	1520 (1509)	1370 (1401)	1350 (1359)	1340 (1329)
34	(5)	4780	0	1470	2590	720	1390 (1429)	1320 (1331)	1290 (1289)	1270 (1264)
21	(4)	4480	0	2750	1290	440	1270 (1314)	1210 (1224)	1180 (1189)	1155 (1167)
126	(4)	4390	0	2200	1890	330	1310 (1291)	1190 (1203)	1160 (1166)	1140 (1146)

(to be continued)

(continued)

"B" Group

No.	N	Δ (km)	X_1 (km)	X_3 (km)	X_5 (km)	X_7 (km)	t_{20} (sec)	t_{25} (sec)	t_{30} (sec)	t_{35} (sec)
121	(4)	5110	620	1590	2220	680	1550 (1520)	1390 (1407)	1350 (1365)	1320 (1340)
221	(4)	5570	1200	870	2820	680	1650 (1648)	1570 (1531)	1500 (1486)	1450 (1461)
138	(4)	5650	1200	930	4620	900	2310 (2278)	2120 (2118)	2050 (2054)	1990 (2011)
207	(3)	5750	2200	430	2820	300	1613 (1653)	1570 (1574)	1500 (1517)	1450 (1488)
116	(3)	5950	2800	900	1870	380	1720 (1714)	1600 (1590)	1550 (1548)	1520 (1517)
216	(3)	5950	2800	900	1870	380	1700 (1714)	1580 (1590)	1530 (1548)	1510 (1517)
238	(3)	5950	2800	800	1870	380	1780 (1714)	1620 (1590)	1550 (1548)	1520 (1517)
127	(3)	7400	2600	1700	2600	500	2170 (2150)	2010 (1989)	1940 (1935)	1890 (1907)
119	(3)	7180	2800	2200	1900	280	2070 (2069)	1910 (1908)	1850 (1864)	1820 (1837)
122	(3)	7180	2800	2200	1900	280	2100 (2069)	1900 (1908)	1840 (1864)	1810 (1837)
111	(4)	9270	1040	1500	5450	1280	2800 (2769)	2565 (1567)	2460 (2479)	2400 (2435)
9	(3)	8500	3200	3500	1500	300	2400 (2437)	2250 (2250)	2200 (2193)	2160 (2167)
10	(3)	8500	3200	3500	1500	300	2430 (2437)	2260 (2250)	2200 (2193)	2180 (2167)
206	(3)	8480	3400	3200	1500	280	2390 (2398)	2220 (2213)	2120 (2166)	2080 (2136)
13	(3)	2100	4700	1700	1490	300	2300 (2300)	2100 (2126)	2060 (2078)	2020 (2054)
227	(3)	8100	4700	1700	1400	300	2320 (2300)	2120 (2126)	2080 (2078)	2050 (2054)
205	(2)	7160	4400	1900	1600	260	2010 (2022)	1880 (1868)	1810 (1829)	1780 (1807)
203	(2)	7290	5350	1250	500	190	2020 (2036)	1890 (1886)	1830 (1853)	1810 (1829)
17	(2)	7400	3800	3150	250	200	2060 (2098)	1920 (1938)	1870 (1887)	1850 (1863)
14	(3)	7670	3810	3160	400	300	2130 (2177)	1990 (2009)	1960 (1965)	1930 (1942)
45	(2)	7660	3810	3250	400	200	2190 (2167)	2000 (2001)	1940 (1952)	1920 (1932)

No: Shock number. N: Dispersion characteristic number.
X_i: Path length along the region "i" (in km).
Δ: Total path length (in km).
t_{20}: Observed and calculated (in bracket) travel-times for the Rayleigh waves with periods of 20 seconds.

region "3", being measured on the division map along the path between the epicenter j to the observation station, V_3 the group velocity of Rayleigh waves in the region "3" and t_j (T_0) the travel-time of Rayleigh waves with the period T_0 along the total path. From these equations,

we can calculate the four unknowns V_1, V_3, V_5 and V_7 for a given period from eleven equations in A area, from twenty-one equations in B area or thirty-two equations for the $A+B$ area respectively.

From the data given in Table 2, the following observational equations can be written.

$$
\begin{array}{ll}
 & T_0: \quad 20 \quad 25 \quad 30 \quad 35 \\
\text{area } A & \left\{\begin{array}{l}
0\frac{1}{V_1}+\ 0\frac{1}{V_3}+2890\frac{1}{V_5}+2960\frac{1}{V_7}=1880,\ 1720,\ 1640,\ 1590 \\
1000\frac{1}{V_1}+1140\frac{1}{V_3}+1160\frac{1}{V_5}+\ 300\frac{1}{V_7}=1040,\ \ 950,\ \ 915,\ \ 890 \\
400\frac{1}{V_1}+1600\frac{1}{V_3}+\ 760\frac{1}{V_5}+1680\frac{1}{V_7}=1410,\ 1275,\ 1220,\ 1195 \\
\vdots\quad\ \vdots\quad\ \vdots\quad\ \vdots\quad\ \vdots\quad\ \vdots\quad\ \vdots\quad\ \vdots \\
0\frac{1}{V_1}+2200\frac{1}{V_3}+1890\frac{1}{V_5}+\ 330\frac{1}{V_7}=1310,\ 1190,\ 1160,\ 1140
\end{array}\right. \\
\text{area } B & \left\{\begin{array}{l}
620\frac{1}{V_1}+1590\frac{1}{V_3}+2220\frac{1}{V_5}+\ 680\frac{1}{V_7}=1500,\ 1390,\ 1350,\ 1320 \\
1200\frac{1}{V_1}+\ 870\frac{1}{V_3}+2820\frac{1}{V_5}+\ 680\frac{1}{V_7}=1650,\ 1570,\ 1500,\ 1450 \\
\vdots\quad\ \vdots\quad\ \vdots\quad\ \vdots\quad\ \vdots\quad\ \vdots\quad\ \vdots\quad\ \vdots \\
3810\frac{1}{V_1}+3250\frac{1}{V_3}+\ 400\frac{1}{V_5}+\ 200\frac{1}{V_7}=2190,\ 2000,\ 1940,\ 1920
\end{array}\right.
\end{array}
$$

.....(2).

The calculations were made for the following three cases: (1) for A area only, (2) for B area only and (3) for $(A+B)$ area. The values of V_1, V_3, V_5 and V_7 calculated from the equations (2) are given in Table 3, and are plotted in the dispersion diagrams of a_2 (for A area), b_3 (for B area) and a_2+b_3 (for $A+B$ area) in Fig. 6 respectively. In these cases, the calculated dispersion dots lie well, in the range of observational errors at least, around the corresponding four dispersion curves. Of course, the writer could not reach this satisfactory result at once. He also obtained some unsuitable results, which are shown in the diagrams of a_1, b_1 and b_2 in Fig. 6. In these cases, the discrepancy between the calculated dots and the observed dispersion curves was very large owing to the great values of $O\sim C$ along every path and

Table 3.

V / T_0	V_1 (km/s)			V_3 (km/s)			V_5 (km/s)			V_7 (km/s)		
		Cal.	Obs.		Cal.	Obs.		Cal.	Obs.		Cal.	Obs.
20 sec	A	3.69		A	3.48		A	3.56		A	2.99	
	B	3.66	3.65	B	3.52	3.45	B	3.34	3.35	B	2.72	3.00
	A+B	3.62		A+B	3.56		A+B	3.32		A+B	2.93	
25 sec	A	3.96		A	3.85		A	3.68		A	3.19	
	B	3.93	3.94	B	3.81	3.78	B	3.48	3.59	B	3.58	3.25
	A+B	3.90		A+B	3.87		A+B	3.56		A+B	3.28	
30 sec	A	4.02		A	3.93		A	3.68		A	3.45	
	B	4.03	4.00	B	3.90	3.88	B	3.70	3.70	B	3.52	3.40
	A+B	3.90		A+B	3.87		A+B	3.56		A+B	3.28	
35 sec	A	4.19		A	3.96		A	3.74		A	3.57	
	B	4.09	4.04	B	3.92	3.93	B	3.87	3.78	B	3.49	3.50
	A+B	4.04		A+B	3.90		A+B	3.72		A+B	3.42	

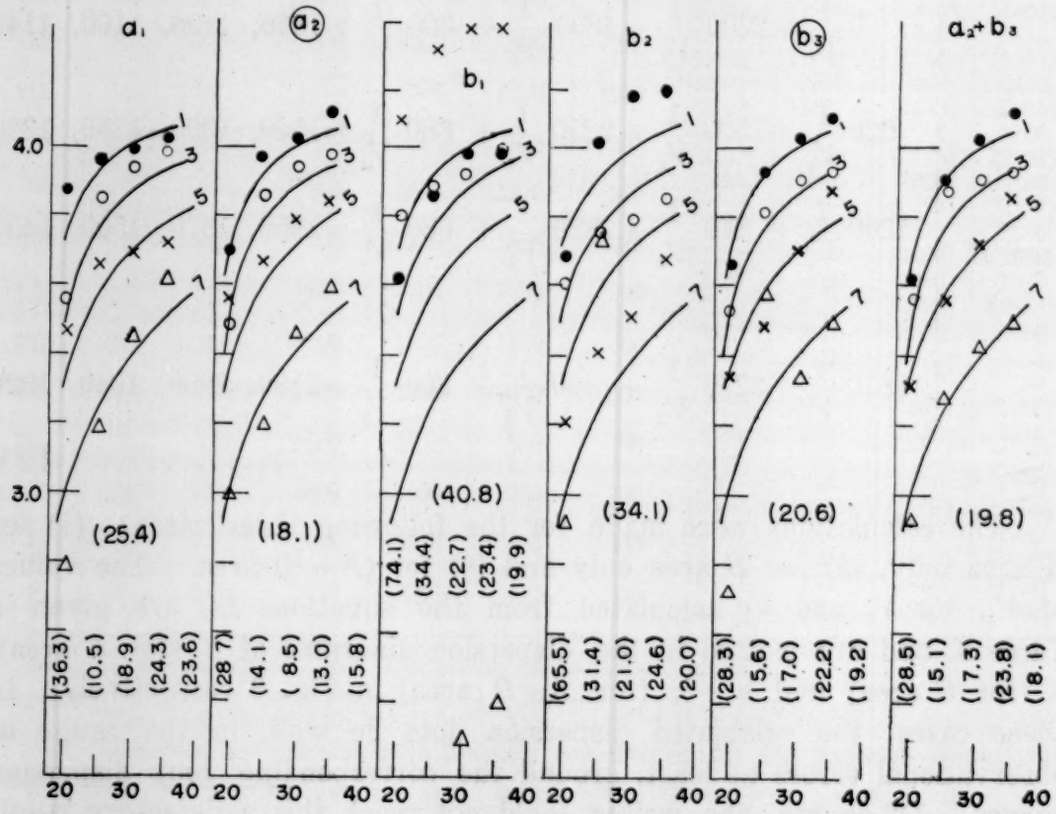

Fig. 6. Calculated dispersion data based on some unsuitable division (a_1, b_1 and b_2) and the final one (a_2, b_3 and a_2+b_3). The black and white circles, crosses and triangles mean the calculated group velocities in the regions "1", "3", "5" and "7" respectively and the smoothed curves mean the observed ones. The numbers in brackets above every period scale and in the centre are the standard deviations of $O\sim C$ in seconds for every period and for the whole periods respectively.

their large standard deviations for every period. (See Table 4 and diagrams in Fig. 6).

Table 4.

$O\sim C$ for "A" Group

	20 sec		25 sec		30 sec		35 sec	
	a_1	a_2	a_1	a_2	a_1	a_2	a_1	a_2
29	32	23	5	5	8	8	19	19
77	15	3	6	8	7	17	18	28
101	41	30	15	1	2	8	3	7
56	27	16	20	0	5	5	10	5
128	37	4	50	21	39	9	48	16
114	25	38	5	13	13	6	10	5
115	27	38	8	13	16	6	12	5
217	51	11	11	31	31	9	9	11
34	39	39	11	11	1	1	6	6
21	59	44	30	14	26	9	25	12
126	19	19	13	13	6	6	6	6
σ	36.8	28.8	10.5	14.1	18.9	8.5	24.4	15.8

$O\sim C$ for "B" Group

	20 sec			25 sec			30 sec			35 sec		
	b_1	b_2	b_3	b_1	b_2	b_3	b_1	b_2	b_3	b_1	b_2	b_3
121	136	86	30	23	23	17	19	19	15	8	8	20
221	68	54	2	84	74	39	51	43	14	34	14	25
138	147	96	32	60	34	2	43	25	4	13	7	7
207	197	197	40	42	42	17	17	17	17	20	38	38
116	27	27	6	10	10	10	2	2	2	3	3	3
216	7	7	14	10	10	10	18	18	18	7	7	7
238	87	87	66	30	30	30	2	2	2	3	3	3
127	45	45	20	21	21	21	5	5	5	17	17	17
119	36	36	1	2	2	2	14	14	14	17	17	17
122	61	61	1	8	8	8	24	24	24	27	27	27
111	89	31	31	22	22	2	9	9	19	23	35	35
9	2	31	31	0	0	0	7	7	7	7	7	7
10	38	38	37	10	10	10	7	7	7	13	13	13
206	29	29	7	7	7	7	34	34	34	56	56	56
13	18	18	8	50	26	26	28	18	18	46	34	34
227	32	32	0	30	30	6	8	8	2	6	6	4
205	24	24	20	0	0	12	27	27	19	6	6	34
203	5	5	16	70	4	4	36	23	25	34	19	19
17	3	38	38	18	18	18	17	17	17	13	13	13
14	10	47	47	33	19	19	15	5	5	15	15	12
45	64	23	23	1	1	1	12	12	12	12	12	12
σ	74.1	65.1	28.3	34.4	31.4	15.6	22.7	21.0	17.0	23.4	24.6	22.2

In Table 4, the $O\sim C$ for $T_0=20$ seconds are remarkably larger than those for other periods. This is owing to the large observational errors

in determining the group velocities in such a short period range where dV/dT is nearly infinitive.

From the final results a_2, b_3 and a_2+b_3 in Fig. 6, we may say that our division of the present area into such regions as is shown in the right map of Fig. 4 is quite a satisfactory one. It means, in other words, that if we divide the present area into such regions "1", "3", "5" and "7" as is shown in the right-hand map given in Fig. 4, all of the resultant dispersion character of Rayleigh waves observed at Tsukuba through the present area can be well explained.

3. Further investigations by using the seismograms at some other observation stations.

The figure of the divided regions, obtained by the method above given, is of course not exact. This method has an inevitable assumption about the kinds and numbers of fundamental regions. Even if the assumption we made were suitable, there remains the uncertainty about the shapes of divided regions due to the restricted dispersion data at the single station, Tsukuba. In other words, as the paths are all concentrated into a single station, the positions or the shapes of the divided region may have some radial uncertainty along the paths.

In order to remove this uncertainty and to correct the figures of regions or to discover some new boundaries which have been blind to the data at Tsukuba, dispersion data along other paths which, if possible, cross nearly perpendicularly the paths to Tsukuba Station are quite desirable. The most suitable stations for this purpose are Hongkong (China), Honolulu (Hawaii) and Suva (Fiji Is.) at which the same instruments as at Tsukuba, the Columbia-type seismographs, have been installed for the I.G.Y. and I.G.C. program.

The Lamont Geological Observatory, Columbia University, U.S.A. favoured the writer by sending him many copies of the seismograms recorded at these stations. From these copies, the writer was able to investigate into many such dispersive characteristics of Rayleigh waves resulting from shocks as are given in Table 5.

a) *General description about dispersion characteristics.*

Fig. 7 shows the dispersion data of Rayleigh waves along shorter paths (diagram (a)) and along longer ones (diagram (b)). From the dispersion characters shown in (a), the crustal conditions in the South

China Sea were newly ascertained. That is, the dispersion data of Rayleigh waves which pass over this area lie quite close along the continental curve "7". But, the dispersion data along the path, from the shock (250) to Hongkong which partly passes over the deep sea region at the middle of the Sea, lie close on the curve "5". This tells

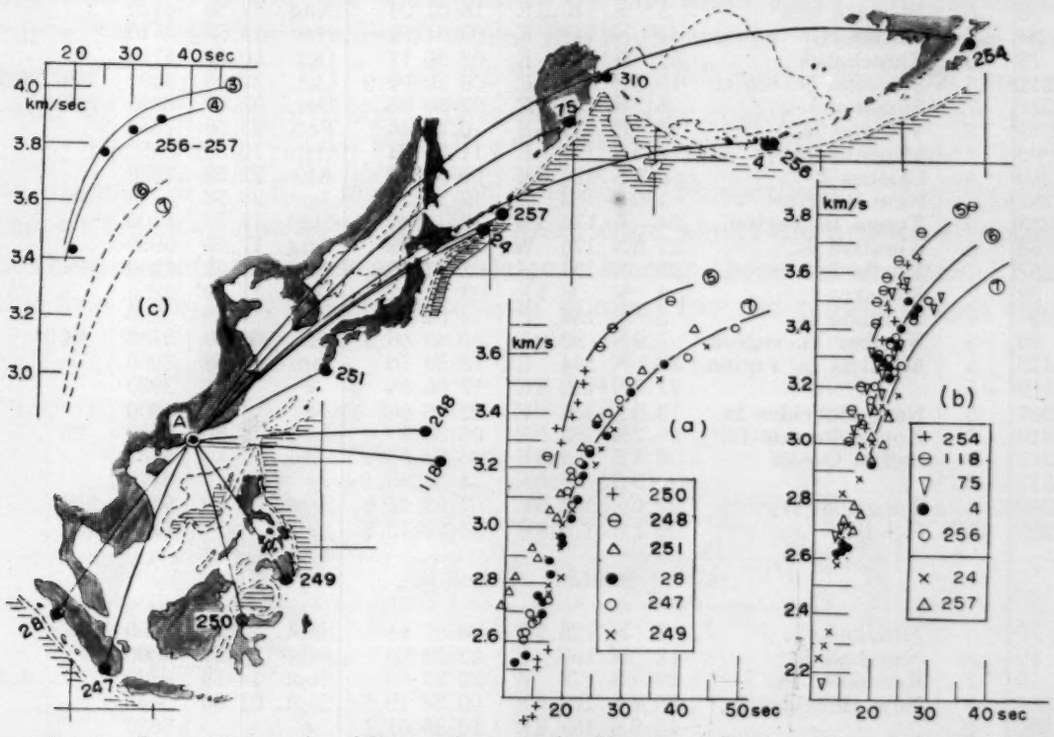

Fig. 7. Travelling paths of Rayleigh waves for Hongkong Station (A), and the dispersion data for every path (diagrams (a) and (b)). The black circles in (c) diagram represent the dispersion data being calculated by the subtraction of travel-times between the two epicenters (256) and (257).

us that there is an oceanic region somewhere in the middle of the South China Sea. The dispersion data of the shock (251) also lie close on the dispersion curve "7" for periods longer than 20 seconds, but they remarkably deviate from it in the short period range. The writer should like to postpone the explanation of this fact to some future time.

The dispersion data along the northern paths traversing the Japan Sea and the East China Sea were given in diagram (b). The dispersion data along the path resulting from the Kurile Islands shocks (24) and (257) lie close on the continental curve "7", though the dispersion data are missing for the periods longer than 25 seconds. On the other hand, in the dispersion data resulting from the Aleutian Islands shocks (4) and (256),

Table 5.

No.	N	District	Epicenter	Origin Time (G.M.T.)	Date	Δ (km)	h (km)	M
			Station: Hongkong					
4	6	Aleutian Is.	51.5N 176.5W	05h53m07s	July 01,58	6660	250	6
76	5	Bismark Sea	3 S 145.5E	18 01 05	Aug. 17,58	4440		
24	7	Kurile Is.	44 N 149 E	05 34 53	Nov. 14,58	4110		
75	6	Kamchatka	53 N 160 E	08 30 17	Oct. 10,58	5110		
211	5	Solomon Is. region	10.3S 161.2E	08 22 00.9	Oct. 22,60	6250	93	6.5
247	7	Sumatra I.	5 S 104 E	07 30 05	Dec. 02,59	6200	250	
249	5	Volcano Is.	24 N 141.5E	10 47 40	Feb. 23,58	2850		
249	7	Mindanao I.	5.5N 127 E	11 35 24	Oct. 10,58	2350		
250	5	Celebes I.	0.5S 120.5E	09 08 13	Apr. 22,58	2620		
252	5	New Britain	4.5S 153 E	19 12 36	Apr. 23,58	5150	100	
253	5	Tonga Is. region	24 S 176.5W	13 15 49	Sept. 14,59	9100		
256	6	Aleutian Is.	21.5N 176 W	09 08 35	Aug. 17,58	6650		
257	7	Kurile Is.	45 N 152 E	02 57 40	Apr. 23,58	4200		
28	7	Sumatra I.	2 N 98.5E	03 21 52	Oct. 12,59	2850		
320	4	Solomon Is.	5 S 154 E	14 56 57	May 1,59	5280		
99	6	Nicobar Is. region	7.9N 92.9E	20 40 06.5	Oct. 08,60	2780	84	
118	5	Mariana Is. region	22 N 144 E	18 38 10	Jan. 30,58	3060		
119	5	〃	21.5N 142.5E	17 56 05	〃	2920		
307	5	Near Hebrides Is.	13.5S 166 E	22 05 06	〃	6900		
310	7	Komandorskie Is.	55.7N 163.9E	05 35 21.0	Aug. 15 60	5360	25	
212	3	Indian Ocean	13.4S 65.8E	06 58 56.4	〃	6580		
213	3	〃	13.5S 67.0E	14 33 38.4	〃	6470		
206	4	Tonga Is. region	27.6S 176.9W	07 53 21.9	Sept. 01 60	9220	500	
205	4	Fiji Is.	16.1S 176.9W	20 02 12.8	〃	8350	184	
			Station: Honolulu					
77	3	Mindanao I.	7 N 126.5E	08 01 45	Sept. 11 58	8250		
19	2	Marshall Is.	12 N 165 E	03 29 58	July 12 58	4060		
9	2	Kermadec Is.	29 S 177 W	22 23 53	Sept. 14 59	8500		6.5
304	2	New Hebrides Is.	16.8S 167.6E	09 28 19.5	Sept. 01 60	5640		
308	2	〃	16.5S 167.6E	10 35 01.1	〃	5620		
138	2	Norfolk Is.	28 S 167.5E	11 12 31	May 20 60	6600		
297		Gulf of California	24 N 108 W	04 11 54	Mar. 06 60	5180		
125	2	Helmahera I.	1 N 129 E	02 22 06	〃	8260		
121	3	Solomon Is.	7.5S 156 E	21 37 05	Feb. 24 05	5920		
101	4	Celebes I.	1 S 123 E	09 34 00	Dec. 02 00	8940		
			Station: Suva					
319	5	Kermadec Is.	29 S 176.5W	10 15 17	Oct. 12 58	1310		
19	1	Marshall Is.	12 N 165 E	03 29 58	July 12 58	3660		
111	5	New Zealand	42 S 173 E	00 46 56	Feb. 21 60	2700		
77	5	Mindanao I.	7 N 126.5E	18 01 45	Sept. 11 58	6340		
29		Java I.	9.5S 112.5E	01 12 30	Oct. 20 58	7150		
28	6	Sumatra I.	2 N 28.5E	03 21 52	Oct. 12 59	8850		

the paths of which cover in addition the oceanic region between the Kurile and Aleutian Islands, lie also on the rather continental characteristic curve "6". As the path resulting from the shock (257) runs quite near the path of the shock (256), we can obtain the dispersion curve for the remaining part, from (256) to (257) by the subtraction of

the travel-times for every period. The result is shown in the diagram (c) given at the left upper part of Fig. 7. This result tells us that the dispersive characteristic number for the region along the path between the two epicenters (256) and (257) is approximately "4". The path from (256) and (257) includes sea region deeper than 4 km which occupies approximately 3/5 of the total path. On the other hand, the dispersion curve "4" can be obtained when Rayleigh waves passed across the regions "3", "2", "1" and "5", "6", "7" with the path length ratio of 3 : 2 respectively. Therefore, if the region deeper than 4 km along the path is region "3", "2" or "1", the remaining part must be region "5", "6", or "7" in this order respectively. Regrettably, the writer does not have sufficient knowledge about the crustal structure of these regions to select a suitable pair among these three cases. But, the first case, *i.e.*, the characteristic number for the region deeper than

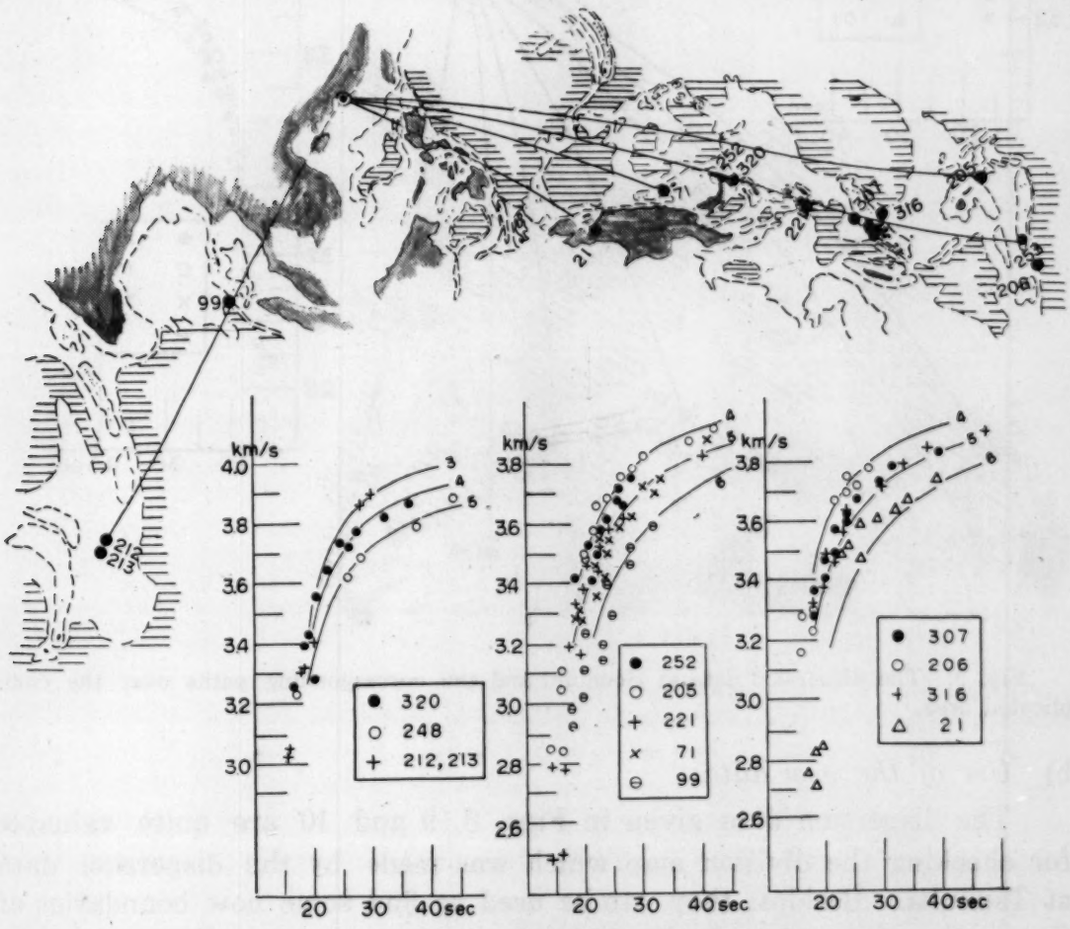

Fig. 8. The dispersion data at Hongkong and the corresponding paths over the complicated area.

4 km along the present path is in an average "3" and accordingly, that for the remainder region is in an average "5" seems to be the most natural.

The dispersion data and the corresponding paths which cover the complicated area are given in Fig. 8 (Hongkong Station), Fig. 9 (Honolulu Station) and Fig. 10 (Suva Station).

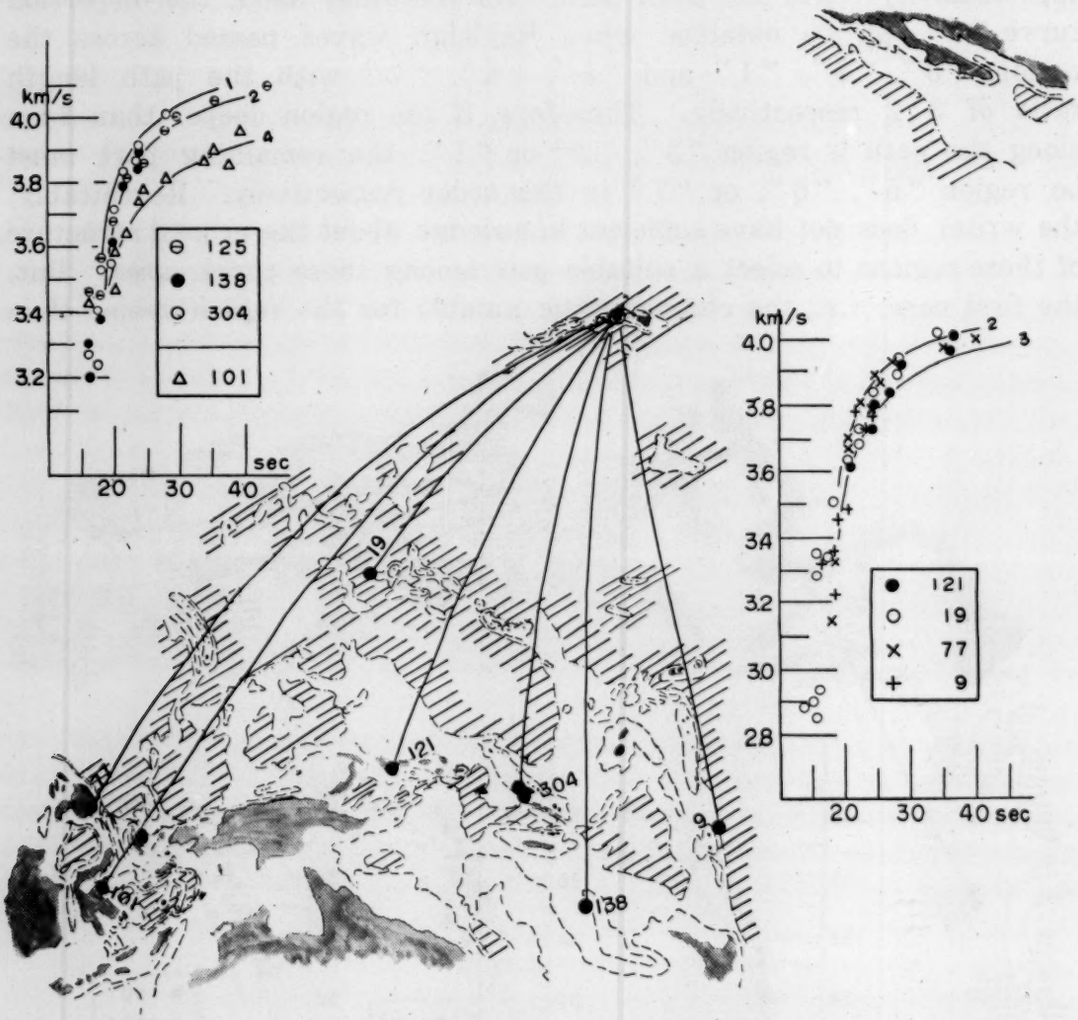

Fig. 9. The dispersion data at Honolulu and the corresponding paths over the complicated area.

b) *Use of the new data.*

The dispersion data given in Figs. 8, 9 and 10 are quite valuable for checking the division map which was made by the dispersion data at Tsukuba. Besides, they can be used to find some new boundaries of the regions for which the Tsukuba data were missing. The paths here used are shown in the left chart of Fig. 11, and the revised map of

the divided regions, based upon the supplementary data, is given on the right hand. The method adopted was quite the same as the previous one. That is, to divide each travelling path into such sections in order to

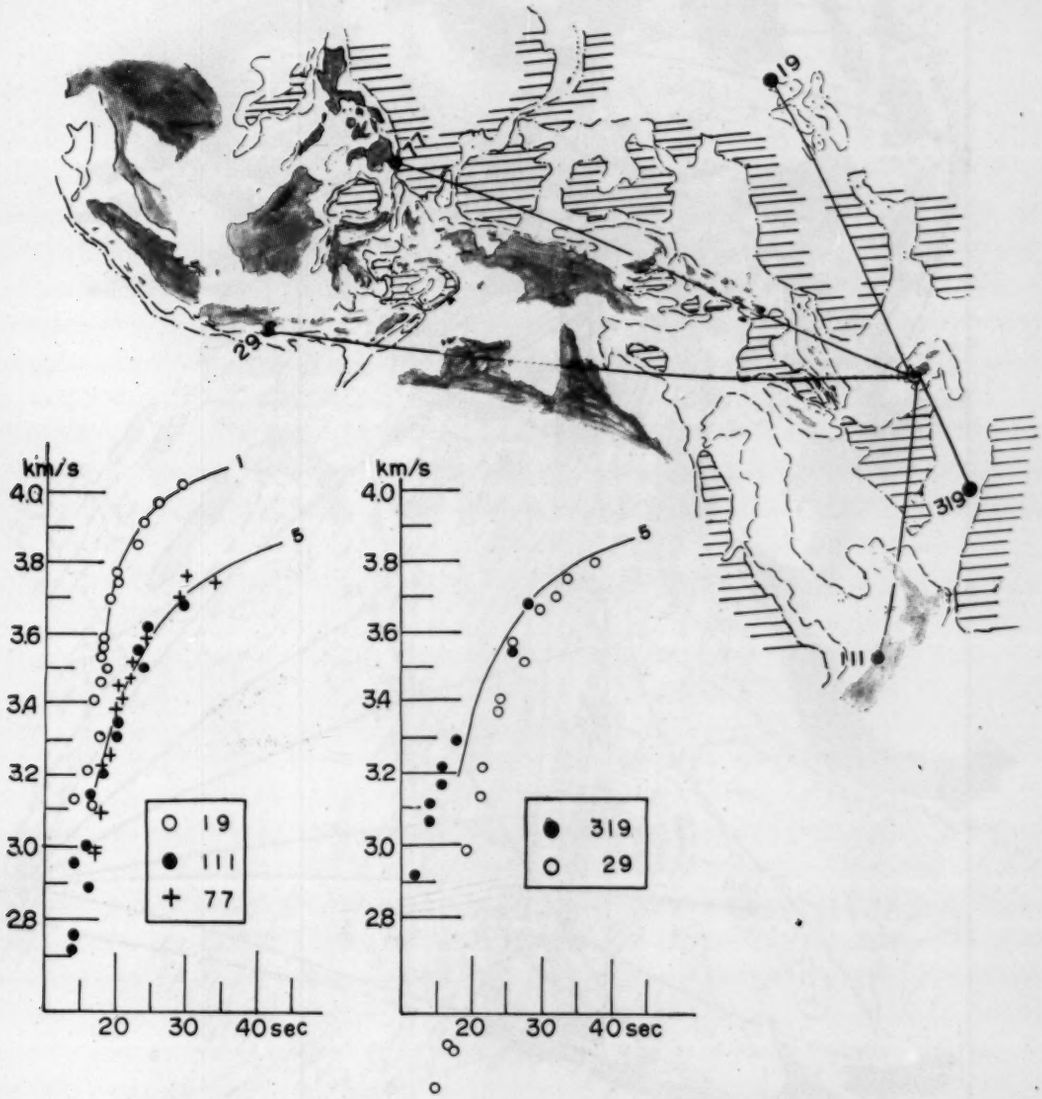

Fig. 10. The dispersion data at Suva and the corresponding paths over the complicated area.

make the differences between the two travelling times $O\sim C$ along each path sufficiently small. In these trials, the previous result, together with the topographical conditions was of course considered. For instance, along the path from 248 (Mariana Is. shock) to Hongkong, the travel distances which cover the regions "1", "3", "5" and "7" becomes 0 km, 830 km, 780 km and 1240 km respectively if we measure them on

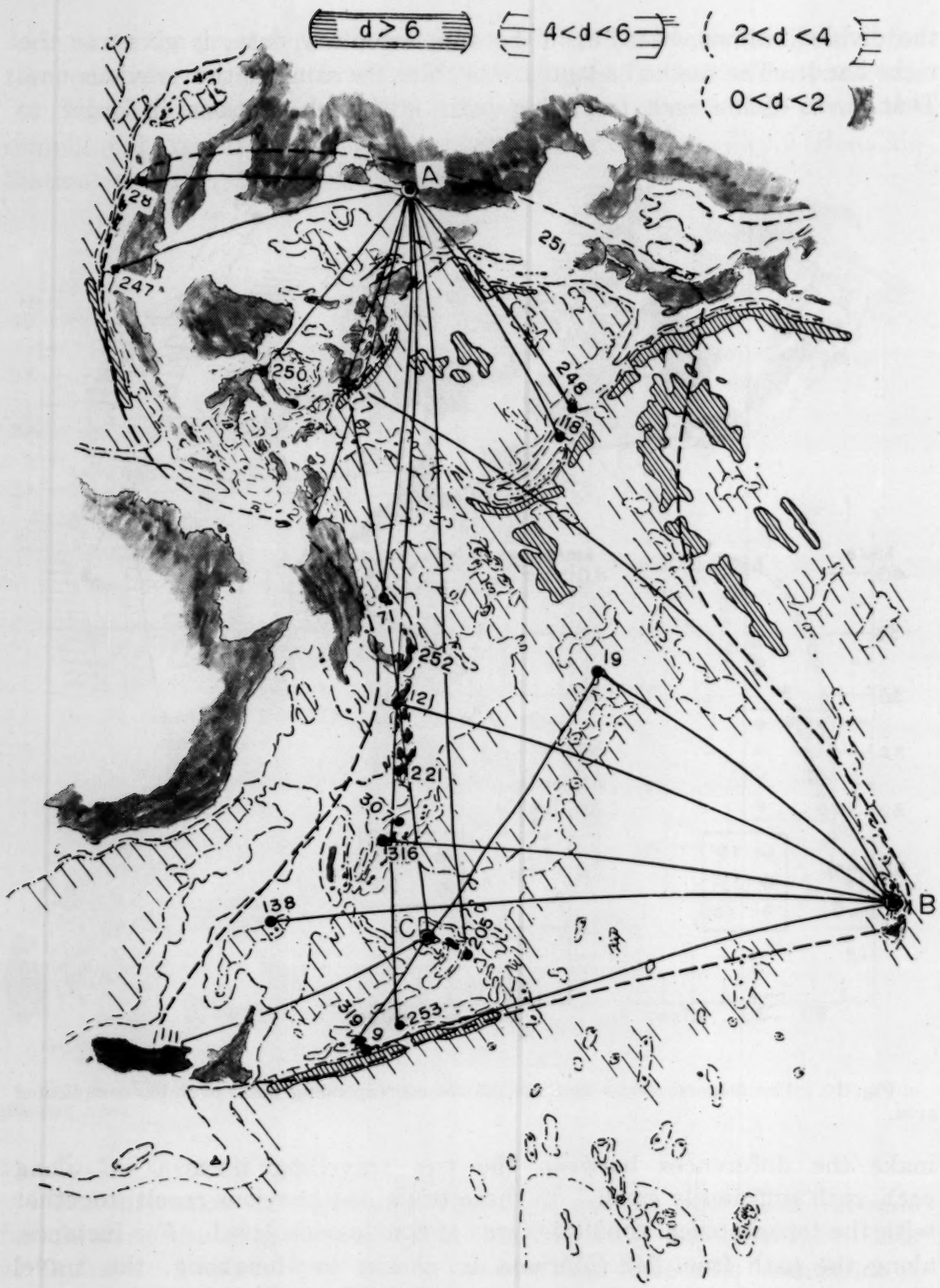

Fig. 11. A division map revised by the new data at Hongkong (A), Honolulu (B) and are the areas deeper than 6 km and broken and chain lines mean the contour line of the

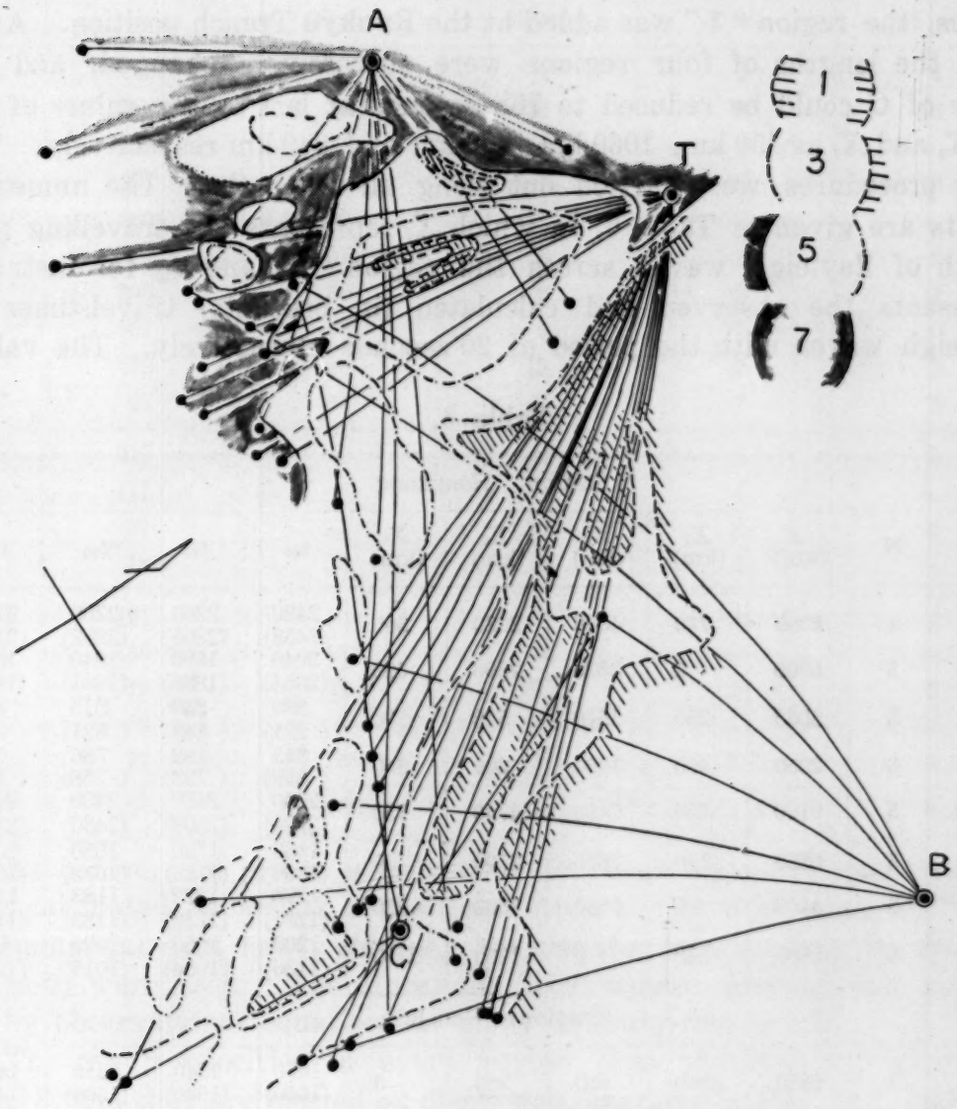

Suva (C), and the ordinary chart of the same area (left). In the left chart, hatched regions depth of 2 km and 4 km respectively.

the division may previously drawn up. If so, the travel-time of Rayleigh waves with the period of 30 seconds along this path was calculated as 789 seconds, which was too large as compared with the observed one, 766 seconds. In order to decrease the difference between these two values, the region "1" was added at the Ryukyu Trench position. After that, the lengths of four regions were successively changed, and the value of C could be reduced to 768 seconds at last by the values of X_1, X_3, X_5 and X_7 as 450 km, 1060 km, 500 km and 840 km respectively. The same procedures were carried out along all the paths. The numerical results are given in Table 6, in which X_i represents the travelling path length of Rayleigh waves across the region "i" and t_{20} for instance, represents the observed and calculated (in brackets) travel-times of Rayleigh waves with the period of 20 seconds respectively. The values

Table 6.

No.	N	Δ (km)	X_1 (km)	X_3 (km)	X_5 (km)	X_7 (km)	t_{20}	t_{25}	t_{30}	t_{35}
Station: Hongkong										
205	4	8350	770	4040	2980	560	2420 (2458)	2260 (2266)	2200 (2202)	2165 (2166)
307	5	6900	0	3630	2390	880	2040 (2058)	1890 (1898)	1840 (1841)	1810 (1808)
118	5	3060	250	1510	510	790	890 (921)	840 (848)	815 (821)	805 (806)
248	5	2850	450	1060	500	840	843 (859)	792 (793)	766 (768)	752 (753)
253	5	9100	150	2480	4740	730	2640 (2790)	2480 (2508)	2430 (2430)	2400 (2387)
221	5	6250	150	2670	2700	730	1850 (1865)	1730 (1723)	1680 (1672)	1650 (1637)
71	5	4400	0	1980	1500	920	1298 (1281)	1222 (1230)	1183 (1185)	1159 (1167)
21	6	3680	230	0	1200	2150	1200 (1136)	1060 (1054)	1020 (1015)	997 (989)
Station: Honolulu										
121	3	5920	3960	980	980	0	1670 (1660)	1540 (1540)	1510 (1506)	1490 (1489)
19	2	4060	3350	710	0	0	1160 (1139)	1060 (1039)	1020 (1021)	1010 (1012)
77	3	8250	5400	1890	890	70	2300 (2371)	2130 (2141)	2085 (2078)	2070 (2071)
Station: Suva										
319	5	1310	0	650	660	0	385 (385)	360 (361)	350 (349)	305 (313)
77	5	6340	80	1850	4050	360	1870 (1888)	1730 (1753)	1700 (1692)	1660 (1666)

of $O\sim C$ are given in Table 7. The regions thus obtained are shown in the right map of Fig. 11.

Table 7.

	No. \ T	20 sec	25 sec	30 sec	35 sec
Hongkong	248	16	1	2	1
	253	51	28	0	13
	252	16	6	5	–
	221	15	7	8	13
	250	35	22	2	–
	71	17	8	2	9
	205	38	6	2	1
	307	18	9	1	0
	118	29	13	7	2
	21	64	7	7	8
Suva	319	0	3	5	8
	111	8	3	4	–
	77	17	20	3	6
	19	33	3	5	–
Honolulu	121	10	7	4	2
	138	15	9	–	–
	19	23	21	2	3
	9	8	1	–	–
	77	17	11	7	1
	σ	27.0	12.1	4.4	6.4

As before, the group velocities of Rayleigh waves in every region were calculated by means of the least square. In this case, not only the numerical data newly obtained but also the data at Tsukuba Station (Table 2) were used. Therefore, the least square method was carried out by observational equations as many as forty-five in all.

The group velocities in every region thus obtained are given in Table 8, and they are plotted on dispersion diagrams in Fig. 12. Judging from the result which shows that the calculated dots lie close, at least in the range of observational errors, on the observational dispersion curves "1", "3", "5" and "7", we can say that our division map is quite satisfactory for explaining all of the Rayleigh waves dispersion characteristics along forty-five paths.

Comparing the revised division map (right map of Fig. 11) with the previous one (Fig. 5), the following points can be noticed.

I) The area west of the Philippines, Mindanao Island and north of Celebes Island, was newly divided into some regions. The effect of the existence of a rather deep sea regions at the South China Sea and the Celebes Sea appears on the dispersion character along the path from the epicenter (250) to Hongkong.

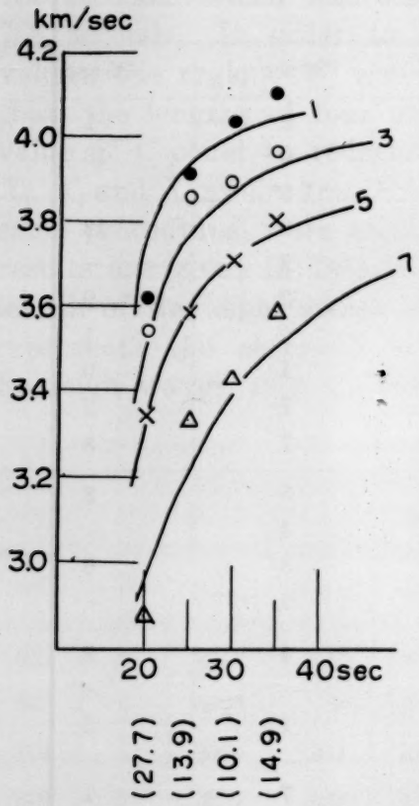

Fig. 12. Calculated dispersion data for the divided four regions and the assumed dispersion curves. The marks of the calculated dots are the same in Fig. 6. Numbers in bracket under the period scale mean the standard deviations of $O-C$ for the corresponding periods.

II) The area around the Ryukyu Islands which also had been left blank was divided. The existence of the Ryukyu Trench also had remarkable effect upon the dispersion character along the paths from (248) and (118) to Hongkong.

III) The sub-oceanic region "3" which was postulated in the Caroline Sea was enlarged eastward in order to explain the dispersion characteristics along the paths from (121), (221), (252), (71), (253) and (205) to Hongkong.

IV) In the Mariana Sea, the shape of region "3" was slightly extended westward. The location and the shape of region "1" could not be sufficiently investigated from the new data.

V) The isolated purely oceanic region "1" which was situated in Micronesia was greatly extended from the Fiji Islands to the Marshall Islands in order to explain the dispersion feature along the path from the epicenter (19) to Suva (C).

VI) The dispersion character in the broad sea area northeast of a

Table 8.

V (km/s) / T (sec)	V_1		V_3		V_5		V_7	
	Cal.	Obs.	Cal.	Obs.	Cal.	Obs.	Cal.	Obs.
20	3.61	3.65	3.54	3.45	3.34	3.35	2.87	3.00
25	3.90	3.94	3.86	3.78	3.58	3.58	3.33	3.25
30	4.04	4.00	3.98	3.88	3.70	3.70	3.42	3.40
35	4.11	4.04	3.89	3.93	3.90	3.78	3.59	3.50

line from the Tongas up to Hawaii, belongs to "1", which is the same as those in the ordinary Pacific Ocean.

4. Crustal models which satisfy the four dispersion curves

The most important problem is that what kind of crustal model can explain each of four dispersion curves in the divided region "1", "3", "5" and "7" respectively.

R. Yamaguchi *et. al.*[4] calculated the theoretical dispersion curves of Rayleigh waves along various crustal models being covered with water. From their results, four models T_1, T_3, T_5 and T_7 given in Fig. 13 were selected as suitable ones which respectively fit best for our

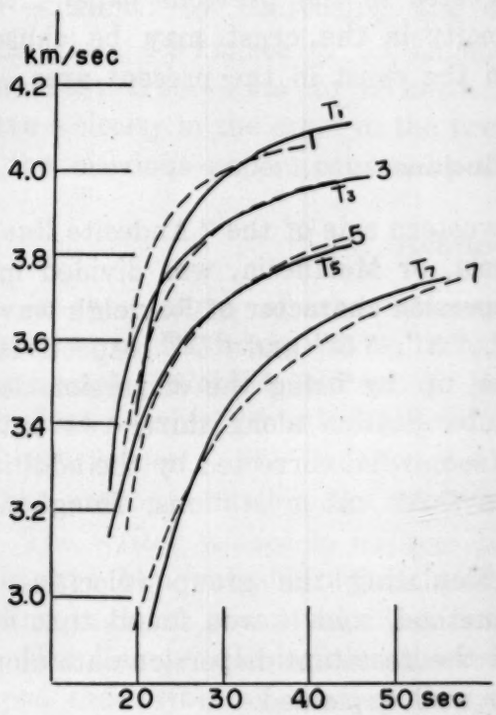

T_1

α	ρ	h
1.52	1.00	6.0
6.90	2.67	6.0
8.10	3.00	∞

T_5

α	ρ	h
1.50	1.00	3.0
5.50	2.80	12.0
7.80	3.00	∞

T_3

α	ρ	h
1.50	1.00	4.5
6.00	2.80	6.75
7.95	3.00	∞

T_7

α	ρ	h
1.50	1.00	0.9
5.00	2.80	18.0
7.95	3.00	∞

Fig. 13. Observed dispersion curves (broken curves) "1", "3", "5" and "7" in the divided regions and the theoretical curves (solid curves) for the models of T_1, T_3, T_5 and T_7 which are given in the right hand.

four observed dispersion curves "1", "3", "5" and "7". The mean value of water depth measured along all of the paths in the region "1" was around 6.8 km. But, as the calculations of the dispersions for

4) R. YAMAGUCHI and T. KIZAWA, "Surface Waves and Layered Structure (Part II)," *Bull. Earthq. Res. Inst.*, **39** (1961), 669.

the crustal models with such deep water layer had not been done, the writer had to compare the observed curve "1" to a theoretical dispersion curve for the model with the water layer of 6 km. If we increase the thickness of the water layer and decrease that of the crust, however, the calculated curve T_1 must be shifted leftward, and the discrepancy between two curves T_1 and "1" will become much smaller. The depth of the water layer in other three models were taken as mean values of those along all of the paths which cover each divided regions respectively.

From these results, we can say at least that the shift of the dispersion curves in these four regions can be explained by both decreasing of the compressional wave velocity in the crust and by increasing the thickness of the crust. As was suggested in the previous paper[5], the decreasing of compressional wave velocity in the crust may be caused by the existence of volcanic layers in the crust in the present area.

5. Conclusions

Intricated structured area in the western side of the "Andesite line", embrasing the Mariana Sea, Micronesia, or Melanesia, was divided into four regions in each of which the dispersion character of Rayleigh waves show the characteristic numbers "1", "3", "5" and "7" respectively.

The first division map was drawn up by using the dispersion data of Rayleigh waves observed at Tsukuba Station along thirty-two paths across the area. Next, this map was somewhat corrected by the addition of thirteen new dispersion data for three other stations, Hongkong, Honolulu and Suva.

These results were checked by calculating the group velocities in every region by the least square method, and it was found that our result was quite satisfactory as all of the resultant dispersion data along forty-five paths across the area were well explained.

Four crustal models which respectively fit the four dispersion curves "1", "3", "5" and "7" were selected, and it was found that the shift of the dispersion character from "1" to "7" could be explained by decreasing the compressional wave velocity in the crust from 6.9 km/sec to 5.0 km/sec and by increasing the thickness of the crust from 5 km to 20 km.

I) As was found in the previous papers, the dispersion character

5) *loc. cit.* 3).

across the sea deeper than 4 km in the Central Pacific Ocean was "1". This circumstance, however, changes in the western side of the "Andesite line". In this area, the dispersion character in the sea deeper than 4 km becomes "3" instead of "1". Roughly speaking, the region "1" in this area, seems to be limited to the regions deeper than 6 km.

II) In the area west of the Philippines, Mindanao Island and north of Celebes Island, the sub-oceanic region "3" could be found only at two locations, the first is at the central part of the South China Sea and the other at the Celebes Sea.

III) Four kinds of dispersion curves in the divided regions were compared with the theoretical ones, and it was found that the shift of the dispersion character from "1" to "7" in the divided regions can be explained by decreasing the compressional waves velocity in the crust from 6.9 km/sec to 5.0 km/sec and by increasing the thickness of the crust from 5 km to 20 km. The decreasing of the compressional wave velocity in the crust in the present area may be, as was suggested in the previous paper, caused by the existence of volcanic layers.

6. Acknowledgement

In the course of the writer's investigations into the dispersion character of Rayleigh waves including the previous three papers, he was greatly indebted to Prof. T. Hagiwara who allowed him to use the abundant records of seismograms recorded at Tsukuba Station under his supervision. The indefatigueable effort of the observational staff of the station including Mr. M. Watanabe must be highly acknowledged.

The writer wishes to express his hearty thanks to Prof. C. Tsuboi who gave him valuable advice and discussed with him the methods of finding regional group velocities from abundant dispersion data.

The Lamont Geological Observatory, Columbia University, U.S.A. helped the writer by sending many copies of seismograms obtained at Hongkong, Honolulu and Suva. The writer's cordial thanks are due to all the people concerned in these institutes and stations.

In selecting some suitable crustal models which fit well for our observed dispersion curves, the writer is greatly indebted to Mr. R. Yamaguchi.

Finally, it must be added that all of the calculations by the least square method were made at the Yulin Computing and Processing Centre, Tokyo.

23. 西南太平洋海域を，夫々の内部でレーリー波が同一の群速度を示す様ないくつかの地区に分けること

東大地震研究所　三　東　哲　夫

前論文で，海洋を伝わつて日本にやつてくるレーリー波の分散曲線を7種に分類したが，これらの分散曲線は，実は夫々独立なものではなくて，例えばレーリー波が，夫々の内部では“1”，“4”，“7”という分散特性を示す様な領域を夫々 3:3:4 の割合で含む径路を通つてきた場合には，全体としての分散特性は“5”になる，といつた具合に，お互いに関連性をもつていることも前論文で示されている（第3図）．この事実を逆に利用することによつて，西南太平洋，特にいわゆる安山岩線の西側の海域を，レーリー波が全く陸的な分散を示す海域“7”，かなり陸的な分散を示す海域“5”，かなり海的な分散を示す海域“3”，完全に海的な分散を示す海域“1”の4つの領域に分割することを試みた．先ず最初は，東大震研の筑波支所の記録から得た合計32本の径路に沿つての分散資料を用い（第4図），次に，これらの径路と交叉する径路をとるものとして，香港，ハワイ，フィジー島の3ヶ所における記録から調べた計13ヶのレーリー波の分散資料を加えて，それによつて前の結果に若干の補正を加えた（第11図）．

逆に，この様にして分けられた 4 つの領域内でのレーリー波の群速度を各周期毎に最小二乗法で求めて見ると，始めに仮定した各領域内のでそれらと，少くとも観測の誤差範囲内でかなりよく合うことが示された（第12図）．

こうして得られた分割図から判断すると，安山岩線の西側は東側に比べてたしかに全体として陸的な構造になつている様に思われる．即ち，東側では，海深4キロ以上の場所ではレーリー波は分散特性“1”，つまり純海洋的な分散特性を示すのに，西側では同じ深さの場所は，やや海的な特性“3”になつている．そして西側で“1”を示すのは僅かに深さ6キロ以上の深海部分に限られている．

また，東支那海，ボルネオ海等を通るレーリー波は，完全に陸的な分散特性“7”を示す．この附近でやや海洋的なのは，僅かに南支那海の中央部と，セレベス海の一部（共に“3”）である．

最後に，これら4種の分散特性“1”，“3”，“5”及び“7”を示す各領域が，どんな地殻構造のモデルで説明できるかを調べて見ると，大凡ではあるが，上部でのP波の速度が約 8 km/s である様な中間層の上に，その内部でのP波の速度，及び厚さが夫々“1”では 6·9 km/s で 5 km，“3”では 6 km/s で 7 km，“5”では 5.5 km/s で 12 km，“7”では 5.0 km/s で 20 km 程度の値をもつ地殻をのせたものになる（第13図）．前の論文でも指摘したように，地殻内における P 波の速度の減少は，おそらく海底火山の溶岩層の存在に原因しているのではないかと思う．

Bulletin of the Earthquake
Research Institute
Vol. 39 (1961), pp. 631-651

24. *Dispersion of Love Waves along Various Paths to Japan (Part 1).*

By Tetsuo A. Santô,

Earthquake Research Institute.

(Read September 26, 1961.—Received September 30, 1961.)

Abstract

The dispersion characters of Love waves along various paths to Japan were investigated by using the seismograms recorded by Columbia-type ultra-long period seismographs at Tsukuba Station, Japan. For the oceanic paths, the dispersion characters were classified into five groups, from I to V. In the central and northern Pacific region, Love waves show the purely and nearly oceanic dispersion character of I and II respectively (Fig. 1, 2). When travelling path comes into the Micronesia region, however, they show a remarkable shift to a continental one with the shift of the path to the west (Fig. 3, 4). This phenomenon is quite similar to that observed in Rayleigh wave dispersion.

Two unexpected results were obtained. That is, 1) clearly dispersive Love wave trains hardly transmitted along the paths which cross the Mariana Sea (Fig. 6), and 2) the shocks which took place in the continent west of Japan did not transmit long-period dispersive trains of Rayleigh waves (Fig. 8).

The dispersion character of Love waves along the oceanic path from Sumatra Island region to Japan was as continental as those along the path from Outer Mongolia or the Sinkiang region to Japan (Fig. 9).

The dispersive characters along the continental paths were classified into five groups (from VII to XI). An interesting result was that the maximum group velocity of Love waves decreases remarkably when Love waves pass in or around the Tibet region (Fig. 12). Such a dispersive character may be explained by the special conditions not only in the earth's crust but also in the upper mantle along this high mountain region.

1. Introduction

In the previous papers[1),2),3)] the author dealt with the dispersion of Rayleigh waves along the various oceanic paths to Japan. Now the dispersion of Love waves will be investigated in the present paper. The seismograms used were, as those used in the previous papers, all obtained at Tsukuba Station by Columbia-type ultra-long period seismographs. In the present paper, only a general description will be given.

2. Conditions for observing the dispersive trains of Love wave

Rayleigh waves should appear on a vertical component record independent both of the azimuth of an epicenter to an observation station and of the crustal structure along the path. Therefore, in the case of Rayleigh waves, if the vertical component seismograph has a suitable period response character for the arriving energy of the surface waves, dispersion data can always be obtained for a considerable period range from the record. In the case of Love waves, however, there are some disadvantageous conditions for observing the dispersive wave train long enough to obtain dispersion data over a period of sufficiently wide range.

These disadvantageous conditions are: (1) When the crustal structure along the travelling path is a purely oceanic one. In this case, Love waves are almost non dispersive for the periods approximately longer than 25 seconds. Therefore, Love waves of these periods reach the observation station approximately at the same time. As a result, the wave form of the Love waves becomes like a pulse.—(2) When the direction of the epicenter from the observation station makes an angle around 45° with the direction of motion of the two perpendicularly installed horizontal seismographs, and further, when the epicentral distance is small. In this case, if the first condition is fulfilled, Rayleigh waves appear not only in the record of the vertical component but in the records of the two horizontal ones. Therefore, if the epicentral distance is

1) T. A. SANTÔ, "Observation of Surface Waves by a Columbia-type Seismograph Installed at Tsukuba Station, Japan (Part 1)—Rayleigh wave dispersions across the Oceanic Basin—," *Bull. Earthq. Res. Inst.*, **38** (1960), 219.

2) T. A. SANTÔ, "Rayleigh Wave Dispersions across the Oceanic Basin around Japan (Part II)," *Bull. Earthq. Res. Inst.*, **38** (1960), 385.

3) T. A. SANTÔ, "Rayleigh Wave Dispersions across the Oceanic Basin around Japan (Part III)—On the Crust of the South-Western Pacific Ocean—," *Bull. Earthq. Res. Inst.*, **39** (1961), 1.

small, the wave train of Love waves will be disturbed by the arrival of Rayleigh waves. For this reason, we cannot measure the group velocities of Love waves for such periods which reach the station later than the arrival of Rayleigh waves.

3. Dispersive features of Love waves along oceanic paths around Japan

On account of the restrictions given in the previous section and of some undiscovered reasons which will be mentioned in a later section, the amounts of the observed dispersion data of Love waves along oceanic paths around Japan were much less than those of Rayleigh waves. The data of the earthquakes for which Love waves dispersion data could be obtained for a sufficiently wide period range are given in Tables 1 (southern oceanic paths), 2 (northern oceanic paths), 3 (continental paths), and 4 (mixed paths).

At first, on account of the condition (1) given in the previous section, the wave form of Love waves along purely oceanic paths, for instance,

Table 1.

No.	District	Epicenter	Origin Time (G. M. T.)	Date	h (in km)	Δ (in km)
			h m s			
13	Tonga Is.	24 S 176.5W	13 15 49	Sept. 14, 59	113	8100
263	〃	28.4 S 176.0W	23 21 42.5	Mar. 12, 61	28	8500
227	〃	24.2 S 176.1W	14 12 21.1	Nov. 23, 60		8130
14	〃	17 S 173 W	21 09 09	Aug. 06, 58		7670
147	Solomon Is.	10 S 161.5E	07 56 15	Apr. 04, 60		5600
44	〃	10.5 S 162.5E	09 46 30	Nov. 17, 58		5770
269	〃	10.7 S 161.6E	01 26 26.1	Mar. 05, 61	99	5660
221	〃	10.3 S 161.2E	08 22 00.9	Oct. 22, 60	90	5570
50	New Hebrides Is.	13 S 167 E	00 06 00	May 19, 58		6230
60	〃	16 S 172.5E	17 55 29	July 03, 59		6650
61	〃	18.5 S 169 E	04 51 30	〃 11, 59		6720
9	Kermadec Is.	29 S 177 W	22 23 53	Sept. 14, 59		8500
10	〃	29 S 176.5W	15 31 57	〃 29, 59		8510
239	Loyality Is.	21.3 S 169.5E	19 43 01.4	Jan. 28, 61		7070
119	Fiji Is.	20 S 174.5E	16 14 47	Nov. 23, 59		7180
112	South Pacific Oc.	54 S 136 W	16 20 34	〃 22, 59		12780
138	Norfolk Is.	28 S 167.5E	11 12 31	May 20, 60		6600
218	Nicobar Is.	7.9N 92.9E	20 40 06.6	Oct. 08, 60		5710
28	Sumatra Is.	2 N 98.5E	03 21 52	〃 12, 59		8850

Table 2.

No.	District	Epicenter	Origin Time (G. M. T.)	Date	h (in km)	△ (in km)
			h m s			
265	Off west coast of Mexico	19.2N 107.3W	08 03 43.9	Mar. 13, 61	49	10630
59	Northern Calif.	41 N 125.5W	01 23 09	July 24, 59		7770
141	Off coast of Calif.	41 N 125 W	07 17 48	June 06, 60		7820
240	Central Alaska	65.2N 149.9W	12 12 39.7	Jan. 30, 61	34	5480
241	Kodiak I. Alaska	55.8N 153.9W	00 48 36.5	〃 31, 61	26	5310
149	Alaska Peninsula	52 N 161.5W	16 07 12	May 13, 60		4830
229	Fox Is., Aleutian	52.7N 168.0W	22 10 06.4	Nov. 06, 60	42	4390
46	〃 〃	52.5N 170 W	13 08 05	July 24, 58		4275
88	And. Is., 〃	51.5N 176.5W	09 08 35	Aug. 17, 58		3830

Table 3.

No.	District	Epicenter	Origin Time (G. M. T.)	Date	h (in km)	△ (in km)
			h m s			
36	Western Sinkiang	51 N 99 E	10 55 31	Apr. 10, 58		3620
39	〃	30.5N 78.5E	04 48 15	June 24, 58		5380
37	Outer Mongolia	46 N 98 E	04 08 56	Apr. 13, 58		3620
38	〃	45 N 98 E	12 27 06	Feb. 24, 58		3550
55	Lake Baikal	52 N 106.5E	17 03 10	Aug. 29, 59		3060
70	Western Sinkiang	44.5N 81 E	05 46 26	Dec. 21, 58		4980
135	Albania—Greece	40 N 20 E	05 10 05	May 26, 60		9560
1	Northern Tibet	36 N 89 E	20 56 12	Nov. 10, 59		4550
26	Burma—Pakistan	23.5N 94.5E	10 11 27	Mar. 22, 58		4500
191	India	26.9N 90.3E	10 42 44.6	July 29, 66	11	4800
202	Western China	32.4N 95.8E	05 29 32.7	Sept. 28, 60	25	4060
222	Western Pakistan	25.5N 67.6E	01 25 35.5	Oct. 29, 60	23	6860
156	Ethiopia	9.8N 40.0E	04 51 10.4	June 02, 61	41	10250
157	〃	10.8N 40.1E	20 32 24.0	〃 14, 61	56	10160
283	Southern Iran	27.8N 56.7E	18 13 40.7	Feb. 13, 61	109	7650
286	Outer Mongolia	41.8N 104.5E	10 45 39.1	Apr. 29, 61	25	3120
287	Sinkiang-China	40.1N 77.8E	16 34 39.1	〃 13, 61	19	5330
279	Sinkiang Province	39.6N 77.7E	15 18 22.8	Feb. 03, 61	21	5370
277	Northern Burma	24.7N 95.3E	08 51 48.9	〃 04, 61	162	4460
161	Ethiopia	9.8N 39.8E	15 23 11.6	June 03, 61	60	10280
164	Iran	28.3N 54.9E	00 24 30.8	〃 13, 61	62	7800
151	Gulf of Aden	11.5N 44.5E	03 21 26.5	〃 20, 61	30	9710
176	Burma-China	24.3N 39.3E	23 29 21.1	〃 11, 61	38	4170

Table 4.

No.	District	Epicenter	Origin Time (G. M. T.)	Date	h (in km)	Δ (in km)
			h m s			
92	Costa Rica	8 N 85 W	09 11 18	June 06, 58		13110
199	Columbia-Panama	6.9N 77.5W	19 01 25.3	Sept. 19, 60		13820
212	Indian Ocean	13.4S 65.8E	06 58 56.4	Aug. 15, 60	15	9510
213	〃	13.5S 67.0E	14 33 38.4	〃	25	9410
87	South Indian Oc.	40 S 45.5E	06 13 50	July 25, 58		12650
33	Antarctic Ocean	57 S 147 E	09 29 43	Oct. 01, 58		10360
62	Indian Ocean	36 S 78 E	12 01 36	July 11, 59		10256
76	Atlantic Ocean	9 N 39.5W	07 20 02	Sept. 25, 58		15000

those originating from shocks in the Easter Is. region (220) or Samoa Is. (270) showed only one or two undulations. (See the upper three examples in Fig. 1).

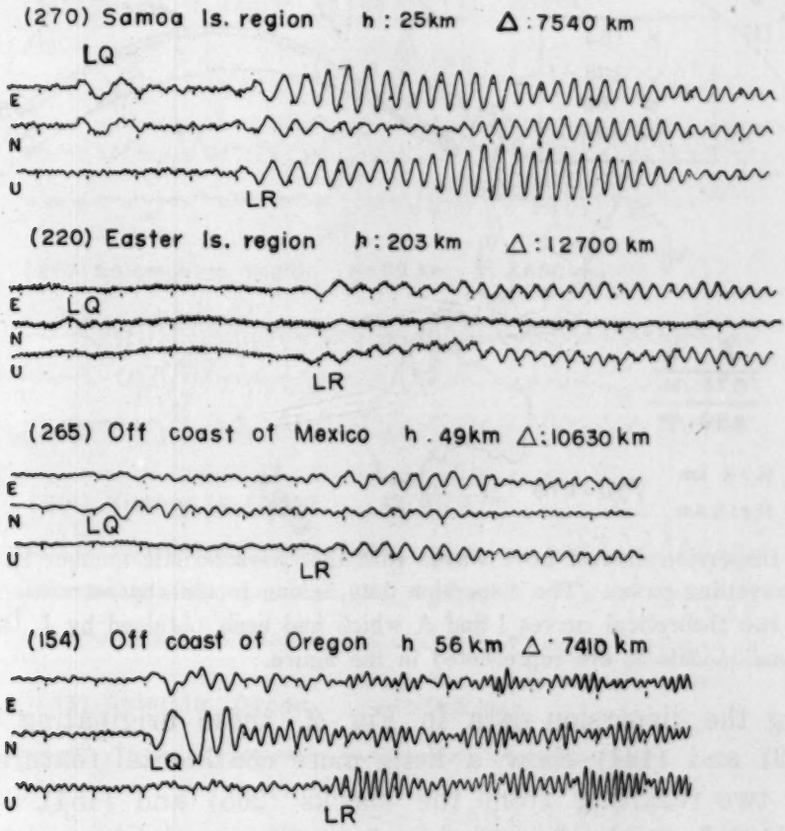

Fig. 1. Examples of seismograms which show a clear dispersive wave train of Rayleigh waves (LR) and a non or poorly dispersive wave train of Love Waves (LQ). The dots on every component represent minute marks.

It means, on the contrary, that the crustal structure along the paths of these shocks is purely oceanic. This result identifies well with the result obtained from the previous investigation into Rayleigh waves dispersions.

The wave form of Love waves caused by the shock which took place off the west coast of Mexico (265) or Oregon (154) showed a short duration (lower two examples in Fig. 1), and the dispersion data for these paths showed little deviation from the purely oceanic one (Fig. 2). The writer named this kind of dispersion character as number (II) in order to classify the dispersion characters of Love waves along the oceanic paths just as was done previously in the case of Rayleigh waves.

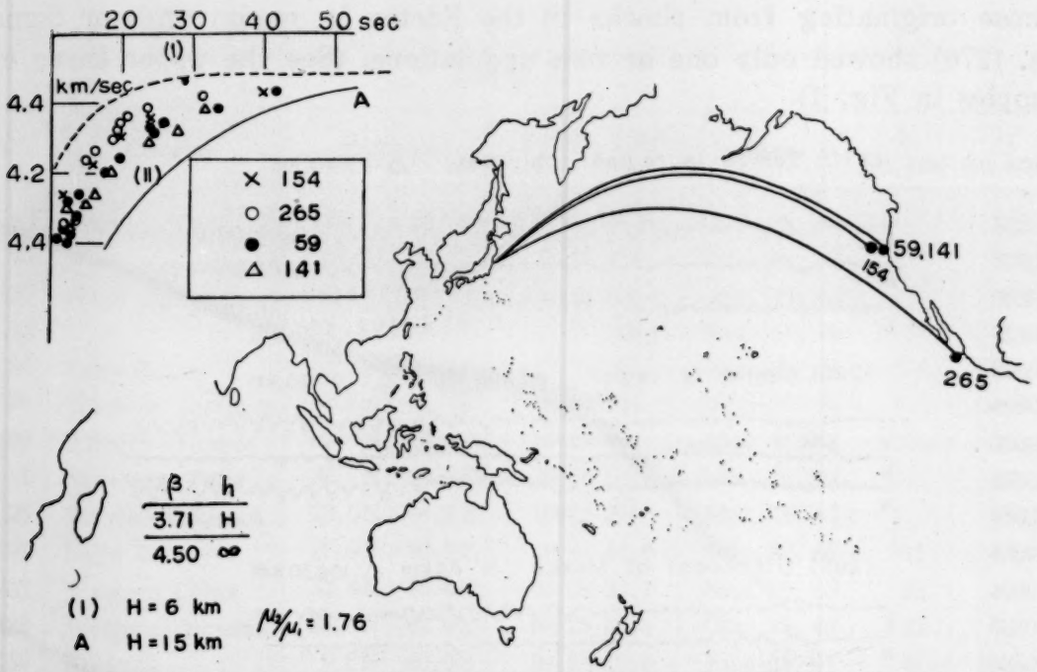

Fig. 2. Dispersion data of Love waves with the characteristic number II, and the corresponding travelling paths. The dispersion data belong to the characteristic number II lie between the two theoretical curves I and A which had been obtained by J. Oliver et. al.[4] by such crustal models as are represented in the figure.

Among the dispersion data in Fig. 2, those originating from two shocks (59) and (141) show a little more continental feature than the remaining two resulting from the shocks (265) and (154). This may have resulted from the fact that the paths due to the former two shocks

4) J. OLIVER, F. PRESS and M. EWING, "Crustal Structure and Surface Wave Dispersion IV: Atlantic and Pacific Ocean Basin," *Bull. Geol. Soc. Amer.*, **66** (1955), 913.

cover the parts much more continental near Aleutian Islands than in the latter two shocks.

For the paths across the Central Pacific Ocean, the writer could not observe any clear dispersive wave train of Love waves. This may be due to the purely oceanic crustal structure of the region. When the path enters into the western side of the "Andesite-line", however,

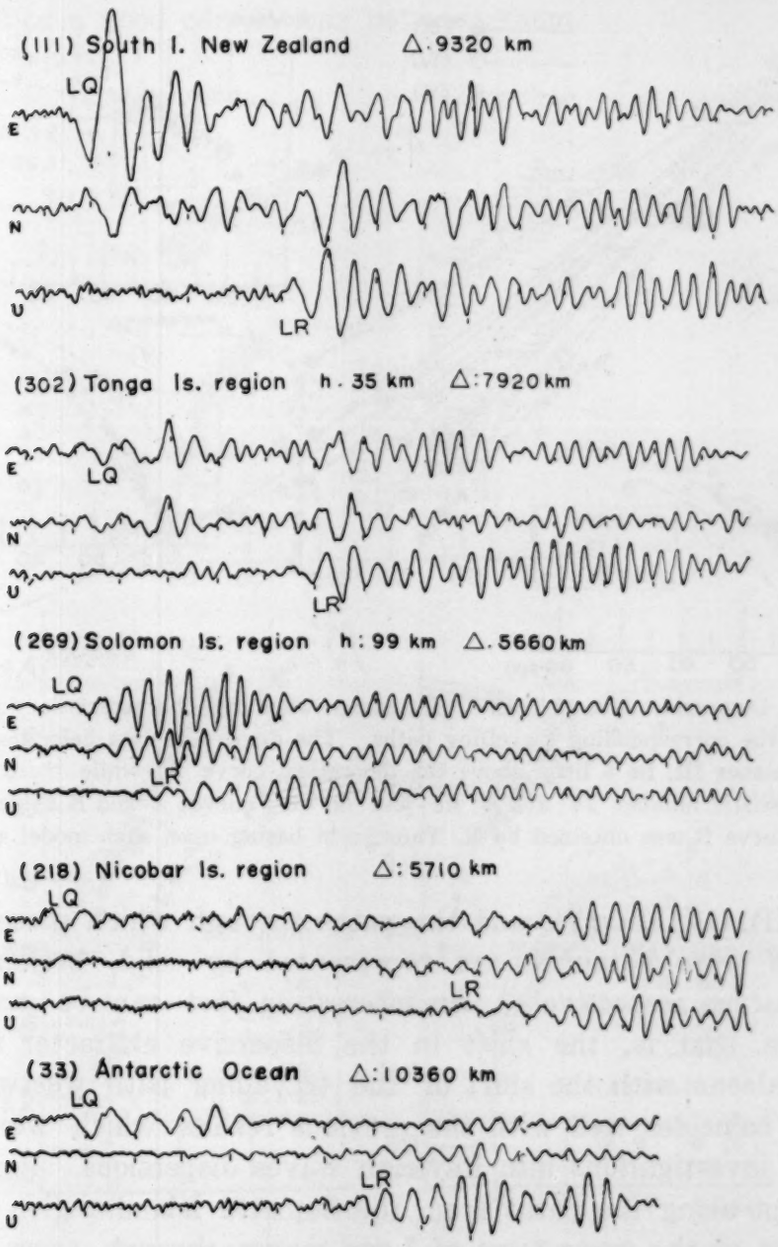

Fig. 3. Examples of seismograms which show dispersive wave trains of both Love and Rayleigh waves.

clear dispersive wave trains of Love waves begin to appear in the seismograms. The examples of the wave forms are shown in Fig. 3 by those caused by the shocks in New Zealand (111), the Tongas (302) and the Solomons (269).

The dispersive characteristic for these paths are represented in Fig. 4. These dispersion characteristics can be classified into three

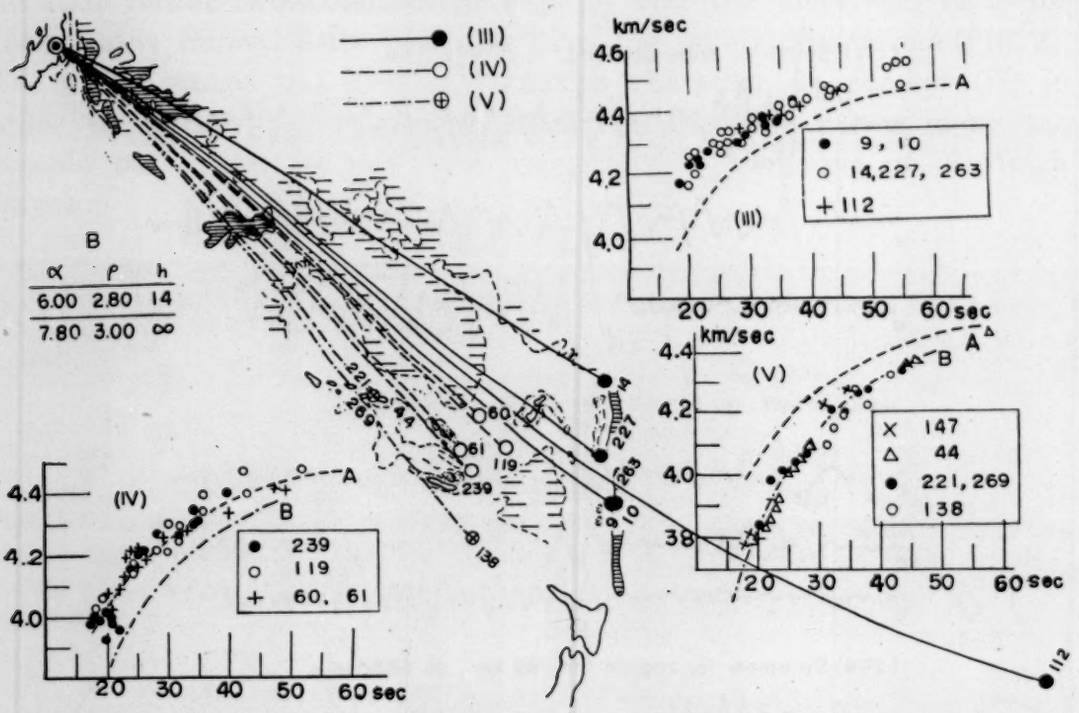

Fig. 4. Dispersion data of both Love waves with the characteristic numbers III, IV and V, and the corresponding travelling paths. The dispersion data belonging to the characteristic number III, lie a little above the theoretical curve A, while those belonging to the characteristic number IV and V lie just on the curves A and B respectively. The theoretical curve B was obtained by R. Yamaguchi basing upon such model as is shown in this figure.

groups (III), (IV) and (V), and the paths through which these dispersive characters were obtained, are represented by solid, broken and half broken curves respectively. An interesting fact can be noticed from this figure, that is, the shift in the dispersive character to rather a continental one with the shift of the travelling path westward. This tendency coincides well with the previous results which were obtained from the investigations into Rayleigh waves dispersions.

Except along the paths from the Sumatra Island region to Tsukuba (the copies of the wave form of Love waves through these paths are given in the lower two examples in Fig. 3), the oceanic paths shown in

Fig. 4 were the special one for which we could obtain dispersion data of Love waves for a sufficiently large period range. Therefore, we can investigate into two kinds of dispersion character of both Love and Rayleigh waves. Some examples are shown in Fig. 5, in which the same marks are used in the dispersion data of Love (LQ) and Rayleigh waves (LR) for each shock. Comparing each mark in every diagrams, we can notice a good correlations between them.

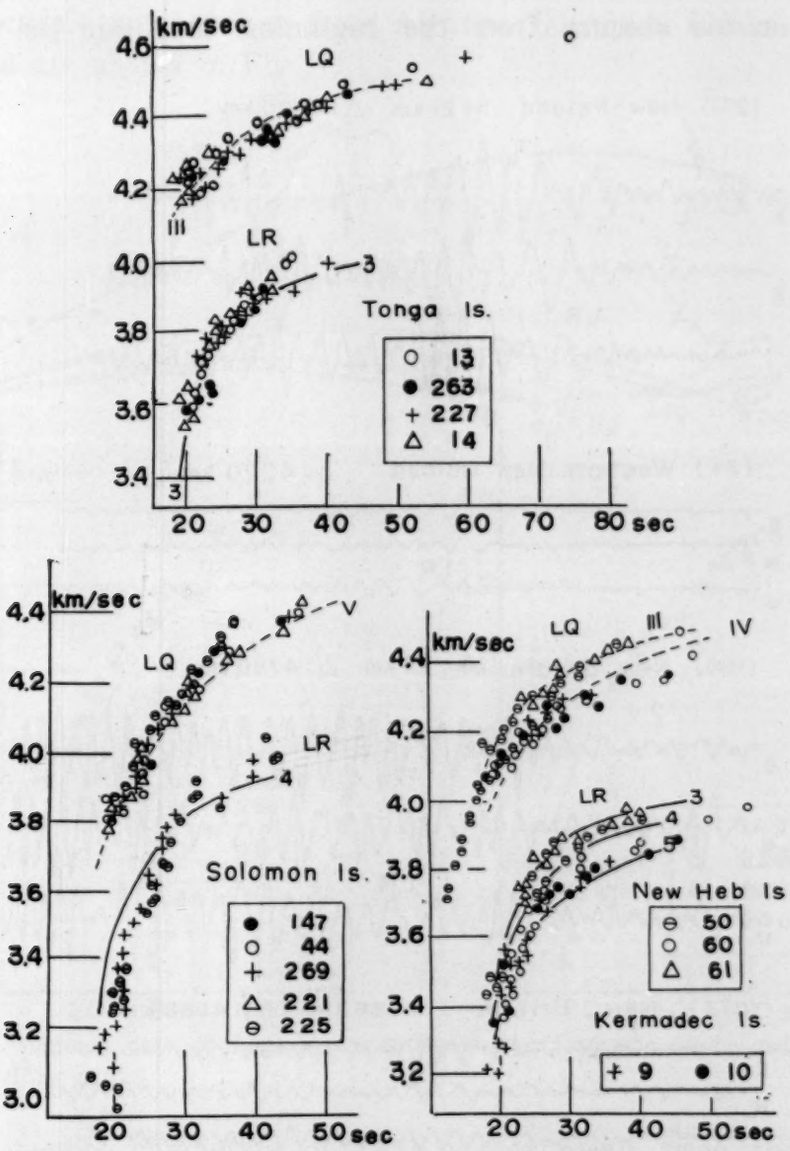

Fig. 5. Dispersion data of both Love and Rayleigh waves. The numbers beside two dispersion curves of LQ and LR respresent the characteristic numbers.

By using these two kinds of dispersion data, we can make, if we want, a more reliable estimation of the average crustal structure along each path between the epicenter and the observation station than by using any of the single type dispersion data. But, the writer did not take this labour, because such estimation for such an intricated structured region has little significance.

Concerning the paths which cover the Mariana Sea, a strange fact was obtained. That is, the wave form of Love waves becomes too irregular or too obscure from the beginning to obtain the dispersion

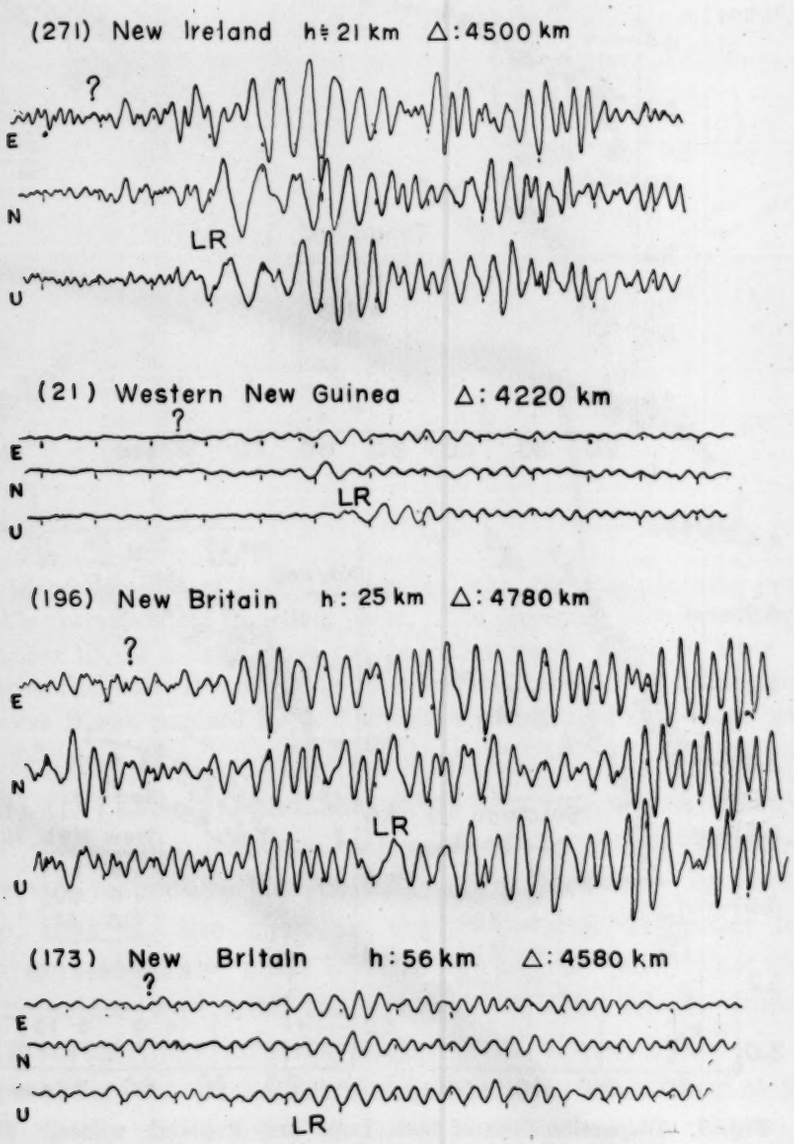

Fig. 6. Examples of seismograms on which Love waves are not apparent.

data. The examples are shown in Fig. 6 from the seismogram data obtained from shocks around New Ireland (271), New Guinea (21) and New Britain (196, 173). As the azimuths of these epicenters are all nearly due south from Tsukuba Station, Love waves should appear clearly in the EW component records. But, as is obvious in all of these examples, they are quite obscure. This unexpected fact cannot be explained at the present stage.

The wave forms and the dispersion characters of Love waves along northern oceanic paths such as from Aleutian Islands or Alaska Peninsula to Tsukuba are shown in Fig. 7.

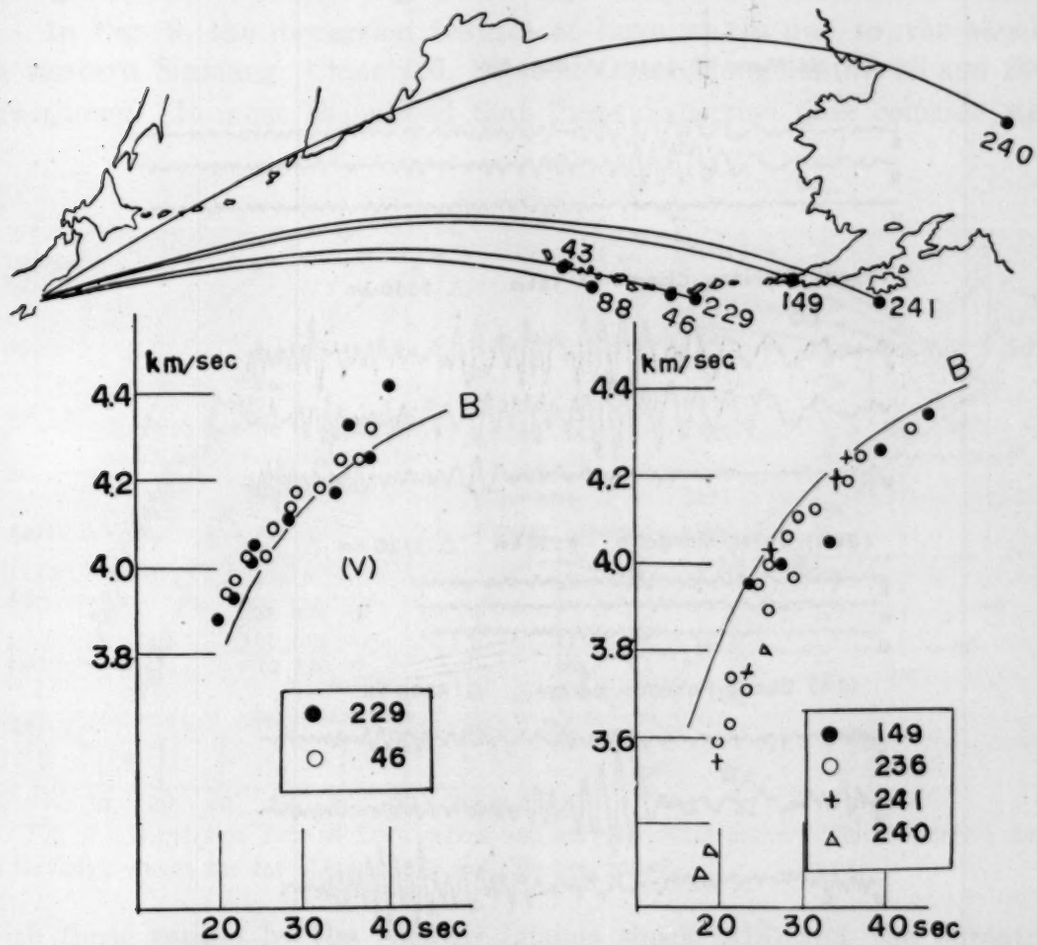

Fig. 7. Dispersion data of Love waves in the northern oceanic region and the corresponding travelling paths.

The dispersion characters of Love waves result from them show rather continental character (V) according to our characteristic number. Together with the result obtained in previous investigations into the

Rayleigh waves dispersions, the crust along these paths is considered to be much thicker than in the central Pacific Ocean.

4. Dispersions along continental paths

On account of the geographical condition, we cannot observe the dispersion of surface waves along purely continental paths in a geographical sense in Japan. "Continental paths" as used here mean, therefore, those due to the shocks which took place in the continent west of the Japanese Islands.

An interesting fact must again be reported here concerning the

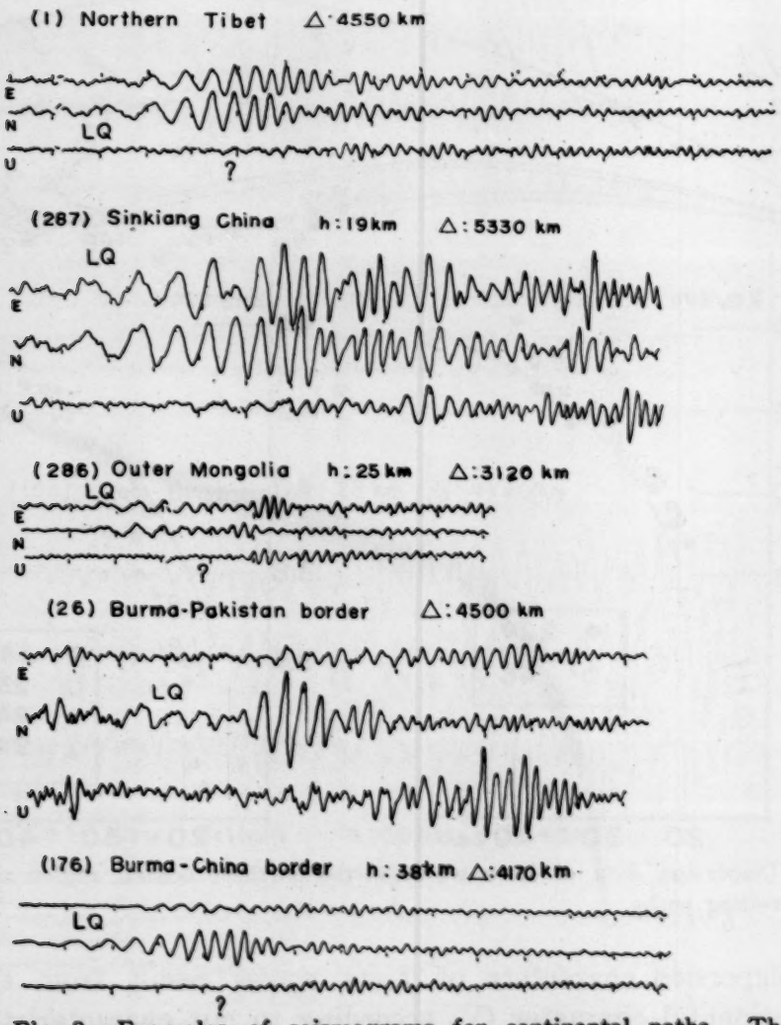

Fig. 8. Examples of seismograms for continental paths. They show clear Love wave trains but poor or else disturbed Rayleigh waves.

propagation of surface waves along the continental paths. That is, quite the oposite to the case of surface wave propagations in the Mariana Sea, the longer period Rayleigh waves were absent or quite obscure in this case in almost all the seismograms. Some examples are given in Fig. 8. For this reason, the writer could not make a complete investigation into the dispersion of Rayleigh waves along the continental paths to Japan.

5. Classification of the dispersive character of Love waves along continental paths

In Fig. 9, the dispersion feature of Love waves due to the shocks in western Sinkiang, China (36, 39) and Outer Mongolia (37, 38 and 286) are shown. It must be noticed that these dispersion data coincide well

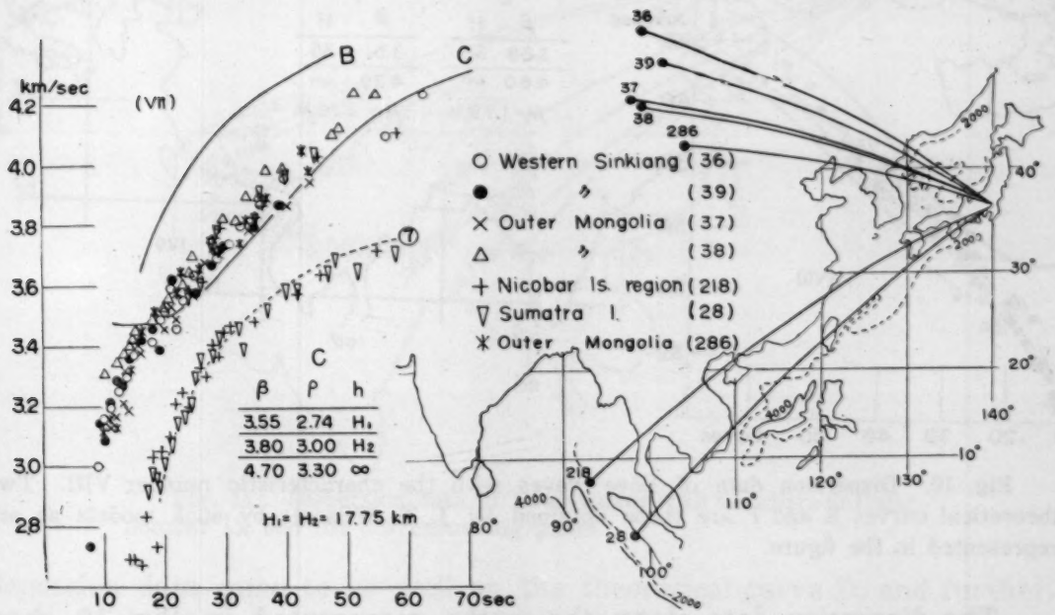

Fig. 9. Dispersion data of Love waves and corresponding paths. The dispersion data of Rayleigh waves for the shocks (218) and (28) are added.

with those caused by the Nicobar Islands shock (218) and the Sumatra Island shock (28). In the previous paper, the writer showed that the crustal structure along the oceanic path from the epicenter (28) to Tsukuba Station is purely continental. Besides, it was found in the present study that the averaged crustal structure along the oceanic path given above is, from the view point of Love wave dispersion at

least, quite similar to that along the continental paths from Sinkiang or the Mongolian region to Tsukuba. These dispersion data approximately lie on a theoretical dispersion curve C (Dorman's case 208).

The discrepancy in the data from the theoretical curve in the short period range may be due to the influence of a sedimentary layer near the observation station. The characteristic number VII was given for this dispersion character.

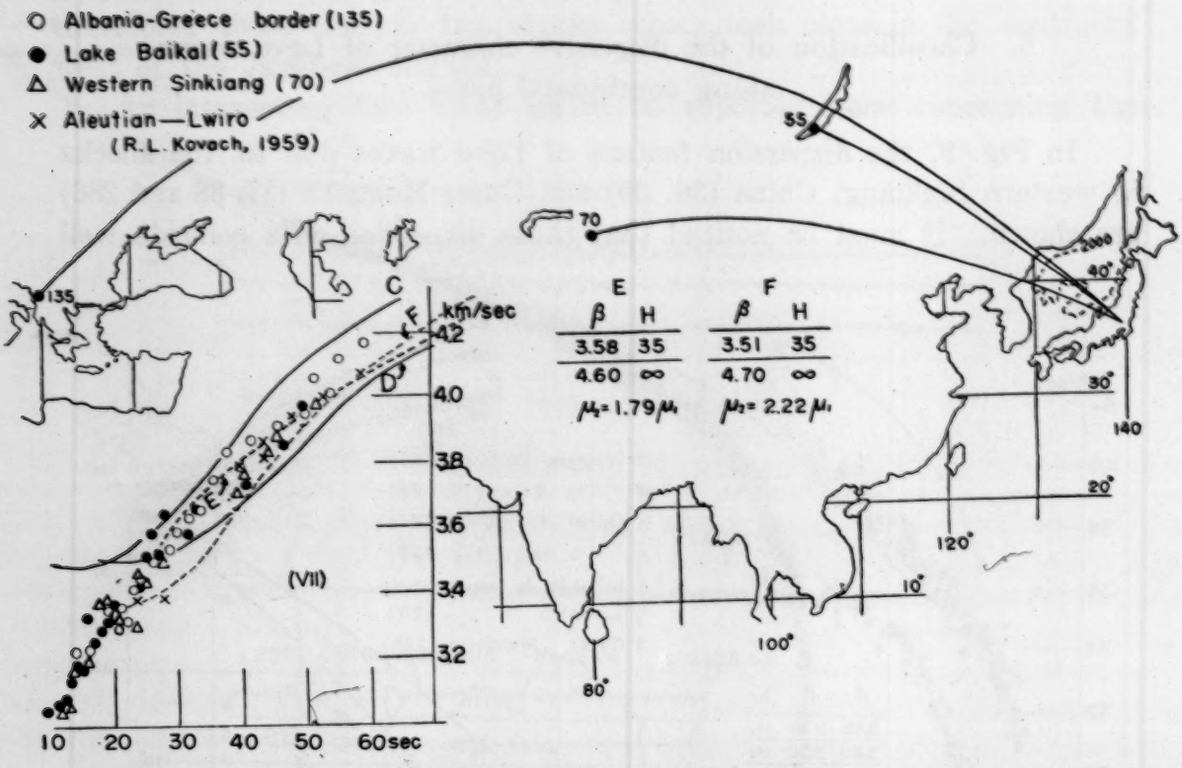

Fig. 10. Dispersion data of Love waves with the characteristic number VIII. Two theoretical curves E and F are those obtained by J. T. Wilson[5] by such models as are represented in the figure.

The dispersion data along the paths represented in Fig. 10 show another group, which lie between the two curves C and D. The curve C is the same as the previous one, and D is the curve when the thickness of the crust is thickened to 45.5 km in Dorman's case 208. The number VIII, was given for these dispersion data.

When the path shifts southward, the group velocities of Love waves gradually decrease, and for such paths as are shown in Fig. 11, the

5) J. T. WILSON, "The Love Waves of the South Atlantic Earthquake of August 28, 1933," *Bull. Seism. Soc. Amer.*, **38** (1940), 273.

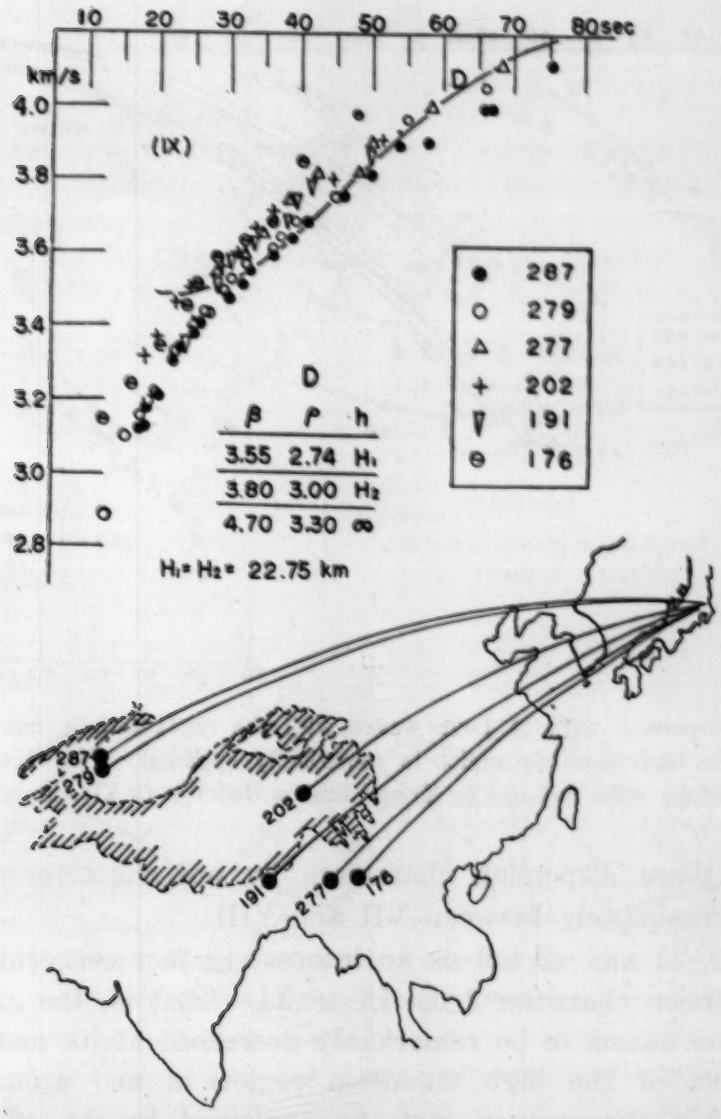

Fig. 11. Dispersion data of Love waves with the characteristic number IX and the corresponding paths.

dispersion data come to lie well on the theoretical curve D, and further, for such paths as are shown in Fig. 12 which include the Tibet Plateau, the dispersion data come beneath the curve D.

In Fig. 13, some other dispersion data of Love waves for the continental paths obtained by other authors[6),7),8)] are shown for comparison.

6) R. S. KOVACH, "Surface Wave Dispersion for an Asio-african and a Eurasian Path," *Journ. Geophys. Res.*, **64** (1959), 805.

7) T. AKIMA,* "On Dispersion Curves of Surface Waves from the Great Assam Earthquake of August 15, 1950," *Bull. Earthq. Res., Inst.*, **30** (1952), 237. (*The same as the present author)

8) J. N. BRUNE, J. E. NAFE and J. E. OLIVER, "A Simplified Method for the Analysis and Synthesis of Dispersed Wave Trains," *Jour. Geophys. Res.*, **65** (1960), 287.

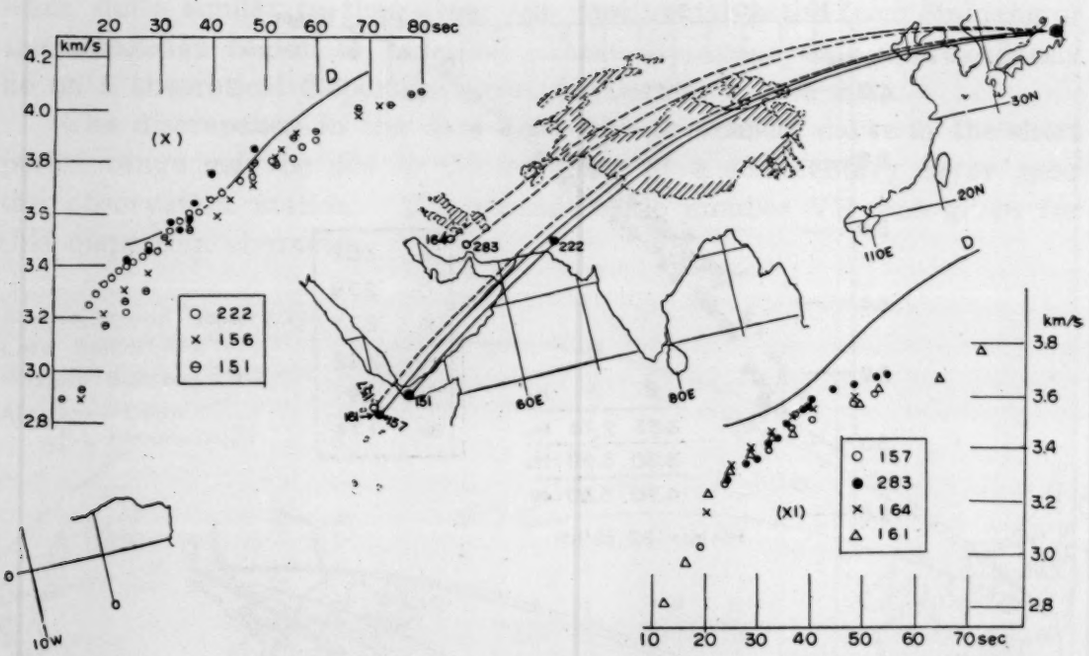

Fig. 12. Dispersion data of Love waves with the characteristic number X and XI. The effect of the high mountain region is remarkably apparent. The corresponding paths are distinguished by solid (belongs to X) and broken (belongs to XI) curves respectively.

Estimating these dispersion characters by our characteristic numbers, they lie approximately between VII and VIII.

Figs. 10, 11 and 12 tell us an interesting fact concerning the shift of the dispersion character from IX to XI. That is, the group velocity of Love waves seems to be remarkably decreased at its maximum value by the effect of the high mountain region in and around the Tibet Plateau. This phenomenon may be explained by the effect of some special conditions not only in the crust but in the upper mantle in these regions.

6. Dispersion data for the mixed paths

The dispersion data for the paths which partly cover the continental region in a geographical sense are shown in Fig. 14, in which, the most continental dispersion character for the oceanic path, hitherto obtained in the present investigations (V) and the most general one for the continental path (VII) are indicated by dotted curves. The list of the shocks used is given in Table IV.

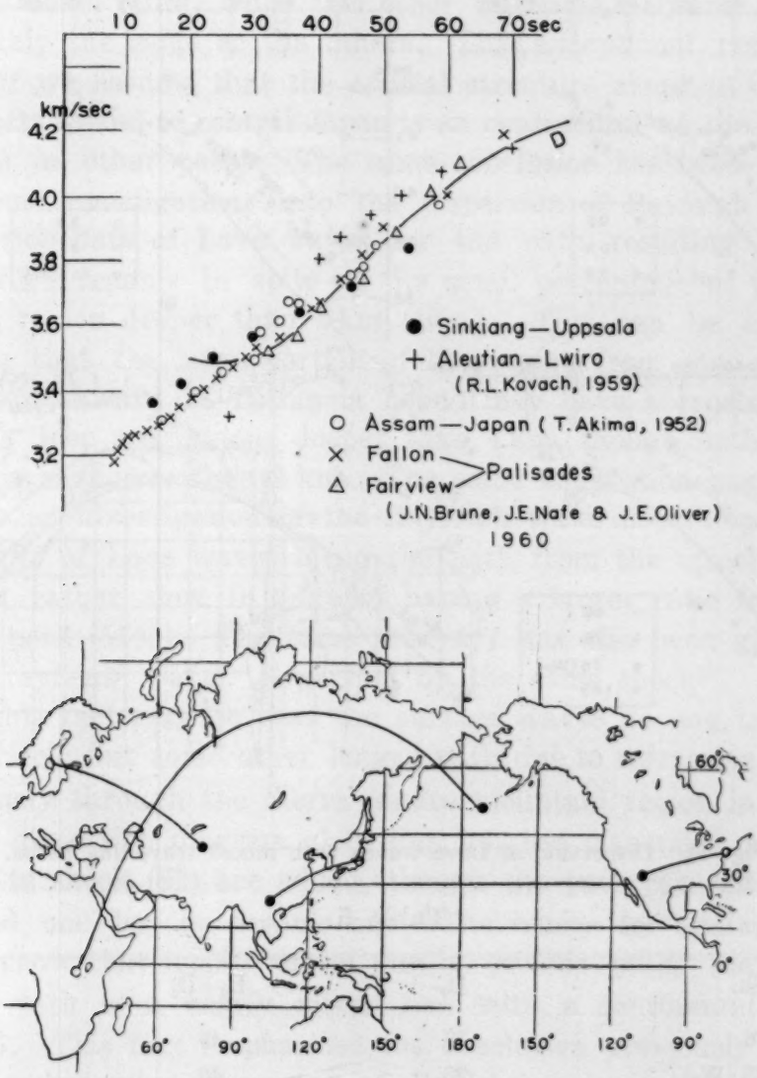

Fig. 13. Dispersion data of Love waves by other authors and the corresponding paths.

It is quite reasonable that these dispersion characters (the writer will give them the characteristic number VI) for the mixed paths lie between V and VII, and that the group velocity for the path, caused by the shock (163) which contains the largest continental portion is slower than the others. A noticeable fact is that most of the dispersion data lie in the same single curve.

In order to explain this, the percentages of the path lengths of a geographically continental region (D_0), a sea region shallower than 2 km (D_2) and one deeper than 4 km (D_4) were measured on every path. The results are given in Table 5. It can be read in this Table, that

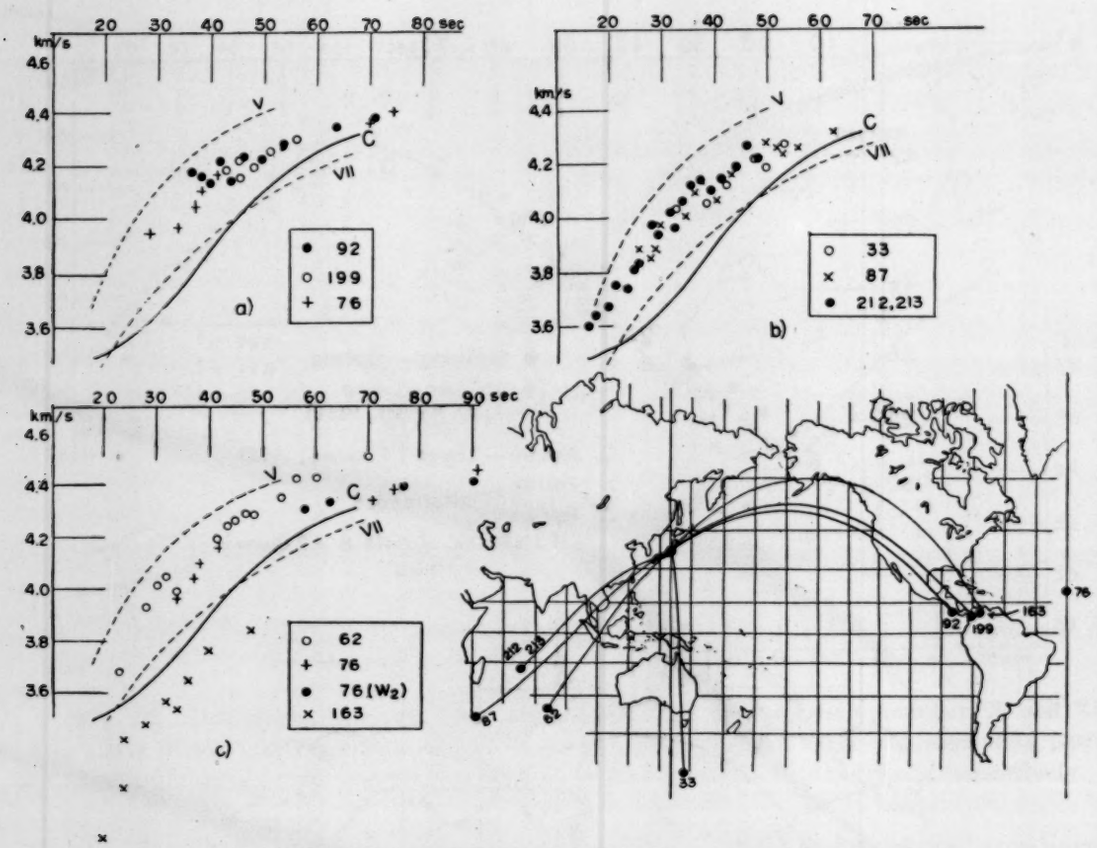

Fig. 14. Dispersion of Love waves with mixed travelling paths.

Table 5.

No.	D_0	D_0+D_2	D_4
76	35	49	33
76 (W_2)	30	40	26
199	31	49	27
92	29	42	51*
212, 213	33	59	32
87	10*	48	39
33	39	51	16*

the values of D_0, D_0+D_2 and D_4 are approximately around 33%, 42% and 30% respectively along most of these paths. Therefore, the similarity in the dispersion character along most of these paths can be explained by the similarity in the percentages of D_0, D_0+D_2 and D_4.

A few exceptional cases, however, can be noticed in Table 5. That is: 1) The value of D_0 along the path from the shock (87) is

remarkably small (10%) while two other values D_0+D_2 and D_4 are both approximately the same as the others. This exceptional result can be explained if we assume that the crustal structure along an oceanic part from Sumatra Island to central Japan is as continental as the continental region (D_0) in other paths. The same conclusion has been obtained in the previous investigations into the dispersion of Rayleigh waves. 2) The dispersion data of Love waves for the path resulting from shock (33) is rather oceanic in spite of its small percentage of path length over a sea region deeper than 4 km (16%). This can be explained if we assume that the large portion of the region from the epicenter to somewhere southward off Tasmania Island may have a crustal structure like that in deep sea regions deeper than 4 km, though bathymetrically the depth is shallower than 4 km. The same suggestion has also been made from an investigation of the Rayleigh wave dispersions[9]. 3) The group velocity of Love waves along the path from the epicenter (92) to Tsukuba is rather slow in spite of having a larger ratio for the deep sea region path (51%). The same tendency has also been given in the study of Rayleigh waves dispersion by the same shock[10]. One explanation of this fact may be that the surface waves do not travel along the great circle but some other longer path due to refraction when they cross obliquely through the Sierra Madre mountain region in Mexico.

In the dispersion diagram c) in Fig. 14, the dispersion data of Love waves due to shock (62) are added, though the path can not be said to be a mixed one but an oceanic one. The reason for adding this data here is to show that inspite of its purely oceanic path, the dispersion along this path is a nearly mixed one with a continental portion of nearly 30%. This fact emphasized the conclusion previously made concerning the dispersion character of Rayleigh waves that the crustal structure between Sumatra Island to Tsukuba along the same path is a nearly continental one with the characteristic number "6".

7. Conclusions

The dispersion of Love waves along various paths to Japan was investigated. Some interesting facts were discovered. Though a detailed analysis of the abundant data is not yet completed, the general conclusions concerning the dispersive character of Love waves around Japan

9) *loc. cit.* 1) p. 229
10) *loc. cit.* 2) p. 395

can be summarized as follows.

a) Love wave propagation is much disturbed along the path which covers the Mariana Sea. On the other hand, the shocks which take place in the Micronesia region, for instance, at the Tongas, Kermadecs, Solomons and New Hebrides can transmit clear dispersive, long trains of Love waves. Further, the Love wave dispersion character along these paths changes gradually with the shift of the paths westward. This tendency is quite the same as with Rayleigh waves.

b) The shocks which take place in the continent west of Japan such as in Mongolia, Sinkiang, India etc. transmit very clear Love waves but not Rayleigh waves.

c) The dispersive characters of Love waves along the continental paths were classfied into four groups. The effect of the special conditions both in the crust and in the upper mantle for the path which covers the Tibet Plateau remarkably appears in the decreasing of the maximum group velocity of Love waves in the long period range.

d) The dispersion character of Love waves from the Sumatra Island region to Japan is as continental as that from Mongolia to Japan.

e) The classified dispersion characteristics of Love waves around Japan are summarized in Fig. 15, in which the broken, dotted and solid curves mean those which were obtained through oceanic, mixed and continental paths respectively.

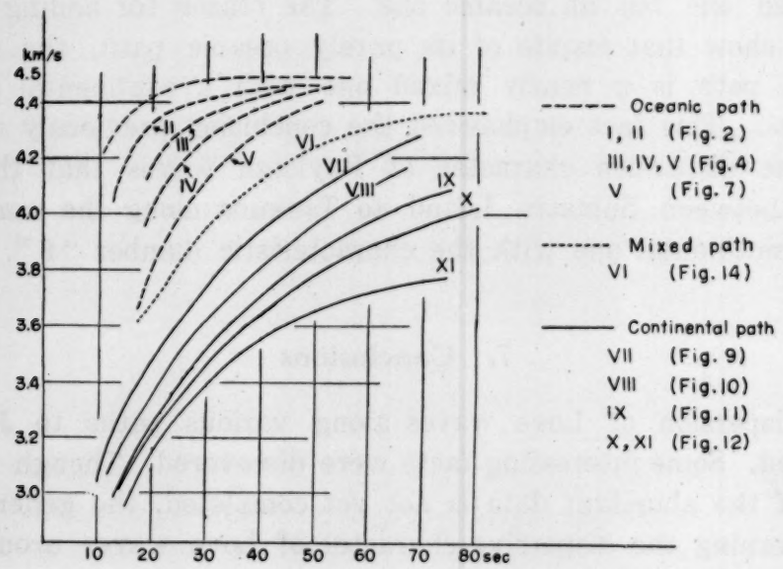

Fig. 15. Summarized figure for the eleven kinds of dispersion curves of Love waves.

24. 日本周辺を伝わるラブ波の分散について

東大地震研究所 三 東 哲 夫

前にレーリー波について調べたのと同様に，地震研究所の筑波支所におかれているコロンビア型地震計の記象を用いて，日本の周辺を伝わるラブ波の分散を調べた．

海洋径路のラブ波の分散は6種に分けられる．このうち，波の伝播径路が，太平洋西部を走るいわゆる「安山岩線」にかからない範囲の広い海域を通るものは，純海洋性（特性 I）か，それに近いもの（特性 II）の何れかに包含されるが，径路がメラネシヤ海域に入ると，レーリー波の場合に見られたと全く同様に，径路が西に移動するにつれて，ラブ波の場合にも分散特性が次第に陸的なものに移つていく傾向がはつきり見られた（第 3, 4 図）．

ただ，意外だつたのは，径路がマリアナ海に入ると，ラブ波の波形が急にひどく乱れたり，またはつきり出なかつたりして（第6図），これらの径路に沿つては分散曲線が全く得られなかつたことである．このことは，アジア大陸方面からやつてくる大陸径路の表面波の場合には，今度は逆に，ラブ波は極めてきれいに現われるのに，レーリー波の方が短周期のものに限られてしまつて（第8図），この場合にはレーリー波に対する分散曲線が十分な周期範囲では得られなくなることと合せて，今後調べて見たい問題である．

スマトラ島附近から日本への径路に沿うレーリー波の分散が大陸的であることは前の論文で示した通りであるが，ラブ波の方でも全くその通りで，その分散性は，外蒙古附近から日本に向う径路に沿つてのそれと全く同一である（第9図）．

大陸径路のラブ波の分散特性は5つに分けた．このうちで特に注目される点は，径路がチベット高原を横切る様になると，ラブ波の群速度の極大値が著しく小さくなる様な傾向を示すことである（第15図）．この特殊な分散傾向が果して地殻内部だけの問題として片づけられるかどうかは残された問題である．

Bulletin of the Earthquake
Research Institute
Vol. 39 (1961), pp. 653-668

25. *Surface Waves and Layered Structures. Part 1. Influence of a low velocity layer and some study on Lg and Rg waves.*

By Rinzo Yamaguchi,

Earthquake Research Institute.

(Read Sept. 26, 1961.—Received Sept. 30, 1961.)

1. Introduction

The nature of surface waves has been investigated by many seismologists from various points of view.[1)-2)] Amongst others, the dispersion of these waves has become one of the most interesting problems in these days.[3)] The reason for this current trend of study lies in the fact that the clarification of regional variation in the crustal structure of the earth has become a central problem of seismology and the usual approach to this problem through the study of travel-time curves of bodily seismic waves in respective parts of the world is hindered by the paucity of adequate seismographic stations, while the study of only a few relevant seismograms of surface waves, transmitted through the region in question, enables us to gain a clue to the problem, because the dispersion of these waves is strongly influenced by the crustal structures concerned. The possibility of the latter approach has hitherto been proved by theoretical calculations as well as actual observations. But there is no method of obtaining a unique solution of the crustal structure from observations of dispersion curves of Lr and Lq waves, since much difficulty has been felt by each investigator in finding even an approximate inference of the actual structure to comply with the observations. Although some investigators have gone so far as to calculate dispersion curves in the cases of complicated crustal structures composed of tens of different layers in accordance

1) Y. Satô, "On Elastic Surface Waves," *Zisin.* [ii], **6** (1953), 13.

2) M. Ewing, W. Jardetzky, and F. Press, *Elastic Waves in Layered Media*, (New York: McGraw-Hill, 1957).

3) e.g. J. Dorman, M. Ewing, and J. Oliver, "Study of the Shear Velocity Distribution in the Upper Mantle by Mantle Rayleigh Waves," *Bull. Seism. Soc. Amer.*, **50** (1960), 87.

with the known earth's structure to explain average dispersion curves. But accurately speaking, there are no true average curves of dispersion for the whole earth, and in addition, the regional variation of them is so remarkable that we have first to derive regional dispersion curves and then find corresponding crustal structures of the first approximation before going into further details.

For such a purpose, we must find the general characteristics of dispersion curves of respective waves of corresponding to particular crustal structures, and then find the main factors whose variation can cover wide variation in velocity, and the other particular features of dispersion curves and the spectral characteristics of the amplitudes, etc.

Recently, long period seismographs of high sensitivity have been accomplished, and long surface waves with periods of hundreds or a thousand seconds are being clearly observed, while remarkable progress of with high speed electronic computers encourage us to proceed into detailed studies involving complicated calculations which would be almost impossible otherwise. In view of these circumstances, the writer ventured to make some contribution to the above mentioned problem by some study on the influence of low velocity layers in the earth's crust on surface waves, and by presenting a systematic calculation of dispersion curves of surface waves covering wide variations of conceivable parameters of the physical constants of the layers along which these waves are propagated.

This paper contains parts of the writer's study touching on such line, and is composed of two parts, the one dedicated to the study of the effect of a low velocity layer on surface waves and some study on Lg and Rg waves, and the other pertaining to the systematic calculation of the dispersion curves of Lr and Lq waves in various layered structures below the ocean bottom.

2. Love waves propagated along the surface of a stratified medium with a low velocity layer.

Our knowledge on the internal structure of the earth has recently advanced from the hypothesis of continuous monotonous increase in velocity v or v/r (r being the radius vector from the earth's centre) up to the core boundary which information was known in the early years of this century. It has been revealed that the crustal structure is

almost certainly subjected to regional variation while the more generally prevalent structure of the mantle also includes some peculiarities other than there hitherto recognized. Some seismologists proposed the hypothesis of the existence of the first order discontinuity while others suggested a minimum in the velocity distribution (a low velocity layer) in the mantle. The existence of two other low velocity layers in the crust has also been pointed out. But crucial tests have yet to be made from points of view other than the time distance curves P and S waves. Verification of the latter hypothesis has recently been made by a comparison of the dispersion curve of the mantle Rayleigh wave as calculated on the suggested earth's structure and that actually observed,[3] and the result seems to be very encouraging.

We have already obtained the velocity equation of Love waves propagated along the surface of a multi-layered media.[4] We shall now examine the effect of a low velocity layer on the dispersion of Love waves and their amplitude distribution within the layers for a reference to the above mentioned verification.

Here we shall study the case where three layers overlie on a semi-infinite medium, and for simplicity, we will assume that the thicknesses of these layers are equal ($=H$) to each other, while the rigidities in the layers and the subjacent medium are in the ratios $1:3:2:4$ respectively and their densities are equal; that is, the third layer is a low velocity layer.

The relevant velocity equation in this case is at once derived from our general formula as follows:

$$\begin{aligned}&\{c_1c_2-\chi_{12}(\tilde{\beta}_1/\tilde{\beta}_2)s_1s_2\}\{c_3-\chi_{34}(\tilde{\beta}_3/\beta_4)s_3\}\\&-\{\chi_{23}(\tilde{\beta}_2/\tilde{\beta}_3)c_1s_2+\chi_{13}(\tilde{\beta}_1/\tilde{\beta}_3)s_1c_2\}\{s_3+\chi_{34}(\tilde{\beta}_3/\beta_4)c_3\}\\&=0\end{aligned}$$

where

$$\begin{aligned}&c_k=\cos\tilde{\beta}_kH_k\ , \qquad s_k=\sin\tilde{\beta}_kH_k\ ,\\&\beta_k=\sqrt{f^2-p^2/V_k^2}=i\tilde{\beta}_k\ , \qquad \chi_{jk}=\mu_j/\mu_k\ ,\\&H_k=\text{thickness of } k\text{ th layer},\\&V_k=\text{shear volocity of } k\text{ th layer},\\&\mu_k=\text{rigidity of } k\text{ th layer},\\&f=\text{wave number},\\&p=\text{frequency}.\end{aligned}$$

4) Y. SATÔ and R. YAMAGUCHI, "Velocity Equation of Love Waves Propagated in Multi-layered Media," *Zisin*, [ii], **12** (1959), 61.

The results of the calculation are represented in Figs. 1 through to 9. Dispersion curves in Fig. 1 show the existence of a very remarkable new branch C other than those of the higher modes (II and III) to the fundamental one (I). The phase velocity of this C branch approaches the shear wave velocity in the low velocity layer as the period decreases to zero. It is also remarkable that the group velocities of the second mode (II) and the branch C, as indicated by the broken lines in the same figure have almost stationary values nearly equal to the

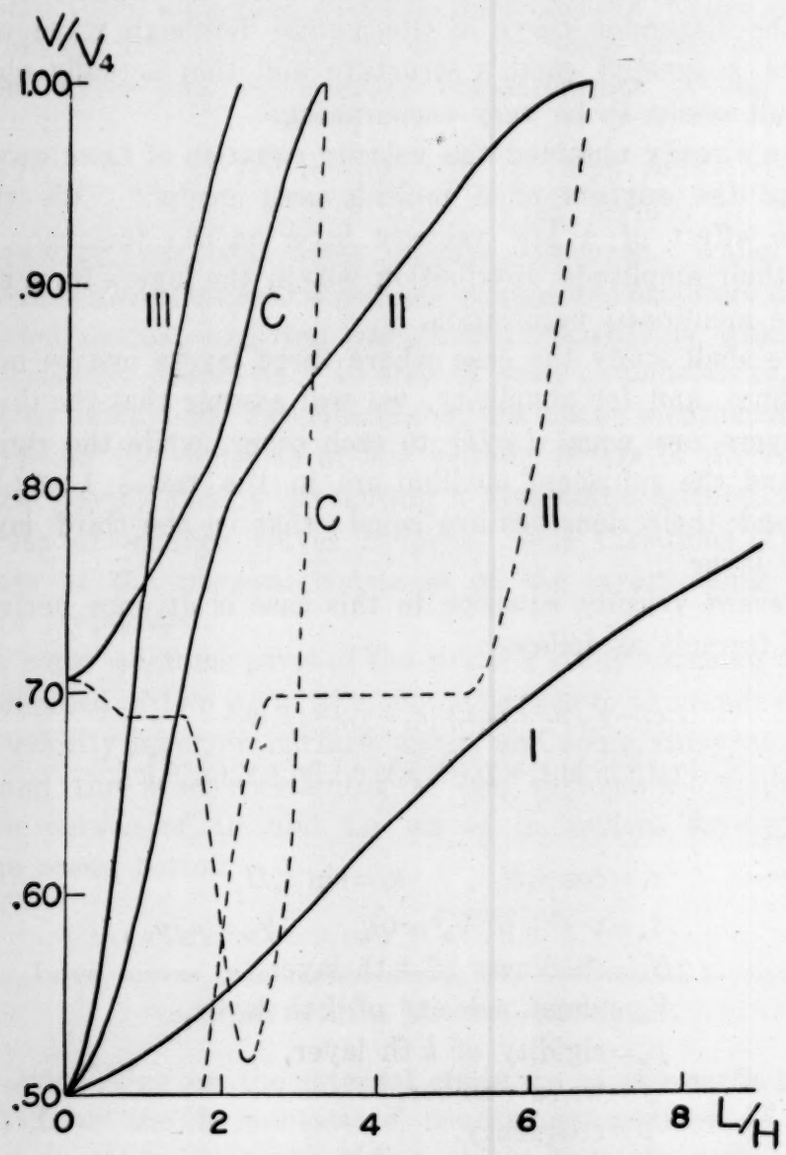

Fig. 1. Phase (solid line) and group (broken line) velocity dispersion curves of Love waves for the case $\mu_1 : \mu_2 : \mu_3 : \mu_4 = 1 : 3 : 2 : 4$, $\rho_1=\rho_2=\rho_3=\rho_4$, $H_1=H_2=H_3=H$.

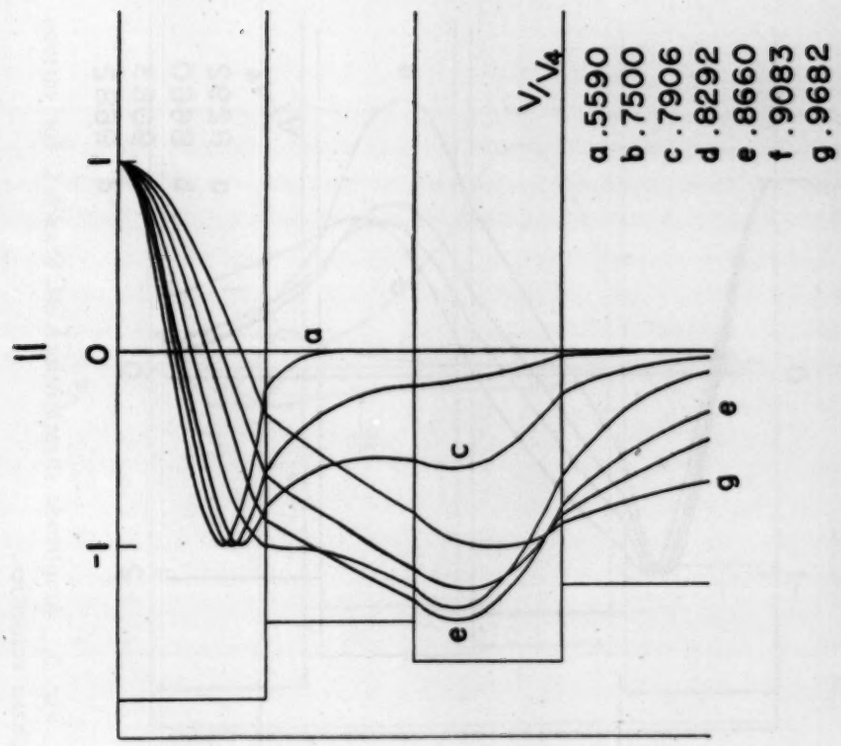

Fig. 3. Amplitude distributions of branch II for various phase velocities.

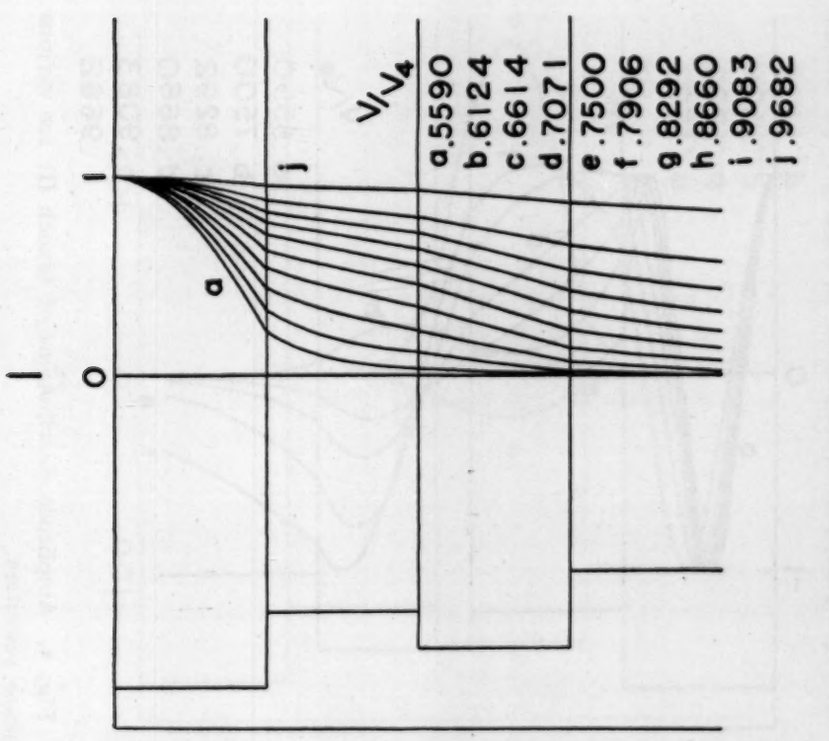

Fig. 2. Amplitude distributions of branch I for various phase velocities.

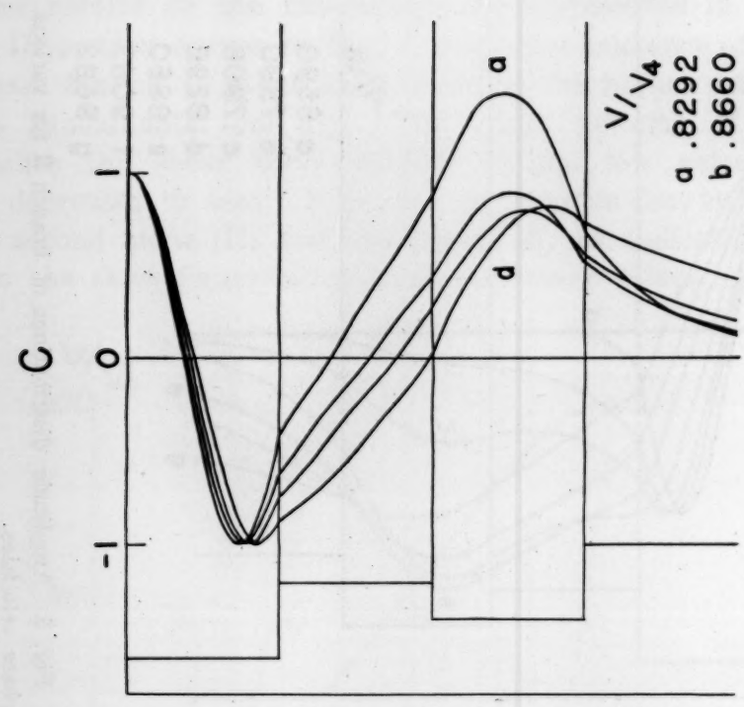

Fig. 5. Amplitude distributions of branch C for various phase velocities.

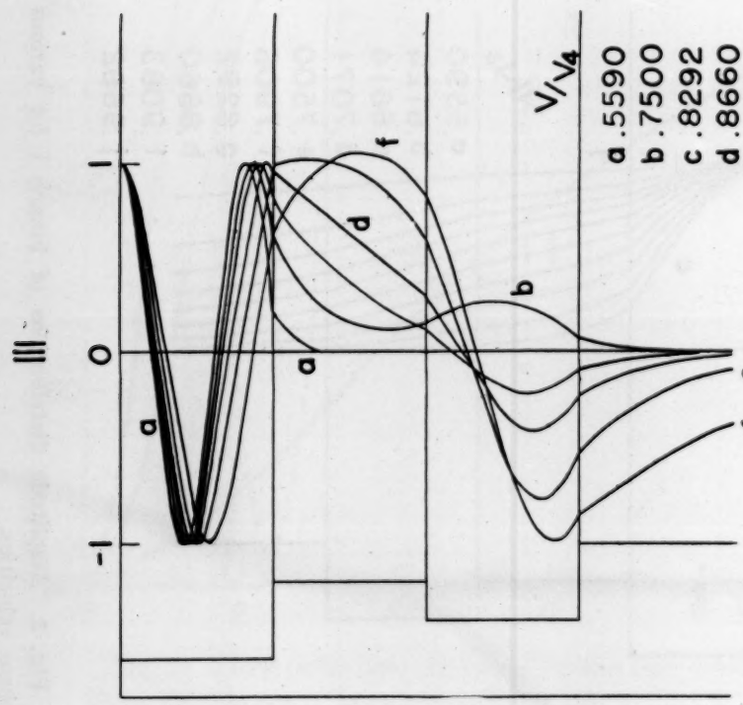

Fig. 4. Amplitude distributions of branch III for various phase velocities.

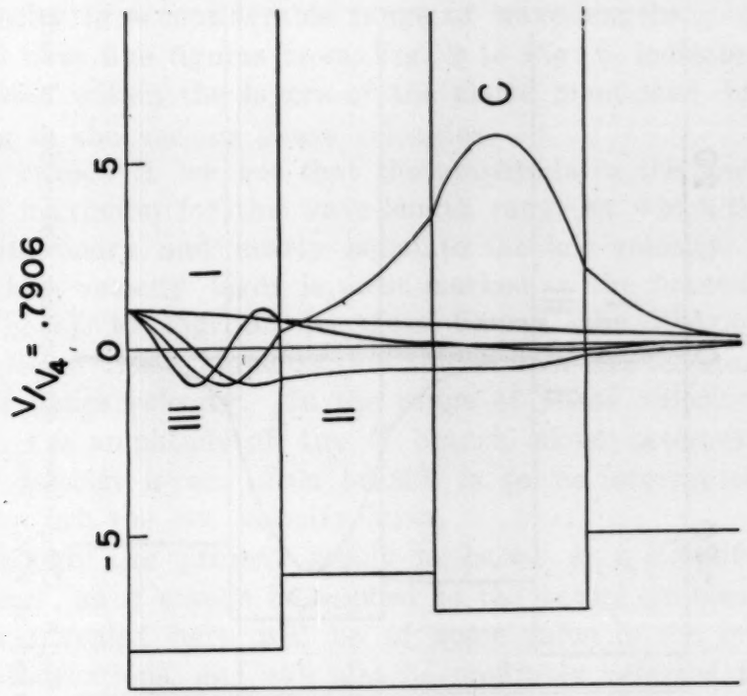

Fig. 7. Comparisons of amplitude distribution of each branch at $V/V_4=0.7906$.

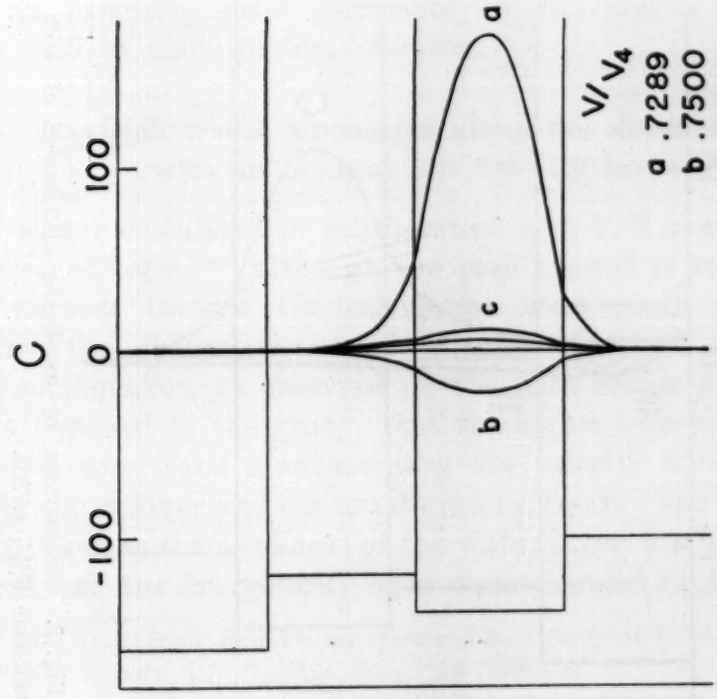

Fig. 6. Amplitude distributions of branch C for various phase velocities.

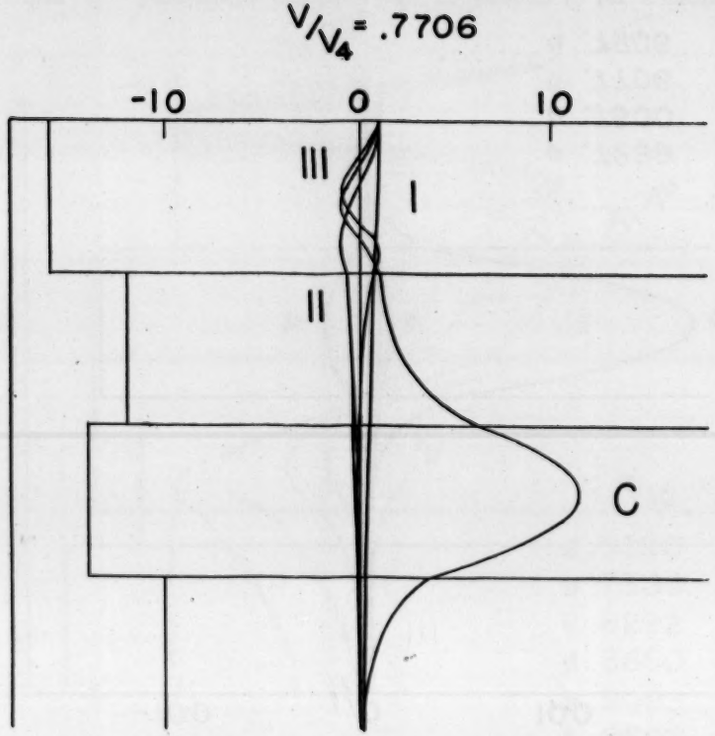

Fig. 8. Comparisons of amplitude distribution of each branch at $V/V_4=.7706$.

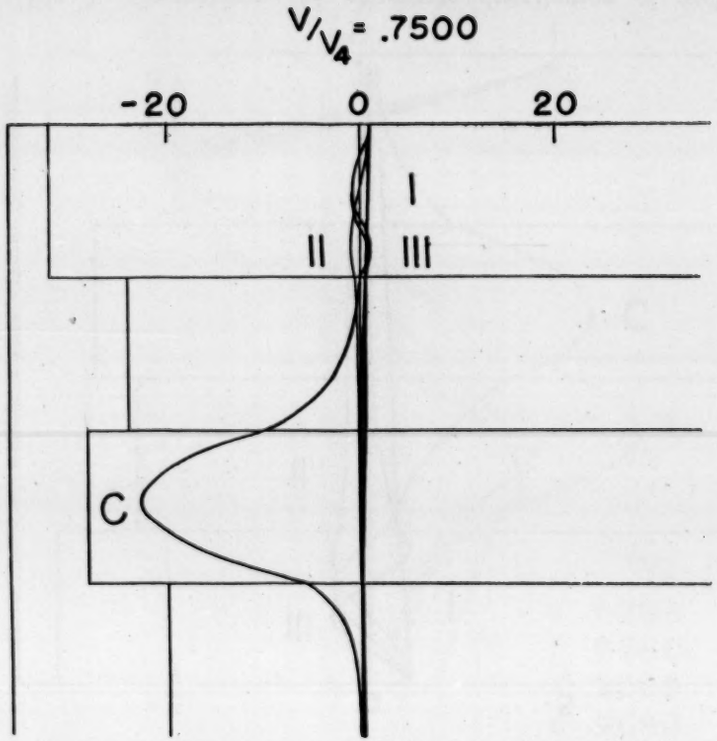

Fig. 9. Comparisons of amplitude distribution of each branch at $V/V_4=.7500$.

low velocity in a considerable range of wave-lengths.

The next five figures from Fig. 2 to Fig. 6 indicate the amplitude distribution within the layers of the above mentioned branches, corresponding to the various phase velocities.

For branch II we see that the amplitude in the low velocity layer becomes maximum for the wave-length range at which the group velocity is stationary and nearly equal to the low velocity. The influence of the low velocity layer is most marked in the branch *C* as is seen from Fig. 7 to Fig. 9. In these figures, the distributions of the amplitudes of these branches, in the layers, are compared at certain levels of phase velocity. In the range of phase velocity near the low velocity, the amplitude of the *C* branch alone becomes very large in the low velocity layer. This branch is to be interpreted as a channel wave through the low velocity layer.

Although the present result is based on a simplified assumption and cannot, as it stands be applied to the actual problem, the general features revealed here will be of some value in the interpretation of actual observations, and will also be profitably referred to in more concrete studies, whenever a low velocity layer is taken into consideration at all.

As an example, some comments on the results we have already reported, will be made in the following.

3. Rayleigh waves propagated along the stratified medium with an internal low velocity layer.

The writer calculated in collaboration with T. Kizawa some examples of the present topic,[5)-6)] although the case treated is too specific for the present purpose because the calculation were made with a view to elucidating the characteristics of actually observed novel phases of volcanic earthquakes, as observed on the path across a shallow bay. It was thus assumed in the study, that the higher velocity surface layer is composed of water, and a sedimentary low velocity layer intervenes between the water layer and the usual granitic layer. The depth of the bay (100 m) is taken as the thickness of the water layer, and the thickness and the velocity of the low velocity layer were changed as parameters. And

5) T. KIZAWA, "Some New Phases Observed in a Study of Earthquake Swarms Relating to Volcanic Activity (I)," *Geophys. Mag.*, **29** (1960), 477.

6) T. KIZAWA and R. YAMAGUCHI, "Some New Phases Observed in a Study of Earthquake Swarms Relating to Volcanic Activity (II)," *Geophs. Mag.*, **30** (1960), 93.

the phase velocities and group velocities of Rayleigh waves in the media were calculated and compared with the observations. We could thus conclude that the observed novel third and fourth phases which accompanied the Usu volcanic earthquakes are to be explained by the fundamental and second modes of Rayleigh waves propagated along the medium of hypothetical structure, with a low velocity layer of velocity $V_p=1$ km/sec, $V_s=0.6$ km/sec and with a thickness of about 300–400 m.

The results of these calculations do not enable a direct comparison with the results mentioned in section 2 of the present paper, but we may almost certainly verify the last conclusion in section 2.

4. Lg and Rg waves

Of late years, the natures of the Lg and Rg phases have been actively discussed,[7)–18)] but no definite conclusion has yet been obtained. It seems to the writer that the segments of the stationary group velocity of the branches of II and C mentioned in section 2 may play some part in the observed Lg phase if a low velocity layer actually exists. There may also be a similar phenomenon in Rayleigh waves in similar circumstances, which is relevant to the interpretation of the Rg phase.

---

7) F. PRESS, M. EWING, "Two Slow-Surface Waves across North America," *Bull. Seis. Soc. Amer.*, **42** (1952), 219.

8) I. LEHMANN, "On the short period surface wave 'Lg' and crustal structure," *Bull. d'Information U.G.G.I.*, **2**. annee, (1953), 248.

9) M. BÅTH, "The Elastic Waves Lg and Rg along Euro-Asiatic Paths," *Arkiv for Geofysik*, **2** (1954), 295.

10) B. GUTENBERG, "Channel Waves in the Earth's Crust," *Geophysics*, **20** (1955), 283.

11) J. OLIVER, M. EWING and F. PRESS, "Crustal Structure of the Arctic Regions from the Lg Phase," *Bull. Geol. Soc. Amer.*, **66** (1955), 1063.

12) F. PRESS, M. EWING and J. OLIVER, "Crustal Structure and Surface Wave Dispersion in Africa," *Bull. Seism. Soc. Amer.*, **46** (1956), 97.

13) M. BÅTH, "Some Consequences of the Existence of Low-Velocity Layers," *Estratto da Annali di Geofisica*, **9** (1956), 411.

14) M. BÅTH, "A Continental Channel Wave, guided by the Intermediate Layer in the Crust," *Geofisica Pura e Applicata*, **38** (1957), 19.

15) I. LEHMANN, "On Lg as Read in North America Records," *Annali di Geofisica*, **10** (1957), No. 1-2, 1.

16) J. OLIVER and M. EWING, "Higher Modes of Continental Rayleigh Waves," *Bull. Seism. Soc. Amer.*, **47** (1957), 187.

17) J. OLIVER and M. EWING, "Normal Mode of Continental Surface Waves," *Bull. Seism. Soc. Amer.*, **48** (1958), 33.

18) T. UTSU, "On the Lg Phase of Seismic Wave Observed in Japan (1)," *Quart. Jour. Seism. Japan Meteor. Agency*, **23** (1958), 61.

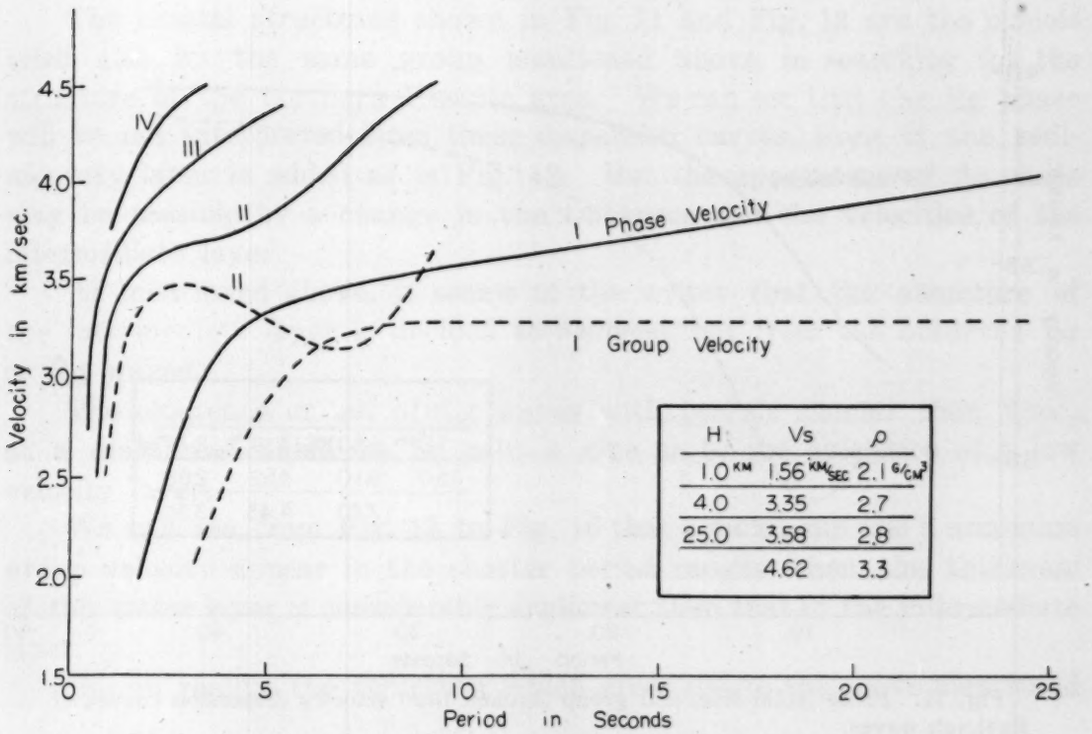

Fig. 10. Phase (solid line) and group (broken line) velocity dispersion curves of Love waves.

On the other hand, the Lg phase will be interpreted when the intermediate layer, with shear wave velocities of 3.5–3.7 km/sec has a thickness as great as five or more times of that of the upper layer.

As an example, we will introduce the model shown in Fig. 10. That model is one of the five models which were tried by the Research Group for Explosion Seismology in Japan, to decide the crustal structure in the northern Kwanto district. From Fig. 10 we can see that a maximum and a minimum group velocity of IInd mode appear in the shorter period range (2 to 7 sec.) and the group velocity of the fundamental mode has a stationary value (about 3.3 km/sec) at periods longer than about 7 sec.

It seems to the writer that the Lg_1 phase corresponds to the maximum and the Lg_2 phase is in agreement with the minimum and the stationary group velocity, since the amplitude at its phase, takes a large value. Perhaps the observed Lg phase in various places will be explained by the models conform to the example as mentioned above.

There may also be a similar phenomenon in the Rayleigh waves. However the fundamental mode brings Rg waves into actual existence in the following.

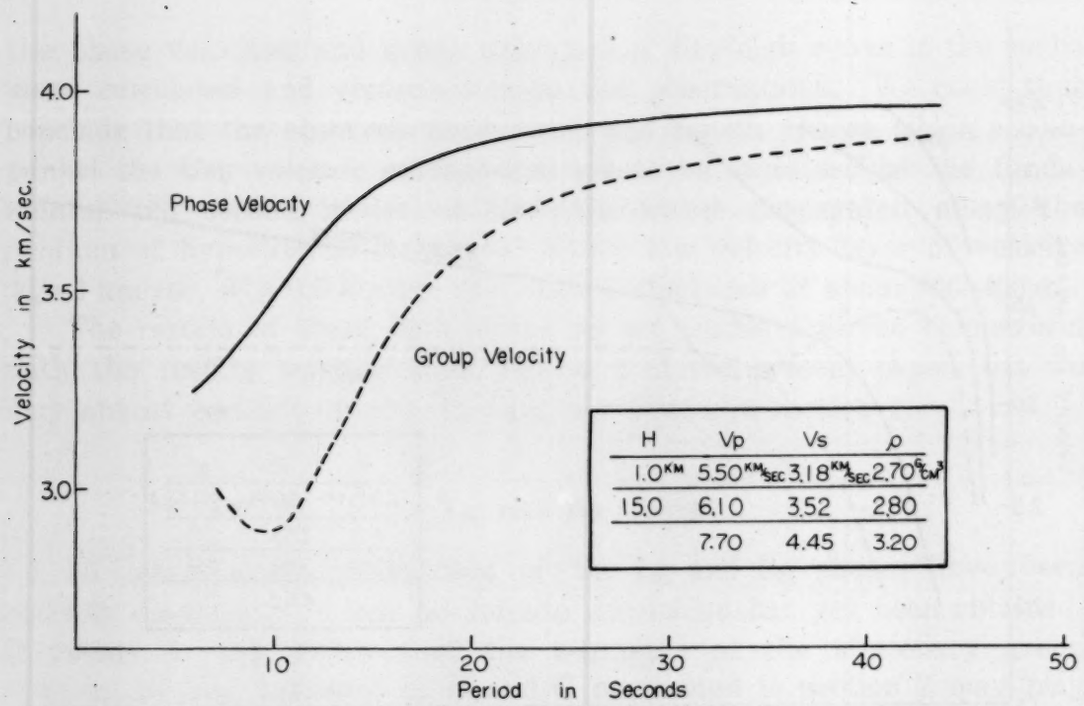

H	Vp	Vs	ρ
1.0 KM	5.50 KM/SEC	3.18 KM/SEC	2.70 G/CM³
15.0	6.10	3.52	2.80
	7.70	4.45	3.20

Fig. 11. Phase (solid line) and group (broken line) velocity dispersion curves of Rayleigh waves.

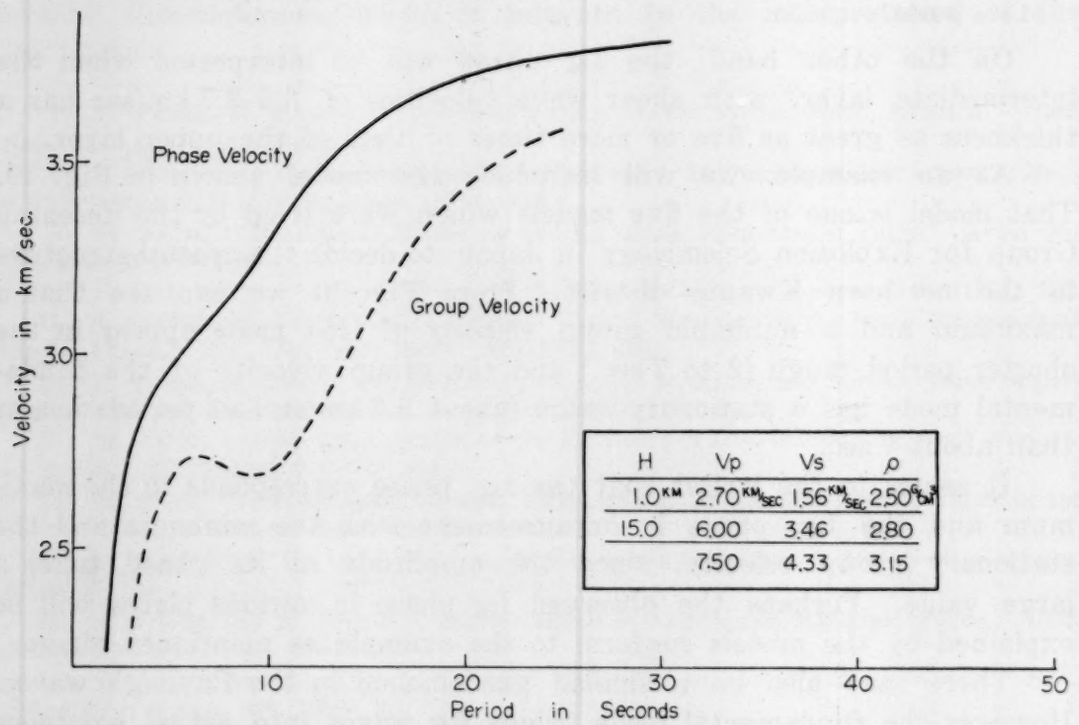

H	Vp	Vs	ρ
1.0 KM	2.70 KM/SEC	1.56 KM/SEC	2.50 G/CM³
15.0	6.00	3.46	2.80
	7.50	4.33	3.15

Fig. 12. Phase (solid line) and group (broken line) velocity dispersion curves of Rayleigh waves.

The crustal structures shown in Fig. 11 and Fig. 12 are the models tried also by the same group mentioned above in searching for the structure of the northern Kwanto area. We can see that the Rg phase will be not interpreted from those dispersion curves, even if the sedimentary layer is added as in Fig. 12. But the appearence of its phase may be possible by a change in the thickness and the velocities of the intermediate layer.

As mentioned above, it seems to the writer that the structure of the intermediate layer is decided to some extent from the observed Lg or Rg waves.

The existence or not of Lg waves with periods shorter than 2 sec. at a distance, enable us to gain a clue as to the existence of a low velocity layer.

We can see from Fig. 13 to Fig. 16 that a maximum and a minimum group velocity appear in the shorter period ranges when the thickness of the water layer is considerably shallower than that of the intermediate layer.

But in reality the structure which gives rise to the above mentioned

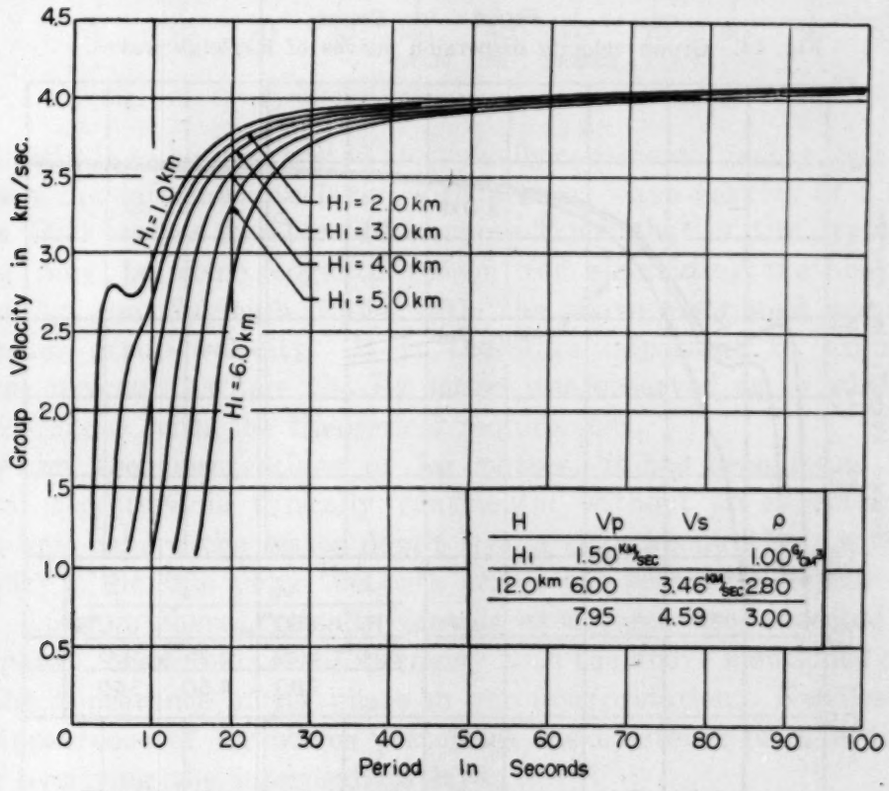

Fig. 13. Group velocity dispersion curves of Rayleigh waves.

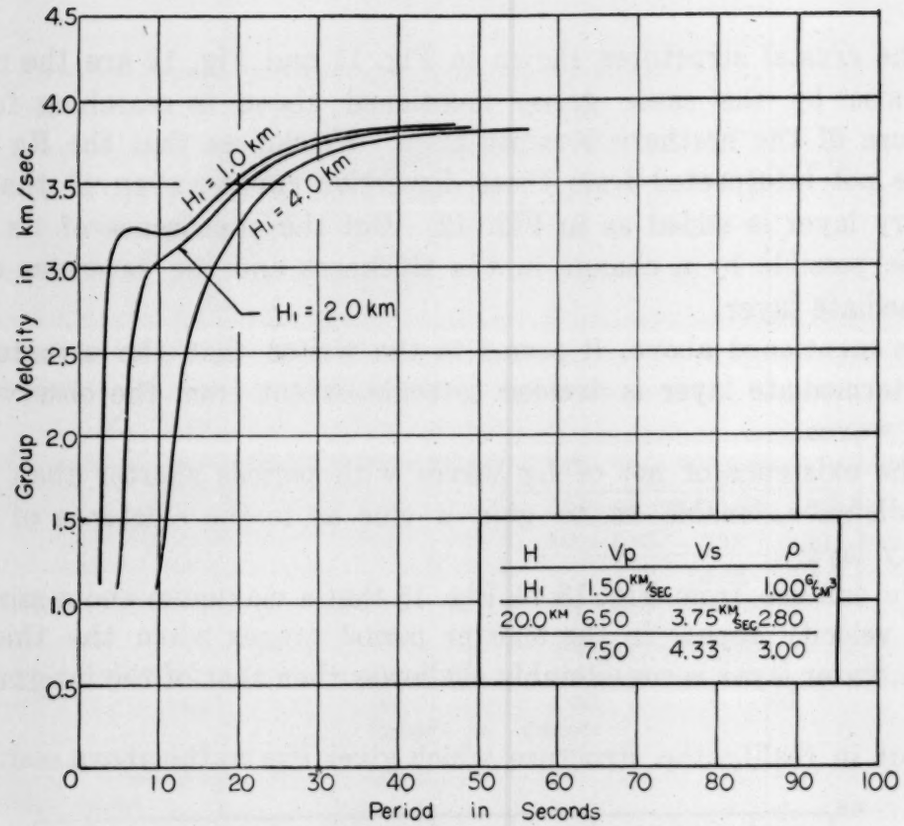

Fig. 14. Group velocity dispersion curves of Rayleigh waves.

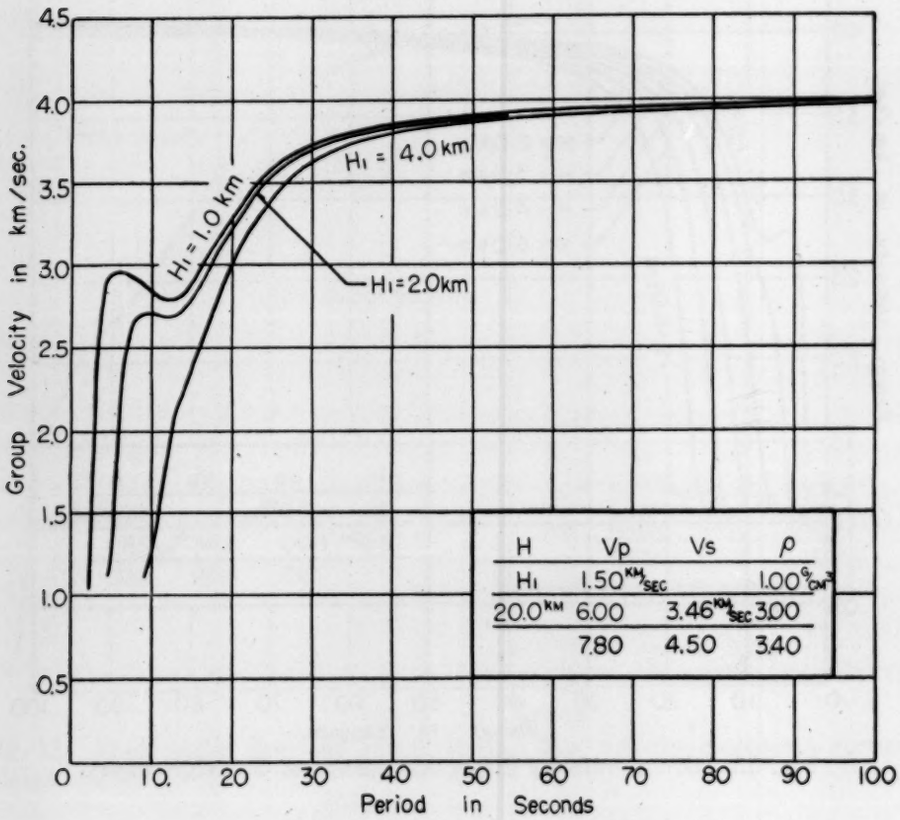

Fig. 15. Group velocity dispersion curves of Rayleigh waves.

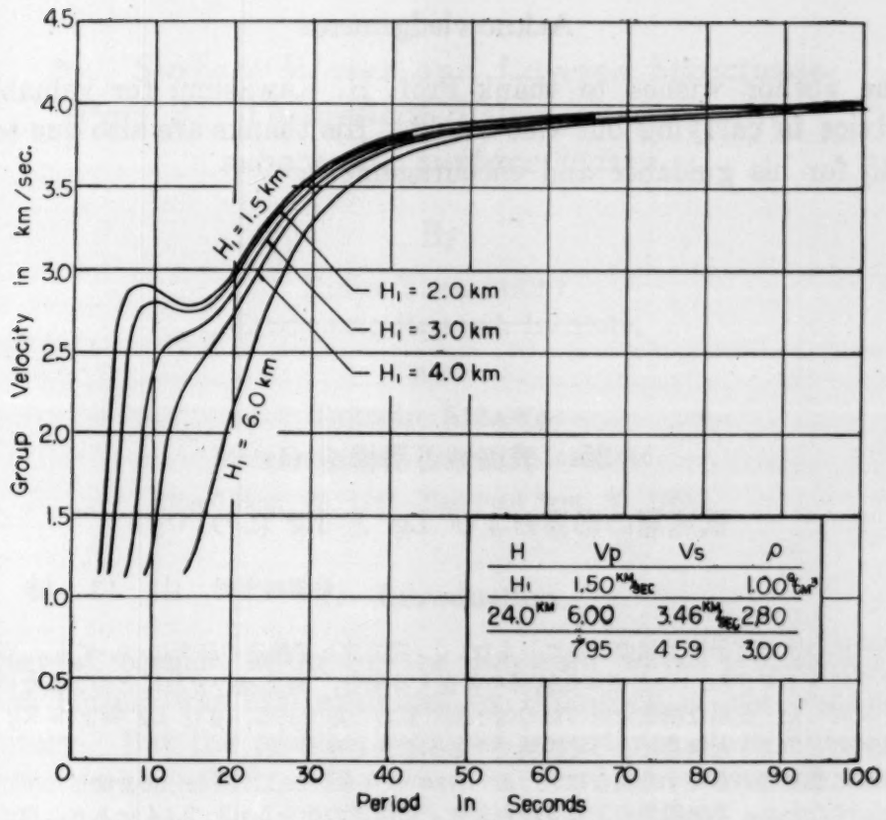

Fig. 16. Group velocity dispersion curves of Rayleigh waves.

peculiarity is to be interpreted as typically continental rather than oceanic, because the intermediate layer with a shear wave velocity of 3.5 km/sec has a thickness as great as 10 or more times that of the water layer. There may be some cognate reason for elucidating the observed Rg phase by the Rayleigh wave with the above mentioned maximum or minimum group velocity. It is therefore important to examine the crustal structure, where the Rg phase was observed as to whether it is in accordance with the theoretical requirement.

From the observations of Lg phases, it has been found that the crustal structure is typically continental without an exception in any large area where the water depth is less than about 2 km, whereas the contrary is the case along the path across the seas with depths of more than 3.5 km, where typically oceanic structures are expected to predominate. These facts are in harmony with the above mentioned condition for the appearance of Rg phase in our interpretation. Needless to say, the appearence of Lg waves postulates the existence of a sedimentary layer overlying the intermediate layer.

Acknowledgements

The author wishes to thank Prof. H. Kawasumi for valuable help and advice in carrying out this study. His thanks are also due to Prof. Y. Satô for his guidance and encouragement.

---

25. 表面波と層構造 (1)

低速層の影響および Lg と Rg について

地震研究所　山　口　林　造

1. 最近における電子計算機の発達にともない，表面波と層構造の研究についても，詳しく議論されるようになつてきた．ここでは低速層の存在する場合，表面波の分散にどのような特徴が現われるかを検討した．簡単な構造に限つたのは手動計算のためである．また Lg および Rg 相について，具体的にどのような構造によつて説明できるかを示した．

2. 一般に低速層の存在する場合における Love 波の分散および振巾分布を簡単な構造を使つて計算した．すなわち，半無限層の上に3層をおき，剛性率の比を 1 : 3 : 2 : 4 にとり，層の厚さおよび密度は等しいとした．したがつて，第3層が低速層になる場合である．注目すべき結果は第1図に示されているごとく，新らしい分枝 C の存在することである．この分枝 C は周期が短かくなると，その位相速度は低速層の速度に近づく．そして振巾分布から分かるごとく，Channel wave の性格を持つているので C 分枝と名付けた．各分枝の振巾分布は第2図から第6図まで，また各分枝の振巾分布の比較を第7図から第9図までに示した．振巾分布から見て面白いことは，分枝Ⅱで群速度のあまり変わらないところで，低速層に振巾が大きく出てくることである．

3. 液体-固体-固体からなる構造で，その中間層にあたる沈澱層の速度を水の層より遅くとつた場合の Rayleigh 波についてはすでに報告してあるが，上述の考えに似た場合を実際問題に適用したものである．

4. Lg および Rg を説明する場合に，もし低速層が地殻のなかに存在するとき，たとえその層がそれほど厚くなくても，その層に準拠して，上述の考察は有力なものとなるであろう．

また一方，中間層がかなり厚く，しかも，その横波の速度が Lg の速度に近いような場合，Lg 相の観測が可能であることを，実例をもつて第10図に示した．群速度の極大，極小およびあまり変わらない点に着目すればよい．

さらに Lg が海の深さ 3.5 km よりも深いような，いわゆる海洋構造では伝わらなくて，2 km より浅くなつて大陸構造になるときに，伝播していくことを，Rayleigh 波の計算において第13図から第16図にわたつて説明した．周期の短かいところで極大，極小が現われるが，それが Rg に対応するものと考えられる．Love 波においては海水層のかわりに沈澱層を考えれば良いわけである．

BULLETIN OF THE EARTHQUAKE
RESEARCH INSTITUTE
Vol. 39 (1961), pp. 669-809

26. *Surface Waves and Layered Structures. Part 2. Theoretical dispersion curves for suboceanic surface waves.*

By

Rinzo YAMAGUCHI,
Earthquake Research Institute,

and

Takashi KIZAWA,
Meteorological Research Institute.

(Read Sept. 26, 1961—Received Sept. 30, 1961.)

1. Introduction

Effect of oceanic water on the Rayleigh waves propagated along the ocean bottom was first examined by Bromwich in the beginning of this century. But the problem regained importance since Stoneley disclosed the marked effect of the ocean on Rayleigh waves of comparatively short periods, with the result that many authors were stimulated to study the problem.[1)-10)] Among these studies, the works of Pekeris,

1) R. STONELEY, "The Effect of the Ocean on Rayleigh Waves," *Mon. Not. Roy. Astron. Soc., Geophys. Suppl.*, **1** (1926), 349.

2) C. L. PEKERIS, "Theory of Propagation of Explosive Sound in Shallow Water," *Geol. Soc. Amer., Memoir*, **27** (1948).

3) F. PRESS and M. EWING, "Low-speed Layer in Water-covered Areas," *Geophysics*, **13** (1948), 404.

4) F. PRESS, M. EWING and I. TOLSTOY, "The Airy Phase of Shallow-focus Submarine Earthquakes," *Bull. Seis. Soc. Amer.*, **40** (1950), 111.

5) F. PRESS and M. EWING, "Propagation of Explosive Sound in a Liquid Layer Overlying a Semi-infinite Elastic Solid," *Geophysics*, **15** (1950), 426.

6) M. EWING and F. PRESS, "Crustal Structure and Surface Wave Dispersion," *Bull. Seism. Soc. Amer.*, **40** (1950), 271.

7) W. S. JARDETZKY and F. PRESS, "Crustal Structure and Surface Wave Dispersion, Part III: Theoretical Dispersion Curves for Suboceanic Rayleigh Waves," *Bull. Seism. Soc. Amer.*, **43** (1953), 137.

8) I. TOLSTOY, "Dispersive Properties of a Fluid Layer Overlying a Semi-infinite Elastic Solid," *Bull. Seism. Soc. Amer.*, **44** (1954), 493.

9) C. L. PEKERIS and I. M. LONGMAN, "Ray Theory Solution of the Problem of Propagation of Explosive Sound in a Layered Liquid," *Jour. Acoust. Soc. Amer.*, **30** (1958), 323.

10) F. F. EVISON, C. E. INGHAM, R. H. ORR and J. H. Le FORT, "Thickness of the Earth's Crust in Antarctica and the Surrounding Oceans," *Geophys. Jour.*, **3** (1960), 289.

Ewing, Press and Tolstoy are representative. However, the complexity of calculation and paucity of observations have prevented progress in the study of crustal structures under the oceans. It is only a short time since a new impetus was given to these studies through the installations of long period seismographs at stations near the margin of oceans. It has recently been revealed that the dispersion curves of the surface waves propagated along the different paths are subjected to conspicuous variation. But the seismologists who discovered such marked features are confronting difficulty in obtaining theoretical dispersion curves complying with the observed ones.

In order to make a contribution, if possible, to such a study, we started to calculate theoretical dispersion curves corresponding to a wide variation of crustal structures, as we had an opportunity to use the electronic computer IBM 704 for a short period. Here a part of the result will be described.

2. Dispersion curves of Rayleigh waves across oceans.

In the present calculation a two-layered structure including the water layer is assumed, and some reference was made to the results of seismic prospecting carried out in some regions of the Pacific, Atlantic and Indian Oceans,[11)-15)] but to cover a possible wider variation of the crustal structure and topography along ridges, trenches etc., the parameters such as the velocities and the densities in the crust and subcrust, and the ratios of the thicknesses of the two layers are chosen from wide ranges, while the ocean depths of 1 km and 5 km were treated in each case. In most of the cases the Poisson's ratio, is taken as 1/4.

---

11) M. EWING, G. H. SUTTON and C. B. OFFICER, "Seismic Refraction Measurements in the Atlantic Oceans, Part VI: Typical Deep Stations, North America Basin," *Bull. Seism. Soc. Amer.*, **44** (1954), 21.

12) R. W. RAITT, "Seismic Refraction Studies of Bikini and Kawahalein Atolls," *Proc. Pap. U. S. Geol. Surv.*, **260** (1954), 507.

13) R. W. RAITT, "Seismic Refraction Studies of the Pacific Ocean Basin Part I: Crustal Thickness of the Central Equatorial Pacific," *Bull. Geol. Soc. Amer.*, **67** (1956), 1623.

14) M. N. Hill, "Recent Geophysical Exploration of the Ocean Floor," *Physics and Chemistry of the Earth*, Vol. **2** (1957), 129.

15) J. EWING and M. EWING, "Seismic-refraction Measurements in the Atlantic Ocean Basin, in the Mediterranean Sea, on the Mid-Atlantic Ridge, and in the Norwegian Sea," *Bull. Geol. Soc. Amer.*, **70** (1959), 291.

The cases treated are grouped and the results are graphically represented in Figs. 1 through 49, and the values of the parameters in the respective groups are tabulated in Table A. The calculated values for every case are shown in Tables 1 to 49. In every case, we have calculated both of the phase and group velocities, but in these figures only the group velocity curves are shown, for simplicity and on the consideration of practical utility. We have chosen a considerable range in each parameter in our calculation, but sometimes an appropriate dispersion curve is missed to keep in harmony with the observational result. In such a case interpolation or extrapolation will easily be made by means of our more or less systematic calculations.

It is also to be stated that we have limited our calculation to the dispersion curve of the fundamental mode, and in addition, branches in the long and short period ranges are not calculated in order to avoid too much complication in the use of the computer. But it is well-known that the dispersion curve in the long period branch approaches asymptotically the velocity of the wave in the semi-infinite substratum, so that our omission of this branch from the calculation is of no importance. In case there is no low velocity layer, a similar asymptotic approach to the lowest velocity in the surface layer is expected in the short period range. More over in the limiting case of the short period, the existence of a boundary wave usually called the Stoneley wave is to be expected. We have already reported the results of our study on the amplitude distribution of such a boundary wave on both sides of the boundary.[16] Stoneley waves propagated along the fluid/solid interface have also been studied by E. Strick et al.[17)-18)] Effects of the limited thicknesses of the layers to such a guided boundary wave is a problem to be studied in the future. Anyhow, the study of the oceanic Rayleigh wave in the period range from 1 to 12 seconds remains at present as an unsolved problem in theory and observation.

Even though our present results is not a complete solution of the problem, the aim of our present calculation is to offer the investigators an immediate clue as to the inference of the crustal structure of the first approximation. In order to discuss the problem thoroughly and

16) R. YAMAGUCHI and Y. SATÔ, "Stoneley Wave—Its Velocity, Orbit and the Distribution of Amplitude," *Bull. Earthq. Res. Inst.*, **33** (1955), 549.

17) E. STRICK and A. S. GINZBARG, "Stoneley Wave Velocities for a Fluid-Solid Interface," *Bull. Seis. Soc. Amer.*, **46** (1956), 281.

18) E. STRICK et al., "Propagation of Elastic Wave Motion from an Impulsive Source along a Fluid/Solid Interface," *Phil. Trans. Roy. Soc.*, [A], **251** (1959), 455.

explain the long period component of the surface wave so called the mantle wave, the more detailed structure of the deeper portion of the subcrust must be taken into consideration, while the short period components of the surface wave are subjected considerably to minor small scaled structures at the upper portion of the crust.

We therefore hope that our present results may be of use in the study of the crustal structure at present based on the current observations of the waves in a narrower range of period than ours which extend from ca. 10 sec. to 100 sec. We believe that the deviations in the observed data from our calculation will give definite clues as to the difference in the crustal structure from our assumption.

Now, in the following a brief explanation of our results will be made. In Figs. 1 through 6 are included the cases partly dealt with by other authors. Our intension of including them is in part to check our calculation to begin with. The cases of $H_1=H_2$ indicated with the others in Figs. 1 and 2 correspond to the cases III and I calculated by Jardetzky and Press. Fig. 3 shows extended cases of their case II with an additional sedimentary layer under the ocean. The difference between their result and the present one in Fig. 3 is found to be very small, so that it will not be possible to detect the difference in these structures from observations, unless they are provided with accuracies less than 0.1 km/sec. in their velocity. It will therefore be necessary to refine observations and find adequate means of correction to the effect of the gradual change in the oceanic depth along the path and to eliminate the effect of refraction at the continental border etc. in the discussion of such a delicate structure.

Figs. 4 and 5 include the cases studied by Mitra for the interpretation of microseisms.[19] From these figures we can clearly observe the difference in the effect on dispersion curves when the sedimentary layer of a lower velocity is replaced by basaltic layer of higher velocity. For the models in Fig. 6 the densities of the solid media are assumed to be nearly equal, while the elastic moduli are those used by Nagamune for the explanation of the waves across the North Pacific basin.[20]

When we approach from the ocean to the continent, we may expect the thickness of the crustal layer to increase gradually. In the regions

19) M. MITRA, "Rayleigh Waves in a Multi-layered Medium with Application to Microseisms," *Mon. Not. Roy. Astr. Soc., Geophys. Suppl.*, **7** (1957), 324.

20) T. NAGAMUNE, "On the Travel Time and the Dispersion of Surface Waves (III): Dispersion of Surface Waves and Structure of North and Central Pacific Basin," *Geophys. Mag.*, **28** (1957), 1.

of not only continental margin, but also near suboceanic ridges and trenches, the intermediate layer may be subjected to some variation while the substratum (or the mantle) undergoes little variation. Therefore, the wide range of variation in the parameters concerning this intermediate layer was chosen for our calculation. Considering the convenience of actual use in comparison with the observations, the cases treated are grouped according to the velocity of the shear wave in the mantle, and are shown in the respective figures.

The cases of ultramafic rock having a compressional wave velocity of 7.95 km/sec in the substratum are shown in Figs. 7 through 12. The observed variation of dispersion curves in different oceanic paths seems to be well explained by these curves, as was actually the case in the sub-oceanic Rayleigh waves along the different paths across the Pacific and in the SE Asian seas.[21] We can see from Fig. 8 that a maximum and a minimum of group velocity appear in the range of the shorter period when the thickness of the intermediate layer is considerably larger than that of the water layer. Such a conspicuous feature is to be certainly correlated to the intermediate layer as is also inferred from the nearness of the velocities.

Figs. 9 through 12 indicate the cases when the solid layer has the characteristics of volcanic or consolidated sediments in which the velocity of the compressional wave takes a value in the range from 3 to 5 km/sec.

The cases in which the velocity of the compressional wave in the substratum, composed of ultra-basic rock is equal to 8.3 km/sec are shown in Figs. 13 through 18. Among these, the first three figures indicate the cases where the velocity Vp_2 of the P-wave in the intermediate layer is equal to 7 km/sec, while the rest indicates the case of $Vp_2=5$ km/sec. As is shown in these figures, the ratios of the densities in the intermediate layer and the subcrust are not the same in all cases. But no remarkable difference can be seen in the variation of the density contrast as above mentioned.

Very precise observation will be required to discriminate the difference in density distribution if desired. The density contrast of the crust to the mantle in the case of Fig. 17 is taken to be larger than that in Fig. 16 and the comparison of the two figures reveals to us

21) T. A. SANTÔ, "Rayleigh Wave Dispersions across the Oceanic Basin around Japan (Part III)—On the Crust of the South-Western Pacific Ocean—," *Bull. Earthq. Res. Inst.*, **39** (1961), 1.

that the increase in the dencity of the intermediate layer is accompanied by a decrease in the group velocity for the wave of long period, although the difference is very slight.

The effect of the density contrast between the water and the solid layers seems, on the contrary, to be seen in the short period range of the Lr wave.

The influence of the variation of the oceanic depth on the group velocity when the crust remains the same will be seen from a comparison of the two curves in Figs. 16 and 18 for (H_1=1.0 km, H_2=25 km) and (H_1=5 km, H_2=25 km). We see in the range of period below 20 sec a remarkable influence from variation in the oceanic depth.

Figs. 19 through 28 illustrate the cases when the velocity Vp_3 of of the compressional wave in the mantle equals 8.1 km/sec. Figs. 29 through 43 and Figs. 44 through 49 represent the cases of Vp_3=7.8 km/sec and 7.5 km/sec respectively.

A brief description of marked features revealed from our calculations will be added here. We have already seen in each figure the effect of the variation of the thickness of the water layer (H_1) or the intermediate layer (H_2) while the other parameters remain constant. It was revealed therefrom that the variation of H_2 has great influence on the dispersion curve. In order to see the influences of the other parameters, we picked out cases for the different values of the parameter while the other parameters remain constant, and showed them side by side in Figs. 50 through 53. In Fig. 50 the effect of H_1 is illustrated. The most interesting feature is the shifting of the dispersion curve to the right (longer period side). As was mentioned in section 4 of Part 1, the second remarkable feature is the appearance of the maximum and minimum group velocities in a short period range when the H_1 become small.

Fig. 51 shows the effect of the variation of the velocity in the mantle. As is already known the most remarkable effect of the velocity in the subcrust is in the asymptotic value of the group velocity (and of course also the phase velocity) which tends to wards the velocity of the wave when the surface layers are removed. But it is rather astonishing that the effect of the variation of the velocity in the mantle is almost invisible in the period range below ca. 15 sec. in the models concerned.

The next Fig. 52 shows the effect of the variation of velocity in the intermediate layer. It is clearly seen that effect is most marked

in the intermediate range of period from 15 to 50 sec. Fig. 53 indicates the effect of the variation of densities in the crust and mantle. As already stated, the conspicuous slightness of the influences of the density variations in both the crust and subcrust is to be specially noted.

3. Guidance in fitting experimental data to theoretical curves.

A consideration of convenience of actual use in comparison with the observations, is outlined in the five figures of Fig. 54 through Fig. 58.

They are grouped according to the thickness of the water layer (H_1) and the value of the group velocity at the period of 30 sec., since there is some relation between those two. That classification is serviceable in finding the most desirable model.

In the figures, the model shown by V60795 R2830 H15 means $Vp_2=6.0$ km/sec, $Vp_3=7.95$ km/sec, $\rho_2=2.8$ g/cm^3, $\rho_3=3.0$ g/cm^3 and $H_2=15$ km, and so on.

From these figures we can see that there are no methods for unique solution of the crustal structure from the utility of the observations of dispersion curves. However, it is important to enable us to get a clue to the problem.

4. Suboceanic Love Waves

Theoretically speaking, a water layer overlying a crust has no effect on the Love wave provided the water is perfect fluid and has no viscosity. But in view of the utility in the practical problem the dispersion curves of Love waves for most of the above cases are calculated and shown graphically in Figs. 1L through 48L. We hope, although the calculation itself involves no particularity, but the results are not barren in the elucidation of some new features in the actual observations.

Acknowledgements

The writers' sincere gratitude is expressed to Prof. H. Kawasumi for his kind guidance.

Their thanks are also due to Dr. H. Itô, chief of the Electronic Computation Center at the Japan Meteorological Agency, by whose courtesy the opportunity of using the IBM 704 electronic computer was given, and also to the other members of the office staff.

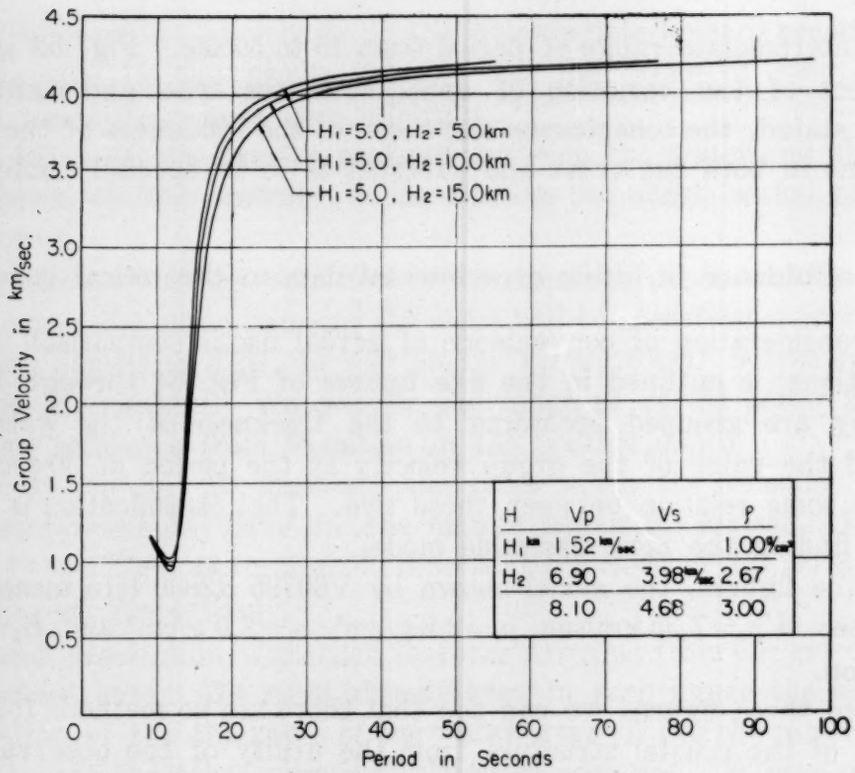

Fig. 1. Group velocity dispersion curves of Rayleigh waves.

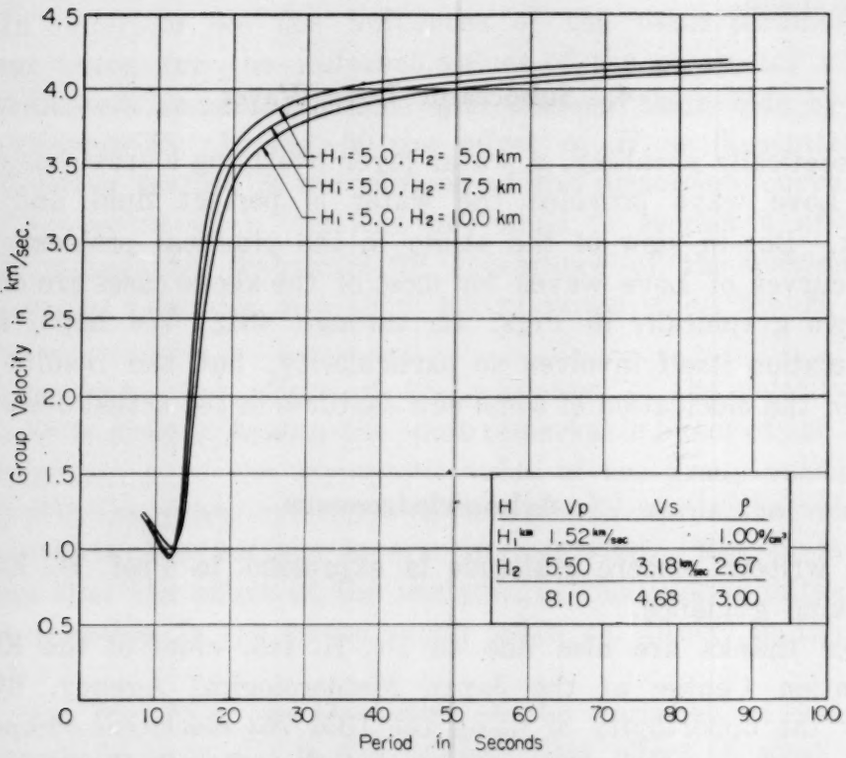

Fig. 2. Group velocity dispersion curves of Rayleigh waves.

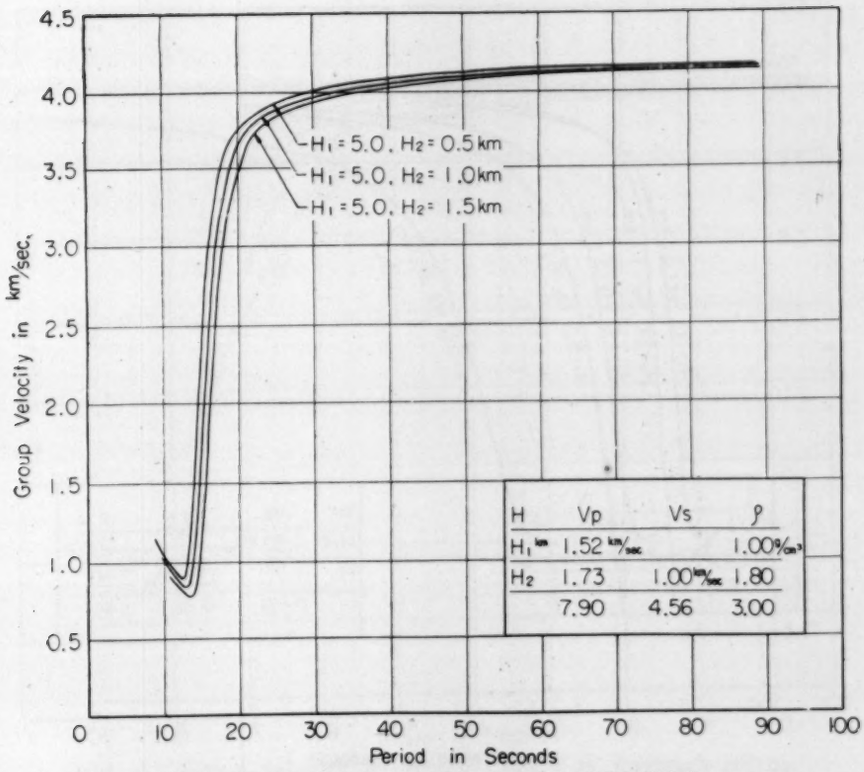

Fig. 3. Group velocity dispersion curves of Rayleigh waves.

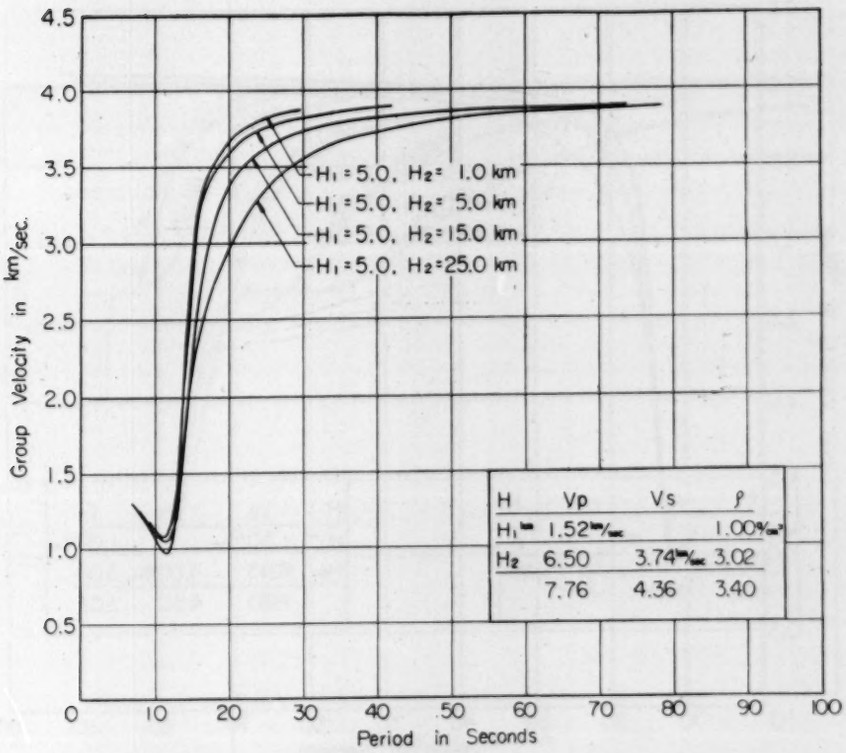

Fig. 4. Group velocity dispersion curves of Rayleigh waves.

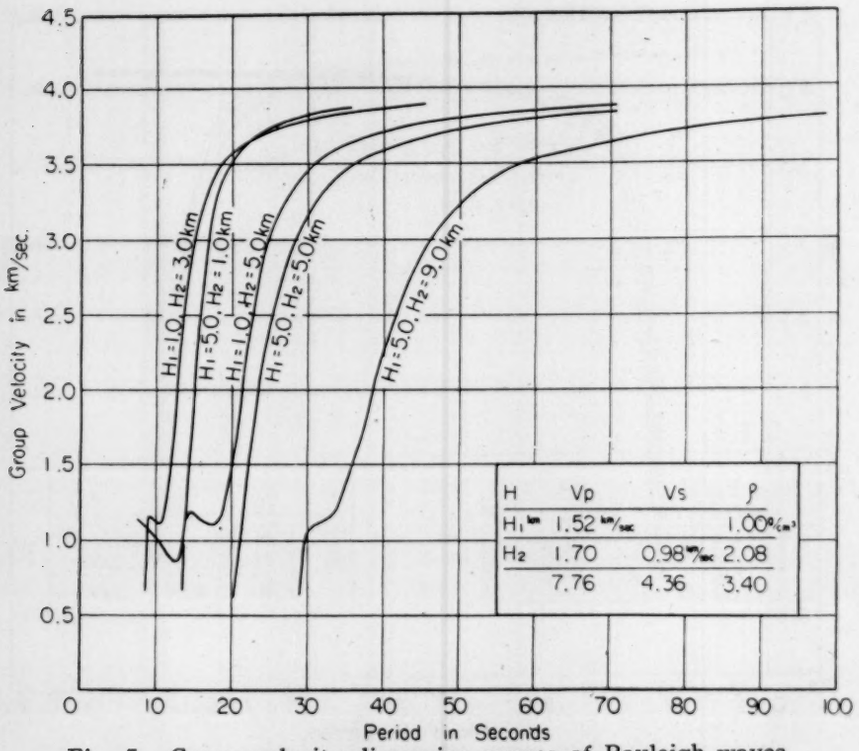

Fig. 5. Group velocity dispersion curves of Rayleigh waves.

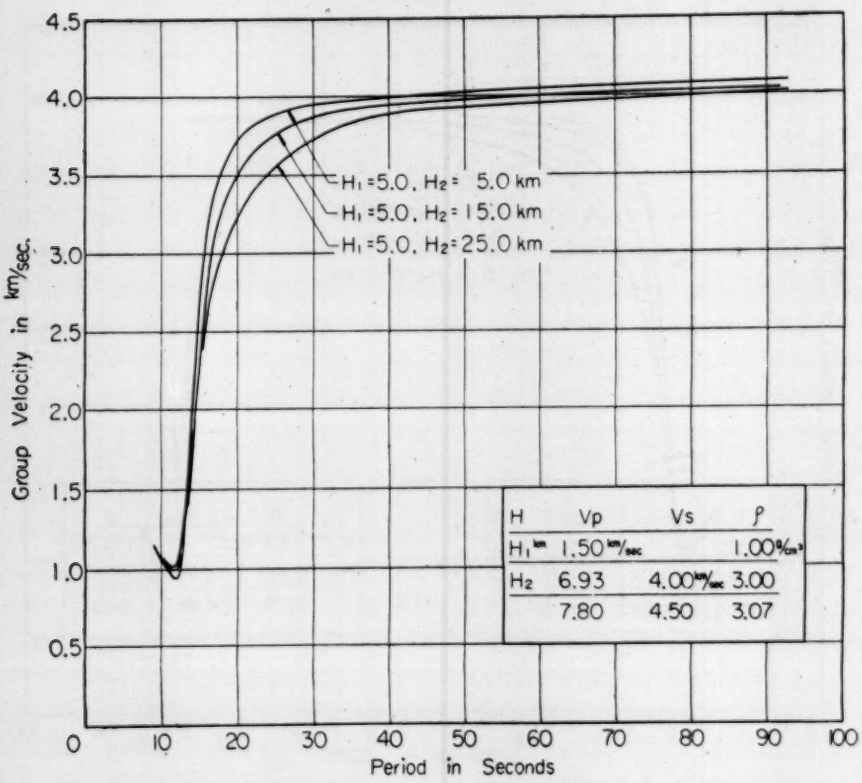

Fig. 6. Group velocity dispersion curves of Rayleigh waves.

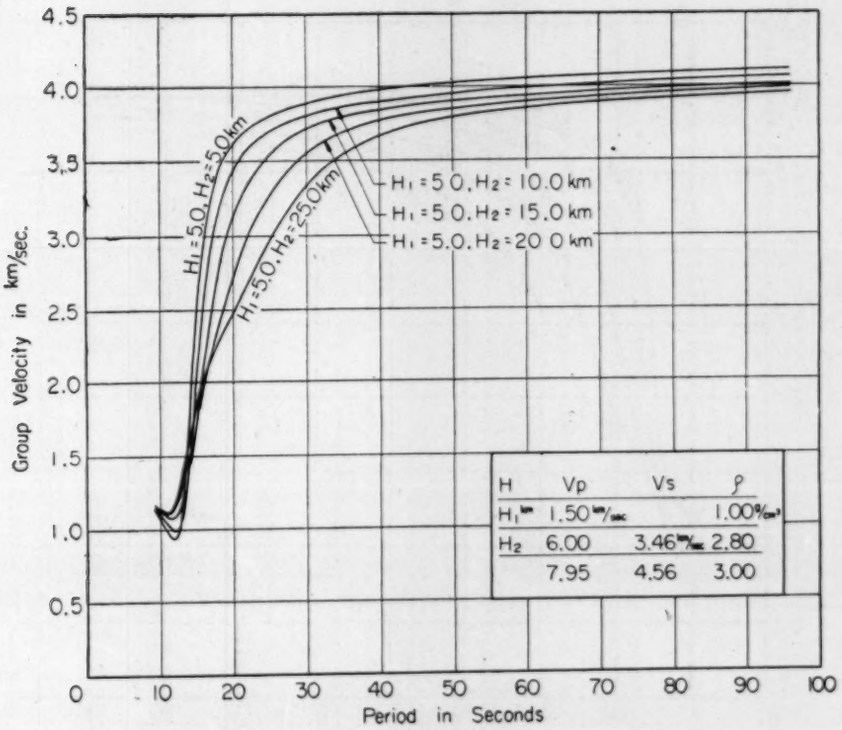

Fig. 7. Group velocity dispersion curves of Rayleigh waves.

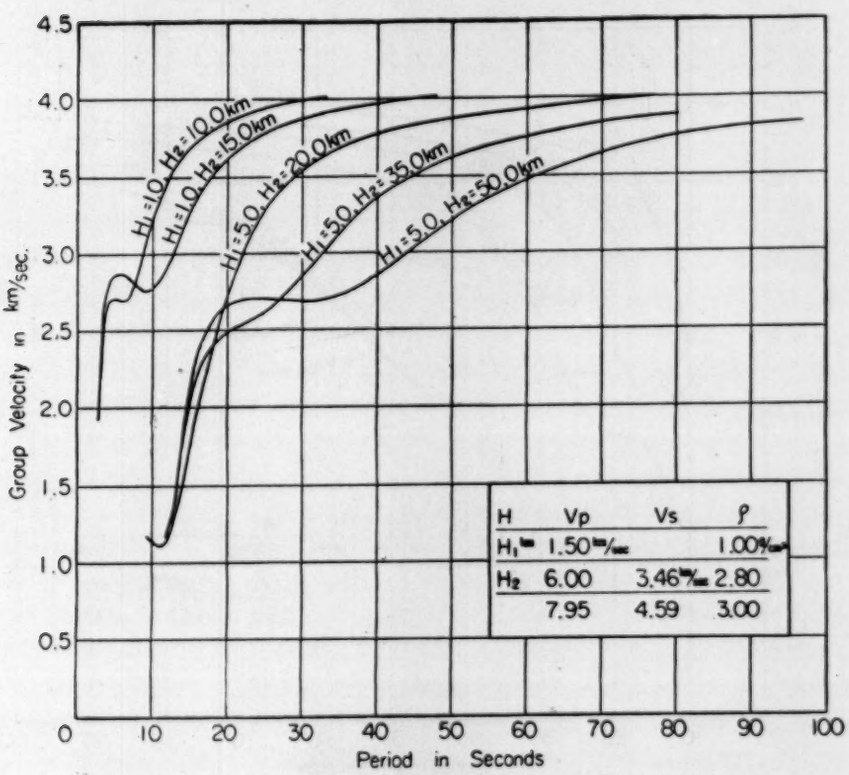

Fig. 8. Group velocity dispersion curves of Rayleigh waves.

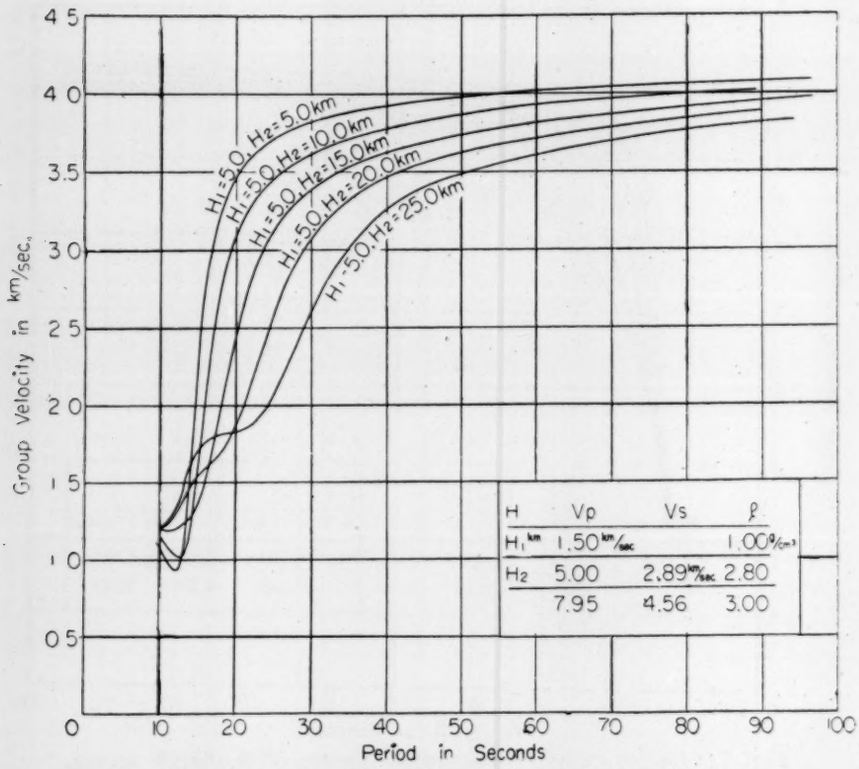

Fig. 9. Group velocity dispersion curves of Rayleigh waves.

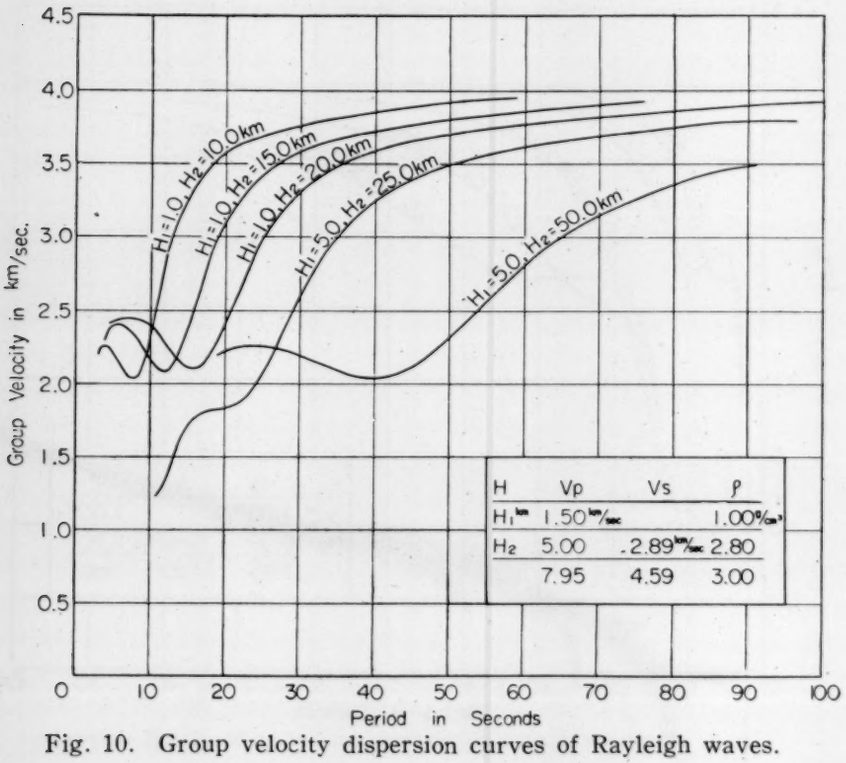

Fig. 10. Group velocity dispersion curves of Rayleigh waves.

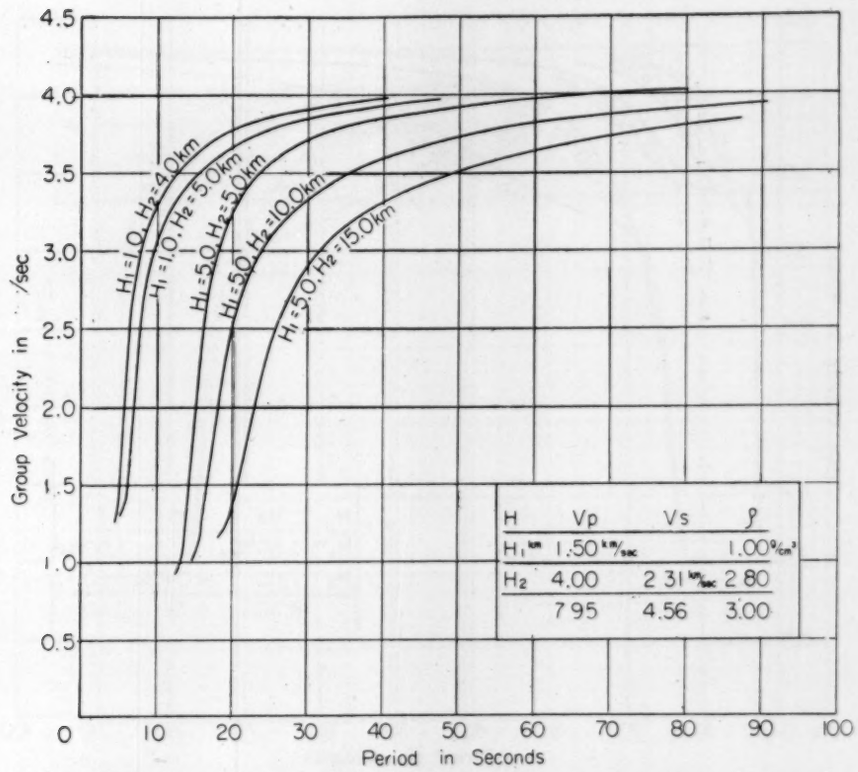

Fig. 11. Group velocity dispersion curves of Rayleigh waves.

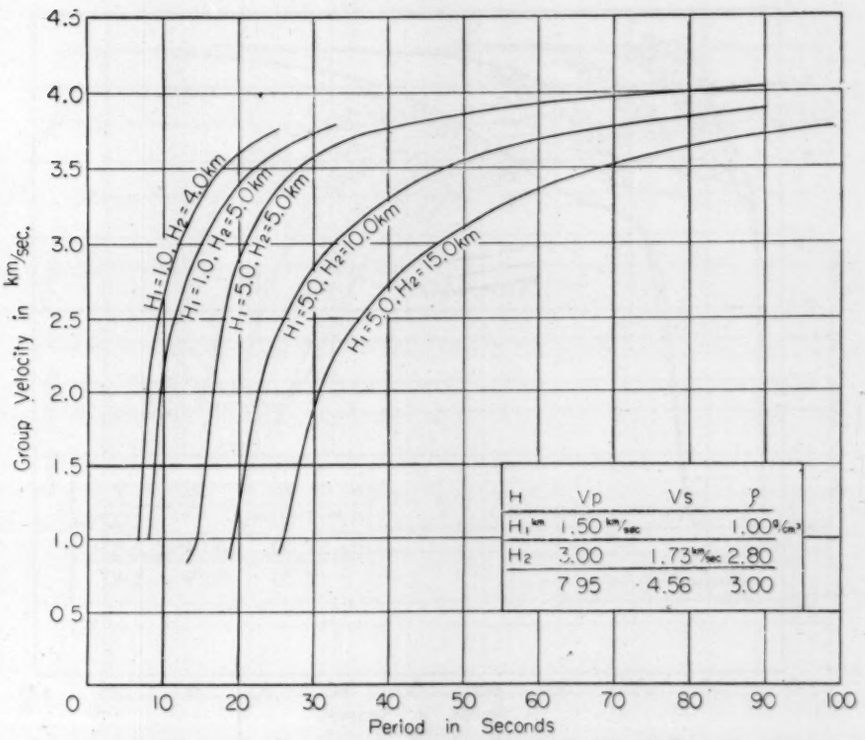

Fig. 12. Group velocity dispersion curves of Rayleigh waves.

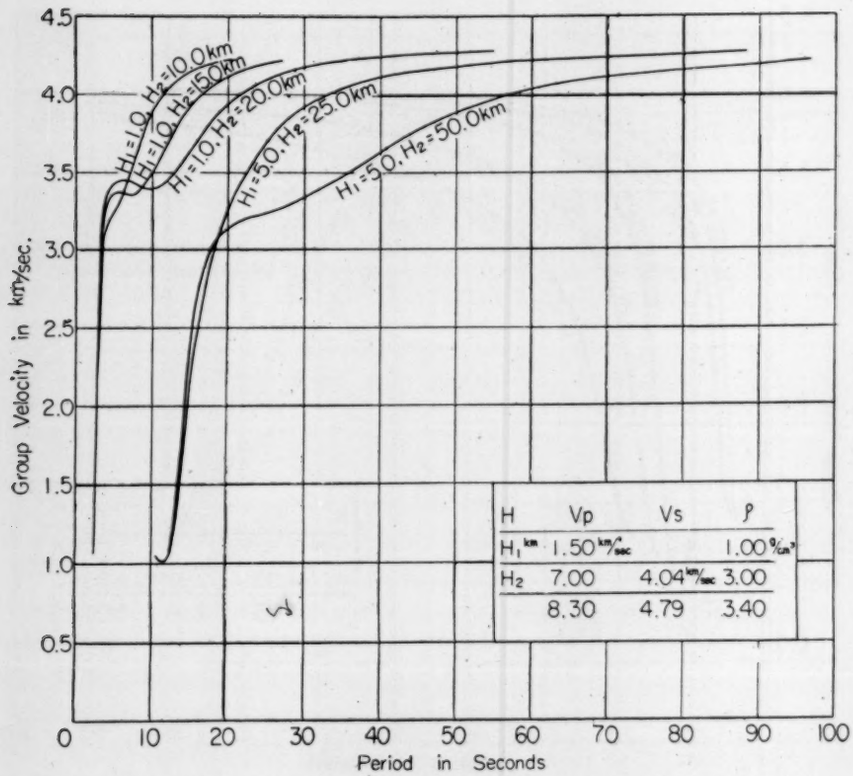

Fig. 13. Group velocity dispersion curves of Rayleigh waves.

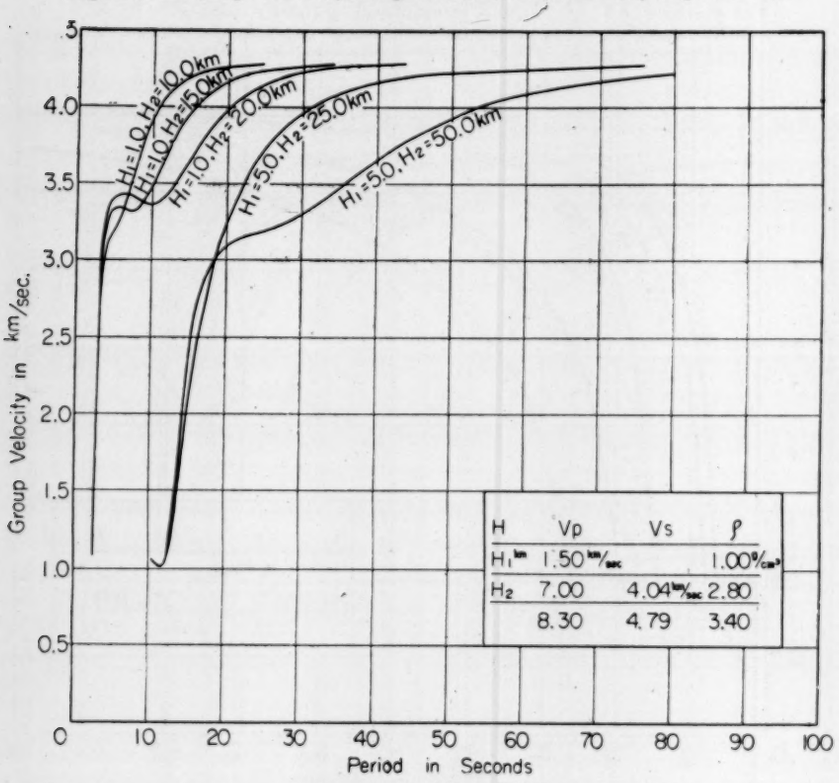

Fig. 14. Group velocity dispersion curves of Rayleigh waves.

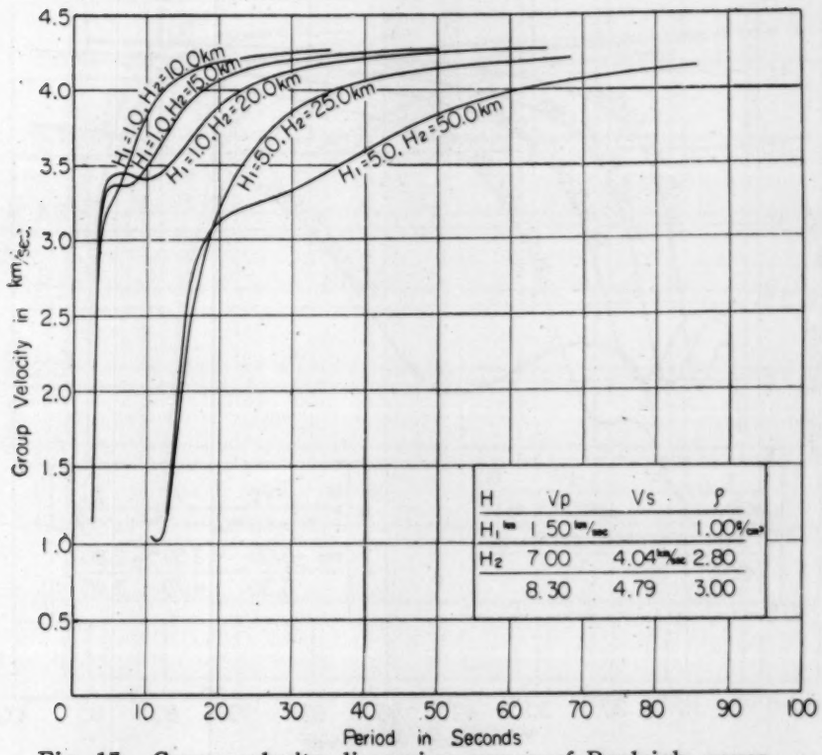

Fig. 15. Group velocity dispersion curves of Rayleigh waves.

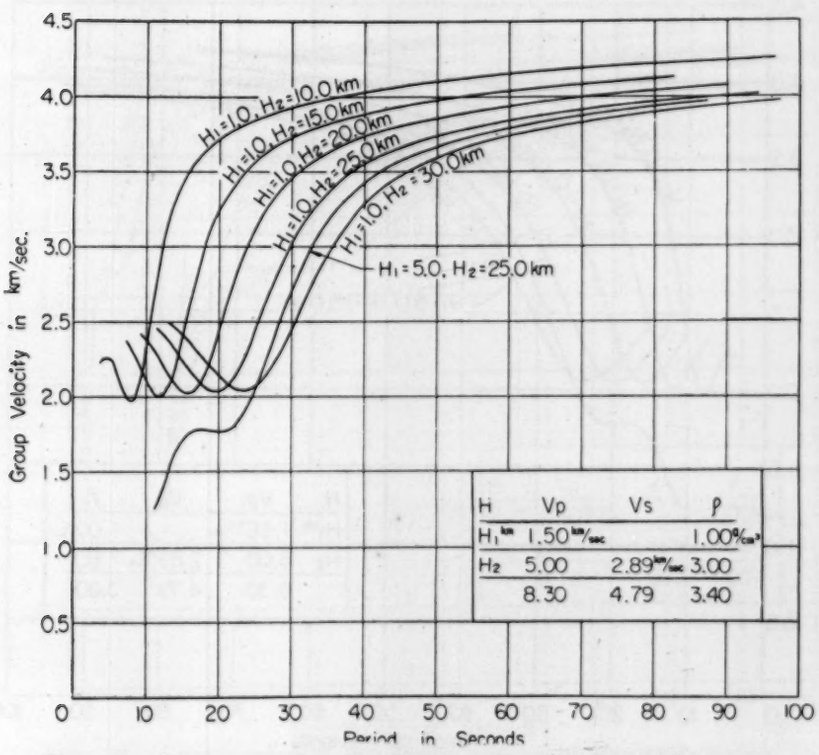

Fig. 16. Group velocity dispersion curves of Rayleigh waves

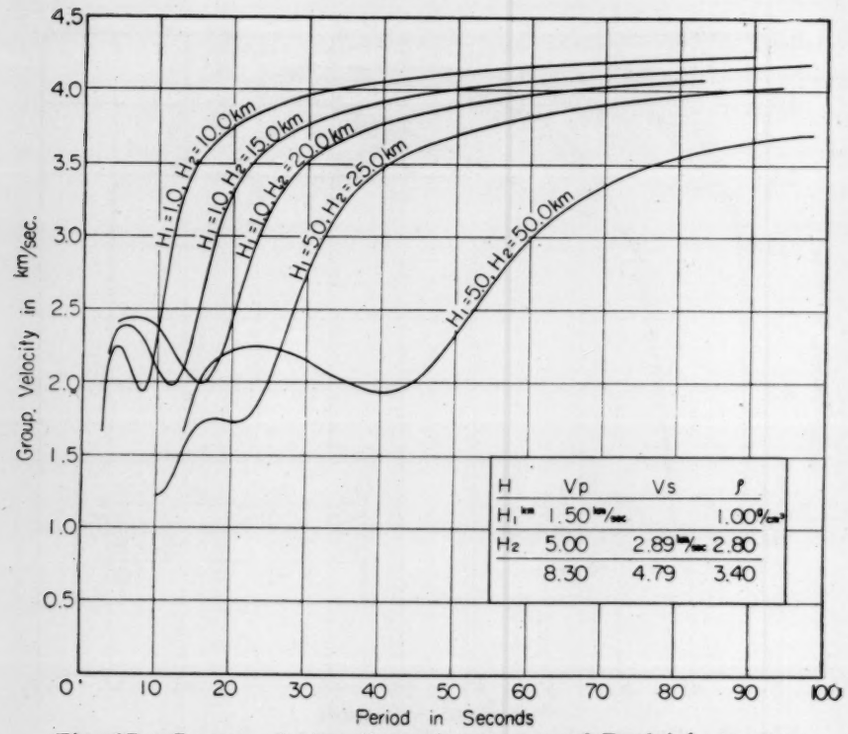

Fig. 17. Group velocity dispersion curves of Rayleigh waves.

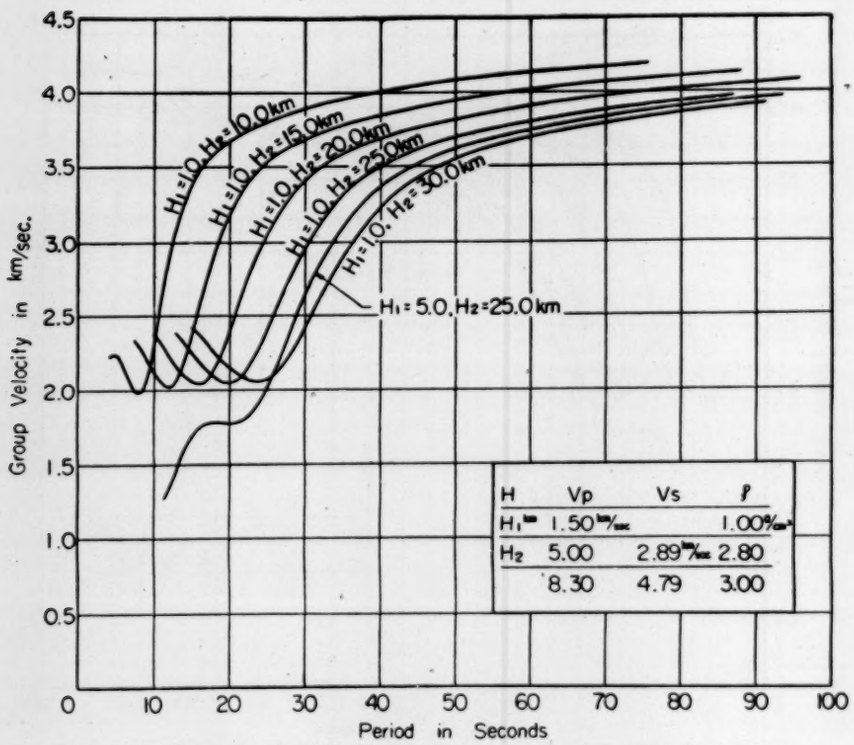

Fig. 18. Group velocity dispersion curves of Rayleigh waves.

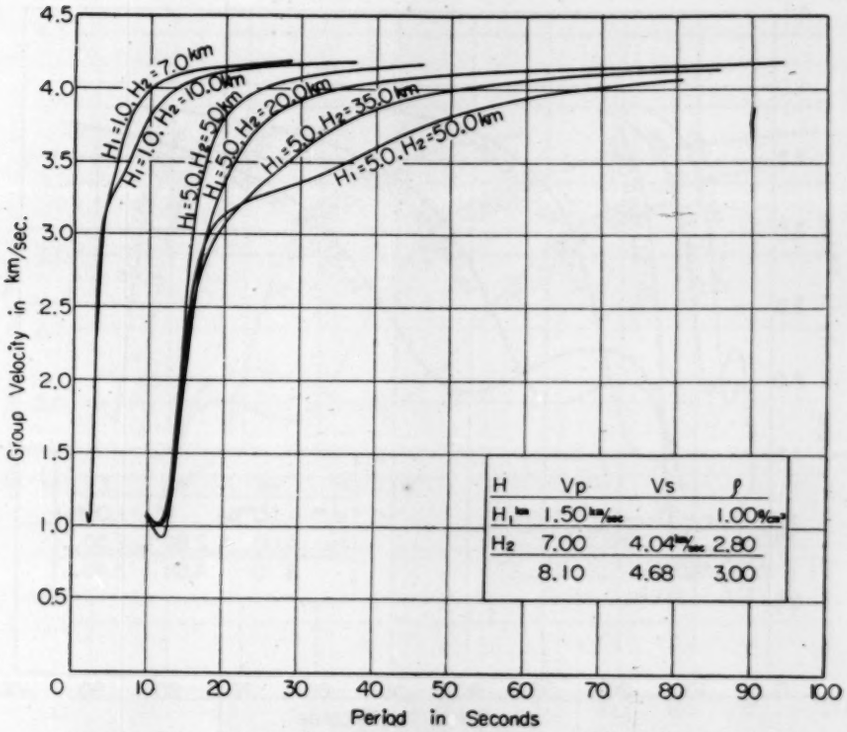

Fig. 19. Group velocity dispersion curves of Rayleigh waves.

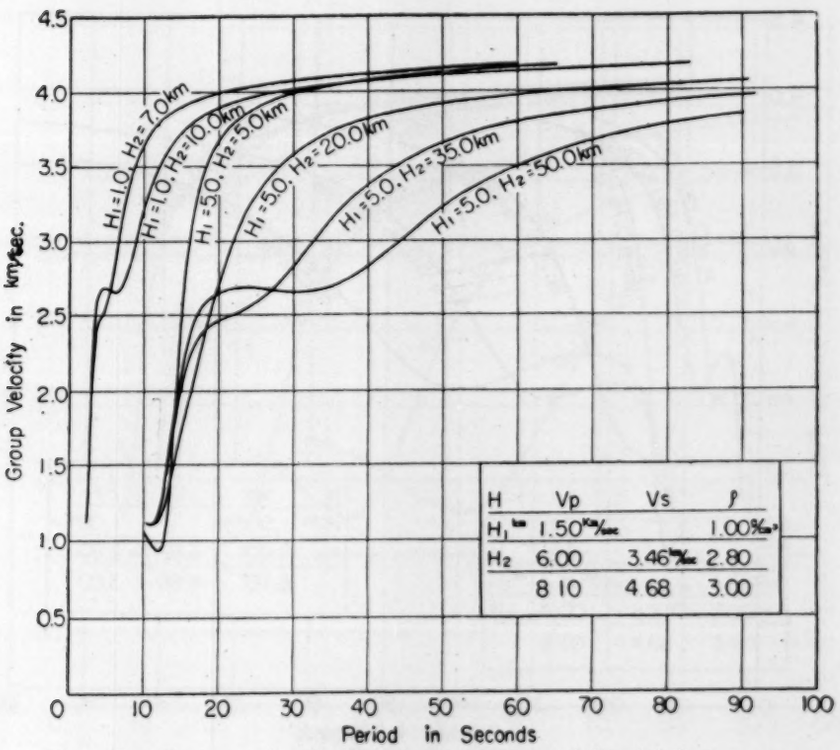

Fig. 20. Group velocity dispersion curves of Rayleigh waves.

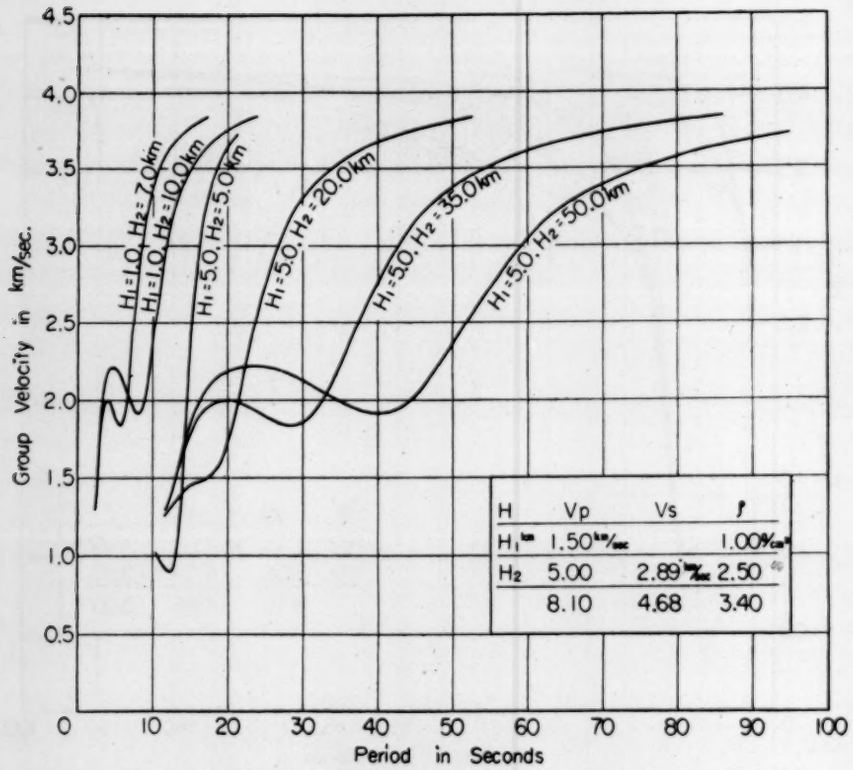

Fig. 21. Group velocity dispersion curves of Rayleigh waves.

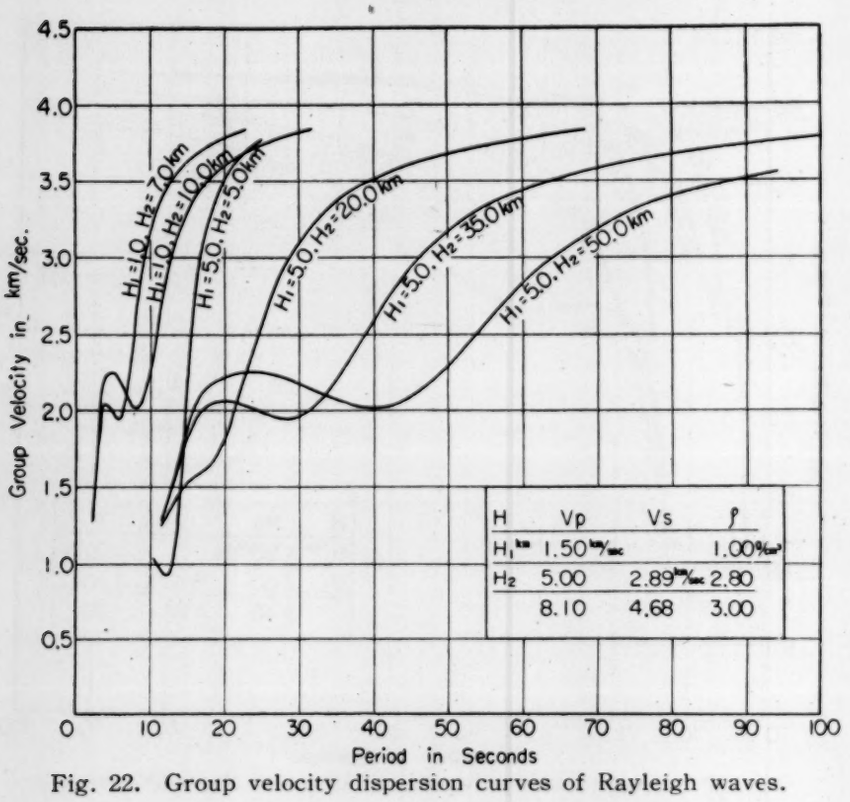

Fig. 22. Group velocity dispersion curves of Rayleigh waves.

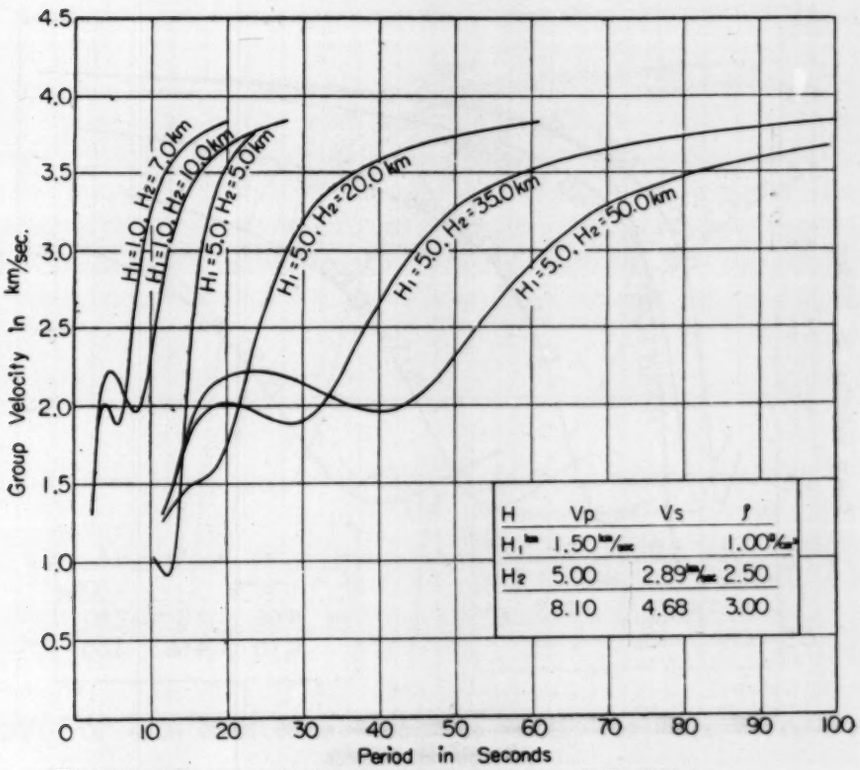

Fig. 23. Group velocity dispersion curves of Rayleigh waves.

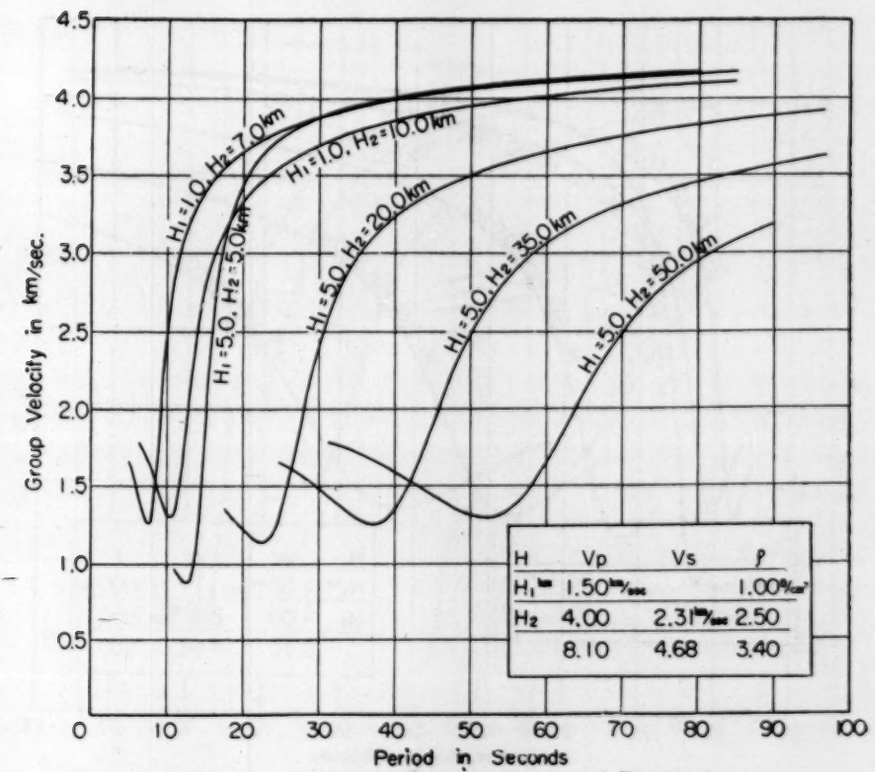

Fig. 24. Group velocity dispersion curves of Rayleigh waves.

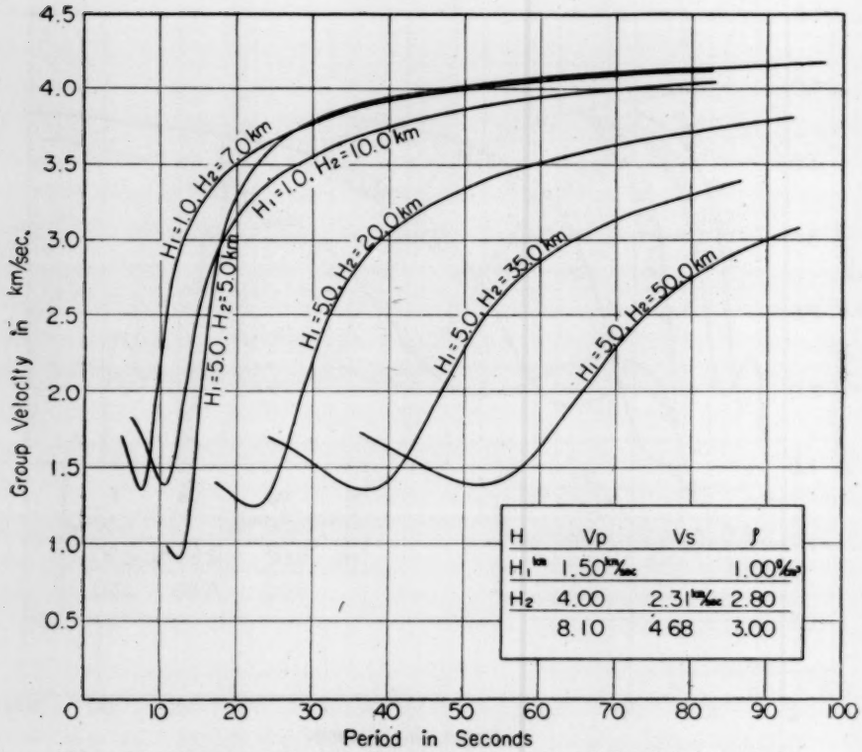

Fig. 25. Group velocity dispersion curves of Rayleigh waves.

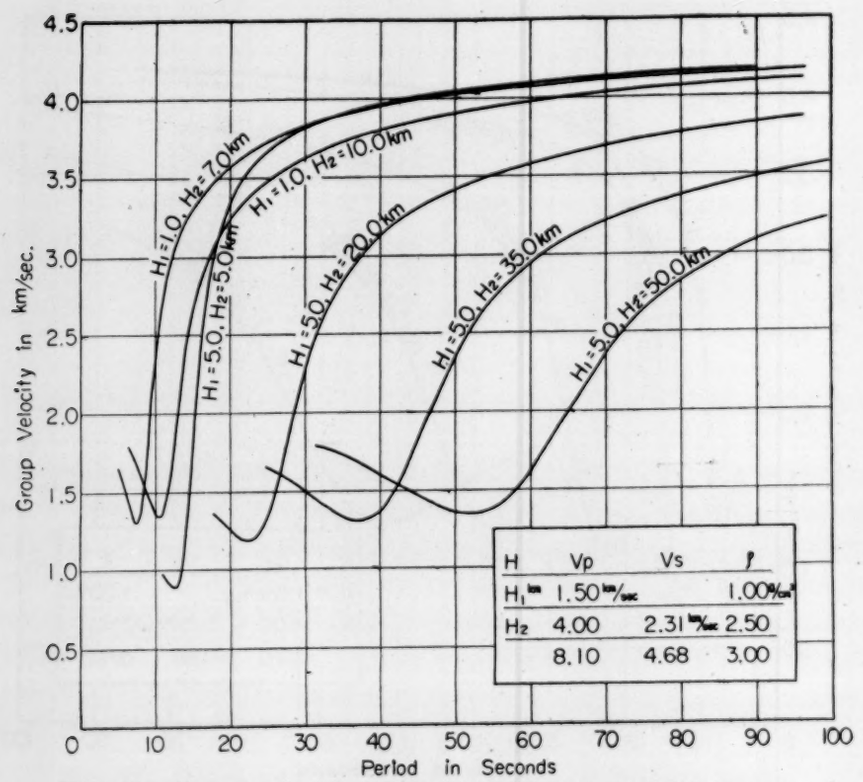

Fig. 26. Group velocity dispersion curves of Rayleigh waves.

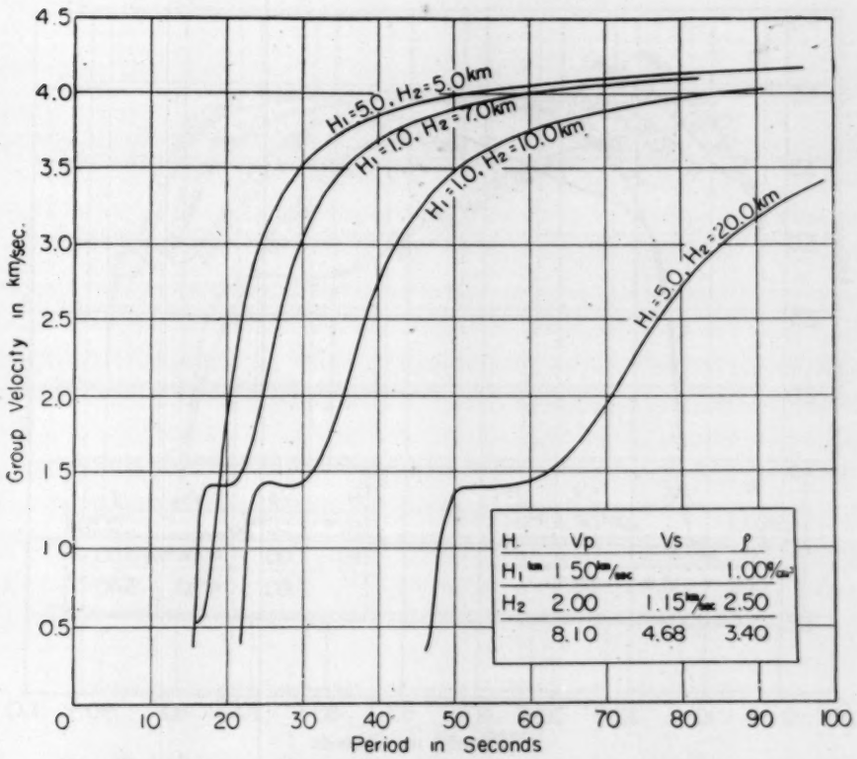

Fig. 27. Group velocity dispersion curves of Rayleigh waves.

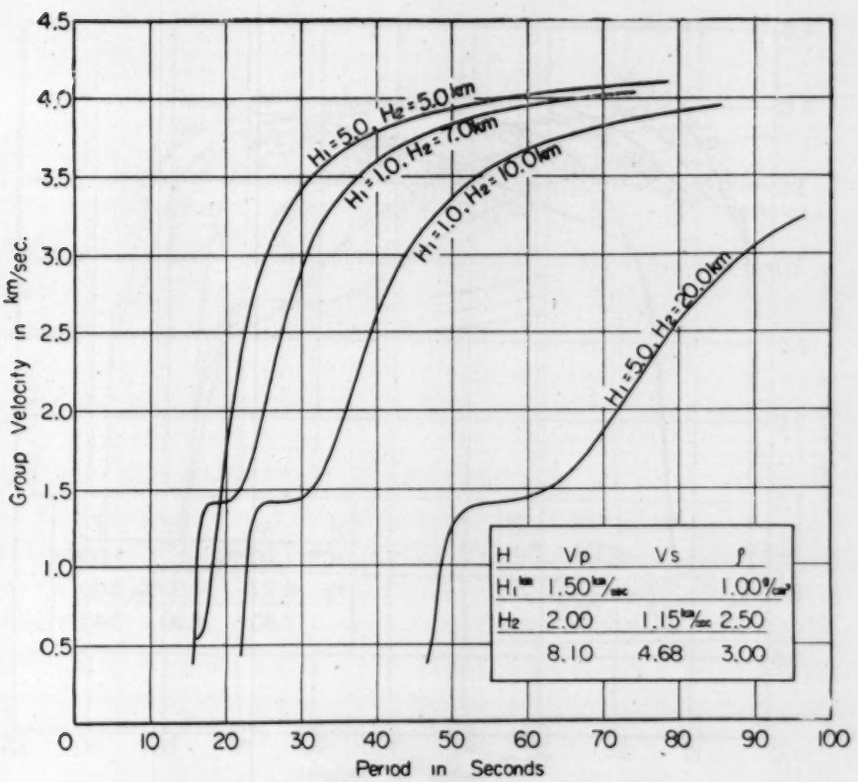

Fig. 28. Group velocity dispersion curves of Rayleigh waves.

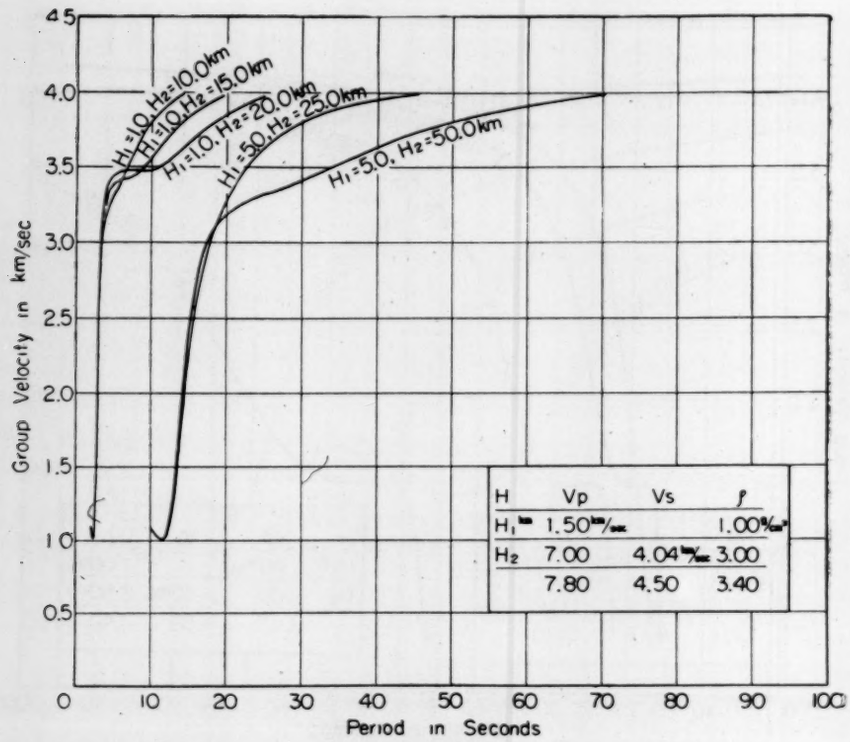

Fig. 29. Group velocity dispersion curves of Rayleigh waves.

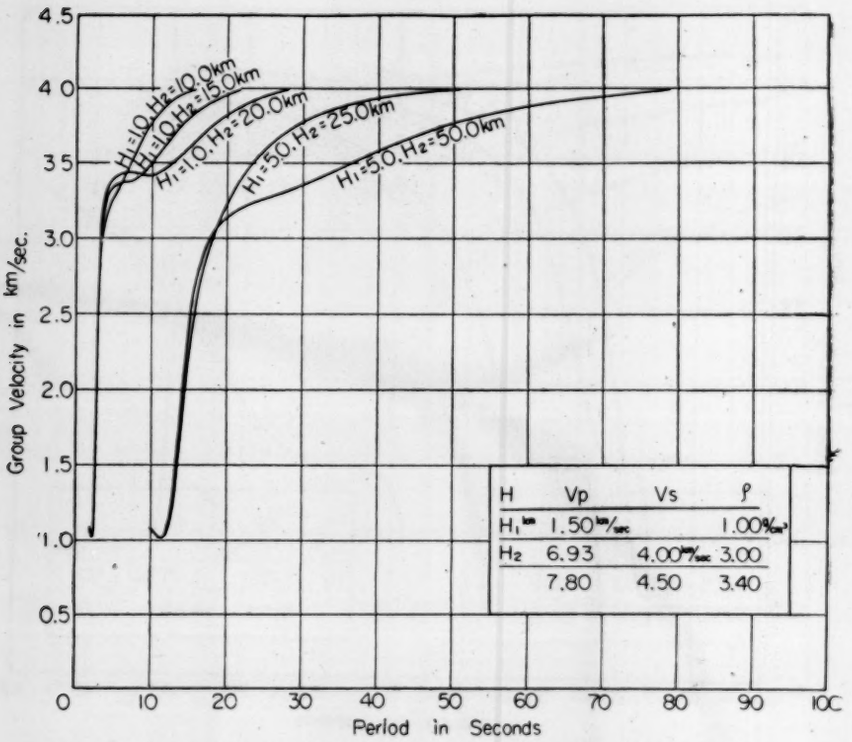

Fig. 30. Group velocity dispersion curves of Rayleigh waves.

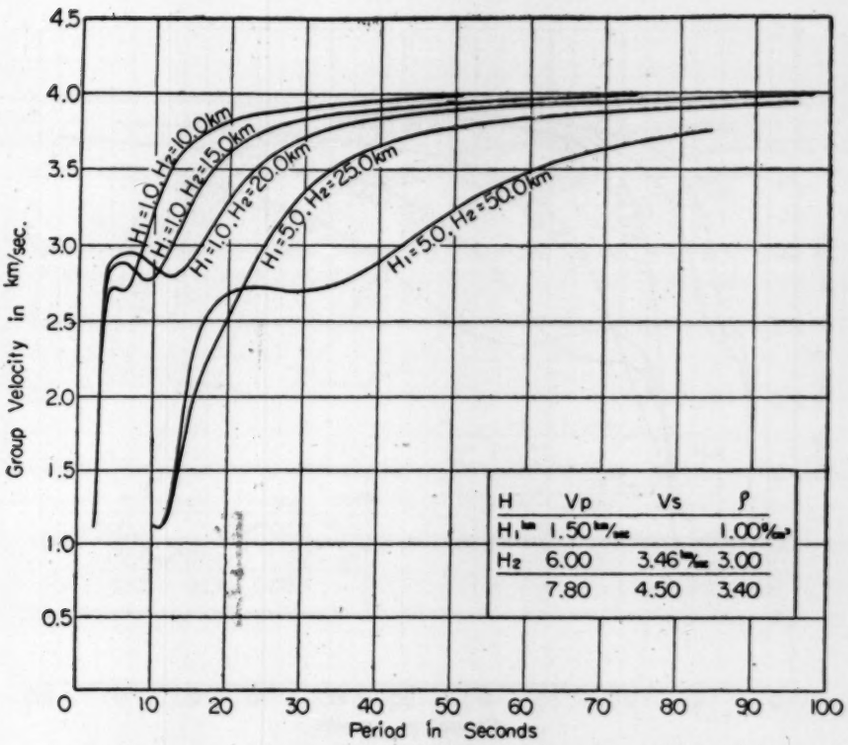

Fig. 31. Group velocity dispersion curves of Rayleigh waves.

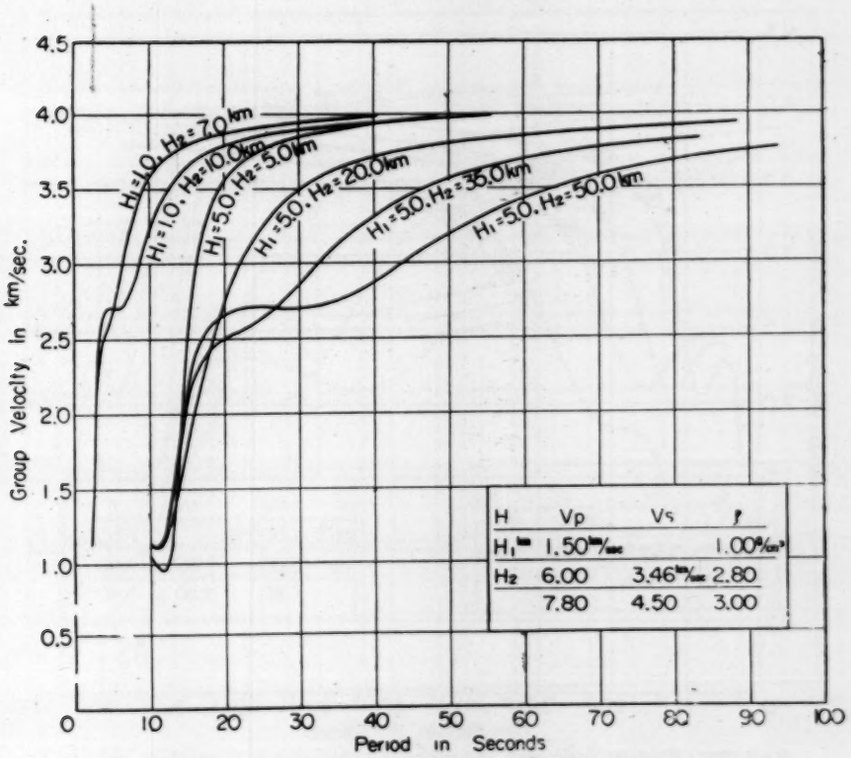

Fig. 32. Group velocity dispersion curves of Rayleigh waves.

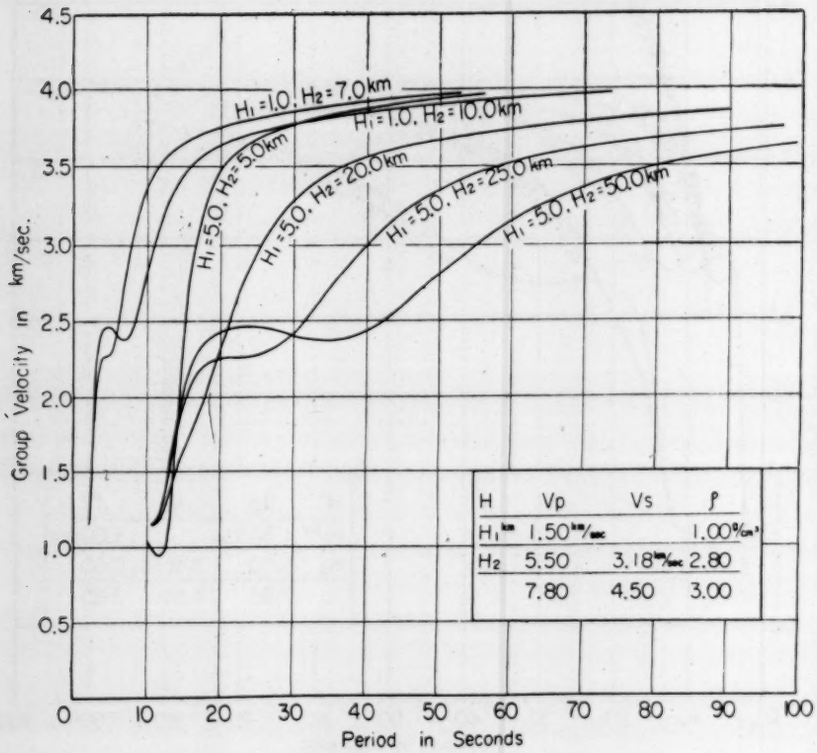

Fig. 33. Group velocity dispersion curves of Rayleigh waves.

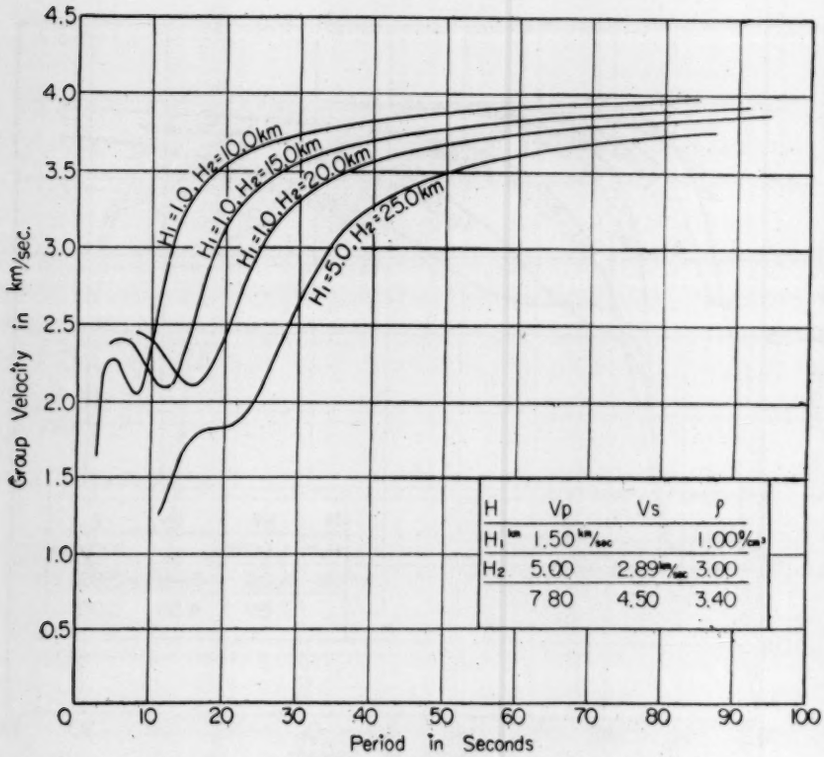

Fig. 34. Group velocity dispersion curves of Rayleigh waves.

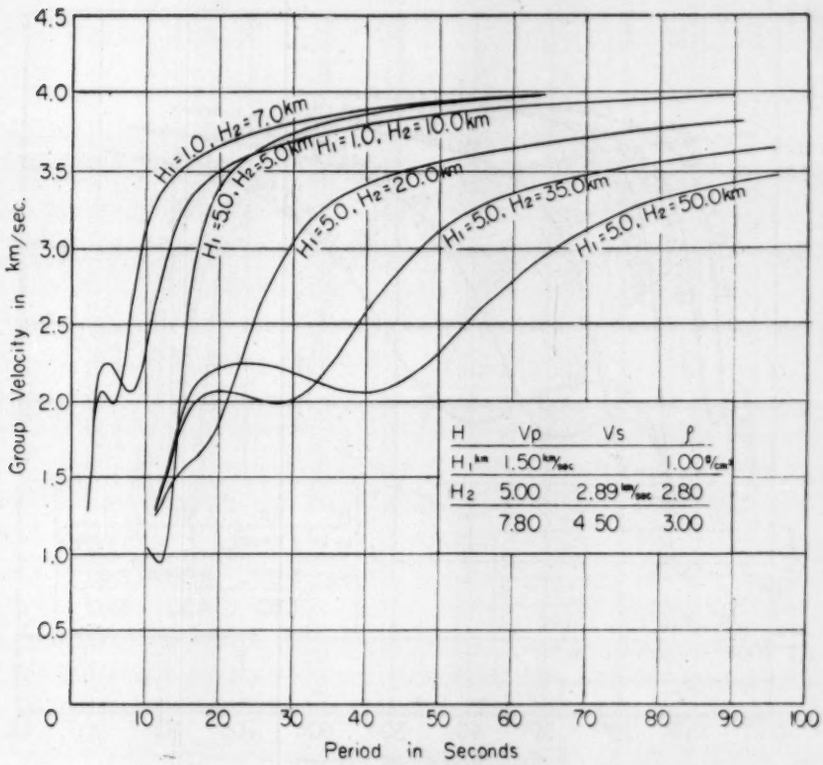

Fig. 35. Group velocity dispersion curves of Rayleigh waves.

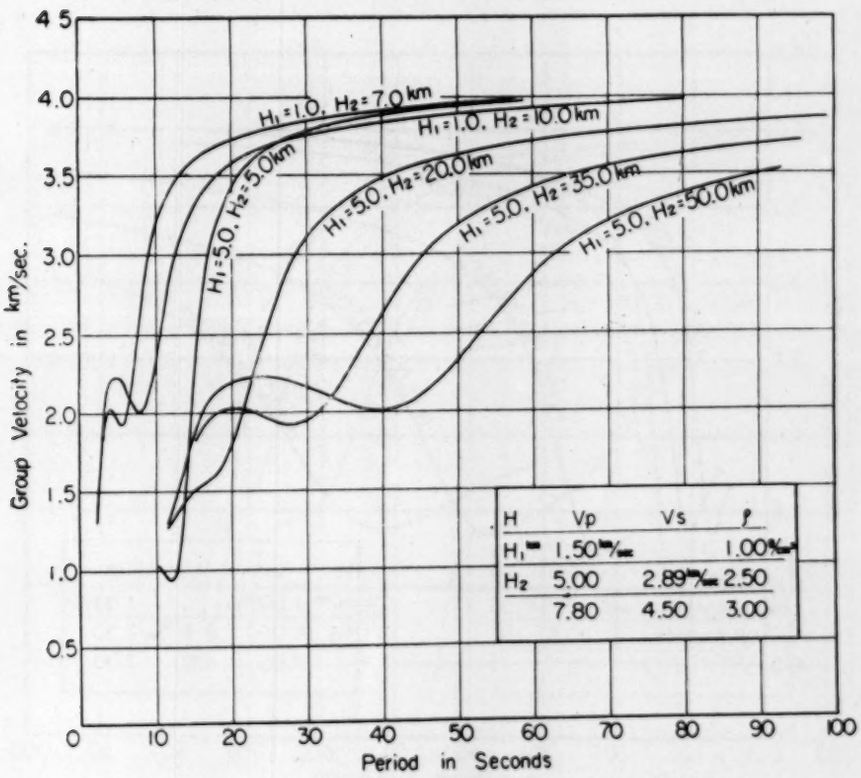

Fig. 36. Group velocity dispersion curves of Rayleigh waves.

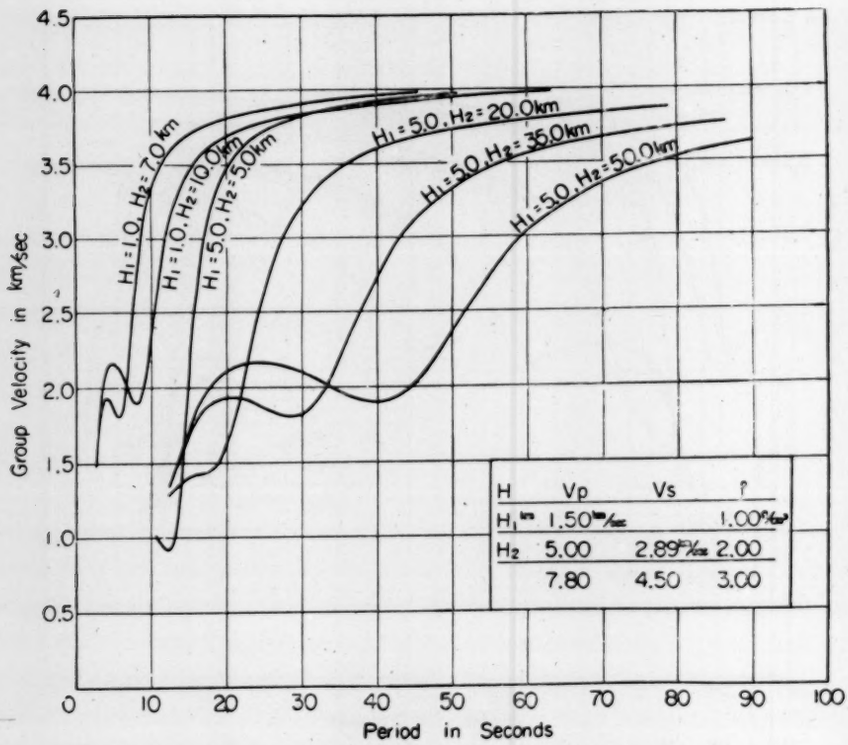

Fig. 37. Group velocity dispersion curves of Rayleigh waves.

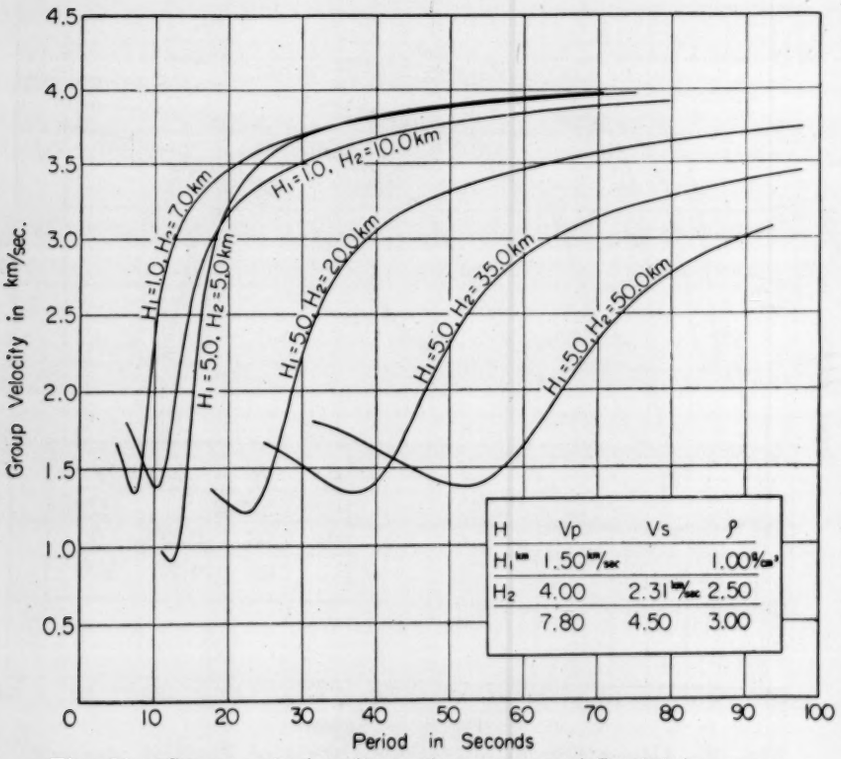

Fig. 38. Group velocity dispersion curves of Rayleigh waves.

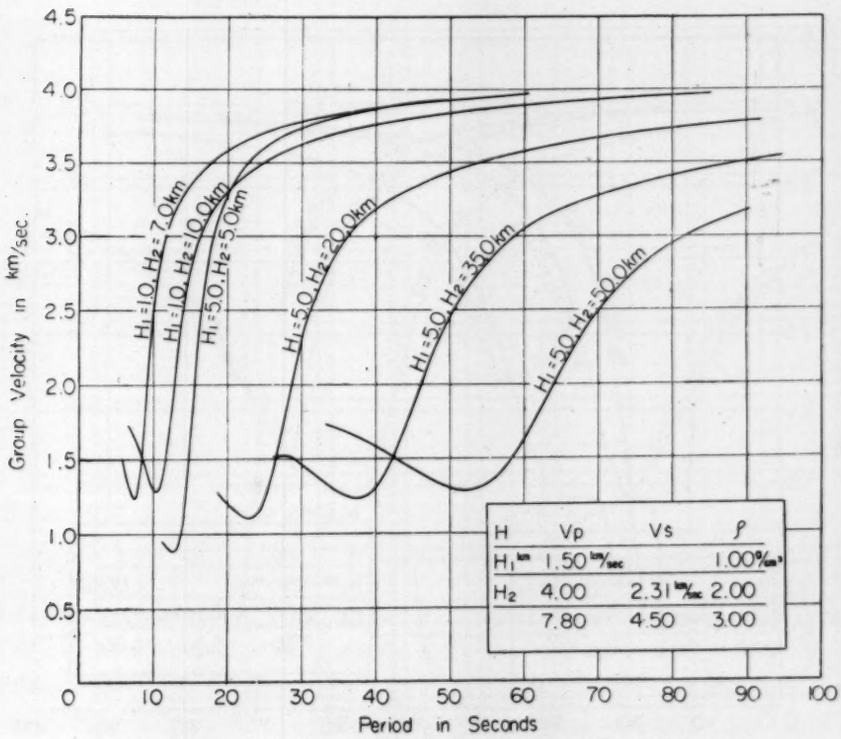

Fig. 39. Group velocity dispersion curves of Rayleigh waves.

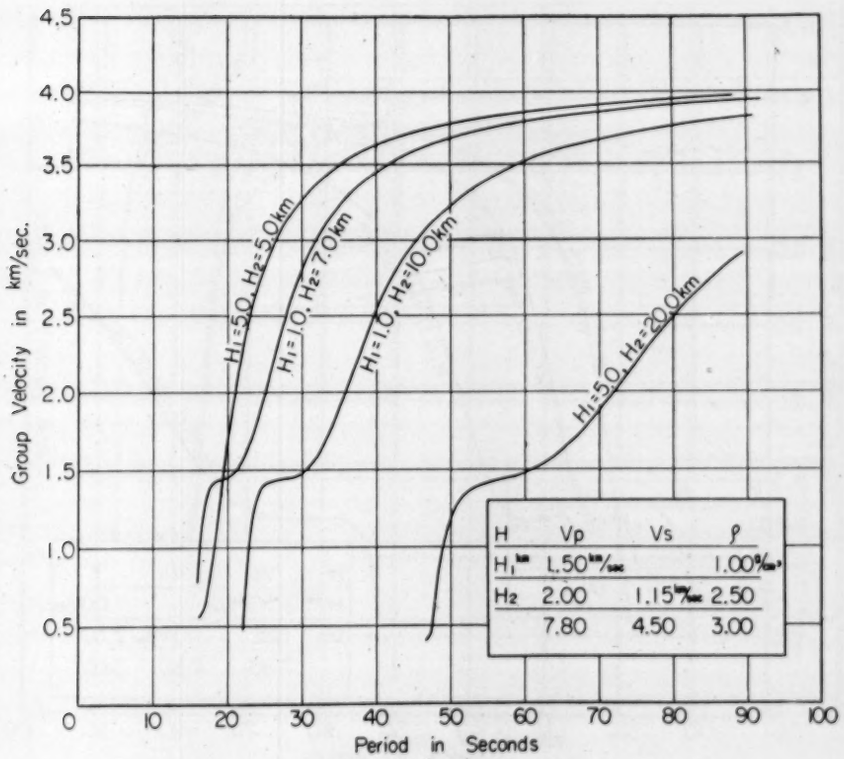

Fig. 40. Group velocity dispersion curves of Rayleigh waves.

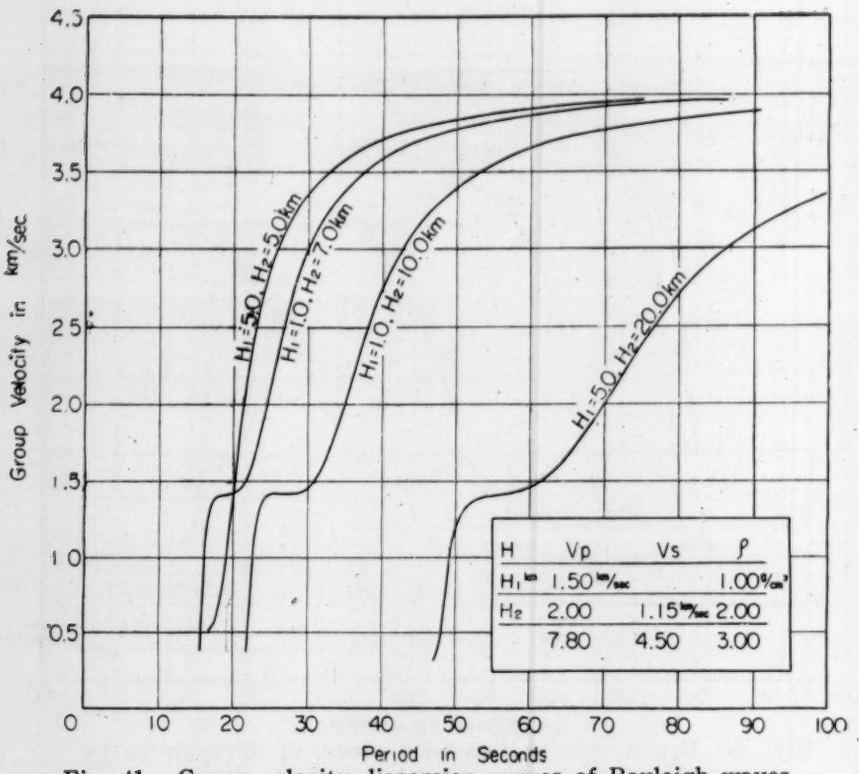

Fig. 41. Group velocity dispersion curves of Rayleigh waves.

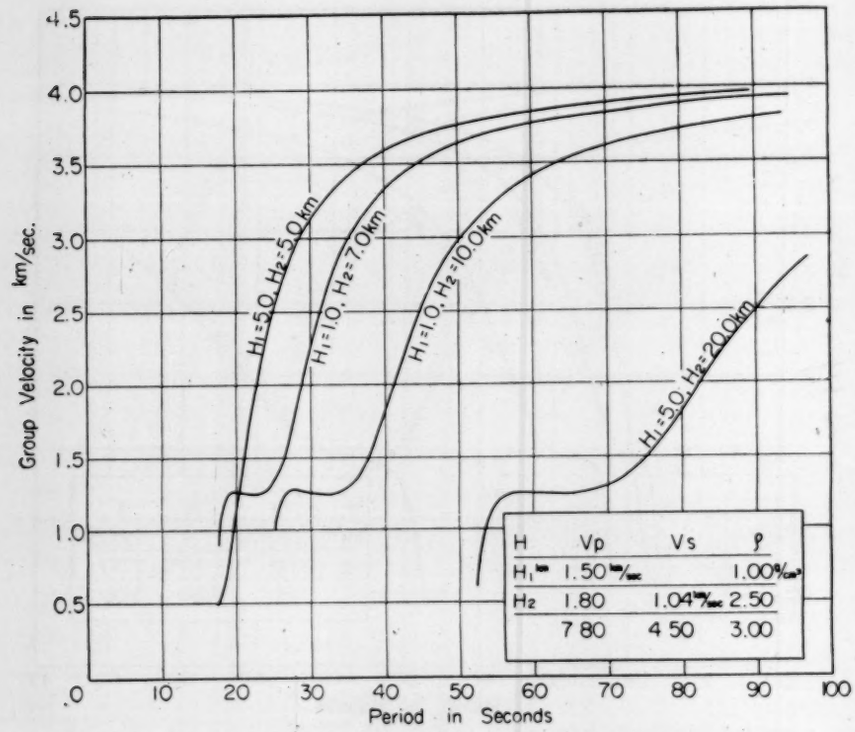

Fig. 42. Group velocity dispersion curves of Rayleigh waves.

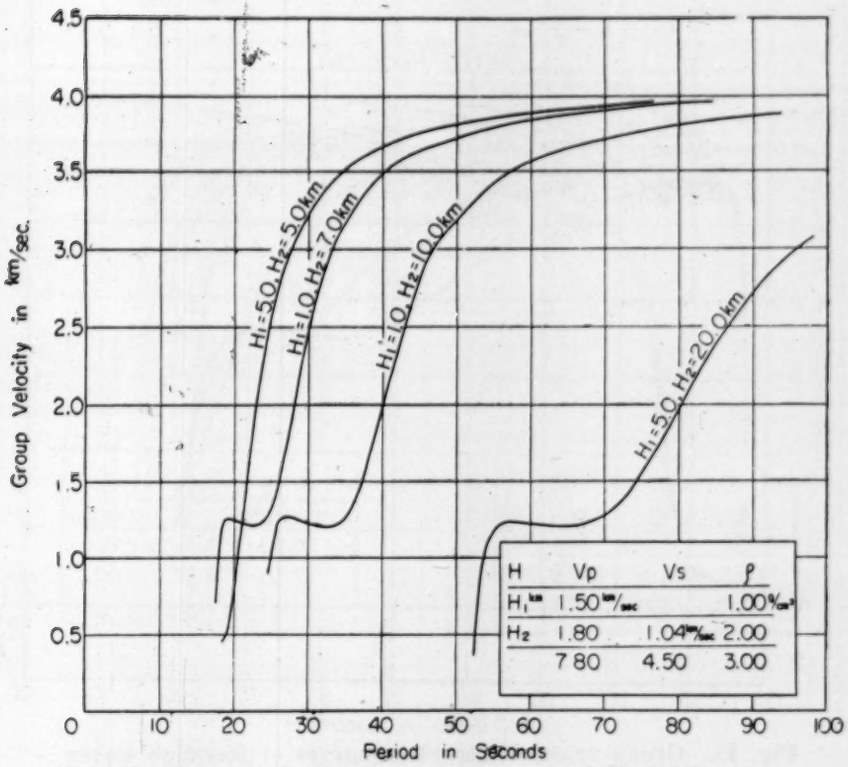

Fig. 43. Group velocity dispersion curves of Rayleigh waves.

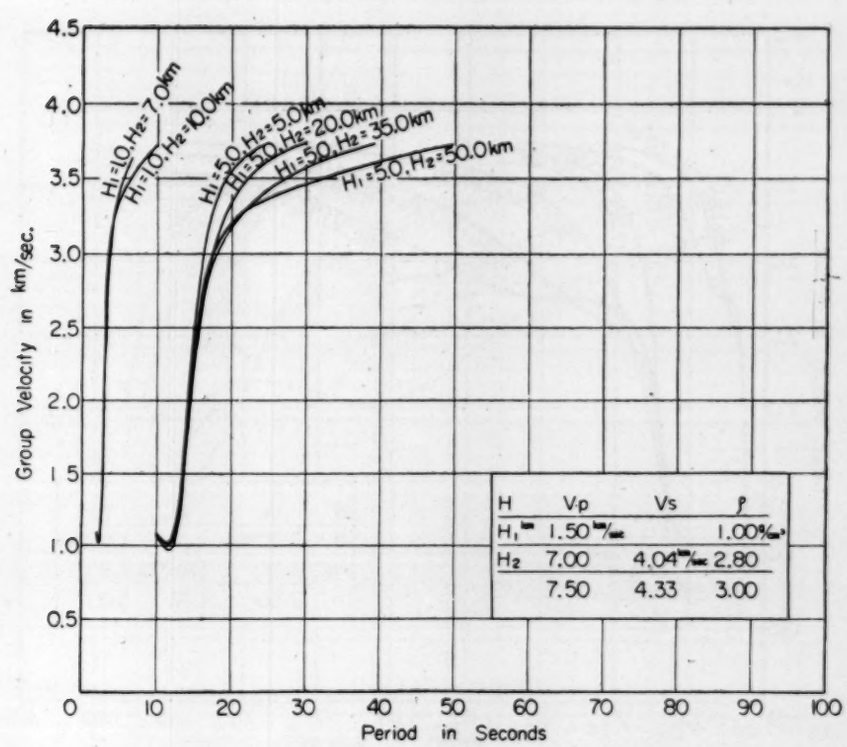

Fig 44. Group velocity dispersion curves of Rayleigh waves.

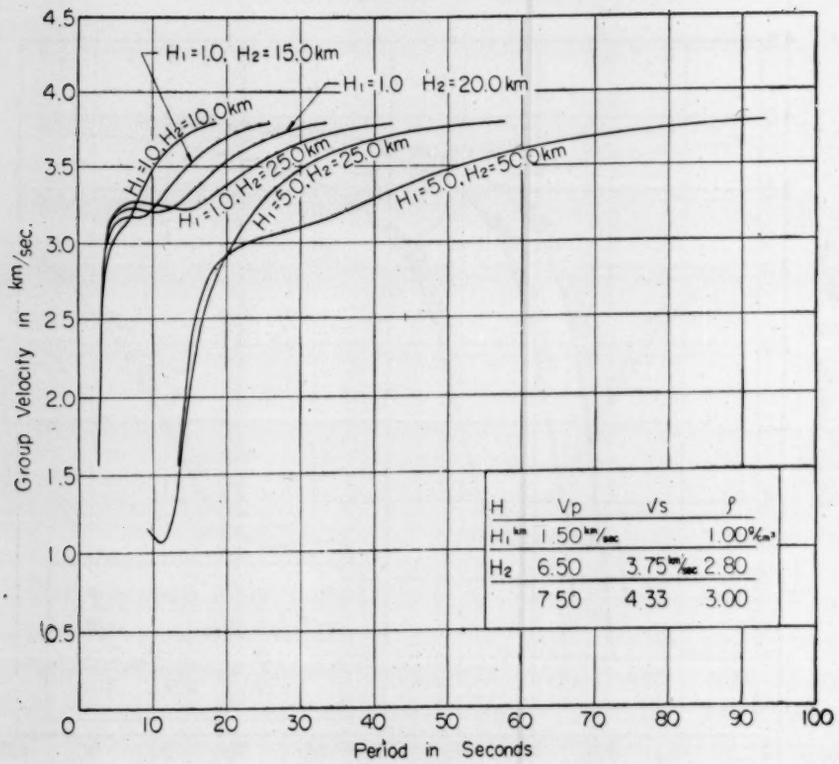

Fig. 45. Group velocity dispersion curves of Rayleigh waves.

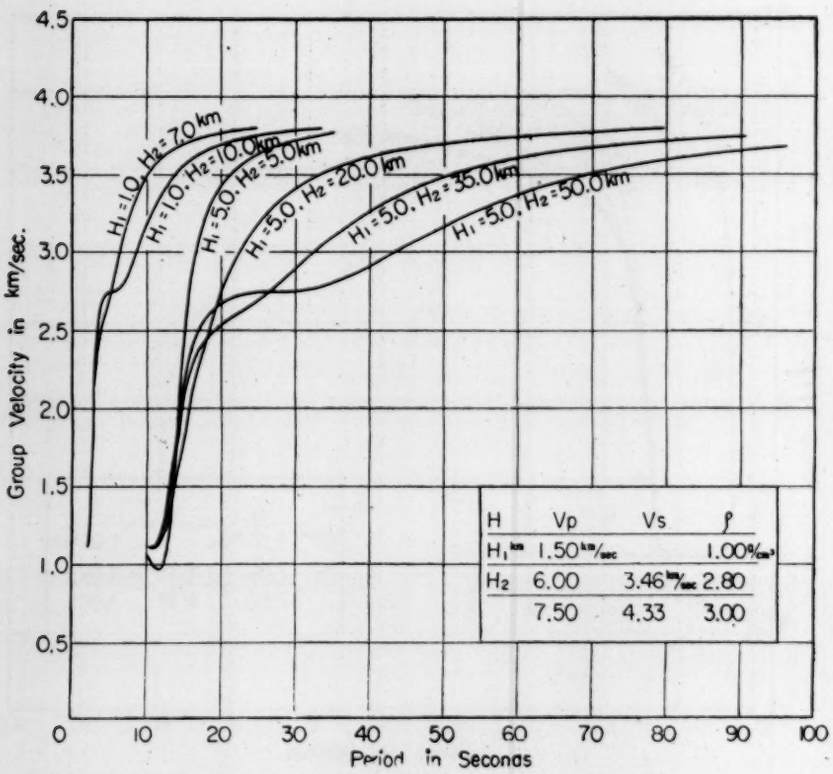

Fig. 46. Group velocity dispersion curves of Rayleigh waves.

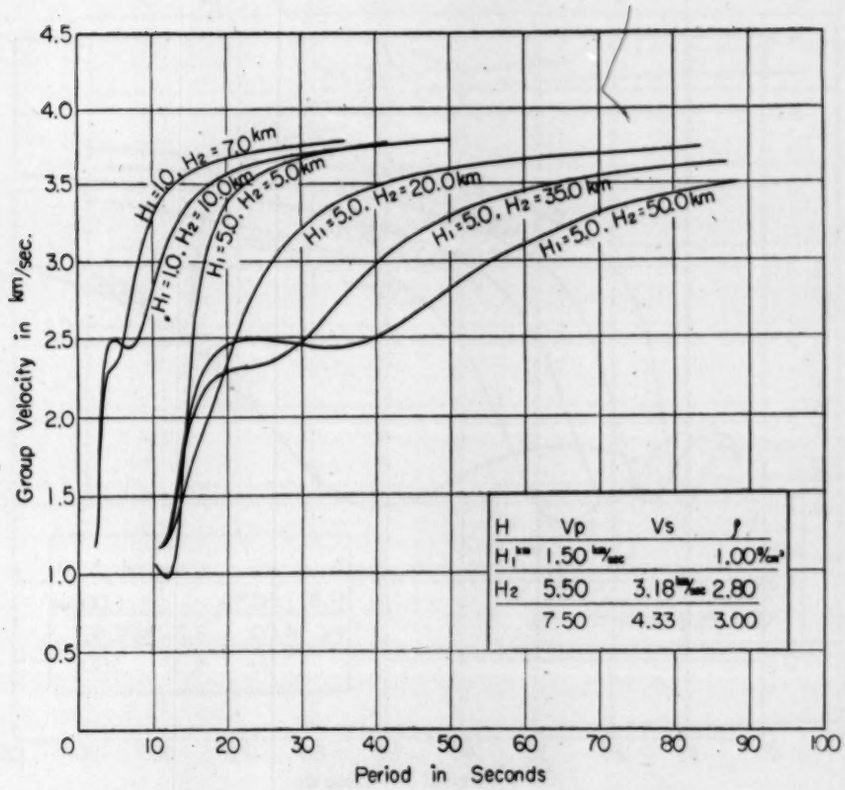

Fig. 47. Group velocity dispersion curves of Rayleigh waves.

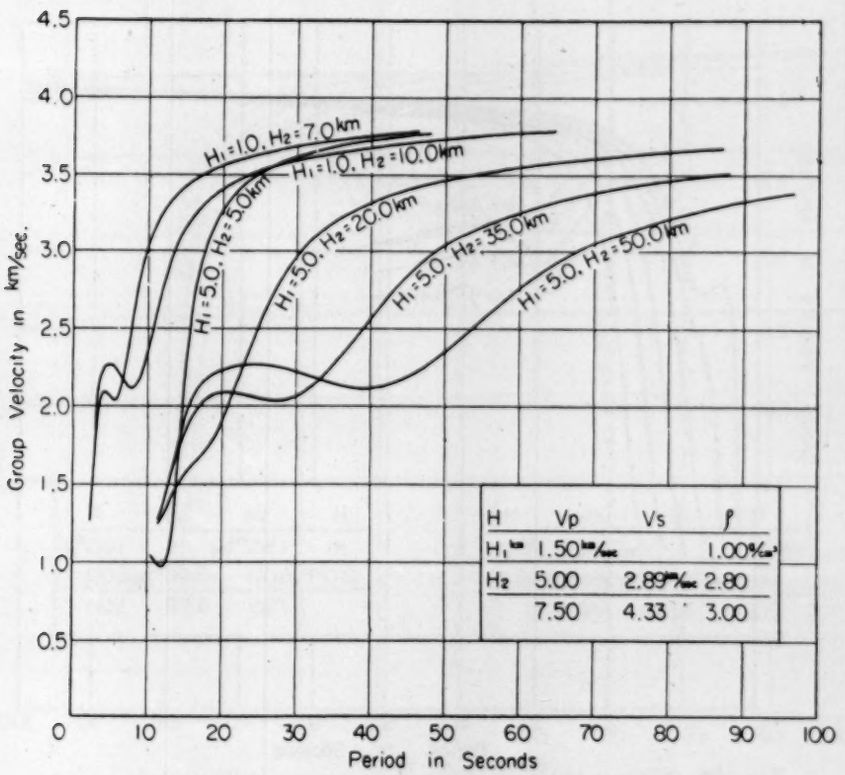

Fig. 48. Group velocity dispersion curves of Rayleigh waves.

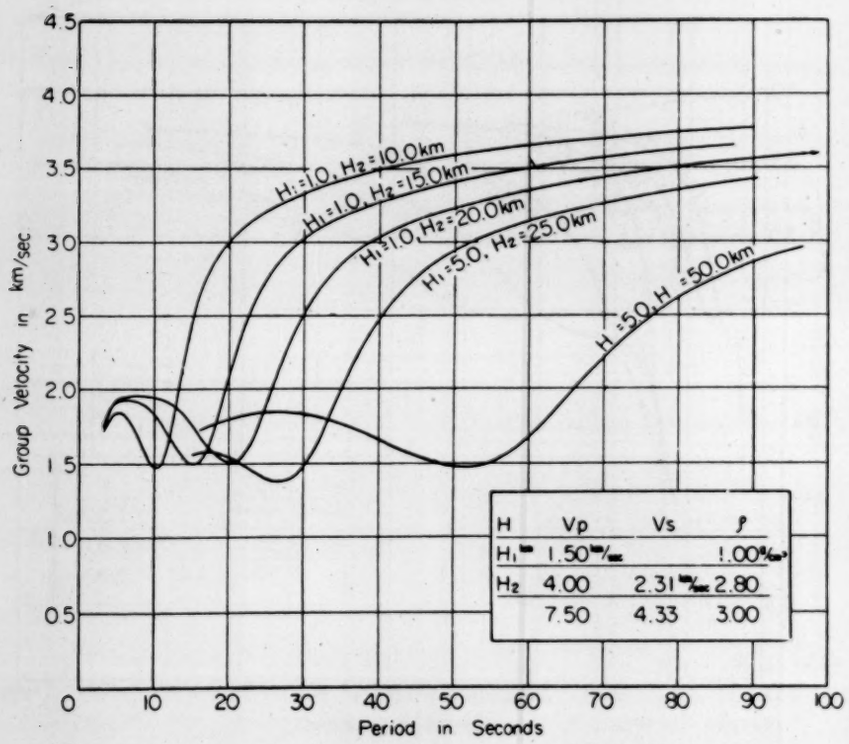

Fig. 49. Group velocity dispersion curves of Rayleigh waves.

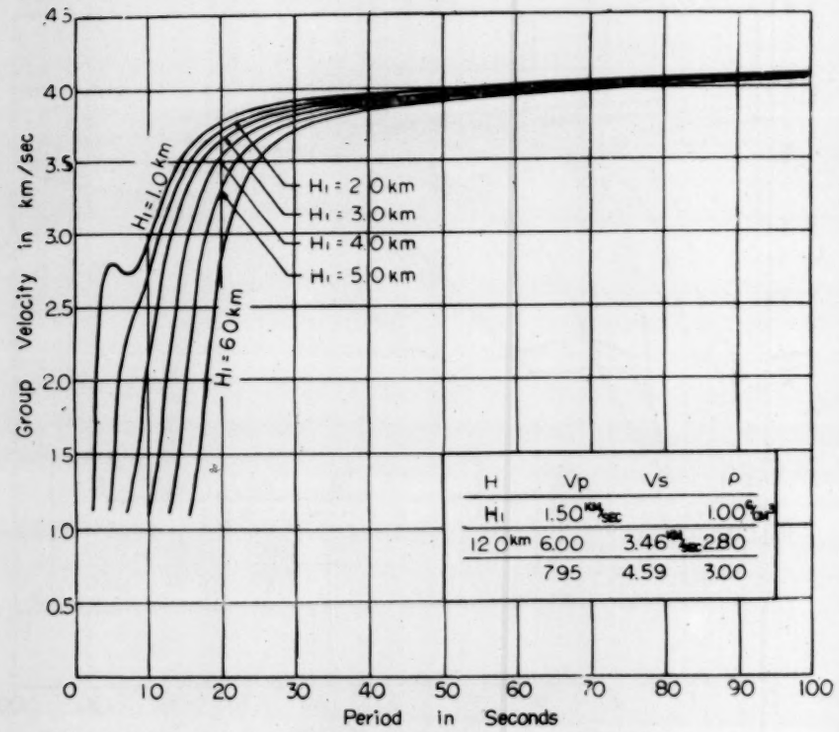

Fig. 50. Group velocity dispersion curves of Rayleigh waves.

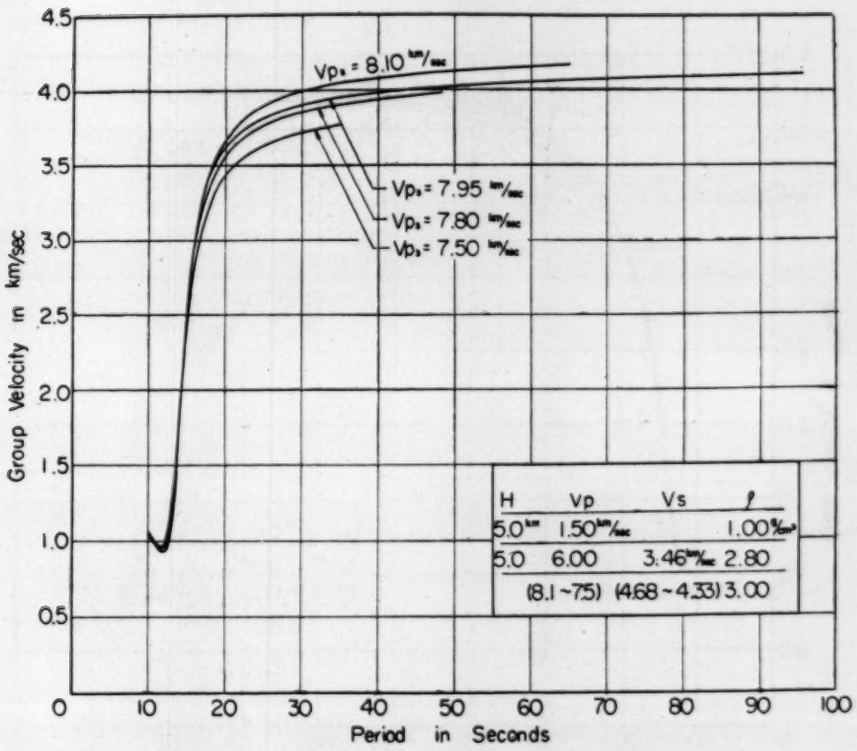

Fig. 51. Group velocity dispersion curves of Rayleigh waves.

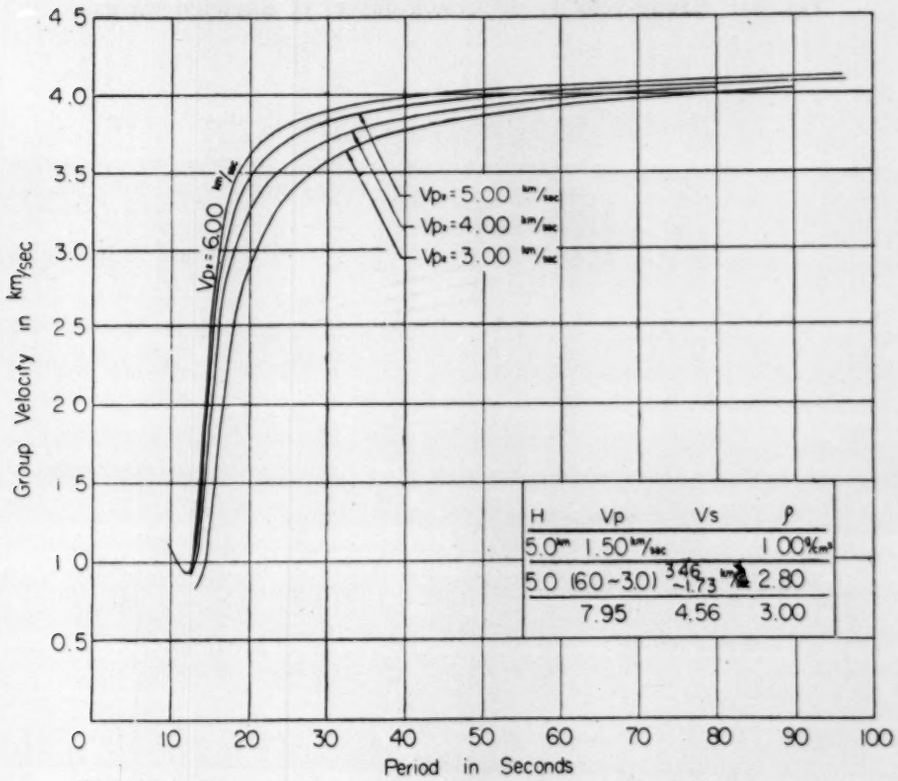

Fig. 52. Group velocity dispersion curves of Rayleigh waves.

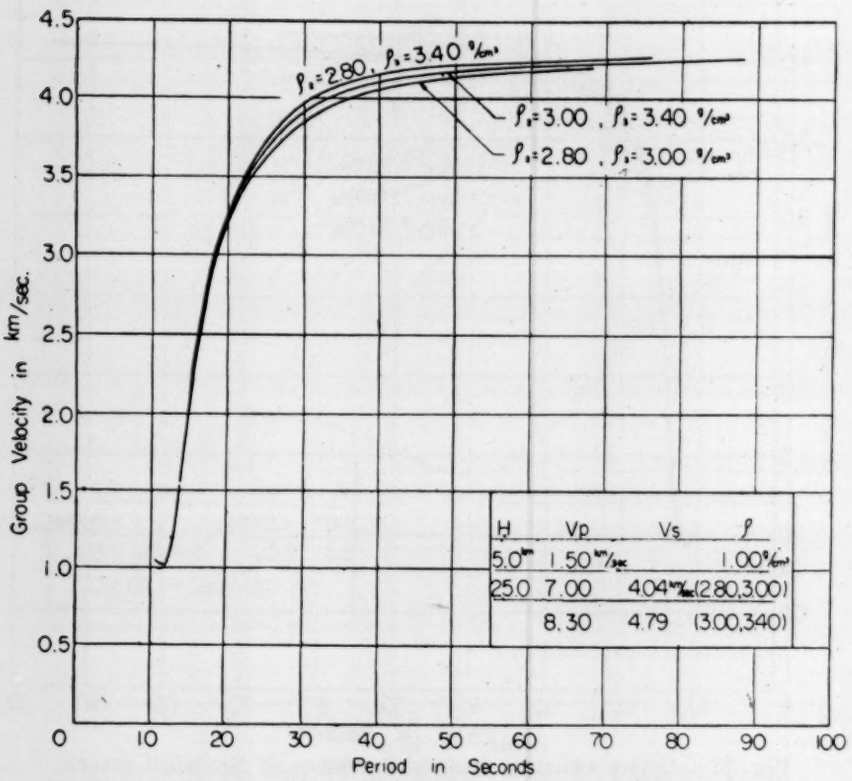

Fig. 53. Group velocity dispersion curves of Rayleigh waves.

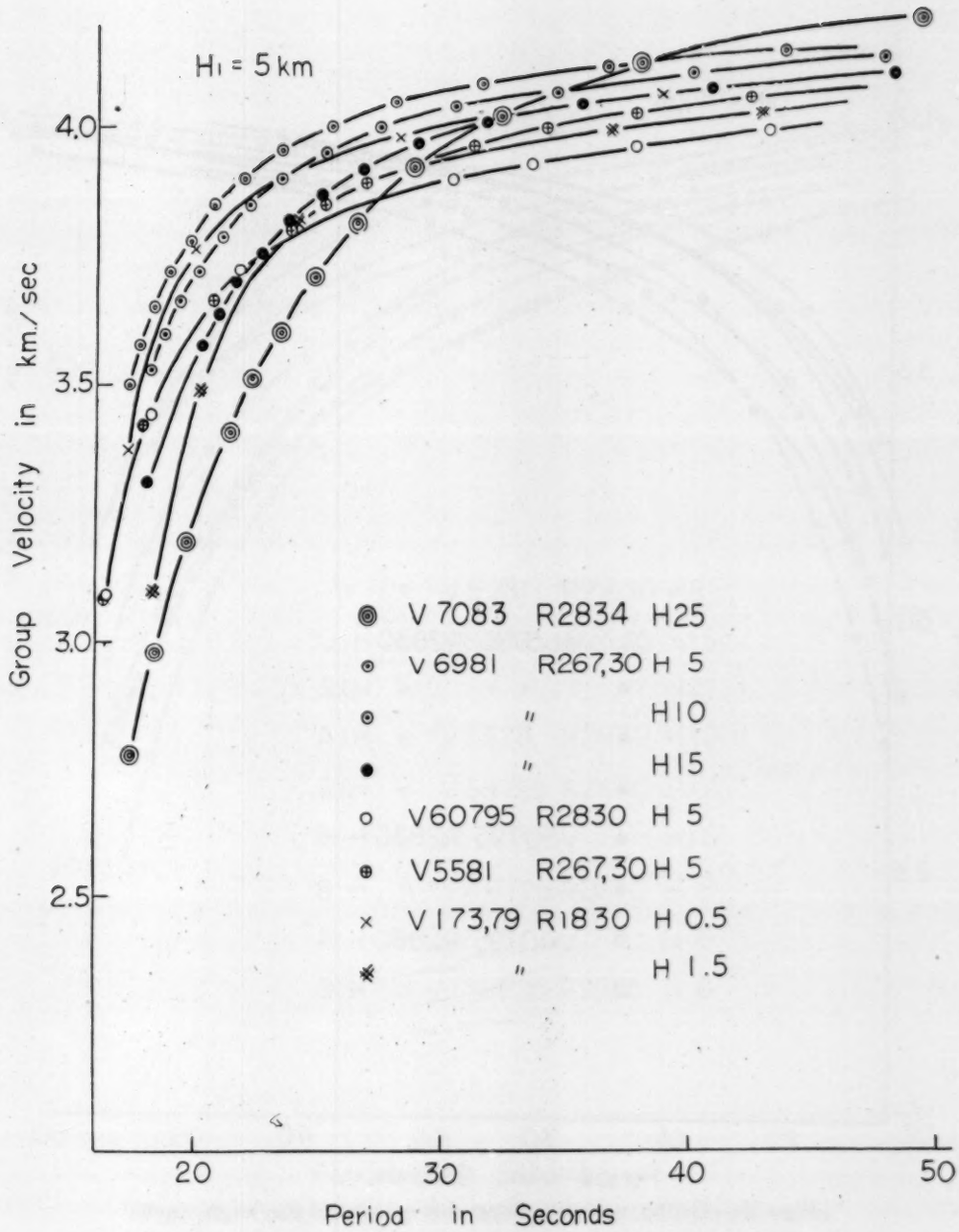

Fig. 54. Group velocity dispersion curves of Rayleigh waves for the various cases.

V7083 R2834 H25 means $Vp_2=7.0$ km/sec, $Vp_3=8.3$ km, $\rho_2=2.8$ g/cm^3, $\rho_3=3.4$ g/cm^3, and $H_2=25$ km.

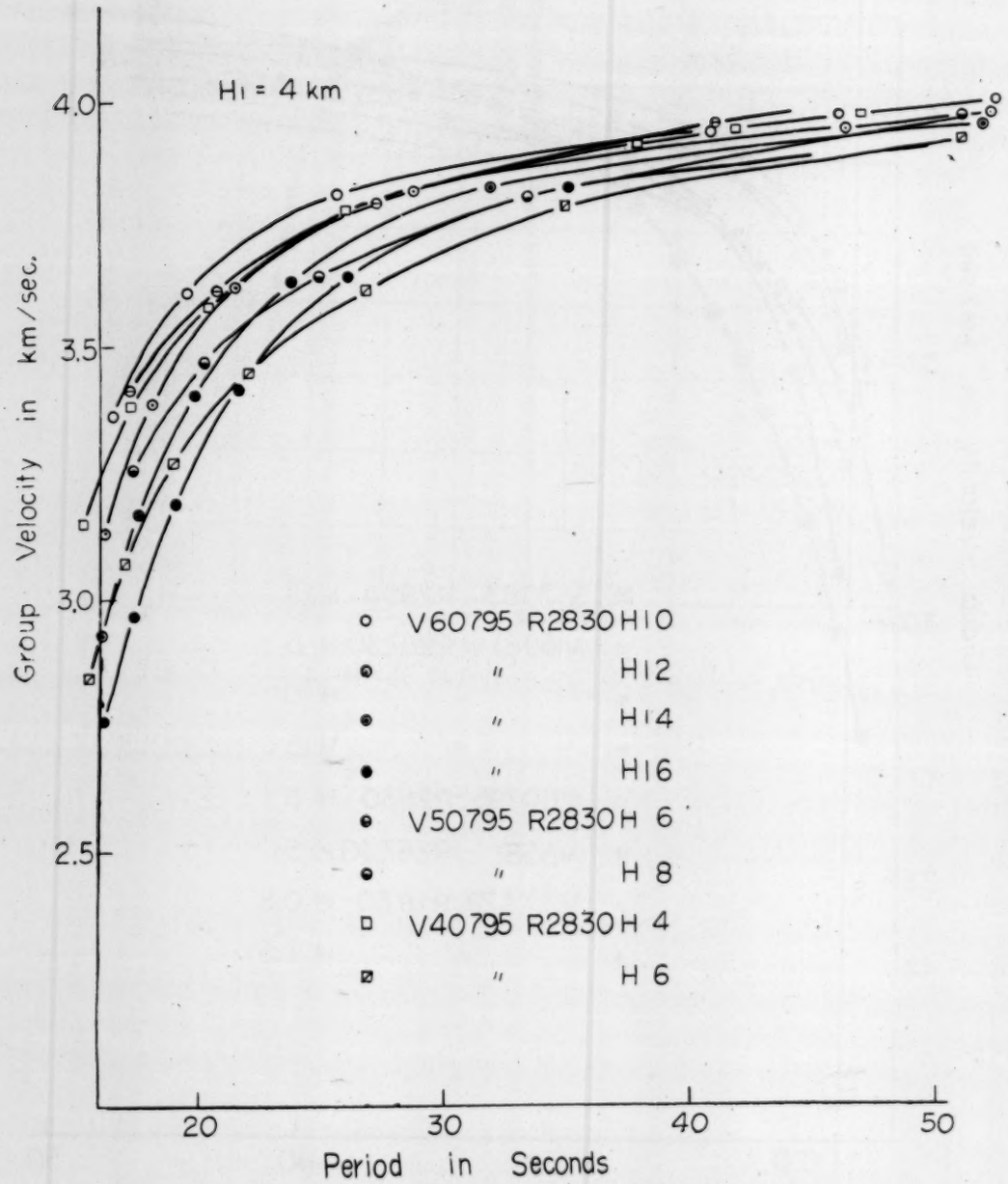

Fig. 55. Group velocity dispersion curves of Rayleigh waves for the various cases.

V60795 R2830 H10 means $Vp_2=6.0$ km/sec, $Vp_3=7.95$ km/sec, $\rho_2=2.8$ g/cm^3, $\rho_3=3.0$ g/cm^3, and $H_2=10$ km.

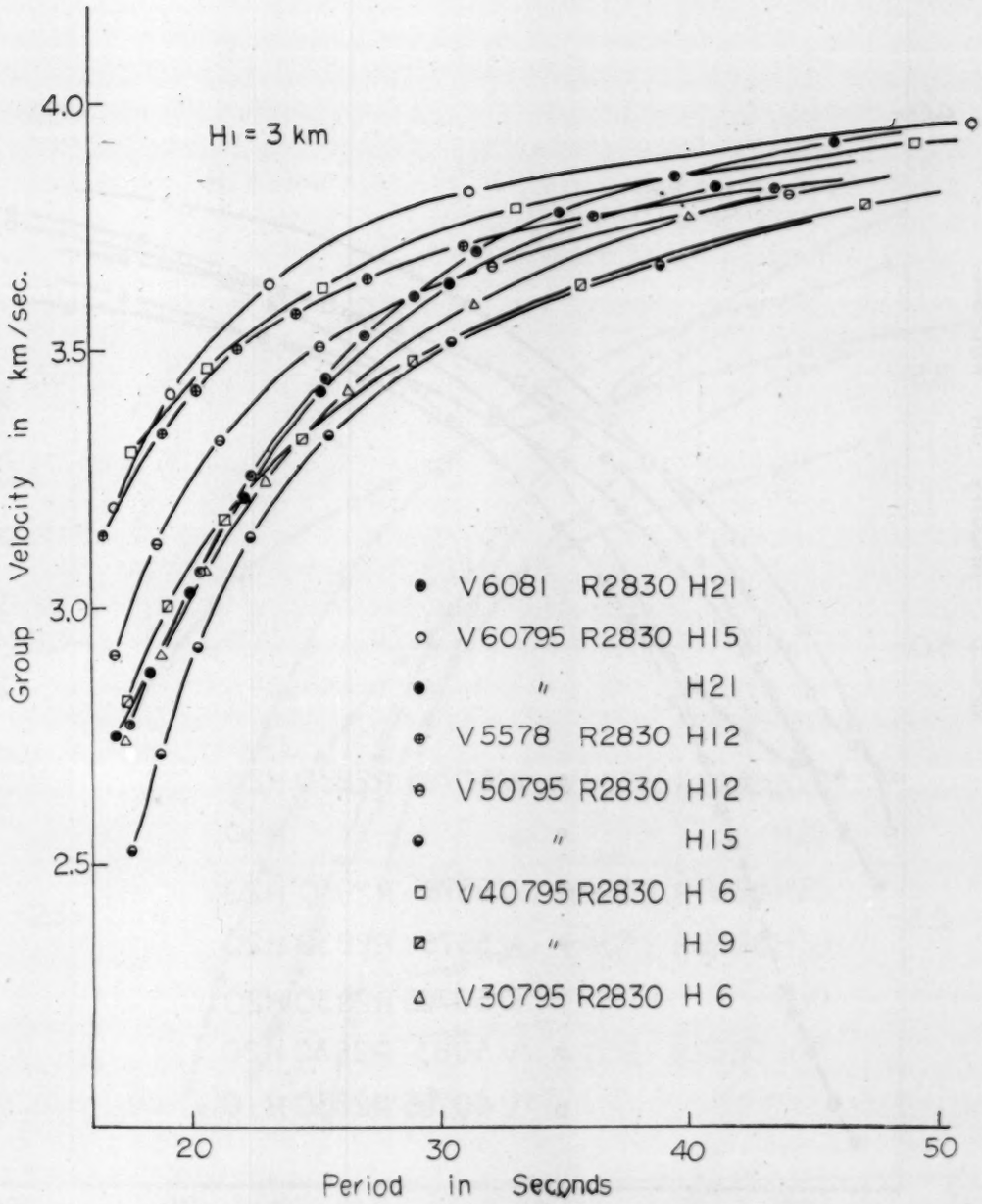

Fig. 56. Group velocity dispersion curves of Rayleigh waves for the various cases.

V6081 R2830 H21 means $Vp_2=6.0$ km/sec, $Vp_3=8.1$ km/sec, $\rho_2=2.8$ g/cm^3, $\rho_3=3.0$ g/cm^3, and $H_2=21$ km.

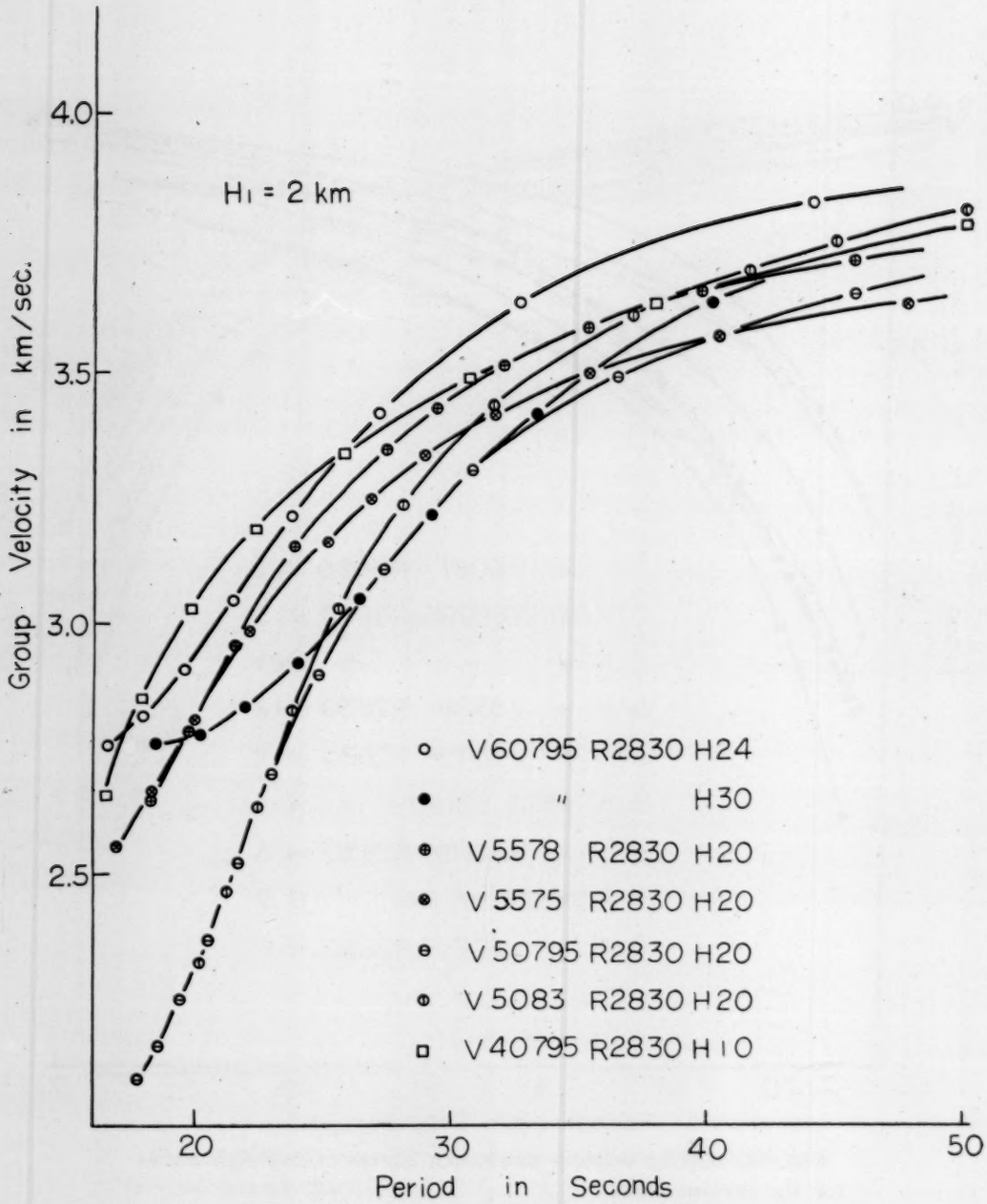

Fig. 57. Group velocity dispersion curves of Rayleigh waves for the various cases.

V60795 R2830 H24 means $Vp_2=6.0$ km/sec, $Vp_3=7.95$ km/sec, $\rho_2=2.8$ g/cm^3, $\rho_3=3.0$ g/cm^3, and $H_2=24$ km.

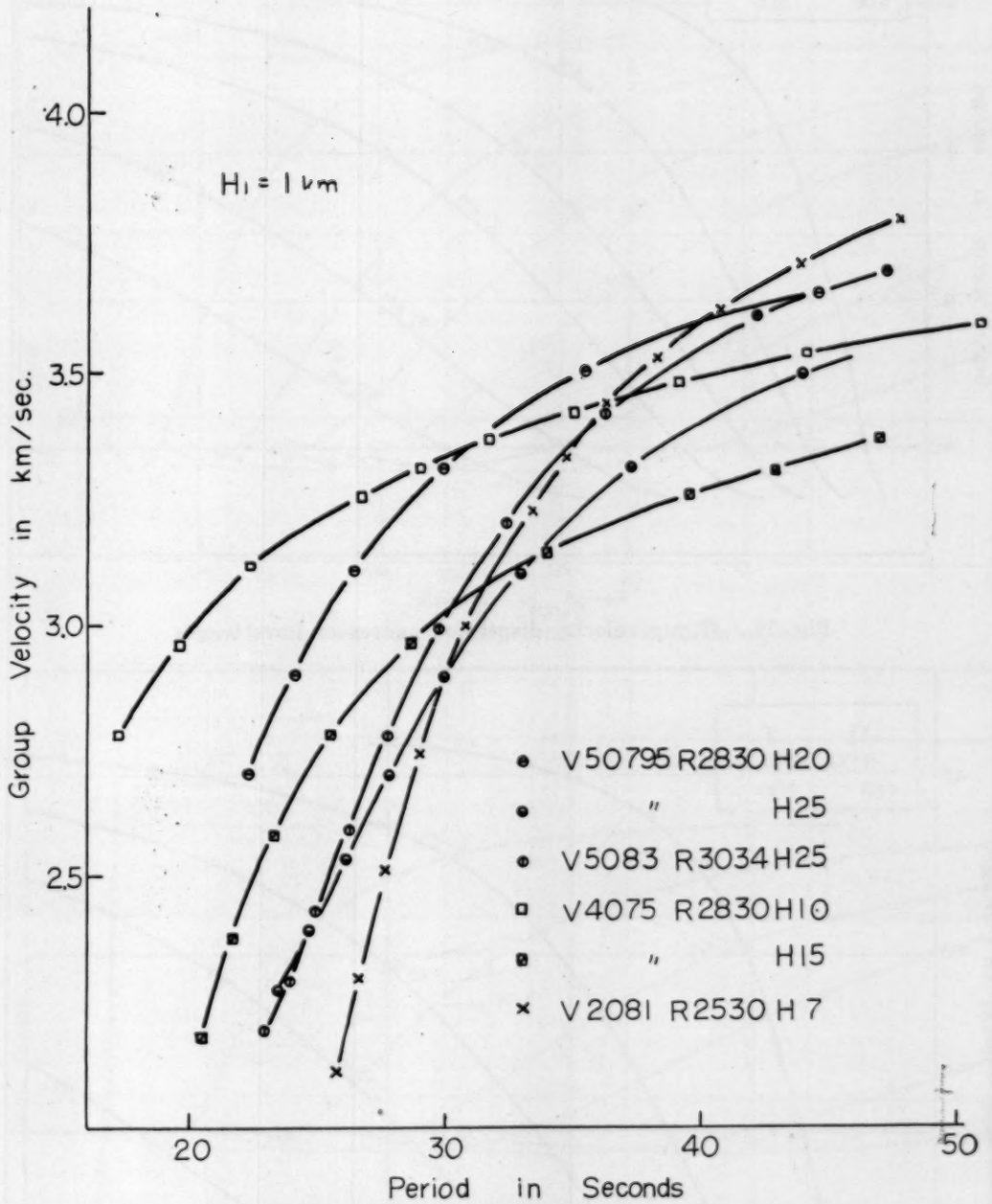

Fig. 58. Group velocity dispersion curves of Rayleigh waves for the various cases.

V50795 R2830 H20 means $Vp_2=5.0$ km/sec, $Vp_3=7.95$ km/sec, $\rho_2=2.8$ g/cm^3, $\rho_3=3.0$ g/cm^3, and $H_2=20$ km.

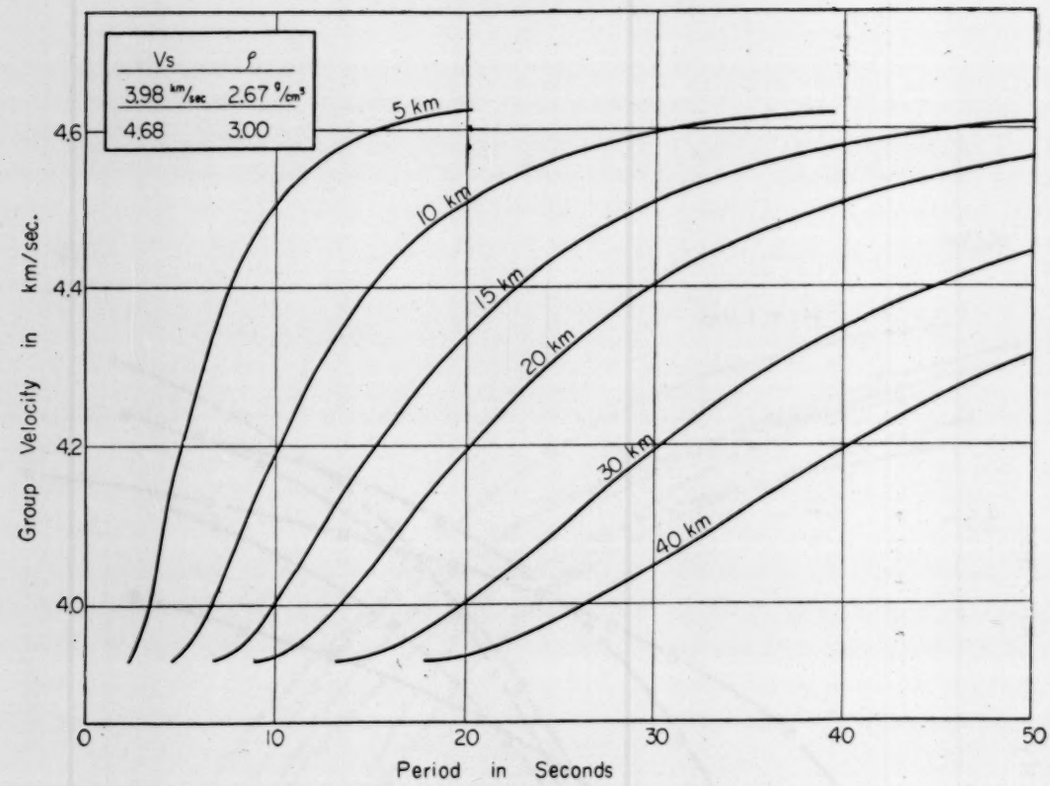

Fig. 1L. Group velocity dispersion curves of Love waves.

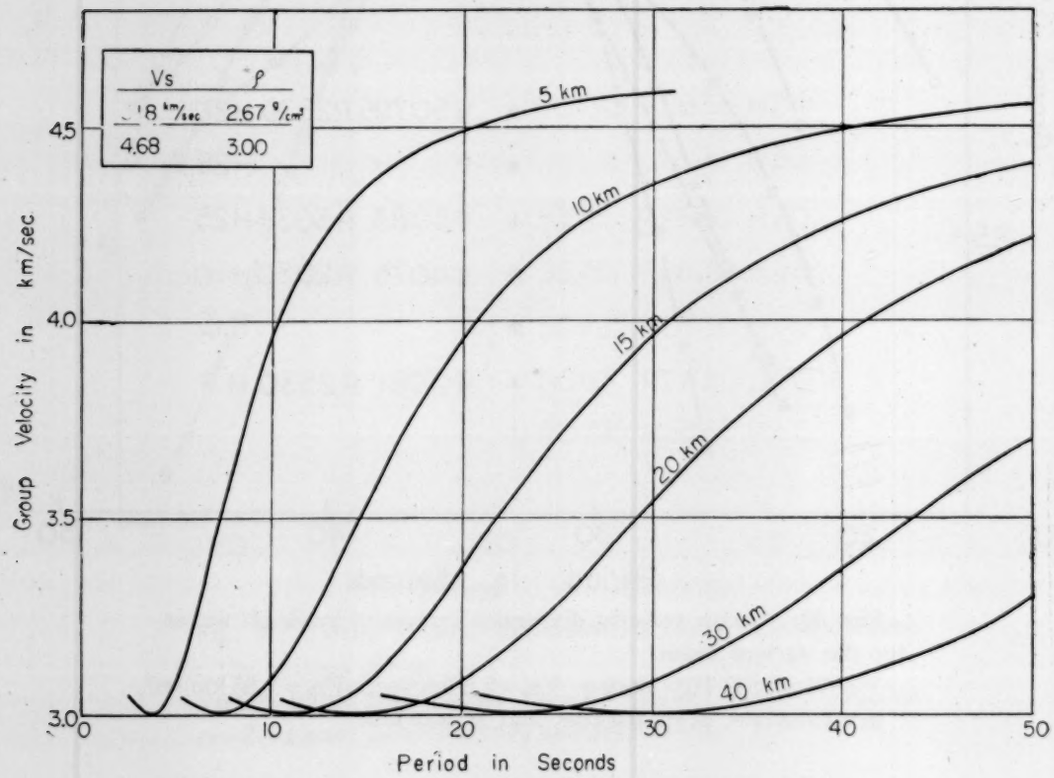

Fig. 2L. Group velocity dispersion curves of Love waves.

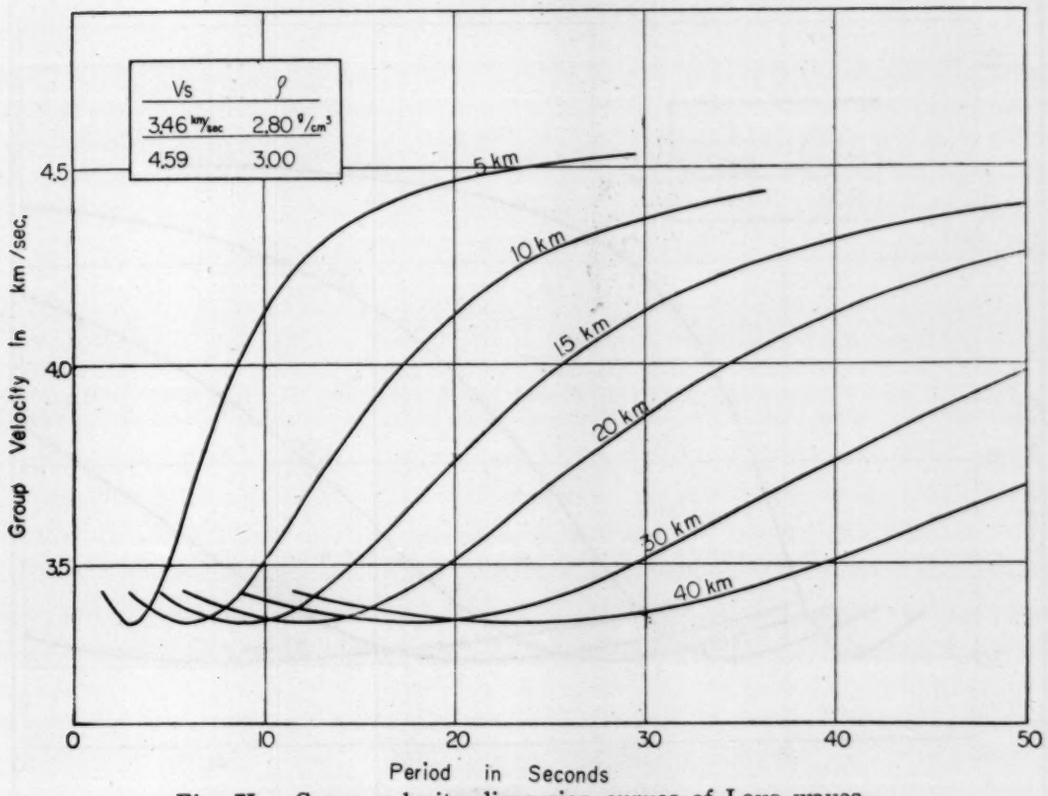

Fig. 7L. Group velocity dispersion curves of Love waves.

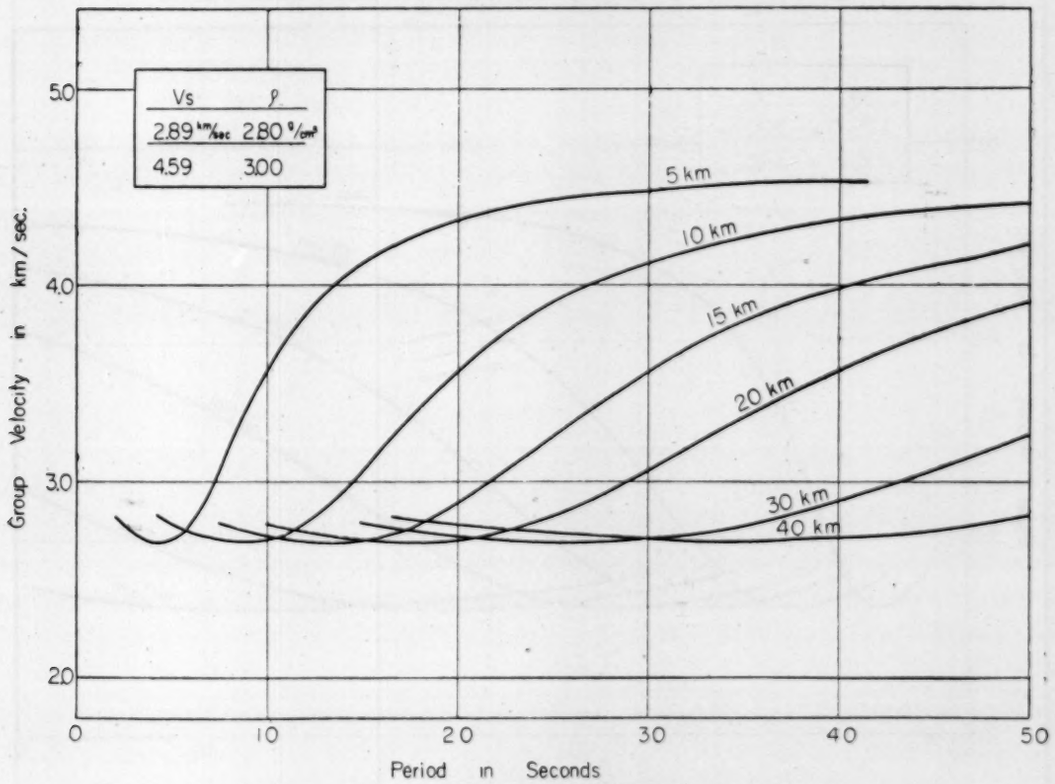

Fig. 9L. Group velocity dispersion curves of Love waves.

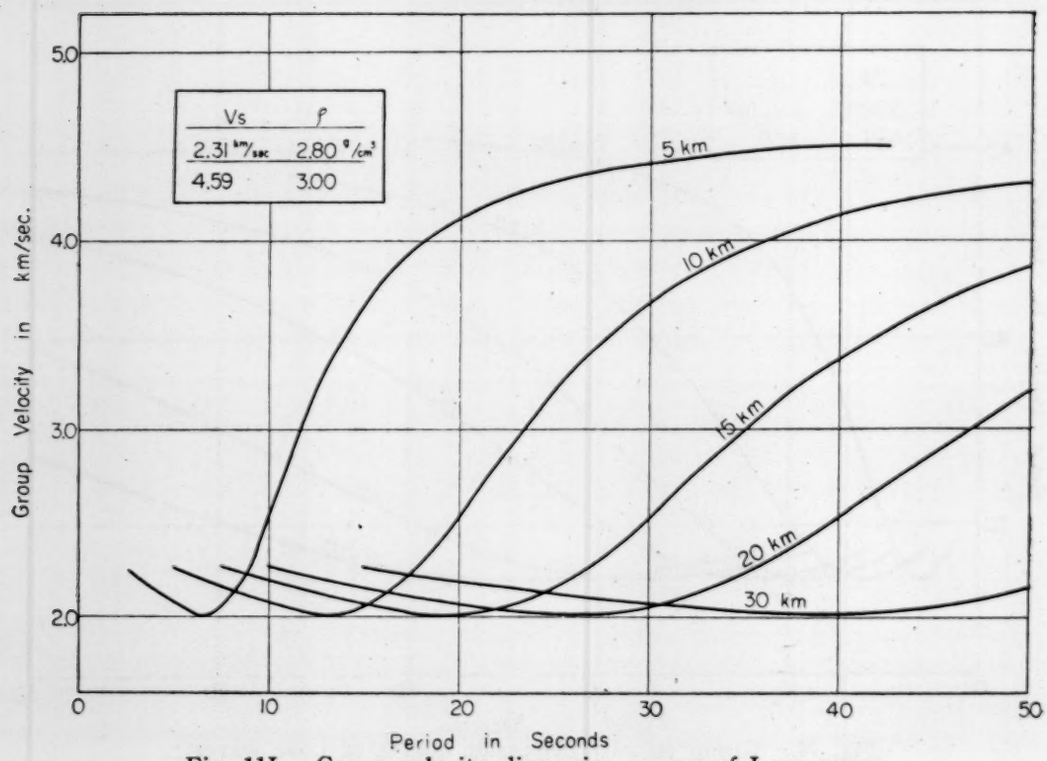

Fig. 11L. Group velocity dispersion curves of Love waves.

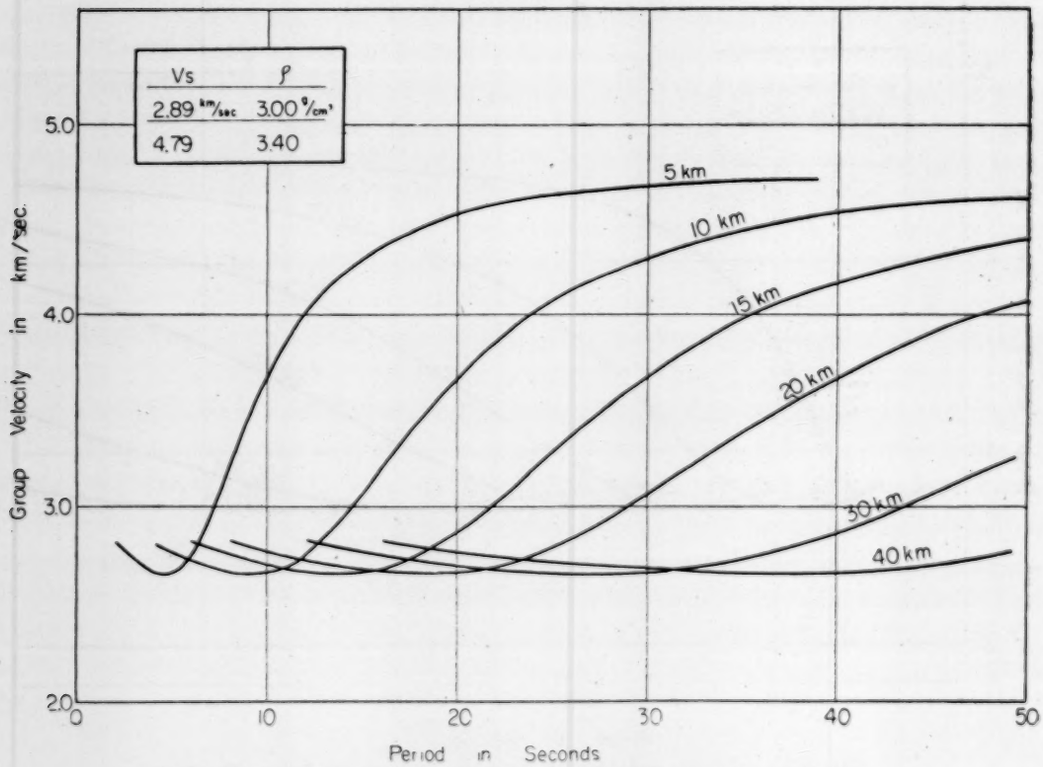

Fig. 16L. Group velocity dispersion curves of Love waves.

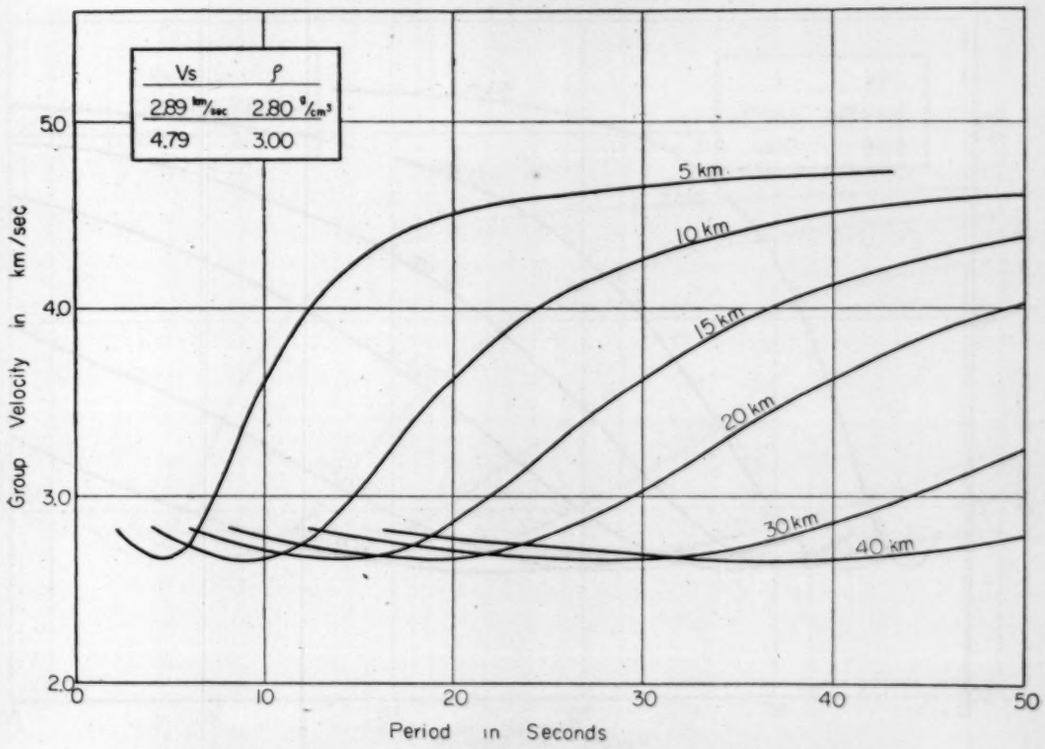

Fig. 18L. Group velocity dispersion curves of Love waves.

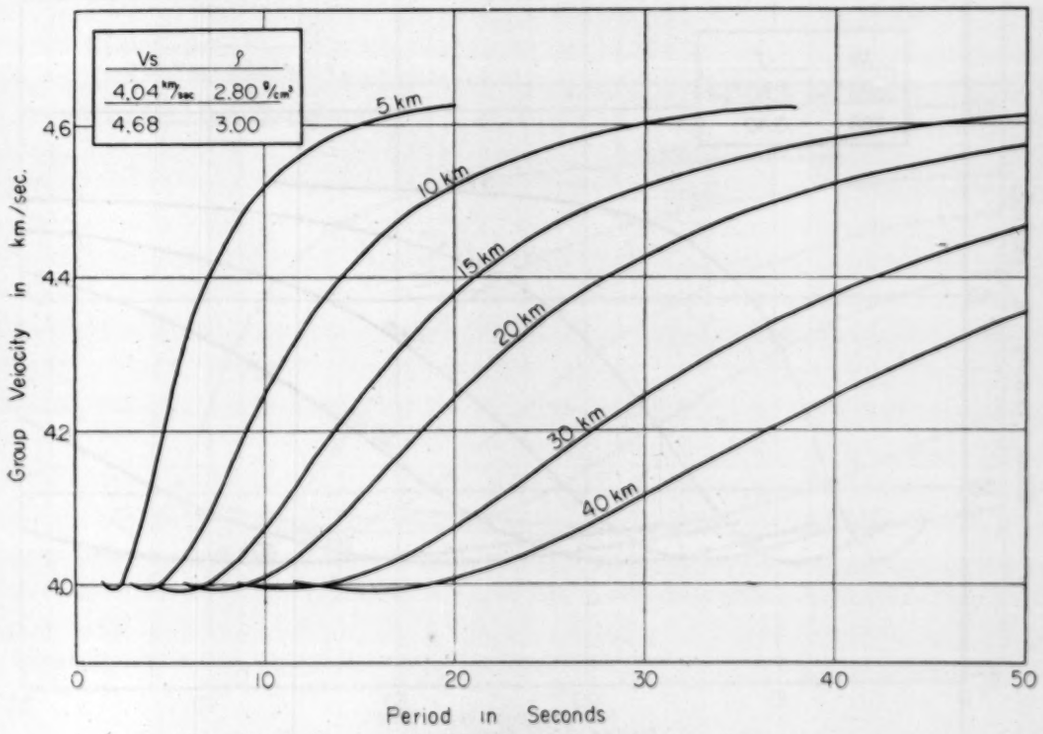

Fig. 19L. Group velocity dispersion curves of Love waves.

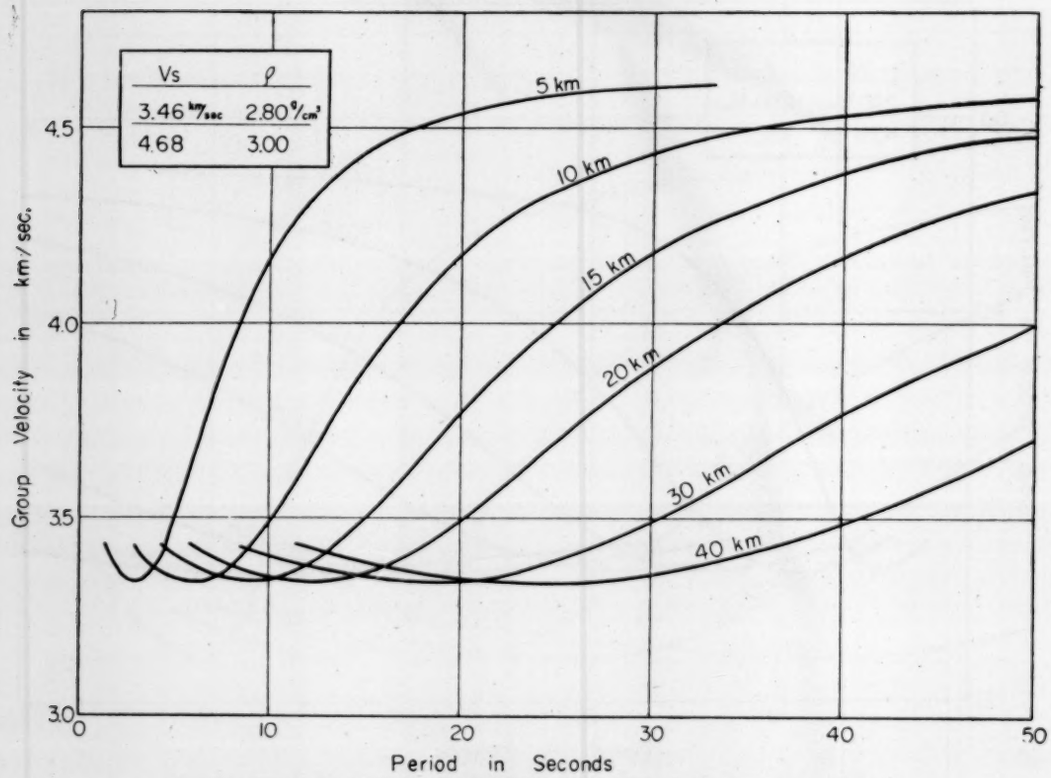

Fig. 20L. Group velocity dispersion curves of Love waves.

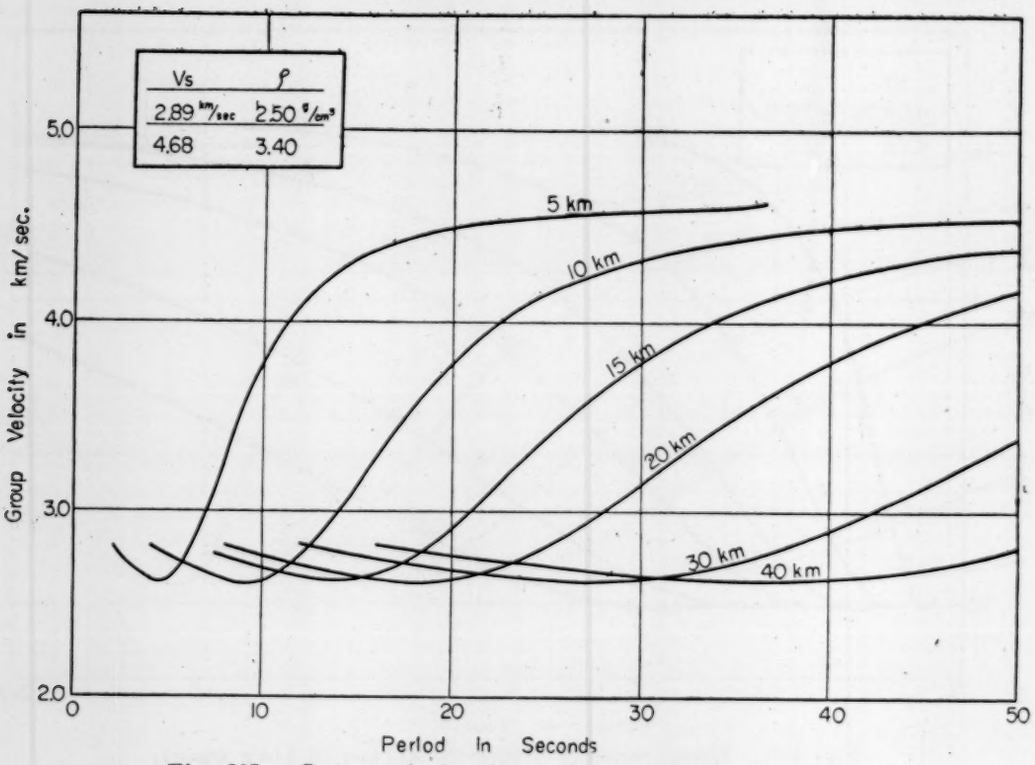

Fig. 21L. Group velocity dispersion curves of Love waves.

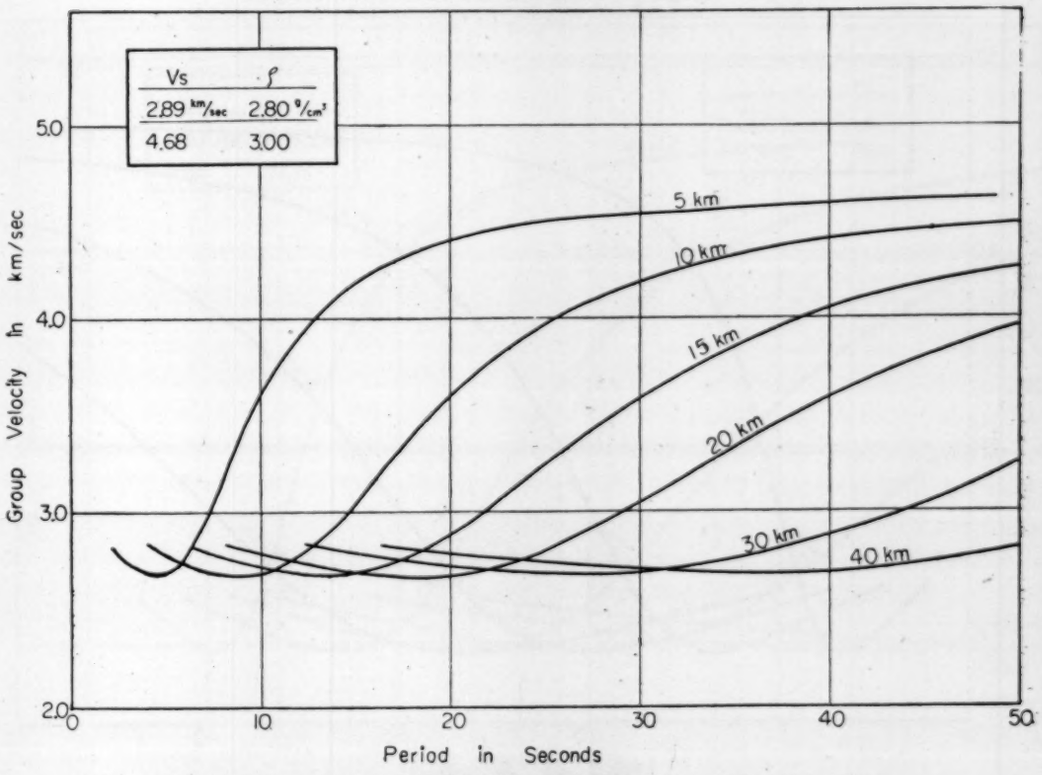

Fig. 22L. Group velocity dispersion curves of Love waves.

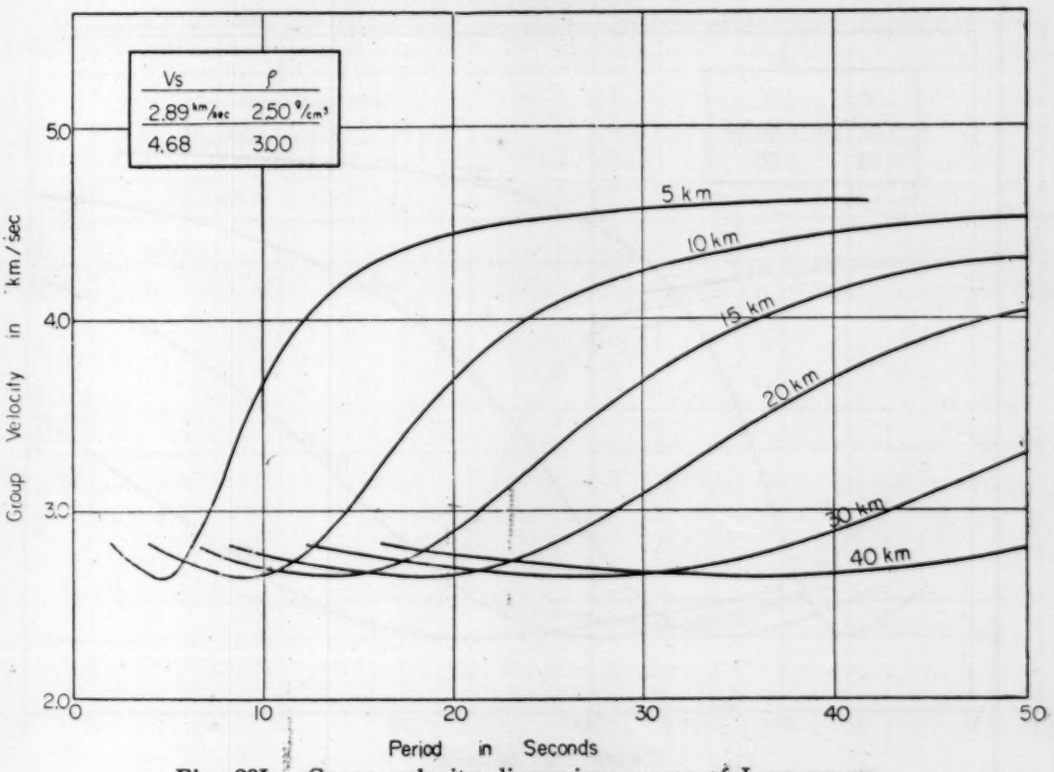

Fig. 23L. Group velocity dispersion curves of Love waves.

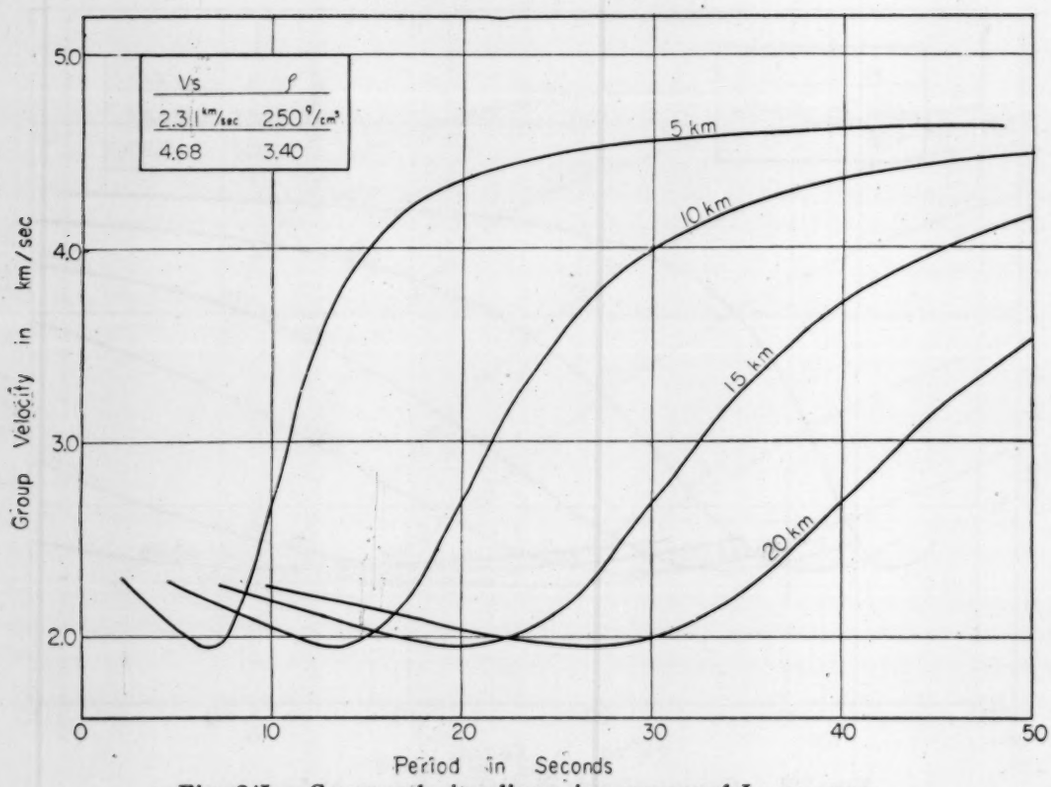

Fig. 24L. Group velocity dispersion curves of Love waves.

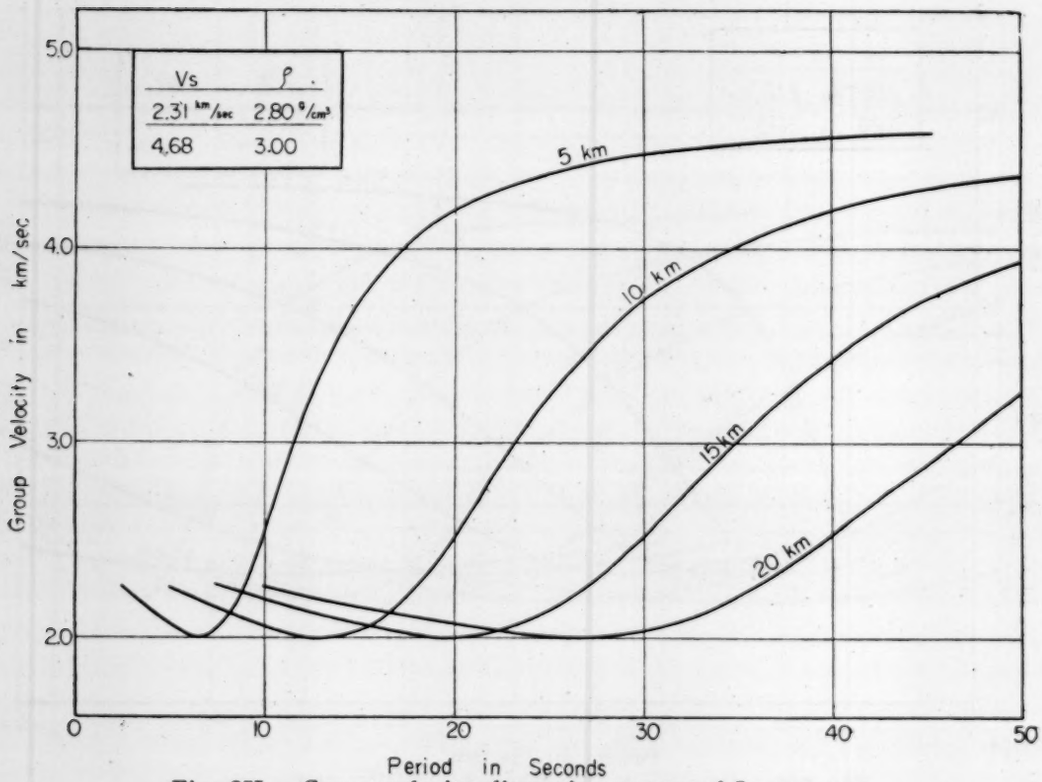

Fig. 25L. Group velocity dispersion curves of Love waves.

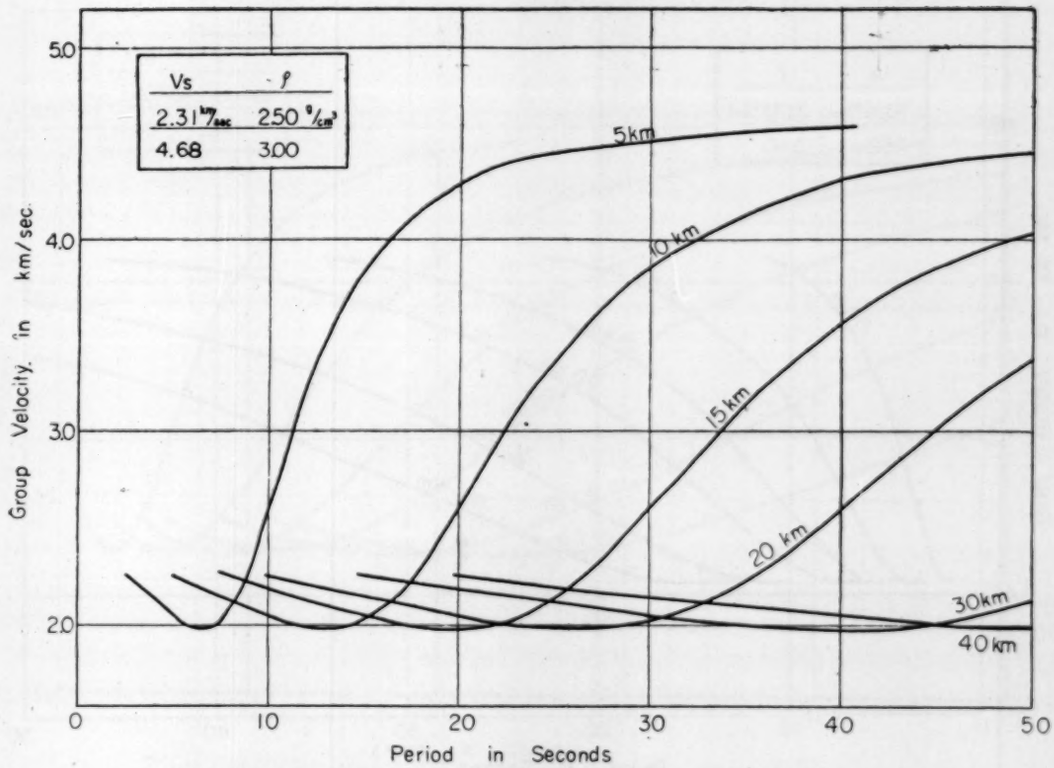

Fig. 26L. Group velocity dispersion curves of Love waves.

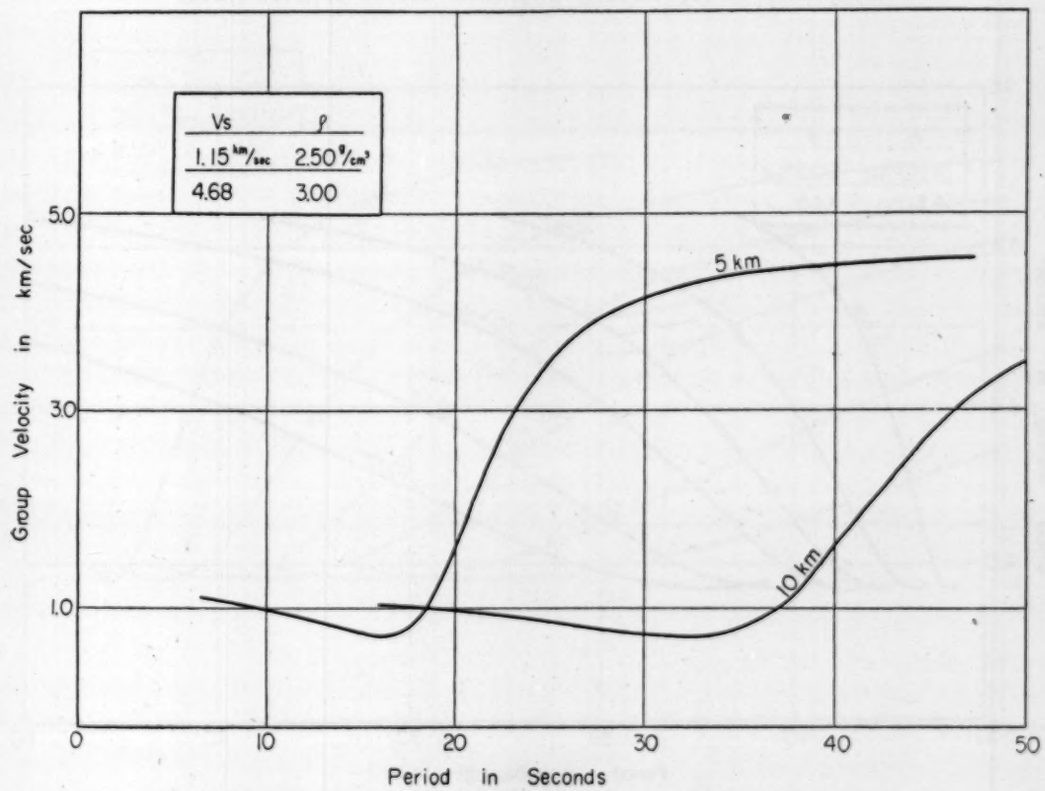

Fig. 28L. Group velocity dispersion curves of Love waves.

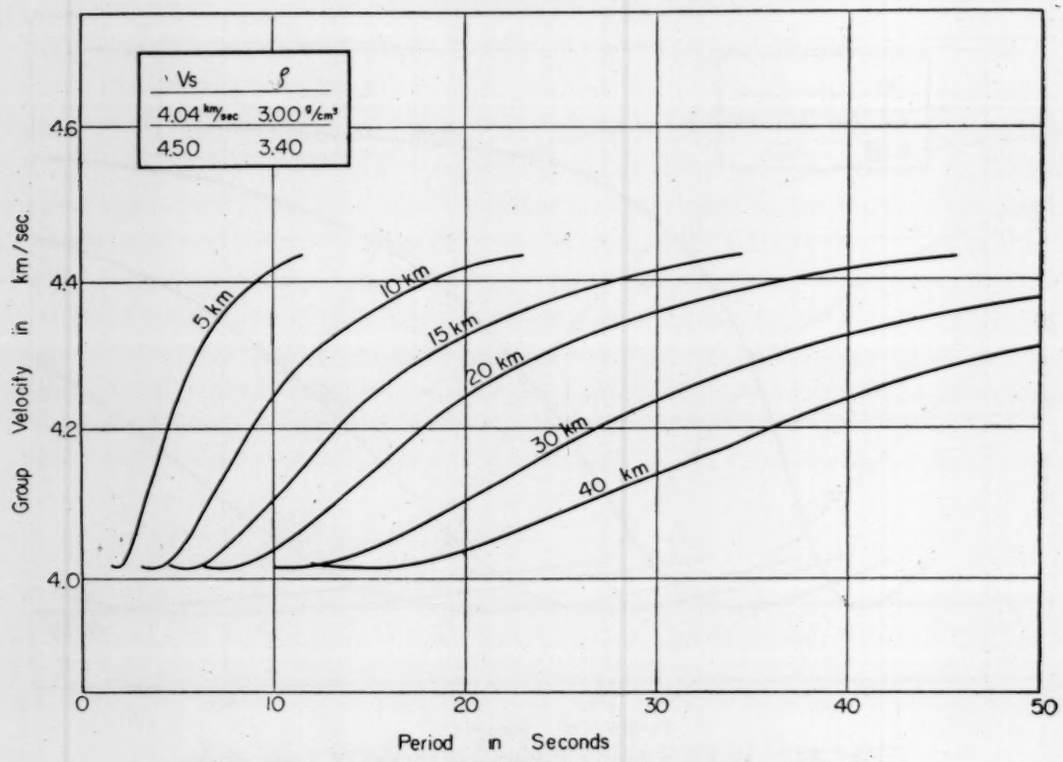

Fig. 29L. Group velocity dispersion curves of Love waves

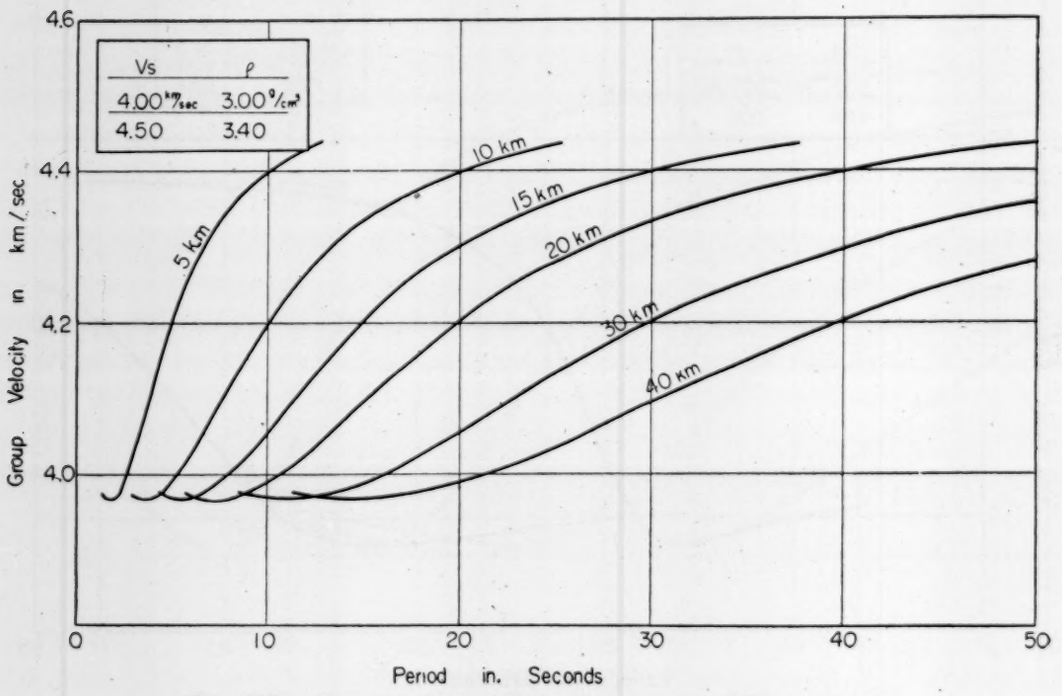

Fig. 30L. Group velocity dispersion curves of Love waves.

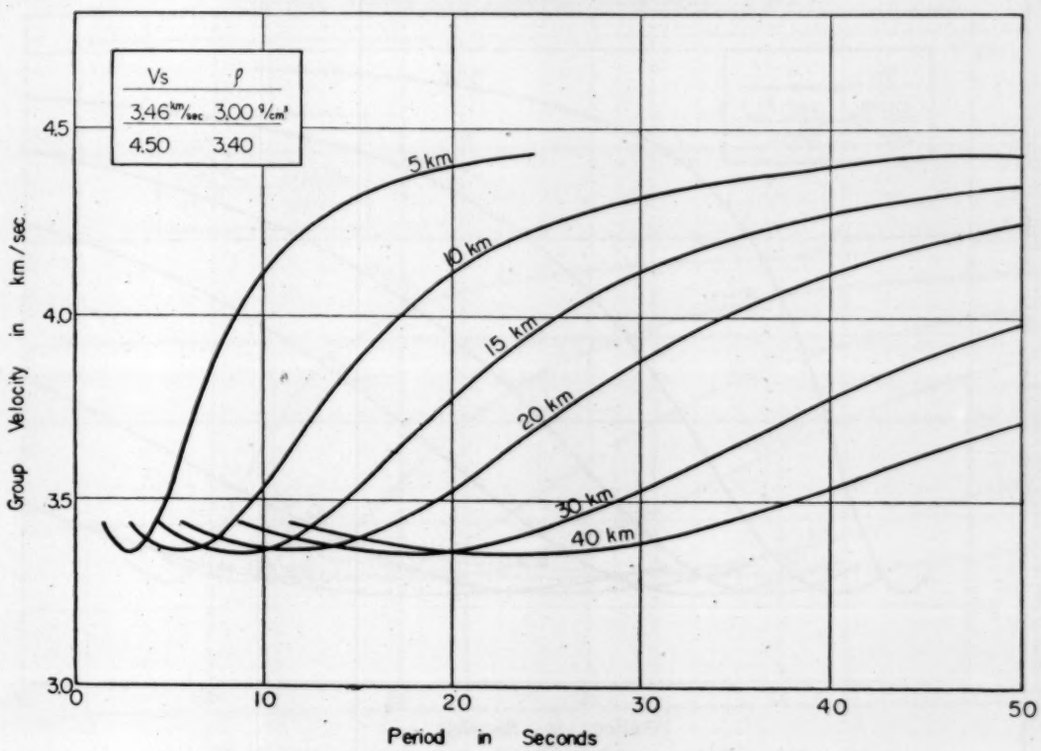

Fig. 31L. Group velocity dispersion curves of Love waves.

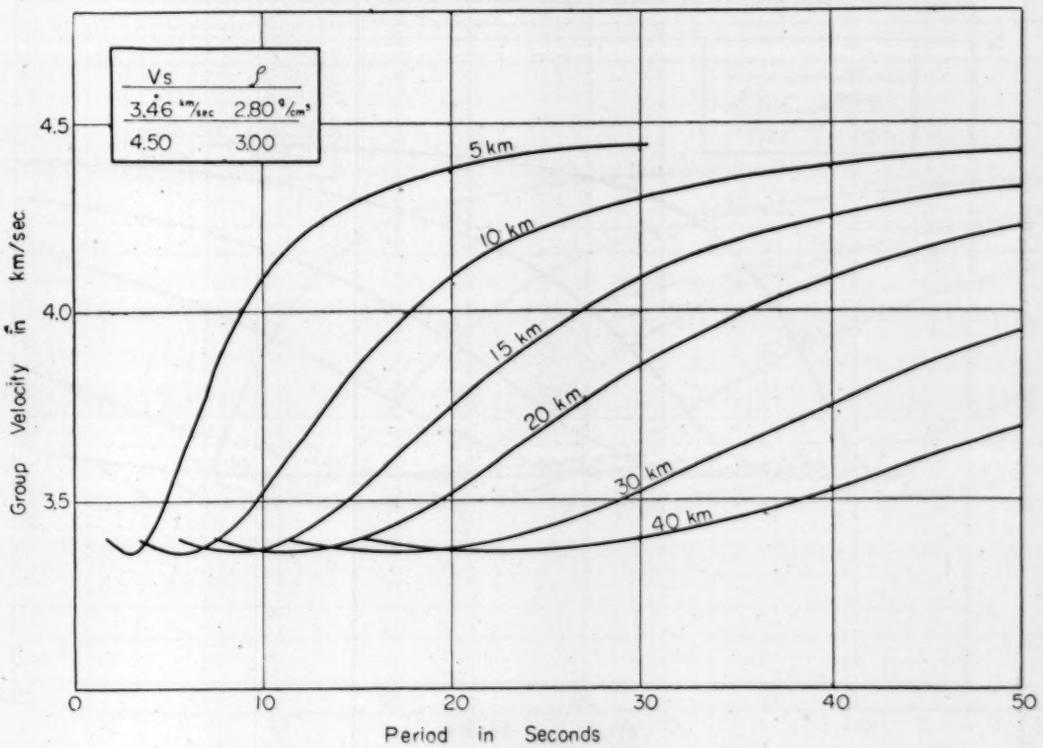

Fig. 32L. Group velocity dispersion curves of Love waves.

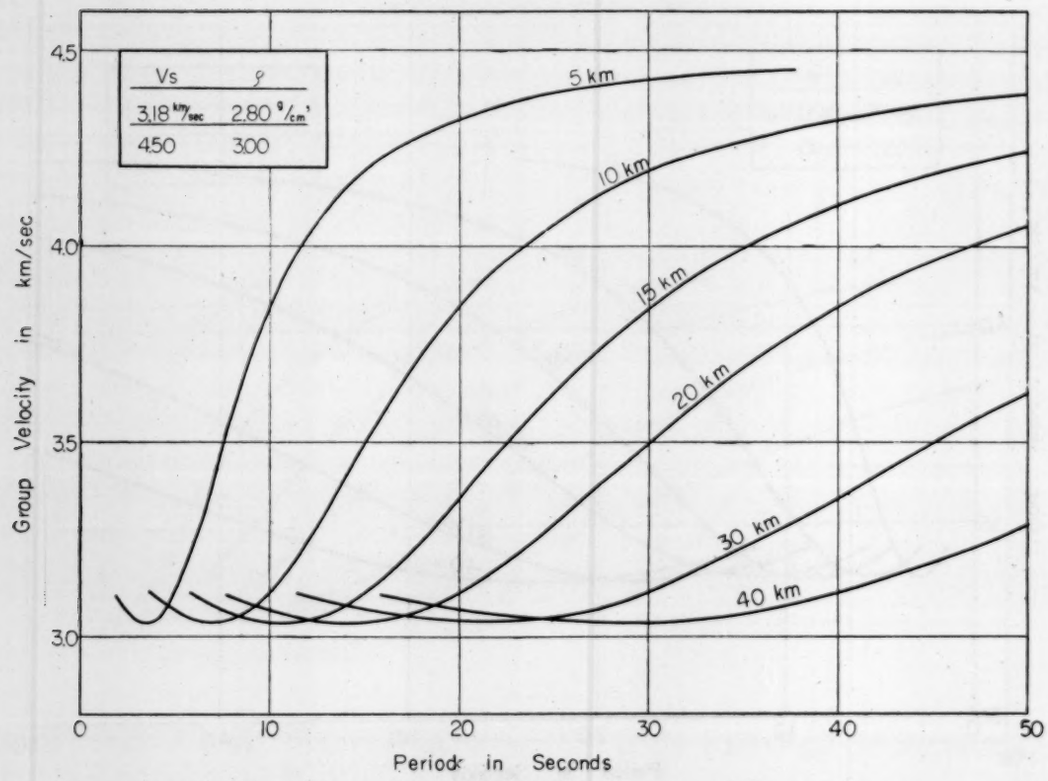

Fig. 33L. Group velocity dispersion curves of Love waves.

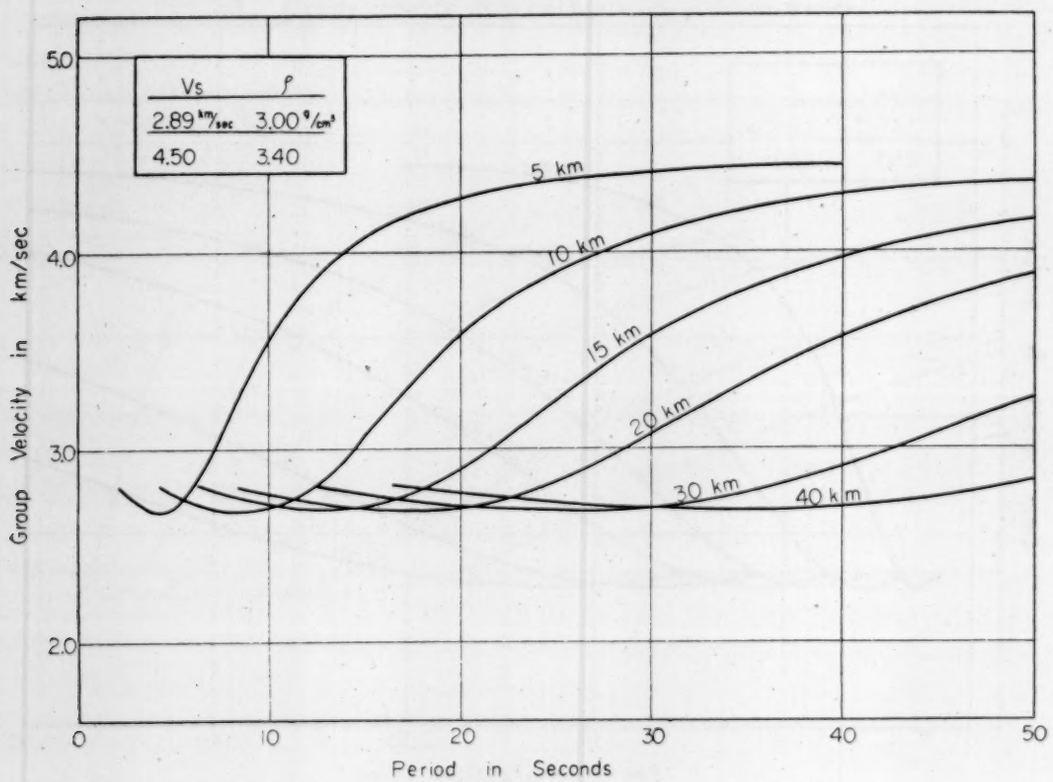

Fig. 34L. Group velocity dispersion curves of Love waves.

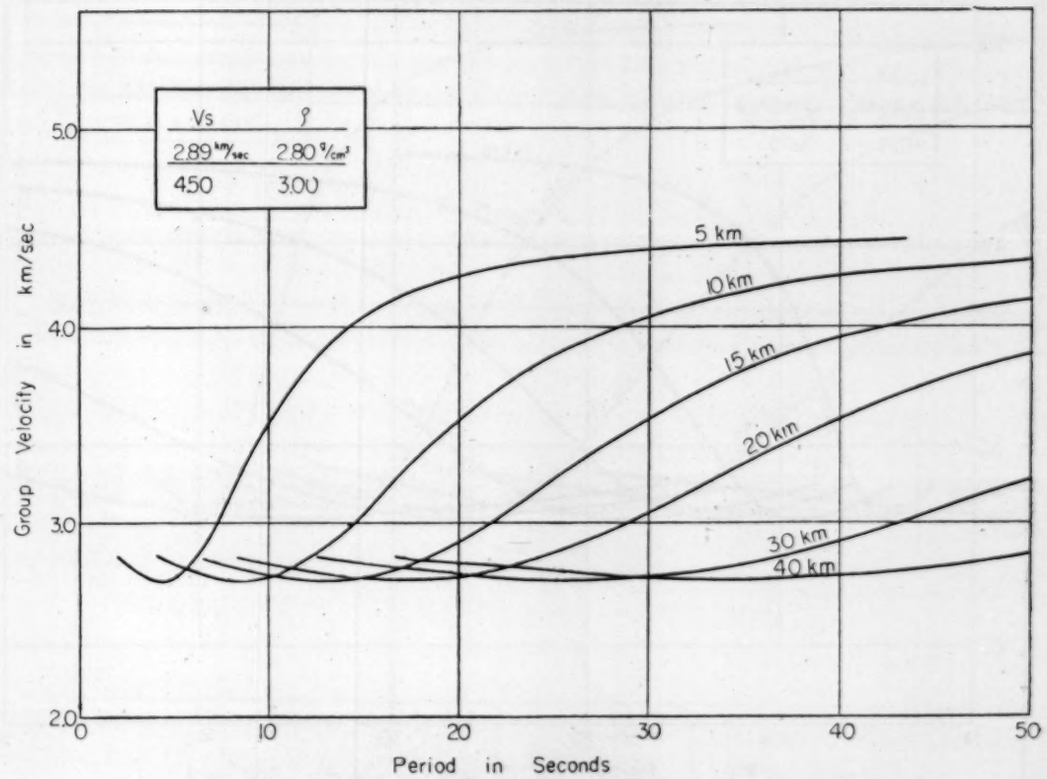

Fig. 35L. Group velocity dispersion curves of Love waves.

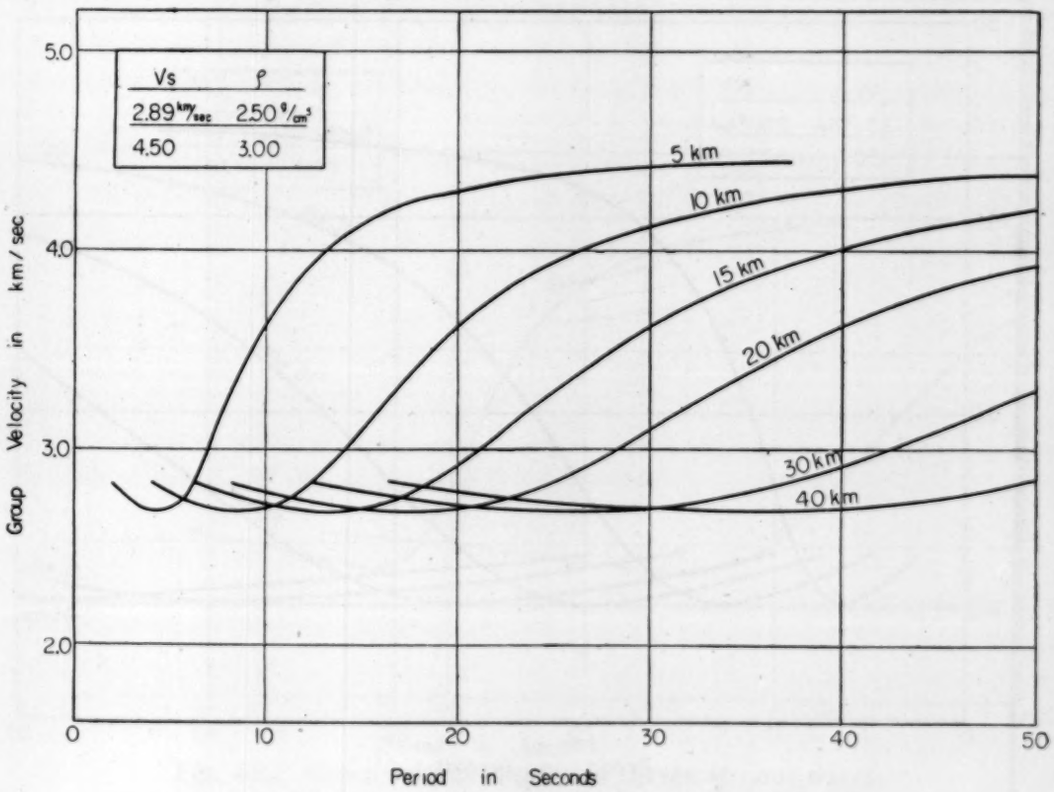

Fig. 36L. Group velocity dispersion curves of Love waves.

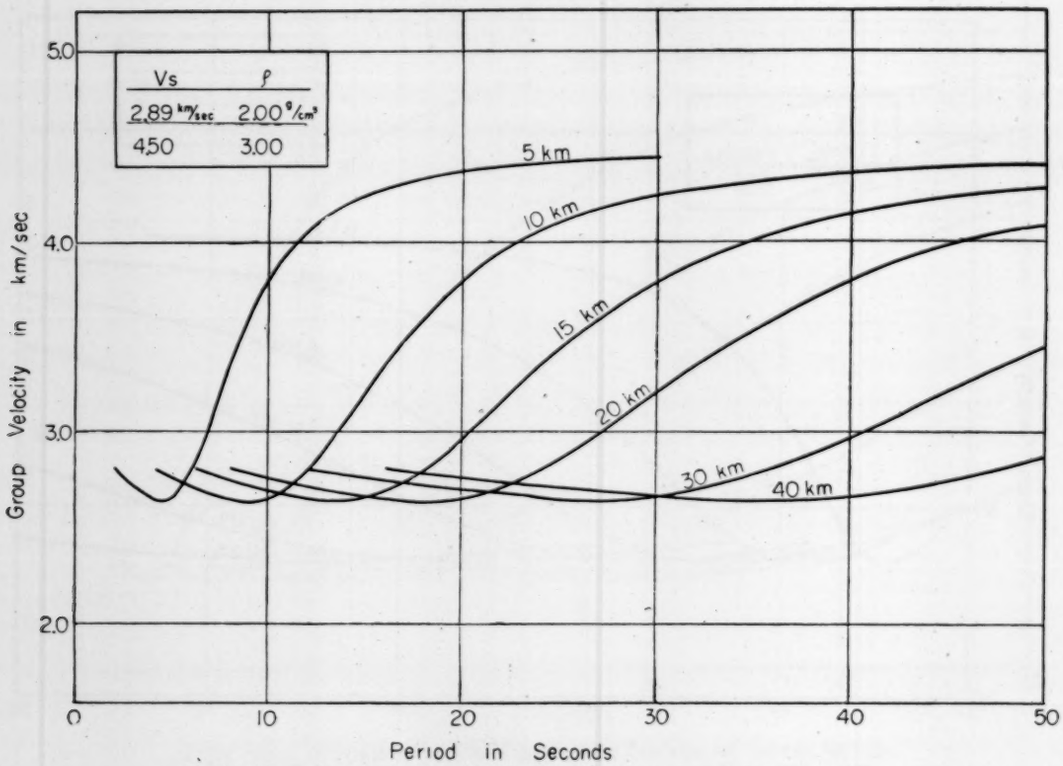

Fig. 37L. Group velocity dispersion curves of Love waves.

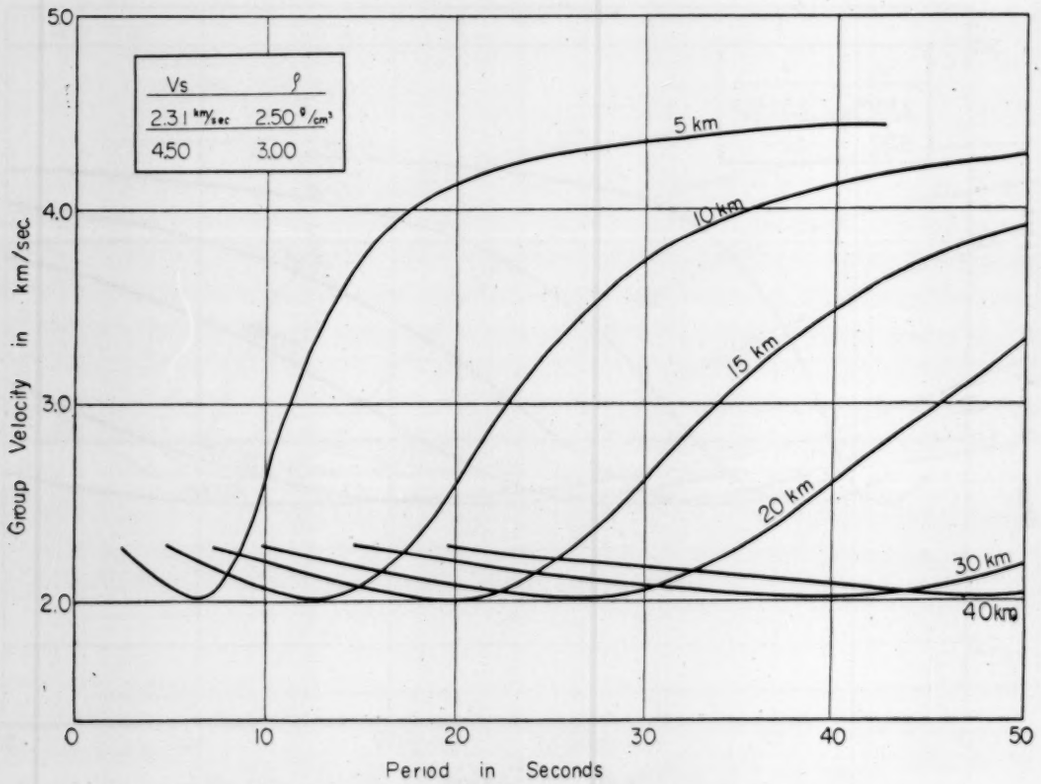

Fig. 38L. Group velocity dispersion curves of Love waves.

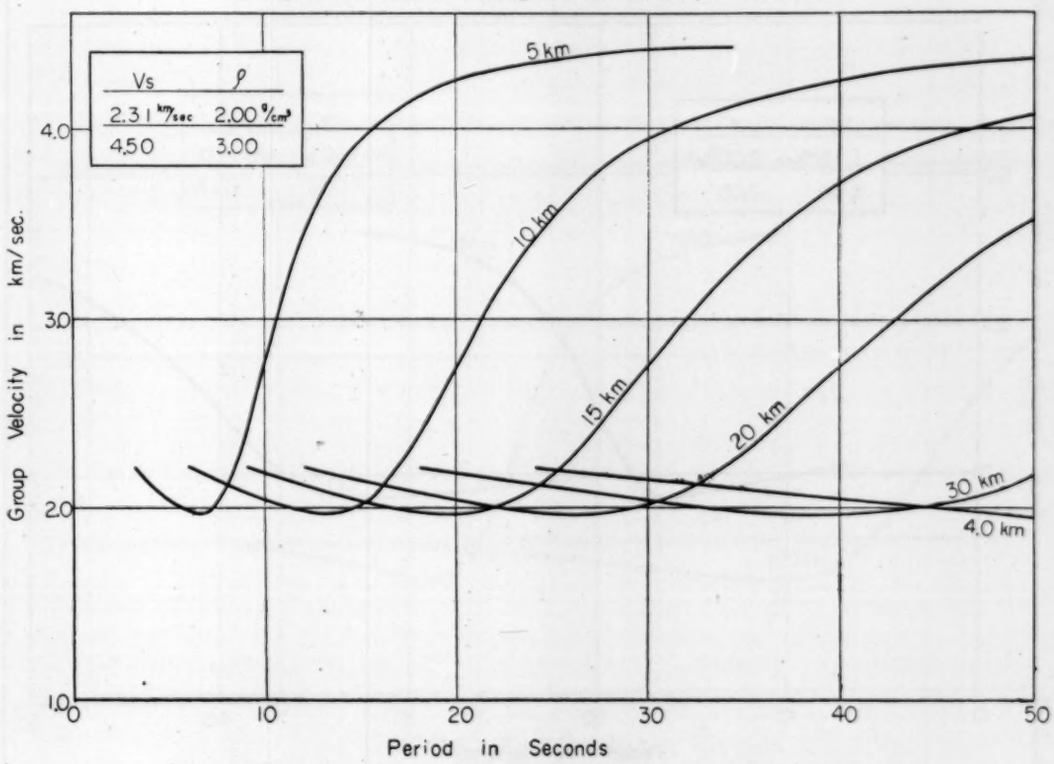

Fig. 39L. Group velocity dispersion curves of Love waves.

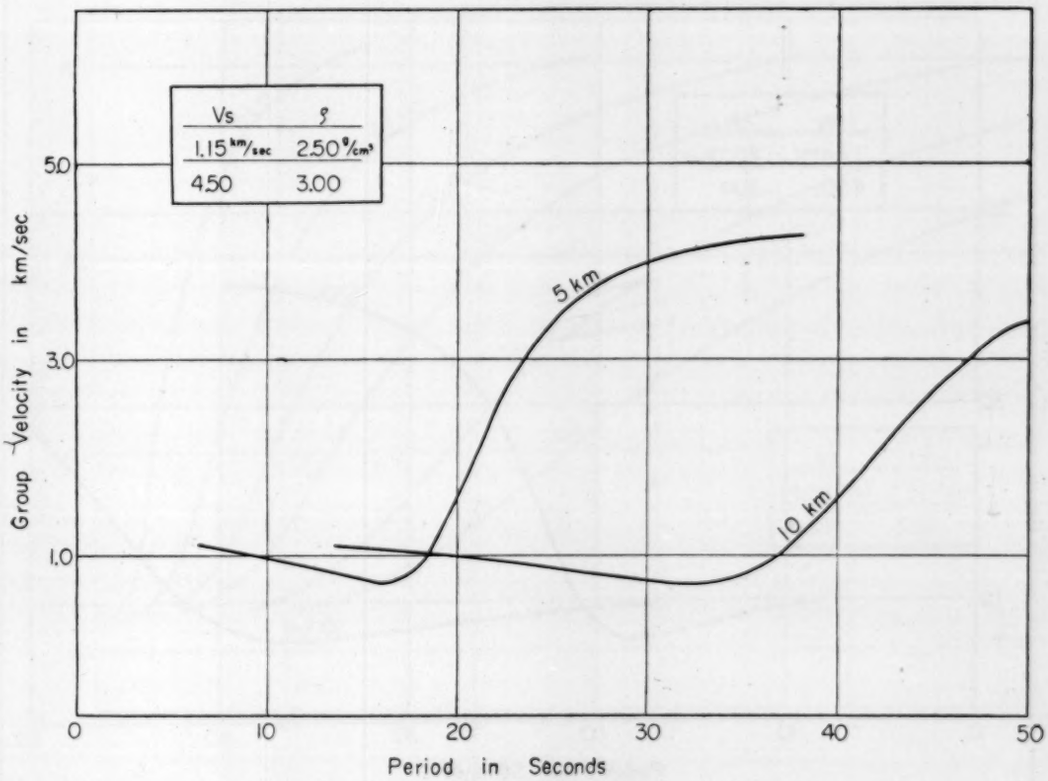

Fig. 40L. Group velocity dispersion curves of Love waves.

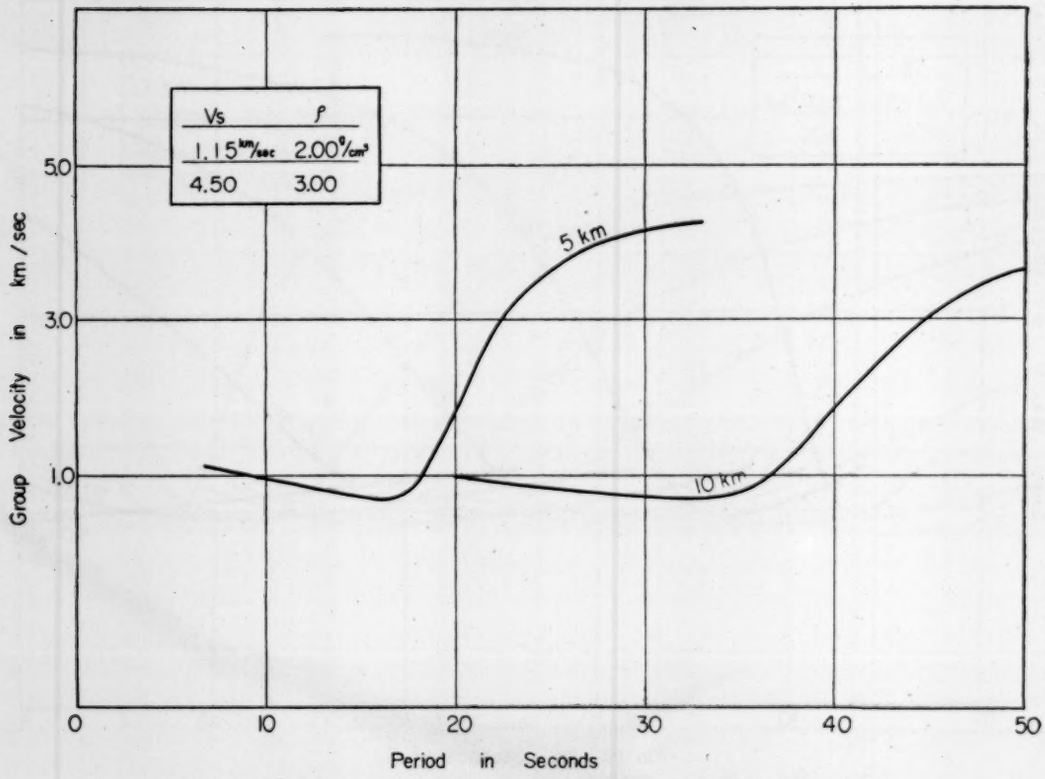

Fig. 41L. Group velocity dispersion curves of Love waves.

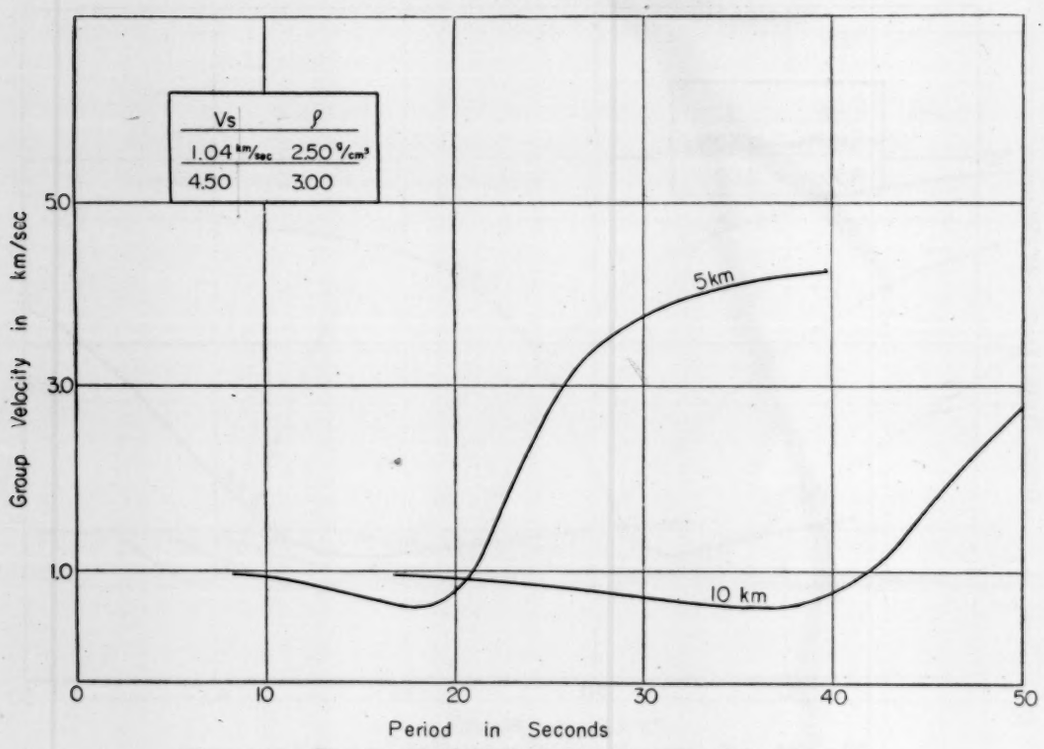

Fig. 42L. Group velocity dispersion curves of Love waves.

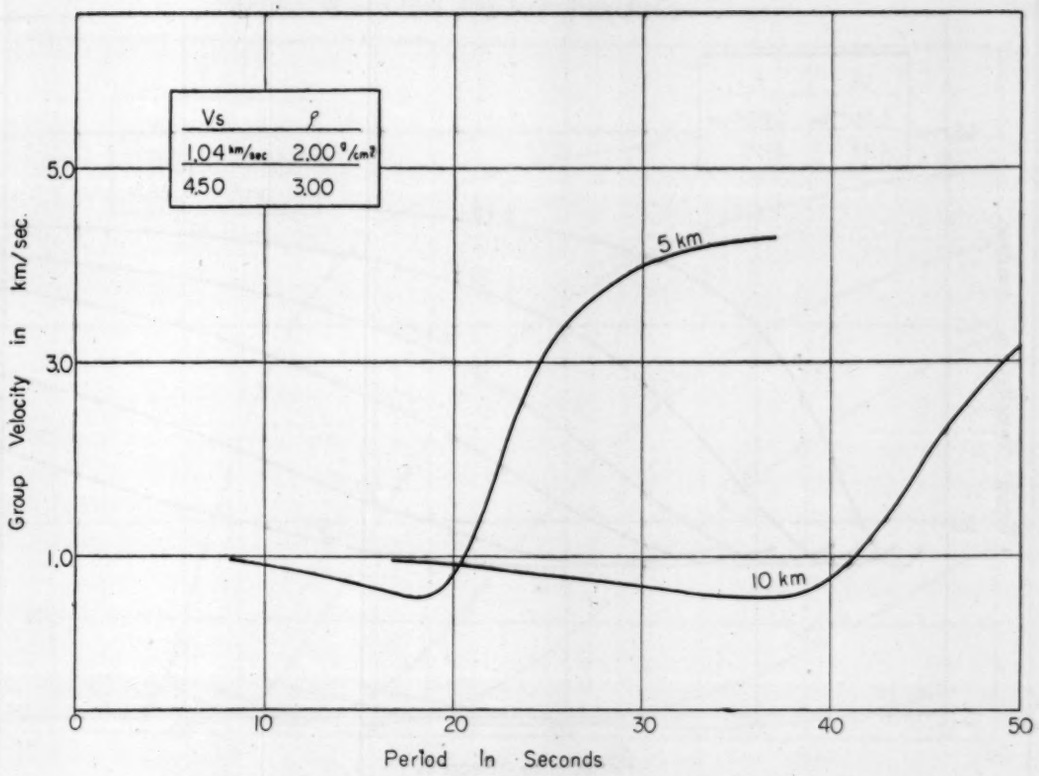

Fig. 43L. Group velocity dispersion curves of Love waves

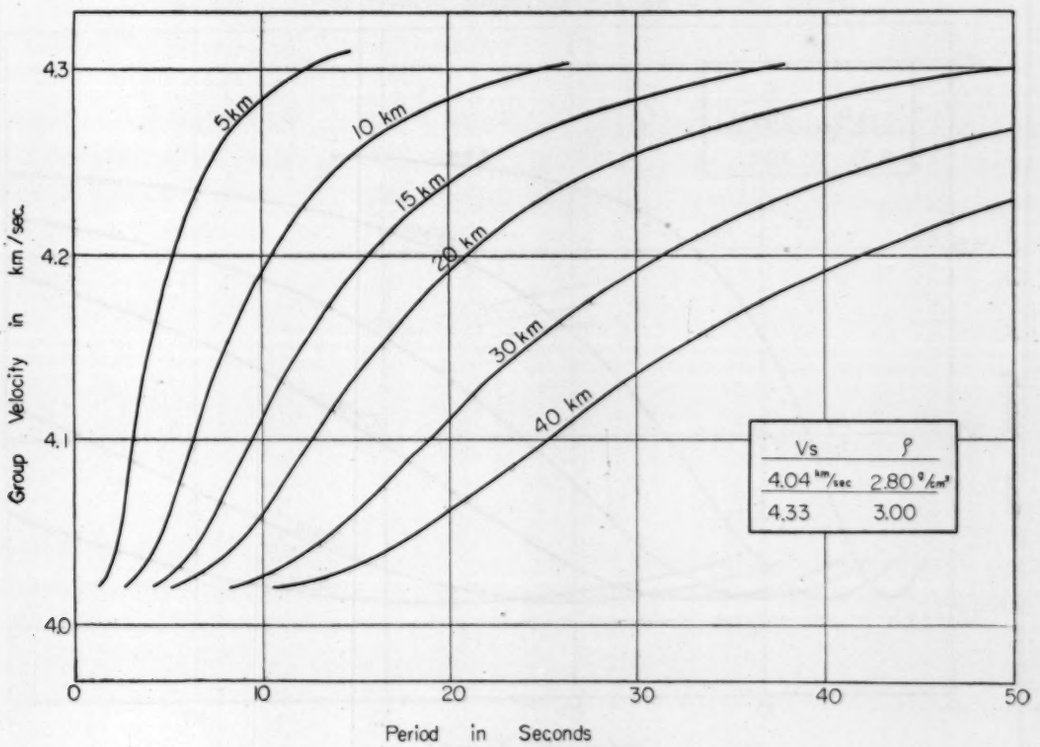

Fig. 44L. Group velocity dispersion curves of Love waves.

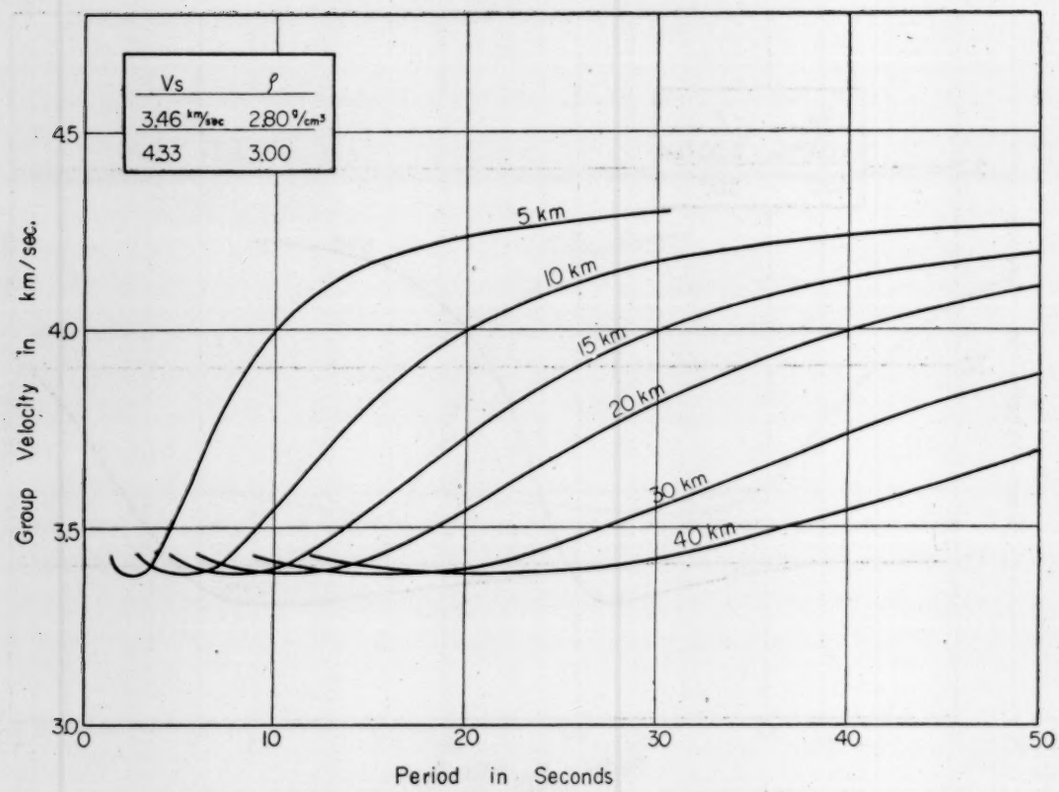

Fig. 46L. Group velocity dispersion curves of Love waves.

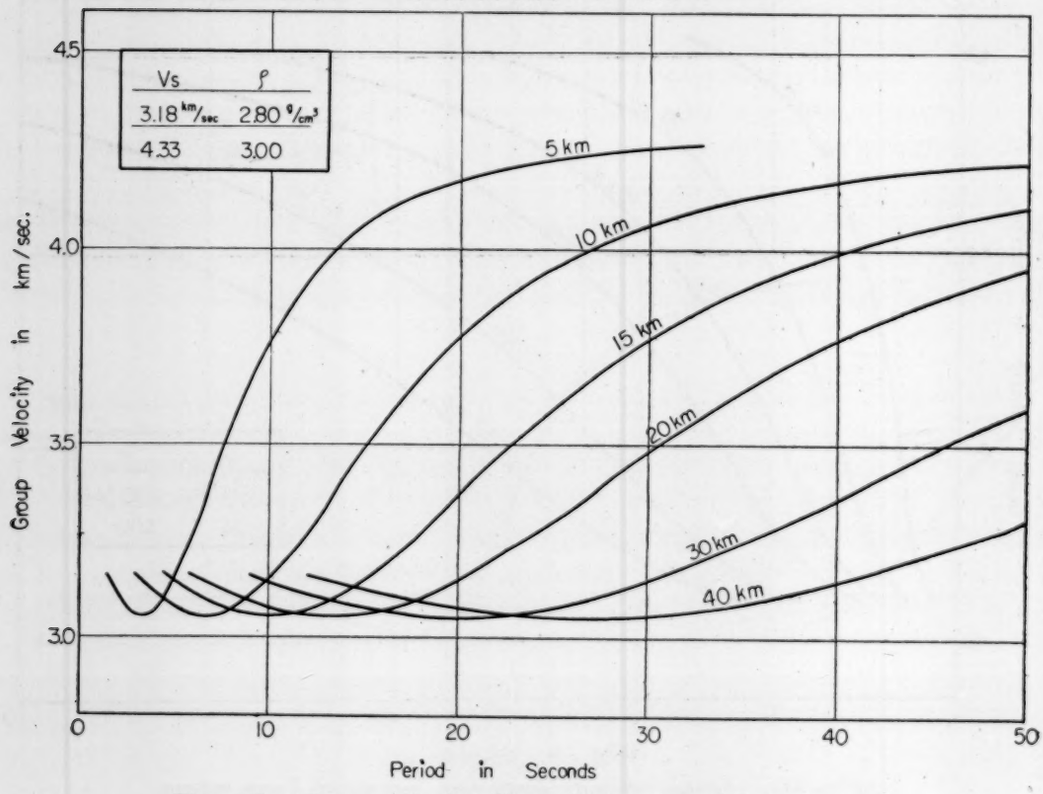

Fig. 47L. Group velocity dispersion curves of Love waves.

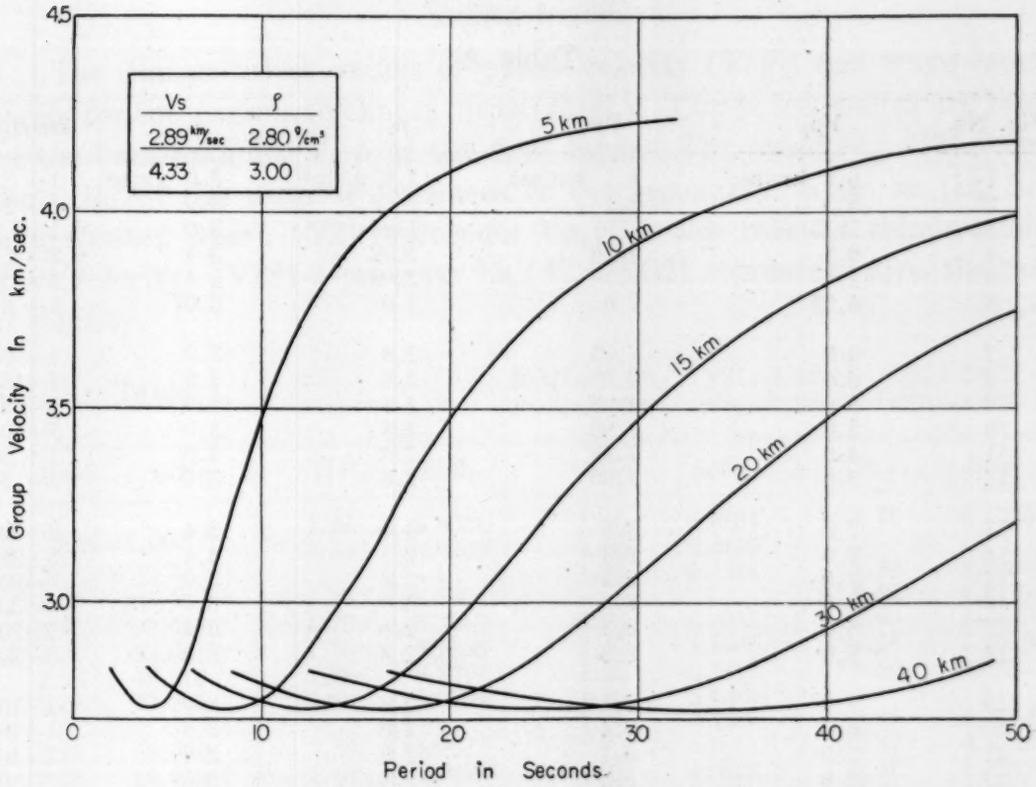

Fig. 48L. Group velocity dispersion curves of Love waves.

Table A

Fig. No.	Vp_2	Vp_3	ρ_2	ρ_3	H_2/H_1
1	6.9 km/sec	8.1 km/sec	2.67 g/cm³	3.0 g/cm³	1— 3
2	5.5	8.1	2.67	3.0	1— 2
3	1.73	7.9	1.8	3.0	0.1—0.3
4	6.5	7.76	3.02	3.4	0.2— 5
5	1.7	7.76	2.08	3.4	0.2— 3
6	6.93	7.8	3.0	3.07	1— 5
7	6.0	7.95	2.8	3.0	1— 5
8	6.0	7.95	2.8	3.0	4—15
9	5.0	7.95	2.8	3.0	1— 5
10	5.0	7.95	2.8	3.0	5—20
11	4.0	7.95	2.8	3.0	1— 5
12	3.0	7.95	2.8	3.0	1— 5
13	7.0	8.3	3.0	3.4	5—20
14	7.0	8.3	2.8	3.4	5—20
15	7.0	8.3	2.8	3.0	5—20
16	5.0	8.3	3.0	3.4	5—30
17	5.0	8.3	2.8	3.4	5—20
18	5.0	8.3	2.8	3.0	5—30
19	7.0	8.1	2.8	3.0	1—10
20	6.0	8.1	2.8	3.0	1—10
21	5.0	8.1	2.5	3.4	1—10
22	5.0	8.1	2.8	3.0	1—10
23	5.0	8.1	2.5	3.0	1—10
24	4.0	8.1	2.5	3.4	1—10
25	4.0	8.1	2.8	3.0	1—10
26	4.0	8.1	2.5	3.0	1—10
27	2.0	8.1	2.5	3.4	1—10
28	2.0	8.1	2.5	3.0	1—10
29	7.0	7.8	3.0	3.4	5—20
30	6.93	7.8	3.0	3.4	5—20
31	6.0	7.8	3.0	3.4	5—20
32	6.0	7.8	2.8	3.0	1—10
33	5.5	7.8	2.8	3.0	1—10
34	5.0	7.8	3.0	3.4	5—20
35	5.0	7.8	2.8	3.0	1—10
36	5.0	7.8	2.5	3.0	1—10
37	5.0	7.8	2.0	3.0	1—10
38	4.0	7.8	2.5	3.0	1—10
39	4.0	7.8	2.0	3.0	1—10
40	2.0	7.8	2.5	3.0	1—10
41	2.0	7.8	2.0	3.0	1—10
42	1.8	7.8	2.5	3.0	1—10
43	1.8	7.8	2.0	3.0	1—10
44	7.0	7.5	2.8	3.0	1—10
45	6.5	7.5	2.8	3.0	5—25
46	6.0	7.5	2.8	3.0	1—10
47	5.5	7.5	2.8	3.0	1—10
48	5.0	7.5	2.8	3.0	1—10
49	4.0	7.5	2.8	3.0	5—20

Vp_i=compressional velocity of ith layer,
Vs_i=shear velocity of ith layer, ($=Vp_i/\sqrt{3}$ for most of the cases)
ρ_i=density of ith layer,
H_i=thickness of ith layer.

Tables 1—49.

The dimensionless values of phase velocity (V/V_1) and wave length (L/H_1) for the various thickness ratios (H_2/H_1). Computed values are based on the constants H, V, ρ of the first layer. For example: H21 represents H_2/H_1, the ratio of thickness of the secondary layer to the first layer (water layer). V21 represents Vp_2/V_1, the ratio of compressional wave velocity. V2S1 represents Vs_2/V_1. RO21 represents ρ_2/ρ_1, the ratio of density.

Table 1.

RO21=2.670 V21=4.540 V2S1=2.621
RO31=3.000 V31=5.329 V3S1=3.077

V/V_1	L/H_1
H21=1.000	
2.82	209.32
2.81	97.466
2.80	63.071
2.79	46.518
2.78	36.895
2.77	30.698
2.76	26.443
2.75	23.393
2.74	21.133
2.73	19.416
2.72	18.084
2.71	17.029
2.70	16.177
2.69	15.479
2.68	14.897
2.67	14.405
2.66	13.984
2.65	13.618
2.63	13.297
2.60	12.321
2.55	11.495
2.50	10.889
2.45	10.401
2.40	9.9819
2.35	9.6074
2.30	9.2634
2.25	8.9400
2.20	8.6320
2.15	8.3349
2.10	8.0461
2.05	7.7636
2.00	7.4856
1.95	7.2107
1.90	6.9381
1.85	6.6669
1.80	6.3962
1.75	6.1252
1.70	5.8533
1.65	5.5797
1.60	5.3034
1.55	5.0237
1.50	4.7395
1.45	4.4494
1.40	4.1520
1.35	3.8451
1.30	3.5256
1.25	3.1897
H21=1.200	
2.70	16.548
2.65	13.797
2.60	12.433
2.55	11.577
2.50	10.954
2.45	10.454
2.40	10.029
2.35	9.649
2.30	9.3011
2.25	8.9751
2.20	8.6642
2.15	8.3651
2.10	8.0746
2.05	7.7901
2.00	7.5108
1.95	7.2346
1.90	6.9608
1.85	6.6884
1.80	6.4165
1.75	6.1444
1.70	5.8715
1.65	5.5968
1.60	5.3195
1.55	5.0388
1.50	4.7534
1.45	4.4624
1.40	4.1638
1.35	3.8557
1.30	3.5349
1.25	3.1975
H21=1.400	
2.70	66.918
2.65	13.986
2.60	12.556
2.55	11.668
2.50	11.027
2.45	10.516
2.40	10.082
2.35	9.6969
2.30	9.3442
2.25	9.0143
2.20	8.7002
2.15	8.3983
2.10	8.1055
2.05	7.8192
2.00	7.5379
1.95	7.2597
1.90	6.9843
1.85	6.7106
1.80	6.4372
1.75	6.1638
1.70	5.8894
1.65	5.6135
1.60	5.3349
1.55	5.0529
1.50	4.7662
1.45	4.4738
1.40	4.1739
1.35	3.8643
1.30	3.5421
1.25	3.2030
H21=1.600	
2.70	17.297
2.65	14.191
2.60	12.694
2.55	11.771
2.50	11.110
2.45	10.586
2.40	10.143
2.35	9.7504
2.30	9.3917
2.25	9.0571
2.20	8.7397
2.15	8.4346
2.10	8.1386
2.05	7.8496
2.00	7.5661
1.95	7.2859
1.90	7.0086
1.85	6.7327
1.80	6.4578
1.75	6.1827

(to be continued)

Table 1. (continued)

V/V_1	L/H_1	V/V_1	L/H_1	V/V_1	L/H_1	V/V_1	L/H_1
1.70	5.9066	1.45	4.4913	2.05	7.9142	2.60	14.216
1.65	5.6291	1.40	4.1883	2.00	7.6244	2.55	12.936
1.60	5.3490	1.35	3.8757	1.95	7.3390	2.50	12.034
1.55	5.0654	1.30	3.5508	1.90	7.0565		
1.50	4.7774	1.25	3.2092	1.85	6.7761	2.45	11.340
						2.40	10.770
1.45	4.4834			1.80	6.4966	2.35	10.280
1.40	4.1820	H21=2.000		1.75	6.2174	2.30	9.8449
1.35	3.8709			1.70	5.9375	2.25	9.4477
1.30	3.5473			1.65	5.6562		
1.25	3.2068	2.82	312.90	1.60	5.3726	2.20	9.0784
		2.81	142.94			2.15	8.7295
		2.80	90.321	1.55	5.0857	2.10	8.3966
H21=1.800		2.79	64.833	1.50	4.7944	2.05	8.0752
		2.78	49.893	1.45	4.4974	2.00	7.7631
				1.40	4.1931		
2.70	17.691	2.77	40.215	1.35	3.8793	1.95	7.4581
2.65	14.416	2.76	33.560			1.90	7.1585
2.60	12.849	2.75	28.818	1.30	3.5532	1.85	6.8626
2.55	11.890	2.74	25.355	1.25	3.2106	1.80	6.5697
2.50	11.205	2.73	22.777			1.75	6.2785
2.45	10.666	2.72	20.819	H21=3.000		1.70	5.9880
2.40	10.211	2.71	19.302			1.65	5.6973
2.35	9.8095	2.70	18.105			1.60	5.4053
2.30	9.4445	2.69	17.142	2.80	117.099	1.55	5.1112
2.25	9.1042	2.68	16.353	2.79	82.678	1.50	4.8137
				2.78	62.445		
2.20	8.7822	2.67	15.696	2.77	49.325	1.45	4.5115
2.15	8.4729	2.66	15.140	2.76	40.362	1.40	4.2029
2.10	8.1734	2.65	14.664			1.35	3.8857
2.05	7.8817	2.64	14.252	2.75	34.080	1.30	3.5570
2.00	7.5949	2.60	13.023	2.74	29.592	1.25	3.2127
				2.73	26.321		
1.95	7.3126	2.55	12.022	2.72	23.881		
1.90	7.0327	2.50	11.318	2.71	22.012		
1.85	6.7547	2.45	10.7540				
1.80	6.4778	2.40	10.2859	2.70	20.544		
1.75	6.2006	2.35	9.8747	2.69	19.363		
				2.68	18.393		
1.70	5.9227	2.30	9.5017	2.67	17.581		
1.65	5.6434	2.25	9.1550	2.66	16.890		
1.60	5.3616	2.20	8.8271				
1.55	5.0763	2.15	8.5132	2.65	16.296		
1.50	4.7867	2.10	8.2099	2.64	15.776		

Table 2.

RO21=2.670 V21=3.61842 V2S1=2.08909
RO31=3.000 V31=5.32894 VS31=3.07667

V/V_1	L/H_1	V/V_1	L/H_1	V/V_1	L/H_1	V/V_1	L/H_1
H21=1.000		H21=1.250		H21=1.500		H21=1.750	
2.80	98.176	2.80	114.29	2.80	130.49	2.80	146.64
2.79	72.528	2.79	84.270	2.79	96.044	2.79	107.83
2.78	57.459	2.78	66.594	2.78	75.770	2.78	84.954
2.77	47.564	2.77	54.963	2.77	62.399	2.77	69.881
2.76	40.592	2.76	46.740	2.76	52.948	2.76	59.188
2.75	35.426	2.75	40.634	2.75	45.914	2.75	51.234
2.74	31.458	2.74	35.933	2.74	40.484	2.74	45.080
2.73	28.327	2.73	32.207	2.73	36.172	2.73	40.192
2.72	25.810	2.72	29.197	2.72	32.681	2.72	36.218
2.71	23.748	2.71	26.721	2.71	29.799	2.71	32.939
2.70	22.041	2.70	24.661	2.70	27.392	2.70	30.192
2.69	20.608	2.69	22.928	2.69	25.360	2.69	27.864
2.68	19.399	2.68	21.454	2.68	23.626	2.68	25.878
2.67	18.368	2.67	20.196	2.67	22.142	2.67	24.171
2.66	17.484	2.66	19.112	2.66	20.859	2.66	22.694
2.65	16.721	2.65	18.175	2.65	19.748	2.65	21.410
2.64	16.059	2.64	17.361	2.64	18.779	2.64	20.289
2.60	14.125	2.60	14.985	2.60	15.950	2.60	17.008
2.55	12.656	2.55	13.210	2.55	13.848	2.55	14.574
2.50	11.705	2.50	12.095	2.50	12.553	2.50	13.086
2.45	11.015	2.45	11.311	2.45	11.662	2.45	12.076
2.40	10.470	2.40	10.708	2.40	10.991	2.40	11.329
2.35	10.012	2.35	10.211	2.35	10.449	2.35	10.733
2.30	9.6085	2.30	9.7805	2.30	9.9862	2.30	10.231
2.25	9.2422	2.25	9.3944	2.25	9.5758	2.25	9.7911
2.20	8.9016	2.20	9.0386	2.20	9.2008	2.20	9.3932
2.15	8.5792	2.15	8.7040	2.15	8.8513	2.15	9.0245
2.10	8.2700	2.10	8.3851	2.10	8.5197	2.10	8.6768
2.05	7.9710	2.05	8.0776	2.05	8.2019	2.05	8.3453
2.00	7.6793	2.00	7.7789	2.00	7.8936	2.00	8.0253
1.95	7.3928	1.95	7.4862	1.95	7.5931	1.95	7.7139
1.90	7.1103	1.90	7.1982	1.90	7.2978	1.90	7.4089
1.85	6.8305	1.85	6.9134	1.85	7.0062	1.85	7.1088
1.80	6.5522	1.80	6.6307	1.80	6.7174	1.80	6.8116
1.75	6.2745	1.75	6.3488	1.75	6.4298	1.75	6.5164
1.70	5.9966	1.70	6.0670	1.70	6.1426	1.70	6.2219
1.65	5.7177	1.65	5.7844	1.65	5.8547	1.65	5.9269
1.60	5.4368	1.60	5.4999	1.60	5.5651	1.60	5.6305
1.55	5.1531	1.55	5.2126	1.55	5.2727	1.55	5.3313
1.50	4.8652	1.50	4.9212	1.50	4.9763	1.50	5.0283
1.45	4.5721	1.45	4.6245	1.45	4.6743	1.45	4.7198
1.40	4.2721	1.40	4.3208	1.40	4.3652	1.40	4.4039
1.35	3.9631	1.35	4.0077	1.35	4.0465	1.35	4.0785
1.30	3.6422	1.30	3.6824	1.30	3.7153	1.30	3.7404
1.25	3.3053	1.25	3.3404	1.25	3.3669	1.25	3.3853

(to be continued)

Table 2. (continued)

V/V_1	L/H_1	V/V_1	L/H_1	V/V_1	L/H_1	V/V_1	L/H_1
H21=2.000		2.70	33.033	2.35	11.069	1.75	6.6076
		2.69	30.421	2.30	10.522		
		2.68	28.184	2.25	10.046	1.70	6.3036
2.80	162.78	2.67	26.260			1.65	5.9996
2.79	119.61	2.66	24.591	2.20	9.6186	1.60	5.6946
2.78	94.167			2.15	9.2263	1.55	5.3870
2.77	77.369	2.65	23.140	2.10	8.8587	1.50	5.0759
2.76	65.456	2.64	21.870	2.05	8.5094		
		2.60	18.148	2.00	8.1742	1.45	4.7595
2.75	56.572	2.55	15.382			1.40	4.4360
2.74	49.708	2.50	13.695	1.95	7.8492	1.35	4.1033
2.73	44.238			1.90	7.5321	1.30	3.7584
2.72	39.793	2.45	12.560	1.85	7.2203	1.25	3.3972
2.71	36.118	2.40	11.727	1.80	6.9126		

Table 3.

RO21=1.800 V21=1.140 V2S1=0.658
RO31=3.000 V31=5.200 V3S1=3.000

V/V_1	L/H_1
H21=0.100	
2.75	133.17
2.74	62.367
2.73	41.722
2.72	32.092
2.71	26.621
2.70	23.149
2.69	20.779
2.65	16.008
2.60	13.642
2.55	12.420
2.50	11.623
2.45	11.028
2.40	10.541
2.35	10.120
2.30	9.7413
2.25	9.3911
2.20	9.0615
2.15	8.7464
2.10	8.4423
2.05	8.1465
2.00	7.8565
1.95	7.5711
1.90	7.2889
1.85	7.0088
1.80	6.7300
1.75	6.4518
1.70	6.1732
1.65	5.8936
1.60	5.6123
1.55	5.3283
1.50	5.0408
1.45	4.7486
1.40	4.4506
1.35	4.1450
1.30	3.8300
1.25	3.5023
1.20	3.1582
1.15	2.7915
1.10	2.3929
1.05	1.9468
H21=0.200	
2.75	159.50
2.74	74.285
2.73	49.279
2.72	37.530
2.71	30.801
2.70	26.506
2.69	23.558
2.65	17.615
2.60	14.720
2.55	13.274
2.50	12.360
2.45	11.692
2.40	11.157
2.35	10.700
2.30	10.294
2.25	9.9211
2.20	9.5721
2.15	9.2404
2.10	8.9217
2.05	8.6121
2.00	8.3101
1.95	8.0133
1.90	7.7205
1.85	7.4309
1.80	7.1430
1.75	6.8564
1.70	6.5701
1.65	6.2836
1.60	5.9959
1.55	5.7065
1.50	5.4144
1.45	5.1190
1.40	4.8192
1.35	4.5137
1.30	4.2011
1.25	3.8797
1.20	3.5470
1.15	3.2001
1.10	2.8355
1.05	2.4496
H21=0.300	
2.75	186.02
2.74	86.377
2.73	57.058
2.72	43.214
2.71	35.243
2.70	30.123
2.69	26.594
2.65	19.426
2.60	15.936
2.55	14.227
2.50	13.173
2.45	12.419
2.40	11.826
2.35	11.328
2.30	10.889
2.25	10.490
2.20	10.119
2.15	9.7679
2.10	9.4321
2.05	9.1076
2.00	8.7915
1.95	8.4821
1.90	8.1778
1.85	7.8772
1.80	7.5793
1.75	7.2833
1.70	6.9884
1.65	6.6940
1.60	6.3992
1.55	6.1034
1.50	5.8061
1.45	5.5065
1.40	5.2038
1.35	4.8970
1.30	4.5853
1.25	4.2676
1.20	3.9425
1.15	3.6086
1.10	3.2647
1.05	2.9103

Table 4.

RO21=3.0197 V21=4.27631 V2S1=2.46052
RO31=3.4030 V31=5.10526 V3S1=2.86842

V/V_1	L/H_1
H21=0.200	
2.61	27.786
2.60	22.869
2.59	19.837
2.58	17.810
2.57	16.373
2.56	15.309
2.55	14.492
2.54	13.845
2.50	12.199
2.45	11.086
2.40	10.374
2.35	9.8405
2.30	9.4021
2.25	9.0194
2.20	8.6719
2.15	8.3482
2.10	8.0406
2.05	7.7448
2.00	7.4570
1.95	7.1754
1.90	6.8978
1.85	6.6229
1.80	6.3495
1.75	6.0768
1.70	5.8036
1.65	5.5293
1.60	5.2527
1.55	4.9729
1.50	4.6889
1.45	4.3992
1.40	4.1022
1.35	3.7959
1.30	3.4773
1.25	3.1423
1.20	2.7845
1.15	2.3930
H21=0.600	
2.61	35.265
2.60	28.086
2.59	23.624
2.58	20.636
2.57	18.534
2.56	16.995
2.55	15.833
2.54	14.930
2.50	12.738
2.45	11.373
2.40	10.556
2.35	9.9705
2.30	9.5028
2.25	9.1014
2.20	8.7420
2.15	8.4093
2.10	8.0955
2.05	7.7948
2.00	7.5033
1.95	7.2185
1.90	6.9383
1.85	6.6613
1.80	6.3863
1.75	6.1119
1.70	5.8375
1.65	5.5619
1.60	5.2843
1.55	5.0037
1.50	4.7189
1.45	4.4287
1.40	4.1313
1.35	3.8247
1.30	3.5060
1.25	3.1711
1.20	2.8136
1.15	2.4230
H21=1.000	
2.61	42.650
2.60	33.235
2.59	27.347
2.58	23.390
2.57	20.613
2.56	18.593
2.55	17.081
2.54	15.925
2.50	13.212
2.45	11.626
2.40	10.721
2.35	10.093
2.30	9.6014
2.25	9.1852
2.20	8.8150
2.15	8.4752
2.10	8.1558
2.05	7.8504
2.00	7.5553
1.95	7.2674
1.90	6.9844
1.85	6.7052
1.80	6.4280
1.75	6.1518
1.70	5.8756
1.65	5.5984
1.60	5.3193
1.55	5.0372
1.50	4.7510
1.45	4.4593
1.40	4.1605
1.35	3.8523
1.30	3.5320
1.25	3.1951
1.20	2.8353
1.15	2.4413
H21=1.400	
2.61	49.928
2.60	38.291
2.59	30.981
2.58	26.065
2.57	22.622
2.56	20.132
2.55	18.287
2.54	16.891
2.50	13.698
2.45	11.905
2.40	10.915
2.35	10.243
2.30	9.7243
2.25	9.2903
2.20	8.9072
2.15	8.5575
2.10	8.2304
2.05	7.9185
2.00	7.6181
1.95	7.3255
1.90	7.0385
1.85	6.7554
1.80	6.4749
1.75	6.1955
1.70	5.9161
1.65	5.6361
1.60	5.3541
1.55	5.0693
1.50	4.7804
1.45	4.4859
1.40	4.1843
1.35	3.8732
1.30	3.5497
1.25	3.2095
1.20	2.8462
1.15	2.4484
H21=1.800	
2.61	57.122
2.60	43.265
2.59	34.544
2.58	28.683
2.57	24.593
2.56	21.659
2.55	19.507
2.54	17.893
2.50	14.258
2.45	12.255
2.40	11.166
2.35	10.438
2.30	9.8830
2.25	9.4236
2.20	9.0224
2.15	8.6586
2.10	8.3198
2.05	7.9985
2.00	7.6898
1.95	7.3901
1.90	7.0969
1.85	6.8083
1.80	6.5224
1.75	6.2384
1.70	5.9547

(to be continued)

Table 4. (continued)

V/V_1	L/H_1
1.65	5.6705
1.60	5.3846
1.55	5.0959
1.50	4.8033
1.45	4.5054
1.40	4.2003
1.35	3.8860
1.30	3.5594
1.25	3.2163
1.20	2.8504
H21=2.200	
2.61	64.240
2.60	48.173
2.59	38.050
2.58	31.263
2.57	26.554
2.56	23.211
2.55	20.781
2.54	18.971
2.50	14.925
2.45	12.697
2.40	11.487
2.35	10.685
2.30	10.081
2.25	9.5872
2.20	9.1602
2.15	8.7758
2.10	8.4210
2.05	8.0865
2.00	7.7666
1.95	7.4575
1.90	7.1559
1.85	6.8598
1.80	6.5674
1.75	6.2772
1.70	5.9882
1.65	5.6990
1.60	5.4085
1.55	5.1157
1.50	4.8193
1.45	4.5179
1.40	4.2098
1.35	3.8928
1.30	3.5639
1.25	3.2190
1.20	2.8516

V/V_1	L/H_1
1.15	2.4510
H21=2.600	
2.61	71.310
2.60	53.033
2.59	41.511
2.58	33.822
2.57	28.529
2.56	24.808
2.55	22.129
2.54	20.143
2.50	15.709
2.45	13.237
2.40	11.883
2.35	10.987
2.30	10.319
2.25	9.7796
2.20	9.3180
2.15	8.9070
2.10	8.5310
2.05	8.1792
2.00	7.8452
1.95	7.5238
1.90	7.2119
1.85	6.9069
1.80	6.6068
1.75	6.3100
1.70	6.0150
1.65	5.7206
1.60	5.4258
1.55	5.1290
1.50	4.8294
1.45	4.5252
1.40	4.2148
1.35	3.8960
1.30	3.5657
1.25	3.2201
1.20	2.8521
1.15	2.4513
H21=3.000	
2.61	78.344
2.60	57.839
2.59	44.938
2.58	36.369

V/V_1	L/H_1
2.57	30.527
2.56	26.458
2.55	23.551
2.54	21.406
2.50	16.600
2.45	13.871
2.40	12.353
2.35	11.345
2.30	10.597
2.25	9.9992
2.20	9.4937
2.15	9.0489
2.10	8.6462
2.05	8.2734
2.00	7.9218
1.95	7.5864
1.90	7.2628
1.85	6.9480
1.80	6.6396
1.75	6.3359
1.70	6.0353
1.65	5.7362
1.60	5.4373
1.55	5.1375
1.50	4.8353
1.45	4.5291
1.40	4.2172
1.35	3.8975
1.30	3.5665
1.25	3.2202
1.20	2.8522
1.15	2.4514
H21=3.400	
2.61	85.326
2.60	62.618
2.59	48.341
2.58	38.916
2.57	32.552
2.56	28.160
2.55	25.041
2.54	22.748
2.50	17.581
2.45	14.589
2.40	12.893
2.35	11.756
2.30	10.913

V/V_1	L/H_1
2.25	10.244
2.20	9.6840
2.15	9.1983
2.10	8.7634
2.05	8.3653
2.00	7.9941
1.95	7.6429
1.90	7.3067
1.85	6.9819
1.80	6.6655
1.75	6.3553
1.70	6.0496
1.65	5.7466
1.60	5.4446
1.55	5.1425
1.50	4.8386
1.45	4.5311
1.40	4.2184
1.35	3.8980
1.30	3.5668
1.25	3.2205
1.20	2.8521
1.15	2.4512
H21=3.800	
2.61	92.303
2.60	67.379
2.59	51.735
2.58	41.467
2.57	34.600
2.56	29.907
2.55	26.591
2.54	24.154
2.50	18.635
2.45	15.377
2.40	13.493
2.35	12.215
2.30	11.263
2.25	10.510
2.20	9.8868
2.15	9.3521
2.10	8.8798
2.05	8.4533
2.00	8.0602
1.95	7.6922
1.90	7.3434

(to be continued)

Table 4. (continued)

V/V_1	L/H_1
1.85	7.0087
1.80	6.6851
1.75	6.3693
1.70	6.0594
1.65	5.7532
1.60	5.4491
1.55	5.1453
1.50	4.8403
1.45	4.5322
1.40	4.2190
1.35	3.8983
1.30	3.5670
1.25	3.2204
1.20	2.8524
1.15	2.4523
H21=4.200	
2.61	99.221
2.60	72.114
2.59	55.111
2.58	44.020
2.57	36.677
2.56	31.693
2.55	28.188
2.54	25.611
2.50	19.746
2.45	16.222
2.40	14.146
2.35	12.717
2.30	11.645
2.25	10.797
2.20	10.099

V/V_1	L/H_1
2.15	9.5075
2.10	8.9931
2.05	8.5351
2.00	8.1190
1.95	7.7341
1.90	7.3730
1.85	7.0296
1.80	6.6994
1.75	6.3790
1.70	6.0659
1.65	5.7574
1.60	5.4517
1.55	5.1469
1.50	4.8412
1.45	4.5326
1.40	4.2193
1.35	3.8984
1.30	3.5669
1.25	3.2205
1.20	2.8525
1.15	2.4524
H21=4.600	
2.61	106.15
2.60	76.814
2.59	58.477
2.58	46.583
2.57	38.772
2.56	33.510
2.55	29.822
2.54	27.110
2.50	20.899
2.45	17.112

V/V_1	L/H_1
2.40	14.843
2.35	13.257
2.30	12.055
2.25	11.100
2.20	10.318
2.15	9.6625
2.10	9.1009
2.05	8.6094
2.00	8.1698
1.95	7.7686
1.90	7.3961
1.85	7.0450
1.80	6.7095
1.75	6.3856
1.70	6.0700
1.65	5.7599
1.60	5.4532
1.55	5.1477
1.50	4.8416
1.45	4.5329
1.40	4.2194
1.35	3.8984
1.30	3.5671
1.25	3.2209
1.20	2.8523
1.15	2.4520
H21=5.000	
2.61	113.09
2.60	81.515
2.59	61.833
2.58	49.156
2.57	40.886

V/V_1	L/H_1
2.56	35.361
2.55	31.486
2.54	28.641
2.50	22.086
2.45	18.038
2.40	15.574
2.35	13.828
2.30	12.489
2.25	11.417
2.20	10.541
2.15	9.8143
2.10	9.2021
2.05	8.6755
2.00	8.2125
1.95	7.7962
1.90	7.4138
1.85	7.0560
1.80	6.7163
1.75	6.3899
1.70	6.0724
1.65	5.7615
1.60	5.4540
1.55	5.1482
1.50	4.8419
1.45	4.5331
1.40	4.2193
1.35	3.8985
1.30	3.5671
1.25	3.2203
1.20	2.8531
1.15	2.4513

Table 5.

RO21=2.0824 V21=1.11842 V2S1=0.64473
RO31=3.403 V31=5.10526 V3S1=2.86842

V/V_1	L/H_1	V/V_1	L/H_1	V/V_1	L/H_1	V/V_1	L/H_1
H21=0.2000		H21=0.600		H21=1.000		H21=1.400	
2.61	34.361	2.61	57.831	2.61	82.281	2.61	106.94
2.60	27.943	2.60	46.291	2.60	65.767	2.60	85.547
2.59	23.940	2.59	38.969	2.59	55.268	2.59	71.908
2.58	21.243	2.58	33.945	2.58	48.043	2.58	62.527
2.57	19.320	2.57	30.307	2.57	42.786	2.57	55.698
2.56	17.895	2.56	27.563	2.56	38.803	2.56	50.522
2.55	16.802	2.55	25.430	2.55	35.697	2.55	46.477
2.54	15.938	2.54	23.729	2.54	33.204	2.54	43.239
2.50	13.777	2.50	19.418	2.50	26.819	2.50	34.926
2.45	12.369	2.45	16.656	2.45	22.633	2.45	29.470
2.40	11.504	2.40	15.060	2.40	20.160	2.40	26.246
2.35	10.879	2.35	13.987	2.35	18.484	2.35	24.058
2.30	10.376	2.30	13.187	2.30	17.235	2.30	22.420
2.25	9.9462	2.25	12.544	2.25	16.243	2.25	21.106
2.20	9.5610	2.20	11.998	2.20	15.415	2.20	20.000
2.15	9.2056	2.15	11.516	2.15	14.700	2.15	19.033
2.10	8.8713	2.10	11.077	2.10	14.066	2.10	18.162
2.05	8.5513	2.05	10.669	2.05	13.493	2.05	17.357
2.00	8.2421	2.00	10.284	2.00	12.966	2.00	16.604
1.95	7.9404	1.95	8.9155	1.95	12.476	1.95	15.890
1.90	7.6448	1.90	9.5599	1.90	12.015	1.90	15.207
1.85	7.3535	1.85	9.2146	1.85	11.577	1.85	14.550
1.80	7.0646	1.80	8.8762	1.80	11.157	1.80	13.923
1.75	6.7778	1.75	8.5445	1.75	10.752	1.75	13.335
1.70	6.4915	1.70	8.2173	1.70	10.358	1.70	12.794
1.65	6.2054	1.65	7.8937	1.65	9.9733	1.65	12.298
1.60	5.9183	1.60	7.5728	1.60	9.5958	1.60	11.833
1.55	5.6296	1.55	7.2536	1.55	9.2236	1.55	11.385
1.50	5.3384	1.50	6.9360	1.50	8.8561	1.50	10.948
1.45	5.0437	1.45	6.6188	1.45	8.4917	1.45	10.518
1.40	4.7445	1.40	6.3018	1.40	8.1297	1.40	10.092
1.35	4.4396	1.35	5.9842	1.35	7.7698	1.35	9.6693
1.30	4.1272	1.30	5.6660	1.30	7.4109	1.30	9.2487
1.25	3.8056	1.25	5.3463	1.25	7.0530	1.25	8.8296
1.20	3.4721	1.20	5.0252	1.20	6.6952	1.20	8.4115
1.15	3.1237	1.15	4.7020	1.15	6.3372	1.15	7.9937
1.10	2.7563	1.10	4.3768	1.10	5.9788	1.10	7.5753
1.05	2.3661	1.05	4.0500	1.05	5.6194	1.05	7.1559
1.00	1.9549	1.00	3.7221	1.00	5.2587	1.00	6.7345
0.95	1.5512	0.95	3.3949	0.95	4.8959	0.95	6.3103
0.90	1.2251	0.90	3.0708	0.90	4.5308	0.90	5.8815
0.85	1.0040	0.85	2.7534	0.85	4.1623	0.85	5.4459
0.80	0.8498	0.80	2.4464	0.80	3.7892	0.80	5.0005
0.75	0.7286	0.75	2.1520	0.75	3.4088	0.75	4.5406
0.70	0.5695	0.70	1.8684	0.70	3.0162	0.70	4.0569

(to be continued)

Table 5. (continued)

V/V_1	L/H_1
H21=1.800	
2.61	131.78
2.60	105.44
2.59	88.677
2.58	77.146
2.57	68.772
2.56	62.417
2.55	57.459
2.54	53.483
2.50	43.300
2.45	36.650
2.40	32.738
2.35	30.090
2.30	28.119
2.25	26.536
2.20	25.200
2.15	24.028
2.10	22.961
2.05	21.972
2.00	21.037
1.95	20.140
1.90	19.273
1.85	18.424
1.80	17.588
1.75	16.764
1.70	15.943
1.65	15.129
1.60	14.338
1.55	13.667
1.50	13.126
1.45	12.615
1.40	12.115
1.35	11.619
1.30	11.127
1.25	10.637
1.20	10.148
1.15	9.6595
1.10	9.1703
1.05	8.6800
1.00	8.1874
0.95	7.6903
0.90	7.1876
0.85	6.6756
0.80	6.1507
0.75	5.6058
0.70	5.0293

V/V_1	L/H_1
H21=2.200	
2.61	156.60
2.60	125.42
2.59	105.52
2.58	91.848
2.57	81.904
2.56	74.390
2.55	68.509
2.54	63.810
2.50	51.787
2.45	43.967
2.40	39.381
2.35	36.293
2.30	33.983
2.25	32.135
2.20	30.564
2.15	29.177
2.10	27.912
2.05	26.730
2.00	25.611
1.95	24.532
1.90	23.487
1.85	22.457
1.80	21.445
1.75	20.440
1.70	19.437
1.65	18.434
1.60	17.426
1.55	16.412
1.50	15.439
1.45	14.756
1.40	14.170
1.35	13.596
1.30	13.027
1.25	12.460
1.20	11.895
1.15	11.330
H21=2.600	
2.61	181.52
2.60	145.40
2.59	122.38
2.58	106.59
2.57	95.128
2.56	86.409

V/V_1	L/H_1
2.55	79.624
2.54	74.210
2.50	60.352
2.45	51.357
2.40	46.099
2.35	42.562
2.30	39.913
2.25	37.787
2.20	35.978
2.15	34.370
2.10	32.899
2.05	31.524
2.00	30.214
1.95	28.953
1.90	27.721
1.85	26.514
1.80	25.321
1.75	24.139
1.70	22.957
1.65	21.770
1.60	20.578
1.55	19.376
1.50	18.158
1.45	16.993
1.40	16.247
1.35	15.587
1.30	14.937
1.25	14.292
1.20	13.648
1.15	13.005
H21=3.000	
2.61	206.32
2.60	165.36
2.59	139.31
2.58	121.37
2.57	108.34
2.56	98.469
2.55	90.779
2.54	84.635
2.50	68.939
2.45	58.773
2.40	52.862
2.35	48.861
2.30	45.878
2.25	43.473
2.20	41.409

V/V_1	L/H_1
2.15	39.579
2.10	37.905
2.05	36.330
2.00	34.827
1.95	33.375
1.90	31.962
1.85	30.577
1.80	29.206
1.75	27.841
1.70	26.479
1.65	25.115
1.60	23.740
1.55	22.348
1.50	20.940
1.45	19.515
1.40	18.350
1.35	17.590
1.30	16.856
1.25	16.129
1.20	15.405
1.15	14.682
H21=3.400	
2.61	231.23
2.60	185.36
2.59	156.26
2.58	136.17
2.57	121.54
2.56	110.55
2.55	101.96
2.54	95.065
2.50	77.555
2.45	66.226
2.40	59.636
2.35	55.191
2.30	51.854
2.25	49.159
2.20	46.862
2.15	44.800
2.10	42.910
2.05	41.143
2.00	39.448
1.95	37.807
1.90	36.215
1.85	34.640
1.80	33.086
1.75	31.542

(to be continued)

Table 5. (continued)

V/V_1	L/H_1
1.70	30.001
1.65	28.456
1.60	26.900
1.55	25.325
1.50	23.726
1.45	22.099
1.40	20.544
1.35	19.600
1.30	18.781
1.25	17.971
1.20	17.166
1.15	16.361
H21=3.800	
2.61	256.08
2.60	205.43
2.59	173.17
2.58	150.93
2.57	134.84
2.56	122.62
2.55	113.14
2.54	105.54
2.50	86.163
2.45	73.703
2.40	66.434
2.35	61.524
2.30	57.851
2.25	54.860
2.20	52.312
2.15	50.028
2.10	47.923
2.05	45.950
2.00	44.062
1.95	42.245
1.90	40.460
1.85	38.708
1.80	36.973
1.75	35.255
1.70	33.528
1.65	31.804
1.60	30.063
1.55	28.301
1.50	26.514
1.45	24.695

V/V_1	L/H_1
1.40	22.872
1.35	21.624
1.30	20.708
1.25	19.815
1.20	18.927
1.15	18.040
H21=4.200	
2.61	280.90
2.60	225.52
2.59	190.05
2.58	165.74
2.57	148.06
2.56	134.71
2.55	124.29
2.54	115.99
2.50	94.818
2.45	81.172
2.40	73.233
2.35	67.858
2.30	63.839
2.25	60.579
2.20	57.768
2.15	55.252
2.10	52.946
2.05	50.765
2.00	48.691
1.95	46.670
1.90	44.711
1.85	42.773
1.80	40.861
1.75	38.961
1.70	37.058
1.65	35.147
1.60	33.223
1.55	31.278
1.50	29.301
1.45	27.288
1.40	25.253
1.35	23.663
1.30	22.641
1.25	21.662
1.20	20.692
1.15	19.720

V/V_1	L/H_1
H21=4.600	
2.61	306.16
2.60	245.38
2.59	206.91
2.58	180.53
2.57	161.31
2.56	146.79
2.55	135.52
2.54	126.45
2.50	103.45
2.45	88.652
2.40	80.025
2.35	74.220
2.30	69.850
2.25	66.291
2.20	63.217
2.15	60.488
2.10	57.953
2.05	55.590
2.00	53.306
1.95	51.104
1.90	48.957
1.85	46.847
1.80	44.749
1.75	42.660
1.70	40.583
1.65	38.495
1.60	36.387
1.55	34.256
1.50	32.096
1.45	29.889
1.40	27.645
1.35	25.722
1.30	24.578
1.25	23.511
1.20	22.457
1.15	21.402

V/V_1	L/H_1
H21=5.000	
2.61	330.71
2.60	265.43
2.59	223.99
2.58	195.32
2.57	174.58
2.56	158.86
2.55	146.64
2.54	136.95
2.50	112.106
2.45	96.156
2.40	86.833
2.35	80.554
2.30	75.830
2.25	71.988
2.20	68.695
2.15	65.720
2.10	62.992
2.05	60.413
2.00	57.932
1.95	55.552
1.90	53.217
1.85	50.910
1.80	48.632
1.75	46.374
1.70	44.111
1.65	41.839
1.60	39.545
1.55	37.238
1.50	34.880
1.45	32.485
1.40	30.040
1.35	27.812
1.30	26.519
1.25	25.361
1.20	24.223
1.15	23.086

Table 6.

RO21=3.000 V21=4.620 V2S1=2.662
RO31=3.072 V31=5.200 V3S1=3.000

V/V_1	L/H_1
H21=1.000	
2.75	196.23
2.74	88.821
2.73	57.108
2.72	42.104
2.71	33.491
2.70	27.994
2.65	16.949
2.60	13.699
2.55	12.202
2.50	11.300
2.45	10.659
2.40	10.152
2.35	9.7229
2.30	9.3426
2.25	8.9945
2.20	8.6684
2.15	8.3584
2.10	8.0596
2.05	7.7698
2.00	7.4859
1.95	7.2066
1.90	6.9305
1.85	6.6565
1.80	6.3834
1.75	6.1106
1.70	5.8371
1.65	5.5622
1.60	5.2849
1.55	5.0045
1.50	4.7195
1.45	4.4291
1.40	4.1312
1.35	3.8238
1.30	3.5041
H21=1.500	
2.75	241.31
2.74	107.79
2.73	68.310
2.72	49.545
2.71	38.739
2.70	31.830
2.65	18.077
2.60	14.207
2.55	12.499
2.50	11.502
2.45	10.810
2.40	10.272
2.35	9.8222
2.30	9.4273
2.25	9.0685
2.20	8.7342
2.15	8.4171
2.10	8.1133
2.05	7.8185
2.00	7.5305
1.95	7.2476
1.90	6.9685
1.85	6.6915
1.80	6.4158
1.75	6.1405
1.70	5.8647
1.65	5.5876
1.60	5.3082
1.55	5.0256
1.50	4.7387
1.45	4.4461
1.40	4.1461
1.35	3.8366
1.30	3.5147
H21=2.000	
2.75	296.11
2.74	126.62
2.73	79.322
2.72	56.831
2.71	43.862
2.70	35.574
2.65	19.270
2.60	14.813
2.55	12.876
2.50	11.766
2.45	11.007
2.40	10.428
2.35	9.9499
2.30	9.5343
2.25	9.1593
2.20	8.8127
2.15	8.4862
2.10	8.1739
2.05	7.8723
2.00	7.5784
1.95	7.2902
1.90	7.0062
1.85	6.7252
1.80	6.4458
1.75	6.1670
1.70	5.8880
1.65	5.6078
1.60	5.3257
1.55	5.0405
1.50	4.7511
1.45	4.4562
1.40	4.1542
1.35	3.8428
1.30	3.5192
H21=2.500	
2.75	330.58
2.74	145.28
2.73	90.254
2.72	64.012
2.71	48.895
2.70	39.259
2.65	20.577
2.60	15.549
2.55	13.356
2.50	12.102
2.45	11.257
2.40	10.620
2.35	10.103
2.30	9.6586
2.25	9.2623
2.20	8.8992
2.15	8.5592
2.10	8.2360
2.05	7.9253
2.00	7.6239
1.95	7.3292
1.90	7.0395
1.85	6.7536
1.80	6.4697
1.75	6.1872
1.70	5.9047
1.65	5.6217
1.60	5.3368
1.55	5.0493
1.50	4.7579
1.45	4.4613
1.40	4.1578
1.35	3.8452
1.30	3.5207
H21=3.000	
2.75	375.43
2.74	163.87
2.73	101.06
2.72	71.123
2.71	53.869
2.70	42.911
2.65	22.007
2.60	16.420
2.55	13.939
2.50	12.512
2.45	11.555
2.40	10.845
2.35	10.276
2.30	9.7951
2.25	9.3715
2.20	8.9874
2.15	8.6310
2.10	8.2951
2.05	7.9736
2.00	7.6636
1.95	7.3618
1.90	7.0663
1.85	6.7753
1.80	6.4872
1.75	6.2011
1.70	5.9157
1.65	5.6301
1.60	5.3432
1.55	5.0541
1.50	4.7612
1.45	4.4635
1.40	4.1592
1.35	3.8460
1.30	3.5211

(to be continued)

Table 6. (continued)

V/V_1	L/H_1	V/V_1	L/H_1	V/V_1	L/H_1	V/V_1	L/H_1
H21=3.500		H21=4.000		H21=4.500		H21=5.000	
2.75	420.18	2.75	464.13	2.75	509.12	2.75	552.87
2.74	182.46	2.74	200.98	2.74	219.50	2.74	237.75
2.73	111.82	2.73	122.52	2.73	133.24	2.73	143.90
2.72	78.165	2.72	85.176	2.72	92.128	2.72	99.080
2.71	58.791	2.71	63.679	2.71	68.547	2.71	73.416
2.70	46.543	2.70	50.172	2.70	53.790	2.70	57.414
2.65	23.549	2.65	25.179	2.65	26.882	2.65	28.635
2.60	17.410	2.60	18.498	2.60	19.662	2.60	20.884
2.55	14.620	2.55	15.383	2.55	16.215	2.55	17.105
2.50	12.990	2.50	13.531	2.50	14.126	2.50	14.765
2.45	11.900	2.45	12.284	2.45	12.702	2.45	13.150
2.40	11.097	2.40	11.372	2.40	11.663	2.40	11.968
2.35	10.464	2.35	10.663	2.35	10.866	2.35	11.070
2.30	9.9379	2.30	10.082	2.30	10.225	2.30	10.361
2.25	9.4813	2.25	9.5882	2.25	9.6879	2.25	9.7790
2.20	9.0729	2.20	9.1520	2.20	9.2229	2.20	9.2840
2.15	8.6979	2.15	8.7571	2.15	8.8076	2.15	8.8489
2.10	8.3475	2.10	8.3918	2.10	8.4278	2.10	8.4562
2.05	8.0149	2.05	8.0485	2.05	8.0743	2.05	8.0934
2.00	7.6960	2.00	7.7211	2.00	7.7397	2.00	7.7525
1.95	7.3874	1.95	7.4060	1.95	7.4191	1.95	7.4279
1.90	7.0860	1.90	7.0999	1.90	7.1093	1.90	7.1152
1.85	6.7905	1.85	6.8008	1.85	6.8071	1.85	6.8112
1.80	6.4989	1.80	6.5063	1.80	6.5108	1.80	6.5133
1.75	6.2098	1.75	6.2151	1.75	6.2181	1.75	6.2198
1.70	5.9222	1.70	5.9259	1.70	5.9280	1.70	5.9290
1.65	5.6347	1.65	5.6374	1.65	5.6386	1.65	5.6392
1.60	5.3465	1.60	5.3482	1.60	5.3490	1.60	5.3493
1.55	5.0563	1.55	5.0573	1.55	5.0578	1.55	5.0579
1.50	4.7628	1.50	4.7633	1.50	4.7637	1.50	4.7638
1.45	4.4646	1.45	4.4649	1.45	4.4649	1.45	4.4650
1.40	4.1598	1.40	4.1599	1.40	4.1600	1.40	4.1601
1.35	3.8462	1.35	3.8464	1.35	3.8465	1.35	3.8464
1.30	3.5821	1.30	3.5213	1.30	3.5214	1.30	3.5214

Table 7—8.

RO21=2.800 V21=4.000 V2S1=2.310
RO31=3.000 V31=5.300 V3S1=3.040

V/V_1	L/H_1
H21=0.500	
2.78	96.952
2.77	61.813
2.76	45.627
2.75	36.394
2.74	30.487
2.73	26.424
2.72	23.491
2.71	21.293
2.70	19.602
2.69	18.270
2.65	14.997
2.60	13.009
2.55	11.889
2.50	11.136
2.45	10.564
2.40	10.095
2.35	9.6877
2.30	9.3211
2.25	8.9818
2.20	8.6619
2.15	8.3562
2.10	8.0607
2.05	7.7730
2.00	7.4911
1.95	7.2131
1.90	6.9379
1.85	6.6647
1.80	6.3924
1.75	6.1201
1.70	5.8472
1.65	5.5728
1.60	5.2960
1.55	5.0159
1.50	4.7316
1.45	4.4417
1.40	4.1446
1.35	3.8384
1.30	3.5200
1.25	3.1857
H21=1.000	
2.78	140.21
2.77	88.333
2.76	64.300
2.75	50.477
2.74	41.533
2.73	35.305
2.72	30.750
2.71	27.293
2.70	24.605
2.69	22.470
2.65	17.212
2.60	14.148
2.55	12.569
2.50	11.591
2.45	10.899
2.40	10.357
2.35	9.9028
2.30	9.5042
2.25	9.1419
2.20	8.8084
2.15	8.4857
2.10	8.1799
2.05	7.8835
2.00	7.5941
1.95	7.3100
1.90	7.0295
1.85	6.7516
1.80	6.4752
1.75	6.1993
1.70	5.9229
1.65	5.6455
1.60	5.3658
1.55	5.0832
1.50	4.7963
1.45	4.5041
1.40	4.2046
1.35	3.8960
1.30	3.5751
1.25	3.2379
H21=1.500	
2.78	183.37
2.77	114.97
2.76	83.167
2.75	64.802
2.74	52.873
2.73	44.522
2.72	38.375
2.71	33.684
2.70	30.011
2.69	27.072
2.65	19.758
2.60	15.512
2.55	13.403
2.50	12.165
2.45	11.328
2.40	10.698
2.35	10.185
2.30	9.7461
2.25	9.3536
2.20	8.9934
2.15	8.6558
2.10	8.3346
2.05	8.0256
2.00	7.7251
1.95	7.4316
1.90	7.1426
1.85	6.8568
1.80	6.5733
1.75	6.2906
1.70	6.0081
1.65	5.7246
1.60	5.4392
1.55	5.1508
1.50	4.8584
1.45	4.5603
1.40	4.2550
1.35	3.9403
1.30	3.6130
1.25	3.2688
H21=2.000	
2.78	226.65
2.77	141.60
2.76	102.03
2.75	79.175
2.74	64.284
2.73	53.846
2.72	46.134
2.71	40.228
2.70	35.589
2.69	31.869
2.65	22.553
2.60	17.134
2.55	14.470
2.50	12.932
2.45	11.915
2.40	11.168
2.35	10.575
2.30	10.076
2.25	9.6387
2.20	9.2431
2.15	8.8768
2.10	8.5316
2.05	8.2020
2.00	7.8842
1.95	7.5746
1.90	7.2718
1.85	6.9733
1.80	6.6782
1.75	6.3847
1.70	6.0920
1.65	5.7991
1.60	5.5045
1.55	5.2075
1.50	4.9067
1.45	4.6008
1.40	4.2879
1.35	3.9658
1.30	3.6317
1.25	3.2815
H21=2.500	
2.78	269.91
2.77	168.26
2.76	120.91
2.75	93.568
2.74	75.727
2.73	63.210
2.72	53.948
2.71	46.839
2.70	41.247
2.69	36.758
2.65	25.513
2.60	18.990
2.55	15.781
2.50	13.921
2.45	12.692

(to be continued)

Table 7—8. (continued)

V/V_1	L/H_1
2.40	11.796
2.35	11.094
2.30	10.512
2.25	10.010
2.20	9.5614
2.15	9.1520
2.10	8.7706
2.05	8.4100
2.00	8.0653
1.95	7.7326
1.90	7.4089
1.85	7.0922
1.80	6.7804
1.75	6.4721
1.70	6.1658
1.65	5.8606
1.60	5.5551
1.55	5.2482
1.50	4.9386
1.45	4.6248
1.40	4.3053
1.35	3.9777
1.30	3.6392
1.25	3.2857
H21=3.000	
2.78	312.90
2.77	194.90
2.76	139.83
2.75	107.98
2.74	
2.73	72.588
2.72	61.784
2.71	53.477
2.70	46.951
2.69	41.701
2.65	28.584
2.60	21.020
2.55	17.294
2.50	15.112
2.45	13.655
2.40	12.587
2.35	11.750
2.30	11.061
2.25	10.471
2.20	9.9511
2.15	9.4811
2.10	9.0484
2.05	8.6445
2.00	8.2626
1.95	7.8977
1.90	7.5462
1.85	7.2054
1.80	6.8727
1.75	6.5465
1.70	6.2249
1.65	5.9066
1.60	5.5901
1.55	5.2740
1.50	4.9570
1.45	4.6374
1.40	4.3133
1.35	3.9825
1.30	3.6418
1.25	3.2869
H21=3.500	
2.78	356.21
2.77	221.57
2.76	158.72
2.75	122.35
2.74	98.662
2.73	81.975
2.72	69.622
2.71	60.138
2.70	52.667
2.69	46.678
2.68	41.803
2.65	31.728
2.60	23.172
2.55	18.953
2.50	16.458
2.45	14.771
2.40	13.521
2.35	12.535
2.30	11.720
2.25	11.023
2.20	10.410
2.15	9.8615
2.10	9.3614
2.05	8.8998
2.00	8.4690
1.95	8.0628
1.90	7.6768
1.85	7.3071
1.80	6.9059
1.75	6.6055
1.70	6.2684
1.65	5.9379
1.60	5.6120
1.55	5.2889
1.50	4.9666
1.45	4.6433
1.40	4.3167
1.35	3.9842
1.30	3.6427
1.25	3.2872
H21=4.000	
2.78	399.32
2.77	248.06
2.76	177.55
2.75	136.78
2.74	110.10
2.73	91.376
2.72	77.460
2.71	66.803
2.70	58.404
2.69	51.663
2.68	46.192
2.65	34.922
2.60	25.404
2.55	20.714
2.50	17.915
2.45	16.001
2.40	14.568
2.35	13.426
2.30	12.473
2.25	11.654
2.20	10.933
2.15	10.288
2.10	9.7038
2.05	9.1700
2.00	8.6780
1.95	8.2214
1.90	7.7951
1.85	7.3936
1.80	7.0128
1.75	6.6488
1.70	6.2982
1.65	5.9577
1.60	5.6248
1.55	5.2968
1.50	4.9712
1.45	4.6459
1.40	4.3180
1.35	3.9849
1.30	3.6429
1.25	3.2873
H21=4.500	
2.78	442.58
2.77	274.81
2.76	196.53
2.75	151.17
2.74	121.60
2.73	100.75
2.72	85.317
2.71	73.479
2.70	64.155
2.69	56.668
2.68	50.606
2.65	38.147
2.60	27.692
2.55	22.539
2.50	19.445
2.45	17.311
2.40	15.698
2.35	14.398
2.30	13.303
2.25	12.353
2.20	11.511
2.15	10.754
2.10	10.070
2.05	9.4491
2.00	8.8841
1.95	8.3695
1.90	7.8985
1.85	7.4639
1.80	7.0596
1.75	6·6792
1.70	6.3174
1.65	5.9695
1.60	5.6317
1.55	5.3006
1.50	4.9735
1.45	4.6469
1.40	4.3186

(to be continued)

Table 7—8. (continued)

V/V_1	L/H_1
1.35	3.9850
1.30	3.6429
1.25	3.2873
H21=5.000	
2.78	486.04
2.77	301.18
2.76	215.27
2.75	165.56
2.74	133.04
2.73	110.15
2.72	93.162
2.71	80.162
2.70	69.906
2.69	61.680
2.68	55.021
2.65	41.393
2.60	30.018
2.55	24.409
2.50	21.027
2.45	18.677
2.40	16.885
2.35	15.428
2.30	14.192
2.25	13.106
2.20	12.134
2.15	11.254
2.10	10.455
2.05	9.7324
2.00	9.0832
1.95	8.5034
1.90	7.9852
1.85	7.5186
1.80	7.0932
1.75	6.6994
1.70	6.3292
1.65	5.9763
1.60	5.6354
1.55	5.3026
1.50	4.9743
1.45	4.6474
1.40	4.3189
1.35	3.9852
1.30	3.6430
1.25	3.2874

V/V_1	L/H_1
H21=5.500	
2.78	529.00
2.73	119.51
2.70	75.638
2.68	59.457
2.65	44.661
2.60	32.370
2.55	26.314
2.50	22.642
2.45	20.080
2.40	18.113
2.35	16.503
2.30	15.122
2.25	13.900
2.20	12.793
2.15	11.780
2.10	10.853
2.05	10.015
2.00	9.2714
1.95	8.6210
1.90	8.0557
1.85	7.5595
1.80	7.1162
1.75	6.7121
1.70	6.3662
1.65	5.9799
1.60	5.6374
1.55	5.3036
1.50	4.9748
H21=6.000	
2.78	572.55
2.73	128.91
2.70	81.404
2.68	63.885
2.65	47.939
2.60	34.743
2.55	28.236
2.50	24.283
2.45	21.508
2.40	19.370
2.35	17.607
2.30	16.084
2.25	14.724
2.20	13.480
2.15	12.327

V/V_1	L/H_1
2.10	11.261
2.05	10.295
2.00	9.4459
1.95	8.7218
1.90	8.1108
1.85	7.5889
1.80	7.1317
1.75	6.7200
1.70	6.3402
1.65	5.9818
1.60	5.6382
1.55	5.3039
1.50	4.9748
H21=6.500	
2.78	614.96
2.73	138.33
2.70	87.167
2.68	68.328
2.65	51.231
2.60	37.129
2.55	30.176
2.50	25.940
2.45	22.957
2.40	20.646
2.35	18.733
2.30	17.070
2.25	15.573
2.20	14.188
2.15	12.890
2.10	11.676
2.05	10.568
2.00	9.6057
1.95	8.8063
1.90	8.1529
1.85	7.6096
1.80	7.1416
1.75	6.7247
1.70	6.3424
1.65	5.9829
1.60	5.6387
1.55	5.3042
1.50	4.9750

V/V_1	L/H_1
H21=7.000	
2.78	659.05
2.73	147.70
2.70	92.926
2.68	72.772
2.65	54.519
2.60	39.524
2.55	32.128
2.50	27.609
2.45	24.419
2.40	21.937
2.35	19.876
2.30	18.074
2.25	16.438
2.20	14.913
2.15	13.465
2.10	12.094
2.05	10.833
2.00	9.7490
1.95	8.8752
1.90	8.1843
1.85	7.6235
1.80	7.1480
1.75	6.7276
1.70	6.3435
1.65	5.9835
1.60	5.6388
H21=7.500	
2.78	702.21
2.73	157.07
2.70	98.662
2.68	77.204
2.65	57.827
2.60	41.925
2.55	34.090
2.50	29.290
2.45	25.893
2.40	23.241
2.35	21.030
2.30	19.088
2.25	17.317
2.20	15.651
2.15	14.051

(to be continued)

Table 7—8. (continued)

V/V_1	L/H_1
2.10	12.514
2.05	11.089
2.00	9.8762
1.95	8.9304
1.90	8.2070
1.85	7.6330
1.80	7.1520
1.75	6.7293
1.70	6.3445
1.65	5.9836
1.60	5.6390
H21=8.000	
2.78	744.89
2.73	166.41
2.70	104.43
2.68	81.662
2.65	61.123
2.60	44.338
2.55	36.057
2.50	30.979
2.45	27.371
2.40	24.554
2.35	22.193
2.30	20.115
2.25	18.208
2.20	16.399
2.15	14.645
2.10	12.934
2.05	11.332
2.00	9.9870
1.95	8.9733
1.90	8.2233
1.85	7.6392
1.80	7.1543
1.75	6.7304
1.70	6.3448
1.65	5.9838
1.60	5.6392
H21=8.500	
2.78	788.24
2.73	175.85
2.70	110.19
2.68	86.117
2.65	64.445
2.60	46.754
2.55	38.034
2.50	32.670
2.45	28.860
2.40	25.872
2.35	23.366
2.30	21.148
2.25	19.105
2.20	17.156
2.15	15.243
2.10	13.353
2.05	11.564
2.00	10.082
1.95	9.0063
1.90	8.2346
1.85	7.6432
1.80	7.1559
1.75	6.7307
1.70	6.3449
1.65	5.9839
1.60	5.6392
H21=9.000	
2.78	831.53
2.73	185.22
2.70	115.95
2.68	90.572
2.65	67.753
2.60	49.175
2.55	40.009
2.50	34.367
2.45	30.351
2.40	27.195
2.35	24.542
2.30	22.187
2.25	20.010
2.20	17.918
2.15	15.848
2.10	13.770
2.05	11.784
2.00	10.163
1.95	9.0313
1.90	8.2425
1.85	7.6457
1.80	7.1567
1.75	6.7313
1.70	6.3449
H21=9.500	
2.78	873.89
2.73	194.60
2.70	121.71
2.68	95.019
2.65	71.064
2.60	51.601
2.55	41.994
2.50	36.073
2.45	31.845
2.40	28.524
2.35	25.722
2.30	23.233
2.25	20.919
2.20	18.685
2.15	16.455
2.10	14.185
2.05	11.990
2.00	10.230
1.95	9.0497
1.90	8.2478
1.85	7.6473
1.80	7.1571
1.75	6.7313
1.70	6.3449
H21=10.000	
2.78	917.50
2.73	204.01
2.70	127.44
2.68	99.463
2.65	74.392
2.60	54.027
2.55	43.974
2.50	37.778
2.45	33.343
2.40	29.854
2.35	26.908
2.30	24.280
2.25	21.833
2.20	19.458
2.15	17.065
2.10	14.597
2.05	12.182
2.00	10.286
1.95	9.0631
1.90	8.2515
1.85	7.6485
1.80	7.1575
H21=10.500	
2.78	962.09
2.73	213.31
2.70	133.24
2.68	103.92
2.65	77.693
2.60	56.457
2.55	45.961
2.50	39.481
2.45	34.847
2.40	31.189
2.35	28.094
2.30	25.332
2.25	22.750
2.20	20.232
2.15	17.676
2.10	15.005
2.05	12.361
2.00	10.331
1.95	9.0730
1.90	8.2533
1.85	7.6494
1.80	7.1579
H21=11.000	
2.78	1003.3
2.73	222.73
2.70	139.00
2.68	108.38
2.65	81.020
2.60	58.886
2.55	47.948
2.50	41.187
2.45	36.348
2.40	32.522
2.35	29.284
2.30	26.386

(to be continued)

Table 7—8. (continued)

V/V_1	L/H_1
2.25	23.668
2.20	21.010
2.15	18.289
2.10	15.409
2.05	12.526
2.00	10.366
1.95	9.0807
1.90	8.2549
H21=11.500	
2.78	1048.3
2.73	232.17
2.70	144.71
2.68	112.80
2.65	84.339
2.60	61.313
2.55	49.939
2.50	42.904
2.45	37.855
2.40	33.861
2.35	30.477
2.30	27.441
2.25	24.591
2.20	21.789
2.15	18.903
2.10	15.811
2.05	12.678
2.00	10.395
1.95	9.0855
1.90	8.2565
H21=12.000	
2.78	1088.20
2.73	241.54
2.70	150.46
2.68	117.27
2.65	87.671
2.60	63.742
2.55	51.934
2.50	44.615
2.45	39.361
2.40	35.199
2.35	31.669
2.30	28.499
2.25	25.515
2.20	22.570
2.15	19.518
2.10	16.206
2.05	12.816
2.00	10.418
1.95	9.0893
1.90	8.2573
H21=12.500	
2.78	1131.2
2.73	250.96
2.70	156.21
2.68	121.71
2.65	90.988
2.60	66.185
2.55	53.925
2.50	46.325
2.45	40.867
2.40	36.539
2.35	32.862
2.30	29.559
2.25	26.441
2.20	23.355
2.15	20.135
2.10	16.599
2.05	12.941
2.00	10.436
1.95	9.0919
1.90	8.2584
H21=13.000	
2.78	1177.8
2.73	260.35
2.70	162.01
2.68	126.19
2.65	94.323
2.60	68.620
2.55	55.917
2.50	48.037
2.45	42.374
2.40	37.883
2.35	34.058
2.30	30.618
2.25	27.366
2.20	24.137
2.15	20.751
2.10	16.986
2.05	13.055
2.00	10.449
H21=13.500	
2.78	1216.8
2.73	269.63
2.70	167.72
2.68	130.61
2.65	97.651
2.60	71.045
2.55	57.918
2.50	49.755
2.45	43.884
2.40	39.223
2.35	35.257
2.30	31.681
2.25	28.295
2.20	24.922
2.15	21.367
2.10	17.369
2.05	13.155
2.00	10.458
H21=14.000	
2.78	1264.7
2.73	278.98
2.70	173.48
2.68	135.06
2.65	100.94
2.60	73.500
2.55	59.914
2.50	51.467
2.45	45.394
2.40	40.571
2.35	36.456
2.30	32.741
2.25	29.224
2.20	25.709
2.15	21.984
2.10	17.746
2.05	13.244
2.00	10.467
H21=14.500	
2.78	1303.1
2.73	288.36
2.70	179.28
2.68	139.53
2.65	104.30
2.60	75.928
2.55	61.902
2.50	53.190
2.45	46.908
2.40	41.912
2.35	37.650
2.30	33.807
2.25	30.152
2.20	26.495
2.15	22.600
2.10	18.119
2.05	13.322
2.00	10.471
H21=15.000	
2.78	1351.0
2.73	297.70
2.70	185.08
2.68	143.98
2.65	107.61
2.60	78.356
2.55	63.901
2.50	54.903
2.45	48.417
2.40	43.257
2.35	38.850
2.30	34.870
2.25	31.084
2.20	27.284
2.15	23.216
2.10	18.489
2.05	13.391
2.00	10.477

Table 9.

RO21=2.800 V21=3.340 V2S1=1.930
RO31=3.000 V31=5.300 V3S1=3.040

V/V_1	L/H_1
H21=0.500	
2.78	115.64
2.77	73.700
2.76	54.278
2.75	43.138
2.74	35.957
2.73	30.962
2.70	22.398
2.65	16.403
2.60	13.801
2.55	12.389
2.50	11.482
2.45	10.823
2.40	10.299
2.35	9.8560
2.30	9.4644
2.25	9.1068
2.20	8.7736
2.15	8.4571
2.10	8.1534
2.05	7.8588
2.00	7.5711
1.95	7.2884
1.90	7.0092
1.85	6.7326
1.80	6.4572
1.75	6.1822
1.70	5.9070
1.65	5.6305
1.60	5.3520
1.55	5.0705
1.50	4.7849
1.45	4.4940
1.40	4.1963
1.35	3.8897
1.30	3.5716
1.25	3.2381
H21=1.000	
2.78	178.29
2.77	112.93
2.76	82.580
2.75	65.055
2.74	53.667
2.73	45.680
2.70	31.673
2.65	21.331
2.60	16.616
2.55	14.107
2.50	12.615
2.45	11.629
2.40	10.911
2.35	10.345
2.30	9.8709
2.25	9.4558
2.20	9.0803
2.15	8.7320
2.10	8.4034
2.05	8.0890
2.00	7.7847
1.95	7.4883
1.90	7.1976
1.85	6.9108
1.80	6.6267
1.75	6.3441
1.70	6.0620
1.65	5.7793
1.60	5.4952
1.55	5.2087
1.50	4.9184
1.45	4.6234
1.40	4.3216
1.35	4.0113
1.30	3.6895
1.25	3.3520
H21=1.500	
2.78	241.09
2.77	152.37
2.76	111.15
2.75	87.329
2.74	71.818
2.73	60.899
2.70	41.634
2.65	27.119
2.60	20.243
2.55	16.466
2.50	14.221
2.45	12.786
2.40	11.793
2.35	11.051
2.30	10.458
2.25	9.9586
2.20	9.5207
2.15	9.1246
2.10	8.7580
2.05	8.4126
2.00	8.0828
1.95	7.7642
1.90	7.4542
1.85	7.1503
1.80	6.8508
1.75	6.5541
1.70	6.2588
1.65	5.9639
1.60	5.6681
1.55	5.3702
1.50	5.0687
1.45	4.7622
1.40	4.4489
1.35	4.1263
1.30	3.7912
1.25	3.4391
H21=2.000	
2.78	303.67
2.77	191.92
2.76	139.83
2.75	109.70
2.74	90.064
2.73	76.255
2.70	51.809
2.65	33.233
2.60	24.287
2.55	19.281
2.50	16.266
2.45	14.340
2.40	13.022
2.35	12.058
2.30	11.306
2.25	10.689
2.20	10.160
2.15	9.6912
2.10	9.2650
2.05	8.8699
2.00	8.4969
1.95	8.1412
1.90	7.7979
1.85	7.4640
1.80	7.1369
1.75	6.8146
1.70	6.4954
1.65	6.1776
1.60	5.8598
1.55	5.5405
1.50	5.2181
1.45	4.8910
1.40	4.5573
1.35	4.2144
1.30	3.8594
1.25	3.4880
H21=2.500	
2.78	366.35
2.77	231.44
2.76	168.48
2.75	132.11
2.74	108.38
2.73	91.685
2.70	62.067
2.65	39.478
2.60	28.527
2.55	22.350
2.50	18.609
2.45	16.210
2.40	14.566
2.35	13.365
2.30	12.433
2.25	11.673
2.20	11.028
2.15	10.463
2.10	9.9534
2.05	9.4858
2.00	9.0490
1.95	8.6356
1.90	8.2401
1.85	7.8581
1.80	7.4865

(to be continued)

Table 9. (continued)

V/V_1	L/H_1
1.75	7.1223
1.70	6.7643
1.65	6.4096
1.60	6.0569
1.55	5.7046
1.50	5.3516
1.45	4.9959
1.40	4.6361
1.35	4.2705
1.30	3.8961
1.25	3.5095
H21=3.000	
2.78	429.29
2.77	270.90
2.76	197.29
2.75	154.57
2.74	126.68
2.73	107.10
2.70	72.343
2.65	45.793
2.60	32.866
2.55	25.557
2.50	21.125
2.45	18.280
2.40	16.328
2.35	14.897
2.30	13.784
2.25	12.874
2.20	12.102
2.15	11.425
2.10	10.816
2.05	10.258
2.00	9.7387
1.95	9.2482
1.90	8.7808
1.85	8.3309
1.80	7.8953
1.75	7.4710
1.70	7.0557
1.65	6.6482
1.60	6.2470
1.55	5.8511
1.50	5.4598
1.45	5.0719
1.40	4.6865
1.35	4.3010
1.30	3.9128
1.25	3.5174
H21=3.500	
2.78	492.55
2.77	310.45
2.76	225.85
2.75	177.00
2.74	145.03
2.73	122.55
2.70	82.659
2.65	52.139
2.60	37.258
2.55	28.836
2.50	23.741
2.45	20.469
2.40	18.222
2.35	16.571
2.30	15.281
2.25	14.225
2.20	13.324
2.15	12.531
2.10	11.817
2.05	11.159
2.00	10.545
1.95	9.9640
1.90	9.4083
1.85	8.8729
1.80	8.3546
1.75	7.8506
1.70	7.3600
1.65	6.8831
1.60	6.4204
1.55	5.9727
1.50	5.5402
1.45	5.1217
1.40	4.7148
1.35	4.3159
1.30	3.9197
1.25	3.5200
H21=4.000	
2.78	555.25
2.77	350.15
2.76	254.69
2.75	199.50
2.74	163.35
2.73	137.99
2.70	92.993
2.65	58.504
2.60	41.674
2.55	32.162
2.50	26.411
2.45	22.727
2.40	20.195
2.35	18.329
2.30	16.870
2.25	15.669
2.20	14.641
2.15	13.734
2.10	12.912
2.05	12.152
2.00	11.438
1.95	10.758
1.90	10.105
1.85	9.4711
1.80	8.8539
1.75	8.2527
1.70	7.6688
1.65	7.1066
1.60	6.5716
1.55	6.0678
1.50	5.5954
1.45	5.1515
1.40	4.7295
1.35	4.3224
1.30	3.9222
1.25	3.5210
H21=4.500	
2.78	617.91
2.77	389.35
2.76	283.28
2.75	221.86
2.74	181.69
2.73	153.46
2.70	103.29
2.65	64.875
2.60	46.118
2.55	35.513
2.50	29.118
2.45	25.028
2.40	22.216
2.35	20.141
2.30	18.513
2.25	17.171
2.20	16.019
2.15	14.998
2.10	14.068
2.05	13.206
2.00	12.391
1.95	11.609
1.90	10.852
1.85	10.112
1.80	9.3839
1.75	8.6697
1.70	7.9751
1.65	7.3130
1.60	6.6976
1.55	6.1375
1.50	5.6311
1.45	5.1679
1.40	4.7365
1.35	4.3252
1.30	3.9233
1.25	3.5212
H21=5.000	
2.78	679.95
2.77	428.93
2.76	312.14
2.75	244.41
2.74	200.05
2.73	168.98
2.70	113.65
2.65	71.251
2.60	50.567
2.55	38.882
2.50	31.849
2.45	27.355
2.40	24.267
2.35	21.985
2.30	20.192
2.25	18.710
2.20	17.434
2.15	16.301
2.10	15.266
2.05	14.301

(to be continued)

Table 9. (continued)

V/V_1	L/H_1	V/V_1	L/H_1	V/V_1	L/H_1	V/V_1	L/H_1
2.00	13.384	1.75	9.0956	1.50	5.6525	1.25	3.5217
1.95	12.500	1.70	8.2743	1.45	5.1767		
1.90	11.637	1.65	7.4986	1.40	4.7399		
1.85	10.784	1.60	6.7985	1.35	4.3262		
1.80	9.9365	1.55	6.1862	1.30	3.9237		

Table 10.

RO21=2.800 V21=3.333 V2S1=1.924
RO31=3.000 V31=5.300 V3S1=3.060

V/V_1	L/H_1
H21=10.000	
2.78	690.71
2.77	526.94
2.76	424.27
2.75	354.49
2.74	303.13
2.73	264.12
2.65	123.29
2.60	89.376
2.55	69.792
2.50	57.866
2.45	50.114
2.40	44.692
2.35	40.603
2.30	37.328
2.25	34.570
2.20	32.160
2.15	29.973
2.10	27.942
2.05	26.008
2.00	24.126
1.95	22.248
1.90	20.331
1.85	18.312
1.80	16.100
1.75	13.558
1.70	10.688
1.65	8.4065
1.60	7.1183
1.55	6.3074
1.50	5.7034
H21=15.000	
2.78	1023.7
2.77	779.88
2.76	628.01
2.75	524.37
2.74	448.20
2.73	390.65
2.65	181.56
2.60	131.41
2.55	102.51
2.50	84.979
2.45	73.626
2.40	65.661
2.35	59.650
2.30	54.833
2.25	50.756
2.20	47.174
2.15	43.922
2.10	40.880
2.05	37.973
2.00	35.118
1.95	32.244
1.90	29.264
1.85	26.045
1.80	22.337
1.75	17.547
1.70	11.520
1.65	8.4626
1.60	7.1268
1.55	6.3098
1.50	5.7038
H21=20.000	
2.78	1353.1
2.77	1031.1
2.76	832.88
2.75	694.06
2.74	593.27
2.73	516.79
2.65	239.96
2.60	173.48
2.55	135.27
2.50	112.14
2.45	97.172
2.40	86.668
2.35	78.739
2.30	72.363
2.25	66.960
2.20	62.217
2.15	57.905
2.10	53.858
2.05	49.968
2.00	46.142
1.95	42.277
1.90	38.232
1.85	33.803
1.80	28.543
1.75	21.063
1.70	11.660
H21=25.000	
2.78	1682.1
2.77	1284.2
2.76	1033.6
2.75	864.78
2.74	738.27
2.73	642.11
2.65	298.39
2.60	215.63
2.55	168.04
2.50	139.30
2.45	120.74
2.40	107.70
2.35	97.837
2.30	89.907
2.25	83.194
2.20	77.273
2.15	71.898
2.10	66.838
2.05	61.977
2.00	57.185
1.95	52.325
1.90	47.209
1.85	41.567
1.80	34.715
1.75	24.130
1.70	11.686
H21=30.000	
2.78	2013.8
2.77	1531.9
2.76	1236.1
2.75	1031.1
2.74	884.40
2.73	768.70
2.65	356.70
2.60	257.75
2.55	200.83
2.50	166.52
2.45	144.30
2.40	128.71
2.35	116.95
2.30	107.43
2.25	99.424
2.20	92.326
2.15	85.887
2.10	79.814
2.05	73.986
2.00	68.220
1.95	62.367
1.90	56.186
1.85	49.317
1.80	40.860
1.75	26.746

Table 11.

RO21=2.800 V21=2.670 V2S1=1.540
RO31=3.000 V31=5.300 V3S1=3.040

V/V_1	L/H_1
H21=0.500	
2.78	131.47
2.77	83.844
2.76	61.784
2.75	49.082
2.74	40.867
2.73	35.132
2.72	30.916
2.71	27.701
2.70	25.178
2.69	23.155
2.65	18.007
2.60	14.796
2.55	13.053
2.50	11.960
2.45	11.191
2.40	10.598
2.35	10.108
2.30	9.6841
2.25	9.3032
2.20	8.9515
2.15	8.6210
2.10	8.3061
2.05	8.0021
2.00	7.7066
1.95	7.4172
1.90	7.1323
1.85	6.8506
1.80	6.5707
1.75	6.2920
1.70	6.0133
1.65	5.7339
H21=1.000	
2.78	210.35
2.77	133.80
2.76	98.210
2.75	77.646
2.74	64.268
2.73	54.880
2.72	47.930
2.71	42.577
2.70	38.335
2.69	34.894
2.65	25.872
2.60	19.889
2.55	16.481
2.50	14.351
2.45	12.928
2.40	11.918
2.35	11.156
2.30	10.547
2.25	10.037
2.20	9.5917
2.15	9.1909
2.10	8.8214
2.05	8.4748
2.00	8.1444
1.95	7.8266
1.90	7.5178
1.85	7.2155
1.80	6.9182
1.75	6.6242
1.70	6.3321
1.65	6.0409
H21=1.500	
2.78	289.33
2.77	183.89
2.76	134.92
2.75	106.59
2.74	88.122
2.73	75.130
2.72	65.511
2.71	58.075
2.70	52.187
2.69	47.383
2.65	34.724
2.60	26.153
2.55	21.111
2.50	17.846
2.45	15.607
2.40	14.011
2.35	12.834
2.30	11.930
2.25	11.208
2.20	10.608
2.15	10.090
2.10	9.6312
2.05	9.2130
2.00	8.8244
1.95	8.4578
1.90	8.1075
1.85	7.7697
1.80	7.4408
1.75	7.1185
1.70	6.8010
1.65	6.4863
H21=2.000	
2.78	368.45
2.77	234.28
2.76	171.75
2.75	135.63
2.74	112.07
2.73	95.513
2.72	83.220
2.71	73.752
2.70	66.219
2.69	60.082
2.65	43.847
2.60	32.791
2.55	26.212
2.50	21.883
2.45	18.865
2.40	16.683
2.35	15.064
2.30	13.828
2.25	12.855
2.20	12.063
2.15	11.395
2.10	10.815
2.05	10.297
2.00	9.8242
1.95	9.3850
1.90	8.9708
1.85	8.5754
1.80	8.1942
1.75	7.8238
1.70	7.4607
1.65	7.1028
H21=2.500	
2.78	447.19
2.77	284.53
2.76	208.64
2.75	164.71
2.74	136.06
2.73	115.95
2.72	101.02
2.71	89.470
2.70	80.312
2.69	72.855
2.65	53.069
2.60	39.566
2.55	31.487
2.50	26.137
2.45	22.380
2.40	19.645
2.35	17.606
2.30	16.051
2.25	14.832
2.20	13.845
2.15	13.020
2.10	12.308
2.05	11.679
2.00	11.108
1.95	10.581
1.90	10.087
1.85	9.6171
1.80	9.1664
1.75	8.7289
1.70	8.3015
1.65	7.8803
H21=3.000	
2.78	526.84
2.77	334.89
2.76	245.45
2.75	193.72
2.74	160.10
2.73	136.42
2.72	118.79
2.71	105.24
2.70	94.461
2.69	85.658

(to be continued)

Table 11. (continued)

V/V_1	L/H_1
2.65	62.337
2.60	46.400
2.55	36.837
2.50	30.491
2.45	26.010
2.40	22.742
2.35	20.302
2.30	18.441
2.25	16.985
2.20	15.810
2.15	14.830
2.10	13.989
2.05	13.246
2.00	12.573
1.95	11.953
1.90	11.373
1.85	10.821
1.80	10.291
1.75	9.7772
1.70	9.2737
1.65	8.7769
H21=3.500	
2.78	606.26
2.77	384.98
2.76	282.35
2.75	222.92
2.74	184.16
2.73	156.88
2.72	136.64
2.71	121.02
2.70	108.61
2.69	98.473
2.65	71.638
2.60	53.256
2.55	42.228
2.50	34.889
2.45	29.699
2.40	25.908

V/V_1	L/A_1
2.35	23.074
2.30	20.916
2.25	19.230
2.20	17.872
2.15	16.742
2.10	15.771
2.05	14.914
2.00	14.139
1.95	13.425
1.90	12.757
1.85	12.120
1.80	11.508
1.75	10.913
1.70	10.328
1.65	9.7486
H21=4.000	
2.78	685.38
2.77	435.10
2.76	319.11
2.75	251.94
2.74	208.14
2.73	177.31
2.72	154.43
2.71	136.78
2.70	122.76
2.69	111.29
2.65	80.943
2.60	60.138
2.55	47.646
2.50	39.313
2.45	33.421
2.40	29.108
2.35	25.887
2.30	23.436
3.25	21.523
2.20	19.985
2.15	18.705
2.10	17.607

V/V_1	L/H_1
2.05	16.639
2.00	15.762
1.95	14.954
1.90	14.196
1.85	13.473
1.80	12.777
1.75	12.099
1·70	11.431
1.65	10.767
H21=4.500	
2.78	764.81
2.77	486.04
2.76	356.21
2.75	281.11
2.74	232.17
2.73	197.89
2.72	172.32
2.71	152.60
2.70	136.93
2.69	124.12
2.65	90.254
2.60	67.029
2.55	53.069
2.50	43.757
2.45	37.161
2.40	32.330
2.35	28.728
2.30	25.984
2.25	23.846
2.20	22.130
2.15	20.702
2.10	19.477
2.05	18.395
2.00	17.418
1.95	16.515
1.90	15.666
1.85	14.859
1.80	14.078

V/V_1	L/H_1
1.75	13.316
1.70	12.564
1.65	11.813
H21=5.000	
2.78	842.42
2.77	535.61
2.76	392.62
2.75	310.26
2.74	256.21
2.73	218.33
2.72	190.14
2.71	168.37
2.70	151.08
2.69	137.00
2.65	99.578
2.60	73.922
2.55	58.497
2.50	48.208
2.45	40.912
2.40	35.569
2.35	31.580
2.30	28.549
2.25	26.188
2.20	24.292
2.15	22.716
2.10	21.366
2.05	20.173
2.00	19.093
1.95	18.095
1.90	17.158
1.85	16.263
1.80	15.398
1.75	14.552
1.70	13.714
1.65	12.877

Table 12.

RO21=2.800 V21=2.000 V2S1=1.155
RO31=3.000 V31=5.300 V3S1=3.040

V/V_1	L/H_1
H21=0.500	
2.78	143.74
2.77	91.816
2.76	67.735
2.75	53.875
2.74	44.887
2.73	38.608
2.72	33.986
2.71	30.450
2.70	27.666
2.65	19.660
2.60	15.981
2.55	13.943
2.50	12.663
2.45	11.771
2.40	11.095
2.35	10.547
2.30	10.080
2.25	9.6670
2.20	9.2901
2.15	8.9393
2.10	8.6072
2.05	8.2889
2.00	7.9810
1.95	7.6809
1.90	7.3866
1.85	7.0963
1.80	6.8091
1.75	6.5238
1.70	6.2392
1.65	5.9546
1.60	5.6690
1.55	5.3816
1.50	5.0913
1.45	4.7972
1.40	4.4980
1.35	4.1920
1.30	3.8774
1.25	3.5518
H21=1.000	
2.78	235.14
2.77	150.06
2.76	110.48
2.75	87.656
2.74	72.772
2.73	62.345
2.72	54.624
2.71	48.687
2.70	43.974
2.65	30.116
2.60	23.380
2.55	19.436
2.50	16.864
2.45	15.065
2.40	13.741
2.35	12.724
2.30	11.914
2.25	11.247
2.20	10.678
2.15	10.181
2.10	9.7343
2.05	9.3251
2.00	8.9437
1.95	8.5831
1.90	8.2385
1.85	7.9057
1.80	7.5822
1.75	7.2656
1.70	6.9543
1.65	6.6464
1.60	6.3410
1.55	6.0368
1.50	5.7328
1.45	5.4279
1.40	5.1210
1.35	4.8109
1.30	4.4963
1.25	4.1756
H21=1.500	
2.78	326.81
2.77	208.56
2.76	153.51
2.75	121.80
2.74	101.10
2.73	86.566
2.72	75.794
2.71	67.513
2.70	60.935
2.65	41.506
2.60	31.964
2.55	26.295
2.50	22.523
2.45	19.824
2.40	17.788
2.35	16.194
2.30	14.910
2.25	13.856
2.20	12.974
2.15	12.225
2.10	11.578
2.05	11.008
2.00	10.497
1.95	10.031
1.90	9.5985
1.85	9.1919
1.80	8.8051
1.75	8.4332
1.70	8.0729
1.65	7.7212
1.60	7.3762
1.55	7.0358
1.50	6.6985
1.45	6.3628
1.40	6.0269
1.35	5.6896
1.30	5.3488
1.25	5.0024
H21=2.000	
2.78	418.81
2.77	267.25
2.76	196.68
2.75	155.98
2.74	129.49
2.73	110.88
2.72	97.098
2.71	86.507
2.70	78.070
2.65	53.124
2.60	40.847
2.55	33.521
2.50	28.623
2.45	25.092
2.40	22.403
2.35	20.275
2.30	18.540
2.25	17.097
2.20	15.884
2.15	14.854
2.10	13.971
2.05	13.207
2.00	12.537
1.95	11.938
1.90	11.393
1.85	10.891
1.80	10.418
1.75	9.9703
1.70	9.5401
1.65	9.1235
1.60	8.7171
1.55	8.3184
1.50	7.9245
1.45	7.5336
1.40	7.1434
1.35	6.7514
1.30	6.3551
1.25	5.9514
H21=2.500	
2.78	510.13
2.77	325.77
2.76	239.96
2.75	190.21
2.74	157.94
2.73	135.31
2.72	118.46
2.71	105.52
2.70	95.230
2.65	64.818
2.60	49.823
2.55	40.867
2.50	34.870
2.45	30.527
2.40	27.209
2.35	24.568
2.30	22.403
2.25	20.590

(to be continued)

Table 12. (continued)

V/V_1	L/H_1
2.20	19.054
2.15	17.745
2.10	16.625
2.05	15.662
2.00	14.824
1.95	14.084
1.90	13.419
1.85	12.811
1.80	12.244
1.75	11.709
1.70	11.198
1.65	10.705
1.60	10.225
1.55	9.7547
1.50	9.2908
1.45	8.8303
1.40	8.3704
1.35	7.9078
1.30	7.4393
1.25	6.9604
H21=3.000	
2.78	602.01
2.77	384.12
2.76	282.97
2.75	224.57
2.74	186.42
2.73	159.65
2.72	139.83
2.71	124.57
2.70	112.46
2.65	76.549
2.60	58.845
2.55	48.267
2.50	41.174
2.45	36.030
2.40	32.092
2.35	28.949
2.30	26.359
2.25	24.183
2.20	22.333
2.15	20.750
2.10	19.393
2.05	18.229
2.00	17.223
1.95	16.340
1.90	15.552
1.85	14.835
1.80	14.170
1.75	13.544
1.70	12.947
1.65	12.372
1.60	11.813
1.55	11.266
1.50	10.725
1.45	10.188
1.40	9.6518
1.35	9.1109
1.30	8.5620
1.25	7.9989
H21=3.500	
2.78	694.63
2.77	442.96
2.76	326.39
2.75	258.91
2.74	214.91
2.73	184.09
2.72	161.30
2.71	143.62
2.70	129.68
2.65	88.303
2.60	67.896
2.55	55.699
2.50	47.505
2.45	41.567
2.40	37.011
2.35	33.369
2.30	30.362
2.25	27.827
2.20	25.663
2.15	23.809
2.10	22.218
2.05	20.853
2.00	19.677
1.95	18.651
1.90	17.737
1.85	16.910
1.80	16.145
1.75	15.426
1.70	14.742
1.65	14.082
1.60	13.442
1.55	12.814
1.50	12.194
1.45	11.578
1.30	10.961
1.35	10.338
1.30	9.7045
1.25	9.0525
H21=4.000	
2.78	785.83
2.77	501.67
2.76	369.50
2.75	293.12
2.74	243.37
2.73	208.56
2.72	182.72
2.71	162.78
2.70	146.94
2.65	100.04
2.60	76.950
2.55	63.132
2.50	53.858
2.45	47.122
2.40	41.953
2.35	37.811
2.30	34.386
2.25	31.495
2.20	29.019
2.15	26.894
2.10	25.070
2.05	23.506
2.00	22.160
1.95	20.989
1.90	19.951
1.85	19.012
1.80	18.146
1.75	17.334
1.70	16.561
1.65	15.816
1.60	15.092
1.55	14.383
1.50	13.682
1.45	12.985
1.40	12.285
1.35	11.579
1.30	10.858
1.25	10.115
H21=4.500	
2.78	876.86
2.77	560.70
2.76	412.77
2.75	327.43
2.74	271.91
2.73	232.90
2.72	204.01
2.71	181.88
2.70	164.18
2.65	111.82
2.60	86.030
2.55	70.596
2.50	60.222
2.45	52.689
2.40	46.908
2.35	42.270
2.30	38.426
2.25	35.180
2.20	32.395
2.15	29.997
2.10	27.939
2.05	26.177
2.00	24.662
1.95	23.346
1.90	22.181
1.85	21.132
1.80	20.164
1.75	19.257
1.70	18.394
1.65	17.563
1.60	16.756
1.55	15.963
1.50	15.180
1.45	14.401
1.40	13.619
1.35	12.828
1.30	12.019
1.25	11.183
H21=5.000	
2.78	969.34
2.77	618.65
2.76	455.91
2.75	361.97
2.74	300.48

(to be continued)

Table 12. (continued)

V/V_1	L/H_1	V/V_1	L/H_1	V/V_1	L/H_1	V/V_1	L/H_1
2.73	257.36	2.35	46.729	1.85	23.260	1.35	14.081
2.72	225.46	2.30	42.472	1.80	22.191	1.30	13.184
2.71	200.90	2.25	38.873	1.75	21.188	1.25	12.254
2.70	181.43	2.20	35.777	1.70	20.235		
2.65	123.58	2.15	33.112	1.65	19.318		
2.60	95.089	2.10	30.820	1.60	18.427		
2.55	78.047	2.05	28.857	1.55	17.551		
2.50	66.596	2.00	27.172	1.50	16.686		
2.45	58.259	1.95	25.712	1.45	15.824		
2.40	51.861	1.90	24.423	1.40	14.959		

Table 13.

RO21=3.000 V21=4.667 V2S1=2.694
RO31=3.400 V31=5.533 V3S1=3.194

V/V_1	L/H_1	V/V_1	L/H_1	V/V_1	L/H_1	V/V_1	L/H_1
H21=5.000		H21=10.000		H21=15.000		H21=20.000	
2.90	136.49	2.90	243.37	2.90	349.91	2.90	455.91
2.88	76.368	2.88	130.44	2.88	184.09	2.88	237.86
2.86	49.746	2.86	82.979	2.86	116.69	2.86	150.55
2.84	37.083	2.84	62.466	2.84	88.592	2.84	114.84
2.82	30.473	2.82	51.955	2.82	74.156	2.82	96.480
2.80	26.494	2.80	45.486	2.80	65.138	2.80	84.909
2.78	23.804	2.78	40.958	2.78	58.765	2.78	76.675
2.76	21.832	2.76	37.538	2.76	53.886	2.76	70.355
2.74	20.304	2.74	34.795	2.74	49.948	2.74	65.212
2.72	19.068	2.72	32.511	2.72	46.640	2.72	60.870
2.70	18.037	2.70	30.549	2.70	43.772	2.70	57.096
2.68	17.157	2.68	28.820	2.68	41.217	2.68	53.728
2.65	16.046	2.65	26.541	2.65	37.816	2.65	49.204
2.60	14.575	2.60	23.298	2.60	32.858	2.60	42.542
2.55	13.421	2.55	20.467	2.55	28.342	2.55	36.348
2.50	12.483	2.50	17.867	2.50	23.879	2.50	29.955
2.45	11.699	2.45	15.449	2.45	19.164	2.45	22.450
2.40	11.034	2.40	13.338	2.40	14.703	2.40	15.180
2.35	10.460	2.35	11.750	2.35	12.091	2.35	12.132
2.30	9.9545	2.30	10.667	2.30	10.759	2.30	10.764
2.25	9.5024	2.25	9.9070	2.25	9.9361		
2.20	9.0909	2.20	9.3275	2.20	9.3380		
2.15	8.7109	2.15	8.8526				
2.10	8.3549	2.10	8.4415				
2.05	8.0176	2.05	8.0706				
2.00	7.6947	2.00	7.7275				
1.95	7.3826	1.95	7.4029				
1.90	7.0790	1.90	7.0916				
1.85	6.7818	1.85	6.7893				
1.80	6.4892	1.80	6.4938				
1.75	6.1996						
1.70	5.9119						
1.65	5.6247						
1.60	5.3368						
1.55	5.0471						
1.50	4.7542						
1.45	4.4566						
1.40	4.1527						

Table 14.

RO21=2.800 V21=4.667 V2S1=2.694
RO31=3.400 V31=5.533 V3S1=3.194

V/V_1	L/H_1	V/V_1	L/H_1	V/V_1	L/H_1	V/V_1	L/H_1
H21=5.000		H21=10.000		H21=15.000		H21=20.000	
2.90	122.82	2.90	214.20	2.90	304.75	2.90	395.03
2.88	65.720	2.88	106.88	2.88	147.74	2.88	188.54
2.86	42.207	2.86	68.419	2.86	95.655	2.86	123.23
2.84	32.332	2.84	53.864	2.84	76.322	2.84	98.946
2.82	27.325	2.82	46.234	2.82	65.930	2.82	85.772
2.80	24.254	2.80	41.316	2.80	59.109	2.80	77.031
2.78	22.126	2.78	37.755	2.78	54.095	2.78	70.558
2.76	20.533	2.76	34.986	2.76	50.148	2.76	65.419
2.74	19.273	2.74	32.720	2.74	46.882	2.74	61.152
2.72	18.239	2.72	30.796	2.72	44.083	2.72	57.485
2.70	17.366	2.70	29.118	2.70	41.620	2.70	54.244
2.68	16.613	2.68	27.620	2.68	39.406	2.68	51.308
2.65	15.650	2.65	25.622	2.65	36.404	2.65	47.313
2.60	14.353	2.60	22.726	2.60	31.956	2.60	41.320
2.55	13.314	2.55	20.161	2.55	27.833	2.55	35.643
2.50	12.453	2.50	17.780	2.50	23.721	2.50	29.720
2.45	11.720	2.45	15.541	2.45	19.357	2.45	22.774
2.40	11.086	2.40	13.541	2.40	15.101	2.40	15.717
2.35	10.527	2.35	11.967	2.35	12.393	2.35	12.452
2.30	10.029	2.30	10.851	2.30	10.970	2.30	10.978
2.25	9.5788	2.25	10.054	2.25	10.093		
2.20	9.1654	2.20	9.4477	2.20	9.4612		
2.15	8.7813	2.15	8.9521				
2.10	8.4205	2.10	8.5256				
2.05	8.0782	2.05	8.1431				
2.00	7.7500	2.00	7.7904				
1.95	7.4331	1.95	7.4581				
1.90	7.1250	1.90	7.1404				
1.85	6.8235	1.85	6.8331				
1.80	6.5272	1.80	6.5327				
1.75	6.2341						
1.70	5.9432						
1.65	5.6531						
1.60	5.3627						
1.55	5.0706						
1.50	4.7756						
1.45	4.4761						
1.40	4.1703						

Table 15.

RO21=2.800 V21=4.667 V2S1=2.694
RO31=3.000 V31=5.533 V3S1=3.194

V/V_1	L/H_1	V/V_1	L/H_1	V/V_1	L/H_1	V/V_1	L/H_1
H21=5.000		H21=10.000		H21=15.000		H21=20.000	
2.90	151.70	2.90	271.62	2.90	390.83	2.90	510.13
2.88	87.866	2.88	152.46	2.88	216.63	2.88	280.96
2.86	58.604	2.86	99.080	2.86	139.76	2.86	180.41
2.84	43.392	2.84	73.030	2.84	103.23	2.84	133.55
2.82	34.941	2.82	59.183	2.82	84.091	2.82	109.12
2.80	29.797	2.80	50.781	2.80	72.394	2.80	94.167
2.78	26.365	2.78	45.060	2.78	64.380	2.78	83.817
2.76	23.892	2.76	40.831	2.76	58.398	2.76	76.097
2.74	22.005	2.74	37.519	2.74	58.678	2.74	69.944
2.72	20.503	2.72	34.811	2.72	49.770	2.72	64.842
2.70	19.268	2.70	32.517	2.70	46.442	2.70	60.477
2.68	18.227	2.68	30.525	2.68	43.524	2.68	56.637
2.65	16.925	2.65	27.939	2.65	39.688	2.65	51.549
2.60	15.230	2.60	24.331	2.60	34.216	2.60	44.224
2.55	13.921	2.55	21.249	2.55	29.344	2.55	37.562
2.50	12.871	2.50	18.471	2.50	24.636	2.50	30.845
2.45	12.005	2.45	15.921	2.45	19.772	2.45	23.193
2.40	11.278	2.40	13.704	2.40	15.183	2.40	15.741
2.35	10.656	2.35	12.022	2.35	12.402	2.35	12.451
2.30	10.114	2.30	10.868	2.30	10.971	2.30	10.979
2.25	9.6348	2.25	10.060	2.25	10.093		
2.20	9.2021	2.20	9.4498	2.20	9.4612		
2.15	8.8057	2.15	8.9533				
2.10	8.4365	2.10	8.5259				
2.05	8.0884	2.05	8.1434				
2.00	7.7566	2.00	7.7904				
1.95	7.4374	1.95	7.4583				
1.90	7.1278	1.90	7.1404				
1.85	6.8253	1.85	6.8331				
1.80	6.5282	1.80	6.5327				
1.75	6.2347						
1.70	5.9436						
1.65	5.6533						
1.60	5.3627						
1.55	5.0706						
1.50	4.7756						
1.45	4.4761						
1.40	4.1702						

Table 16.

RO21=3.000 V21=3.333 V2S1=1.924
RO31=3.400 V31=5.533 V3S1=3.194

V/V_1	L/H_1
H21=5.000	
2.90	338.54
2.88	216.41
2.86	157.99
2.84	123.54
2.82	100.85
2.80	84.769
2.78	72.762
2.76	63.470
2.74	56.121
2.72	50.195
2.70	45.342
2.68	41.334
2.66	38.012
2.65	36.569
2.60	30.936
2.55	27.145
2.50	24.443
2.45	22.401
2.40	20.770
2.35	19.406
2.30	18.226
2.25	17.173
2.20	16.211
2.15	15.312
2.10	14.461
2.05	13.642
2.00	12.845
1.95	12.059
1.90	11.277
1.85	10.493
1.80	9.7020
1.75	8.9081
1.70	8.1233
1.65	7.3755
1.60	6.6970
1.55	6.1017
1.50	5.5812
1.45	5.1163
1.40	4.6883
2.35	4.2817
H21=10.000	
2.90	652.86
2.88	417.25
2.86	304.42
2.84	237.77
2.82	193.82
2.80	162.60
2.78	139.31
2.76	121.30
2.74	107.05
2.72	95.522
2.71	90.599
2.70	86.131
2.69	82.058
2.68	78.375
2.67	75.030
2.66	71.978
2.65	69.183
2.64	66.646
2.60	58.395
2.55	51.177
2.50	46.029
2.45	42.129
2.40	38.999
2.35	36.375
2.30	34.082
2.25	32.016
2.20	30.108
2.15	28.314
2.10	26.585
2.05	24.892
2.00	23.202
1.95	21.490
1.90	19.706
1.85	17.799
1.80	15.672
1.75	13.182
1.70	10.337
1.65	8.1536
1.60	6.9474
H21=15.000	
2.90	968.24
2.88	618.06
2.86	451.03
2.84	352.16
2.82	286.91
2.80	240.43
2.78	205.92
2.76	179.17
2.74	157.99
2.72	140.98
2.71	133.64
2.70	127.02
2.69	121.03
2.68	115.53
2.67	110.60
2.66	106.07
2.65	101.93
2.64	98.181
2.60	86.039
2.55	75.392
2.50	67.826
2.45	62.068
2.40	57.457
2.35	53.554
2.30	50.164
2.25	47.094
2.20	44.244
2.15	41.558
2.10	38.961
2.05	36.404
2.00	33.838
1.95	31.206
1.90	28.431
1.85	25.377
1.80	21.800
1.75	17.051
1.70	11.045
H21=20.000	
2.90	1280.4
2.88	818.57
2.86	596.57
2.84	466.23
2.82	379.92
2.80	318.67
2.78	272.68
2.76	237.24
2.74	209.13
2.72	186.36
2.71	176.72
2.70	167.92
2.69	159.95
2.68	152.71
2.67	146.17
2.66	140.17
2.65	134.71
2.64	129.73
2.60	113.71
2.55	99.628
2.50	89.635
2.45	82.045
2.40	75.926
2.35	70.781
2.30	66.261
2.25	62.188
2.20	58.416
2.15	54.832
2.10	51.381
2.05	47.950
2.00	44.514
1.95	40.965
1.90	37.186
1.85	32.985
1.80	27.903
1.75	20.445
1.70	11.143
H21=25.000	
2.90	1594.5
2.88	1021.3
2.86	743.38
2.84	581.21
2.82	472.91
2.80	396.43
2.78	339.08
2.76	295.00
2.74	260.12
2.72	231.81
2.71	219.74
2.70	208.87
2.69	198.87
2.68	189.93
2.67	181.75
2.66	174.36
2.65	167.55

(to be continued)

Table 16. (continued)

V/V_1	L/H_1	V/V_1	L/H_1	V/V_1	L/H_1	V/V_1	L/H_1
2.64	161.35	1.90	45.964	2.78	405.80	2.45	122.04
2.60	141.28	1.85	40.598	2.76	352.74	2.40	112.92
2.55	123.92	1.80	33.974	2.74	311.05	2.35	105.27
				2.72	277.37	2.30	98.530
2.50	111.43	1.75	23.339				
2.45	102.00			2.71	262.83	2.25	92.442
2.40	94.423			2.70	249.73	2.20	86.782
2.35	87.992			2.69	237.87	2.15	81.443
2.30	82.381	H21=30.000		2.68	227.09	2.10	76.214
				2.67	217.42	2.05	71.078
2.25	77.332						
2.20	72.602	2.90	1906.4	2.66	208.38	2.00	65.881
2.15	68.128	2.88	1225.5	2.65	200.36	1.95	60.493
2.10	63.791	2.86	891.75	2.64	192.93	1.90	54.739
2.05	59.508	2.84	694.06	2.60	169.05	1.85	48.216
		2.82	566.62	2.55	148.11	1.80	40.027
2.00	55.189						
1.95	50.725	2.80	474.48	2.50	133.32	1.75	25.827

Table 17.

RO21=2.800 V21=3.333 V2S1=1.924
RO31=3.400 V31=5.533 V3S1=3.194

V/V_1	L/H_1	V/V_1	L/H_1	V/V_1	L/H_1	V/V_1	L/H_1
H21=5.000		H21=10.000		H21=15.000		H21=20.000	
2.90	316.75	2.90	610.58	2.90	904.60	2.90	1194.2
2.88	202.41	2.88	384.35	2.88	575.75	2.88	763.68
2.86	147.48	2.86	283.28	2.86	419.49	2.86	555.25
2.84	115.23	2.84	221.10	2.84	327.01	2.84	432.54
2.82	93.961	2.82	179.91	2.82	266.00	2.82	352.31
2.80	78.884	2.80	150.86	2.80	222.82	2.80	294.80
2.78	67.673	2.78	129.10	2.78	190.57	2.78	252.19
2.76	59.034	2.76	112.33	2.76	165.72	2.76	219.22
2.74	52.213	2.74	99.156	2.74	146.19	2.74	193.29
2.70	42.304	2.70	79.987	2.70	117.81	2.70	155.65
2.65	34.386	2.65	64.769	2.65	95.301	2.65	125.88
2.60	29.374	2.60	55.221	2.60	81.250	2.60	107.34
2.55	26.016	2.55	48.858	2.55	71.898	2.55	94.984
2.50	23.610	2.50	44.292	2.50	65.196	2.50	86.117
2.45	21.772	2.45	40.789	2.45	60.039	2.45	79.322
2.40	20.289	2.40	37.950	2.40	55.844	2.40	73.774
2.35	19.036	2.35	35.535	2.35	52.272	2.35	69.043
2.30	17.940	2.30	33.404	2.30	49.110	2.30	64.851
2.25	16.953	2.25	31.468	2.25	46.234	2.25	61.036
2.20	16.045	2.20	29.668	2.20	43.550	2.20	57.466
2.15	15.193	2.15	27.960	2.15	40.991	2.15	54.050
2.10	14.380	2.10	26.308	2.10	38.507	2.10	50.736
2.05	13.596	2.05	24.683	2.05	36.047	2.05	47.453
2.00	12.829	2.00	23.056	2.00	33.569	2.00	44.125
1.95	12.070	1.95	21.399	1.95	31.020	1.95	40.686
1.90	11.314	1.90	19.674	1.90	28.323	1.90	37.011
1.85	10.555	1.85	17.825	1.85	25.359	1.85	32.921
1.80	9.7879	1.80	15.771	1.80	21.893	2.80	27.981
1.75	9.0148	1.75	13.380	1.75	17.349	1.75	20.858
1.70	8.2457	1.70	10.638	1.70	11.511	1.70	11.647
1.65	7.5033	1.65	8.4032				
1.60	6.8176	1.60	7.1179				
1.55	6.2075						
1.50	5.6708						
1.45	5.1914						
1.40	4.7511						
1.35	4.3350						

Table 18.

RO21=2.800 V21=3.333 V2S1=1.924
RO31=3.000 V31=5.533 V3S1=3.194

V/V_1	L/H_1
H21=5.000	
2.90	360.75
2.88	230.86
2.86	168.54
2.84	132.06
2.82	107.91
2.80	90.760
2.78	78.002
2.76	68.106
2.74	60.235
2.72	53.859
2.70	48.632
2.68	44.281
2.66	40.644
2.65	39.060
2.60	32.816
2.55	28.585
2.50	25.570
2.45	23.305
2.40	21.514
2.35	20.034
2.30	18.761
2.25	17.635
2.20	16.616
2.15	15.671
2.10	14.781
2.05	13.929
2.00	13.103
1.95	12.295
1.90	11.494
1.85	10.694
1.80	8.8908
1.75	9.0855
1.70	8.2897
1.65	7.5269
1.60	6.8285
1.55	6.2121
1.50	5.6724
1.45	5.1919
1.40	4.7511
1.35	4.3352
H21=10.000	
2.90	695.19
2.88	444.03
2.86	324.21
2.84	253.51
2.82	206.91
2.80	173.80
2.78	148.99
2.76	129.90
2.74	114.66
2.72	102.29
2.70	92.151
2.68	83.754
2.66	76.760
2.65	73.717
2.60	61.758
2.55	53.688
2.50	47.979
2.45	43.674
2.40	40.248
2.35	37.407
2.30	34.948
2.25	32.753
2.20	30.740
2.15	28.857
2.10	27.059
2.05	25.307
2.00	23.569
1.95	21.816
1.90	20.000
1.85	18.071
1.80	15.939
1.75	13.474
1.70	10.665
1.65	8.4043
1.60	7.1183
H21=15.000	
2.90	1028.6
2.88	657.87
2.86	479.25
2.84	374.94
2.82	305.72
2.80	256.85
2.78	220.08
2.76	191.66
2.74	169.07
2.72	150.82
2.70	135.80
2.68	123.40
2.66	113.00
2.65	108.46
2.60	90.850
2.55	79.003
2.50	70.594
2.45	64.237
2.40	59.212
2.35	55.010
2.30	51.365
2.25	48.101
2.20	45.113
2.15	42.295
2.10	39.594
2.05	36.951
2.00	34.315
1.95	31.620
1.90	28.793
1.85	25.707
1.80	22.121
1.75	17.453
1.70	11.517
H21=20.000	
2.90	1361.7
2.88	871.81
2.86	635.46
2.84	496.45
2.82	405.04
2.80	339.88
2.78	291.20
2.76	253.51
2.74	223.52
2.72	199.44
2.70	179.42
2.68	163.05
2.66	149.28
2.65	143.23
2.60	119.99
2.55	104.31
2.50	93.219
2.45	84.836
2.40	78.215
2.35	72.651
2.30	67.826
2.25	63.502
2.20	59.519
2.15	55.773
2.10	52.182
2.05	48.639
2.00	45.100
1.95	41.467
1.90	37.621
1.85	33.371
1.80	28.271
1.75	20.966
H21=25.000	
2.90	1695.4
2.88	1083.2
2.86	789.93
2.84	618.06
2.82	504.03
2.80	423.01
2.78	362.58
2.76	315.39
2.74	277.99
2.72	248.03
2.70	223.25
2.68	202.71
2.66	185.63
2.65	178.13
2.60	149.14
2.55	129.61
2.50	115.84
2.45	105.48
2.40	97.219
2.35	90.263
2.30	84.281
2.25	78.886
2.20	73.937
2.15	69.272
2.10	64.767
2.05	60.334
2.00	55.899
1.95	51.324
1.90	46.455
1.85	41.033
1.80	34.388
1.75	24.033

(to be continued)

Table 18. (continued)

V/V_1	L/H_1	V/V_1	L/H_1	V/V_1	L/H_1	V/V_1	L/H_1
H21=30.000		2.78	433.70	2.55	154.96	2.10	77.350
		2.76	377.58	2.50	138.48		
		2.74	332.76	2.45	126.06	2.05	72.033
2.90	2032.9	2.72	296.50	2.40	116.18	2.00	66.701
2.88	1299.8			2.35	107.95	1.95	61.183
2.86	946.87	2.70	266.97			1.90	55.303
2.84	739.54	2.68	242.43	2.30	100.75	1.85	48.698
2.82	603.28	2.66	221.71	2.25	94.285		
		2.65	213.05	2.20	88.355	1.80	40.481
2.80	505.82	2.60	178.23	2.15	82.742	1.75	26.664

Table 19.

RO21=2.800 V21=4.667 V2S1=2.694
RO31=3.000 V31=5.400 V3S1=3.118

V/V_1	L/H_1	V/V_1	L/H_1	V/V_1	L/H_1	V/V_1	L/H_1
H21=1.000		H21=4.000		H21=7.000		H21=10.000	
2.84	68.684	2.84	156.95	2.84	243.57	2.84	330.20
2.82	38.867	2.82	79.638	2.82	118.88	2.82	157.81
2.80	27.494	2.80	49.963	2.80	71.981	2.80	94.126
2.78	21.820	2.78	35.918	2.78	51.345	2.78	67.379
2.76	18.590	2.76	28.609	2.76	41.089	2.76	54.302
2.74	16.580	2.74	24.338	2.74	35.078	2.74	46.552
2.72	15.237	2.72	21.558	2.72	31.053	2.72	41.279
2.70	14.282	2.70	19.591	2.70	28.108	2.70	37.363
2.68	13.567	2.68	18.116	2.68	25.816	2.68	34.268
2.66	13.007	2.66	16.958	2.66	23.949	2.66	31.707
2.64	12.554	2.64	16.020	2.64	22.381	2.64	29.522
2.62	12.176	2.62	15.238	2.62	21.026	2.62	27.605
2.60	11.852	2.60	14.576	2.60	19.835	2.60	25.888
2.58	11.568	2.58	14.005	2.58	18.772	2.58	24.324
2.55	11.198	2.55	13.277	2.55	17.360	2.55	22.185
2.50	10.682	2.50	12.308	2.50	15.379	2.50	19.008
2.45	10.247	2.45	11.544	2.45	13.758	2.45	16.192
2.40	9.8611	2.40	10.914	2.40	12.443	2.40	13.809
2.35	9.5098	2.35	10.376	2.35	11.400	2.35	12.054
2.30	9.1814	2.30	9.9021	2.30	10.581	2.30	10.878
2.25	8.8700	2.25	9.4752	2.25	9.9254	2.25	10.064
2.20	8.5708	2.20	9.0832	2.20	9.3839	2.20	9.4511
2.15	8.2807	2.15	8.7174	2.15	8.9201	2.15	8.9537
2.10	7.9976	2.10	8.3715	2.10	8.5087	2.10	8.5259
2.05	7.7194	2.05	8.0408	2.05	8.1344	2.05	8.1434
2.00	7.4451	2.00	7.7219	2.00	7.7857	2.00	7.7904
1.95	7.1735	1.95	7.4125	1.95	7.4557	1.95	7.4583
1.90	6.9037	1.90	7.1099	1.90	7.1391	1.90	7.1404
1.85	6.6348	1.85	6.8129	1.85	6.8324	1.85	6.8329
1.80	6.3661	1.80	6.5196	1.80	6.5324	1.80	6.5327
1.75	6.0969	1.75	6.2290	1.75	6.2373		
1.70	5.8265	1.70	5.9397	1.70	5.9451		
1.65	5.5543	1.65	5.6509	1.65	5.6540		
1.60	5.2793	1.60	5.3613	1.60	5.3632		
1.55	5.0007	1.55	5.0698	1.55	5.0708		
1.50	4.7175	1.50	4.7751	1.50	4.7758		
1.45	4.4284	1.45	4.4758				
1.40	4.1318	1.40	4.1702				
1.35	3.8256	1.35	3.8560				

Table 20.

RO21=2.800 V21=4.000 V2S1=2.309
RO31=3.000 V31=5.400 V3S1=3.118

V/V_1	L/H_1	V/V_1	L/H_1	V/V_1	L/H_1	V/V_1	L/H_1
H21=1.000		H21=4.000		H21=7.000		H21=10.000	
2.84	97.684	2.84	280.16	2.84	462.71	2.84	645.01
2.82	55.232	2.82	153.85	2.82	252.61	2.82	351.01
2.80	38.438	2.80	103.08	2.80	168.14	2.80	232.99
2.78	29.586	2.78	75.756	2.78	122.55	2.78	169.27
2.76	24.238	2.76	58.798	2.76	94.250	2.76	129.78
2.74	20.749	2.74	47.459	2.74	75.437	2.74	103.51
2.72	18.359	2.72	39.558	2.72	62.463	2.72	85.564
2.70	16.660	2.70	33.929	2.70	53.350	2.70	73.022
2.68	15.413	2.68	29.830	2.68	46.791	2.68	64.068
2.66	14.470	2.66	26.775	2.66	41.945	2.66	57.482
2.64	13.737	2.64	24.439	2.64	38.246	2.64	52.443
2.62	13.149	2.62	22.602	2.62	35.326	2.62	48.467
2.60	12.667	2.60	21.118	2.60	32.962	2.60	45.222
2.58	12.262	2.58	19.893	2.58	30.988	2.58	42.519
2.55	11.757	2.55	18.400	2.55	28.555	2.55	39.174
2.50	11.095	2.50	16.513	2.50	25.413	2.50	34.812
2.45	10.569	2.45	15.088	2.45	22.965	2.45	31.385
2.40	10.126	2.40	13.945	2.40	20.934	2.40	28.497
2.35	9.7300	2.35	12.989	2.35	19.162	2.35	25.948
2.30	9.3739	2.30	12.162	2.30	17.565	2.30	23.597
2.25	9.0397	2.25	11.431	2.25	16.079	2.25	21.355
2.20	8.7226	2.20	10.774	2.20	14.667	2.20	19.139
2.15	8.4187	2.15	10.175	2.15	13.308	2.15	16.873
2.10	8.1250	2.10	9.6257	2.10	12.004	2.10	14.513
2.05	7.8368	2.05	9.1159	2.05	10.792	2.05	12.170
2.00	7.5550	2.00	8.6420	2.00	9.7346	2.00	10.295
1.95	7.2783	1.95	8.1978	1.95	8.8725	1.95	9.0717
1.90	7.0020	1.90	7.7801	1.90	8.1855	1.90	8.2574
1.85	6.7284	1.85	7.3845	1.85	7.6254	1.85	7.6519
1.80	6.4542	1.80	7.0073	1.80	7.1497	1.80	7.1602
1.75	6.1821	1.75	6.6459	1.75	6.7293		
1.70	5.9075	1.70	6.2966	1.70	6.3448		
1.65	5.6327	1.65	5.9572	1.65	5.9844		
1.60	5.3544	1.60	5.6246	1.60	5.6396		
1.55	5.0741	1.55	5.2969				
1.50	4.7885	1.50	4.9715				
1.45	4.4977	1.45	4.6462				
1.40	4.1994	1.40	4.3183				
1.35	3.8917	1.35	3.9851				

Table 21.

RO21=2.500 V21=3.333 V2S1=1.924
RO31=3.400 V31=5.400 V3S1=3.118

V/V_1	L/H_1	V/V_1	L/H_1	V/V_1	L/H_1	V/V_1	L/H_1
H21=1.000		H21=4.000		H21=7.000		H21=10.000	
2.72	19.095	2.72	49.303	2.72	81.094	2.72	113.00
2.70	17.262	2.70	42.632	2.70	69.843	2.70	97.190
2.68	15.906	2.68	37.516	2.68	61.241	2.68	85.083
2.66	14.876	2.66	33.538	2.66	54.562	2.66	75.765
2.64	14.074	2.64	30.409	2.64	49.333	2.64	68.461
2.62	13.437	2.62	27.925	2.62	45.208	2.62	62.709
2.60	12.917	2.60	25.929	2.60	41.904	2.60	58.121
2.58	12.483	2.58	24.301	2.58	39.222	2.58	54.415
2.56	12.115	2.56	22.957	2.56	37.015	2.56	51.349
2.55	11.950	2.55	22.371	2.55	36.050	2.55	50.016
2.50	11.262	2.50	20.043	2.50	32.224	2.50	44.708
2.45	10.724	2.45	18.376	2.45	29.470	2.45	40.886
2.40	10.273	2.40	17.089	2.40	27.328	2.40	37.900
2.35	9.8766	2.35	16.037	2.35	25.562	2.35	35.427
2.30	9.5168	2.30	15.137	2.30	24.035	2.30	33.283
2.25	9.1821	2.25	14.340	2.25	22.670	2.25	31.357
2.20	8.8651	2.20	13.616	2.20	21.415	2.20	29.576
2.15	8.5608	2.15	12.944	2.15	20.235	2.15	27.897
2.10	8.2661	2.10	12.311	2.10	19.104	2.10	26.273
2.05	7.9780	2.05	11.705	2.05	18.003	2.05	24.681
2.00	7.6956	2.00	11.120	2.00	16.914	2.00	23.089
1.95	7.4168	1.95	10.549	1.95	15.822	1.95	21.473
1.90	7.1406	1.90	9.9885	1.90	14.711	1.90	19.790
1.85	6.8659	1.85	9.4347	1.85	13.560	1.85	17.999
1.80	6.5923	1.80	8.8850	1.80	12.351	1.80	16.023
1.75	6.3185	1.75	8.3390	1.75	11.066	1.75	13.755
1.70	6.0441	1.70	7.7970	1.70	9.7207	1.70	11.155
1.65	5.7681	1.65	7.2622	1.65	8.4213	1.65	8.8542
1.60	5.4899	1.60	6.7394	1.60	7.3398	1.60	7.4339
1.55	5.2085	1.55	6.2340	1.55	6.5177		
1.50	4.9230	1.50	5.7506	1.50	5.8769		
1.45	4.6322	1.45	5.2901	1.45	5.3432		
1.40	4.3345	1.40	4.8506				
1.35	4.0279	1.35	4.4269				

Table 22.

RO21=2.800 V21=3.333 V2S1=1.924
RO31=3.000 V31=5.400 V3S1=3.118

V/V_1	L/H_1	V/V_1	L/H_1	V/V_1	L/H_1	V/V_1	L/H_1
H21=1.000		H21=4.000		H21=7.000		H21=10.000	
2.72	22.724	2.72	64.045	2.72	106.49	2.72	149.00
2.70	20.248	2.70	55.389	2.70	91.862	2.70	128.47
2.68	18.369	2.68	48.632	2.68	80.445	2.68	112.36
2.66	16.912	2.66	43.239	2.66	71.299	2.66	99.474
2.64	15.764	2.64	38.857	2.64	63.918	2.64	89.089
2.62	14.844	2.62	35.266	2.62	57.860	2.62	80.586
2.60	14.097	2.60	32.302	2.60	52.868	2.60	73.599
2.58	13.479	2.58	29.837	2.58	48.742	2.58	67.812
2.56	12.961	2.56	27.773	2.56	45.291	2.56	62.992
2.55	12.733	2.55	26.866	2.55	43.772	2.55	60.892
2.50	11.805	2.50	23.273	2.50	37.805	2.50	52.571
2.45	11.115	2.45	20.762	2.45	33.635	2.45	46.771
2.40	10.565	2.40	18.898	2.40	30.534	2.40	42.444
2.35	10.100	2.35	17.434	2.35	28.082	2.35	39.020
2.30	9.6906	2.30	16.230	2.30	26.047	2.30	36.164
2.25	9.3190	2.25	15.200	2.25	24.292	2.25	33.697
2.20	8.9736	2.20	14.293	2.20	22.726	2.20	31.483
2.15	8.6471	2.15	13.472	2.15	21.291	2.15	29.444
2.10	8.3349	2.10	12.716	2.10	19.950	2.10	27.527
2.05	8.0326	2.05	12.007	2.05	18.666	2.05	25.681
2.00	7.7382	2.00	11.333	2.00	17.418	2.00	23.866
1.95	7.4494	1.95	10.685	1.95	16.183	1.95	22.046
1.90	7.1649	1.90	10.058	1.90	14.937	1.90	20.178
1.85	6.8832	1.85	9.4452	1.85	13.659	1.85	18.200
1.80	6.6033	1.80	8.8447	1.80	12.322	1.80	16.026
1.75	6.3243	1.75	8.2562	1.75	10.908	1.75	13.519
1.70	6.0452	1.70	7.6813	1.70	9.4470	1.70	10.677
1.65	5.7652	1.65	7.1242	1.65	8.1026	1.65	8.4062
1.60	5.4833	1.60	6.5908	1.60	7.0597	1.60	7.1187
1.55	5.1986	1.55	6.0859	1.55	6.2953	1.55	6.3068
1.50	4.9102	1.50	5.6113	1.50	5.7008	1.50	5.7036
1.45	4.6165	1.45	5.1646	1.45	5.2012		
1.40	4.3162	1.40	4.7401				
1.35	4.0071	1.35	4.3309				

Table 23.

RO21=2.500 V21=3.333 V2S1=1.924
RO31=3.000 V31=5.400 V3S1=3.118

V/V_1	L/H_1	V/V_1	L/H_1	V/V_1	L/H_1	V/V_1	L/H_1
H21=1.000		H21=4.000		H21=7.000		H21=10.000	
2.72	21.269	2.72	56.988	2.72	94.037	2.72	131.15
2.70	19.065	2.70	49.265	2.70	81.033	2.70	112.88
2.68	17.405	2.68	43.280	2.68	70.937	2.68	98.711
2.66	16.130	2.66	38.545	2.66	62.955	2.66	87.513
2.64	15.131	2.64	34.744	2.64	56.587	2.64	78.597
2.62	14.331	2.62	31.676	2.62	51.439	2.62	71.393
2.60	13.682	2.60	29.174	2.60	47.274	2.60	65.586
2.58	13.142	2.58	27.120	2.58	43.864	2.58	60.859
2.56	12.688	2.56	25.413	2.56	41.049	2.56	56.928
2.55	12.486	2.55	24.664	2.55	39.817	2.55	55.221
2.50	11.657	2.50	21.715	2.50	34.965	2.50	48.490
2.45	11.027	2.45	19.641	2.45	31.545	2.45	43.743
2.40	10.514	2.40	18.076	2.40	28.951	2.40	40.140
2.35	10.073	2.35	16.826	2.35	26.863	2.35	37.226
2.30	9.6804	2.30	15.778	2.30	25.097	2.30	34.748
2.25	9.3204	2.25	14.868	2.25	23.547	2.25	32.567
2.20	8.9830	2.20	14.055	2.20	22.145	2.20	30.585
2.15	8.6628	2.15	13.310	2.15	20.845	2.15	28.734
2.10	8.3549	2.10	12.616	2.10	19.614	2.10	26.973
2.05	8.0560	2.05	11.960	2.05	18.427	2.05	25.262
2.00	7.7641	2.00	11.331	2.00	17.265	2.00	23.569
1.95	7.4771	1.95	10.722	1.95	16.108	1.95	21.859
1.90	7.1941	1.90	10.128	1.90	14.938	1.90	20.098
1.85	6.9135	1.85	9.5458	1.85	13.734	1.85	18.231
1.80	6.6343	1.80	8.9708	1.80	12.477	1.80	16.185
1.75	6.3559	1.75	8.4029	1.75	11.148	1.75	13.847
1.70	6.0772	1.70	7.8421	1.70	9.7631	1.70	11.186
1.65	5.7974	1.65	7.2924	1.65	8.4368	1.65	8.8587
1.60	5.5157	1.60	6.7579	1.60	7.3442	1.60	7.4339
1.55	5.2313	1.55	6.2444	1.55	6.5185		
1.50	4.9429	1.50	5.7559	1.50	5.8765		
1.45	4.6495	1.45	5.2925	1.45	5.3435		
1.40	4.3494	1.40	4.8517				
1.35	4.0405	1.35	4.4273				

Table 24.

RO21=2.500 V21=2.667 V2S1=1.540
RO31=3.400 V31=5.400 V3S1=3.118

V/V_1	L/H_1	V/V_1	L/H_1	V/V_1	L/H_1	V/V_1	L/H_1
H21=1.000		H21=4.000		H21=7.000		H21=10.000	
2.84	116.59	2.84	373.31	2.84	629.86	2.84	888.06
2.82	67.021	2.82	213.82	2.82	361.05	2.82	508.21
2.80	47.286	2.80	149.92	2.80	253.36	2.80	356.55
2.78	36.755	2.78	115.68	2.78	195.32	2.78	274.96
2.76	30.247	2.76	94.209	2.76	159.04	2.76	223.99
2.74	25.855	2.74	79.520	2.74	134.21	2.74	188.96
2.72	22.722	2.72	68.861	2.72	116.15	2.72	163.53
2.70	20.392	2.70	60.738	2.70	102.42	2.70	144.13
2.68	18.611	2.68	54.357	2.68	91.593	2.68	128.92
2.66	17.217	2.66	49.201	2.66	82.837	2.66	116.56
2.64	16.107	2.64	44.966	2.64	75.636	2.64	106.41
2.62	15.207	2.62	41.411	2.62	69.587	2.62	97.885
2.60	14.469	2.60	38.404	2.60	64.453	2.60	90.626
2.58	13.854	2.58	35.828	2.58	60.041	2.58	84.369
2.55	13.102	2.55	32.600	2.55	54.508	2.55	76.561
2.50	12.162	2.50	28.483	2.50	47.444	2.50	66.544
2.45	11.459	2.45	25.485	2.45	42.284	2.45	59.252
2.40	10.898	2.40	23.245	2.40	38.443	2.40	53.824
2.35	10.425	2.35	21.519	2.35	35.505	2.35	49.669
2.30	10.009	2.30	20.143	2.30	33.167	2.30	46.375
2.25	9.6308	2.25	19.000	2.25	31.231	2.25	43.654
2.20	9.2801	2.20	18.019	2.20	29.576	2.20	41.326
2.15	8.9490	2.15	17.151	2.15	28.113	2.15	39.265
2.10	8.6320	2.10	16.363	2.10	26.782	2.10	37.388
2.05	8.3257	2.05	15.634	2.05	25.548	2.05	35.648
2.00	8.0271	2.00	14.947	2.00	24.382	2.00	34.004
1.95	7.7344	1.95	14.292	1.95	23.266	1.95	32.427
1.90	7.4462	1.90	13.660	1.90	22.185	1.90	30.894
1.85	7.1611	1.85	13.044	1.85	21.127	1.85	29.387
1.80	6.8779	1.80	12.439	1.80	20.079	1.80	27.893
1.75	6.5958	1.75	11.839	1.75	19.032	1.75	26.394
1.70	6.3139	1.70	11.241	1.70	17.974	1.70	24.874
1.65	6.0316	1.65	10.638	1.65	16.895	1.65	23.310
1.60	5.7478	1.60	10.028	1.60	15.780	1.60	21.681
1.55	5.4617	1.55	9.4031	1.55	14.608	1.55	19.943
1.50	5.1725	1.50	8.7568	1.50	13.349	1.50	18.037
1.45	4.8789	1.45	8.0810	1.45	11.957	1.45	15.844
1.40	4.5798	1.40	7.3659	1.40	10.353	1.40	13.116
1.35	4.2733	1.35	6.6029	1.35	8.4537	1.35	9.5052

Table 25.

RO21=2.800 V21=2.667 V2S1=1.540
RO31=3.000 V31=5.400 V3S1=3.118

V/V_1	L/H_1	V/V_1	L/H_1	V/V_1	L/H_1	V/V_1	L/H_1
H21=1.000		H21=4.000		H21=7.000		H21=10.000	
2.84	143.89	2.84	469.81	2.84	795.79	2.84	1119.9
2.82	82.582	2.82	269.09	2.82	456.31	2.82	642.11
2.80	58.113	2.80	188.71	2.80	319.86	2.80	451.03
2.78	44.990	2.78	145.40	2.78	246.23	2.78	347.03
2.76	36.821	2.76	118.26	2.76	200.34	2.76	282.38
2.74	31.268	2.74	99.613	2.74	168.74	2.74	237.77
2.72	27.263	2.72	86.045	2.72	145.75	2.72	205.33
2.70	24.247	2.70	75.703	2.70	128.12	2.70	180.68
2.68	21.906	2.68	67.559	2.68	114.29	2.68	161.07
2.66	20.045	2.66	60.945	2.66	103.06	2.66	145.20
2.64	18.540	2.64	55.496	2.64	93.797	2.64	132.10
2.62	17.305	2.62	50.906	2.62	85.958	2.62	121.10
2.60	16.278	2.60	46.996	2.60	79.300	2.60	111.67
2.58	15.416	2.58	43.617	2.58	73.523	2.58	103.51
2.55	14.359	2.55	39.349	2.55	66.236	2.55	93.195
2.50	13.044	2.50	33.807	2.50	56.731	2.50	79.764
2.45	12.091	2.45	29.658	2.45	49.602	2.45	69.660
2.40	11.360	2.40	26.498	2.40	44.178	2.40	61.992
2.35	10.769	2.35	24.056	2.35	39.991	2.35	56.063
2.30	10.269	2.30	22.128	2.30	36.700	2.30	51.426
2.25	9.8302	2.25	20.571	2.25	34.049	2.25	47.690
2.20	9.4338	2.20	19.274	2.20	31.953	2.20	44.591
2.15	9.0675	2.15	18.163	2.15	29.973	2.15	41.946
2.10	8.7233	2.10	17.185	2.10	28.314	2.10	39.609
2.05	8.3955	2.05	16.304	2.05	26.821	2.05	37.502
2.00	8.0795	2.00	15.493	2.00	25.442	2.00	35.559
1.95	7.7725	1.95	14.735	1.95	24.150	1.95	33.732
1.90	7.4724	1.90	14.016	1.90	22.920	1.90	31.988
1.85	7.1773	1.85	13.326	1.85	21.732	1.85	30.304
1.80	6.8858	1.80	12.656	1.80	20.571	1.80	28.648
1.75	6.5965	1.75	12.000	1.75	19.424	1.75	27.009
1.70	6.3084	1.70	11.350	1.70	18.276	1.70	25.362
1.65	6.0206	1.65	10.701	1.65	17.115	1.65	23.682
1.60	5.7322	1.60	10.046	1.60	15.920	1.60	21.941
1.55	5.4419	1.55	9.3795	1.55	14.670	1.55	20.094
1.50	5.1488	1.50	8.6927	1.50	13.330	1.50	18.074
1.45	4.8517	1.45	7.9753	1.45	11.845	1.45	15.742
1.40	4.5492	1.40	7.2179	1.40	10.121	1.40	12.798
1.35	4.2395	1.35	6.4134	1.35	8.0693	1.35	8.8866

Table 26.

RO21=2.500 V21=2.667 V2S1=1.540
RO31=3.000 V31=5.400 V3S1=3.118

V/V_1	L/H_1
H21=1.000	
2.84	132.18
2.82	75.917
2.80	53.489
2.78	41.483
2.76	34.029
2.74	28.982
2.72	25.352
2.70	22.345
2.68	20.540
2.66	18.884
2.64	17.553
2.62	16.464
2.60	15.565
2.58	14.813
2.56	14.176
2.54	13.630
2.52	13.158
2.50	12.745
2.48	12.379
2.46	12.053
2.44	11.759
2.42	11.491
2.40	11.245
2.38	11.016
2.36	10.804
2.34	10.604
2.32	10.415
2.30	10.235
2.28	10.064
2.26	9.8997
2.24	9.7411
2.22	9.5881
2.20	9.4398
2.18	9.2955
2.15	9.0852
2.10	8.7499
2.05	8.4278
2.00	8.1168
1.95	7.8134
1.90	7.5160
1.85	7.2229
1.80	6.9329
1.75	6.6646
1.70	6.3574
1.65	6.0701
1.60	5.7828
1.55	5.4921
1.50	5.1994
1.45	4.9027
1.40	4.6007
1.35	4.2916
H21=4.000	
2.84	423.43
2.82	242.33
2.80	170.01
2.78	131.01
2.76	106.62
2.74	89.885
2.72	77.719
2.70	68.454
2.68	61.145
2.66	55.246
2.64	50.374
2.62	46.291
2.60	42.820
2.58	39.827
2.56	37.238
2.54	34.967
2.52	32.978
2.50	31.215
2.48	29.658
2.46	28.269
2.44	27.031
2.42	25.927
2.40	24.932
2.38	24.040
2.36	23.229
2.34	22.493
2.32	21.823
2.30	21.209
2.28	20.642
2.26	20.114
2.24	19.624
2.22	19.165
2.20	18.731
2.18	18.322
2.15	17.745
2.10	16.864
2.05	16.060
2.00	15.312
1.95	14.605
1.90	13.929
1.85	13.276
1.80	12.637
1.75	12.010
1.70	11.386
1.65	10.761
1.60	10.130
1.55	9.4860
1.50	8.8229
1.45	8.1309
1.40	7.4012
1.35	6.6249
H21=7.000	
2.84	713.70
2.82	409.29
2.80	286.91
2.78	221.10
2.76	180.00
2.74	151.67
2.72	131.13
2.70	115.43
2.68	103.03
2.66	93.044
2.64	84.786
2.62	77.818
2.60	71.908
2.58	66.812
2.56	62.381
2.54	58.512
2.52	55.095
2.50	52.072
2.48	49.393
2.46	47.018
2.44	44.886
2.42	42.996
2.40	41.291
2.38	39.765
2.36	38.384
2.34	37.131
32	35.996
2.30	34.952
2.28	33.988
2.26	33.097
2.24	32.270
2.22	31.490
2.20	30.764
2.18	30.071
2.15	29.100
2.10	27.614
2.05	26.255
2.00	24.984
1.95	23.786
1.90	22.633
1.85	21.508
1.80	20.407
1.75	19.311
1.70	18.212
1.65	17.094
1.60	15.943
1.55	14.739
1.50	13.450
1.45	12.028
1.40	10.396
1.35	8.4705
H21=10.000	
2.84	1004.5
2.82	576.52
2.80	404.27
2.78	311.27
2.76	253.36
2.74	213.61
2.72	184.49
2.70	162.47
2.68	145.06
2.66	130.93
2.64	119.25
2.62	109.48
2.60	101.09
2.58	93.899
2.56	87.633
2.54	82.150
2.52	77.313
2.50	73.047
2.48	69.257
2.46	65.895

(to be continued)

Table 26. (continued)

V/V_1	L/H_1	V/V_1	L/H_1	V/V_1	L/H_1	V/V_1	L/H_1
2.44	62.893	2.26	46.261	2.00	34.839	1.60	21.902
2.42	60.221			1.95	33.141	1.55	20.120
2.40	57.808	2.24	45.100	1.90	31.508	1.50	18.171
2.38	55.657	2.22	44.008			1.45	15.936
2.36	53.715	2.20	42.979	1.85	29.917	1.40	13.165
		2.18	42.008	1.80	28.349		
2.34	51.937	2.15	40.634	1.75	26.779	1.35	9.5118
2.32	50.336			1.70	25.200		
2.30	48.861	2.10	38.545	1.65	23.583		
2.28	47.511	2.05	36.627				

Table 27.

RO21=2.500 V21=1.333 V2S1=0.7697
RO31=3.400 V31=5.400 V3S1=3.118

V/V_1	L/H_1	V/V_1	L/H_1	V/V_1	L/H_1	V/V_1	L/H_1
H21=1.000		H21=4.000		H21=7.000		H21=10.000	
2.84	139.67	2.84	466.74	2.84	792.85	2.84	1119.9
2.82	81.577	2.82	273.90	2.82	466.23	2.82	659.90
2.80	58.669	2.80	197.57	2.80	336.95	2.80	476.06
2.78	46.522	2.78	157.12	2.78	268.42	2.78	379.59
2.76	39.061	2.76	132.26	2.76	226.11	2.76	320.34
2.74	34.042	2.74	115.55	2.74	197.85	2.74	280.35
2.72	30.449	2.72	103.58	2.72	177.61	2.72	251.87
2.70	27.755	2.70	94.687	2.70	162.60	2.70	230.61
2.68	25.665	2.68	87.734	2.68	150.87	2.68	213.93
2.66	23.992	2.66	82.202	2.66	141.47	2.66	200.86
2.64	22.624	2.64	77.691	2.64	133.92	2.64	190.13
2.62	21.483	2.62	73.928	2.62	127.51	2.62	181.14
2.60	20.514	2.60	70.719	2.60	122.17	2.60	173.70
2.58	19.678	2.58	67.955	2.58	117.52	2.58	167.13
2.55	18.615	2.55	64.461	2.55	111.55	2.56	161.30
2.50	17.206	2.50	59.784	2.50	103.67	2.55	158.79
2.45	16.100	2.45	56.084	2.45	97.426	2.50	147.64
2.40	15.192	2.40	52.989	2.40	92.151	2.45	138.78
2.35	14.423	2.35	50.313	2.35	87.609	2.40	131.36
2.30	13.754	2.30	47.922	2.30	83.493	2.35	124.88
2.25	13.159	2.25	45.722	2.25	79.707	2.30	119.10
2.20	12.622	2.20	43.679	2.20	76.178	2.25	113.75
2.15	12.130	2.15	41.747	2.15	72.849	2.20	108.72
2.10	11.673	2.10	39.878	2.10	69.617	2.15	103.98
2.05	11.245	2.05	38.080	2.05	66.494	2.10	99.382
2.00	10.840	2.00	36.321	2.00	63.439	2.05	94.896
1.95	10.453	1.95	34.591	1.95	60.424	2.00	90.543
1.90	10.080	1.90	32.877	1.90	57.436	1.95	86.246
1.85	9.7199	1.85	31.172	1.85	54.451	1.90	82.003
1.80	9.3686	1.80	29.473	1.80	51.480	1.85	77.743
1.75	9.0252	1.75	27.776	1.75	48.492	1.80	73.498
1.70	8.6877	1.70	26.093	1.70	45.496	1.75	69.242
1.65	8.3551	1.65	24.464	1.65	42.508	1.70	64.924
1.60	8.0261	1.60	23.056	1.60	39.643	1.65	60.629
1.55	7.7000	1.55	21.977	1.55	37.251	1.60	56.429
1.50	7.3762	1.50	21.063	1.50	35.480	1.55	52.720
1.45	7.0537	1.45	20.212	1.45	33.970	1.50	49.992
1.40	6.7323	1.40	19.383	1.40	32.551	1.45	47.787
1.35	6.4115	1.35	18.565	1.35	31.160	1.40	45.754
						1.35	43.792

Table 28.

RO21=2.500 V21=1.333 V2S1=0.7697
RO31=3.000 V31=5.400 V3S1=3.118

V/V_1	L/H_1	V/V_1	L/H_1	V/V_1	L/H_1	V/V_1	L/H_1
H21=1.000		H21=4.000		H21=7.000		H21=10.000	
2.84	157.99	2.84	527.59	2.84	899.23	2.84	1265.3
2.82	91.967	2.82	308.14	2.82	525.65	2.82	742.10
2.80	65.858	2.80	221.44	2.80	377.25	2.80	534.16
2.78	51.967	2.78	175.22	2.78	299.12	2.78	423.01
2.76	43.392	2.76	146.64	2.76	250.69	2.76	354.78
2.74	37.612	2.74	127.36	2.74	217.95	2.74	308.58
2.72	33.461	2.72	113.56	2.72	194.53	2.72	275.49
2.70	30.339	2.70	103.21	2.70	176.95	2.70	250.84
2.68	27.916	2.68	95.170	2.68	163.40	2.68	231.73
2.66	25.977	2.66	88.732	2.66	152.54	2.66	216.41
2.64	24.389	2.64	83.466	2.64	143.60	2.64	203.81
2.62	23.066	2.62	79.080	2.62	136.17	2.62	193.33
2.60	21.941	2.60	75.344	2.60	129.94	2.60	184.55
2.58	20.973	2.58	72.162	2.58	124.54	2.58	176.99
2.55	19.746	2.55	68.093	2.55	117.62	2.56	170.32
2.50	18.127	2.50	62.722	2.50	108.57	2.55	167.29
2.45	16.864	2.45	58.501	2.45	101.45	2.50	154.44
2.40	15.836	2.40	55.020	2.40	95.545	2.45	144.45
2.35	14.970	2.35	52.030	2.35	90.441	2.40	136.14
2.30	14.222	2.30	49.393	2.30	85.947	2.35	128.94
2.25	13.562	2.25	47.011	2.25	81.878	2.30	122.55
2.20	12.970	2.20	44.811	2.20	78.063	2.25	116.77
2.15	12.431	2.15	42.739	2.15	74.519	2.20	111.35
2.10	11.934	2.10	40.768	2.10	71.094	2.15	106.28
2.05	11.471	2.05	38.867	2.05	67.826	2.10	101.45
2.00	11.036	2.00	37.027	2.00	64.611	2.05	96.752
1.95	10.624	1.95	35.228	1.95	61.475	2.00	92.204
1.90	10.230	1.90	33.452	1.90	58.395	1.95	87.776
1.85	9.8516	1.85	31.696	1.85	55.322	1.90	83.363
1.80	9.4849	1.80	29.956	1.80	52.266	1.85	78.983
1.75	9.1280	1.75	28.227	1.75	49.227	1.80	74.623
1.70	8.7790	1.70	26.514	1.70	46.175	1.75	70.255
1.65	8.4362	1.65	24.867	1.65	43.141	1.70	65.881
1.60	8.0985	1.60	23.415	1.60	40.258	1.65	61.522
1.55	7.7648	1.55	22.255	1.55	37.780	1.60	57.272
1.50	7.4342	1.50	21.283	1.50	35.884	1.55	53.501
1.45	7.1057	1.45	20.393	1.45	34.293	1.50	50.590
1.40	6.7791	1.40	19.538	1.40	32.816	1.45	48.252
1.35	6.4533	1.35	18.700	1.35	31.388	1.40	46.135
						1.35	44.111

Table 29.

RO21=3.000 V21=4.667 V2S1=2.694
RO31=3.400 V31=5.200 V3S1=3.000

V/V_1	L/H_1	V/V_1	L/H_1	V/V_1	L/H_1	V/V_1	L/H_1
H21=5.000		H21=10.000		H21=15.000		H21=20.000	
2.72	65.717	2.72	96.672	2.72	127.85	2.72	159.63
2.70	36.825	2.70	56.963	2.70	78.674	2.70	100.74
2.68	27.836	2.68	44.844	2.68	62.866	2.68	81.099
2.66	23.498	2.66	38.345	2.66	54.022	2.66	69.859
2.64	20.819	2.64	33.996	2.64	47.952	2.64	62.029
2.62	18.942	2.62	30.748	2.62	43.309	2.62	55.996
2.60	17.522	2.60	28.140	2.60	39.515	2.60	51.009
2.58	16.395	2.58	25.949	2.58	36.258	2.58	46.694
2.56	15.470	2.56	24.039	2.56	33.362	2.56	42.803
2.54	14.690	2.54	22.331	2.54	30.704	2.54	39.186
2.52	14.023	2.52	20.775	2.52	28.199	2.52	35.718
2.50	13.443	2.50	19.335	2.50	25.786	2.50	32.280
2.48	12.933	2.48	17.993	2.48	23.415	2.48	28.770
2.45	12.272	2.45	16.146	2.45	19.892	2.45	23.154
2.40	11.379	2.40	13.590	2.40	14.811	2.40	15.207
2.35	10.669	2.35	11.823	2.35	12.100	2.35	12.132
2.30	10.082	2.30	10.689	2.30	10.760		
2.25	9.5812	2.25	9.9137	2.25	9.9363		
2.20	9.1405	2.20	9.3298	2.20	9.3379		
2.15	8.7418	2.15	8.8535				
2.10	8.3748	2.10	8.4420				
2.05	8.0300	2.05	8.0711				
2.00	7.7022	2.00	7.7274				
1.95	7.3876	1.95	7.4029				
1.90	7.0820	1.90	7.0917				
1.85	6.7838	1.85	6.7892				
1.80	6.4902	1.80	6.4936				
1.75	6.2004	1.75	6.2023				
1.70	5.9122	1.70	5.9135				
1.65	5.6249						
1.60	5.3368						
1.55	5.0471						
1.50	4.7543						
1.45	4.4567						
1.40	4.1526						
1.35	3.8399						

Table 30.

RO21=3.000 V21=4.620 V2S1=2.662
RO31=3.400 V31=5.200 V3S1=3.000

V/V_1	L/H_1	V/V_1	L/H_1	V/V_1	L/H_1	V/V_1	L/H_1
H21=5.000		H21=10.000		H21=15.000		H21=20.000	
2.72	75.264	2.72	116.65	2.72	156.95	2.72	197.21
2.70	41.054	2.70	63.924	2.70	88.258	2.70	113.00
2.68	30.048	2.68	48.803	2.68	68.552	2.68	88.531
2.66	24.981	2.66	41.243	2.66	58.311	2.66	75.543
2.64	21.953	2.64	36.384	2.64	51.561	2.64	66.864
2.62	19.871	2.62	32.843	2.62	46.532	2.62	60.345
2.60	18.316	2.60	30.052	2.60	42.498	2.60	55.069
2.58	17.090	2.58	27.734	2.58	39.108	2.58	50.594
2.56	16.088	2.56	25.742	2.56	36.133	2.56	46.648
2.54	15.246	2.54	23.974	2.54	33.448	2.54	43.040
2.52	14.524	2.52	22.374	2.52	30.954	2.52	39.654
2.50	13.896	2.50	20.897	2.50	28.592	2.50	36.387
2.48	13.342	2.48	19.519	2.48	26.300	2.48	33.150
2.45	12.625	2.45	17.595	2.45	22.906	2.45	28.134
2.40	11.652	2.40	14.762	2.40	17.293	2.40	18.934
2.35	10.880	2.35	12.575	2.35	13.218	2.35	13.341
2.30	10.246	2.30	11.124	2.30	11.272	2.30	11.283
2.25	9.7093	2.25	10.175	2.25	10.216		
2.20	9.2411	2.20	9.4996	2.20	9.5130		
2.15	8.8223	2.15	8.9708				
2.10	8.4393	2.10	8.5271				
2.05	8.0828	2.05	8.1354				
2.00	7.7461	2.00	7.7779				
1.95	7.4239	1.95	7.4432				
1.90	7.1126	1.90	7.1242				
1.85	6.8096	1.85	6.8167				
1.80	6.5124	1.80	6.5165				
1.75	6.2192	1.75	6.2217				
1.70	5.9286	1.70	5.9301				
1.65	5.6391						
1.60	5.3492						
1.55	5.0579						
1.50	4.7638						
1.45	4.4650						
1.40	4.1600						
1.35	3.8466						

Table 31.

RO21=3.000 V21=4.000 V2S1=2.310
RO31=3.400 V31=5.200 V3S1=3.000

V/V_1	L/H_1	V/V_1	L/H_1	V/V_1	L/H_1	V/V_1	L/H_1
H21=5.000		H21=10.000		H21=15.000		H21=20.000	
2.72	182.14	2.72	340.69	2.72	499.34	2.72	658.88
2.70	111.53	2.70	206.22	2.70	300.79	2.70	395.69
2.68	76.911	2.68	140.31	2.68	203.57	2.68	266.91
2.66	56.948	2.66	102.57	2.66	148.32	2.66	193.91
2.64	44.704	2.64	80.040	2.64	115.58	2.64	151.19
2.62	36.977	2.62	66.214	2.62	95.787	2.62	125.42
2.60	31.898	2.60	57.290	2.60	83.014	2.60	108.84
2.58	28.384	2.58	51.112	2.58	74.184	2.58	97.352
2.56	25.810	2.56	46.557	2.56	67.666	2.56	88.824
2.54	23.838	2.54	43.022	2.54	62.563	2.54	82.171
2.52	22.258	2.52	40.166	2.52	58.446	2.52	76.773
2.50	20.958	2.50	37.778	2.50	54.974	2.50	72.235
2.45	18.473	2.45	33.116	2.45	48.154	2.45	63.257
2.40	16.639	2.40	29.546	2.40	42.890	2.40	56.284
2.35	15.175	2.35	26.583	2.35	38.455	2.35	50.398
2.30	13.944	2.30	23.959	2.30	34.482	2.30	45.084
2.25	12.871	2.25	21.525	2.25	30.717	2.25	39.984
2.20	11.914	2.20	19.158	2.20	26.933	2.20	34.776
2.15	11.050	2.15	16.766	2.15	22.857	2.15	28.957
2.10	10.269	2.10	14.285	2.10	18.056	2.10	21.346
2.05	9.5653	2.05	11.869	2.05	12.928		
2.00	8.9356	2.00	10.033	2.00	10.190		
1.95	8.3750	1.95	8.8786				
1.90	7.8745	1.90	8.1128				
1.85	7.4237	1.85	7.5396				
1.80	7.0115	1.80	7.0691				
1.75	6.6290	1.75	6.6576				
1.70	6.2681	1.70	6.2822				
1.65	5.9229						
1.60	5.5888						
1.55	5.2616						
1.50	4.9381						
1.45	4.6151						
1.40	4.2901						
1.35	3.9595						

Table 32.

RO21=2.800 V21=4.000 V2S1=2.309
RO31=3.000 V31=5.200 V3S1=3.000

V/V_1	L/H_1	V/V_1	L/H_1	V/V_1	L/H_1	V/V_1	L/H_1
H21=1.000		H21=4.000		H21=7.000		H21=10.000	
2.72	60.150	2.72	162.91	2.72	265.59	2.72	368.18
2.70	39.215	2.70	101.35	2.70	163.59	2.70	225.75
2.68	29.181	2.68	71.192	2.68	113.50	2.68	155.81
2.66	23.449	2.66	53.550	2.66	84.369	2.66	115.24
2.64	19.857	2.64	42.372	2.64	66.101	2.64	89.979
2.62	17.470	2.62	34.981	2.62	54.295	2.62	73.877
2.60	15.814	2.60	29.960	2.60	46.416	2.60	63.199
2.58	14.619	2.58	26.422	2.58	40.913	2.58	55.792
2.56	13.725	2.56	23.831	2.56	36.891	2.56	50.362
2.54	13.034	2.54	21.858	2.54	33.806	2.54	46.181
2.52	12.482	2.52	20.301	2.52	31.352	2.52	42.838
2.50	12.028	2.50	19.037	2.50	29.335	2.50	40.080
2.48	11.645	2.48	17.984	2.48	27.628	2.48	37.741
2.45	11.168	2.45	16.684	2.45	25.487	2.45	34.778
2.40	10.536	2.40	15.014	2.40	22.647	2.40	30.811
2.35	10.030	2.35	13.730	2.35	20.368	2.35	27.576
2.30	9.5981	2.30	12.686	2.30	18.422	2.30	24.756
2.25	9.2135	2.25	11.805	2.25	16.687	2.25	22.171
2.20	8.8610	2.20	11.040	2.20	15.090	2.20	19.696
2.15	8.5309	2.15	10.364	2.15	13.586	2.15	17.227
2.10	8.2160	2.10	9.7570	2.10	12.171	2.10	14.700
2.05	7.9135	2.05	9.2072	2.05	10.879	2.05	12.237
2.00	7.6191	2.00	8.7037	2.00	9.7736	2.00	10.309
1.95	7.3310	1.95	8.2390	1.95	8.8882	1.95	9.0747
1.90	7.0472	1.90	7.8069	1.90	8.1914	1.90	8.2578
1.85	6.7666	1.85	7.4015	1.85	7.6275	1.85	7.6519
1.80	6.4878	1.80	7.0183	1.80	7.1506	1.80	7.1602
1.75	6.2102	1.75	6.6525	1.75	6.7295	1.75	6.7332
1.70	5.9322	1.70	6.3005	1.70	6.3450	1.70	6.3465
1.65	5.6534	1.65	5.9594	1.65	5.9844		
1.60	5.3727	1.60	5.6260	1.60	5.6398		
1.55	5.0889	1.55	5.2976	1.55	5.3047		
1.50	4.8013	1.50	4.9719	1.50	4.9756		
1.45	4.5081	1.45	4.6463	1.45	4.6482		
1.40	4.2080	1.40	4.3184				
1.35	3.8987	1.35	3.9851				

Table 33.

RO21=2.800 V21=3.667 V2S1=2.117
RO31=3.000 V31=5.200 V3S1=3.000

V/V_1	L/H_1	V/V_1	L/H_1	V/V_1	L/H_1	V/V_1	L/H_1
H21=1.000		H21=4.000		H21=7.000		H21=10.000	
2.72	69.688	2.72	203.77	2.72	338.01	2.72	471.87
2.70	45.525	2.70	129.74	2.70	214.25	2.70	298.70
2.68	33.819	2.68	93.348	2.68	153.46	2.68	213.51
2.66	27.001	2.66	71.728	2.66	117.19	2.66	162.72
2.64	22.622	2.64	57.474	2.64	93.307	2.64	129.16
2.62	19.633	2.62	47.490	2.62	76.622	2.62	105.86
2.60	17.512	2.60	40.264	2.60	64.608	2.60	89.119
2.58	15.962	2.58	34.912	2.58	55.807	2.58	76.897
2.56	13.796	2.56	30.892	2.56	49.240	2.56	67.837
2.54	13.899	2.54	27.813	2.54	44.275	2.54	60.907
2.52	13.190	2.52	25.415	2.52	40.408	2.52	55.698
2.50	12.617	2.50	23.508	2.50	37.344	2.50	51.492
2.48	12.143	2.48	21.957	2.48	34.847	2.48	48.060
2.45	11.564	2.45	20.104	2.45	31.845	2.45	43.924
2.40	10.824	2.40	17.828	2.40	28.118	2.40	38.773
2.35	10.252	2.35	16.154	2.35	25.323	2.35	34.884
2.30	9.7778	2.30	14.838	2.30	23.072	2.30	31.723
2.25	9.3642	2.25	13.745	2.25	21.159	2.25	29.008
2.20	8.9913	2.20	12.804	2.20	19.463	2.20	26.576
2.15	8.6455	2.15	11.970	2.15	17.904	2.15	24.316
2.10	8.3197	2.10	11.214	2.10	16.433	2.10	22.139
2.05	8.0076	2.05	10.519	2.05	15.010	2.05	19.971
2.00	7.7059	2.00	9.8720	2.00	13.605	2.00	17.739
1.95	7.4114	1.95	9.2666	1.95	12.201	1.95	15.345
1.90	7.1228	1.90	8.6972	1.90	10.814	1.90	12.744
1.85	6.8380	1.85	8.1625	1.85	9.5205	1.85	10.299
1.80	6.5555	1.80	7.6597	1.80	8.4416	1.80	8.6662
1.75	6.2744	1.75	7.1878	1.75	7.6102	1.75	7.6723
1.70	5.9937	1.70	6.7441	1.70	6.9661	1.70	6.9842
1.65	5.7124	1.65	6.3254	1.65	6.4404		
1.60	5.4296	1.60	5.9276	1.60	5.9861		
1.55	5.1439	1.55	5.5469	1.55	5.5758		
1.50	4.8546	1.50	5.1786	1.50	5.1923		
1.45	4.5601	1.45	4.8186	1.45	4.8251		
1.40	4.2588	1.40	4.4628				
1.35	3.9486	1.35	4.1070				

Table 34.

RO21=3.000 V21=3.333 V2S1=1.924
RO31=3.400 V31=5.200 V3S1=3.000

V/V_1	L/H_1	V/V_1	L/H_1	V/V_1	L/H_1	V/V_1	L/H_1
H21=5.000		H21=10.000		H21=15.000		H21=20.000	
2.72	276.91	2.72	532.83	2.72	787.03	2.72	1043.6
2.70	178.42	2.70	342.60	2.70	507.01	2.70	670.21
2.68	130.02	2.68	249.23	2.68	368.18	2.68	486.87
2.66	101.16	2.66	193.39	2.66	285.57	2.66	377.58
2.64	81.998	2.64	156.26	2.64	230.48	2.64	304.86
2.62	68.388	2.62	129.90	2.62	191.49	2.62	253.21
2.60	58.287	2.60	110.35	2.60	162.54	2.60	214.79
2.58	50.570	2.58	95.488	2.58	140.45	2.58	185.52
2.56	44.574	2.56	83.923	2.56	123.43	2.56	162.91
2.54	39.856	2.54	74.910	2.54	110.10	2.54	145.30
2.52	36.108	2.52	67.794	2.52	99.590	2.52	131.45
2.50	33.107	2.50	62.110	2.50	91.262	2.50	120.42
2.48	30.675	2.48	57.505	2.48	84.519	2.48	111.56
2.45	27.800	2.45	52.105	2.45	76.595	2.45	101.10
2.40	24.366	2.40	45.651	2.40	67.119	2.40	88.647
2.35	21.938	2.35	41.054	2.35	60.379	2.35	79.747
2.30	20.080	2.30	37.516	2.30	55.152	2.30	72.832
2.25	18.572	2.25	34.614	2.25	50.870	2.25	67.161
2.20	17.289	2.20	32.115	2.20	47.163	2.20	62.260
2.15	16.158	2.15	29.881	2.15	43.840	2.15	57.839
2.10	15.128	2.10	27.821	2.10	40.768	2.10	53.733
2.05	14.171	2.05	25.873	2.05	37.829	2.05	49.814
2.00	13.262	2.00	23.977	2.00	34.956	2.00	45.977
1.95	12.386	1.95	22.089	1.95	32.074	1.95	42.096
1.90	11.528	1.90	20.163	1.90	29.084	1.90	38.039
1.85	10.681	1.85	18.130	1.85	25.848	1.85	33.594
1.80	9.8364	1.80	15.892	1.80	22.099	1.80	28.276
1.75	8.9966	1.75	13.296	1.75	17.177	1.75	20.572
1.70	8.1755	1.70	10.364	1.70	11.049	1.70	11.136
1.65	7.4022	1.65	8.1554				
1.60	6.7084	1.60	6.9474				
1.55	6.1060	1.55	6.1830				
1.50	5.5828						
1.45	5.1169						
1.40	4.6885						
1.35	4.2818						

Table 35.

RO21=2.800 V21=3.333 V2S1=1.924
RO31=3.000 V31=5.200 V3S1=3.000

V/V_1	L/H_1	V/V_1	L/H_1	V/V_1	L/H_1	V/V_1	L/H_1
H21=1.000		H21=4.000		H21=7.000		H21=10.000	
2.72	78.573	2.72	241.11	2.72	403.51	2.72	566.62
2.70	51.530	2.70	155.86	2.70	260.59	2.70	365.36
2.68	38.349	2.68	113.99	2.68	190.05	2.68	266.25
2.66	30.607	2.66	88.990	2.66	148.01	2.66	207.21
2.64	25.558	2.64	72.394	2.64	120.12	2.64	167.88
2.62	22.049	2.62	60.584	2.62	100.17	2.62	139.81
2.60	19.503	2.60	51.785	2.60	85.326	2.60	118.98
2.58	17.604	2.58	45.037	2.58	73.954	2.58	102.96
2.56	16.154	2.56	39.742	2.56	65.039	2.56	90.473
2.54	15.024	2.54	35.531	2.54	57.979	2.54	80.596
2.52	14.129	2.52	32.151	2.52	52.341	2.52	72.688
2.50	13.406	2.50	29.411	2.50	47.787	2.50	66.337
2.48	12.813	2.48	27.170	2.48	44.079	2.48	61.180
2.45	12.098	2.45	24.512	2.45	39.687	2.45	55.085
2.40	11.210	2.40	21.331	2.40	34.454	2.40	47.836
2.35	10.548	2.35	19.103	2.35	30.779	2.35	42.722
2.30	10.016	2.30	17.424	2.30	27.986	2.30	38.829
2.25	9.5641	2.25	16.085	2.25	25.732	2.25	35.673
2.20	9.1634	2.20	14.963	2.20	23.821	2.20	32.991
2.15	8.7973	2.15	13.989	2.15	22.140	2.15	30.615
2.10	8.4558	2.10	13.119	2.10	20.612	2.10	28.441
2.05	8.1319	2.05	12.324	2.05	19.188	2.05	26.395
2.00	7.8202	2.00	11.581	2.00	17.828	2.00	24.429
1.95	7.5181	1.95	10.880	1.95	16.501	1.95	22.481
1.90	7.2229	1.90	10.208	1.90	15.181	1.90	20.507
1.85	6.9323	1.85	9.5585	1.85	13.838	1.85	18.438
1.80	6.6452	1.80	8.9284	1.80	12.444	1.80	16.184
1.75	6.3602	1.75	8.3152	1.75	10.982	1.75	13.603
1.70	6.0759	1.70	7.7204	1.70	9.4815	1.70	10.699
1.65	5.7916	1.65	7.1486	1.65	8.1131	1.65	8.4078
1.60	5.5058	1.60	6.6048	1.60	7.0621	1.60	7.1190
1.55	5.2180	1.55	6.0933	1.55	6.2960	1.55	6.3071
1.50	4.9267	1.50	5.6148	1.50	5.7014		
1.45	4.6305	1.45	5.1662	1.45	5.2015		
1.40	4.3279	1.40	4.7407	1.40	4.7546		
1.35	4.0168	1.35	4.3311				

Table 36.

RO21=2.500 V21=3.333 V2S1=1.924
RO31=3.000 V31=5.200 V3S1=3.000

V/V_1	L/H_1	V/V_1	L/H_1	V/V_1	L/H_1	V/V_1	L/H_1
H21=1.000		H31=4.000		H21=7.000		H21=10.000	
2.72	72.516	2.72	216.52	2.72	360.75	2.72	505.22
2.70	47.575	2.70	139.54	2.70	231.86	2.70	324.46
2.68	35.458	2.68	101.67	2.68	168.54	2.68	235.29
2.66	28.376	2.66	79.139	2.66	130.77	2.66	182.37
2.64	23.791	2.64	64.221	2.64	105.62	2.64	147.15
2.62	20.634	2.62	53.630	2.62	87.860	2.62	122.20
2.60	18.367	2.60	45.811	2.60	74.740	2.60	103.73
2.58	16.691	2.58	39.878	2.58	64.774	2.58	89.810
2.56	15.421	2.56	35.294	2.56	57.122	2.56	79.124
2.54	14.437	2.54	31.707	2.54	51.173	2.54	70.828
2.52	13.659	2.52	28.875	2.52	46.507	2.52	64.356
2.50	13.030	2.50	26.612	2.50	42.799	2.50	59.228
2.48	12.511	2.48	24.775	2.48	39.801	2.48	55.083
2.45	11.879	2.45	22.607	2.45	36.276	2.45	50.218
2.40	11.081	2.40	20.012	2.40	32.039	2.40	44.354
2.35	10.473	2.35	18.163	2.35	29.008	2.35	40.152
2.30	9.9742	2.30	16.746	2.30	26.655	2.30	36.879
2.25	9.5437	2.25	15.591	2.25	24.716	2.25	34.165
2.20	9.1577	2.20	14.607	2.20	23.043	2.20	31.810
2.15	8.8021	2.15	13.740	2.15	21.544	2.15	29.693
2.10	8.4682	2.10	12.955	2.10	20.165	2.10	27.726
2.05	8.1492	2.05	12.227	2.05	18.864	2.05	25.860
2.00	7.8419	2.00	11.542	2.00	17.609	2.00	24.038
1.95	7.5424	1.95	10.890	1.95	16.378	1.95	22.226
1.90	7.2496	1.90	10.259	1.90	15.145	1.90	20.377
1.85	6.9608	1.85	9.6462	1.85	13.889	1.85	18.435
1.80	6.6747	1.80	9.0459	1.80	12.586	1.80	16.322
1.75	6.3905	1.75	8.4573	1.75	11.215	1.75	13.924
1.70	6.1070	1.70	7.8800	1.70	9.7974	1.70	11.211
1.65	5.8230	1.65	7.3167	1.65	8.4493	1.65	8.8613
1.60	5.5379	1.60	6.7725	1.60	7.3472	1.60	7.4345
1.55	5.2503	1.55	6.2524	1.55	6.5190		
1.50	4.9592	1.50	5.7598				
1.45	4.6634	1.45	5.2944				
1.40	4.3610	1.40	4.8524				
1.35	4.0503	1.35	4.4277				

Table 37.

RO21=2.000 V21=3.333 V2S1=1.924
RO31=3.000 V31=5.200 V3S1=3.000

V/V_1	L/H_1	V/V_1	L/H_1	V/V_1	L/H_1	V/V_1	L/H_1
H21=1.000		H21=4.000		H21=7.000		H21=10.000	
2.72	62.463	2.72	175.43	2.72	288.84	2.72	402.00
2.70	41.078	2.70	112.29	2.70	184.09	2.70	255.93
2.68	30.785	2.68	81.314	2.68	132.59	2.68	184.01
2.66	24.845	2.66	62.930	2.66	101.98	2.66	141.19
2.64	21.068	2.64	50.851	2.64	81.904	2.64	113.03
2.62	18.520	2.62	42.469	2.62	67.955	2.62	93.572
2.60	16.724	2.60	36.446	2.60	57.987	2.60	79.742
2.58	15.415	2.58	32.039	2.58	50.785	2.58	69.768
2.56	14.429	2.56	28.762	2.56	45.481	2.56	62.481
2.54	13.665	2.54	26.289	2.54	41.515	2.54	57.039
2.52	13.057	2.52	24.375	2.52	38.466	2.52	52.883
2.50	12.559	2.50	22.862	2.50	36.063	2.50	49.599
2.48	12.142	2.48	21.634	2.48	34.115	2.48	46.934
2.45	11.623	2.45	20.170	2.45	31.779	2.45	43.745
2.40	10.946	2.40	18.365	2.40	28.880	2.40	39.760
2.35	10.408	2.35	17.022	2.35	26.699	2.35	36.740
2.30	9.9545	2.30	15.949	2.30	24.928	2.30	34.278
2.25	9.5531	2.25	15.039	2.25	23.412	2.25	32.157
2.20	9.1864	2.20	14.240	2.20	22.060	2.20	30.255
2.15	8.8449	2.15	13.516	2.15	20.818	2.15	28.494
2.10	8.5203	2.10	12.846	2.10	19.646	2.10	26.819
2.05	8.2089	2.05	12.214	2.05	18.521	2.05	25.200
2.00	7.9063	2.00	11.609	2.00	17.424	2.00	23.601
1.95	7.6108	1.95	11.024	1.95	16.334	1.95	21.989
1.90	7.3205	1.90	10.453	1.90	15.237	1.90	20.334
1.85	7.0337	1.85	9.8908	1.85	14.114	1.85	18.595
1.80	6.7489	1.80	9.3346	1.80	12.950	1.80	16.713
1.75	6.4657	1.75	8.7826	1.75	11.729	1.75	14.611
1.70	6.1828	1.70	8.2324	1.70	10.453	1.70	12.238
2.65	5.8994	1.65	7.6853	1.65	9.1712	1.65	9.8972
1.60	5.6144	1.60	7.1440	1.60	8.0067	1.60	8.2035
1.55	5.3269	1.55	6.6121	1.55	7.0571	1.55	7.1022
1.50	5.0359	1.50	6.0952	1.50	6.3066	1.50	6.3169
1.45	4.7403	1.45	5.5972	1.45	5.6907		
1.40	4.4383	1.40	5.1201	1.40	5.1581		
1.35	4.1280	1.35	4.6612				

Table 38.

RO21=2.500 V21=2.667 V2S1=1.540
RO31=3.000 V31=5.200 V3S1=3.000

V/V_1	L/H_1	V/V_1	L/H_1	V/V_1	L/H_1	V/V_1	L/H_1
H21=1.000		H21=4.000		H21=7.000		H21=10.000	
2.72	86.461	2.72	274.43	2.72	462.71	2.72	650.88
2.70	57.160	2.70	180.68	2.70	304.64	2.70	428.93
2.68	42.880	2.68	134.59	2.68	226.83	2.68	319.38
2.66	34.447	2.66	107.18	2.66	180.68	2.66	254.11
2.64	28.917	2.64	89.009	2.64	149.92	2.64	210.98
2.62	25.028	2.62	76.052	2.62	128.04	2.62	180.07
2.60	22.166	2.60	66.347	2.60	111.61	2.60	156.95
2.58	19.988	2.58	58.790	2.58	98.832	2.58	138.99
2.56	18.286	2.56	52.753	2.56	88.604	2.56	124.51
2.54	16.930	2.54	47.819	2.54	80.204	2.54	112.70
2.52	15.832	2.52	43.711	2.52	73.234	2.52	102.84
2.50	14.931	2.50	40.245	2.50	67.336	2.50	94.520
2.48	14.182	2.48	37.295	2.48	62.300	2.48	87.412
2.45	13.273	2.45	33.615	2.45	56.026	2.45	78.540
2.40	12.146	2.40	28.974	2.40	48.094	2.40	67.343
2.35	11.325	2.35	25.629	2.35	42.385	2.35	59.288
2.30	10.682	2.30	23.162	2.30	38.193	2.30	53.394
2.25	10.152	2.25	21.276	2.25	35.005	2.25	48.905
2.20	9.6941	2.20	19.779	2.20	32.485	2.20	45.367
2.15	9.2851	2.15	18.545	2.15	30.409	2.15	42.457
2.10	8.9094	2.10	17.487	2.10	28.634	2.10	39.958
2.05	8.5579	2.05	16.556	2.05	27.063	2.05	37.754
2.00	8.2238	2.00	15.712	2.00	25.640	2.00	35.748
1.95	7.9024	1.95	14.932	1.95	24.318	1.95	33.881
1.90	7.5912	1.90	14.197	1.90	23.069	1.90	32.115
1.85	7.2867	1.85	13.498	1.85	21.871	1.85	30.415
1.80	6.9871	1.80	12.822	1.80	20.708	1.80	28.762
1.75	6.6913	1.75	12.163	1.75	19.560	1.75	27.122
1.70	6.3976	1.70	11.513	1.70	18.415	1.70	25.481
1.65	6.1049	1.65	10.865	1.65	17.261	1.65	23.810
1.60	5.8121	1.60	10.214	1.60	16.078	1.60	22.084
1.55	5.5183	1.55	9.5536	1.55	14.843	1.55	20.262
1.50	5.2221	1.50	8.8750	1.50	13.529	1.50	18.275
1.45	4.9222	1.45	8.1701	1.45	12.084	1.45	16.007
1.40	4.6175	1.40	7.4282	1.40	10.430	1.40	13.201
1.35	4.3059	1.35	6.6416	1.35	8.4830	1.35	9.5186

Table 39.

RO21=2.000 V21=2.667 V2S1=1.540
RO31=3.000 V31=5.200 V3S1=3.000

V/V_1	L/H_1	V/V_1	L/H_1	V/V_1	L/H_1	V/V_1	L/H_1
H21=1.000		H21=4.000		H21=7.000		H21=10.000	
2.72	73.865	2.72	223.99	2.72	374.61	2.72	525.01
2.70	48.976	2.70	147.40	2.70	246.51	2.70	345.36
2.68	36.897	2.68	109.85	2.68	183.54	2.68	257.31
2.66	29.828	2.66	87.609	2.66	146.29	2.66	205.23
2.64	25.230	2.64	72.861	2.64	121.68	2.64	170.55
2.62	22.037	2.62	62.417	2.62	104.11	2.62	145.90
2.60	19.718	2.60	54.606	2.60	90.972	2.60	127.47
2.58	17.974	2.58	48.577	2.58	80.809	2.58	113.17
2.56	16.630	2.56	43.773	2.56	72.713	2.56	101.76
2.54	15.569	2.54	39.878	2.54	66.132	2.54	92.482
2.52	14.718	2.52	36.664	2.52	60.678	2.52	84.819
2.50	14.022	2.50	33.988	2.50	56.128	2.50	78.415
2.48	13.442	2.48	31.728	2.48	52.290	2.48	73.010
2.45	12.733	2.45	28.964	2.45	47.584	2.45	66.390
2.40	11.836	2.40	25.551	2.40	41.789	2.40	58.219
2.35	11.156	2.35	23.137	2.35	37.717	2.35	52.496
2.30	10.605	2.30	21.348	2.30	34.715	2.30	48.290
2.25	10.134	2.25	19.951	2.25	32.382	2.25	45.020
2.20	9.7163	2.20	18.808	2.20	30.477	2.20	42.360
2.15	9.3346	2.15	17.831	2.15	28.850	2.15	40.084
2.10	8.9786	2.10	16.968	2.10	27.412	2.10	38.068
2.05	8.6407	2.05	16.185	2.05	26.105	2.05	36.235
2.00	8.3168	2.00	15.458	2.00	24.888	2.00	34.524
1.95	8.0028	1.95	14.773	1.95	23.736	1.95	32.906
1.90	7.6967	1.90	14.118	1.90	22.630	1.90	31.334
1.85	7.3959	1.85	13.485	1.85	21.551	1.85	29.806
1.80	7.0993	1.80	12.866	1.80	20.491	1.80	28.298
1.75	6.8053	1.75	12.257	1.75	19.439	1.75	26.793
1.70	6.5129	1.70	11.651	1.70	18.380	1.70	25.275
1.65	6.2210	1.65	11.046	1.65	17.307	1.65	23.719
1.60	5.9289	1.60	10.436	1.60	16.203	1.60	22.105
1.55	5.6354	1.55	9.8148	1.55	15.052	1.55	20.400
1.50	5.3396	1.50	9.1775	1.50	13.831	1.50	18.549
1.45	5.0402	1.45	8.5161	1.45	12.502	1.45	16.460
1.40	4.7361	1.40	7.8228	1.40	11.010	1.40	13.958
1.35	4.4255	1.35	7.0875	1.35	9.2874	1.35	10.775

Table 40.

RO21=2.500 V21=1.333 V2S1=0.7697
RO31=3.000 V31=5.200 V3S1=3.000

V/V_1	L/H_1	V/V_1	L/H_1	V/V_1	L/H_1	V/V_1	L/H_1
H21=1.000		H21=4.000		H21=7.000		H21=10.000	
2.72	105.88	2.72	354.20	2.72	603.28	2.72	852.75
2.70	71.180	2.70	238.83	2.70	406.96	2.70	574.98
2.68	54.357	2.68	182.91	2.68	311.95	2.68	440.83
2.66	44.477	2.66	150.08	2.66	256.23	2.66	362.27
2.64	38.023	2.64	128.54	2.64	219.85	2.64	311.05
2.62	33.489	2.62	113.47	2.62	194.26	2.62	275.31
2.60	30.141	2.60	102.35	2.60	175.43	2.60	248.66
2.58	27.570	2.58	93.817	2.58	160.89	2.58	228.16
2.56	25.530	2.56	87.022	2.56	149.51	2.56	212.03
2.54	23.877	2.54	81.546	2.54	140.17	2.54	198.95
2.52	22.508	2.52	76.994	2.52	132.51	2.52	188.05
2.50	21.351	2.50	73.147	2.50	126.01	2.50	179.02
2.45	19.108	2.45	65.695	2.45	113.43	2.45	161.33
2.40	17.469	2.40	60.209	2.40	104.21	2.40	148.18
2.35	16.197	2.35	55.928	2.35	96.897	2.35	137.95
2.30	15.166	2.30	52.385	2.30	90.924	2.30	129.56
2.25	14.302	2.25	49.371	2.25	85.772	2.25	122.23
2.20	13.558	2.20	46.711	2.20	81.224	2.20	115.76
2.15	12.902	2.15	44.287	2.15	77.088	2.15	109.87
2.10	12.316	2.10	42.047	2.10	73.228	2.10	104.41
2.05	11.783	2.05	39.947	2.05	69.604	2.05	99.290
2.00	11.292	2.00	37.945	2.00	66.134	2.00	94.368
1.95	10.836	1.95	36.012	1.95	62.783	1.95	89.560
1.90	10.406	1.90	34.130	1.90	59.519	1.90	84.903
1.85	9.9986	1.85	32.293	1.85	56.300	1.85	80.344
1.80	9.6089	1.80	30.478	1.80	53.129	1.80	75.819
1.75	9.2331	1.75	28.692	1.75	49.984	1.75	71.299
1.70	8.8688	1.70	26.941	1.70	46.861	1.70	66.840
1.65	8.5135	1.65	25.259	1.65	43.769	1.65	62.393
1.60	8.1653	1.60	23.750	1.60	40.830	1.60	58.079
1.55	7.8228	1.55	22.511	1.55	38.270	1.55	54.195
1.50	7.4848	1.50	21.480	1.50	36.248	1.50	51.120
1.45	7.1500	1.45	20.548	1.45	34.569	1.45	48.654
1.40	6.8177	1.40	19.666	1.40	33.039	1.40	46.455
1.35	6.4873	1.35	18.808	1.35	31.572	1.35	44.372

Table 41.

RO21=2.000 V21=1.333 V2S1=0.7697
RO21=3.000 V31=5.200 V3S1=3.000

V/V_1	L/H_1	V/V_1	L/H_1	V/V_1	L/H_1	V/V_1	L/H_1
H21=1.000		H21=4.000		H21=7.000		H21=10.000	
2.72	89.979	2.72	290.41	2.72	491.33	2.72	692.94
2.70	60.893	2.70	197.30	2.70	334.58	2.70	471.35
2.68	46.873	2.68	152.48	2.68	258.86	2.68	365.05
2.66	38.712	2.66	126.31	2.66	214.90	2.66	303.35
2.64	33.409	2.64	109.28	2.64	186.25	2.64	263.31
2.62	29.709	2.62	97.440	2.62	166.25	2.62	235.16
2.60	26.985	2.60	88.714	2.60	151.62	2.60	214.57
2.58	24.903	2.58	82.014	2.58	140.45	2.58	198.95
2.56	23.257	2.56	76.746	2.56	131.61	2.56	186.57
2.54	21.922	2.54	72.455	2.54	124.47	2.54	176.52
2.52	20.817	2.52	68.905	2.52	118.52	2.52	168.18
2.50	19.884	2.50	65.888	2.50	113.47	2.50	161.11
2.48	19.083	2.48	63.311	2.48	109.17	2.48	155.08
2.45	18.070	2.45	60.030	2.45	103.67	2.45	147.37
2.40	16.735	2.40	55.657	2.40	96.317	2.40	137.13
2.35	15.692	2.35	52.165	2.35	90.492	2.35	128.83
2.30	14.839	2.30	49.250	2.30	85.513	2.30	121.86
2.25	14.116	2.25	46.698	2.25	81.217	2.25	115.76
2.20	13.485	2.20	44.397	2.20	77.294	2.20	110.25
2.15	12.923	2.15	42.290	2.15	73.666	2.15	105.10
2.10	12.411	2.10	40.293	2.10	70.240	2.10	100.22
2.05	11.938	2.05	38.393	2.05	66.951	2.05	95.545
2.00	11.494	2.00	36.565	2.00	63.779	2.00	91.030
1.95	11.075	1.95	34.782	1.95	60.686	1.95	86.595
1.90	10.673	1.90	33.029	1.90	57.632	1.90	82.276
1.85	10.286	1.85	31.303	1.85	54.609	1.85	77.950
1.80	9.9116	1.80	29.584	1.80	51.604	1.80	73.649
1.75	9.5458	1.75	27.884	1.75	48.588	1.75	69.347
1.70	9.1876	1.70	26.223	1.70	45.579	1.70	65.042
1.65	8.8353	1.65	24.683	1.65	42.615	1.65	60.732
1.60	8.4880	1.60	23.427	1.60	39.824	1.60	56.558
1.55	8.1444	1.55	22.423	1.55	37.595	1.55	53.007
1.50	7.8036	1.50	21.521	1.50	35.896	1.50	50.376
1.45	7.4650	1.45	20.660	1.45	34.395	1.45	48.195
1.40	7.1278	1.40	19.816	1.40	32.963	1.40	46.155
1.35	6.7915	1.35	18.987	1.35	31.567	1.35	44.183

Table 42.

RO21=2.500 V21=1.200 V2S1=0.6928
RO31=3.000 V31=5.200 V3S1=3.000

V/V_1	L/H_1	V/V_1	L/H_1	V/V_1	L/H_1	V/V_1	L/H_1
H21=1.000		H21=4.000		H21=7.000		H21=10.000	
2.72	107.31	2.72	360.14	2.72	613.64	2.72	866.53
2.70	72.357	2.70	243.71	2.70	415.63	2.70	587.58
2.68	55.453	2.68	187.39	2.68	319.86	2.68	451.98
2.66	45.554	2.66	154.40	2.66	264.12	2.66	373.63
2.64	39.097	2.64	133.00	2.64	227.55	2.64	322.26
2.62	34.575	2.62	118.03	2.62	202.33	2.62	286.72
2.60	31.238	2.60	106.99	2.60	183.54	2.60	260.27
2.58	28.676	2.58	98.560	2.58	169.27	2.58	240.22
2.56	26.650	2.56	91.868	2.56	158.10	2.56	224.27
2.54	25.005	2.54	86.478	2.54	148.93	2.54	211.64
2.52	23.639	2.52	82.029	2.52	141.42	2.52	200.96
2.50	22.488	2.50	78.272	2.50	135.14	2.50	192.04
2.48	21.497	2.48	75.054	2.48	129.70	2.48	184.38
2.45	20.246	2.45	70.984	2.45	122.88	2.45	174.84
2.40	18.596	2.40	65.628	2.40	113.80	2.40	162.07
2.35	17.306	2.35	61.440	2.35	106.73	2.35	152.03
2.30	16.250	2.30	57.953	2.30	100.81	2.30	143.68
2.25	15.357	2.25	54.973	2.25	95.687	2.25	136.54
2.20	14.578	2.20	52.317	2.20	91.159	2.20	130.08
2.15	13.887	2.15	49.907	2.15	87.019	2.15	124.11
2.10	13.262	2.10	47.652	2.10	83.140	2.10	118.66
2.05	12.690	2.05	45.528	2.05	79.469	2.05	113.43
2.00	12.161	2.00	43.490	2.00	75.951	2.00	108.43
1.95	11.667	1.95	41.531	1.95	72.526	1.95	103.57
1.90	11.203	1.90	39.613	1.90	69.211	1.90	98.832
1.85	10.764	1.85	37.732	1.85	65.930	1.85	94.119
1.80	10.346	1.80	35.876	1.80	62.697	1.80	89.535
1.75	9.9453	1.75	34.035	1.75	59.486	1.75	84.926
1.70	9.5582	1.70	32.192	1.70	56.271	1.70	80.365
1.65	9.1824	1.65	30.355	1.65	53.051	1.65	75.730
1.60	8.8156	1.60	28.502	1.60	49.806	1.60	71.125
1.55	8.4562	1.55	26.648	1.55	46.529	1.55	66.439
1.50	8.1021	1.50	24.821	1.50	43.233	1.50	61.687
1.45	7.7526	1.45	23.187	1.45	40.012	1.45	56.998
1.40	7.4063	1.40	21.973	1.40	37.298	1.40	52.815
1.35	7.0625	1.35	20.979	1.35	35.359	1.35	49.814

Table 43.

RO21=2.000 V21=1.200 V2S1=0.6928
RO31=3.000 V31=5.200 V3S1=3.000

V/V_1	L/H_1	V/V_1	L/H_1	V/V_1	L/H_1	V/V_1	L/H_1
H21=1.000		H21=4.000		H21=7.000		H21=10.000	
2.72	91.282	2.72	295.61	2.72	500.50	2.72	706.64
2.70	62.002	2.70	201.76	2.70	342.60	2.70	483.03
2.68	47.952	2.68	156.83	2.68	266.58	2.68	376.59
2.66	39.797	2.66	130.77	2.66	222.71	2.66	314.47
2.64	34.516	2.64	113.87	2.64	194.35	2.64	274.78
2.62	30.832	2.62	102.13	2.62	174.65	2.62	247.31
2.60	28.125	2.60	93.551	2.60	160.23	2.60	227.09
2.58	26.053	2.58	87.004	2.58	149.25	2.58	211.76
2.56	24.417	2.56	81.842	2.56	140.68	2.56	199.54
2.54	23.086	2.54	77.649	2.54	133.71	2.54	189.86
2.52	21.980	2.52	74.197	2.52	127.92	2.52	181.81
2.50	21.045	2.50	71.275	2.50	123.03	2.50	174.99
2.48	20.239	2.48	68.750	2.48	118.85	2.48	169.08
2.45	19.217	2.46	66.555	2.46	115.21	2.46	163.86
2.40	17.859	2.44	64.622	2.44	111.96	2.44	159.34
2.35	16.785	2.42	62.871	2.42	109.02	2.42	155.23
2.30	15.900	2.40	61.297	2.40	106.36	2.40	151.50
2.25	15.141	2.38	59.840	2.38	103.95	2.38	148.11
2.20	14.476	2.35	57.880	2.35	100.59	2.35	143.36
2.15	13.878	2.30	54.982	2.30	95.715	2.30	136.49
2.10	13.334	2.25	52.445	2.25	91.392	2.25	130.35
2.05	12.829	2.20	50.148	2.20	87.433	2.20	124.74
2.00	12.357	2.15	48.000	2.15	83.762	2.15	119.59
1.95	11.910	2.10	45.990	2.10	80.287	2.10	114.61
1.90	11.484	2.05	44.056	2.05	76.950	2.05	109.87
1.85	11.074	2.00	42.190	2.00	73.710	2.00	105.23
1.80	10.677	1.95	40.364	1.95	70.538	1.95	100.72
1.75	10.291	1.90	38.570	1.90	67.416	1.90	96.288
1.70	9.9131	1.85	36.795	1.85	64.316	1.85	91.862
1.65	9.5426	1.80	35.032	1.80	61.241	1.80	87.490
1.60	9.1775	1.75	33.270	1.75	58.173	1.75	83.083
1.55	8.8165	1.70	31.502	1.70	55.076	1.70	78.674
1.50	8.4595	1.65	29.726	1.65	51.971	1.65	74.242
1.45	8.1049	1.60	27.933	1.60	48.824	1.60	69.736
1.40	7.7526	1.55	26.125	1.55	45.631	1.55	65.162
1.35	7.4014	1.50	24.373	1.50	42.401	1.50	60.527
		1.45	23.044	1.45	39.260	1.45	55.909
		1.40	22.065	1.40	36.922	1.40	51.996
		1.35	21.151	1.35	35.266	1.35	49.447

Table 44.

RO21=2.800 V21=4.667 V2S1=2.694
RO31=3.000 V31=5.000 V3S1=2.887

V/V_1	L/H_1	V/V_1	L/H_1	V/V_1	L/H_1	V/V_1	L/H_1
H21=1.000		H21=4.000		H21=7.000		H21=10.000	
2.60	24.243	2.60	30.440	2.60	38.744	2.60	48.461
2.58	18.919	2.58	23.138	2.58	30.249	2.58	38.352
2.56	16.172	2.56	19.526	2.56	25.597	2.56	32.478
2.54	14.537	2.54	17.318	2.54	22.497	2.54	28.384
2.52	13.458	2.52	15.802	2.52	20.209	2.52	25.230
2.50	12.689	2.50	14.684	2.50	18.415	2.50	22.656
2.48	12.106	2.48	13.821	2.48	16.956	2.48	20.471
2.46	11.643	2.46	13.128	2.46	15.741	2.46	18.577
2.44	11.262	2.44	12.557	2.44	14.716	2.44	16.928
2.42	10.938	2.42	12.076	2.42	13.847	2.42	15.507
2.40	10.656	2.40	11.662	2.40	13.108	2.40	14.311
2.38	10.406	2.38	11.301	2.38	12.477	2.38	13.326
2.35	10.075	2.35	10.833	2.35	11.696	2.35	12.188
2.30	9.6021	2.30	10.192	2.30	10.712	2.30	10.915
2.25	9.1940	2.25	9.6635	2.25	9.9863	2.25	10.075
2.20	8.8265	2.20	9.2080	2.20	9.4133	2.20	9.4548
2.15	8.4868	2.15	8.8011	2.15	8.9346	2.15	8.9550
2.10	8.1660	2.10	8.4283	2.10	8.5162	2.10	8.5270
2.05	7.8586	2.05	8.0792	2.05	8.1381	2.05	8.1435
2.00	7.5614	2.00	7.7482	2.00	7.7876	2.00	7.7906
1.95	7.2714	1.95	7.4302	1.95	7.4568	1.95	7.4581
1.90	6.9866	1.90	7.1218	1.90	7.1398	1.90	7.1405
1.85	6.7051	1.85	6.8209	1.85	6.8325	1.85	6.8330
1.80	6.4259	1.80	6.5249	1.80	6.5326		
1.75	6.1480	1.75	6.2323	1.75	6.2374		
1.70	5.8699	1.70	5.9419	1.70	5.9450		
1.65	5.5911	1.65	5.6522	1.65	5.6540		
1.60	5.3106	1.60	5.3621	1.60	5.3632		
1.55	5.0270	1.55	5.0703	1.55	5.0708		
1.50	4.7394	1.50	4.7753	1.50	4.7758		
1.45	4.4466	1.45	4.4760				
1.40	4.1465	1.40	4.1703				
1.35	3.8373	1.35	3.8560				

Table 45.

RO21=2.800 V21=4.333 V2S1=2.502
RO31=3.000 V31=5.000 V3S1=2.887

V/V_1	L/H_1	V/V_1	L/H_1	V/V_1	L/H_1	V/V_1	L/H_1
H21=5.000		H21=10.000		H21=15.000		H21=20.000	
2.60	66.613	2.60	109.96	2.60	153.14	2.60	196.38
2.58	43.933	2.58	72.009	2.58	100.77	2.58	129.65
2.56	33.473	2.56	55.675	2.56	78.571	2.56	101.62
2.54	27.823	2.54	46.759	2.54	66.330	2.54	86.016
2.52	24.276	2.52	40.971	2.52	58.246	2.52	75.616
2.50	21.801	2.50	36.771	2.50	52.298	2.50	67.941
2.48	19.942	2.48	33.499	2.48	47.619	2.48	61.828
2.46	18.475	2.46	30.825	2.46	43.739	2.46	56.750
2.44	17.273	2.44	28.546	2.44	40.392	2.44	52.335
2.42	16.261	2.42	26.551	2.42	37.423	2.42	48.385
2.40	15.390	2.40	24.759	2.40	34.710	2.40	44.754
2.38	14.629	2.38	23.121	2.38	32.186	2.38	41.336
2.35	13.645	2.35	20.870	2.35	28.610	2.35	36.414
2.30	12.319	2.30	17.484	2.30	22.810	2.30	27.994
2.25	11.273	2.25	14.478	2.25	16.911	2.25	18.372
2.20	10.429	2.20	12.102	2.20	12.638	2.20	12.721
2.15	9.7339	2.15	10.544	2.15	10.649		
2.10	9.1484	2.10	9.5500	2.10	9.5749	H21=25.000	
2.05	8.6427	2.05	8.8502	2.05	8.8569		
2.00	8.1950	2.00	8.3063	2.00	8.3082	2.60	239.52
1.95	7.7894	1.95	7.8053	1.95	7.8517	2.58	158.67
1.90	7.4142	1.90	7.4477			2.56	124.72
1.85	7.0613	1.85	7.0801			2.54	105.74
1.80	6.7247	1.80	6.7353			2.52	93.027
1.75	6.4001	1.75	6.4059			2.50	83.612
1.70	6.0841	1.70	6.0872			2.48	76.086
1.65	5.7734	1.65	5.7750			2.46	69.783
1.60	5.4661	1.60	5.4671			2.44	64.300
1.55	5.1601					2.42	59.368
1.50	4.8534					2.40	54.821
1.45	4.5441					2.38	50.502
1.40	4.2299					2.35	44.216
1.35	3.9085					2.30	33.018
1.30	3.5763					2.25	19.040
1.25	3.2294						

Table 46.

RO21=2.800 V21=4.000 V2S1=2.309
RO31=3.000 V31=5.000 V3S1=2.887

V/V_1	L/H_1	V/V_1	L/H_1	V/V_1	L/H_1	V/V_1	L/H_1
H21=1.000		H21=4.000		H21=7.000		H21=10.000	
2.60	37.432	2.60	91.088	2.60	144.47	2.60	197.76
2.58	27.317	2.58	61.593	2.58	95.915	2.58	130.22
2.56	21.774	2.56	45.308	2.56	69.530	2.56	93.879
2.54	18.408	2.54	35.620	2.54	54.309	2.54	73.297
2.52	16.225	2.52	29.584	2.52	45.089	2.52	60.989
2.50	14.733	2.50	25.617	2.50	39.093	2.50	52.994
2.48	13.665	2.48	22.848	2.48	34.887	2.48	47.370
2.46	12.868	2.46	20.806	2.46	31.749	2.46	43.143
2.44	12.249	2.44	19.229	2.44	29.285	2.44	39.808
2.42	11.751	2.42	17.965	2.42	27.275	2.42	37.060
2.40	11.339	2.40	16.921	2.40	25.585	2.40	34.740
2.38	10.990	2.38	16.037	2.38	24.127	2.38	32.718
2.35	10.548	2.35	14.931	2.35	22.251	2.35	30.093
2.30	9.9563	2.30	13.479	2.30	19.679	2.30	26.436
2.25	9.4740	2.25	12.340	2.25	17.537	2.25	23.305
2.20	9.0576	2.20	11.406	2.20	15.657	2.20	20.442
2.15	8.6833	2.15	10.613	2.15	13.948	2.15	17.685
2.10	8.3374	2.10	9.9262	2.10	12.382	2.10	14.933
2.05	8.0112	2.05	9.3203	2.05	10.985	2.05	12.315
2.00	7.6993	2.00	8.7783	2.00	9.8184	2.00	10.325
1.95	7.3971	1.95	8.2874	1.95	8.9054	1.95	9.0778
1.90	7.1026	1.90	7.8381	1.90	8.1980	1.90	8.2578
1.85	6.8131	1.85	7.4213	1.85	7.6301	1.85	7.6522
1.80	6.5273	1.80	7.0303	1.80	7.1516	1.80	7.1602
1.75	6.2434	1.75	6.6599	1.75	6.7298	1.75	6.7332
1.70	5.9606	1.70	6.3050	1.70	6.3453	1.70	6.3465
1.65	5.6773	1.65	5.9620	1.65	5.9844	1.65	5.9851
1.60	5.3928	1.60	5.6274	1.60	5.6396		
1.55	5.1060	1.55	5.2984	1.55	5.3049		
1.50	4.8155	1.50	4.9722	1.50	4.9755		
1.45	4.5200	1.45	4.6466				
1.40	4.2177	1.40	4.3184				
1.35	3.9066	1.35	3.9853				

Table 47.

RO21=2.800 V21=3.667 V2S1=2.117
RO31=3.000 V31=5.000 V3S1=2.887

V/V_1	L/H_1	V/V_1	L/H_1	V/V_1	L/H_1	V/V_1	L/H_1
H21=1.000		H21=4.000		H21=7.000		H21=10.000	
2.60	44.380	2.60	122.66	2.60	201.09	2.60	279.43
2.58	32.260	2.58	85.615	2.58	139.26	2.58	193.04
2.56	25.448	2.56	64.317	2.56	103.78	2.56	143.31
2.54	21.184	2.54	50.701	2.54	81.114	2.54	111.58
2.52	18.336	2.52	41.463	2.52	65.878	2.52	90.435
2.50	16.353	2.50	35.009	2.50	55.389	2.50	75.944
2.48	14.922	2.48	30.401	2.48	47.984	2.48	65.817
2.46	13.858	2.46	27.028	2.46	42.620	2.46	58.501
2.44	13.043	2.44	24.487	2.44	38.597	2.44	53.013
2.42	12.399	2.42	22.514	2.42	35.472	2.42	48.753
2.40	11.878	2.40	20.941	2.40	32.967	2.40	45.327
2.38	11.444	2.38	19.651	2.38	30.894	2.38	42.485
2.35	10.911	2.35	18.087	2.35	28.364	2.35	39.003
2.30	10.221	2.30	16.124	2.30	25.119	2.30	34.499
2.25	9.6804	2.25	14.640	2.25	22.598	2.25	30.962
2.20	9.2254	2.20	13.445	2.20	20.497	2.20	27.986
2.15	8.8248	2.15	12.435	2.15	18.660	2.15	25.339
2.10	8.4602	2.10	11.554	2.10	16.984	2.10	22.882
2.05	8.1200	2.05	10.766	2.05	15.404	2.05	20.498
2.00	7.7974	2.00	10.050	2.00	13.877	2.00	18.092
1.95	7.4870	1.95	9.3910	1.95	12.373	1.95	15.555
1.90	7.1854	1.90	8.7826	1.90	10.907	1.90	12.833
1.85	6.8904	1.85	8.2188	1.85	9.5613	1.85	10.317
1.80	6.5996	1.80	7.6952	1.80	8.4553	1.80	8.6681
1.75	6.3118	1.75	7.2094	1.75	7.6145	1.75	7.6723
1.70	6.0256	1.70	6.7568	1.70	6.9673	1.70	6.9842
1.65	5.7393	1.65	6.3324	1.65	6.4407	1.65	6.4456
1.60	5.4524	1.60	5.9316	1.60	5.9863		
1.55	5.1632	1.55	5.5490	1.55	5.5760		
1.50	4.8709	1.50	5.1794	1.50	5.1925		
1.45	4.5738	1.45	4.8190				
1.40	4.2700	1.40	4.4632				
1.35	3.9577	1.35	4.1070				

Table 48.

RO21=2.800 V21=3.333 V2S1=1.924
RO31=3.000 V31=5.000 V3S1=2.887

V/V_1	L/H_1	V/V_1	L/H_1	V/V_1	L/H_1	V/V_1	L/H_1
H21=1.000		H21=4.000		H21=7.000		H21=10.000	
2.60	51.045	2.60	151.73	2.60	252.76	2.60	353.61
2.58	37.163	2.58	108.10	2.58	179.47	2.58	250.84
2.56	29.273	2.56	82.885	2.56	137.17	2.56	191.40
2.54	24.236	2.54	66.480	2.54	109.53	2.54	152.64
2.52	20.797	2.52	54.998	2.52	90.207	2.52	125.53
2.50	18.341	2.50	46.583	2.50	76.079	2.50	105.65
2.48	16.532	2.48	40.249	2.48	65.476	2.48	90.818
2.46	15.166	2.46	35.390	2.46	57.375	2.46	79.491
2.44	14.113	2.44	31.611	2.44	51.118	2.44	70.793
2.42	13.283	2.42	28.641	2.42	46.231	2.42	64.020
2.40	12.615	2.40	26.271	2.40	42.355	2.40	58.653
2.38	12.068	2.38	24.355	2.38	39.229	2.38	54.336
2.35	11.407	2.35	22.089	2.35	35.539	2.35	49.235
2.30	10.580	2.30	19.367	2.30	31.091	2.30	43.083
2.25	9.9566	2.25	17.423	2.25	27.882	2.25	38.619
2.20	9.4492	2.20	15.925	2.20	25.373	2.20	35.116
2.15	9.0132	2.15	14.700	2.15	23.295	2.15	32.189
2.10	8.6230	2.10	13.656	2.10	21.485	2.10	29.636
2.05	8.2644	2.05	12.734	2.05	19.856	2.05	27.309
2.00	7.9273	2.00	11.896	2.00	18.340	2.00	25.127
1.95	7.6055	1.95	11.121	1.95	16.892	1.95	23.011
1.90	7.2953	1.90	10.390	1.90	15.474	1.90	20.902
1.85	6.9926	1.85	9.6950	1.85	14.050	1.85	18.721
1.80	6.6958	1.80	9.0271	1.80	12.589	1.80	16.369
1.75	6.4030	1.75	8.3837	1.75	11.068	1.75	13.700
1.70	6.1121	1.70	7.7655	1.70	9.5203	1.70	10.724
1.65	5.8222	1.65	7.1760	1.65	8.1245	1.65	8.4096
1.60	5.5321	1.60	6.6203	1.60	7.0649	1.60	7.1183
1.55	5.2403	1.55	6.1013	1.55	6.2965	1.55	6.3071
1.50	4.9455	1.50	5.6187	1.50	5.7010		
1.45	4.6463	1.45	5.1679	1.45	5.2013		
1.40	4.3411	1.40	4.7415				
1.35	4.0277	1.35	4.3315				

Table 49.

RO21=2.800 V21=2.667 V2S1=1.5395
RO31=3.000 V31=5.000 V3S1=2.887

V/V_1	L/H_1	V/V_1	L/H_1	V/V_1	L/H_1	V/V_1	L/H_1
H21=5.000		H21=10.000		H21=15.000		H21=20.000	
2.60	248.06	2.60	479.70	2.60	711.92	2.60	944.44
2.58	180.73	2.58	349.67	2.58	518.87	2.58	688.13
2.56	141.91	2.56	274.52	2.56	406.89	2.56	540.10
2.54	116.56	2.54	225.36	2.54	334.23	2.54	442.96
2.52	98.662	2.52	190.71	2.52	282.66	2.52	374.89
2.50	85.388	2.50	164.87	2.50	244.41	2.50	323.72
2.48	75.087	2.48	144.87	2.48	214.73	2.48	284.53
2.46	66.899	2.46	128.94	2.46	191.06	2.46	253.06
2.44	60.222	2.44	115.95	2.44	171.74	2.44	227.65
2.42	54.676	2.42	105.17	2.42	155.69	2.42	206.22
2.40	50.016	2.40	96.083	2.40	142.23	2.40	188.33
2.38	46.047	2.38	88.349	2.38	130.71	2.38	173.07
2.35	41.128	2.35	78.763	2.35	116.48	2.35	154.15
2.30	34.974	2.30	66.769	2.30	98.662	2.30	130.54
2.25	30.592	2.25	58.272	2.25	86.059	2.25	113.90
2.20	27.392	2.20	52.102	2.20	76.927	2.20	101.74
2.15	24.966	2.15	47.426	2.15	70.001	2.15	92.625
2.10	23.043	2.10	43.735	2.10	64.542	2.10	85.374
2.05	21.458	2.05	40.686	2.05	60.025	2.05	79.395
2.00	20.099	2.00	38.062	2.00	56.149	2.00	74.242
1.95	18.896	1.95	35.732	1.95	52.689	1.95	69.660
1.90	17.804	1.90	33.604	1.90	49.526	1.90	65.461
1.85	16.789	1.85	31.619	1.85	46.568	1.85	61.532
1.80	15.828	1.80	29.727	1.80	43.743	1.80	57.775
1.75	14.905	1.75	27.890	1.75	40.997	1.75	54.118
1.70	14.004	1.70	26.082	1.70	38.272	1.70	50.487
1.65	13.113	1.65	24.264	1.65	35.530	1.65	46.814
1.60	12.219	1.60	22.405	1.60	32.703	1.60	43.011
1.55	11.307	1.55	20.457	1.55	29.703	1.55	38.961
1.50	10.362	1.50	18.344	1.50	26.389	1.50	34.432
1.45	9.3618	1.45	15.930	1.45	22.450	1.45	28.915
1.40	8.2796	1.40	12.908	1.40	16.930	1.40	20.439
1.35	7.0993	1.35	8.9245				
1.30	5.8882						
1.25	4.8411						

Tables 1L.—48L.

The values of phase velocity in km/sec and the dimensionless values of wave length (L/H_1). H_1 is the thickness of the upper layer. VS1 and RO1 represent the shear velocity (km/sec) and the density (g/cm^3) of the upper layer respectively.

Table 1L.

VS1=3.984 RO1=2.670
VS2=4.677 RO2=3.000

V	L/H_1	V	L/H_1	V	L/H_1	V	L/H_1
4.67	27.926	4.62	9.4717	4.57	6.6612	4.35	3.0129
4.66	17.809	4.61	8.6749	4.55	6.0160	4.30	2.5965
4.65	14.042	4.60	8.0336	4.50	4.8752	4.25	2.2246
4.64	11.917	4.59	7.5020	4.45	4.0935	4.20	1.8801
4.63	10.503	4.58	7.0509	4.40	3.4984	4.15	1.5491

Table 2L.

VS1=3.176 RO1=2.670
VS2=4.677 RO2=3.000

V	L/H_1	V	L/H_1	V	L/H_1	V	L/H_1
4.67	55.070	4.57	14.000	4.10	5.3293	3.60	2.7037
4.66	35.329	4.55	12.824	4.05	4.9971	3.55	2.4788
4.65	28.024	4.50	10.792	4.00	4.6901	3.50	2.2524
4.64	23.929	4.45	9.4511	3.95	4.4032	3.45	2.0218
4.63	21.221	4.40	8.4709	3.90	4.1326	3.40	1.7835
4.62	19.259	4.35	7.7061	3.85	3.8752	3.35	1.5321
4.61	17.752	4.30	7.0816	3.80	3.6282		
4.60	16.547	4.25	6.5543	3.75	3.3896		
4.59	15.555	4.20	6.0974	3.70	3.1572		
4.58	14.718	4.15	5.6931	3.65	2.9291		

Table 7L.

VS1=3.464 RO1=2.800
VS2=4.590 RO2=3.000

V	L/H_1	V	L/H_1	V	L/H_1	V	L/H_1
4.58	38.134	4.45	9.7554	4.10	4.2864	3.70	1.8935
4.57	26.887	4.40	8.2040	4.05	3.9210	3.65	1.6206
4.56	21.888			4.00	3.5864		
4.55	18.898	4.35	7.1358	3.95	3.2751	3.60	1.3338
4.54	16.850	4.30	6.3311	3.90	2.9814	3.55	1.0172
		4.25	5.6883			3.50	0.6252
4.53	15.333	4.20	5.1528	3.85	2.7006		
4.52	14.149	4.15	4.6924	3.80	2.4285		
4.50	12.393			3.75	2.1609		

Table 9L.

VS1=2.887 RO1=2.800
VS2=4.590 RO2=3.000

V	L/H_1	V	L/H_1	V	L/H_1	V	L/H_1
4.58	53.708	4.35	10.825	3.85	5.3736	3.35	2.9283
4.57	37.985	4.30	9.7781	3.80	5.0841	3.30	2.7079
4.56	31.018	4.25	8.9537	3.75	4.8103	3.25	2.4858
4.55	26.864	4.20	8.2771	3.70	4.5495	3.20	2.2598
4.54	24.027	4.15	7.7042	3.65	4.2993	3.15	2.0272
4.53	21.932	4.10	7.2073	3.60	4.0579	3.10	1.7843
4.52	20.301	4.05	6.7679	3.55	3.8236	3.05	1.5249
4.50	17.895	4.00	6.3730	3.50	3.5949	3.00	1.2380
4.45	14.312	3.95	6.0133	3.45	3.3703	2.95	0.8979
4.40	12.235	3.90	5.6819	3.40	3.1486		

Table 11L.

VS1=2.309 RO1=2.800
VS2=4.590 RO2=3.000

V	L/H_1	V	L/H_1	V	L/H_1	V	L/H_1
4.58	66.588	4.15	10.655	3.50	6.0828	2.85	3.3522
4.57	47.242			3.45	5.8499	2.80	3.1479
4.56	38.697	4.10	10.086	3.40	5.6235	2.75	2.9405
4.55	33.616	4.05	9.5848			2.70	2.7287
4.54	30.155	4.00	9.1366	3.35	5.4029	2.65	2.5109
		3.95	8.7304	3.30	5.1871		
4.53	27.606	3.90	8.3581	3.25	4.9755	2.60	2.2847
4.52	25.628			3.20	4.7673	2.55	2.0471
4.50	22.718	3.85	8.0136	3.15	4.5619	2.50	1.7931
4.45	18.416	3.80	7.6922			2.45	1.5143
4.40	15.947	3.75	7.3902	3.10	4.3586	2.40	1.1936
		3.70	7.1045	3.05	4.1568		
4.35	14.284	3.65	6.8327	3.00	3.9560	2.35	0.7831
4.30	13.058			2.95	3.7554		
4.25	12.098	3.60	6.5729	2.90	3.5544		
4.20	11.315	3.55	6.3234				

Table 16L.

VS1=2.887 RO1=3.000
VS2=4.792 RO2=3.400

V	L/H_1	V	L/H_1	V	L/H_1	V	L/H_1
4.78	50.003	4.50	10.270	3.95	5.4084	3.40	3.0175
4.77	36.986	4.45	9.4590	3.90	5.1565	3.35	2.8167
4.76	30.712	4.40	8.7943	3.85	4.9157		
4.75	26.843	4.35	8.2321			3.30	2.6139
4.74	24.155			3.80	4.6842	3.25	2.4076
		4.30	7.7450	3.75	4.4606	3.20	2.1961
4.73	22.147	4.25	7.3148	3.70	4.2434	3.15	1.9766
4.72	20.574	4.20	6.9287	3.65	4.0317	3.10	1.7456
4.70	18.236	4.15	6.5775	3.60	3.8242		
4.65	14.729	4.10	6.2545			3.05	1.4969
4.60	12.687			3.55	3.6200	3.00	1.2198
		4.05	5.9546	3.50	3.4181	2.95	0.8884
4.55	11.300	4.00	5.6736	3.45	3.2176		

Table 18L.

VS1=2.887 RO1=2.800
VS2=4.792 RO2=3.000

V	L/H_1	V	L/H_1	V	L/H_1	V	L/H_1
4.78	52.841	4.50	10.676	3.95	5.5285	3.40	3.0530
4.77	39.055	4.45	9.8123	3.90	5.2652	3.35	2.8475
4.76	32.404	4.40	9.1051	3.85	5.0141		
4.75	28.302	4.35	8.5078			3.30	2.6403
4.74	25.449			3.80	4.7732	3.25	2.4299
		4.30	7.9910	3.75	4.5409	3.20	2.2145
4.73	23.317	4.25	7.5353	3.70	4.3158	3.15	1.9915
4.72	21.646	4.20	7.1270	3.65	4.0967	3.10	1.7571
4.70	19.160	4.15	6.7564	3.60	3.8824		
4.65	15.428	4.10	6.4162			3.05	1.5054
4.60	13.252			3.55	3.6719	3.00	1.2253
		4.05	6.1009	3.50	3.4642	2.95	0.8913
4.55	11.773	4.00	5.8061	3.45	3.2582		

Table 19L.

VS1=4.0410 RO1=2.800
VS2=4.6765 RO2=3.000

V	L/H_1	V	L/H_1	V	L/H_1	V	L/H_1
4.67	28.034	4.60	7.7025	4.35	2.7120	4.10	0.8119
4.66	17.457	4.55	5.7069	4.30	2.2897		
4.65	13.664	4.50	4.5751	4.25	1.9084		
4.64	11.547	4.45	3.7964	4.20	1.5492		
4.63	10.145	4.40	3.2007	4.15	1.1935		

Table 20L.

VS1=3.4640 RO1=2.800
VS2=4.6765 RO2=3.000

V	L/H_1	V	L/H_1	V	L/H_1	V	L/H_1
4.67	50.122	4.50	9.1417	4.15	4.4180	3.80	2.3743
4.66	31.383	4.45	7.9174			3.75	2.1194
4.65	24.702	4.40	7.0166	4.10	4.0693	3.70	1.8626
4.64	20.994			4.05	3.7481	3.65	1.5986
4.63	18.552	4.35	6.3091	4.00	3.4482		
		4.30	5.7277	3.95	3.1647	3.60	1.3193
4.60	14.344	4.25	5.2336	3.90	2.8935	3.55	1.0090
4.55	10.985	4.20	4.8024	3.85	2.6312	3.50	0.6222

Table 21L.

VS1=2.8870 RO1=2.500
VS2=4.6765 RO2=3.400

V	L/H_1	V	L/H_1	V	L/H_1	V	L/H_1
4.67	54.397	4.50	11.013	3.90	5.0117	3.35	2.7628
4.66	34.298	4.45	9.8008			3.30	2.5671
4.65	27.181	4.40	8.9184	3.85	4.7787	3.25	2.3677
4.64	23.257			3.80	4.5556	3.20	2.1626
4.63	20.686	4.35	8.2315	3.75	4.3406	3.15	1.9493
		4.30	7.6710	3.70	4.1323		
4.62	18.837	4.25	7.1975	3.65	3.9293	3.10	1.7242
4.61	17.425	4.20	6.7867			3.05	1.4811
4.60	16.302	4.15	6.4226	3.60	3.7304	3.00	1.2092
4.59	15.381			2.55	3.5347	2.95	0.8827
4.58	14.607	4.10	6.0944	3.50	3.3411		
		4.05	5.7943	3.45	3.1486		
4.57	13.945	4.00	5.5165	3.40	2.9562		
4.55	12.865	3.95	5.2568				

Table 22L.

VS1=2.8870 RO1=2.800
VS2=4.6765 RO2=3.000

V	L/H_1	V	L/H_1	V	L/H_1	V	L/H_1
4.67	68.861	4.45	11.606	3.90	5.4810	3.35	2.8910
4.66	43.241	4.40	10.449	3.85	5.2013	3.30	2.6768
4.65	34.134	4.35	9.5517	3.80	4.9360		
4.64	29.094	4.30	8.8237			3.25	2.4601
4.63	25.783			3.75	4.6826	3.20	2.2390
		4.25	8.2130	3.70	4.4392	3.15	2.0109
4.62	23.395	4.20	7.6873	3.65	4.2040	3.10	1.7719
4.61	21.567	4.15	7.2253	3.60	3.9757	3.05	1.5160
4.60	20.109	4.10	6.8125	3.55	3.7528		
4.59	18.910	4.05	6.4385			3.00	1.2322
4.55	15.626			3.50	3.5340	2.95	0.8949
		4.00	6.0956	3.45	3.3183		
4.50	13.198	3.95	5.7779	3.40	3.1044		

Table 23L.

VS1=2.8870 RO1=2.500
VS2=4.6765 RO2=3.000

V	L/H_1	V	L/H_1	V	L/H_1	V	L/H_1
4.67	61.552	4.35	8.8741	3.85	4.9839	3.35	2.8253
4.66	38.718	4.30	8.2316	3.80	4.7403	3.30	2.6206
4.65	30.614	4.25	7.6910	3.75	4.5067	3.25	2.4128
4.64	26.136	4.20	7.2241	3.70	4.2814	3.20	2.2000
4.63	23.198	4.15	6.8124	3.65	4.0628	3.15	1.9795
4.60	18.174	4.10	6.4430	3.60	3.8497	3.10	1.7475
4.55	14.218	4.05	6.1070	3.55	3.6408	3.05	1.4982
4.50	12.081	4.00	5.7976	3.50	3.4350	3.00	1.2205
4.45	10.682	3.95	5.5097	3.45	3.2313	2.95	0.8887
4.40	9.6643	3.90	5.2395	3.40	3.0284		

Table 24L.

VS1=2.3090 RO1=2.500
VS2=4.6765 RO2=3.400

V	L/H_1	V	L/H_1	V	L/H_1	V	L/H_1
4.67	66.654	4.30	10.400	3.55	5.8251	2.80	3.0384
4.66	42.202	4.25	9.8600	3.50	5.6265	2.75	2.8455
4.65	33.580	4.20	9.3938	3.45	5.4320	2.70	2.6473
4.64	28.842	4.15	8.9824	3.40	5.2411	2.65	2.4423
4.63	25.749	4.10	8.6130	3.35	5.0532	2.60	2.2282
4.62	23.532	4.05	8.2767	3.30	4.8676	2.55	2.0019
4.61	21.844	4.00	7.9669	3.25	4.6840	2.50	1.7586
4.60	20.504	3.95	7.6787	3.20	4.5019	2.45	1.4897
4.59	19.409	3.90	7.4083	3.15	4.3208	2.40	1.1784
4.58	18.491	3.85	7.1527	3.10	4.1401	2.35	0.7765
4.55	16.432	3.80	6.9095	3.05	3.9596		
4.50	14.261	3.75	6.6770	3.00	3.7786		
4.45	12.851	3.70	6.4535	2.95	3.5966		
4.40	11.831	3.65	6.2377	2.90	3.4131		
4.35	11.041	3.60	6.0285	2.85	3.2273		

Table 25L.

VS1=2.3090 RO1=2.800
VS2=4.6765 RO2=3.000

V	L/H_1	V	L/H_1	V	L/H_1	V	L/H_1
4.67	84.314	4.35	12.689	3.60	6.4363	2.85	3.3279
4.66	53.110	4.30	11.852	3.55	6.2012	2.80	3.1268
4.65	42.053	4.25	11.153	3.50	5.9734	2.75	2.9224
4.64	35.952	4.20	10.554	3.45	5.7518	2.70	2.7134
4.63	31.955	4.15	10.030	3.40	5.5355	2.65	2.4981
4.62	29.079	4.10	9.5632	3.35	5.3239	2.60	2.2743
4.61	26.883	4.05	9.1422	3.30	5.1163	2.55	2.0389
4.60	25.136	4.00	8.7578	3.25	4.9120	2.50	1.7869
4.59	23.703	3.95	8.4033	3.20	4.7104	2.45	1.5099
4.58	22.501	3.90	8.0735	3.15	4.5109	2.40	1.1909
4.57	21.473	3.85	7.7644	3.10	4.3131	2.35	0.7819
4.55	19.796	3.80	7.4729	3.05	4.1164		
4.50	16.932	3.75	7.1962	3.00	3.9201		
4.45	15.070	3.70	6.9324	2.95	3.7237		
4.40	13.725	3.65	6.6796	2.90	3.5265		

Table 26L.

VS1=2.3090 RO1=2.500
VS2=4.6765 RO2=3.000

V	L/H_1	V	L/H_1	V	L/H_1	V	L/H_1
4.67	75.389	4.10	9.0742	3.35	5.1850	2.60	2.2509
4.66	47.590	4.05	8.6968	3.30	4.9888	2.55	2.0201
4.65	37.761	4.00	8.3508	3.25	4.7951	2.50	1.7725
4.64	32.346	3.95	8.0304	3.20	4.6036	2.45	1.4997
4.63	28.805	3.90	7.7312	3.15	4.4136	2.40	1.1846
4.60	22.779	3.85	7.4497	3.10	4.2246	2.35	0.7792
4.55	18.079	3.80	7.1831	3.05	4.0362		
4.50	15.566	3.75	6.9292	3.00	3.8477		
4.45	13.932	3.70	6.6862	2.95	3.6587		
4.40	12.753	3.65	6.4525	2.90	3.4686		
4.35	11.842	3.60	6.2268	2.85	3.2765		
4.30	11.105	3.55	6.0080	2.80	3.0817		
4.25	10.488	3.50	5.7952	2.75	2.8832		
4.20	9.9571	3.45	5.5876	2.70	2.6797		
4.15	9.4908	3.40	5.3845	2.65	2.4697		

Table 28L.

VS1=1.1547 RO1=2.500
VS2=4.6765 RO2=3.000

V	L/H_1	V	L/H_1	V	L/H_1	V	L/H_1
4.65	49.783	4.40	21.656	3.20	11.661	1.95	5.7198
4.64	43.463	4.39	21.437	3.15	11.407	1.90	5.4799
4.63	39.387	4.35	20.652	3.10	11.155	1.85	5.2375
4.62	36.494	4.30	19.828	3.05	10.907	1.80	4.9922
4.61	34.310	4.25	19.127	3.00	10.661	1.75	4.7434
4.60	32.589	4.20	18.514	2.95	10.417	1.70	4.4903
4.59	31.190	4.15	17.967	2.90	10.175	1.65	4.2321
4.58	30.023	4.10	17.470	2.85	9.9343	1.60	3.9675
4.57	29.032	4.05	17.013	2.80	9.6956	1.55	3.6953
4.56	28.176	4.00	16.587	2.75	9.4584	1.50	3.4132
4.55	27.426	3.95	16.188	2.70	9.2224	1.45	3.1186
4.54	26.762	3.90	15.810	2.65	8.9874	1.40	2.8075
4.53	26.169	3.85	15.451	2.60	8.7534	1.35	2.4734
4.52	25.635	3.80	15.107	2.55	8.5202	1.30	2.1055
4.51	25.150	3.75	14.776	2.50	8.2875	1.25	1.6817
4.50	24.706	3.70	14.457	2.45	8.0554	1.20	1.1422
4.49	24.298	3.65	14.148	2.40	7.8235		
4.48	23.921	3.60	13.847	2.35	7.5918		
4.47	23.571	3.55	13.554	2.30	7.3600		
4.46	23.245	3.50	13.268	2.25	7.1280		
4.45	22.940	3.45	12.988	2.20	6.8956		
4.44	22.653	3.40	12.714	2.15	6.6626		
4.43	22.383	3.35	12.445	2.10	6.4288		
4.42	22.128	3.30	12.179	2.05	6.1939		
4.41	21.886	3.25	11.918	2.00	5.9577		

Table 29L.

VS1=4.041 RO1=3.000
VS2=4.504 RO2=3.400

V	L/H_1	V	L/H_1	V	L/H_1	V	L/H_1
4.49	13.516	4.44	5.9694	4.30	2.6704		
4.48	10.213	4.43	5.4817	4.25	2.1302		
4.47	8.4859	4.42	5.0783	4.20	1.6751		
4.46	7.3746	4.40	4.4403	4.15	1.2590		
4.45	6.5786	4.35	3.3760	4.10	0.8389		

Table 30L.

VS1=4.001 RO1=3.000
VS2=4.504 RO2=3.400

V	L/H_1	V	L/H_1	V	L/H_1	V	L/H_1
4.49	14.637	4.44	6.5040	4.30	2.9943	4.05	0.7439
4.48	11.072	4.43	5.9811	4.25	2.4332		
4.47	9.2105	4.42	5.5491	4.20	1.9688		
4.46	8.0141	4.40	4.8674	4.15	1.5559		
4.45	7.1581	4.35	3.7366	4.10	1.1616		

Table 31L.

VS1=3.464 RO1=3.000
VS2=4.504 RO2=3.400

V	L/H_1	V	L/H_1	V	L/H_1	V	L/H_1
4.49	28.622	4.42	11.447	4.10	4.4349	3.80	2.4480
4.48	21.803	4.40	10.218			3.75	2.1742
4.47	18.268	4.35	8.2406	4.05	4.0274	3.70	1.9022
4.46	16.013			4.00	3.6629	3.65	1.6260
4.45	14.412	4.30	7.0080	3.95	3.3302	3.60	1.3369
		4.25	6.1302	3.90	3.0209		
4.44	13.198	4.20	5.4530	3.85	2.7286	3.55	1.0187
4.43	12.235	4.15	4.9017			3.50	0.6257

Table 32L.

VS1=3.464 RO1=2.800
VS2=4.503 RO2=3.000

V	L/H_1	V	L/H_1	V	L/H_1	V	L/H_1
4.49	31.369	4.42	12.097	4.10	4.5793	3.75	2.2107
4.48	23.502	4.40	10.770	4.05	4.1483		
4.47	19.552	4.35	8.6437	4.00	3.7641	3.70	1.9302
4.46	17.066	4.30	7.3223			3.65	1.6464
4.45	15.315	4.25	6.3835	3.95	3.4146	3.60	1.3507
				3.90	3.0907	3.55	1.0267
4.44	13.994	4.20	5.6611	3.85	2.7858	3.50	0.6287
4.43	12.950	4.15	5.0745	3.80	2.4942		

Table 33L.

VS1=3.175 RO1=2.800
VS2=4.503 RO2=3.000

V	L/H_1	V	L/H_1	V	L/H_1	V	L/H_1
4.49	38.731	4.30	9.3916	3.80	3.9213	3.30	1.2902
4.48	29.072	4.25	8.2831	3.75	3.6363	3.25	0.9639
4.47	24.230	4.20	7.4388	3.70	3.3644	3.20	0.5309
4.46	21.189	4.15	6.7606	3.65	3.1024		
4.45	19.051	4.10	6.1943	3.60	2.8475		
4.44	17.440	4.05	5.7076	3.55	2.5971		
4.43	16.170	4.00	5.2794	3.50	2.3484		
4.42	15.134	3.95	4.8955	3.45	2.0983		
4.40	13.527	3.90	4.5458	3.40	1.8430		
4.35	10.967	3.85	4.2230	3.35	1.5767		

Table 34L.

VS1=2.887 RO1=3.000
VS2=4.504 RO2=3.400

V	L/H_1	V	L/H_1	V	L/H_1	V	L/H_1
4.49	41.471	4.30	10.847	3.80	5.1375	3.30	2.7095
4.48	31.696	4.25	9.6726	3.75	4.8513	3.25	2.4865
4.47	26.646	4.20	8.7817	3.70	4.5807	3.20	2.2599
4.46	23.435	4.15	8.0693	3.65	4.3229	3.15	2.0270
4.45	21.163	4.10	7.4771	3.60	4.0756	3.10	1.7838
4.44	19.445	4.05	6.9703	3.55	3.8366	3.05	1.5244
4.43	18.088	4.00	6.5265	3.50	3.6043	3.00	1.2376
4.42	16.980	3.95	6.1306	3.45	3.3769	2.95	0.8976
4.40	15.261	3.90	5.7720	3.40	3.1530		
4.35	12.525	3.85	5.4429	3.35	2.9311		

Table 35L.

VS1=2.887 RO1=2.800
VS2=4.503 RO2=3.000

V	L/H_1	V	L/H_1	V	L/H_1	V	L/H_1
4.49	45.452	4.30	11.343	3.80	5.2638	3.30	2.7433
4.48	34.168	4.25	10.084	3.75	4.9636	3.25	2.5148
4.47	28.520	4.20	9.1312	3.70	4.6806	3.20	2.2831
4.46	24.978	4.15	8.3704	3.65	4.4116	3.15	2.0456
4.45	22.491	4.10	7.7393	3.60	4.1541	3.10	1.7982
4.44	20.621	4.05	7.2003	3.55	3.9059	3.05	1.5348
4.43	19.148	4.00	6.7294	3.50	3.6652	3.00	1.2444
4.42	17.948	3.95	6.3103	3.45	3.4301	2.95	0.9012
4.40	16.091	3.90	5.9316	3.40	3.1992		
4.35	13.145	3.85	5.5848	3.35	2.9708		

Table 36L.

VS1=2.887 RO1=2.500
VS2=4.504 RO2=3.000

V	L/H_1	V	L/H_1	V	L/H_1	V	L/H_1
4.49	39.218	4.34	11.602	4.19	8.3171	3.45	3.3273
4.48	30.001	4.33	11.264	4.15	7.7929	3.40	3.1099
4.47	25.243	4.32	10.953	4.10	7.2359	3.35	2.8940
4.46	22.220	4.31	10.666	4.05	6.7583	3.30	2.6779
4.45	20.082	4.30	10.399	4.00	6.3392	3.25	2.4600
4.44	18.467	4.29	10.150	3.95	5.9646	3.20	2.2381
4.43	17.192	4.28	9.9169	3.90	5.6244	3.15	2.0095
4.42	16.151	4.27	9.6982	3.85	5.3115	3.10	1.7704
4.41	15.280	4.26	9.4922	3.80	5.0204	3.05	1.5146
4.40	14.537	4.25	9.2976	3.75	4.7470	3.00	1.2311
4.39	13.893	4.24	9.1134	3.70	4.4879	2.95	0.8942
4.38	13.328	4.23	8.9385	3.65	4.2405		
4.37	12.826	4.22	8.7721	3.60	4.0025		
4.36	12.377	4.21	8.6135	3.55	3.7721		
4.35	11.971	4.20	8.4620	3.50	3.5475		

Table 37L.

VS1=2.887 RO1=2.000
VS2=4.504 RO2=3.000

V	L/H_1	V	L/H_1	V	L/H_1	V	L/H_1
4.49	31.586	4.30	8.9214	3.80	4.6396	3.30	2.5741
4.48	24.273	4.25	8.0673	3.75	4.4076	3.25	2.3727
4.47	20.513	4.20	7.4159	3.70	4.1857	3.20	2.1662
4.46	18.132	4.15	6.8905	3.65	3.9718	3.15	1.9518
4.45	16.453	4.10	6.4495	3.60	3.7641	3.10	1.7257
4.44	15.189	4.05	6.0679	3.55	3.5613	3.05	1.4820
4.43	14.192	4.00	5.7298	3.50	3.3619	3.00	1.2097
4.42	13.381	3.95	5.4244	3.45	3.1648	2.95	0.8829
4.40	12.126	3.90	5.1444	3.40	2.9686		
4.35	10.138	3.85	4.8841	3.35	2.7722		

Table 38L.

VS1=2.310 RO1=2.500
VS2=4.504 RO2=3.000

V	L/H_1	V	L/H_1	V	L/H_1	V	L/H_1
4.49	49.309	4.05	9.5669	3.35	5.1145	2.55	2.0300
4.48	37.853	4.00	9.0856	3.25	4.9073	2.50	1.7784
4.47	31.959	3.95	8.6579	3.20	4.7035	2.45	1.5016
4.46	28.227	3.90	8.2719	3.15	4.5024	2.40	1.1823
4.45	25.595	3.85	7.9191	3.10	4.3034	2.35	0.7712
4.44	23.613	3.80	7.5932	3.05	4.1058		
4.43	22.051	3.75	7.2894	3.00	3.9089		
4.42	20.780	3.70	7.0039	2.95	3.7123		
4.40	18.817	3.65	6.7336	2.90	3.5151		
4.35	15.718	3.60	6.4764	2.85	3.3165		
4.30	13.838	3.55	6.2301	2.80	3.1157		
4.25	12.532	3.50	5.9932	2.75	2.9117		
4.20	11.549	3.45	5.7642	2.70	2.7031		
4.15	10.766	3.40	5.5422	2.65	2.4883		
4.10	10.119	3.35	5.3259	2.60	2.2650		

Table 39L.

VS1=2.310 RO1=2.000
VS2=4.504 RO2=3.000

V	L/H_1	V	L/H_1	V	L/H_1	V	L/H_1
4.49	39.775	4.05	8.6395	3.30	4.8793	2.55	1.9961
4.48	30.703	4.00	8.2535	3.25	4.6924	2.50	1.7525
4.47	26.058	3.95	7.9072	3.20	4.5075	2.45	1.4832
4.46	23.128	3.90	7.5918	3.15	4.3241	2.40	1.1709
4.45	21.070	3.85	7.3008	3.10	4.1415		
4.44	19.524	3.80	7.0295	3.05	3.9594		
4.43	18.310	3.75	6.7743	3.00	3.7772		
4.42	17.324	3.70	6.5325	2.95	3.5942		
4.40	15.805	3.65	6.3017	2.90	3.4098		
4.35	13.417	3.60	6.0803	2.85	3.2233		
4.30	11.970	3.55	5.8667	2.80	3.0340		
4.25	10.962	3.50	5.6597	2.75	2.8407		
4.20	10.199	3.45	5.4583	2.70	2.6422		
4.15	9.5878	3.40	5.2616	2.65	2.4369		
4.10	9.0780	3.35	5.0688	2.60	2.2226		

Table 40L.

VS1=1.155 RO1=2.500
VS2=4.504 RO2=3.000

V	L/H_1	V	L/H_1	V	L/H_1	V	L/H_1
4.45	36.074	4.20	20.283	3.00	10.786	1.75	4.7579
4.44	33.786	4.19	20.091	2.95	10.533	1.70	4.5029
4.43	31.999	4.15	19.398	2.90	10.283	1.65	4.2429
4.42	30.556	4.10	18.655	2.85	10.035	1.60	3.9767
4.41	29.359	4.05	18.012	2.80	9.7888	1.55	3.7028
4.40	28.346	4.00	17.443	2.75	9.5449	1.50	3.4193
4.39	27.474	3.95	16.930	2.70	9.3028	1.45	3.1232
4.38	26.713	3.90	16.459	2.65	9.0621	1.40	2.8107
4.37	26.041	3.85	16.024	2.60	8.8227	1.35	2.4752
4.36	25.441	3.80	15.616	2.55	8.5845	1.30	2.1059
4.35	24.902	3.75	15.232	2.50	8.3471	1.25	1.6806
4.34	24.413	3.70	14.867	2.45	8.1105	1.20	1.1390
4.33	23.966	3.65	14.518	2.40	7.8745		
4.32	23.556	3.60	14.183	2.35	7.6389		
4.31	23.178	3.55	13.860	2.30	7.4034		
4.30	22.827	3.50	13.547	2.25	7.1680		
4.29	22.500	3.45	13.244	2.20	6.9324		
4.28	22.194	3.40	12.949	2.15	6.6963		
4.27	21.907	3.35	12.660	2.10	6.4596		
4.26	21.637	3.30	12.378	2.05	6.2220		
4.25	21.381	3.25	12.102	2.00	5.9832		
4.24	21.139	3.20	11.831	1.95	5.7428		
4.23	20.910	3.15	11.564	1.90	5.5006		
4.22	20.691	3.10	11.301	1.85	5.2560		
4.21	20.482	3.05	11.042	1.80	5.0087		

Table 41L.

VS1=1.155 RO1=2.000
VS2=4.504 RO2=3.000

V	L/H_1	V	L/H_1	V	L/H_1	V	L/H_1
4.45	30.846	4.20	18.784	3.00	10.527	1.75	4.7156
4.44	29.106	4.19	18.632	2.95	10.288	1.70	4.4652
4.43	27.750	4.15	18.077	2.90	10.052	1.65	4.2095
4.42	26.656	4.10	17.476	2.85	9.8172	1.60	3.9475
4.41	25.749	4.05	16.948	2.88	9.5839	1.55	3.6776
4.40	24.981	4.00	16.475	2.75	9.3518	1.50	3.3978
4.39	24.320	3.95	16.044	2.70	9.1209	1.45	3.1054
4.38	23.742	3.90	15.644	2.65	8.8910	1.40	2.7963
4.37	23.232	3.85	15.270	2.60	8.6619	1.35	2.4641
4.36	22.775	3.80	14.917	2.55	8.4334	1.30	2.0979
4.35	22.364	3.75	14.582	2.50	8.2053	1.25	1.6755
4.34	21.991	3.70	14.260	2.45	7.9776	1.20	1.1367
4.33	21.649	3.65	13.951	2.40	7.7501		
4.32	21.334	3.60	13.652	2.35	7.5226		
4.31	21.043	3.55	13.362	2.30	7.2949		
4.30	20.773	3.50	13.080	2.25	7.0669		
4.29	20.520	3.45	12.804	2.20	6.8384		
4.28	20.283	3.40	12.535	2.15	6.6091		
4.27	20.060	3.35	12.271	2.10	6.3789		
4.26	19.849	3.30	12.011	2.05	6.1476		
4.25	19.650	3.25	11.756	2.00	5.9147		
4.24	19.460	3.20	11.504	1.95	5.6801		
4.23	19.280	3.15	11.256	1.90	5.4433		
4.22	19.107	3.10	11.010	1.85	5.2039		
4.21	18.942	3.05	10.767	1.80	4.9616		

Table 42L.

VS1=1.0393 RO1=2.500
VS2=4.504 RO2=3.000

V	L/H_1	V	L/H_1	V	L/H_1	V	L/H_1
4.45	37.577	4.20	21.919	3.00	12.057	1.75	5.6533
4.44	35.308	4.19	21.726	2.95	11.787	1.70	5.3903
4.43	33.538	4.15	21.028	2.90	11.520	1.65	5.1239
4.42	32.110	4.10	20.277	2.85	11.255	1.60	4.8535
4.41	30.926	4.05	19.623	2.80	10.992	1.55	4.5781
4.40	29.924	4.00	19.042	2.75	10.731	1.50	4.2967
4.39	29.062	3.95	18.515	2.70	10.472	1.45	4.0078
4.38	28.309	3.90	18.031	2.65	10.214	1.40	3.7096
4.37	27.644	3.85	17.581	2.60	9.9584	1.35	3.3995
4.36	27.051	3.80	17.158	2.55	9.7036	1.30	3.0737
4.35	26.517	3.75	16.757	2.50	9.4499	1.25	2.7266
4.34	26.032	3.70	16.376	2.45	9.1971	1.20	2.3485
4.33	25.590	3.65	16.011	2.40	8.9451	1.15	1.9213
4.32	25.183	3.60	15.660	2.35	8.6936	1.10	1.4011
4.31	24.808	3.55	15.320	2.30	8.4425		
4.30	24.459	3.50	14.991	2.25	8.1917		
4.29	24.134	3.45	14.670	2.20	7.9410		
4.28	23.829	3.40	14.358	2.15	7.6902		
4.27	23.543	3.35	14.052	2.10	7.4391		
4.26	23.274	3.30	13.753	2.05	7.1876		
4.25	23.019	3.25	13.460	2.00	6.9353		
4.24	22.777	3.20	13.171	1.95	6.6820		
4.23	22.547	3.15	12.887	1.90	6.4275		
4.22	22.328	3.10	12.607	1.85	6.1715		
4.21	22.119	3.05	12.330	1.80	5.9136		

Table 43L.

VS1=1.0393 RO1=2.000
VS2=4.504 RO2=3.000

V	L/H_1	V	L/H_1	V	L/H_1	V	L/H_1
4.45	32.406	4.00	18.084	2.75	10.532	1.50	4.2692
4.44	30.686	3.95	17.637	2.70	10.285	1.45	3.9840
4.43	29.347	3.90	17.222	2.65	10.038	1.40	3.6893
4.42	28.267	3.85	16.832	2.60	9.7919	1.35	3.3825
4.41	27.371	3.80	16.462	2.55	9.5468	1.30	3.0599
4.40	26.613	3.75	16.110	2.50	9.3023	1.25	2.7157
4.39	25.960	3.70	15.771	2.45	9.0583	1.20	2.3405
4.38	25.389	3.65	15.445	2.40	8.8147	1.15	1.9159
4.37	24.883	3.60	15.129	2.35	8.5713	1.10	1.3982
4.36	24.431	3.55	14.821	2.30	8.3280		
4.35	24.023	3.50	14.522	2.25	8.0846		
4.34	23.652	3.45	14.229	2.20	7.8410		
4.33	23.313	3.40	13.942	2.15	7.5970		
4.32	23.000	3.35	13.660	2.10	7.3524		
4.31	22.710	3.30	13.383	2.05	7.1070		
4.30	22.440	3.25	13.110	2.00	6.8607		
4.29	22.187	3.20	12.841	1.95	6.6131		
4.28	21.950	3.15	12.575	1.90	6.3641		
4.27	21.727	3.10	12.312	1.85	6.1133		
4.26	21.516	3.05	12.051	1.80	5.8604		
4.25	21.315	3.00	11.793	1.75	5.6049		
4.20	20.443	2.95	11.538	1.70	5.3465		
4.15	19.726	2.90	11.284	1.65	5.0845		
4.10	19.113	2.85	11.032	1.60	4.8182		
4.05	18.572	2.80	10.781	1.55	4.5468		

Table 44L.

VS1=4.041 RO1=2.800
VS2=4.330 RO2=3.000

V	L/H_1	V	L/H_1	V	L/H_1	V	L/H_1
4.325	15.591	4.300	6.0411	4.275	4.2101	4.18	1.8855
4.320	10.915	4.295	5.5312	4.26	3.5925	4.16	1.6182
4.315	8.8211	4.290	5.1156	4.24	2.9979	4.14	1.3755
4.310	7.5599	4.285	4.7674	4.22	2.5504	4.12	1.1482
4.305	6.6901	4.280	4.4695	4.20	2.1900	4.10	0.9276

Table 46L.

VS1=3.464 RO1=2.800
VS2=4.330 RO2=3.000

V	L/H_1	V	L/H_1	V	L/H_1	V	L/H_1
4.32	30.920	4.05	4.9168	3.55	1.0505		
4.31	21.760	4.00	4.3317	3.50	0.6373		
4.30	17.681	3.95	3.8400				
4.29	15.236	3.90	3.4119				
4.28	13.559	3.85	3.0284				
4.27	12.313	3.80	2.6763				
4.25	10.550	3.75	2.3455				
4.20	8.0393	3.70	2.0274				
4.15	6.6152	3.65	1.7137				
4.10	5.6460	3.60	1.3938				

Table 47L.

VS1=3.175 RO1=2.800
VS2=4.330 RO2=3.000

V	L/H_1	V	L/H_1	V	L/H_1	V	L/H_1
4.32	39.800	4.05	6.8407	3.55	2.7147		
4.31	28.075	4.00	6.1470	3.50	2.4406		
4.30	22.866	3.95	5.5737	3.45	2.1692		
4.29	19.751	3.90	5.0837	3.40	1.8956		
4.28	17.619	3.85	4.6539	3.35	1.6139		
4.27	16.039	3.80	4.2688	3.30	1.3143		
4.25	13.811	3.75	3.9176	3.25	0.9769		
4.20	10.664	3.70	3.5921	3.20	0.5348		
4.15	8.9018	3.65	3.2863				
4.10	7.7184	3.60	2.9953				

Table 48L.

VS1=2.887 RO1=2.800
VS2=4.330 RO1=3.000

V	L/H_1	V	L/H_1	V	L/H_1	V	L/H_1
4.31	33.846	4.00	7.8642	3.50	3.8421	3.05	1.5580
4.30	27.613	3.95	7.2145	3.45	3.5790	3.00	1.2592
4.29	23.894	3.90	6.6642	3.40	3.3239	2.95	0.9088
4.28	21.351	3.85	6.1861	3.35	3.0746		
		3.80	5.7622	3.30	2.8288		
4.25	16.825	3.75	5.3798	3.25	2.5844		
4.20	13.108	3.70	5.0299	3.20	2.3388		
4.15	11.044	3.65	4.7059	3.15	2.0890		
4.10	9.6686	3.60	4.4025	3.10	1.8308		
4.05	8.6571	3.55	4.1157				

26. 表面波と層構造 (2)

海洋構造を伝わる表面波の理論的分散曲線

地震研究所 山口林造
気象研究所 木沢綏

1. 長周期地震計が世界各地に設備され，海洋構造を伝わる表面波についても，次第にその観測記録について論議されるようになってきた．然しながら，その観測から地殻構造を求めるに必要な理論的分散曲線が未だに充分計算されていない．その要求に答えて，電子計算機の使用に不自由な我国ではあるが，IBM 704 を使用する機会を得たので，計算結果をできるだけ使用に便利な様に図示した．

2. 計算した構造については Table A に一括して並べ，第 1 図から第 49 図まで各構造について，Rayleigh 波の群速度についての分散曲線を図示した．位相速度に関しては第 1 表から第 49 表まで同順序で整理されている．夫々の図から海水層と中間層の厚さの割合に応じて変化する様子が明瞭に分る．

又それらの図の組合せで，いろいろな比較が出来るわけであるが，ここでは簡単に海水層の変化に着目した第 50 図，Mantle の速度の変化に応じたものが第 51 図に，Crust の速度を変えて比較したのが第 52 図に表わされている．又第 53 図には密度の多少の変化では，それ程影響を受けないことが図示されている．

3. 実際の観測から，それに合致する様な構造を容易に探せる様，第 54 図から第 58 図までを用意した．その分類の方法としては周期 30 秒での群速度に着目した．そのことは又今迄の観測から特別な場合を除き，大体海の深さに於ても整理できる可能性があるからである．

それらの図からも分る如く，単に観測された分散曲線から一義的に構造を決めることは現在の観測精度だけを考慮しても難しい，然し大凡の見当をつけることは，充分可能であるし，真の構造を見つける為には有力な手懸りになることには異論はないであろう．

4. 最後に海水層を無視して，夫々の構造に対応した Love 波の分散曲線を求めた．群速度に関しては第 1L 図から第 48L 図まで，又位相速度については第 1L 表から第 48L 表までに示した．全部に亘ることは出来なかったが，Rayleigh 波のものとともに使用して，或程度役立ち得るものと思う．

Bulletin of the Earthquake
Research Institute
Vol. 39 (1961), pp. 811-822

27. *The Dispersion of Love Waves in Heterogeneous Half Space overlain by a Homogeneous Layer.*

By Takehito Takahashi*,

Earthquake Research Institute.

(Read Sept. 26, 1961.—Received Sept. 30, 1961.)

1. Introduction

The author once treated the dispersion of surface waves in heterogeneous half space[1]. Formulation was made in a general form, and a scheme was presented for determining the structure of the medium from the dispersion curve of Love waves. However, the assumption of slowly varying material constants of the medium has prevented us from applying the theory to many practical problems. The numerical example at the end of [I], where the discontinuity structure was replaced by a continuous layer, has to be understood as a mere trial.

In order to get numerically precise results, it might be most adequate to divide the medium into several parts, each of which satisfies the above mentioned assumption.

As such we shall consider here the heterogeneous half space having a homogeneous upper layer, and shall treat the dispersion of Love waves.

Such a problem has already been solved by several authors[2] assuming special functions for density and rigidity. Our treatment will be nothing but the generalization of their results. We shall treat the case when density and shear velocity in the lower layer are given only numerically, and show that the scheme for the inverse problem still holds under certain restrictions.

---

* Professor in Rikkyo University, Toshima-ku, Tokyo.

1) T. Takahashi, *Bull. Earthq. Res. Inst.*, **33** (1955) 287; **35** (1957) 297. Cited as I and II respectively in this paper.

2) T. Matsuzawa, *Bull. Earthq. Res. Inst.*, **6** (1929) 213.
H. Jeffreys, M. N. R. S. *Geophys. Suppl.*, **2** (1928) 101.
Y. Satô, *Bull. Earthq. Res. Inst.*, **30** (1952) 1.
J. T. Wilson, *Bull. Seism. Soc. Amer.*, **30** (1940) 273.

Notations are as follows:

T period
L wave-length
$p=2\pi/T$
$f=2\pi/L$
$v_Q=p/f=L/T$ phase velocity
$U=dp/df$ group velocity
$V(z)$ amplitude
$\rho(z)$ density
$\mu(z)$ rigidity
$v_s(z)=\sqrt{\mu/\rho}$ shear velocity
$\kappa(z)=(v_Q/v_s(z))^2=p^2\rho/f^2\mu$
H zero point of $\kappa-1$. Then $\kappa(H)=1$, or $v_Q=v_s(H)$.
$\mu(0)$, $\kappa(0)$ etc. are written merely as μ_0, κ_0 etc.

2. Recapitulation of the formulas of the previous papers

Consider the differential equation

$$\frac{1}{\mu}\frac{d}{dz}\left(\mu\frac{dV}{dz}\right)+f^2(\kappa-1)V=0\,, \tag{1}$$

where μ and κ are slowly varying functions of z, and $d\kappa/dz$ is assumed to be negative.

Then the approximate solution of (1) which is valid for large f and converges to zero at $z=\infty$, is expressed as

$$V(z)=\left(\frac{-\varphi}{\mu\sqrt{\kappa-1}}\right)^{1/2}K_{1/3}(-i\varphi)\,, \tag{2}$$

where $K_{1/3}$ means modified Bessel function of order 1/3, and φ is defined by

$$\varphi(z)=f\int_z^H\sqrt{\kappa-1}\,dz\,. \tag{3}$$

Next we introduce a function $H(\varphi)$:

$$H(\varphi)=\frac{d}{d\varphi}\log\{\varphi^{1/2}K_{1/3}(-i\varphi)\}\,. \tag{4}$$

The asymptotic expression of $H(\varphi)$ for large φ is

$$H(\varphi) \sim \tan\left(\frac{\pi}{4}-\varphi\right), \tag{5}$$

which is useful for calculating higher modes.

From (2) and (4) we obtain

$$\frac{V'(0)}{V(0)}=-\frac{\mu_0'}{2\mu_0}-\frac{\kappa_0'}{4(\kappa_0-1)}-f\sqrt{\kappa_0-1}\ H(\varphi_0), \tag{6}$$

where the letters with prime are derivatives with respect to z.

When κ_0 becomes very near to 1, equation (6) is transformed into

$$\frac{V'(0)}{V(0)}=-\frac{\mu_0'}{2\mu_0}-0.72904\,f^{2/3}(-\kappa_0')^{1/3}+1.10554\,\frac{f^{4/3}(\kappa_0-1)}{(-\kappa_0')^{1/3}}+\frac{\kappa_0''+5f^2(\kappa_0-1)^2}{10(-\kappa_0')}+\cdots, \tag{7}$$

where

$$0.72904=9^{-1/3}\Gamma(2/3)/\Gamma(4/3)\ ,\quad 1.10554=9^{-1/3}\{\Gamma(2/3)/\Gamma(4/3)\}^2\ .$$

Usually κ is defined only for $z\geqq 0$. Accordingly, if $\kappa_0<1$, we cannot determine H, and $\varphi(z)$ must have some expression other than (3). (See Appendix.) The expression (7) is proved to hold both for $\kappa_0>1$ and $\kappa_0<1$.

Lastly, if κ_0 is fairly small as compared with 1, we can use the asymptotic expansion of $K_{1/3}(|\varphi|)$ and obtain

$$\frac{V'(0)}{V(0)}=-\frac{\mu_0'}{2\mu_0}-f\sqrt{1-\kappa_0}\left(1-\frac{\kappa_0'}{4(1-\kappa_0)^{3/2}}-\frac{5}{32f^2}\,\frac{\kappa_0'^2}{(1-\kappa_0)^3}-\frac{1}{8f^2}\,\frac{\kappa_0''}{(1-\kappa_0)^2}-\cdots\right). \tag{8}$$

3. Equation of dispersion

We shall discuss the theory of Love wave propagation in media consisting of a homogeneous upper layer of thickness h and a heterogeneous lower layer, where rigidity and density are slowly varying functions of the depth. The shear velocity is assumed to be increasing with the depth.

The z-axis is taken vertically downward, and the origin at the interface of two layers. Then the free surface is indicated by the equation $z=-h$.

The letters with suffix 1, such as ρ_1, μ_1, κ_1 and $V_1(z)$ are used to denote that they belong to the upper layer. Shear velocity in the upper layer is expressed merely as v_1. ρ_1, μ_1, κ_1 and v_1 are all constants, and $v_1 < v_s(0)$.

The amplitude $V(z)$ of the Love wave satisfies (1). Then, in the lower layer we can employ the expression (2).

The boundary conditions are such that the stress shall vanish at the free surface, and at the interface displacement and stress shall be continuous with those given by (2). That is

$$V_1'(-h)=0\ , \tag{9}$$

and

$$\frac{V'(0)}{V(0)}=\frac{\mu_1 V_1'(0)}{\mu_0 V_1(0)}\ . \tag{10}$$

It is easily verified that in the homogeneous layer,

$$V_1(z)=A\cos\{f\sqrt{\kappa_1-1}(z+h)\} \tag{11}$$

is the solution of (1) which satisfies (9).

Substituting (11) in (10), we obtain

$$\frac{V'(0)}{V(0)}=-\frac{\mu_1}{\mu_0}f\sqrt{\kappa_1-1}\tan(fh\sqrt{\kappa_1-1})\ . \tag{12}$$

This is the equation of dispersion, and has three different expressions corresponding to the various values of κ_0.

i) $\kappa_0>1$ $(v_Q>v_s(0))$.

From (6) and (12) we have

$$H(\varphi_0)=\frac{\mu_1\sqrt{\kappa_1-1}}{\mu_0\sqrt{\kappa_0-1}}\tan(fh\sqrt{\kappa_1-1})+\frac{1}{4f(\kappa_0-1)^{3/2}}\left\{(2-\kappa_0)\frac{\mu_0'}{\mu_0}-\kappa_0\frac{\rho_0'}{\rho_0}\right\}\ . \tag{13}$$

To solve (13), we transform (13) into

$$H(\varphi_0)=\frac{\mu_1\sqrt{\kappa_1-1}}{\mu_0\sqrt{\kappa_0-1}}\tan\left(\varphi_0\frac{h\sqrt{\kappa_1-1}}{\varphi}\right)+\frac{1}{\varphi_0}\frac{\varphi}{4(\kappa_0-1)^{3/2}}\left\{(2-\kappa_0)\frac{\mu_0'}{\mu_0}-\kappa_0\frac{\rho_0'}{\rho_0}\right\}\ , \tag{14}$$

where

$$\bar{\varphi}=\varphi_0/f=\int_0^H \sqrt{\kappa-1}\, dz\ .$$

When $v_s(z)$ is given, fix a value of v_Q and calculate $\bar{\varphi}$, κ_0 and κ_1. Assuming that μ_1/μ_0, h, μ_0'/μ_0 and ρ_0'/ρ_0 are all known, we can determine φ_0 from (14), then $f=\varphi_0/\varphi$ is the wave number corresponding to v_Q.

A brief table of $H(\varphi)$ for real φ is given in [II]. The more precise one (Table 1) is calculated, using the table of Airy functions.[3] (See Appendix (A3))

Table 1

φ	$H(\varphi)$	$\varphi H(\varphi)$	φ	$H(\varphi)$	$\varphi H(\varphi)$
.00	∞	.16667	.50	.53195	.26598
.02	10.51098	.21022	.52	.49598	.25791
.04	5.81366	.23255	.54	.46151	.24922
.06	4.15550	.24933	.56	.42836	.23988
.08	3.32878	.26630	.58	.39641	.22992
.10	2.73762	.27376	.60	.36553	.21932
.12	2.35715	.28286	.62	.33632	.20852
.14	2.07403	.29036	.64	.30653	.19618
.16	1.85316	.29651	.66	.27954	.18450
.18	1.67467	.30144	.68	.25065	.17044
.20	1.52635	.30527	.70	.22370	.15659
.22	1.40048	.30811	.72	.19729	.14205
.24	1.29166	.31000	.74	.17141	.12684
.26	1.19622	.31102	.76	.14596	.11093
.28	1.11148	.31121	.78	.12093	.09433
.30	1.03538	.31061	.80	.09623	.07698
.32	.96642	.30925	.82	.07185	.05892
.34	.90342	.30716	.84	.04772	.04008
.36	.84543	.30435	.86	.02385	.02051
.38	.79174	.30086	.88	.00018	.00016
.40	.74171	.29668	.90	−.02332	−.02099
.42	.69486	.29184	.92	−.04670	−.04296
.44	.65077	.28634	.94	−.07996	−.07516
.46	.60911	.28019	.96	−.09315	−.08942
.48	.56958	.27340	.98	−.11633	−.11400
			1.00	−.13951	−.13951

ii) $\kappa_0 \fallingdotseq 1$ $(v_Q \fallingdotseq v_s(0))$.

From (7) and (12) we have

$$\tan(fh\sqrt{\kappa_1-1})=\frac{\mu_0}{\mu_1\sqrt{\kappa_1-1}}\left\{\frac{\mu_0'}{2f\mu_0}+0.72904\left(\frac{-\kappa_0'}{f}\right)^{1/3}\right.$$

3) A. D. SMIRNOV, *Tables of Airy Functions* (Pergamon Press, 1960).

$$-1.10554\frac{f^{1/3}(\kappa_0-1)}{(-\kappa_0')^{1/3}}-\frac{\kappa_0''+5f^2(\kappa_0-1)^2}{10f(-\kappa_0')}+\cdots\Big\}. \quad (15)$$

When $\kappa_0=1$ ($v_Q=v_s(0)$), (15) becomes

$$\xi\tan\xi=\frac{\mu_0}{\mu_1}\frac{h}{2}\left(\frac{\mu_0'}{\mu_0}-\frac{\kappa_0''}{5(-\kappa_0')}\right)+0.72904\frac{\mu_0}{\mu_1}\left(\frac{h(-\kappa_0')}{\kappa_1-1}\right)^{1/3}\xi^{2/3}. \quad (16)$$

where

$$\xi=fh\sqrt{\kappa_1-1}\ .$$

iii) $\kappa_0<1$ $(v_s(0)>v_Q>v_1)$.

From (8) and (12) we have

$$\tan(fh\sqrt{\kappa_1-1})=\frac{\mu_0\sqrt{1-\kappa_0}}{\mu_1\sqrt{\kappa_1-1}}\Big\{1+\frac{\mu_0'}{2f\mu_0\sqrt{1-\kappa_0}}-\frac{\kappa_0'}{4f(1-\kappa_0)^{3/2}}$$
$$-\frac{5}{32f^2}\frac{\kappa_0'^2}{(1-\kappa_0)^3}-\frac{\kappa_0''}{8f^2(1-\kappa_0)^2}-\cdots\Big\}. \quad (17)$$

(15) and (17) are solved by iteration.

4. Explicit expression of $\bar{\varphi}$

Examples of the explicit expression of $\bar{\varphi}$ are given in this section.

i) When ρ/μ is a linear function of z, we put

$$\rho/\mu=(\rho_0/\mu_0)(1-\beta z)\ ,$$

or

$$\kappa=\kappa_0(1-\beta z)\ . \quad (18)$$

From $\kappa(H)=1$, β is expressed by H as

$$\beta=(\kappa_0-1)\kappa_0^{-1}H^{-1}\ . \quad (19)$$

The calculation of $\bar{\varphi}$ is easily performed:

$$\bar{\varphi}=\int_0^H\sqrt{\kappa-1}dz=\frac{2}{3}H\sqrt{\kappa_0-1}\ . \quad (20)$$

We add expressions for $d\bar{\varphi}/d\kappa_0$, κ_0' and κ_0''.

$$\frac{1}{\bar{\varphi}}\frac{d\bar{\varphi}}{d\kappa_0}=\frac{3}{2(\kappa_0-1)}-\frac{1}{\kappa_0}\ , \quad (21)$$

$$\frac{-\kappa_0'}{\kappa_0}=\beta=\frac{\kappa_0-1}{H\kappa_0}\,,\qquad \kappa_0''=0\,. \tag{22}$$

ii) When $\sqrt{\mu/\rho}$ is a linear function of z, we put

$$\sqrt{\mu/\rho}=\sqrt{\mu_0/\rho_0}(1+\gamma z)\,,$$

or

$$\kappa=\kappa_0(1+\gamma z)^{-2}\,. \tag{23}$$

From $\kappa(H)=1$, γ is expressed by H as

$$\gamma=(\sqrt{\kappa_0}-1)H^{-1}\,. \tag{24}$$

If we put

$$\sqrt{\kappa}=\cosh\theta\,, \tag{25}$$

the calculation of $\bar{\varphi}$ is easily carried out:

$$\bar{\varphi}=H(\theta_0\cosh\theta_0-\sinh\theta_0)(\cosh\theta_0-1)^{-1}\,. \tag{26}$$

We add expressions for $d\bar{\varphi}/d\kappa_0$, κ_0' and κ_0''.

$$\frac{d\bar{\varphi}}{d\kappa_0}=\frac{H}{2}\frac{\theta_0}{\cosh\theta_0(\cosh\theta_0-1)}\,, \tag{27}$$

$$-\frac{\kappa_0'}{\kappa_0}=\frac{2}{H}(\sqrt{\kappa_0}-1)\,,\qquad \frac{\kappa_0''}{\kappa_0}=\frac{6}{H^2}(\kappa_0-1)^2\,. \tag{28}$$

iii) When μ/ρ is a linear function of z, we put

$$\mu/\rho=(\mu_0/\rho_0)(1+\delta z)\,,$$

or

$$\kappa=\kappa_0(1+\delta z)^{-1}\,. \tag{29}$$

From $\kappa(H)=1$, δ is expressed by H as

$$\delta=(\kappa_0-1)H^{-1}\,. \tag{30}$$

If we put

$$\frac{2}{\kappa}-1=\cos\omega\,, \tag{31}$$

the calculation of $\bar{\varphi}$ is easily performed:

$$\bar{\varphi}=H(\omega_0-\sin\omega_0)(1-\cos\omega_0)^{-1} \tag{32}$$

We add the expressions for $d\bar{\varphi}/d\kappa_0$, κ_0' and κ_0''.

$$\frac{d\bar{\varphi}}{d\kappa_0}=\frac{H}{2}\frac{\sin\omega_0(1+\cos\omega_0)}{1-\cos\omega_0}, \tag{33}$$

$$\frac{-\kappa_0'}{\kappa_0}=\frac{\kappa_0-1}{H}, \qquad \frac{\kappa_0''}{\kappa_0}=2\left(\frac{\kappa_0-1}{H}\right)^2. \tag{34}$$

5. Group velocity

We have only to differentiate the period equation with f in order to obtain the equation for the group velocity U.

From the relation

$$\kappa_0 \propto p^2/f^2$$

we obtain

$$\frac{1}{\kappa}\frac{d\kappa}{df}=\frac{1}{\kappa'}\frac{d\kappa'}{df}=\frac{1}{\kappa''}\frac{d\kappa''}{df}=\frac{2}{f}\left(\frac{U}{v_Q}-1\right).$$

Then the differentiation can be carried out easily, and only the results are listed.

i) When $\kappa_0>1$, we have from (13)

$$\frac{U}{v_Q}=1-\left\{-\sqrt{\kappa_0-1}\,\frac{dH}{d\varphi_0}\varphi_0-\sqrt{\kappa_0-1}\,H(\varphi_0)+\frac{\mu_1}{\mu_0}\sqrt{\kappa_1-1}\,(\tan\xi+\xi\sec^2\xi)\right\}$$
$$\div\left\{-2f\kappa_0\sqrt{\kappa_0-1}\,\frac{d\bar{\varphi}}{d\kappa_0}\frac{dH}{d\varphi_0}-\frac{\kappa_0}{\sqrt{\kappa_0-1}}H(\varphi_0)\right.$$
$$\left.+\frac{\mu_1}{\mu_0}\frac{\kappa_1}{\sqrt{\kappa_1-1}}(\tan\xi+\xi\sec^2\xi)-\frac{(-\kappa_0')}{2f(\kappa_0-1)^2}\right\}. \tag{35}$$

When $\bar{\varphi}$ has explicit expression, $d\bar{\varphi}/d\kappa_0$ can be computed easily. However, in case $\bar{\varphi}$ is obtained by numerical integration, it would be better to give up the use of (35) and return to the usual method of numerical (or graphical) differentiation of v_Q.

ii) When $\kappa_0=1$, we have from (15)

$$\frac{v_Q}{U}=1-\left\{0.72904\frac{2h}{3}\frac{\mu_0}{\mu_1}\left(\frac{f}{-\kappa_0'}\right)^{-1/3}-\frac{1}{f}(\tan\xi+\xi\sec^2\xi)\right\}$$

$$\div\left\{1.10554\cdot 2h\frac{\mu_0}{\mu_1}\left(\frac{f}{-\kappa_0'}\right)^{1/3}+\frac{1}{f(\kappa_1-1)}(\tan\xi+\xi\sec^2\xi)\right\}. \quad (36)$$

iii) When $\kappa_0<1$, we have from (17)

$$\frac{U}{v_Q}=1-\left\{\xi(\tan\xi+\xi\sec^2\xi)+\frac{5}{32}\frac{\kappa_0'}{f(1-\kappa_0)^{5/2}}+\frac{\kappa_0''}{8f}\frac{1}{(1-\kappa_0)^{3/2}}-\mu_0\sqrt{1-\kappa_0}\right\}$$
$$\div\left\{\frac{\kappa_1}{\kappa_1-1}\xi(\tan\xi+\xi\sec^2\xi)+\frac{\mu_0\kappa_0}{\sqrt{1-\kappa_0}}+\frac{\kappa_0'}{2(1-\kappa_0)^2}\right.$$
$$\left.+\frac{5\kappa_0'^2}{32f^2}\frac{(4+\kappa_0)}{(1-\kappa_0)^{7/2}}+\frac{\kappa_0''}{8f}\frac{(2+\kappa_0)}{(1-\kappa_0)^{5/2}}\right\}. \quad (37)$$

6. Numerical results

As an example of calculation, it will be desirable to take up the case when the distribution of shear velocity is given only numerically. And a knowledge of the accurate results, if we could have them, would be useful for checking our calculation.

N. Kobayashi and H. Takeuchi[4] treated the dispersion of mantle Love waves. Their computation was based on the method of variation which is considered to have fairly good accuracy, therefore their results would be able to be taken as our criterion.

Table 2

case	T	v_Q	v_Q*	U	U*
	65.5	4.35	4.36	3.95	4.01
1	174.0	4.76	4.80		
2	181.2	4.76	4.82	4.29	4.24
3	176.7	4.76	4.81	(4.33)	4.23
4	175.5	4.76	4.81	4.26	4.23
1	346.6	5.32	5.41		
2	330.6	5.32	5.36	4.37	4.36
3	312.8	5.32	5.30	(4.46)	4.34
4	306.6	5.32	5.28	4.29	4.33

v_Q* (or U*) means phase (or group) velocity read from the results of Kobayashi and Takeuchi.

case 1. $\bar{\varphi}$ is calculated numerically.

case 2. $\bar{\varphi}=\frac{2}{3}H\sqrt{\kappa_0-1}$

case 3. $\bar{\varphi}=H(\theta_0\cosh\theta_0-\sinh\theta_0)/(\cosh\theta_0-1)$, $\quad\cosh\theta_0=\sqrt{\kappa_0}$

case 4. $\bar{\varphi}=H(\omega_0-\sin\omega_0)/(1-\cos\omega_0)$, $\quad\cos\omega_0=\frac{2}{\kappa_0}-1$

4) N. KOBAYASHI and T. TAKEUCHI, *Zisin* (*Journ. Seism. Soc. Japan*), **13** (1960) 232.

We performed the calculation using the same data as theirs for the case of the Jeffreys-Bullen's model, with the homogeneous upper layer of $h=35$ km, $v_1=3.5$ km/sec and $\rho=2.7$ gm/cm^3. The results are shown in Table 2.

We choose the values of v_Q equal to those of shear velocity at depths as 35 km (interface), 300 km and 500 km. Besides the values of $\bar{\varphi}$ obtained by numerical integration (case 1), we tentatively made use of the explicit expressions given in section 4, using the value of H gained from the given data (case 2, 3 and 4).

Group velocity was calculated from (35) or (36). However, the use of (36) can not always be appropriate for the present treatment, where the structure is not precisely the same as assumed in (i), (ii) or (iii) of section 4.

We see from Table 2 that, for $v_Q=5.32$ km/sec, the error of case 1 is greatest and reaches nearly 2%. As we understand, cases 2, 3 and 4 are only approximation of case 1, so that the above result seems to be somewhat queer.

Presumably, it might be that we have reached the limit of our theory, which clearly does not hold for extremely long waves.

7. Analysis of the dispersion curve

Assuming that ρ_1, μ_1, ρ_0, μ_0, ρ_0' μ_0' and h are already known, we can determine the function $v_s(z)$ from the dispersion curve. The process is essentially the same as the one discussed in [I].

For an assigned value of v_Q, f is determined from the dispersion curve. And, after calculating the right side of (13), we obtain φ_0 from the table of $H(\varphi)$. After all, we get $\bar{\varphi}=\varphi_0/f$ as a function of v_Q:

$$\bar{\varphi}\equiv\int_0^H\left\{\left(\frac{v_Q}{v_s(z)}\right)^2-1\right\}^{1/2}dz=I(v_Q)\,,$$

which is the same integral equation as I(26). Its solution was given by I(30)–(32).

For relatively short wave-lengths, assuming that we can use the conventional calculation of $\bar{\varphi}$ as in the case 2 to 4 of the former section, the approximate value of H is immediately determined.

For example, using the formula of case 2, we have

$$H=\frac{3}{2}(\kappa_0-1)^{-1/2}\bar{\varphi}\ .$$

As $v_Q(H)=v_q$, the function $v_s(z)$ is fully determined.

The present research is carried out as a continuation or completion of the previous work.[5] We hope it might include practically useful results.

We acknowledge kind assistance of Mr. Rinzo Yamaguchi in the numerical calculations.

Appendix

We shall give the expression of our dispersion equation making use of the Airy function.

The Airy function may be defined as

$$A_i(-\zeta)=\frac{1}{\sqrt{3}\,\pi}\zeta^{1/2}K_{1/3}\left(\frac{2}{3}\zeta^{3/2}\right)\ . \tag{A1}$$

For real arguement we have the expression

$$A_i(x)=\frac{1}{\pi}\int_0^\infty \cos\left(tx-\frac{1}{3}t^3\right)dt\ . \tag{A2}$$

From (A1) we easily obtain

$$\begin{aligned}H(\varphi)&=\frac{d}{d\varphi}\log\{\varphi^{1/2}K_{1/3}(-i\varphi)\}\\&=\frac{1}{6\varphi}+\left(\frac{2}{3\varphi}\right)^{1/3}\frac{A_i'\left\{\left(\frac{3}{2}\varphi\right)^{2/3}\right\}}{A_i\left\{\left(\frac{3}{2}\varphi\right)^{2/3}\right\}}\ .\end{aligned} \tag{A3}$$

Putting (A3) in (6), we get

$$\frac{V'(0)}{V(0)}=-\frac{\mu_0'}{\mu_0}-\frac{\kappa_0'}{4(\kappa_0-1)}-\frac{f\sqrt{\kappa_0-1}}{6\varphi_0}-f\sqrt{\kappa_0-1}\left(\frac{2}{3\varphi_0}\right)^{1/3}\frac{A_i'\left\{\left(\frac{3}{2}\varphi_0\right)^{2/3}\right\}}{A_i\left\{\left(\frac{3}{2}\varphi_0\right)^{2/3}\right\}}\ . \tag{A4}$$

5) An interesting paper of L. Knopoff appeared recently which treated the perturbation in the dispersion curves of Love waves due to an additional inhomogeneity of density or modulus:
L. KNOPOFF, *Geophys. J.*, **4** (1961) 161.

The left side of (A4) being replaced by the right side of (12), we have the dispersion equation.

Now we can write

$$\kappa=\kappa_0+z\kappa_0'+\frac{z^2}{2}\kappa_0''+\cdots\cdots,$$

and

$$1=\kappa_0+H\kappa_0'+\frac{H^2}{2}\kappa_0''+\cdots\cdots$$

By the iteration method, we solve the last equation for H

$$H=\frac{\kappa_0-1}{(-\kappa_0')}+\frac{(\kappa_0-1)\kappa_0''}{2(-\kappa_0')^3}+\cdots.$$

From these expressions, we obtain after some calculation

$$\bar{\varphi}=\int_0^H\sqrt{\kappa-1}\,dz=\frac{2}{3}\frac{(\kappa_0-1)^{3/2}}{(-\kappa_0')}\left\{1+\frac{2}{5}\frac{(\kappa_0-1)\kappa_0''}{(-\kappa_0')^2}+\cdots\right\}. \quad \text{(A5)}$$

Then we can deduce the following expression of (A4), valid when κ_0 is near 1:

$$\frac{V'(0)}{V(0)}=-\frac{\mu_0'}{2\mu_0}+\frac{\kappa_0''}{10(-\kappa_0')}-(-f^2\kappa_0')^{1/3}\left\{1-\frac{2}{15}\frac{\kappa_0''(\kappa_0-1)}{(-\kappa_0')^2}\right\}\frac{A_i'\left\{\left(\frac{3}{2}\varphi_0\right)^{2/3}\right\}}{A_i\left\{\left(\frac{3}{2}\varphi_0\right)^{2/3}\right\}}. \quad \text{(A6)}$$

In [II] we defined φ_0 for $\kappa_0<1$, as

$$\varphi_0=\frac{2i}{3}\frac{f(1-\kappa_0)^{3/2}}{(-\kappa_0')}\left\{1-\frac{2}{5}\frac{(1-\kappa_0)\kappa_0''}{(-\kappa_0')^2}\right\}. \quad \text{(A7)}$$

If the use of (A7) is understood, (A6) can be applied for $\kappa_0>1$, $\kappa_0<1$ and $\kappa_0=1$. We observe that (A6) is the refinement of (7).

---

27. 均質な表面層のある不均質な半平面における Love 波の分散

地震研究所　高　橋　健　人

不均質な部分の ρ と μ の変化がゆるやかで，μ/ρ が深さとともに増加する場合の一般的な取扱いを行ない，例として，Jeffreys-Bullen の模型に対して計算し，変分法による結果と比べた．

BULLETIN OF THE EARTHQUAKE
RESEARCH INSTITUTE
Vol. 39 (1961), pp. 823-830

28. *Dispersion Curves for the Higher Modes of Surface Waves in Heterogeneous Media.*

By Takehito TAKAHASHI*,

Earthquake Research Institute.

(Read Sept. 26, 1961.—Received Sept. 30, 1961.)

1. Higher modes of surface waves

In the previous papers[1] concerning the dispersion of surface waves in heterogeneous media, we treated only fundamental mode. Turning to higher modes, we readily see that the dispersion formula becomes rather simple, owing to the fact that the parameter φ_0 is now very large and we have only to use the first term in the asymptotic expansion of the solution for large argument.

For Love waves, we can use I (11):

$$\tan\left(\frac{\pi}{4}-\varphi_0\right)=\frac{1}{4f(\kappa_0-1)^{3/2}}\left\{(2-\kappa_0)\frac{\mu_0'}{\mu_0}-\kappa_0\frac{\rho_0'}{\rho_0}\right\}, \qquad (1)$$

instead of I (17).

In the dispersion equation for Rayleigh wave II (52), the left side is written merely as $\tan\left(\frac{\pi}{4}-\varphi_0\right)$:

$$\tan\left(\frac{\pi}{4}-\varphi_0\right)=\frac{\left(1-\frac{\kappa_0}{2}\right)^2}{\sqrt{(\kappa_0-1)(1-\eta_0)}}-\frac{\kappa_0'}{f\kappa_0}\Delta_\sigma(\kappa_0)-\frac{\rho_0'}{f\rho_0}\frac{\Delta_\rho(\kappa_0)}{\sqrt{1-\kappa_0}}. \qquad (2)$$

Using (1) and (2) we have drawn the dispersion curves for the second mode of both Love and Rayleigh waves, assuming that ρ be constant and μ be linear, and have confirmed the coincidence with the results achieved by Y. Satô.[2]

---

* Professor in Rikkyo University, Toshima-ku, Tokyo.

1) T. TAKAHASHI, *Bull. Earthq. Res. Inst.*, **33** (1955) 287; **35** (1957) 297. Cited as I and II respectively in this paper.

2) Y. SATÔ, *Bull. Seism. Soc. Amer.*, **49** (1959) 57.

In the following we shall treat the case where a low velocity layer exists. Wave number f is assumed to be very large, so that the first approximation is obtained by putting $1/f=0$. For (1) we have

$$\varphi_0 \doteqdot \left(n+\frac{1}{4}\right)\pi . \qquad (n=1, 2, \ldots) \tag{3}$$

2. Higher modes of Love waves in media having a low velocity zone

We use the following notations:

v_Q phase velocity

$v_s(z)$ shear velocity

$\kappa(z)=(v_Q/v_s(z))^2$, $\kappa(H)=1$.

When $\kappa>1$ $(v_Q>v_s(z))$, we define $\varphi_{\alpha\beta}$ by

$$\varphi_{\alpha\beta}=f\int_\alpha^\beta \sqrt{\kappa-1}\,dz . \tag{4}$$

Similarly for $\kappa<1$ $(v_Q<v_s(z))$, we define $\psi_{\alpha\beta}$ by

$$\psi_{\alpha\beta}=f\int_\alpha^\beta \sqrt{1-\kappa}\,dz . \tag{5}$$

Then the asymptotic expression of the amplitude $V(z)$ of the Love wave is

$$\mu^{-1/2}(1-\kappa)^{-1/4}e^{\pm\psi_{\alpha z}} \qquad (\kappa<1), \tag{6}$$

or

$$\mu^{-1/2}(\kappa-1)^{-1/4}\begin{matrix}\cos\\ \sin\end{matrix}\left(\frac{\pi}{4}-\varphi_{\alpha z}\right) \qquad (\kappa>1). \tag{7}$$

In case $(\kappa-1)$ changes sign at $z=\alpha$, there exist the so-called connection formulas of H. Jeffreys[3] which are expressed as

$$2(\kappa-1)^{-1/4}\cos\left(\frac{\pi}{4}-|\varphi_{z\alpha}|\right) \longleftrightarrow (1-\kappa)^{-1/4}e^{-|\psi_{\alpha z}|} , \tag{8}$$

$$(\kappa-1)^{-1/4}\sin\left(\frac{\pi}{4}-|\varphi_{z\alpha}|\right) \longleftrightarrow (1-\kappa)^{-1/4}e^{|\psi_{\alpha z}|} . \tag{9}$$

$V(z)$ must converge to zero at infinity. Then, near the surface,

3) H. JEFFREYS, *Proc. Cam. Phil. Soc.*, **52** (1956) 61.

$V(z)$ takes the form

$$\mu^{-1/2}(\kappa-1)^{-1/4}\cos\left(\frac{\pi}{4}-\varphi_{za}\right), \tag{10}$$

when $(\kappa-1)$ has only one zero point. (1) is the immediate result of applying the boundary condition

$$\frac{d}{dz}V(0)=0 \tag{11}$$

to (10).

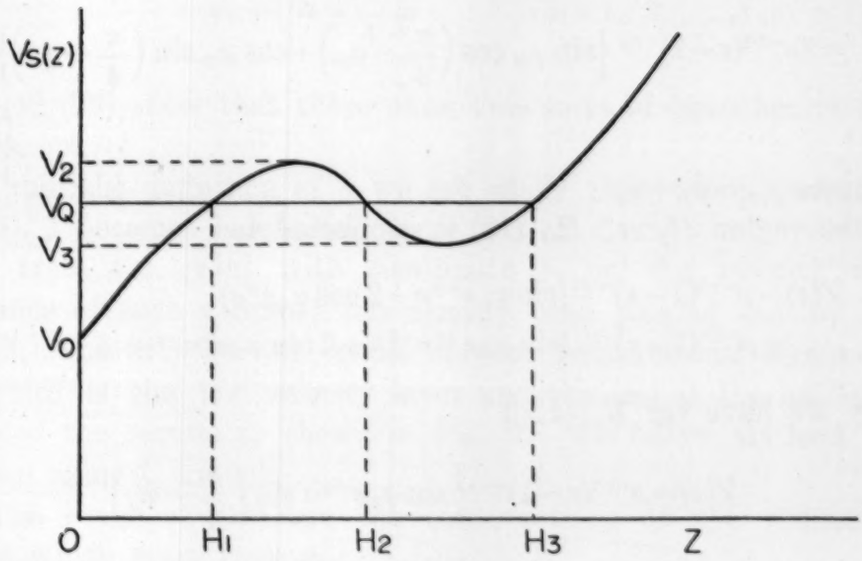

Fig. 1

Now we assume that there exists a low velocity internal layer as shown in Fig. 1. For $v_3<v_Q<v_2$, $(\kappa-1)$ has three zero-points H_1, H_2 and H_3, v_2 or v_3 being the maximum or minimum value of $v_s(z)$.

We observe

$$\begin{aligned}
&\kappa-1>0 \quad \text{for} \quad H_1>z\geqq 0\,,\\
&\kappa-1<0 \quad \text{for} \quad H_2>z>H_1\,,\\
&\kappa-1>0 \quad \text{for} \quad H_3>z>H_2\,,\\
&\kappa-1<0 \quad \text{for} \quad z>H_3\,.
\end{aligned}$$

We further assume that in the above four regions, the asymptotic expression as (6) or (7) holds, which may be allowed for fairly large f and for v_Q not too near to v_2 or v_3.

Following the treatment of H. Jeffreys,[4] we proceed as follows: When $z>H_3$, we have

$$V(z)\sim\mu^{-1/2}(1-\kappa)^{-1/4}e^{-\psi_{3z}}\,, \tag{12}$$

where ψ_{3z} means ψ_{H_3z}.

By the connection formula, we have for $H_3>z>H_2$

$$\begin{aligned}V(z)&\sim 2\mu^{-1/2}(\kappa-1)^{-1/4}\cos\left(\frac{\pi}{4}-\varphi_{z3}\right)\\&=2\mu^{-1/2}(\kappa-1)^{-1/4}\cos\left(\frac{\pi}{4}+\varphi_{2z}-\varphi_{23}\right)\\&=2\mu^{-1/2}(\kappa-1)^{-1/4}\left\{\sin\varphi_{23}\cos\left(\frac{\pi}{4}-\varphi_{2z}\right)+\cos\varphi_{23}\sin\left(\frac{\pi}{4}-\varphi_{2z}\right)\right\}\,,\end{aligned} \tag{13}$$

where $\varphi_{23}\equiv\varphi_{H_2H_3}=\varphi_{2z}+\varphi_{z3}$.

In the region $H_2>z>H_1$, (12) is connected to

$$\begin{aligned}V(z)&\sim\mu^{-1/2}(1-\kappa)^{-1/4}\{\sin\varphi_{23}e^{-\psi_{z2}}+2\cos\varphi_{23}e^{\psi_{z2}}\}\\&=\mu^{-1/2}(1-\kappa)^{-1/4}\{\sin\varphi_{23}e^{-\psi_{12}+\psi_{1z}}+2\cos\varphi_{23}e^{\psi_{12}-\psi_{1z}}\}\,.\end{aligned} \tag{14}$$

Similarly we have for $H_1>z>0$

$$\begin{aligned}V(z)\sim\mu^{-1/2}(\kappa-1)^{-1/4}&\left\{\sin\varphi_{23}e^{-\psi_{12}}\sin\left(\frac{\pi}{4}-\varphi_{1z}\right)\right.\\&\left.+4\cos\varphi_{23}e^{\psi_{12}}\cos\left(\frac{\pi}{4}-\varphi_{1z}\right)\right\}\,.\end{aligned} \tag{15}$$

3. Appearance of C branch

Putting (15) in the boundary condition (11), we obtain the dispersion equation

$$\frac{-\frac{1}{4}\tan\varphi_{23}e^{-2\psi_{12}}+\tan\left(\frac{\pi}{4}-\varphi_{01}\right)}{\frac{1}{4}\tan\varphi_{23}\tan\left(\frac{\pi}{4}-\varphi_{01}\right)e^{-2\psi_{12}}+1}=\frac{-1}{2f\sqrt{\kappa_0-1}}\left(\frac{\mu_0'}{\mu_0}+\frac{\kappa_0'}{2(\kappa_0-1)}\right). \tag{16}$$

As $1/f$ is assumed to be very small, we have approximately

4) H. JEFFREYS, M.N.R.A.S. *Geophys. Suppl.*, **7** (1957) 332.

$$\tan\varphi_{23}\cot\left(\frac{\pi}{4}-\varphi_{01}\right)\fallingdotseq 4e^{2\psi_{12}}\ . \tag{17}$$

For large f, $e^{2\psi_{12}}$ becomes very large, then at least one of the factors of the left side, $\tan\varphi_{23}$ or $\cot\left(\frac{\pi}{4}-\varphi_{01}\right)$, must be very large. And we have as a rough estimation

$$\varphi_{23}\fallingdotseq\left(n+\frac{1}{2}\right)\pi \qquad (n=1,\ 2,\ \ldots)\ , \tag{18}$$

or

$$\varphi_{01}\fallingdotseq\left(m+\frac{1}{4}\right)\pi \qquad (m=1,\ 2,\ \ldots)\ . \tag{19}$$

(18) and (19) show that there exist two sorts of branches of dispersion curves.

From the definition of φ we see easily that when v_Q approaches v_3 in (18), f becomes indefinitely large, which means that these branches start from the point with coordinate v_3 on the velocity axis. The existence of such a branch has already been pointed out by R. Yamaguchi[5], who treated the model of four homogeneous layers, of which the third is the low velocity layer and the last is the half-space, and obtained the results as shown in Fig. 2. We follow his lead in adapting the name C branch.

The branches (19) are the continuations of the ordinary higher modes which start from v_0.

To see the nature of these branches, we write

$$\varphi_{01}=f\int_0^{H_1}\sqrt{\kappa-1}\,dz=fH_1\sqrt{\bar{\kappa}_0-1}\ , \tag{20}$$

$$\varphi_{23}=f\int_{H_2}^{H_3}\sqrt{\kappa-1}\,dz=fH_{23}\sqrt{\bar{\kappa}_3-1}\ , \tag{21}$$

where $\bar{\kappa}_0$ and $\bar{\kappa}_3$ are some mean values of κ in the corresponding region and $H_{23}=H_3-H_2$.

If we adopt the approximate values of φ_{01} and φ_{23} given by (18) and (19), we have

$$\sqrt{\bar{\kappa}_0-1}=\frac{\pi}{fH_1}\left(m+\frac{1}{4}\right),\qquad \sqrt{\bar{\kappa}_3-1}=\frac{\pi}{fH_{23}}\left(n+\frac{1}{2}\right), \tag{22}$$

5) R. YAMAGUCHI, *Bull. Earthq. Res. Inst.*, **39** (1961), 653.

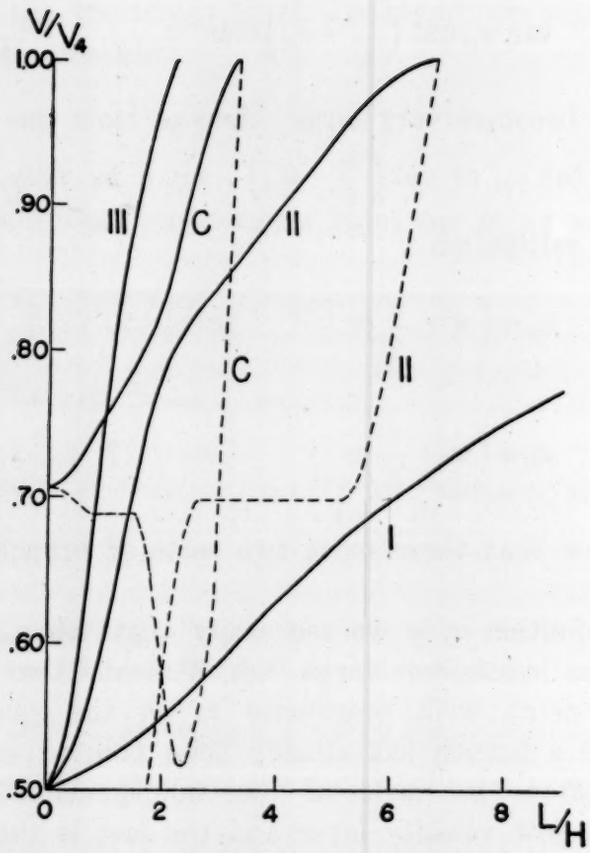

Fig. 2. Phase (solid line) and group (broken line) velocity dispersion curves of Love waves due to R. Yamaguchi. Rigidity, density and thickness of the respective layers are taken as $\mu_1 : \mu_2 : \mu_3 : \mu_4 = 1 : 3 : 2 : 4$, $\rho_1=\rho_2=\rho_3=\rho_4$, $H_1=H_2=H_3=H$.

or

$$v_Q=\bar{v}_0\sqrt{1+\frac{L^2}{4H_1^2}\left(m+\frac{1}{4}\right)^2}\ , \qquad v_Q=\bar{v}_3\sqrt{1+\frac{L^2}{4H_{23}^2}\left(n+\frac{1}{2}\right)^2}\ . \tag{23}$$

These are the equations of dispersion curves. Notice that $\bar{v}_0$, $\bar{v}_3$, H_1 and H_{23} are all functions of v_Q.

The condition that these branches should intersect is expressed as

$$\sqrt{\frac{\bar{\kappa}_0-1}{\bar{\kappa}_3-1}}=\frac{H_{23}}{H_1}\frac{m+\frac{1}{4}}{n+\frac{1}{2}}\ . \tag{24}$$

Putting $n=1$, $H_{23}=H_1$, (24) is written as

$$\frac{\left(\frac{4m+1}{6}\right)^2-1}{\left(\frac{4m+1}{6}\right)-(\bar{v}_3/\bar{v}_0)^2}=\bar{\kappa}_3>1\,. \tag{25}$$

As we assume $v_3/v_0>1$, it is easy to see that (25) is not satisfied when $m=1$. That is, the first C branch ($n=1$) does not intersect the ordinary second mode ($m=1$).

For $m\geqq 2$, the numerator of (25) being positive, the denominator must be positive and smaller than the numerator. Then we have

$$\bar{v}_3/\bar{v}_0<\frac{4m+1}{6}\qquad (m=2,\ 3,\ \ldots)\,. \tag{26}$$

This is the condition required for the first C branch to intersect the ordinary $(m+1)$-th mode.

For example, if

$$\frac{3}{2}>\bar{v}_3/\bar{v}_0>1\,,$$

we can expect that the first C branch intersects the ordinary branches of $m\geqq 2$.

The above is a rough explanation of Yamaguchi's curves of Fig. 2.

When (18) holds, from (15) and (17) we obtain

$$\mu_0^{1/2}(\kappa_0-1)^{1/4}V(0)\fallingdotseq\sin\varphi_{23}e^{-\psi_{12}}\left\{\sin\left(\frac{\pi}{4}-\varphi_{01}\right)+\cos\left(\frac{\pi}{4}-\varphi_1\right)\cot\left(\frac{\pi}{4}-\varphi_1\right)\right\}$$

$$=\frac{\sin\varphi_{23}}{\sin\left(\frac{\pi}{4}-\varphi_{01}\right)}e^{-\psi_{12}}\,. \tag{27}$$

For the ordinary $(m+1)$-th mode, $\sin\left(\frac{\pi}{4}-\varphi_{01}\right)$ being nearly zero, we transform (27) into

$$\mu_0^{1/2}(\kappa_0-1)^{1/4}V(0)\fallingdotseq\frac{4\cos\varphi_{23}}{\cos\left(\frac{\pi}{4}-\varphi_{01}\right)}e^{\psi_{12}}\,. \tag{28}$$

These relations show that, even if the amplitudes in the lower layer are the same, at free surface the amplitude of the C branch

becomes very small compared with that of the ordinary higher modes.

4. The case of Rayleigh waves

If we want to treat Rayleigh waves under the same assumptions as those in the former section, we have only to replace $H(\varphi_0)$ of II(52) by the left side of (16):

$$\frac{-\frac{1}{4}\tan\varphi_{23}e^{-\psi_{12}}+\tan\left(\frac{\pi}{4}-\varphi_{01}\right)}{1+\frac{1}{4}\tan\varphi_{23}\tan\left(\frac{\pi}{4}-\varphi_{01}\right)e^{-2\psi_{12}}}$$

$$=\frac{\left(1-\frac{\kappa_0}{2}\right)^2}{\sqrt{(\kappa_0-1)(1-\gamma_0)}}-\frac{\kappa_0'}{f\kappa_0}\Delta_\sigma(\kappa_0)-\frac{\rho_0'}{f\rho_0}\frac{\Delta_\rho(\kappa_0)}{\sqrt{1-\kappa_0}}\,, \qquad (29)$$

which is the dispersion equation for $v_2>v_Q>v_3$.

In (29) we observe that, if $\tan\varphi_{23}$ is not great $\tan\varphi_{23}e^{-2\psi_{12}}$ becomes very small and we can write

$$\tan\left(\frac{\pi}{4}-\varphi_{01}\right)\fallingdotseq\frac{\left(1-\frac{\kappa_0}{2}\right)^2}{\sqrt{(\kappa_0-1)(1-\gamma_0)}}-\frac{\kappa_0'}{f\kappa_0}\Delta_\sigma(\kappa_0)-\frac{\rho_0'}{f\rho_0}\frac{\Delta_\rho(\kappa_0)}{\sqrt{1-\kappa_0}}\,, \qquad (30)$$

which is similar to (2).

Another alternative is that $\tan\varphi_{23}$ takes a large value and $\tan\varphi_{23}{}^{-2\psi_{12}}$ becomes comparable with the right side. In this case we have

$$\varphi_{23}\fallingdotseq\left(n+\frac{1}{2}\right)\pi\,. \qquad (31)$$

From (30) and (31) we can expect branches similar to those of Love waves to appear.

---

28. 不均質な媒質における表面波の Higher Modes の分散曲線

地震研究所　高　橋　健　人

特に低速層がある場合を極めて近似的に取り扱い，山口林造が見出した分散曲線の新しい分枝について説明した．

Bulletin of the Earthquake
Research Institute
Vol. 39 (1961), pp. 831-847

29. *Seismicity of Taiwan (Formosa).**

By Hsu Ming-Tung,

Taiwan Weather Bureau,
Taipei, Taiwan, China.

(Read Sept. 26, 1961.—Received Sept. 30, 1961.)

1. Historical sketch of seismological observation

Taiwan is located in the Circum-Pacific Seismic Zone, and has suffered great damage from a number of destructive earthquakes throughout her history. Seismological observation was first recorded in Taiwan at Anping. Many weather stations were established in 1896. Later, seismographs of the Gray-Milne type were set up at Taipei, Tainan and Penghu, and instrumental observations began. A complete network for making seismic observations was then formed. In 1928, Wiechert type seismometers were installed at Taipei.

The most destructive earthquake recorded by scientific instruments occurred in Taiwan on April 21st of 1935. After this earthquake, seismological observation was strengthened and the Hsinchu seismological station was then established. During the decade of 1928 to 1938, a Wiechert's seismometer and other seismographs were installed at other seismological stations on the islands. Seismological observation made remarkable progress during these years. Before World War II, a seismic network of 17 stations had been established throughout the Taiwan Islands. At the end of the war, many seismic stations were destroyed by airraids and seismological observation had almost ceased.

After the year 1945, six seismic stations were reestablished at Taipei, Ilan, Hwalien, Alishan, Tainan and Taitung. Seismometers have been continuously in operation since then.

On October 22nd of 1951, a severe earthquake occurred at Hwalien and Taitung. A toll of 856 wounded and 68 persons dead was reported in this earthquake. About 2,382 houses were damaged. Close to the Hwalien Earthquake another big earthquake occurred around Taitung on November 25th of the same year. Twenty persons were killed, 326 persons were hurt and more than 1,500 houses were damaged.

* Communicated by T. Hagiwara.

Table 1. List of the Seismological Stations, Taiwan, China

Station	φ; N	λ; E	φ'	Altitude	Subsoil	a	b	c	Seismographs	Year of Establishment
Alishan (阿里山)	23°31′	120°48′	23°22′	2,406.1m	Miocene Sandstone	−0.4700	+0.7885	+0.3966	$W(H, V)$, O, S_1	1933
Hengchun (恒春)	22 00	120 45	21 52	22.3	Alluvium	4745	7976	3724	$W(H, V)$, S_1	1907
Hsinkong (新港)	23 06	121 22	22 58	36.5	Alluvium	4793	7862	3901	$W(H, V)$, S_1	1941
Hsinchu (新竹)	24 48	120 58	24 39	32.8	Alluvium	4677	7793	4171	P_1, S_2	1938
Hwalien (花蓮)	23 58	121 37	23 49	17.6	Diluvium	4796	7791	4038	$W(H, V)$, P_1, S_2, A_2	1914
Ilan (宜蘭)	24 46	121 45	24 37	7.4	Alluvium	4784	7731	4165	$W(H, V)$,P_1, S_1	1936
Kaohsiung (高雄)	22 37	120 16	22 29	33.1	Limestone	4657	7981	3824	P_1, S_1	1931
Lanyu (蘭嶼)	22 02	121 33	21 54	332.2	Basalt	4881	7950	3730	P_2	1961
Penghu (澎湖)	23 32	119 33	23 23	9.4	Basalt	4527	7985	3969	P_1	1900
Taipei (台北)	25 02	121 31	24 53	8.0	Alluvium	4742	7733	4208	$W(H, V)$, O, P_3, S_1, A_1	1896
Tawu (大武)	22 21	120 54	22 13	7.6	Alluvium	4754	7944	3781	$W(H, V)$, S_1	1942
Taitung (台東)	22 45	121 09	22 37	8.9	Alluvium	4775	7900	3846	$W(H, V)$, S_2	1906
Tainan (台南)	23 00	120 13	22 52	12.7	Alluvium	4637	7962	3886	$W(H, V)$, P_1, S_1, A_1	1898
Taichung (台中)	24 09	120 41	24 00	77.1	Alluvium	4662	7856	4067	$W(H, V)$, P_1, S_2	1902
Yushan (玉山)	23 29	120 57	23 21	3,850.0	Miocene Sandstone	4722	7873	3964	P_1	1944

Notation

λ: Longitude
φ: Geographical Latitude
φ': Geocentric Latitude
$W(H)$: Wiechert's horizontal seismograph
$W(V)$: Wiechert's vertical seismograph
O: Omori's horizontal seismograph
P_1: Portable horizontal seismograph
P_2: Three component portable seismograph
P_3: Higuti's portable horizontal seismograph
S_1: C.M.O type three component strong motion seismograph
S_2: Higuti's three component strong motion seismograph
A_1: Ishimoto's three component acceleration seismograph
A_2: Higuti's three component strong motion asseleration seismograph

$a=\cos\varphi'\cos\lambda$, $b=\cos\varphi'\sin\lambda$, $c=\sin\varphi'$

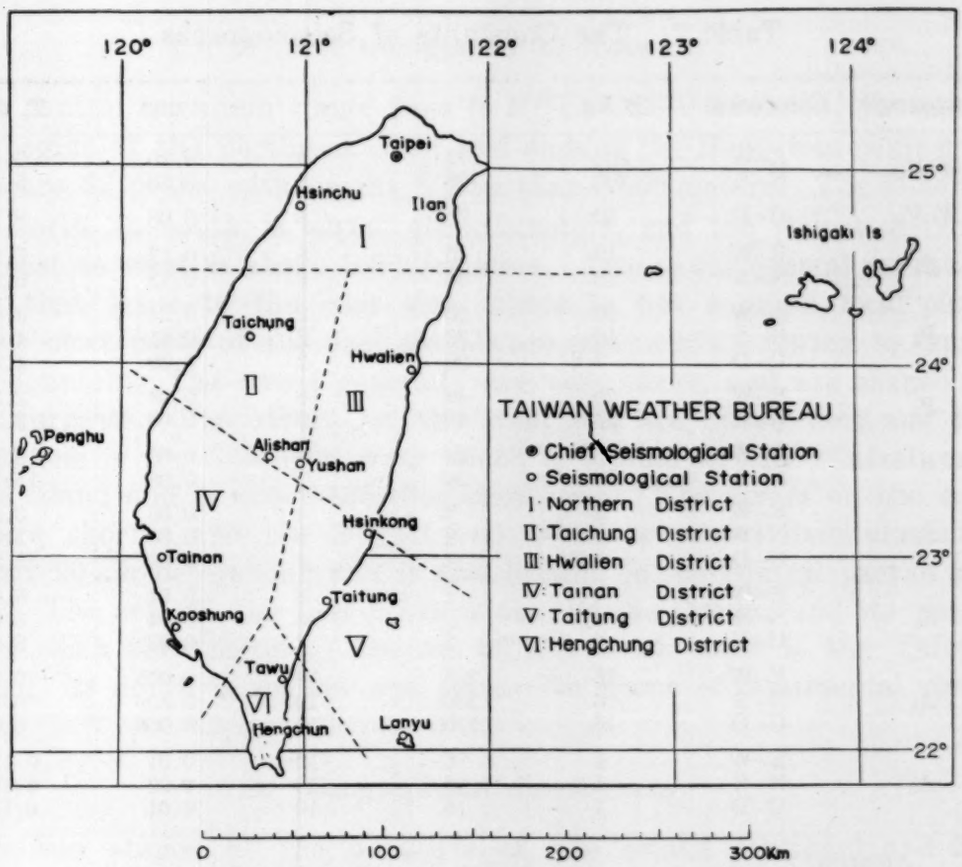

Fig. 1. The network of seismological station in Taiwan.

For the purpose of solving earthquake engineering problems, some new types of strong motion seismographs and acceleration seismographs were introduced. From 1955 to 1957, new type seismographs such as Higuti's three component strong motion seismograph, Higuti's portable horizontal seismograph, Ishimoto's three component acceleration seismograph were installed at important stations.

Since 1954, the quarterly Seismological Bulletin of the Taiwan Weather Bureau has been published. More than 150 observatories have their names on its mailing list.

The Taiwan Weather Bureau is now maintaning a network of 15 seismological stations in a satisfactory manner. The geographic coordinates of these stations and the seismographs in use are indicated in Table 1, and a map also showing the distribution of location is given in Fig. 1. The coefficients of seismographs are listed in Table 2.

The scale of seismic intensity of 0–VI in Table 3 is customarily adopted for use in Taiwan.

Table 2. The Constants of Seismographs

Seismograph	Component	M kg	V	v	r mm	T_0 sec
$W(H)$	E-W	200	77	9	0.10	5.1
	N-S	200	78	9	0.13	5.1
$W(V)$	U-D	80	75	8	0.08	5.1
P_1	E-W	18	40	8	0.13	5.1
	N-S	18	40	8	0.13	5.1
P_2	E-W	10	20	2	0.24	4.0
	N-S	10	20	2	0.41	4.0
	U-D	7.5	20	2	0.29	4.0
P_3	E-W	20	49	10	0.08	2.2
	N-S	20	49	10	0.08	2.3
0	E-W	15	20	3	0.05	15.7
	N-S	15	20	3	0.08	15.1
S_1	E-W	2	2	4	0.06	3.8
	N-S	2	2	4	0.06	3.8
	U-D	1.5	2	8	0.06	3.5
S_2	E-W	4	1	8	0.04	6.0
	N-S	4	1	8	0.04	6.0
	U-D	2	1	8	0.03	5.0
A_1	E-W	16	220	10	0.005	0.10
	N-S	16	220	10	0.009	0.10
	U-D	16	170	10	0.006	0.08
A_2	E-W	1	16	10	0.01	0.11
	N-S	1	16	10	0.02	0.10
	U-D	1	16	10	0.01	0.11

Notation

M: Mass
V: Magnification
v: Damping ratio
r: Friction
T_0: Proper period

Table 3. Scales of Seismic Intensity

0; No Feeling: Shocks too weak to cause human feelings, registered only by seismographs. (Acceleration smaller than 0.8 gal)

I; Slight: Extremely feeble shocks only felt by persons at rest or by those who are observant of earthquakes. (0.8–2.5 gal)

II; Weak: Shocks felt by most persons, slight shaking of doors. (2.5–8.0 gal)

III; Rather Strong: Slight shaking of houses and buildings, rattling of doors, swinging of hanging objects such as electric lamps, moving of liquids in vessels. (8.0–25.0 gal)

IV; Strong shaking of houses and buildings, overturning of unstable objects, spilling of liquids out of vessels. (25.0–80.0 gal)

V; Very Strong: Cracks in the walls, overturning of gravestones, stone lanterns etc., damaging of chimneys and stone walls. (80.0–250 gal)

VI; Disastrous: Demolition of houses, landslides, faults, fissures on the ground. (larger than 250 gal)

2. The topography of Taiwan

A central mountain range runs in NNE to SSW direction, the north edge begins at the northeast coast and ends at the Hengchun peninsula. There are 62 peaks with height higher than 3,000 meters. The distance from north to south is about 400 kilometers, and the widest distance from east to west is about 160 kilometers. Due to the central mountain range that leans to the east side, there is but a small local plane because most parts of the east seaside are steep cliffs. Owing to many high mountains, the rivers generally are very short, and are shaped by rapid currents. The rivers on the west side are rather long and the longest one is the Choshichi river which is located at the central part of the island and is about 165 kilometers long. The rivers on the east side are shorter and the longest one, which is named Hsiukuluanchi, is about 90 kilometers long and is also located in the central part of the island. The sea off the east coast is the Pacific Ocean, and its depth is more than 2,000 meters. The sea off the west coast is the Taiwan Channel, its depth is shallow and forms the shape of continental shelf.

3. Geographical distribution

Taiwan stands at the outskirts of the asiatic continent and lies right on the Circum-Pacific Seismic Zone where earthquakes are frequently felt. Taiwan experienced earthquakes about 1,265 times in an average year as calculated from 1930 to 1960. Among them 1,037 times were unfelt earthquake and 238 times were felt earthquake. The number changed considerebly from year to year as in Fig. 2. The maximum number occurred in 1922 amounting to 3,224 times, while the minimum in 1910 was only 264 times. The fomer was caused by an earthquake swarm which occurred near Suau, on northeastern coast of Taiwan.

The geographical distribution of the number which could be felt by persons is shown in Fig. 3 which was made on the basis of data from 1933 to 1958.

For the sake of convenience we divided Taiwan into six districts as in Fig. 1, and the annual monthly mean numbers of felt and unfelt earthquake are shown in Table 4 and Table 5 respectively. The number of earthquakes counted in the tables occurred within 300 kms from the coast of Taiwan. As the number of unfelt earthquakes increases with the magnification of the seismagraphs, so the number of unfelt earth-

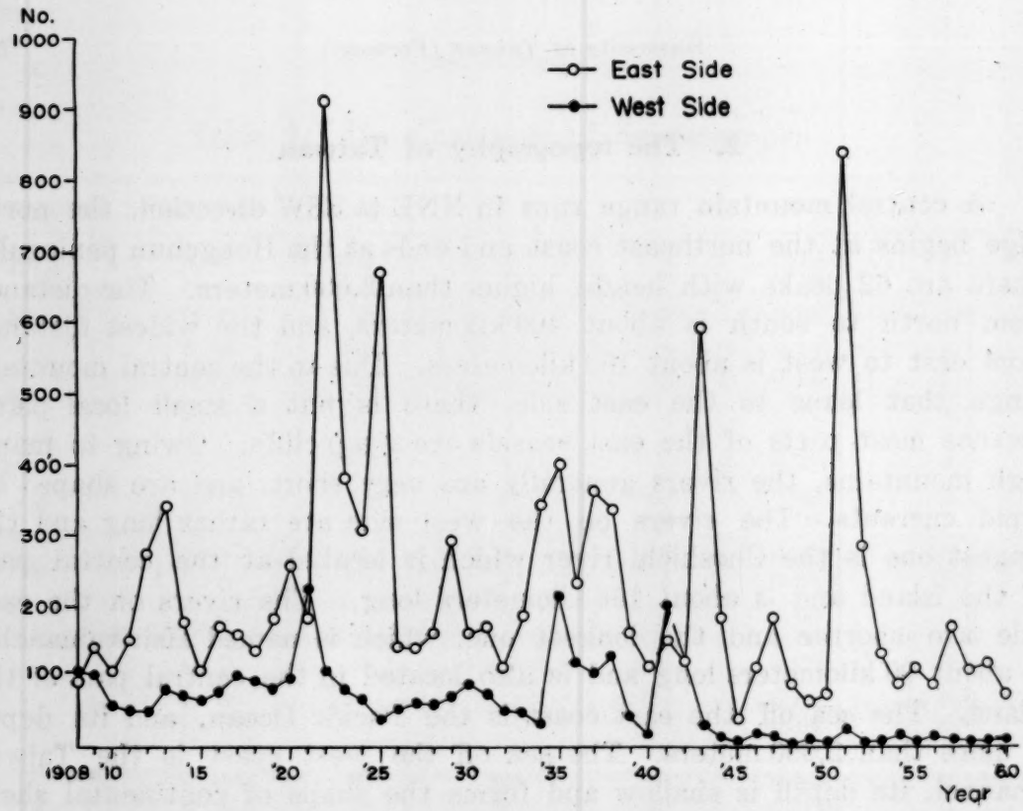

Fig. 2. The secular change of the number of earthquakes in Taiwan in the years from 1909 to 1960.

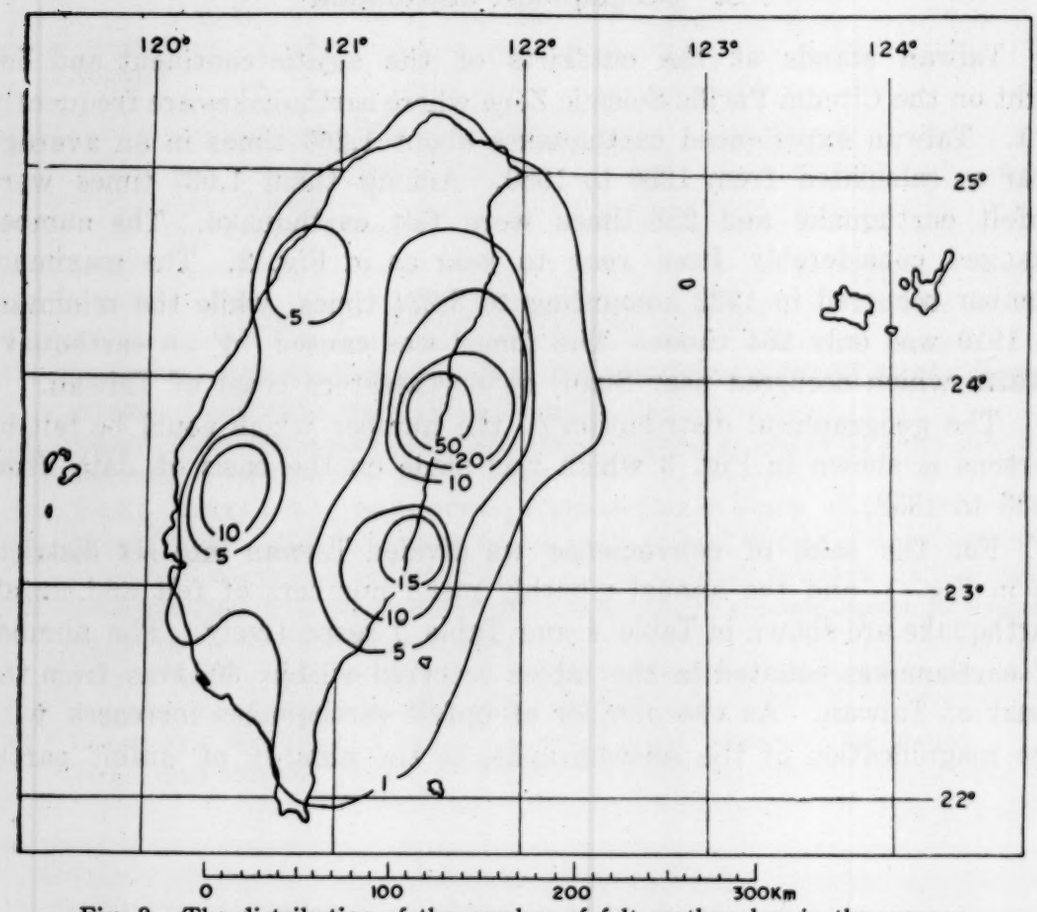

Fig. 3. The distribution of the number of felt earthquakes in the average year from 1933 to 1958.

Table 4. Number of Annual Monthly Mean Felt Earthquakes from 1913 to 1958.

District	Jan.	Feb.	Mar.	Apr.	May	Jun.	Jul.	Aug.	Sept.	Oct.	Nov.	Dec.	Year	Monthly Mean	Ratio of District per Total Area. %
Northern	4.0	3.3	3.4	4.0	3.4	2.9	3.7	4.7	12.6	5.7	5.3	4.0	57.3	4.8	19.8
Taichung	2.1	1.5	1.2	1.4	1.0	1.2	3.5	1.5	1.4	1.4	1.9	0.8	18.7	1.5	6.2
Hwalien	10.5	8.8	12.2	8.0	8.5	17.4	6.0	7.0	8.8	17.7	15.4	7.7	128.1	10.7	44.0
Tainan	4.5	2.5	2.5	2.8	2.1	2.6	1.6	2.5	3.0	2.6	1.8	7.3	35.8	3.0	12.3
Taitung	4.6	2.5	3.1	3.3	2.8	4.2	2.7	3.5	4.1	3.4	4.1	7.3	45.7	3.8	15.6
Hengchun	0.5	0.4	0.6	1.3	0.6	0.3	0.8	0.6	0.3	0.2	0.3	0.3	5.9	0.5	2.1
Total Taiwan	26.2	19.0	23.0	20.8	18.4	28.6	18.0	19.8	30.2	31.0	28.8	27.4	291.5	24.3	100.0

Table 5. Number of Annual Monthly Mean Unfelt Earthquakes from 1930 to 1958.

District	Jan.	Feb.	Mar.	Apr.	May	Jun.	Jul.	Aug.	Sept.	Oct.	Nov.	Dec.	Year	Monthly Mean	Ratio of District per Total Area. %
Northern	13.1	11.7	10.3	13.6	15.2	13.3	15.2	20.5	31.3	22.2	13.6	13.3	193.3	16.1	18.6
Taichung	4.0	3.7	3.7	4.8	3.5	3.8	3.8	3.5	6.7	5.1	3.8	3.8	50.2	4.2	4.9
Hwalien	23.5	40.5	31.2	24.3	23.4	22.9	18.4	21.3	36.7	71.7	48.8	29.2	391.9	32.7	37.8
Tainan	20.4	8.2	8.1	10.1	4.4	3.3	3.4	4.9	6.2	4.1	5.8	18.0	96.9	8.1	9.4
Taitung	15.5	16.1	15.1	14.6	17.3	14.8	14.7	15.8	20.0	18.0	22.1	44.8	228.8	19.1	22.0
Hengchun	3.9	6.5	6.5	8.7	7.0	4.4	5.0	9.8	8.7	5.2	5.1	5.2	76.0	6.3	7.3
Total Taiwan	80.4	86.7	74.9	76.1	70.8	62.5	60.5	75.8	109.6	126.3	99.2	114.3	1037.1	86.5	100.0

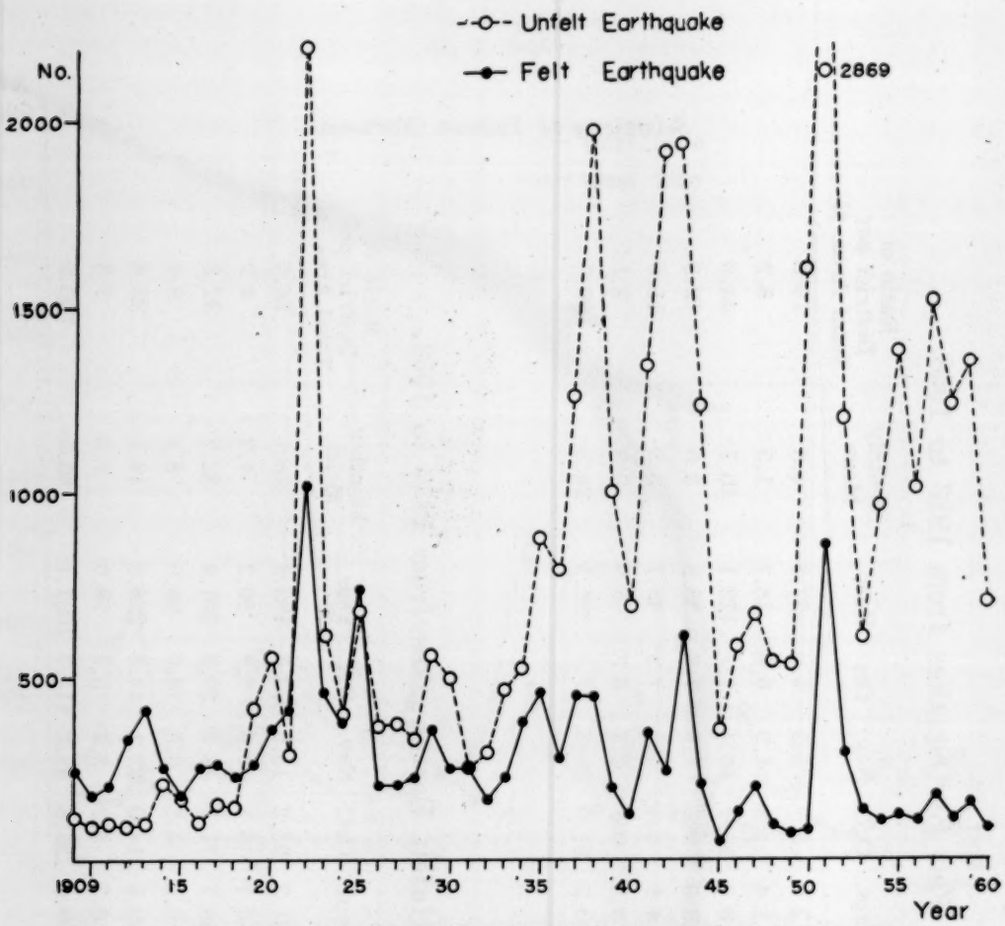

Fig. 4. The secular change of the number of felt earthquakes in Eastside Seismic Zone and the Westside Seismic Zone from 1908 to 1960.

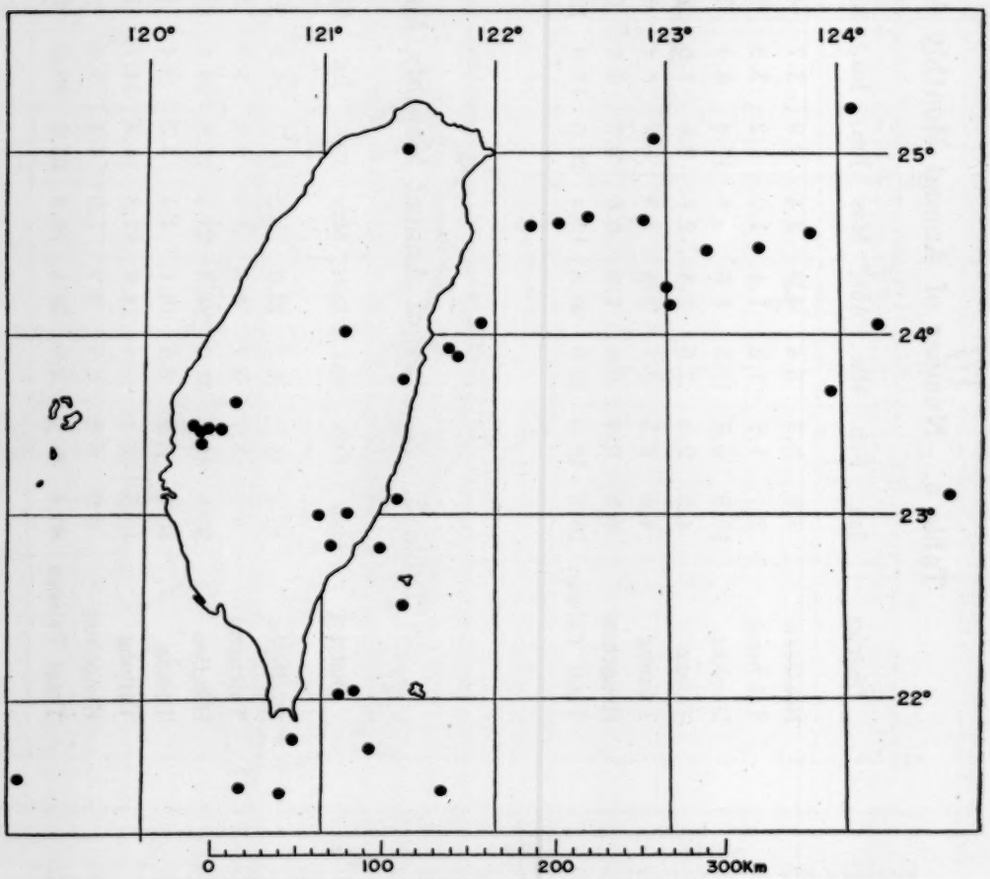

Fig. 5. The distribution of the epicentres of remarkable earthquake which occurred during the years from 1900 to 1960.

quakes were counted from the year 1930 when the Wiechert's seismographs were installed at main seismological stations. These figures and tables indicate that the most frequently affected region is that along the east coast of Taiwan, and the quietest is the southwestern part of Taiwan. The largest number of felt earthquakes was observed at the Hwalien District which ammount to 128 times per year as the mean value from 1913 to 1958. This value is equal to 44% of the total felt earthquakes in Taiwan.

As mentioned above, the region most frequently affected lies along the east coast of Taiwan suggesting that there is a seismic zone in this area. We called it the Eastside Seismic Zone. On the other hand, in the west plane near Hsinchu and Chai area earthquakes also frequently occurred. We called it the Westside Seismic Zone.

In the case of earthquake occurring in the Eastside Zone. in case

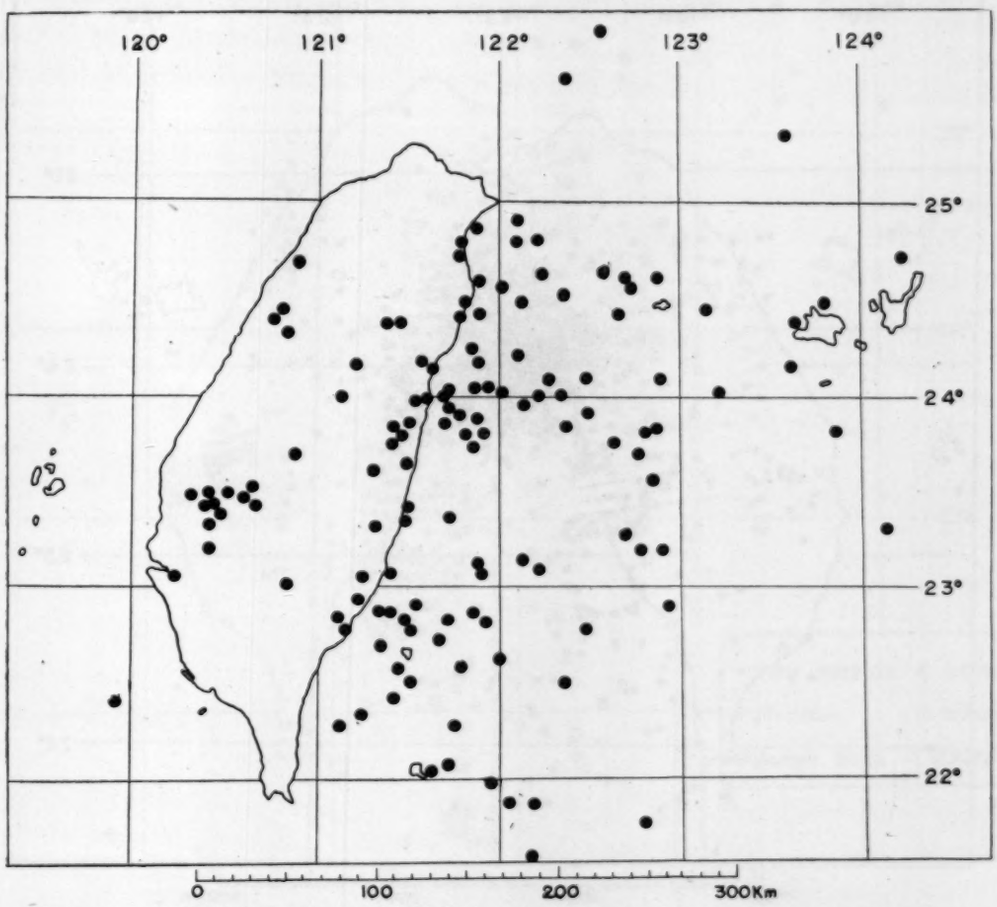

Fig. 6. The distribution of the epicentres of moderate earthquake which occurred during the years from 1900 to 1960.

the epicentre is located on land its magnitude is small and the depth of the hypocentre is about 10 to 30 km but they occur frequently and continuously. In case the epicentre located at sea, its magnitude is larger and the depth of the hypocentre is deeper, namely 40 to 100 km, so that little damage and crustal deformation occurs on land.

In the Westside Zone many destructive earthquakes have occurred throughout history. Owing to the depth of the hypocentres being very shallow, that is 0 to 10 km, great damage and accompaning remarkable crustal deformation such as fault, fissure and landslide occurs.

The number of felt earthquakes which have occurred in the East and West sides Seismic Zones are shown in Fig. 4. The seismic activety was vigourous in the years 1913, 1922, 1925, 1929, 1935, 1937, 1943, and 1951 in the eastside and 1908, 1913, 1917, 1921, 1930, 1935, 1938

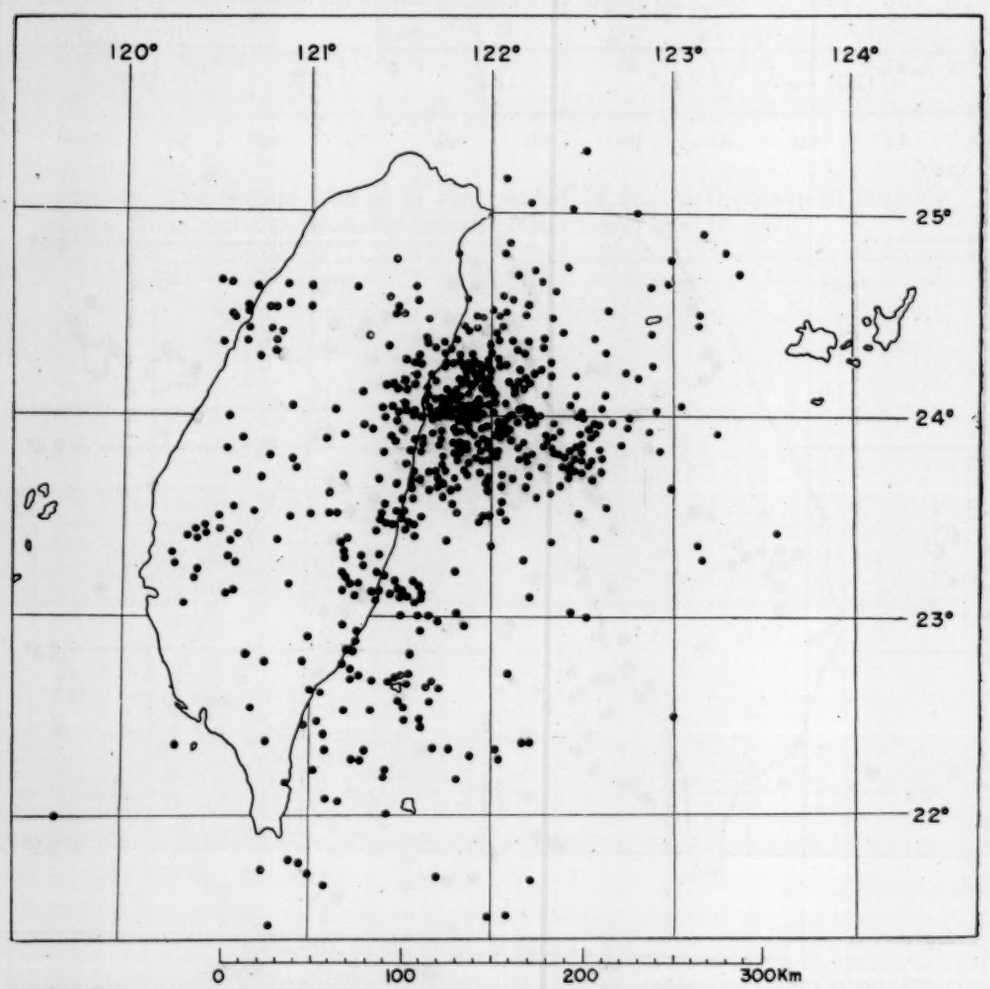

Fig. 7. The distribution of the epicentres of earthquakes of limited felt area which occurred during the years from 1931 to 1960.

and 1941, in the westside. It is very difficult to find periodicity in both sides.

The magnitude of an earthquake is classified according to the radius of the felt area under the assumption of a circle as follows:

i) Remarkable earthquake; The radius of the felt area is greater than 300 km. (M is larger than 6.4)

ii) Moderate earthquake: The radius is smaller than 300 km but greater than 200 km. (M=6.4–5.7)

iii) Earthquake of limited felt area: The radius is smaller than 200 km but greater than 100 km. (M=5.7–4.8)

iv) Local earthquake: The radius is smaller than 100 km. (M is smaller than 4.8)

According to the "Guide of Seismometry" (Zishin Kansokuho) published

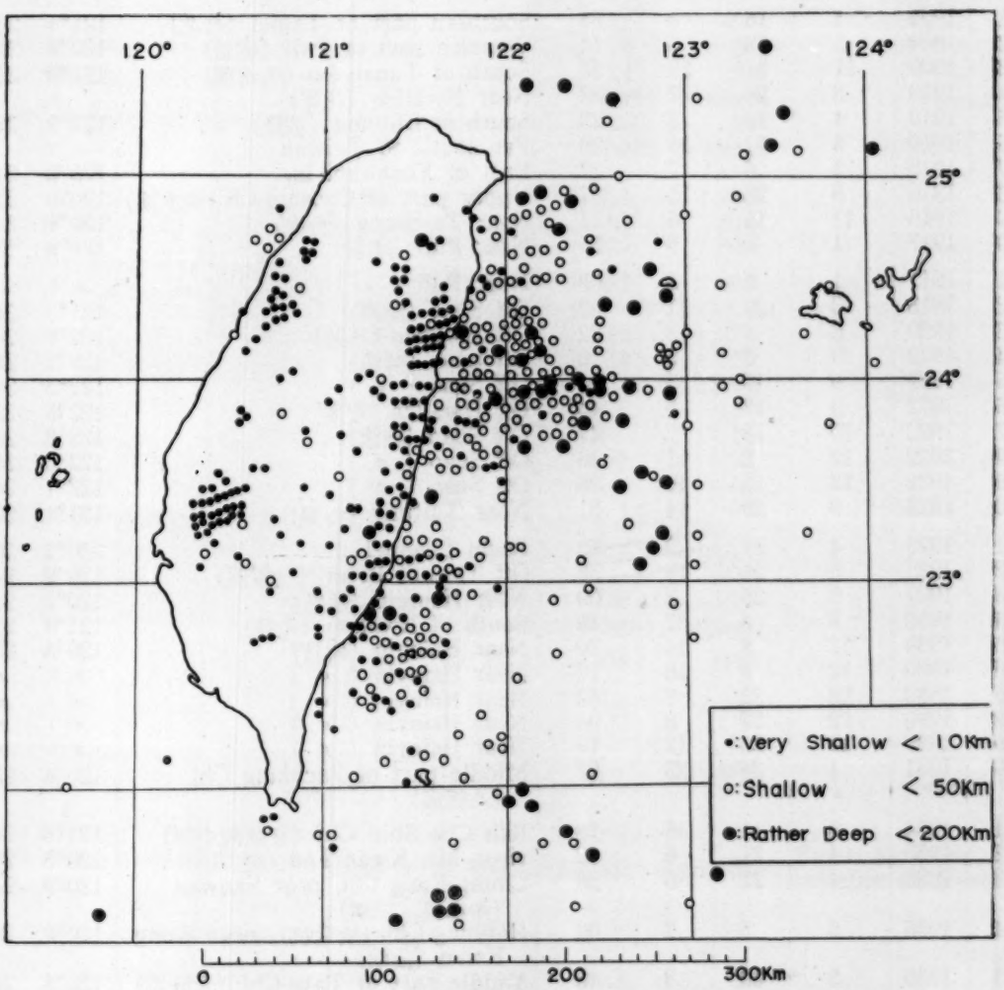

Fig. 8. The distribution of earthquakes of magnitude larger than local earthquakes, classified by the depth of the hypocentre (1909–1958).

Table 6. List of Disastrous

No.	Origin Time					Location of epicentre		
	Year	Month	Day	Hour	Minute	Place	Lat. (N)	Long. (E)
1	1901	6	7	8	05	Near Ilan (宜蘭)		
2	1904	4	24	14	39	Upper part of Pachang-Chi (八埃溪)	120°5	23°5
3	1904	11	6	4	25	Lower part of Peikang-Chi (北港溪)	120°3	23°5
4	1906	3	17	6	42	Near Minhsung (民雄)	120°5	23°6
5	1906	3	26	11	29	Near Touliu (斗六)	120°5	23°7
6	1906	4	5	0	52	Near Tian-tze Kou (店仔口)	120°4	23°4
7	1906	4	8	6	40	Near Tian-tze Kou (〃)	〃	〃
8	1906	4	14	3	18	Near Tian-tze Kou (〃)	〃	〃
9	1906	4	14	7	52	Near Tian.ize Kou (〃)	〃	〃
10	1908	1	11	11	35	Near Patzai (拔子)	121°4	23°7
11	1909	4	15	3	54	Southern part of Taipei (台北)	121°5	25°0
12	1909	5	23	6	44	Western part of Puli (埔里)	120°9	24°0
13	1909	11	21	15	36	South of Tanan-Ao (大南澳)	121°8	24°4
14	1910	3	26	2	38	Near Hwalien (花蓮)		
15	1910	4	12	8	23	South of Chilung (基隆)	122°9	25°1
16	1910	6	17	13	28	Far south off Taiwan		
17	1915	1	6	7	27	East of Yonakuni Is.	123°2	24°4
18	1916	8	28	15	27	Upper part of Choshui-Chi (濁水溪)	120°9	23°7
19	1916	11	15	6	31	Near Taichung (台中)	120°7	24°1
20	1917	1	5	0	55	Near Puli (埔里)	120°9	23°9
21	1917	1	7	2	08	Near Puli (〃)	〃	〃
22	1918	3	27	11	52	Off Suao (蘇澳)	121°9	24°6
23	1920	6	5	12	22	Off Hwalien (花蓮)	122°0	24°0
24	1922	9	2	3	16	Off Suao (蘇澳)	122°2	24°6
25	1922	9	15	3	32	Off Suao (〃)	122°3	24°6
26	1922	9	17	6	44	Off Hwalien (花蓮)	122°5	23°9
27	1922	10	15	7	47	Off Suao (蘇澳)	122°3	24°6
28	1922	12	2	11	46	Off Suao (〃)	122°0	24°6
29	1922	12	13	19	26	Off Suao (〃)	122°1	24°6
30	1923	9	29	14	51	Near Taitung (台東)	121°1	22°8
31	1925	4	17	3	53	Bashi Channel	120°2	20°4
32	1925	6	24	13	38	Off Takkili River (立霧溪)	120°8	24°1
33	1927	8	25	2	09	Near Hsinyin (新営)	120°3	23°3
34	1930	8	8	7	49	South of Hwalien (花蓮)	121°3	23°2
35	1930	12	8	14	20	Near Hsinyin (新営)	120°4	23°3
36	1930	12	8	16	10	Near Hsinyin (〃)	〃	〃
37	1930	12	22	7	52	Near Hsinyin (〃)	〃	〃
38	1930	12	22	8	08	Near Hsinyin (〃)	〃	〃
39	1930	12	22	12	19	Near Hsinyin (〃)	〃	〃
40	1931	1	24	23	02	Middle part of Pachiang Chi (八埃溪)	120°4	23°4
41	1934	8	11	16	18	Ilan Cho Shui Chi (宜蘭濁水溪)	121°8	24°8
42	1935	4	21	6	02	Near Mt. Kwan-Tao (関刀山)	120°8	24°3
43	1935	4	21	6	26	Chung-Kang-Chi, near Sanwan (中港溪, 三湾)	120°9	24°7
44	1935	5	5	7	02	Houlung-Chi (後竜溪), near Kung Kwan (公館)	120°8	24°5
45	1935	5	30	3	43	Middle part of Tatu-Chi (大肚溪)	120°8	24°1

Earthquakes in Taiwan (1900–1960).

Magnitude	Depth of Hypocentre	Damage				
		No. of lives lost	No. of wounded	No. of houses totally destroyed	No. of houses damaged	Crustal deformation
m				1	57	
m		3	10	66	840	
m		145	158	661	3,197	Fissure, sand-crater
r		1,258	2,385	6,769	14,218	Fault, fissure and sand crater
l		1	5	29	529	
m		1	6	63	283	Landslide
m						
r		15	84	1,794	10,037	Fissure, sand-crater landslide
r						
m		2		3	5	Fissure, landslide
r		9	51	122	1,050	
s			6	10	32	
m			4	14	39	
s				Slight	damages	
r				13	59	
r				Slight	damages	
r				〃	〃	
m		16	159	614	4,885	
s		1	20	97	972	
s		54	85	130	625	
s			21	187	498	
m			3		6	
r		5	20	273	1,275	
r		5	7	14	161	
r			5	24	389	
m			1	6	197	
m		6	2		14	
m		1	2	1	33	
s			1		13	
s			1	1	80	
r				Slight	damages	
s			1		339	
r		11	63	439	984	
s				Slight	damages	
m		4	25	214	449	
r						
r			14	545	2,295	
r						
s						
s					698	
m	S		3	7	11	
m	5	3,276	12,053	17,907	36,781	Fault, landslide, collapse of ground
m	S					
s	S		38	28	571	
s	S			2	24	

(to be continued)

No.	Origin Time					Location of spicentre		
	Year	Month	Day	Hour	Minute	Piace	Lat. (N)	Long. (E)
46	1935	6	7	10	51	Near Wuchi (悟棲)	120°5	24°2
47	1935	7	17	0	19	Near Houlung-Chi (後竜溪)	120°7	24°6
48	1935	9	4	9	38	50 km E of Taitung (台東)	121°5	22°5
49	1936	8	22	14	51	45 km E of Hengchun (恒春)	121°1	22°0
50	1937	12	8	16	32	Near Hsing-Kong (新港)	121°4	23°1
51	1938	9	7	12	03	30 km SE of Hwalien (花蓮)	121°8	23°8
52	1938	11	2	14	40	S of Mt. Hohuan 20 km (合歓山)	121°2	24°1
53	1939	11	7	11	53	Near Cholan, Hsinchu (卓蘭, 新竹)	120°8	24°4
54	1942	12	17	3	19	SE of Chiayi (嘉義), near Chung Pu (中埔)	120°4	23°4
55	1943	10	23	0	01	15 km SW of Hwalien (花蓮)	121°5	23°8
56	1943	10	23	0	15	15 km SW of Hwalien (〃)	〃	〃
57	1943	11	3	0	51	30 km E of Hwalien (〃)	121°8	24°0
58	1943	11	24	5	51	5 km ENE of Hwalien (花蓮)	119°3	21°6
59	1943	12	2	13	09	20 km S of Lutao (緑島, former 火焼島)	121°5	22°5
60	1944	2	6	1	20	25 km SW of Hwalien (花蓮)	121°4	23°8
61	1946	12	5	6	47	Near Hsin-Hwa (新化)	120°1	23°1
62	1951	10	22	5	34	15 km ESE of Hwalien (花蓮)	121°7	23°8
63	1951	10	22	11	29	30 km E of Hwalien (花蓮)	121°8	24°1
64	1951	11	25	2	47	35 km NW of Taitung (台東)	120°9	23°0
65	1955	4	4	12	11	30 km SSE of Hengchung (恒春)	120°9	21°8
66	1959	4	27	4	41	145 km ENE of Hwalien (花蓮)	123°0	24°1
67	1959	8	15	16	57	67 km ESE of Hengchun (恒春)	121°2	21°5
68	1959	8	17	16	25	35 km E of Tawu (大武)	121°2	22°3
69	1959	8	18	8	34	98 km E of Hengchun (恒春)	121°7	22°1
70	1959	9	25	10	37	50 km E of Hengchun (〃)	121°2	22°1

Notation:
r : remarkable earthquake
m : moderate earthquake
s : earthquake of limited felt area
l : local earthquake
S : shallow earthquake
Note: 120° E.M.T. is used

by the Japan Meteorological Agency, there is a relation between the radius of a felt earthquake (r) and the Richter and Gutenberg magnitend (M) in the form, $r=2.3(M-1.3)^3-1.7$

The distribution of the epicentre of remarkable earthquakes is shown in Fig. 5. The number amounts to 41 times during the year from 1900 to 1960. It indicates that remarkable earthquake frequently occurred along the east coast and the Chai district. The distribution of the epicentre of moderate earthquakes is shown in Fig. 6. The number amounts to 136 times. This also shows that the district of their frequent occurrence is along the east coast and Chai district. The distribution

(continued)

Magnitude	Depth of Hypocentre	Damage				
		No. of lives lost	No. of wounded	No. of houses totally destroyed	No. of houses damaged	Crustal deformation
s	S		2	5	190	
m	30	44	391	1,754	6,167	
m	S				114	
r			3	Slight	damages	
r				Slight	damages	Landslide
m				Slight	damages	
m				Slight	damages	
s	S			4	20	
m	10	358	733	4,520	11,086	Landslide
m	5	1	1	1	148	Road collapse
m						
s					87	
m					479	
r	40	3	11	139	284	Landslide
m	5			2	388	Fissure
s	0	74	482	1,954	2,084	Landslide
r	0	68	856		2,382	Landslide, fissure
r	20					Damage was confusedly included in (62)
r	5	20	326	1,016	582	Landslide, fissure
r	5	5	7	22	171	
r	30		1	9	4	
r	20	16	63	789	752	
m	40		3			
m	15			32	5	
r	10		3	3	65	

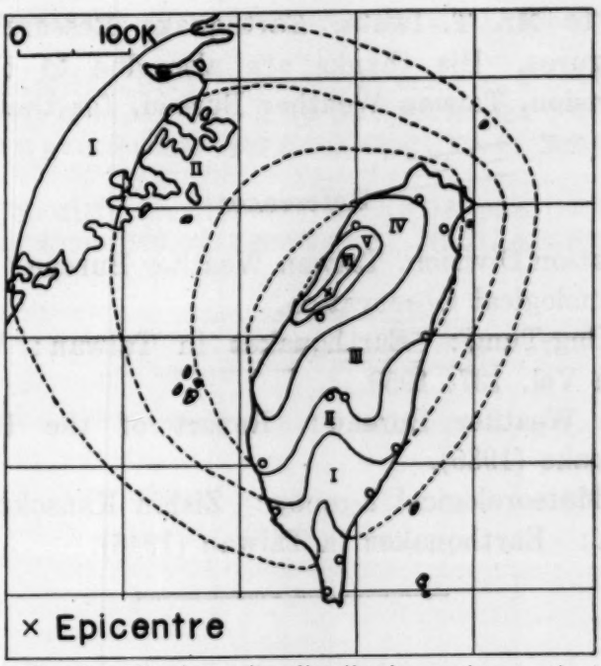

Fig. 9. The intensity distribution owing to the Hsinchu-Taichung Earthquake of 1935.

of earthquakes of limited felt area is shown in Fig. 7. The number amounts to 581 times during the years from 1931 to 1960. The area of their most frequent occurrence is off the coast of Hwalien.

The distribution of earthquakes of magnitude larger than local earthquakes, classified by the depth of the hypocentre is shown in Fig. 8. It shows that the depth of the hypocentres in the westside is shallower than those occurring in the eastside.

The earthquakes which caused damage in Taiwan since 1900 have amounted to 70 in number (see Table 6). The earthquake which caused the greatest number of casualties in Taiwan was the Hsinch-Taichung earthquake of 1935 in which 54,688 houses were destroyed and 15,329 persons where either killed or hurt. It's intensity scale is shown in Fig. 9. The next is the Chai earthquake of 1906 in which 20,987 houses were destroyed and 3,643 persons were killed or hurt. These two earthquakes were accompanied by very remarkable crustal deformation such as fault, fissure, landslide, sand-crator and collapse of the ground.

Acknowledgement

The author expresses his hearty thanks to Director Kenneth T. C. Cheng who gave him continuous encouragement. He is also much obliged to Dr. T. Hagiwara, Earthquake Research Institute, Tokyo University, for checking the manuscript and writing the Japanese summary, and to Mr. T. Iwata, Earthquake Research Institute, for drawing the figures. His thanks are also due to the staff of the Observation Division, Taiwan Weather Bureau, for their assistance.

References

1. Observation Division, Taiwan Weather Bureau: Annual Ledger of Seismological Observation.
2. Hsu Ming-Tung: Earthquakes in Taiwan: Weather Bureau Bulletin Vol. 137, 1959.
3. Taiwan Weather Bureau: Report of the Hsinchu-Taichung Earthquake (1936).
4. Japan Meteorological Agency: Zishin Kansokuho (1952).
5. Y. Oka: Earthquakes in Taiwan (1946).

29. 台湾の地震活動

中華民国 台湾省気象所 徐 明 同

第2次世界戦争前，台湾にはウィヘルト地震計を備えた17の地震観測があつたが，戦争のとき空襲によつてその多くを失い，地震観測はほとんど中断した．1945年には6カ所の地震観測所(台北，宜蘭，花蓮，阿里山，台南，台中）が復活した．

1951年10月22日花蓮，台中地方に地震が起こり，破壊家屋 2,382，死者 68，負傷者 856 を生じた．同年11月25日これに近い地域に再び地震が起こり，破壊家屋 1,500，死者 20，負傷者 326，を生じた．これに刺激されて，地震工学上の目的から重要な観測所に加速度地震計や強震計が付加えられるようになつた．

1954年以後，台湾省気象所から地震報告が発行され，現在では同省は15の地震観測所の維持に当つている．これらの観測所の位置は第1表及び第1図に示してある．第2表は地震計の常数を示す．

台湾は 1930～1960 年の間に，平均年間有感地震 238 回，無感地震 1,037 回を経験した．年間回数は年により大いに異り，最大は有感無感合せて，1922 年の 3,224 回，最小は 1910 年の 264 回である．第3図に 1933～1958 年の有感地震の震央分布を示す．

便宜上，台湾を6箇の地区に分け(第1図)，区域別の有感，無感地震の月別年平均を示した(第3，第4図)．地震は台湾の海岸から 300 km 以内に起こつたものを採つてある．1930年後無感地震回数が増加しているのは，ウィヘルト地震計が主要な観測所に置かれたためである．この表から分るように，地震回数の最も多いのは，台湾の東海岸に沿つた地域であり，少いのは台湾の西南地域である．1913年～1958年の期間に，花蓮(元の花蓮港)地方では平均年間 128 回の有感地震があつたが，これは全島有感地震回数の 44% に当る．

東海岸に沿う地震の多く起こる地帯を「東側地震帯」，これに対して新竹及び嘉義付近の平地の地震頻発地帯を「西側地震帯」と名付けた．東側地震帯では，震央が陸地の場合は，magnitude は小さく，深さは 10～30 km，時間に対し連続的に起こつている．この地震帯で，震央が海の場合は，magnitude が比較的大きいが，深さは 40～100 km より深く，災害や地形変動を起こすことは稀である．西側地震帯では有史以来多くの破壊地震が起こつている．震源の深さは 0～10 km で，大きな災害と断層，地割，山崩れなど地形変動を生じることが多い．

第4図に，両地震帯の有感回数の時間的変化を示すが，周期性を見出すことは困難である．

第5図に顕著地震の震央分布を示す．顕著地震の多くは，台湾の東海岸と嘉義地方に起こつている。

第6図に稍顕著地震の震央分布を示す．顕著地震と同じ地域に多く起こつている．

第7図に小区域の地震の震央分布を示す．この多くは花蓮の沖に起こつている．

第8図に，局発地震以上の大きい地震の深さ別の分布を示してある．震央の深さは，西側の方が東側より浅い．

1900年以後の破壊地震の数は70である(第6表)．最も大きい被害を生じたのは 1935 年の新竹台中地震である．これに次ぐものは 1906 年の嘉義地震である．両地震とも顕著な地形変動を伴つた．

地震研究所彙報
第39号(1961) 849-856頁

30. 昭和36年8月19日白山国定公園附近に発生した地震の調査概報

地震研究所　吉山良一

(昭和36年9月26日発表—昭和36年9月30日受理)

緒　言

走時曲線と発震機巧に関する調査は気象庁から当研究所え非公式に知らされた資料に基づくものである．其等の資料は気象庁において速報と名付け，精度には自ら疑問ありとされている様で，一つにはその故に非公式となつているものと思われる．目下同庁地震課において地震記象を再調査中とのことであるから，ここに述べる事柄も将来幾分かは修正を免れない．然し乍らまた考うるに，周知の如く地震記象は極めて複雑で，余りに微細な点に惹かれては却つてその基調ともいうべきものを見失うことも起り得る様に思はれる．速報の精度に疑問ありとする因子は多々あろうが，もし幸いにしてその主たるものが，限られた時間内に報告を迫られ，微細な初動の検出に拘つて居られないことだけにあつて，それから後の器械的な計算手続きに誤りがないならば，速報資料に基づく調査の結果もまたこの地震の一面を伝えることになる筈である．本調査において，福井，金沢，富山，岐阜，名古屋，松本，飯田等の発震時は震央，震源の決定に重要な影響を与えるので，少くとも上述の計算手続には誤りがないことをたしかめておく必要があつた．そのため，折角全般的な再調査を進めて居られる気象庁地震課にお願いして特に抽き出して検討して頂いた．高山測候所の資料は現地調査に立寄つた際頂いたもので気象庁と測候所の好意により本調査のためには最も重要な資料となつた．また名古屋，金沢両気象台においては初動の判定から，発震時，初期微動継続時間の算出に至る経過に就いて説明して頂いたのでその観測精度に関し正しく評価することが出来た，このことは走時曲線の解析に大きな便宜を与えた．銘記して何れ方にも謝意を表する次第である．

次に現地調査のためとつた道順は金沢市から白峰－市ノ瀬（三ッ谷）－白山－別山往復であつた．その被害の外観的報告は他の方々によるものと重複することが多いと思われるので大部分を省略し写真の説明に止めることにしたが，調査に当つて資料の提供，案内等に援助をして下さつた，金沢県庁，白峰村役場，北国新聞社，白山頂上室堂等現地の方々に深甚の謝意を表する．

震央ならびに震源の深さに就いて

第1図は震央の決定に重要な気象台，測候所及び目標となる村落，山岳の位置を示すものである．また高山測候所に関しては後に述べる様に強震計の記象に基づき地震動の水平成分合成の結果を，福井，金沢に就いてはP波初動の方向を記入してある．P波初動の方向によれば，震央は福井からは東微北(引き)，金沢からは南微東(押し)，名古屋からは北微

西(引き)にあると見られ，これに高山における初動方向を併せ考えると，第1図でいえば別山，市ノ瀬，三ッ谷，小池でかこまれる範囲，すなわち 36°06′～03′N, 136°46′～42′E の範囲に限定される．福井，高山，金沢における初期微動継続時間が 6～7 秒，名古屋におけるものが約 14 秒であることもこの推定を支持する．そこで 36°05′N, 136°44′E を震央とした時のP波走時曲線を第2図に示す．見掛けの速度は明らかに約 6.～6.5 km/sec となる．すなわち震央距離が 150 km の舞鶴，松代の辺り迄を考えると 6 km/sec となり震央距離 100 km の名古屋，松本，飯田辺りまでをとれば約 6.3 km/sec，それでも 6.5 km/sec 以上とは考えられない．震央は同図右下の附図からも推定される様に最悪 2 km 動くとは思われない．敦賀，彦根の発震時が著しく前者は遅く，後者は早すぎることに疑問が残るだけである．

さて本研究所特別事業の一つとして爆破地震動による地殻構造の解明が進められつつあるが，幸いにしてここに仮定した震央の東北東約 15 km にある御母衣(福島谷)を起点とする調査が繰返し行われ，その結果は爆破グループの方々によつて詳細に本彙報あるいは地震学会誌「地震」に発表されている．それに依ればこの辺りでいわゆる Moho- 不連続面の深さは約 30 km にあり，その上にはP波の速度 6 km/sec の層が厚く，地域的には 5.5 km/sec 層が数キロの厚さで存在し，Moho- 不連続面直下の速度は 7.5～7.7 km/sec となつている．また御母衣を起点として東方測線と西方測線とを比べた場合，ここに取扱つている震央距離の範囲内で且つ自然地震の観測精度で検出される程の違いは認められないこと等が明らかにされている．第2図で震央距離 150 km に近い舞鶴，亀山，輪島の発震時までが 6 km/sec の延長上にあることは後に述べる様にむしろ解釈に苦しむのであるが少くとも震央距離，50 km～100 km の間に約 6 km/sec～6.5 km/sec の線を仮定することは上記爆破グループの調査結果とも非常によく合致する．従つて震央もここに仮定した点でよいと思はれるのである．

震源の深さは先づ走時曲線の見掛けの速度から推定されるが，Moho- 不連続面より深くないことだけは直ちに想像される．不連続面の深さ約 30 km という前記爆破グループの調査結果に従えば 30 km より深くないことになるが，たとえそれにとらわれないとしても，また震央距離 50 km～100 km の間で見掛けの速度が 6.5 km/sec に近いとしても，6 km/sec 層が主なものである限り，40 km よりも深くはならない．震源が Moho- 不連続面から上方にどれほど離れているかは，7.5～7.7 km/sec の速度をもつと思はれる Pn 波の線が第2図でどこから始つているかによつて定まる．若しこの線が舞鶴，松代等に至つて漸く始まるとすればその隔りは，震源の深さを 40 km, 30 km, 20 km, 0 km と仮定するに従つてそれぞれ約 9 km, 12 km, 17 km, 25 km となる，すなわちそれぞれの仮定に対して Moho- 不連続面の深さは 49 km, 42 km, 37 km, 25 km と計算される．若し Pn の線が震央距離 100 km で始まるとすればこれ等の数字はそれぞれ約 3 km, 5 km, 8 km, 17 km と約 43 km, 35 km, 28 km, 17 km, となる．これ等の数字から考えると推定される震源の深さとしては，20 km, あるいは表面層の影響を考慮に入れると多分 25 km 位いが浅い方の限界とも，またもつともらしい値とも考えられる．

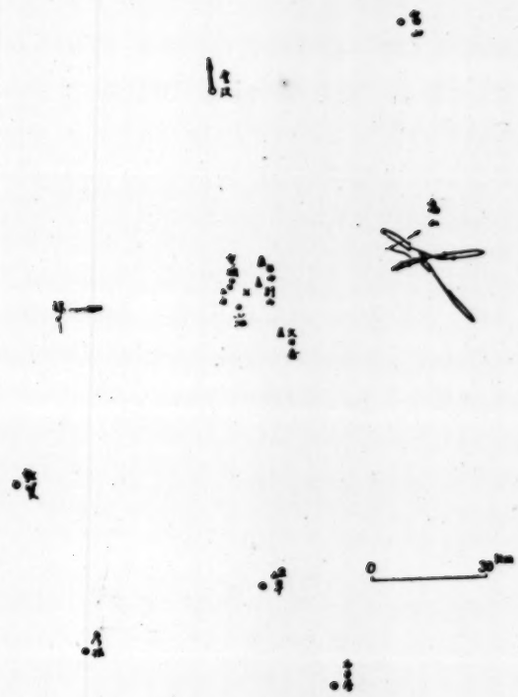

第 1 図　震央附近を囲む観測所

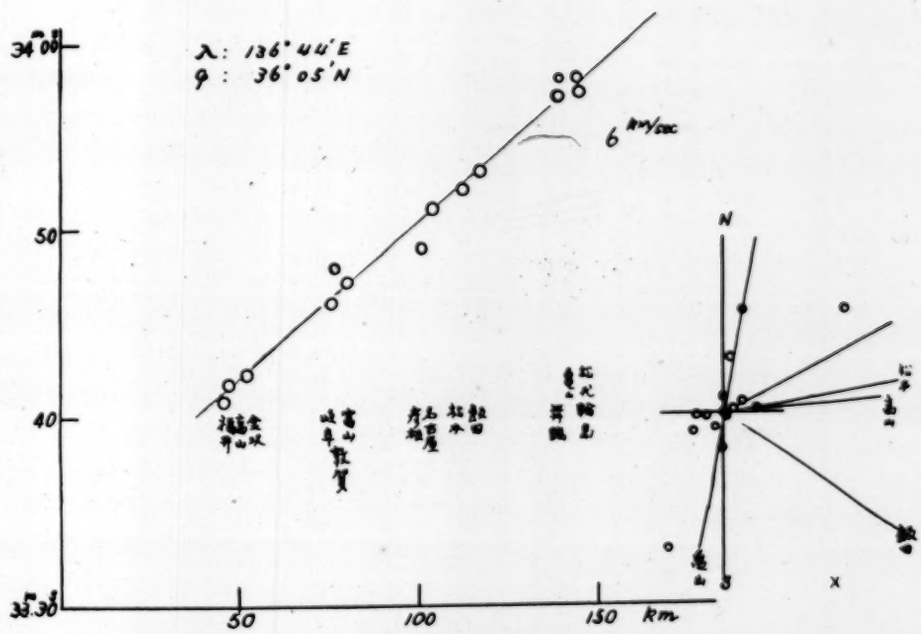

第 2 図　P 波走時曲線．右下の図は各観測点の平均値からのずれを吟味して震央の位置を検討するためのもので，走時曲線での距離標尺を 5 倍して現わしてある．

Pn 波の線が富山の震央距離 80 km の辺りから始まつているとしてもそれは名古屋の震央距離約 100 km のところで 6 km/sec の線から僅かに 0.7 秒外れるに過ぎない．この時間差を現在の観測精度で検出することは困難であろう．しかし後にP波初動の“押し引き”分布から推定される様に Pn 波の線が震央距離 100 km 前後から始つているならば震央距離 150 km のところではその差は 1.5 秒には達するから当然検出し得る筈である．すなわち舞鶴，松代，亀山等における発震時の確認が望ましいと思うのである．上に出したいろいろの数字，爆破グループの調査結果，また高山における初期微動継続時間や初動の入射角を考え併せると，走時曲線からきめられる震源の深さとしては 5 km 刻みに考えるだけの精度はないし 30 km±10 km，が考えられる．深い方の限界は上に記した震源の深さと Moho- 不連続面の深さとの関係を示す数字と爆破グループの方々による調査結果とを併せ考えると多分も少し縮まるものと思われる．

所謂発震機巧について

第 3 図はP波初動の“押し引き”分布であるがほとんどすべての観測所が引きで，ただ震央の南側では亀山，津，汐岬，その北側では金沢，輪島がP波の nodal line に近い記象型ではあるが明瞭な押しとなつていて，岐阜は引きと見られる．この様な初動分布を象限型の機巧で説明することは困難で，石本博士によつて提唱された円錐型のものでなければならない．S 波を精査するまで確認することは出来ないが，この判定が正しいならば昭和23年

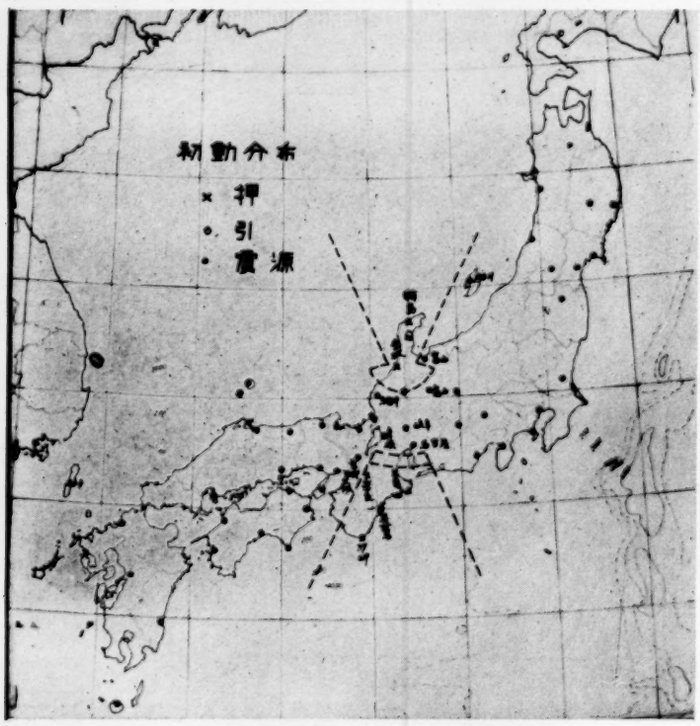

第 3 図

6 月の福井地震が象限型であつたのと異り，この地震の発震機巧がどちらかといえば非常に類例の少くない円錐型の機巧に属することは注意すべきことと思われる．なお Pn 波による“押し”の部分が巾のせまい部分だけに現はれたことから考えると多分了解されていると思うがここにいう震源は Moho- 不連続面内にあつて P 波の Node を与える円錐面が不連続面にほとんどすれすれに切り込んでいることを示す．定量的計算を行つて未知の量を一つ一つ押えて行くほど観測精度はよくないが，雑多な計算の結果沢山出て来た数字をいろいろ按配して考えた結果不連続面と震源の位置，円錐の向きを想像して見たものを第 4 図に示す．現在与えられた資料でこの想定図にもつとも都合の悪いことは，既に走時曲線のところで述べた様に震央距離 150 km に近い舞鶴，松代等の諸点までが 6 km/sec の延長上にあることであつてこの疑点はそれ等の発震時を再検討して見るまでは解決されない．また金沢が“押し”であるのに富山が“引き”であることに合せるには富山が転向円外にあるとせねば説明されない．富山の震央距離は 78 km である．ところが震央の南側において若し岐阜，彦根，名古屋までが速報に従つて“引き”，奈良，亀山が“押し”であるとすれば名古屋あるいは彦根に当る震央距離 100 km の辺りに転向円の境があることになる．従つて Moho- 不連続面は南の方で深い様に思はれる．若し“押し引き”の分布から，更に，走時曲線のところでふれた様に亀山，舞鶴等の発震時からこの方面で転向円の半径が 100 km を越すことにでもなるならば，それをもつとも簡単に説明するには単なる南下りの傾斜よりもはなはだ不自然とは思うが断層的喰違いを併せ想像する方が容易らしく見える．略 5 km の落差で説明がつく筈である．今後の検討を必要とし，その際は輪島，富山，岐阜，名古屋，奈良，彦根，亀山，尾鷲，津，汐岬等の一層詳しい観測資料が特に決定的な役目をすることになるであろう．第 4 図に断層の如く書いてあるのはこれ等の問題点を現わしたに過ぎないので，この様な地殻構造を考えるよりも，むしろ現在は初動の検出精度に疑問をおく方が自然であろう．

第 5 図は高山測候所強震計の記象複写，第 6 図はこれを読み取つて拡大し，東西，上下

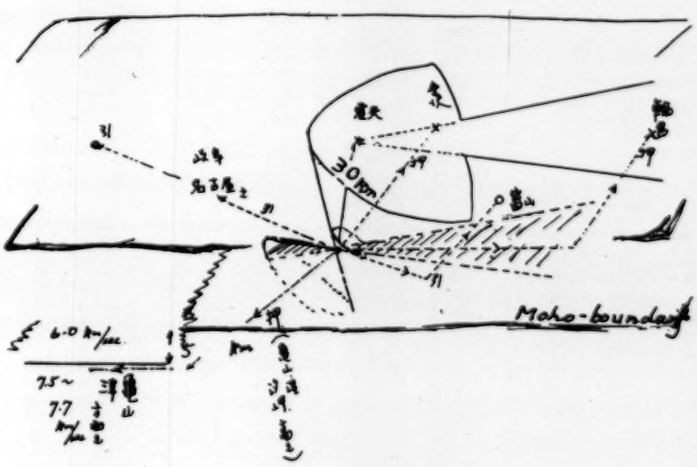

第 4 図　震源における発震機巧の想定図

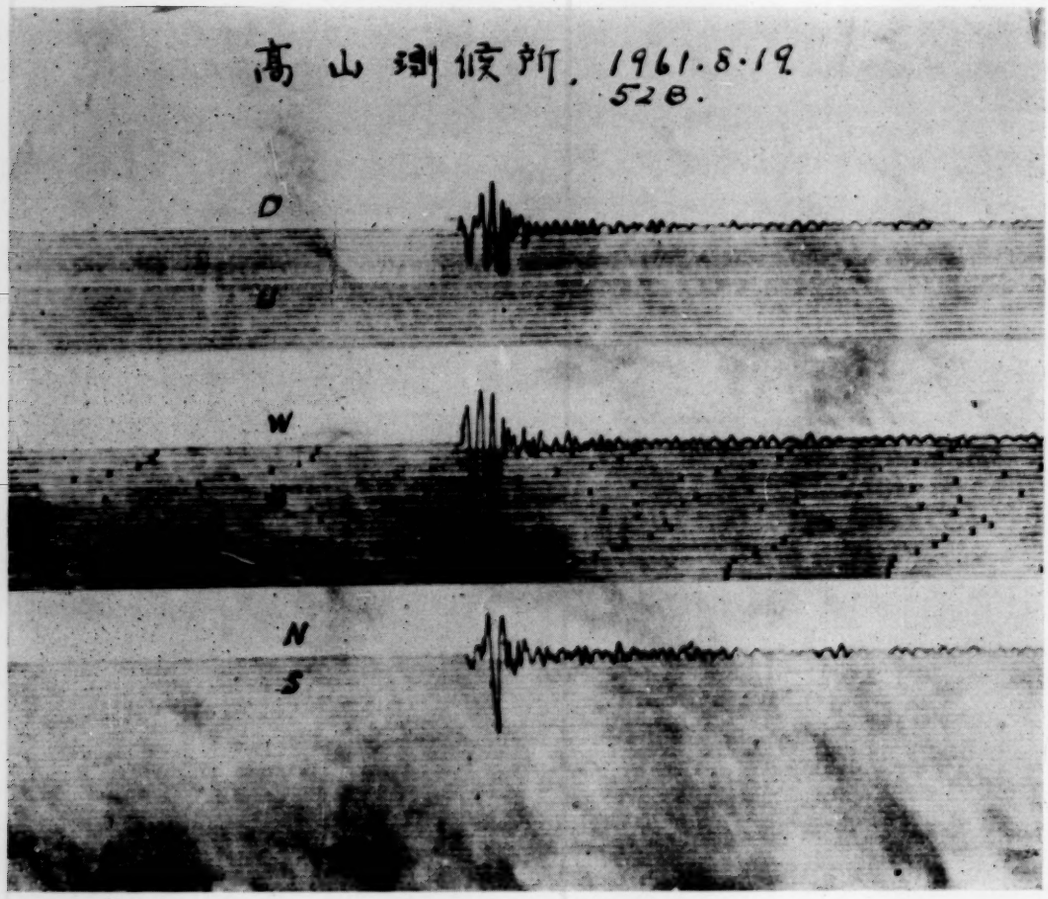

第 5 図　高山測候所における 1 倍強震計の記象.
地震計常数（気象庁提供）

	U-D	E-W	N-S
T	6.8	6.0	5.1
v	8	8	9

（此の写真の縮率：約 0.73）

両成分を合成したものと水平両成分を合成したもので，後者は既に第 1 図に記入してある．地震計の特性による補正を行つていないから，変位とも速度ともあるいは加速度ともいえないものではあるが，三成分の地震計の特性が略ゝ同じであるからその運動方向に著しい歪みは起らない筈である，とすれば特に水平成分の図にＳ波の到来が非常に明瞭に現われ，その震動方向も上記発震機巧に著しく矛盾するものでないことだけはいえる．すなわち第 4 図の推定に従えば震源で略ゝ北，上方に向う“押し”の円錐内でＰ波最大の点，すなわちＳ波の節点が震央のほぼ北 20～30 km ところに現はれ，Ｓ波はそこに集る様に向

く筈である．

地震の発震機巧すなわち“押し引き”分布がその地震の原因として本質的なものとどれほどの関連をもつか，まだ不明確な点が多いが，原因らしいものを想像して地震を分類するとすれば今のところこの“押し引き”分布によるよりほかはない．従つて既に述べた通り今回の地震が断層を伴つた福井地震，あるいはその他の多くの所謂破壊的地震に現われた象限型と異つた発震機巧に属することは注目すべきことと思われる．現地調査では著しい断層が見られなかつたが測地学的に検出されるかどうか，興味あることである．震源の深さに就いては走時曲線からきめられるものは前節に述べた通りであるが震度分布の面から深いところでは 100 km までまだ数々の異論がある．とはいつても震度分布からの異論に対しては，この辺りの特殊な地殻構造すなわち単一に 6 km/sec 層が非常に厚いことや，震源が丁度 Moho- 不連続面にあつて伝播に都合のよい境界波が発生したのではないかと云うことも考えねばならぬ．また高山の周期の長い地震記象から判断すると震源域も可なり大きかつたのではないかと考えられる．最後の点に就いては筆者が前に験震学的に下した定義によるものについても気象庁から再調査の資料が発表されるのを待つて追究して見度いと思う．

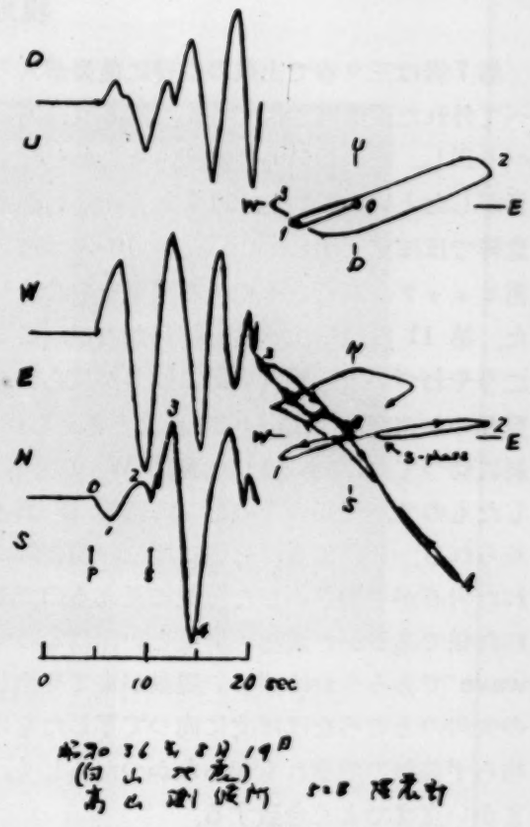

第 6 図

以上走時曲線からと“押し引き”分布からと，もちろん互いに全く独立では有り得ないが，二方面から震源の深さに就いて考えた．走時曲線からはどちらかといえば Moho- 不連続面から少し上となるし，発震機巧からはどうしても不連続面内という方が適当に思はれる．この二つを併せ考えると震源は深さ 20 km～25 km の辺りから，地表下約 30 km と推定される Moho- 不連続面の少し下までのひろがりを持ち，しかも点源に還元される単なる球波面よりも，複雑さを一つ増したという意味で，prolate spheroid, あるいは oblate spheroid の波面で始つたと考えて見るのも興味あることに思はれる．斯うすれば同時に第 4 図に示した断層の如きものを小さくすることも出来る．もちろん現在は斯うした思考を可能とする様な精度の観測が一日も早く得られることを渇望するに止まるべき段階であろうが，今後の研究目標として敢えて言及した次第である．

現地調査

第7図は三ツ谷で土蔵の白壁に亀裂が入り前廂がこわれたもの．右の家の廂の支柱はすべて外れたが修理されていた．第8図は同じく三ツ谷で屋内にあつた石造水槽が屋外にすべり出し，家の腰廻りの石積みをこわしたもの．又三ツ谷で本震の直前白山の方で大きな音がしたといつていたのはもちろん前震があつたものと解釈される．第9図は市ノ瀬の記念碑でほぼ東えずれている．第 10 図は市ノ瀬から白山えの途中にある，通称高飯場の県営ヒュッテ．石壁とその上の屋根をのせるためのコンクリートの枠台に亀裂が入つていた．第 11 図は白山室堂で崩れた石垣，ここでは主な震動は N50°W の方を指し器物の亡りやわづか乍ら物置小屋の亡りが見られ，食堂の食卓が向きによつて倒れたというので震動の加速度は 0.15～0.20 g 位と考えられた．第 12 図は白山から別山えの途中尾根を斜に切つて N，あるいは N10°W の方向に出来た地割れ，第 13 図はそこの地形を遠望したもので，矢印の下のところに第 12 図と同様な砕岩が写真でも他のところと区別して見られる．この亀裂は北国新聞社の踏査隊が最初に発見し，尾根を切つて，しかも破砕された岩石が“湧き出した”様に見えるので普通の地亡りとは違い断層ではないかと考えられた様であるが，通称大屏風といはれるこの辺りの特殊地形のところに，多分 shear wave であろうかはげしい震動が来て発生したものと思はれた．第12図は第13図の左端の矢印のところをほぼ北に向つて写したものである．その辺りはこの様に急峻な地形にも拘らず差程の地崩れも起らなかつたらしく，一，二年前の登山案内書に見られる写真とこまかい点までよく合致する．

30. Earthquake near the National Park Hakusan on August 19th, 1961.

By Ryoichi YOSHIYAMA,
Earthquake Research Institute.

Epicentre of the earthquake is determined,

$$\lambda = 136°44'\mathrm{E},\quad \varphi = 36°05'\mathrm{N},$$

and the depth of the hypocentre,

$$h = 30\ \mathrm{km} \pm 10\ \mathrm{km},$$

probably in the Mohorovicic boundary.

The mechanism of the earthquake will be explained by the “Cone type”, and probably will never be explained by the “Quadrant type”, although the “Quadrant type” is used with success in the case of the Fukui earthquake and many other destructive earthquakes accompanying fault.

Discussing the hypocentral depth in two ways, one from the time-distance curve, and the other from the “push and pull” distribution, the magnitude of the hypocentral region is roughly estimated.

第 7 図　三ツ谷における土蔵の被害．白壁の亀裂と前廂の破損．

第 8 図　三ツ谷．屋内にあつた石の水槽が辷り出して家の下半部をこわしたところ．

（震研彙報　第三十九号　図版　吉山）

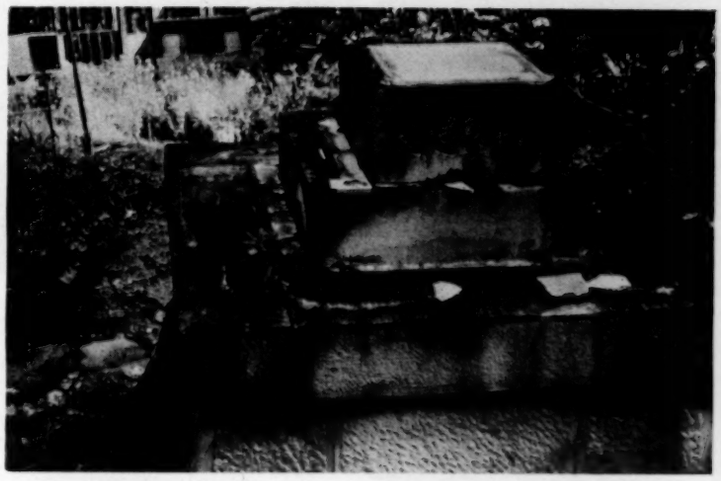

第 9 図　市ノ瀬の永井旅館裏手にある記念碑で東へ辷つて転倒したもの.

第 10 図　市ノ瀬から白山えの登山道の途中，県営高飯場ヒュッテの石壁の亀裂.

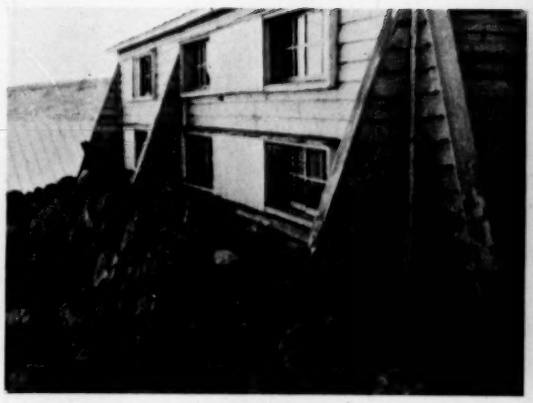

第 11 図　白山室堂小屋をかこむ石垣のくずれたもの，ここでは多くの石垣がくずれた．

第 12 図　白山から別山への途中，所謂天池の近くに発生した地割れ，第 13 図の左端矢印の辺りから北（白山）の方を向いて写したもの．

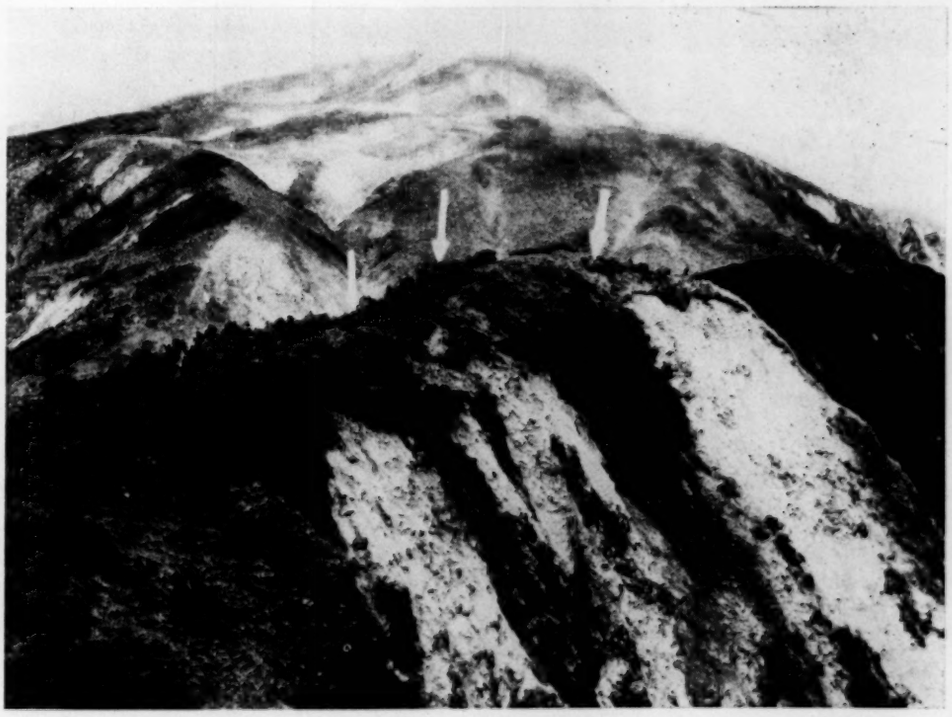

第 13 図　第 12 図の場所を別山の方から遠望したもので後は白山御前峰．矢印の下に第 12 図に示す砕岩の地割れが尾根道を横切つて雁行的に見られる．（北国新聞社提供）

Bulletin of the Earthquake
Research Institute
Vol. 39 (1961), pp. 857-868

31. *Field Studies of the Kita Mino Earthquake on August 19, 1961.*

By Fuyuhiko Kishinouye and Isao Onda,

Earthquake Research Institute.

(Read on Sept. 26, 1961.—Received on Sept. 26, 1961.)

The Kita Mino Earthquake occurred near the borders of three Prefectures, Gifu, Fukui and Ishikawa. The time of occurrence was 14 h 33 m in J.S.T. on August 19, 1961. In the seismic area none could walk during the main shocks which lasted about thirty or forty seconds.

One house completely collapsed under an earth flow at Koike, but many houses in the seismic area are built so rigidly (Fig. 1) that damage to the houses was small. The piteous loss of life was rather more :—8 killed, and 36 injured. The unfortunate loss was due to rock-falls which fell on men as they moved about.

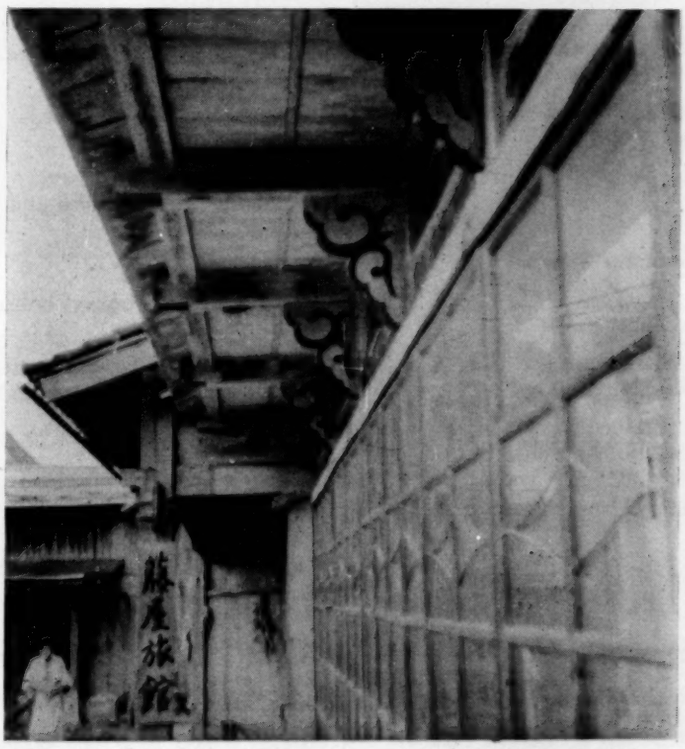

Fig. 1. Rigid structure of a wooden house at Itoshiro.

Fig. 2. Epicentre.

The seismic magnitude was reported by the Japan Meteorological Agency as 7.2, but comparing the relation between the seismic intensity and epicentral distance of past earthquakes, this earthquake was close to the Mikawa Earthquake of Jan. 13, 1945, which occurred about 120 km south. Both earthquakes occurred in the middle part of Honshu Island, Japan, so the results of observations may be compared. The latter earthquake was reported as 6.9 or 7.1 in earthquake magnitude, then the magnitude of the present earthquake may be estimated as 7.

Past earthquakes in the vicinity.

In this region strong earthquakes were frequently recorded near the shore of the Japan Sea. In the mountain area several earthquakes only were recorded in historical records, as seen from Table I.

Characteristic features of earthquakes in this region were (i) damage to house, slight, (ii) loss of life, small, (iii) damaged area, small, (iv) numbers of felt after-shocks, small.

Table I. Past earthquakes in the neighbourhood.

Data	Locality	Damage
1855 3 18	Hida-Shirakawa, Omaki and Hokiwaki Villages	Loss of life, landslide at Hokiwaki and after-shocks.
1858 4 9	Hida, Etchū, Echigo and Kaga Provinces	209 killed, 711 collapsed houses, many landslides.
1891 10 28	Mino and Owari Provinces	7,273 killed, 142,177 collapsed houses, many after-shocks and earthquake faults.
1934 8 18	Gujō-Hachiman Town	
1945 1 13	Mikawa Province (Mikawa Earthquake)	1,961 killed, 12,142 collapsed houses and earthquake faults.
1948 6 28	Echizen Province (Fukui Earthquake)	3,895 killed, 35,420 collapsed houses, 3960 burnt houses and earthquake faults.
1952 3 7	Japan Sea off the coast of Daishoji	

After-shocks.

The numbers of after-shocks observed at the Gifu, Fukui, Kanazawa and other stations of the Japan Meteorological Agency were published by them, and some temporary observation stations were set up after August 24, by the members of our institute. A record of the after-

shocks felt near the epicentre was made at Oshirakawa by a member of the Second Station of the Miboro Electric Powers Station, and is shown in Table II through the kindness of the Dengen-Kaihatsu Company.

Table II. After-shocks felt at Oshirakawa on Aug. 19 and 20.

Aug. 19,	14 h	34 m	(The principal shock)		5 h	15 m
	**	**				20
	17	06				35
		50			6	00
	18	00				04
	19	50				10
	20	24				58 Strong
	21	05			8	45
		47			10	30
	22	10	Moderate		11	53
		34			12	40
	23	13			13	35
		18				50
		55	Violent		15	50
20,	0	10			16	15
		30			17	23
	1	33				26
		43				44
	2	51				54
		53			20	11
	3	54				47
	4	00				54
		05			21	06
		09				11
		28				58
		48				

Information about the earthquakes from inhabitants and writers is listed below: At Nagataki, a woman speaking about the earthquake said that the principal shock was felt in mostly vertical motions, and glass bottles in her house were thrown down. On the next day she felt the strongest shock at 15 h. Considering that in reports from the seismological stations the strongest after-shock was reported at 17 h 07 m on August 20, the writers feel that her memory about the time might be mistaken.

The writers felt three after-shocks at Shiratori at about 13 h on Aug. 23, *P* waves were distinguished from main motions, and they

considered that Shiratori is not very near the epicentre.

On the next day, Aug. 24, the road from Shiratori to Itoshiro was cleared of fallen rocks, and the writers could get to Itoshiro. Dwellers overtaken by the main earthquake stated that the earthquake motion began with loud sound and was prolonged. The senior writer had a similar experience in the case of the Idu earthquake of 1930 at Aziro, and the long duration of the vibrations may be a noticeable feature of strong earthquakes. After-shocks were felt by the writers like the report of a gun close at hand. And they thought Itoshiro was probably the nearest place to the origin of the after-shocks (see, Table III).

Table III. After-shocks felt at Itoshiro by the writers.

Time	Intensity (Japanese Intensity Scale)
Aug. 24 20 h 01 m	III
20 41	II
25 4 15	II
5 50	II
52	III

On Aug. 27 the writers went to Koike, Ōno City, Fukui Prefecture. They felt an after-shock at 13 h 05 m (intensity III) in a house at Okubira, the entrance to Koike, and others at 14 h 21 m and 22 m (Intensity both III) in front of a small shrine above Simo Koike village. In the latter shocks, narrow cracks appeared in the surface soil there, and seemed to close and reopen instantly with the earthquakes.

A postman who encountered the main earthquake by chance at Koike told about his experience: He was about to leave this village at the time of the main earthquake, and could not walk, so returned to the village. He felt many earthquakes there soon after the main earthquake, about one after-shock every five minutes, and the frequency gradually decreased.

Although the number of felt after-shocks from this earthquake was thought to be small, past earthquakes which have occurred in the neighbourhood were similar in the minority of the frequency of their after-shocks.

Rock-falls and Landslides.

The loss of life in this case was unfortunately caused by rock-falls on mountain climbers, and other damage caused by the earthquake was also mostly due to rock-falls, and landslides, or in this case the sliding down of superficial soils and fragments of rocks (Fig. 3). Places where rock-falls and landslides occurred are shown in Fig. 4.

Rock-fall may be a characteristic feature of earthquake damage in this region as recorded in historical materials.

Thin piled layers of cracked volcanic rock, agglomerate and soil are cut out by the rivers and form such steep cliffs that they overhang locally. In such conditions, rock-falls are liable to take place when earthquake motion is strong. The area of rock-falls was roughly in a circle with the radius of about 10 km. This dimension was nearly equal to the area where there was a shifting of gravestones as mentioned below.

A large earth flow occurred at Koike, in the upper reaches of the River Uchinami, and one house was totally destroyed. Fortunately, the dwellers were safely out of doors.

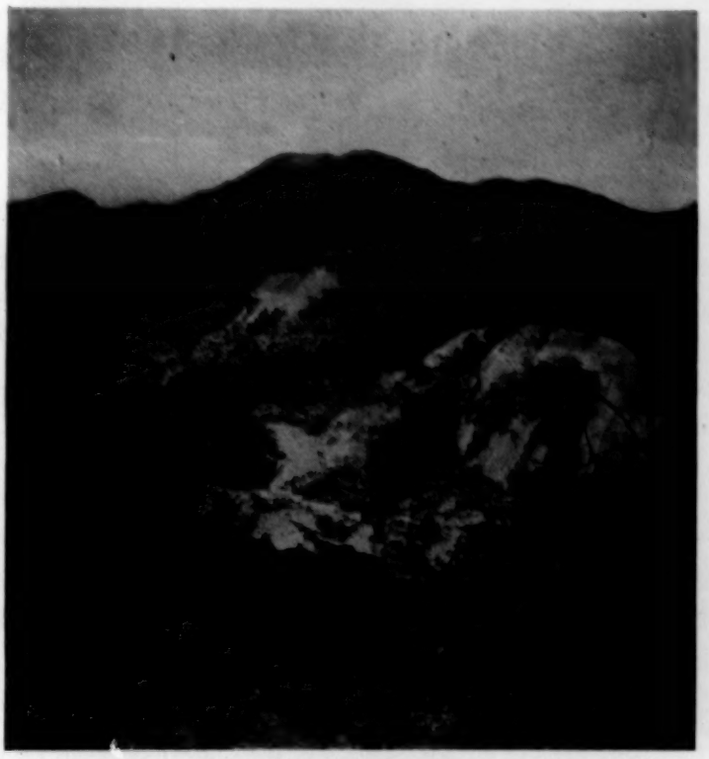

Fig. 3. Landslide and rock-fall at teh western side of Mt. Gankyōji from Koike.

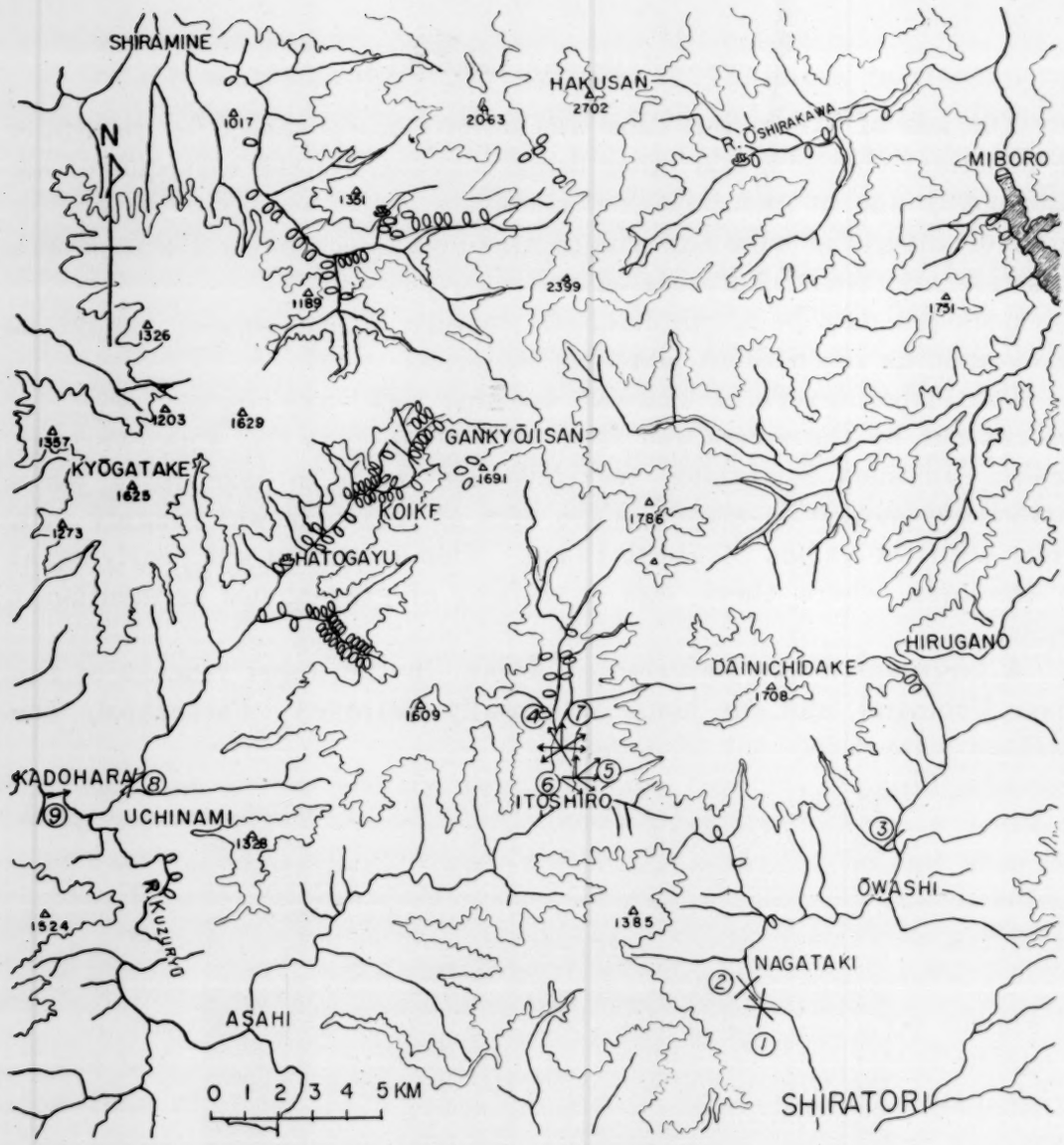

Fig. 4. Rock-falls, landslides (in oblong circle) and displacements of gravestones (in arrow).

Earth Fissures.

Many roads follow the rivers in this region. The surface of the roads was levelled by cutting into the mountain side in some places and raising the level along the river banks (Fig. 5). In June of this year heavy rains fell in this region, and flood waters tore the earth from the sides of the river banks. Then at many places the roads were unstable when the earthquake took place. The soil fell in at the cuttings

and earth fissures opened parallel to the river.

Upstream of the River Uchinami the writers found some earth fissures which were not parallel either to a road or to a river. Near the fissures greyish clay was found, so the writers doubted that these fissures were a manifestation at a geological fault moved by the earthquake. They could not find a clear extension of fault there, because the road was covered with grass at the cutting in the mountain side and with pebbles at the opposite river side, but on the opposite cliff of the river soil and rock slipped off, and there the direction of the river changed along the fissure. Further study of the fissure by geologists is requested.

Overturning and Rotation of Gravestone.

The area damaged by an earthquake is in general proportionate to the magnitude of the earthquake. In the present case the area of the overturning and rotation of gravestones was small; about 20 km in diameter. Since the diameter of the affected area was small, the depth

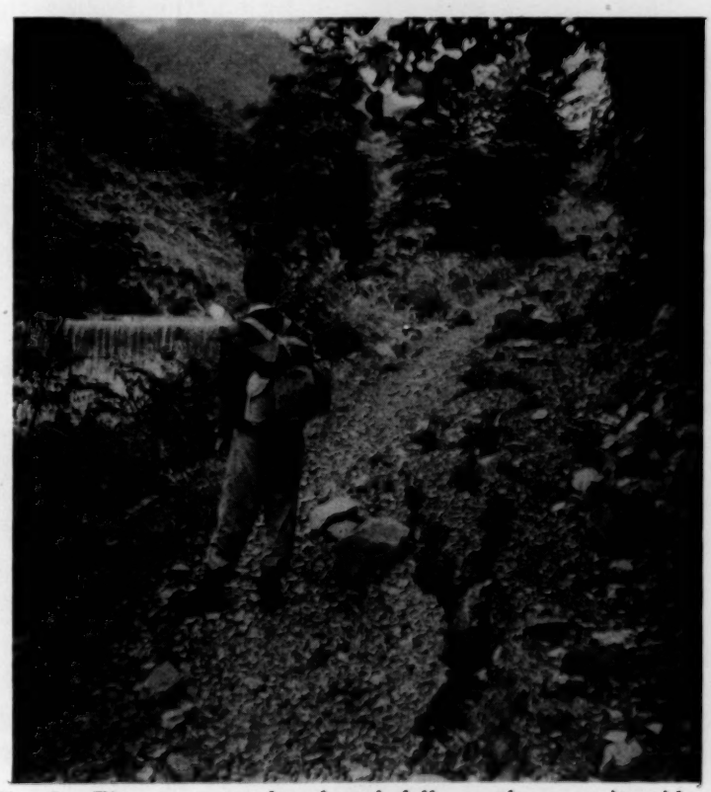

Fig. 5. Fissure on road and rock-falls on the opposite side of the river between Hatogayu and Koike.

of the earthquake might have been shallow. The rotation of gravestones was thought to be rather more numerous than actual overturning. The writers consider that the ground is hard and the amplitude of the earthquake motion was not sufficiently large to overturn the gravestones but only to rotate them. (Figs. 6 and 7).

In the map in Fig. 4 the overturned direction is indicated by an arrow, and final direction of an edge of the rotated stones by a thick line. In Table IV, the places are indicated by using the same numbers as in Fig. 4; 3rd column is the dimension of the mentioned gravestones; 4th column the ratio of breadth (b) and height (h) of the gravestone and 5th column the rotated directions of one face of gravestones before and after the earthquake, or the overturned direction estimated with traces remaining at the face of gravestones. The data obtained were too limited for the epicentre to be deduced from them.

The acceleration of the earthquake motion near the epicentre might estimated about $0.4\,g$ by West's formula.

Change in Underground Water.

Oshirakawa hot spring stopped spouting after the earthquake, and

Fig. 6. Gravestones at Nagataki, Shiratori.

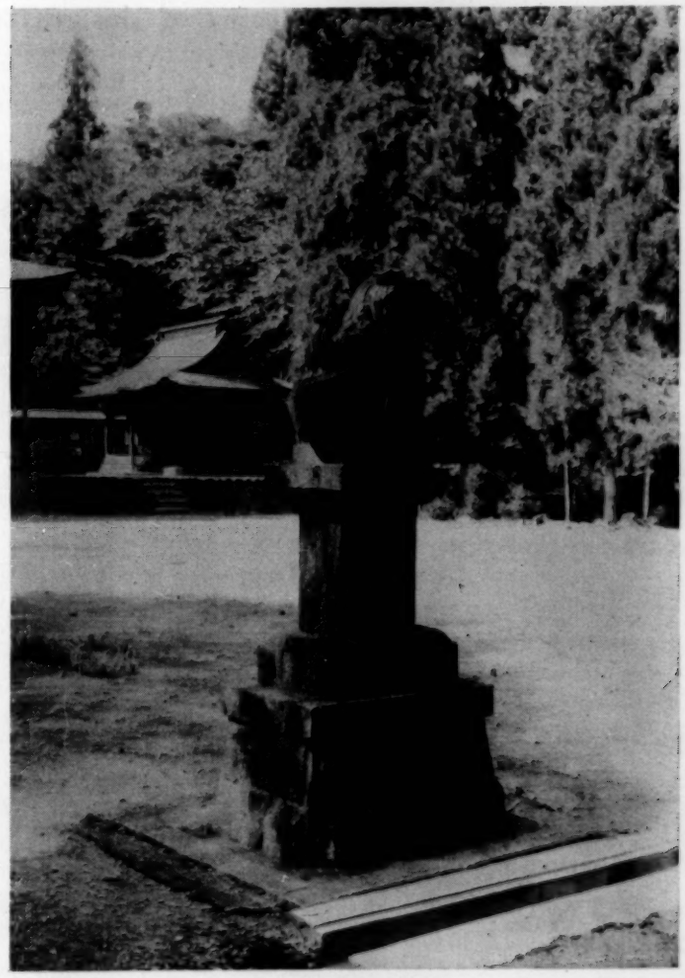

Fig. 7. Rotation of Komainu at Hakusan Shrine, Shiratori.

the mineral spring at Hatogayu and the well at Nagataki, Shiratori, became milky. Most villages used river water which was disturbed by earth flows in many places.

Disturbance of Water in the Reservoir at Miboro.

At the duration of the earthquake the mayor of the town Shiratori, happened to be standing on Miboro Dam and saw water waves proceed with white crests from west to east over the reservoir. A water level meter set at the side of the dam showed traces of the motion of water as large as 40 cm from the mean level of water.

Table IV. The rotation and overturning of the gravestones, etc.

No.	Place	Kind	Dimension	b/h	Rotation or Overturning	Translation
1)	Nagataki (Ashihara In)	Gravestone	18×24×52	0.42	N70W→N80W	
			30×30×77	0.36		6 cm, N45W
			14×20×53	0.35	N50W→N75W	
			15×24×59	0.38	N40E→N65E	
			24×26×70	0.35		2.5 cm, N50W
			28×28×75	0.35		2.5 cm, N 5E
2)	Nagataki (Hakusan Shrine)	Komainu			N50E→N40E	
		Komainu			N50E→N35E	
3)	Owashi	Gravestone	15×22×50	0.40	N35E→N40E	
4)	Itoshiro (Kamizaisho cemetry)	Gravestone	21×21×57	0.35	S50W	
			21×21×59	0.35	W	
			28×21×73	0.36	E	
			26×39×68	0.39	W	
			26×29×68	0.40	E	
			23×20×53	0.40	N	
			24×24×57	0.39	N	
			21×23×53	0.40	?	
			—	—	N50E	
			—	—	S30E	
			—	—	N30W	
5)	Itoshiro (Taishido)	Stone-lantern	—	0.05	S60E	
			—	—	N	
			—	—	S	
6)	Itoshiro (Kubinashi Zuka)	Stone Monument	H=1.5m	—	S60E	
			H=1.0m	—	S80E	
7)	Itoshiro (Chūkyo Shrine)	Komainu	—	—	E	3 cm, W
8)	Shimo Uchinami	Gravestone	26×36×130	0.27		2 cm, N50E
			34×35×140	0.24		5.5 cm, N30E
			25×31×79	0.37		4 cm, N60E
			25×25×49	0.47	N60E→N70E	
			30×45×129	0.33	N20E→N25E	
			40×40×140	0.27	N20E→N25E	6 cm, N25E
			21×21×44	0.43	N20E→N45E	
			—	—	N60E→N70E	
			—	—	N50E→N55E	
			—	—		5.5 cm, N60E
9)	Kadohara	Stature	—	—	N70E	

In concluding this report the writers wish to express their thanks to the Gifu Prefectural Authorities, and people who helped in the study of the earthquake.

31. 1961 年8月 19 日北美濃地震踏査概報

地震研究所 { 岸 上 冬 彦
音 田 功

岐阜，福井，石川の三県の境付近に表題の強震が起り，死者8名，負傷者36名を出した．人体感覚による震度と震央距離との関係は，1940年1月13日の三河地震とほぼ同様であるので，これより類推すると，今回の地震は $M=7$ 程度である．

われわれは8月22日より1週間にわたつて主に岐阜，福井の両県にまたがつて震災地を踏査した．

i) この付近に起つた過去の地震（第1表）

この地方の地震活動性を調べると，日本海に近いところは地震はときどき起るが，大地震は比較的少ない．しかし，日本中部地震帯といわれ，ときどき大地震が若狭湾，伊勢湾，琵琶湖により陸地が狭められた地域を南北に分布して起つている．これらの地震における特徴は落石や山崩れによる被害が非常に多いことである．

ii) 余 震

震央近くにおける余震の観察は電源開発 K. K. 御母衣第二発電所の大白川ダム建設地で行なつていたので，同会社の好意によつて第2表に載せた．

一方，筆者らは踏査期間中各地で余震を感じた．岐阜県下においては，白鳥町市街地で初期微動を感じ（23日），石徹白で急激な shocks を感じた（24日）．余震からの類推ではあるが，震央は石徹白近辺と考えられた．福井県下では，打波川上流の鳩ヶ湯で石徹白で感じたものより周期が長いように思われ（26日），さらに上流の小池でも同様の感じを受けた．

これらの期間における余震においては推定震度Ⅲが最大で，震動の継続時間は数秒以内であつた，現地の人々の話すところによると，本震は長いあいだ揺れていて歩行困難になつたとのことであり，筆者の一人がかつて同様のことを経験しており，大地震の本質の一部を表わすものと考えられる．

余震の頻度は鳩ヶ湯の下流中村で19日には30分ごとに起つていたが，踏査当日（26日）には10回くらい感じている．小池では19日夜10時ころまでに 4～5 回強い余震を感じている．これらのことを考えると，いままでの経験から，この地震は多少深いのか，あるいは，この付近の地質による震動特性の違いによるのか問題である．

iii) 落石，山崩（第4図）

この地震の特徴は大きな石の落ちたところが多く，それが原因となつて山崩れを起したところが少なくなかつた．鉛直に近く，またときにはのしかかるような傾斜の急なところの大きな割目をもつ岩石が地震動によつて落ちたのはむしろ当然といえるものが多かつたが，この地震による被害のほとんど全部，特に死者や負傷者はすべてこれら落石，山崩れや土砂崩れによるものであつた．

第4図は筆者らの踏査したもののほか，ほかから聞いたもののうち確定できたものは加えてある．しかし，あまり小さなものは省略してある．この分布を見ると，約 20km の直径の円内に入り，墓石や石碑の移動とほぼ同じ範囲となつている．地質との関係は別に述べられるであろう．

iv) 地割れ，地震断層

川に沿つた道の切取面の落石と片盛部分に川と平行に入つた地割れが到るところで見られた．これらの地割れのなかには，この地震の前にあつた同年6月 24—29 日の集中豪雨のため堤の土砂が川水にけずられ，土の摩擦による安定を欠いたところも少なくなかつた．

しかし，打波川の上流で小池のわずか下流付近で，道路に直角に入つた地割れが二個所で見られた．粘土状の泥があり，古い断層が今回の地震によつて少し動いたものと思われた．道路に見えた斜めの割目は 10m くらい追跡できたが，その両端は，すなわち川原では転石によつて，他方，山側では草木の繁茂によつて追跡することは不可能であつたが，ただ対岸にも崩れたところがあつて，果して地震断層か否かは地質の研究にまかせる．

v) 石碑，墓石などの移動および転倒（第4表，第4図）

大きな地震ほど被害を受ける範囲は広くなることは衆知のことであるが，この地震の墓石などの

転倒した地域は直径約 20km で，いままでの地震と比べて広くなかつた．このことは震源の深さが深くなかつたとも考えられ，iii) で述べた深いということと矛盾するので，結局，今回の地震は大きなものではなく，また震源の深さも深いものではないだろう．地震動が地質に影響されて，振巾が小さく，そして周期が短かいために墓石などは転倒し難く，回転が多く見られたのであろうと思われる．

この地方では，墓石にほぞがつけてあつたり，また新らしいものはセメントで土台に固定してあるものが少なからずあつて，また地震後，直ちに復旧したものが多かつたが，倒れたときにつけられたと思われる墓石の面や角の新らしい傷跡を見て倒れた方向を推定できた．同時にその大きさも測つてきたが，West の公式によつて推定した水平最大加速度は 0.4 g という値が石徹白で見出された．

倒れた方向や回転したあとの方向は震央の近くでは複雑であるが，そこでは上下動が大きかつたと考えれば説明できよう．ここで回転方向というのは，一つの面が地震のあとにどう向いているかを示すものであつて，地震波が短形柱を振動させるときには波の進向方向が短形柱の一つの面と平行になるように回転させると考えると，筆者らの測定した方向か，あるいはそれに直交する方向から墓石の移動や転倒に寄与した波がやつてきたことになる．この考えによれば，震央は石徹白のやや西方となる．

vi) その他

この地域には地下水の湧出しているところが数カ所見られるが，著しい変化を起したのは，大白川上流の大白川温泉で地震直後湧水が止まり，筆者らの行なつた 1 週間後にあつても湧水はみられなかつた．

また，鳩ケ湯の湧水は地震いらい濁つて，1 週間を過ぎてやつと濁りがとれ始めた．そのほか白山北方の温泉には異常はなかつたようである．

白鳥町長滝にある農業組合の井戸水は濁つた．

その他に，注目される現象は，御母衣ダムの貯水池の水に波が立つたことである．同ダムは約 $3\times10^8 m^3$ の水を貯めているが，その表面に波長約 2m の進行波が観察されたが，残念なことに器械による記録はなされなかつた．このことはダムに対して湛水の影響についての新らしい資料であろう．なお，このダムは震央に近かつたにもかかわらず，地震のあとには漏水は減り，またダムの頂が 5cm 沈下したとのことである．

以上の調査については，岐阜県庁，白鳥町役場，電源開発株式会社その他多くの方々から便宜を与えられた．厚く感謝の意を表する次第である．

地震研究所彙報
第39号(1961)869-872頁

32. 北美濃地震における家屋の被害について

地震研究所　大　沢　　胖

(昭和 36 年 9 月 26 日発表—昭和 36 年 9 月 30 日受理)

今回の地震は山間の人家の少ない地域におこつたため，家屋の被害は比較的僅少であつた．筆者の踏査した範囲では，修復不可能と思われるほど大被害をうけた家屋は，山崩れのため倒壊したものを入れて2戸にとどまり，そのほか壁のひびわれ程度の被害をうけたものまで入れた家屋被害数は約 20 戸であつた．筆者の見たのは，小池，中洞，中村，石徹白，勝原等震源地付近のおもな部落を含んでいるので，この地震による被害全体としても，あまり上の数字を出るものとは思われない．

家屋被害の特徴としては，地震動により家屋が大きくゆれてそのため生じた直接被害のほかに，家屋の基礎地盤が一部崩れたため不同沈下をおこして生じたといつたような，間接的な被害も多くみられたことがあげられる．もつともこの種の被害は間接的とはいつても，従来の震害にしばしばみられたもので，地震による被害として重要なものであることはいうまでもない．

以下に，筆者の踏査した範囲で，家屋被害の状況を述べることとする．

小池は最も被害の大きかつたところで，全戸数 10 戸がいずれも大なり小なり被害をうけた．このうち7戸は下小池と称して一団となつており山あいの大きくくぼんだ盆地状のところに建てられている．大被害をうけたものとして1戸は山崩れにより上方から土砂でつぶされて全壊し，2 戸は震動のため大傾斜した．

家屋は大部分，100年前後を経過したもので，その構造は，ふつうのかやぶき木造平家建(一部中2階つき)で，土台をまわさず直接石の上に柱を立てている．そのため外柱では，震動により柱が石から 5～10 cm 位ずれて，上部の柱梁接合部がはずれかかつたり外壁の板がはずれたりしたものが多くみれた．(Fig. 5 参照) 一方家屋内部では，柱・梁接合部で柱が折れている例があつた．内柱は外柱とちがつて柱脚の拘束が大きいので，柱脚がずれたための2次的被害というよりも，地震動により建物上部に水平力がはたらいて接合部に曲げモーメントがかかり，この曲げ応力にたえられなくなつて折れたものと考えられる．そのほか内部の板戸がはずれてバラバラになるといつた被害がみられた．

家屋の構造上ただひとつの例外は，打波小・中学校分校である．これは数年前建てられた木造2階建で，見たところ基礎に土台をまわし筋かいも十分に入つていると思われる近代建築であるが．この建物は1階の壁になめのひびわれを生じているだけでこの部落では最も被害が少なかつた．(Fig. 4)

中洞・中村では基礎が崩れたため生じた間接的被害が多くみられた．この部落は打波川に沿つた傾斜地にあり．大部分の家屋は斜面の一部をけずり，一部を埋立ててならした上に建てられている．この埋立てた部分は外側に石を積んであるが，この石積みが崩れ落

ち，その上の基礎が下がつて不同沈下をおこし，上部構造にも被害を生じている．

この部落では平坦地に建つた家屋が壁のひびわれ程度の小被害ですんでいるので，地震動そのものはそれほど大きくなかつたと思われる．

石徹白では被害はきわめて軽微で，土壁やタイルのひびわれが，2, 3 の家にみられた程度であつた．この部落は一見したところ程度の良い家が多く，大体土台がまわしてあり，壁も（板壁が多い）十分に配置されているようであつた．建具の被害，瓦の落下は全くみられず，町役場への報告も皆無であつた．

その他勝原では，がけの上に建つていた家が，がけ崩れのため一部不同沈下をおこし被害をうけた例があつた．(Fig. 6, 7) また鳩ケ湯の旅館も基礎地盤の一部が崩れたため基礎構造及び上部柱・梁・建具等に被害をうけた．

Fig. 1. 下小池の住家の被害状況

Fig. 2. 同左．柱が上の方で折れている．

Fig. 3. たまたま空家になつていた家屋の被害状況．(下小池)

Fig. 4. 下小池の小中学校分校．内部の壁にひびわれがあつた程度で被害軽微．

Fig. 5. 奥平小池の住家．土台石の上で柱がずれている．

Fig. 6. ガケ崩れで家屋の一部が不同沈下し被害を生じた例．(勝原)
(森本良平氏撮影)

Fig. 7. ガケ崩れで家屋の一部が不同沈下し被害を生じた例．(勝原)
(Fig. 6 の家屋に同じ) (森本良平氏撮影)

32. On the Damage to Buildings during the Kita Mino Earthquake of August 19, 1961.

By Yutaka Osawa,
Earthquake Research Institute.

This report describes the damage to dwelling-houses during the Kita Mino Earthquake of August 19, 1961. As this earthquake occurred in the mountain area and was not of very high intensity, the damage to dwelling-houses was comparatively small.

Two types of damage were observed; one is produced directly from the vibration due to ground motion, and the other is caused by foundation failure. The latter was mostly seen in the houses built on the filled ground.

地震研究所彙報
第39号(1961)873-879頁

33. 1961年8月19日北美濃地震とその余震観測概説

地震研究所　萩原尊礼
東京大学大学院
地球物理専門課程　茅野一郎

(昭和36年9月26日発表—昭和36年9月30日受理)

1961年8月19日14時33分頃本州中部に強い地震を感じた．有感区域は，東は関東地方から，西は中国地方に及ぶ広い地域にわたつた．震央は，岐阜．福井県境白山南方山地で，気象庁により，北美濃地震と名付けられた．

Table 1.

	J.M.A.	U.S.C.G.S.
	h m s	h m s
Origin Time	05 33 32	05 33 30 6
Epicentre	36.0°N, 136.8°E	36.0°N, 136.5°E
Depth	40 km	about 17 km
Magnitude	7.2	7½

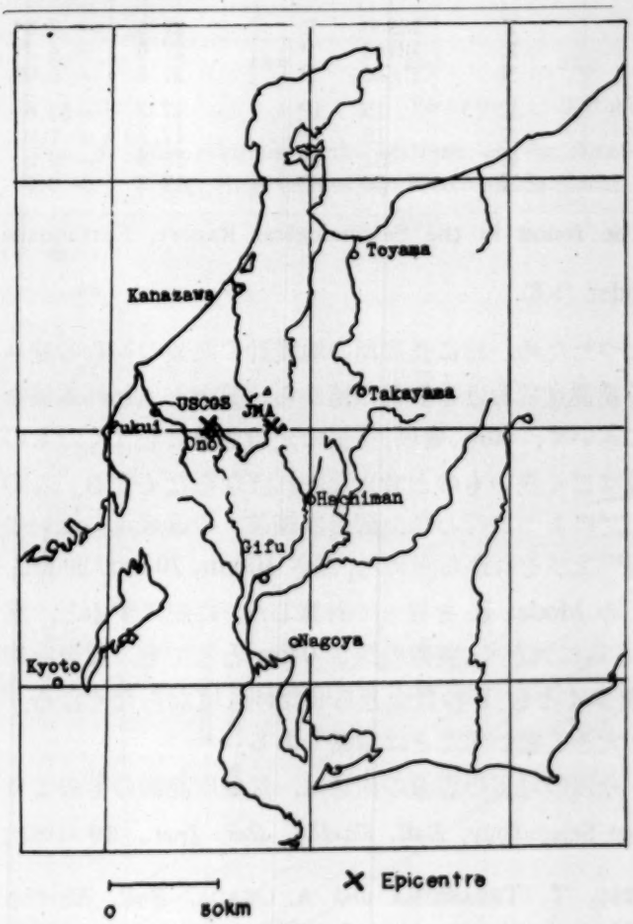

Fig. 1.

気象庁及びアメリカ合衆国沿岸測地局 (United States Coast and Geodetic Survey) の発表による，震央位置，震源の深さ，発震時刻，マグニチュードは，第1表の通りである．両者の発表による震央位置は，第1図に示してあるが，気象庁発表のそれの方が妥当だと思われる．また発震時刻は，USCGS 発表のそれは早過ぎると思われる．しかし，震央位置及び深さに関しては，なお検討の余地があり，本報告中でも論及されよう．

地震研究所の各観測所における，初動の検測の結果を第2表に示す．この地震が起る五分余り前から，たまたま，ペルーに起つた大きい地震

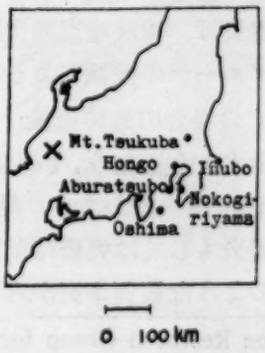

Fig. 2. Distribution of the stations of the Earthquake Research Institute.

Table 2. Observations of the Kita Mino Earthquake, 19 Augugt, 1961, by the Earthquake Research Institute.

Station	Seismograph	Component	V_{max}	Phase	Time	Amplitude
					h m s	
Mt. Tsukuba 36°13′N 140°07′E	Anderson-Wood	E	2000	P	14 34 17 9	− 3.2*
		N	2400	P	18 4	+ 1.0*
	HES 1-1	Z	37000	iP	17 8	−47.5*
		E	29000	iP	17 8_5	−58.0*
		N	29000	P	18 0_5	+ 2.9*
	Columbia Long Period	Z	627	P	16 8	−
		E	697	P	17 2	−
		N	432	P	18 4	+
Nokogiriyama 35°10′N 139°50′E	HES 1-1	Z	3180	iP	18 5	− 5.3*
		E	3120			
		N	3390	P	18 6	+ 1.9*
Aburatsubo 35°09′N 139°37′E	Anderson-Wood	E	2000	eP	15 9	− 2.7*
		N	2400	eP	16 2	+ 1.5*
Oshima 34°44′N 139°22′E	HES 1-1	Z	1400	P	15 9	− 3.8*
		E	1200	eP	15 8	− 1.5*
		N	1100	eP	16 9	+ 0.7*
Inubo 35°42′N 140°52′E	HES 1-1	Z	10900	P	27 6	− 7.3*
		E	12145	P	27 6	− 4.7*
		N	11540	P	27 8	+ 2.0*
Hongo, Tokyo 35°43′N 139°46′E	Omori	E	15	iP	17 3	−53.6
		N	15	iP	17 7	+ 7.0
	Hagiwara	E	31	iP	18 8	− 9.0
		N	30	eP	17 7	+ 0.5

The characteristic curves would be found in the Seismological Report, Earthquake Research Institute, Tokyo University.

* Amplitude on the microfilm reader (×8).

を記録しつつあり，両者の波動が重なつたため，特に長周期の地震計の記象の初動の読みとり値の精度は落ちると思われる．各観測点における数個の値から，妥当と思われる値をとつて，気象庁発表の震央，発震時に基いて，和達，鷺坂，益田の走時曲線に記入したものが第3図である．これによると．震源はごく浅いものと考えなければならなくなる．この地震の震央は，爆破地震動実験グループによつて行われた御母衣(ミボロ)爆破[1]の爆破点に近いので，同グループの観測による走時曲線[2]及びそれから求めた，深さ 10 km, 20 km, 30 km, 35.6 km の場合の走時曲線（簡単のため Model II を採つて計算した）に記入すると，第4図に示すようになり，その食違いはさらに大きく，震源の深さ 0 km としても，震央を約 10 km 以上西へ動かすか，発震時刻を少くとも 1 秒以上遅らせなければならなくなる．しかし震央もしくは発震時刻をあまり大きく動かすことは困難である．

上記のような観測事実からみると，今回の地震の震源の深さは，気象庁発表のものより

1) The Research Group for Explosion Seismology, *Bull. Earthq. Res. Inst.*, **39** (1961), 285～326.

2) T. Mikumo, M. Otsuka, T. Utsu, T. Terashima and A. Okada, *Bull. Earthq. Res. Inst.*, **39** (1961), 327～349.

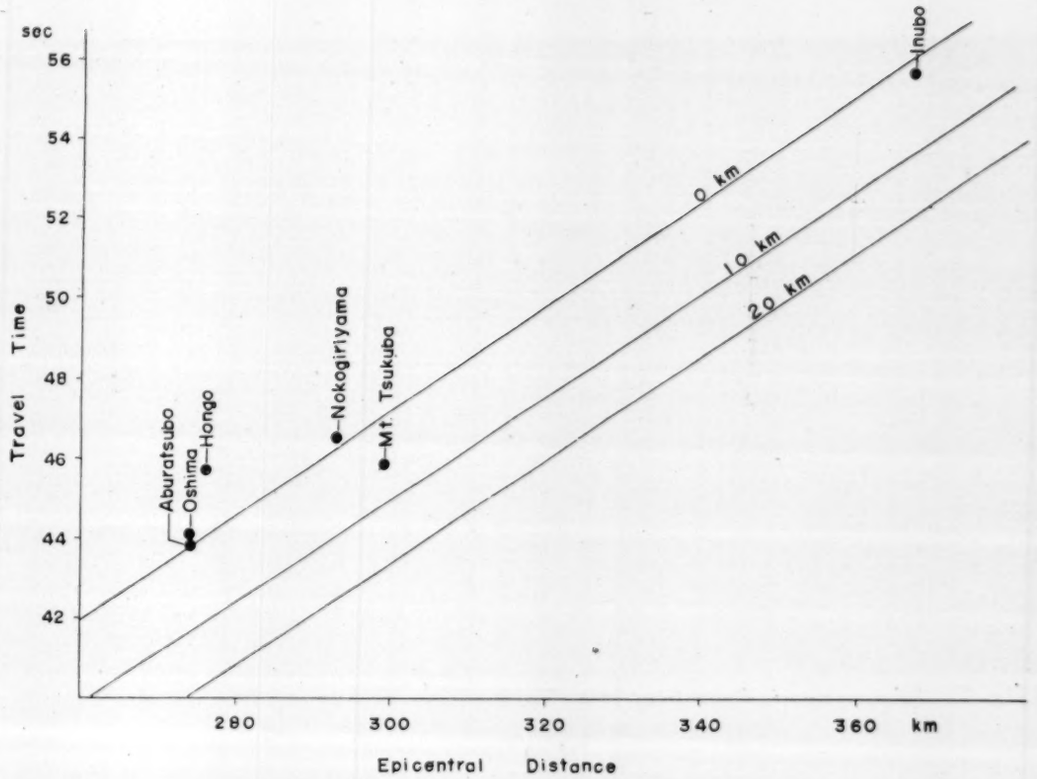

Fig. 3. Observations at the stations of the Earthquake Research Institute with the travel time curves by Wadachi, Sagisaka and Masuda.

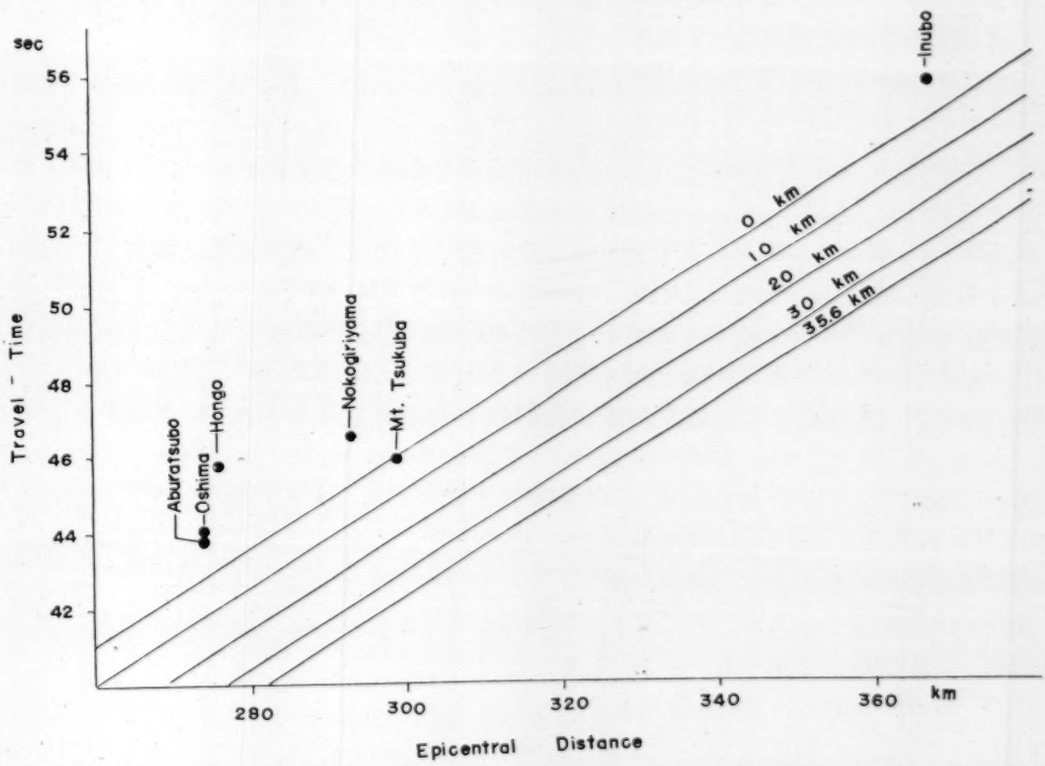

Fig. 4. Observations at the stations of the Earthquake Research Institute with the travel time curves derived from the observations of the Miboro Explosion conducted by the Research Group for Explosion Seismology.

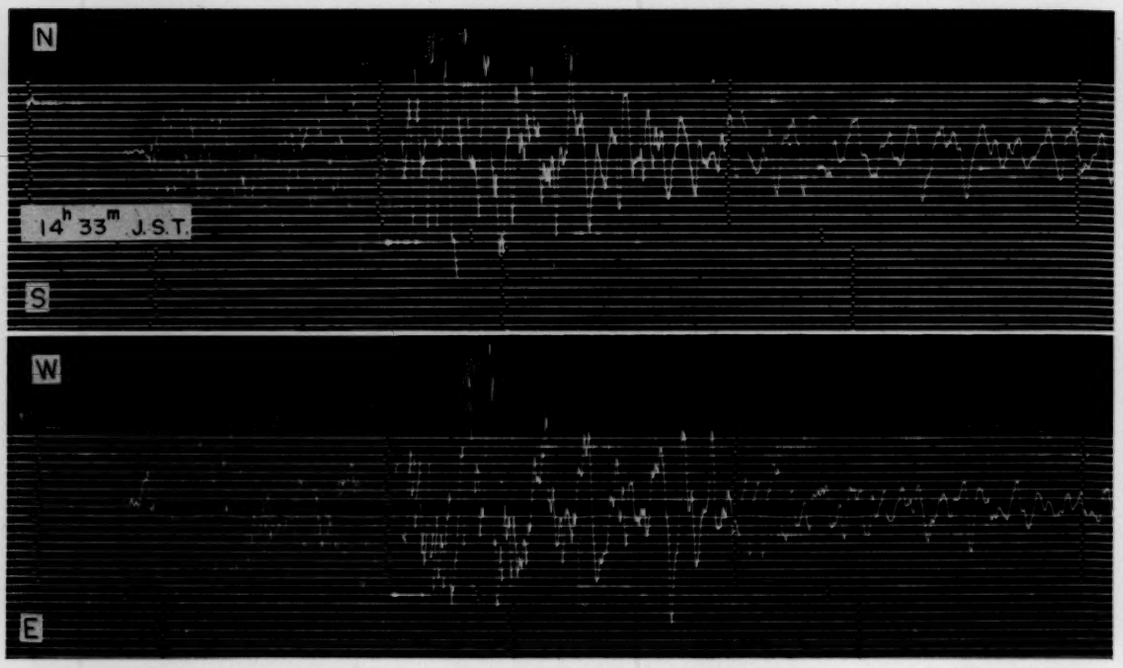

Fig. 5. Seismograms of the Kita Mino Earthquake, 19 August, 1961, at Mt. Tsukuba.
Anderson-Wood seismograph $T=0.80^{sec}$, $h=0.8$

も，さらに浅いのではないかと思われる．この点は，気象庁でも，さらに，観測結果を検討しているので，やがて解決されるものと期待している．

なお，筑波山における発現時刻が，他の観測点におけるそれにくらべて明かに早いが，これは爆破地震動観測の際にも認められたところである．

筑波山の Anderson-Wood 地震計の記象を第 5 図に示す．この最大振巾より Richter の公式によつてマグニチュードを求めると，6～6¼ となつて，著るしく小さい値を与える．Pasadena 及び Berkeley で定められた日本の地震のマグニチュードと比較して松本[3] が決めた公式によると，さらに幾分小さい値が得られる．

第 6 図に，気象庁の観測に基く震度分布を，第 10 図に，震央距離と震度との関係を示す．第 10 図より，河角マグニチュードを求めると，$M_k=4.7$ となり，これを，河角の公式によつて Richterのマグニチュードに換算すると $M=7.2$ となる．比較のため，1948 年 6 月 28 日の福井地震 ($M=7.3$)，1945 年 1 月 13 日の三河地震 ($M=7.1$)，1934 年 8 月 18 日の岐阜県郡上八幡地震 ($M=6.1$) の震度分布を第 7 図～第 9 図に示す．また，第 11 図には，各地の初動の押し引きの分布を示した．主として，気象庁の観測結果に基いているが，地震研究所の観測結果も盛りこんである．銚子では，気象庁は速報で Up と発表しているが，われわれの観測に基いて Down と図示した．この分布が，何型に属するかの論議は次の機会に譲り，ここでは事実の報告にとどめる．

震央が山地であつたため，崖くずれ等は随所に見られたが，土木建築物の損害及び人的被害は，比較的軽少であつた．

3) T. MATSUMOTO, in preparation.

Fig. 6. Isoseismal map of the Kita Mino Earthquake, August 19, 1961.
M:7.2 (After J.M.A.)

Fig. 7. Isoseismal map of the Fukui Earthquake, June 28, 1948.
M:7.3 (After T. Hirono)

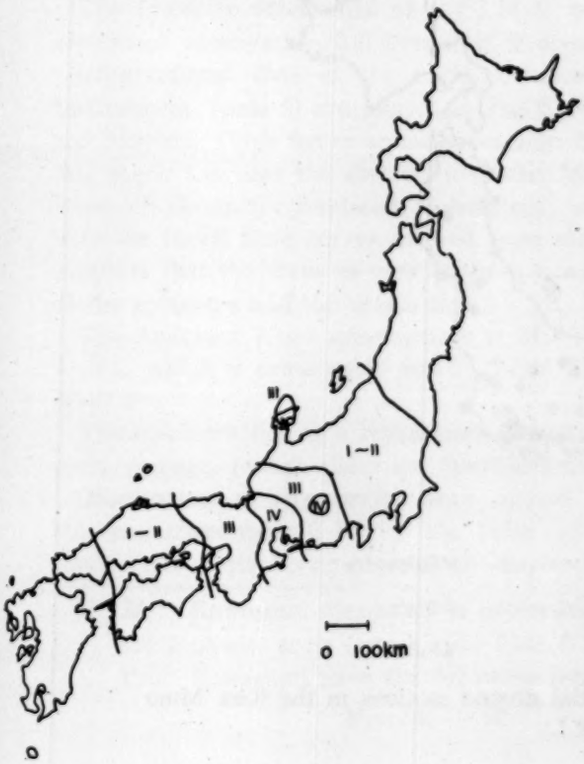

Fig. 8. Isoseismal map of the Mikawa Earthquake, January 13, 1945.
M:7.1

Fig. 9. Isoseismal map of the Gujo-Hachiman Earthbuake, August 18, 1934.
M:6.1 (After T. Miura)

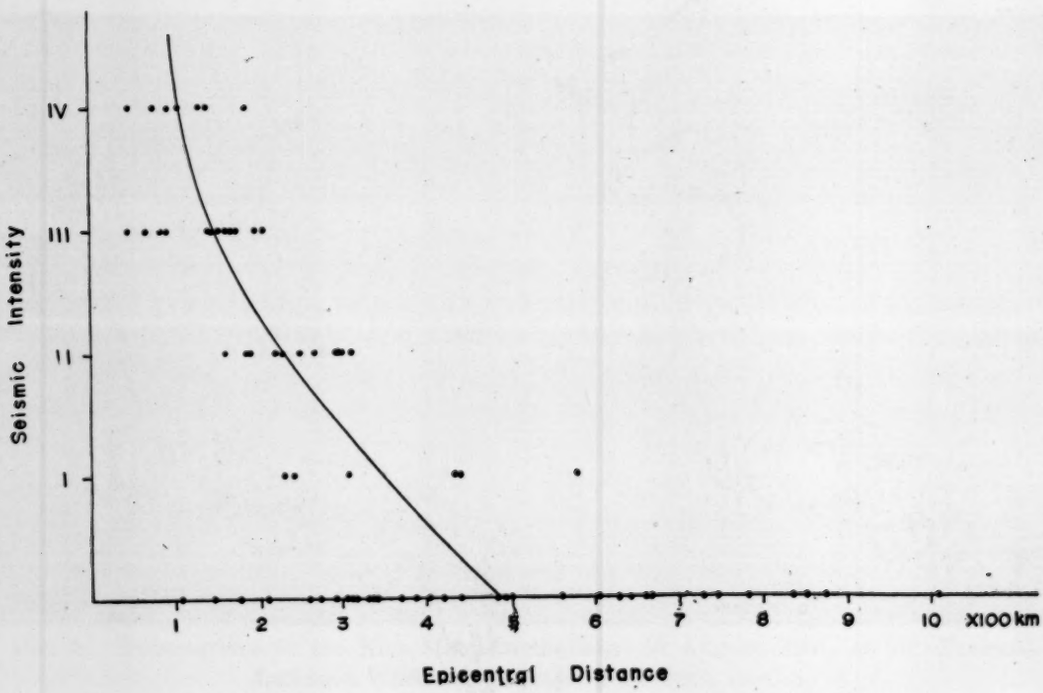

Fig. 10. Relation between seismic intensity and epicentral distance.

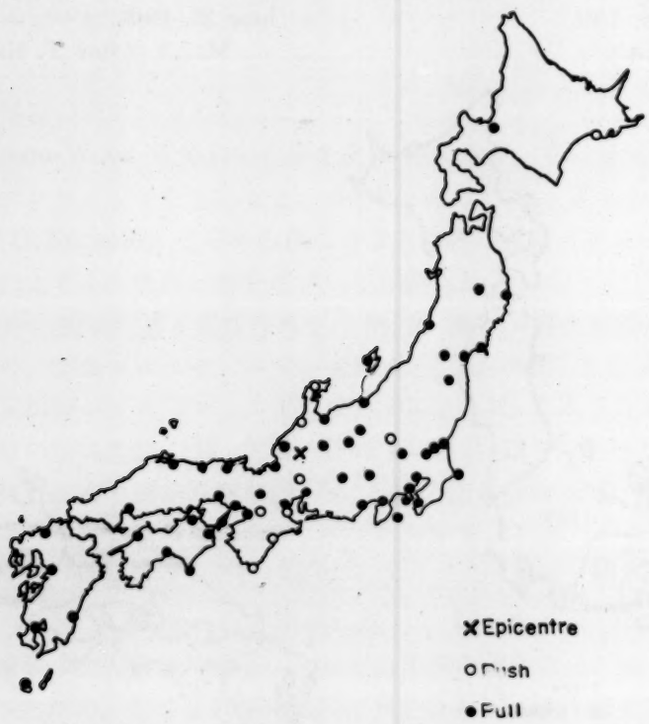

Fig. 11. Push-Pull distribution of initial ground motions in the Kita Mino Earthquake (After J.M.A. and E.R.I.)

余震活動はあまり盛んでないように思われたが，地震研究所においては，福井県大野市勝原(カドハラ)で HES (Hagiwara Electromagnetic Seismograph) によつて出張観測をすることにきまり，8 月 26 日から観測を開始した．同時に，岐阜県郡上郡八幡町で三点観測を開始した．ややおくれて，岐阜県大野郡高鷲村において HES による観測が開始されたが，9 月 16 日の第二室戸台風により器械が被水したため，旬日を出でずして観測を中止するの止むなきに至つた．勝原及び郡上八幡における観測は 9 月 20 日まで行つた．

HES による余震観測は，余震観測班としては最初である．観測開始まで，本震より約一週間経過していたにもかかわらず，高倍率の地震計を用いたため，かなり多数の余震を記録することができた．勝原と高鷲村における観測，および郡上八幡の三点観測は，それぞれの担当者が題を改めて報告することにした．

33. Seismological Observations of the Kita Mino Earthquake, August 19, 1961 and its Aftershocks.

By Takahiro HAGIWARA,
Earthquake Research Institute,
and Ichiro KAYANO,
Graduate School, University of Tokyo.

Seismological data of the Kita Mino earthquake occurred at about 14^h33^m J.S.T. (05^h33^m G.M.T.), August 19, 1961, in the central part of Japan are as follows:

$05^h33^m32^s$ 36.0°N, 136.8°E d: 40 km M: 7.2 (J.M.A.)
$05^h33^m30.2^s$ 36.0°N, 136.5°E d: about 17 km M: $7^1/_4$ (U.S.C.G.S.)

The epicentre determined by the J.M.A. is more reasonable from macroseismic data and aftershock observation, but even that is open to discussion.

Observational data of the initial motions at the stations of the Earthquake Research Institute (in Table 2) are plotted in Fig. 3 with the travel time curves by Wadachi, Sagisaka and Masuda. This figure seems to suggest that the focal depth is small. The epicentre of this shock lies near the shot point of the Miboro explosion which was conducted by the Research Group for Explosion Seismology, so the observed values are plotted in Fig. 4 with the travel time curves derived from that given by the R.G.E.S.. This figure, too, supports that the focus is very shallow, even if there are some errors in the determination of the epicentre and the origin time.

The Anderson-Wood seismograms at Mt. Tsukuba (shown in Fig. 5) gives the magnitude $6-6^1/_4$, which is remarkably small. From Fig. 10, we get $M_k=4.7$, which is reduced to $M=7.2$[1].

The epicentre lies in a mountaneous region, so there are few casualties and little property damage, though there are landslides and cracks in many places.

Observations of aftershocks were carried out at Kadohara (August 25—September 20), Hirugano (September 8-16) by the Seismograph HES 1-1 and tripartite observations were carried out at Hachiman (August 26—September 20).

1) M_k: Kawasumi magnitude is determined as the number representing the intensity on the Japanese scale (which runs from 0 to 6) at an epicetral distance of 100 kilometres. Prof. Kawasumi gave the following relation:

$$M_k=2M-9.70$$

地震研究所彙報
第39号(1961) 881-894 頁

34. 北美濃地震余震観測
——勝原(カドハラ)および蛭ケ野における観測

地震研究所 表 俊一郎
唐鎌郁夫
中島直吉
斎藤貞夫
東京大学大学院 地球物理専門課程 茅野一郎

(昭和36年9月26日，昭和36年10月24日発表—昭和36年10月31日受理)

1. 緒　　言

1961年8月19日午後2時33分頃，福井，石川，岐阜三県の県境に近いあたりにかなりの被害を伴つた地震が発生した．気象庁から発表された所によると，発震時 1961 VIII 19d 14h 32m 32s 頃，震央 36.0°N, 136.8°E, 深さ約 40 km, M=7.2 である．この地震の余震を観測するため，主として経費の都合で，地震研究所から余震観測班2班を派遣することが定められ，われわれはその一班を受持つて福井県大野市勝原において，宮村その他[1]が他の一班を受持つて岐阜県郡上八幡において，それぞれ観測を行うこととなつた．しかし今回の余震観測を行うにあたつては，余震発生回数が比較的に少ないことが本震直後の現地からの報告で知らされていたので感度の高い HES[2] 3成分を携行することとし，25日から勝原において観測が開始された．さて実際に観測を開始してみると，まだ日々相当数の余震が記録されることが判明したので，少くともう一点観測点を設置することが必要且つ可能であるとして蛭ケ野に観測点を設置することとなり9月13日から観測が開始された．

勝原観測点の余震観測は八幡観測点と同様9月20日迄継続された．しかしこの間9月17日台風8号がこの地方に来襲したため2日間交流電源の供給が停止された．勝原では直ちに停電対策装置が始動して観測が継続されたが，停電の時間が長かつた為蓄電池の電圧降下により約1日間欠測を生じた．蛭ケ野観測点は上記台風のため，観測を行つていた家屋が大被害をうけて17日以降の観測は中止しなくてはならなかつた．

勝原観測点は唐鎌，中島の両名で観測を始めた．9月6日以降新らたな観測点を増設するため唐鎌は蛭ケ野へ移つた．蛭ケ野観測点の地震計設置には斎藤が協力した．観測結果の解析には茅野，表が当つた．

観測結果を読み取つて余震震央をきめるためには八幡観測班の協力を得た．すなわち八幡のモニター用地震計の記象から得られた全部の地震の発震時及びp-s時を提供していただいた．

今回の地震に際して金井，長田[3]は地盤の振動特性を研究するため石徹白(イトシロ)で8月25日

1) 宮村摂三，堀実，安芸敬一，松本英照，安藤誠一　地震研究所彙報 **39** (1961), 895～908.
2) T. HAGIWARA, *"HES" electromagnetic seismograph and its recording system*, Earthq, Res. Inst., Univ. Tokyo., 1960.
3) K. KANAI and K. OSADA, *Bull. Earthq. Res. Inst.*, **39** (1961), 943～951.

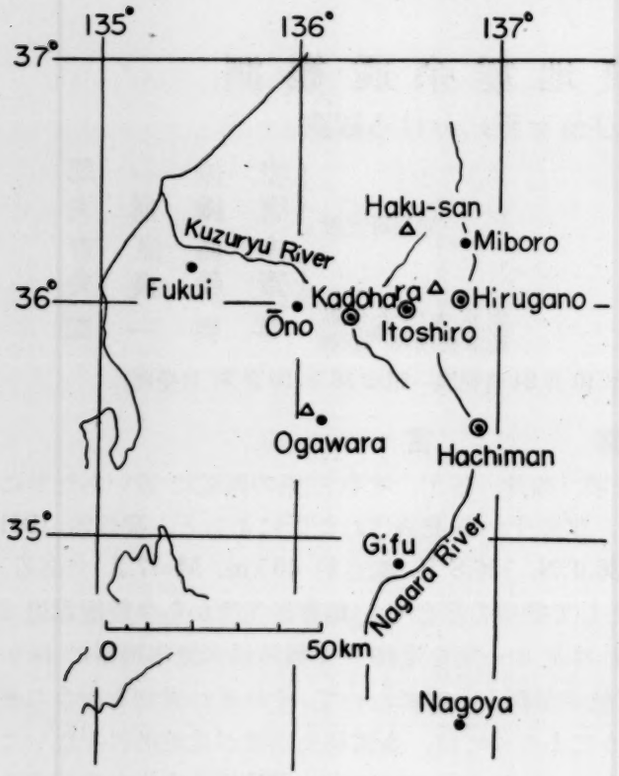

Fig. 1.

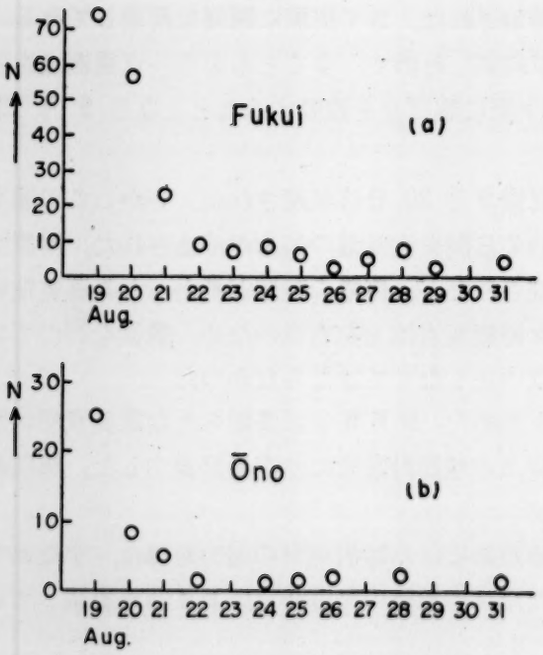

Fig. 2. (a) Daily number of aftershocks recorded on the seismograms at the Fukui observatory of J.M.A.
(b) Daily number of felt aftershocks at Ōno. (By the courtesy of J.M.A.).

4) 三宅恒夫 oral communication.

—31 日に至る間石本式加速度計により余震観測を行つた．その観測結果からも発震時とp-s時とがわれわれのために提供せられたので，これらの貴重な資料を加えてここに余震の震央を求めることとした．これら観測点の位置は第1図に示されている．

2. 余震の数の消長

北美濃地震に伴う余震について，われわれの観測班が記録し得たものは8月25日以降のものである．従つて本震直後4～5日間の余震発生の有様はわれわれの観測からは知り得ないこととなるが，この期間の余震の数の消長は福井気象台[4]が福井及び大野において得ている資料を引用することにより知ることが出来る．本震震央からほぼ 52 km の福井市において福井気象台の14年式簡単微動計（自己周期約2秒，倍率約55倍）の記録から求められた毎日の余震回数は第2-a図に示す通りである．また震央から略々28 km の所には福井気象台管下の大野通報所が置かれていて，本震直後人体感覚のあつた余震は，業務として忠実にその発震時が記録に止められていたので，1日毎の有感覚地震の数は充分の信頼度をもつて知ることが出来た．その結果が第2-b図に示されている．第2図 a, b 共に各1日は暦の上で0時から 24 時までであるから8月19日の余震数は本震（14 h 30 m

頃) 後から 24 時まで約9時間の間の回数をあたえるものとなる.

本震の magnitude は JMA により 7.2 と発表せられている. この余震の発生回数を, M=7.3 であつた福井地震[5] (28, June, 1948) の場合と較べると今回の地震に伴つて発生した余震の数が著るしく少なかつたことは特に注目に値いする. また余震の減り方も極めて急激であつて震央から 28 km 位しか距つていない大野においてさえ大地震後僅か4日目にすでに有感覚余震の数が1日1回位となつてしまつていることには特に注意がひかれる.

われわれが勝原及び蛭ケ野において観測した余震の1日毎の回数は**第3図 a, b** に示す通りである. なお比較のため大野における有感覚余震の数が同じ図に×印で記入されている. これらの図をもとめるにあたつては p-s 時のよみとれなかつたような小さな地震は数えられていないが, われわれの観測点においては地震計の倍率をほぼ 1 万倍にして観測をしているので, 本震後8日目にあたる 28 日においてもなお1日約 60 個の余震が記録せられたことが知られる.

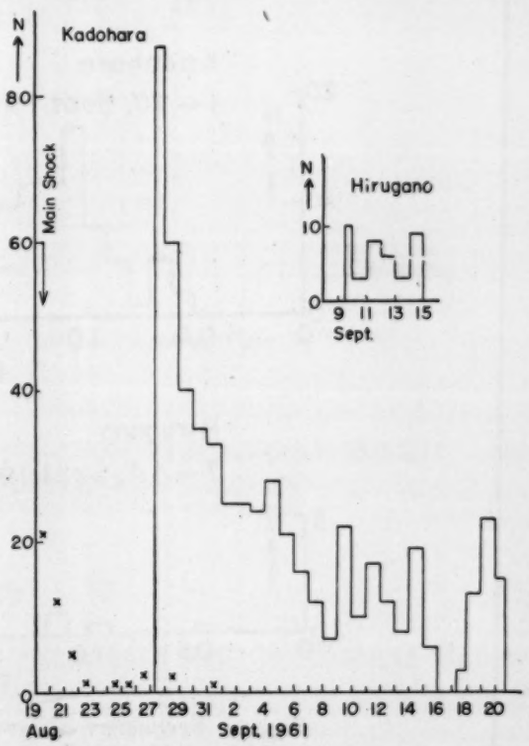

Fig. 3. Daily frequency of aftershocks recorded at Kadohara and Hirugano stations, and crosses indicate daily frequency of aftershock felt at Ono.

3. p-s 時頻度分布

勝原で観測された余震の中 p-s 時が明らかに読みとられたものについて p-s 時頻度分布を求めた結果が**第4図 a, b** に示されている. a は観測を始めた8月 25 日から 31 日までの 7 日間, b は 9 月 1 日から観測の終つた 20 日までのものである. a, b に共通に見られる特徴として次のような点をあげることが出来るであろう. (1) p-s 時の頻度極大は 1.0 sec の所に見られる. (2) p-s 時の短い地震については, 0.5 sec 位の余震が a, b いづれの期間についても 2—3 個宛は観測されている. (3) p-s 時の長い方のものについては, 3 sec 位までの余震は非常に多いが 4 sec, 5 sec 位のものになると僅かに 1～2 個位宛観測されているに過ぎない.

a, b 各期間の差違として目立つ点は, 後の期間 (b) で p-s 時 1.8 sec あたりにもう一つ極大が現れてきている点である. 本震後日数が経つにつれて p-s 時の長い地震が幾分多くなつたと考えられるようである. 勝原から見て余震震源までの距離が遠いものが多

5) S. Omote et al., *The Fukui Earthquake of Jane 28, 1948* (1950), 37-78.

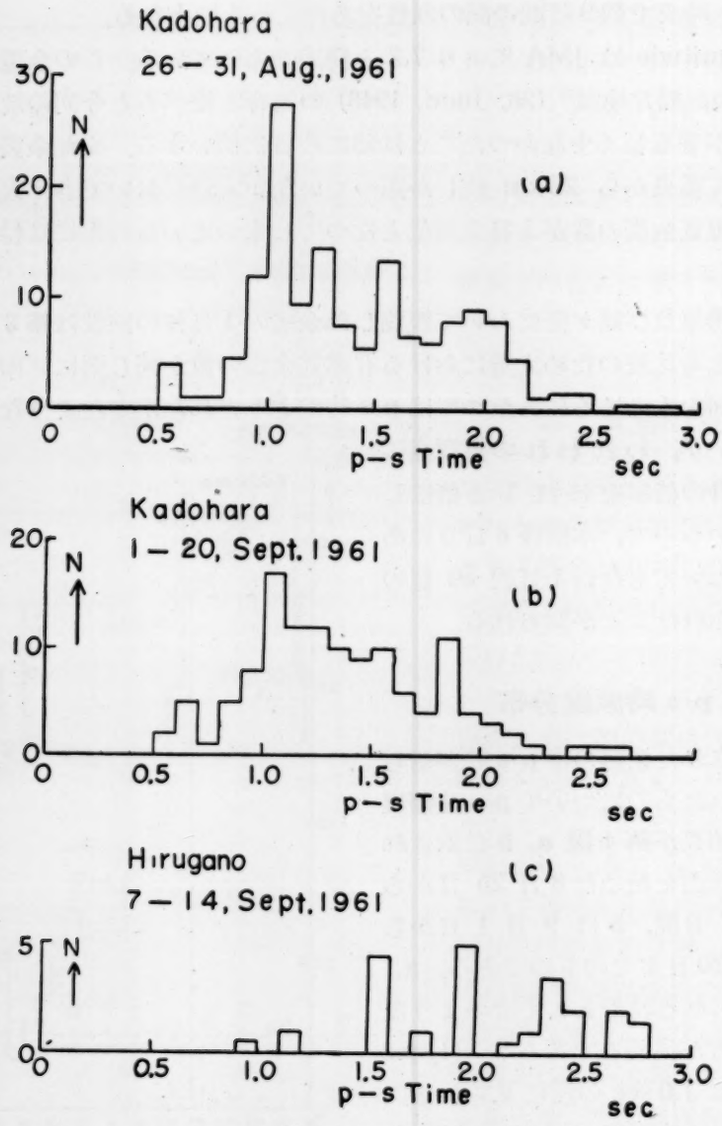

Fig. 4. Frequency diagram of the p-s duration times

くなつたことを意味する訳であるが震央距離が大きくなつたものであるか震源の深さが深い地震が多くなつたことによるものであるかはこの図からは明らかでない.

蛭ケ野の観測から得られたp-s時の頻度分布図が第4図cに示されている. ここは観測期間が短かかつたため p-s 時 頻度も統計的議論に耐える程充分な数に達していないが, 勝原観測点にくらべp-s時の長い地震が多いことは確かである. p-s時の頻度極大は約2sec 位の所にあるといえるであろう.

勝原, 蛭ケ野のp-s時と較べるため, 八幡, 石徹白のp-s時頻度分布が第5図 a, b に示されている. これを見ると八幡ではp-s時 4～5 sec のものが非常に多いことが明らかに見られる. 勝原で多く見られた様な 1sec 位の短い p-s 時をもつ地震がほとんど観測

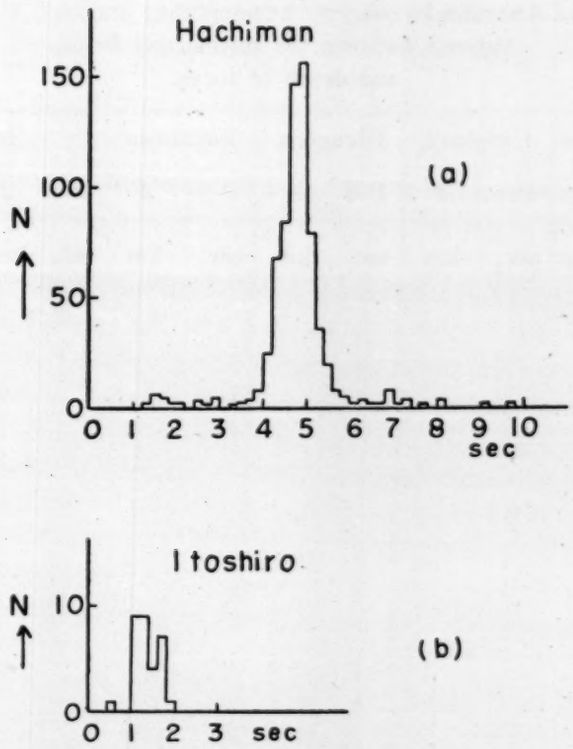

Fig. 5. Frequency diagram of p-s duration time
(a): after Miyamura et al.

されていないことは著るしいことである．これとは反対に石徹白の p-s 時頻度図は 1 sec 付近のものが大部分であつて八幡のものと著るしい対照をなしている．

4. k の 値

すでにのべたように，今回の余震観測に際しては，勝原及び蛭ケ野においては HES 地震計により約1万倍の倍率で，八幡においては磁気テープ地震計により約 10 万倍の倍率で，また石徹白では短期間石本加速度計により約 150 倍の倍率で観測が行われた．これらの中，いづれか3ケ所の観測点で p-s 時が明瞭によみとられたものをひろい上げた結果が**第1表**に示されている．

第1表をみると，観測点相互の間に観測期間のズレがあるため4つの観測点で同時に観測されている余震はない．従つて3点で観測された p-s 時から震源を求めなくてはならないということになる．このためにはいわゆる大森係数 k の値を適当な仮定の下で推定しなくてはならない．k の値はすでに多くの余震の場合について求められていて一般には裏日本の地震の場合には比較的大きな値となることが特徴的であることが知られている．しかし場所々々でいくらかずつ異つた値を与えているので付近に起きた他の地震の場合の値をそのまま用いるという訳には行かない．

Table 1 Aftershocks observed at temporary stations: P-S time, distance between the station and focus, and depth of focus.

Earthq. No.	Origin time	Kadohara		Hirugano		Hachiman		Itoshiro				focal depth
		P-S	Δ	P-S	Δ	P-S	Δ	P-S	Δ	P-S	Δ	
	VIII d h m	sec.	km	sec.	km	sec.	km	sec.	km	sec.	km	km
1	27 19 26	1.65	14.7			4.4	38.2			1.0	8.9	7.6
2	28 20 22	1.7	15.1			4.62	40.1	1.0	8.9	1.05	9.4	7.6
3	〃 21 31	1.3	11.6			4.75	41.3	1.1	9.8	1.0	8.9	5.1
4	29 00 49	1.2	10.7			4.44	38.5	1.0	8.5	1.2	10.7	6.7
5	〃 02 13	1.2	10.7			4.77	41.4	1.3	11.6	1.3	11.6	6.7
6	〃 09 33	1.9	16.9					1.0	8.9	1.0	8.9	9.0
	IX											
7	9 13 52	1.0	8.8	2.55	22.7	4.8	40.8					6.8
8	〃 14 46	1.3	11.6	2.2	19.6	5.4	38.2					7.5
9	〃 19 06	1.9	10.9	1.7	15.1	5.1	47.1					
10	10 00 25	1.5	13.4	2.2	19.6	4.9	42.6					2.3
11	〃 23 51	1.7	15.1	2.1	18.8	4.7	40.8					7.9
12	11 01 40	2.25	20.0	1.8	16.0	3.8	32.8					12.0
13	〃 09 47	1.15	10.2	2.25	20.0	4.4	38.2					6.7
14	〃 13 10	1.5	13.4	2.1	18.8	4.5	39.0					6.1
15	12 04 57	1.5	13.4	2.4	21.4	4.8	41.7					9.0
16	〃 05 16	0.9	8.0	2.1	18.8	4.6	40.0					0
17	〃 14 05	1.0	8.9	2.0	17.8	4.4	38.2					0
18	〃 17 45	1.3	11.6	2.9	25.8	4.3	37.3					10.0
19	〃 17 48	1.1	9.8	2.6	23.2	4.4	38.2					8.3
20	13 12 48	1.1	9.8	2.5	22.2	4.9	42.9					5.4
21	14 02 30	1.2	10.7	2.2	19.6	4.9	42.6					0
22	〃 16 04	1.3	11.6	2.1	18.7	4.3	37.3					6.9
23	〃 20 51	1.6	14.2	2.4	21.4	4.25	31.8					11.4

k の値はその場所の地下構造とp波及びs波の速度とが知られれば直ちに求めることが出来る．幸にして，今回の地震域は御母衣(ミボロ)大爆破が行われた際に爆破地震動研究グループ[6]により観測が行われた地域に当つているので波の伝播速度については充分信頼の置ける値が得られているばかりでなく，大爆破観測のときの観測点，石徹白，大河原，岐阜等は第1図にみるようにわれわれの余震観測網の付近に分布しているので余震観測地域の地下構造についてもかなり確かな推定を行うことが出来ることとなる．爆破地震動観測

6) The Research Group for Explosion Seismology, *Bull. Earthq. Res. Inst.*, **39** (1961), 285-326.

T. MIKUMO, M. OTSUKA, T. UTSU, T. TERASHIMA and A. OKADA, *Bull. Earthq. Res. Inst.*, **39** (1961), 327-349.

の結果によると，概略的にいえばこのあたりでは表面に薄い 5.5 km/sec の層がありその下に 6.0 km/sec の比較的厚い層がみられる．ことに御母衣の近くでは 5.5 km/sec の第1層の厚さは極めて薄くて，石徹白では略々1 km，大河原ではこの層はなくなつていて 6.0 km/sec の層が直接地表まで出ていると考えられている．従つてわれわれの場合においても勝原，蛭ケ野などでは5.5 km/secの第1層はなくなつていて6.0 km/sec の層が直接地表にまで出ているものと考えることとする．この p に対する s の速度として，先ず始め

Fig. 6. Seismograms of aftershocks of the Kita Mino Earthquake recorded at Kadohara by the seismograph HES 1-1 (N-S)
(T_1: 1.0 sec, T_2: 1.0 sec, h_1: 1.0, h_2: 1.0)
A) 29-30 August, 1961.
B) 30-31 August, 1961.

にこの地域に完全弾性体の仮定が成り立つと考えてポアソン比 σ を $\sigma=1/4$ とおいてs波の速度 Vs をもとめ

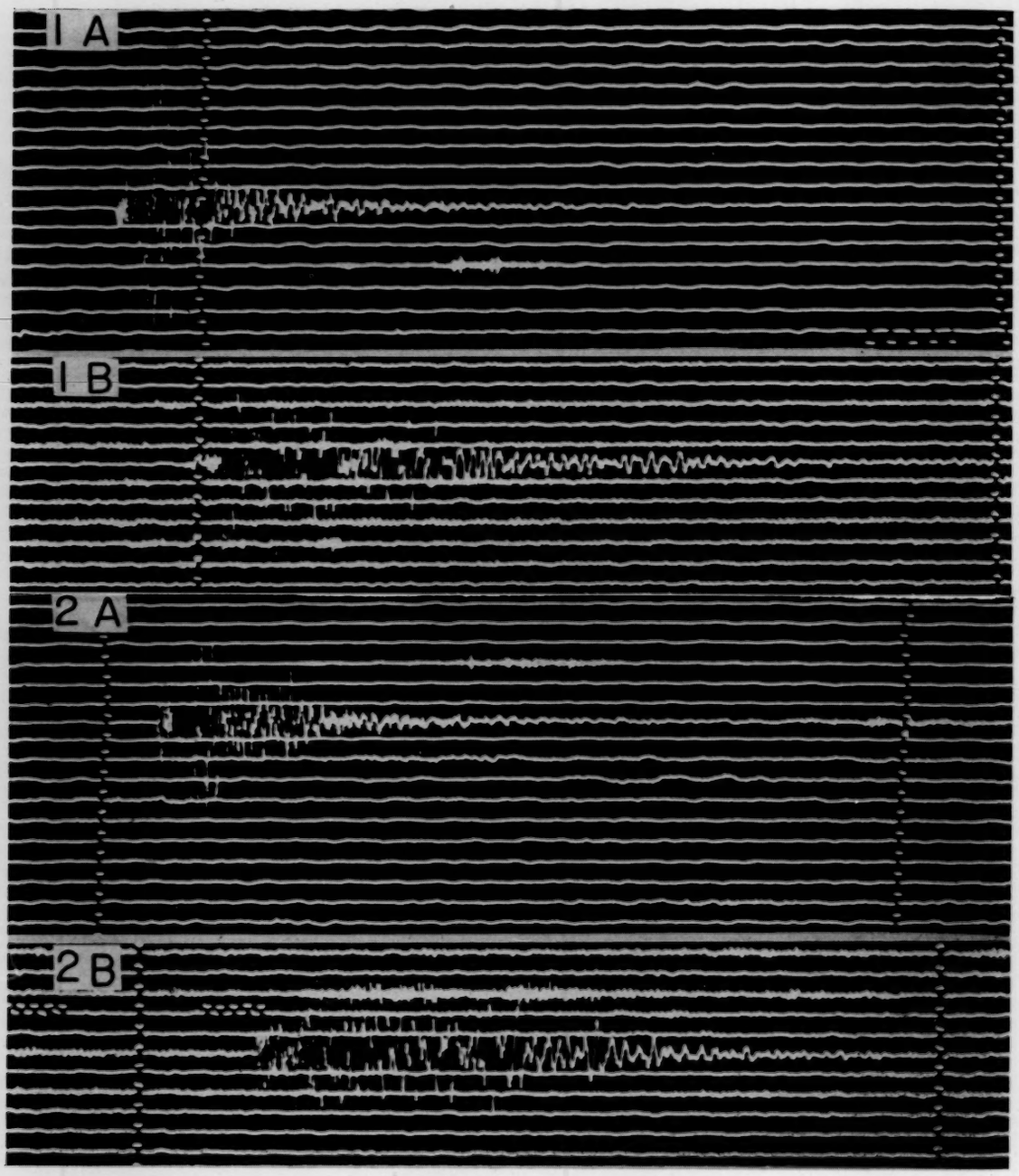

Fig. 7. Seismograms of the aftershocks recorded at Kadohara (A) and Hirugano (B).
1) 05 h 16 m JST, 12 September, 1961
2) 17 h 48 m JST, 12 September, 1961

$$Vs=3.5\ \mathrm{km/sec}$$

と考え，この2つの速度を組合せて k の値を求めれば

$$k=8.24$$

となる．さてこの k を用いて震央距離を求めようとしたのであつたが，例えば第1表No. 16の地震についてみると，勝原の p-s 時 0.9 sec，蛭ケ野の p-s 時 2.1 sec となつていて両者の和は僅かに 3.0sec にしかならない．これに対して勝原，蛭ケ野間の直距離は 26.4 km であるので，上に求めた k の値をとることは，少くともこの地震に関しては不合理なこととなる．しかし第7図 a の写真に見るようにこの地震の p,s は極めて明瞭であるので，p-s 時として別の値を与えることは困難である．更に No. 17 の地震についてもこれと同様なことが認められる．従つてこのような矛盾を取り去るためには，どうしてももう少し大きな k の値を与えなくてはならないこととなる．しかし p の値はこれを変更する根拠に乏しいので上に仮定した s の値を再び検討しよう．上において s の値を推定するにあたつては $\sigma=1/4$ と仮定している．地表近い岩石でこの仮定をおくことが無理であることはすでに多くの著者が指摘しているところである．例へば吉山[7]は近畿地方の浅い地震を調べた際に Vp/Vs の値として，完全弾性体の場合に期待される値 1.73 よりは相当に小さい値が得られることを報告していて，その際に得られた値として $Vp/Vs=1.67$ を与えている．今われわれもこの値を借用して $Vp=6.0\ \mathrm{km/sec}$ に対する Vs の値を求めると

$$Vs=3.6\ \mathrm{km/sec}$$

を得る．これらから k を求めれば

$$k=8.9$$

となる．われわれはこの k の値を用いて震源を作図的に求めることとした．

しかし第1表の地震について，それぞれの観測点で求められている p-s 時にこの k の値を乗じて震源距離を算出し震央を作図してみると，k の値が大きくなつたため，八幡からの震源距離が増大して勝原及び蛭ケ野をそれぞれ中心としてそれぞれの震源距離を半径とする2つの円が交わることによつて出来る弦が，八幡を中心とする円と交わらないという場合がいくつも生じてくるのが見られた．

このようなことが生じた原因としてむろんいろいろの理由が考えられるであろう．その1つとして，われわれが p-s 時として読み取つているものが各観測点について同一の位相であるか否かの問題がある．しかし現在の資料からはこれ以上に立ち入ることは難かしいので p のあとの大きな明瞭な位相の始めを s の始めと考えることとした．p-s 時をこのように定義する限りにおいては，観測された p-s 時から八幡の震源距離を算出するにあたつては，勝原，蛭ケ野の場合に仮定したような簡単な地下構造では都合が悪いと考えるのが至当であると思われる．しかし，御母衣大爆破の観測点は御母衣一八幡の方向には配置せられていないのでその結果から直接八幡の地下構造を知ることは出来ないが，八幡から南々西約40 km の岐阜では御母衣爆破の観測が行われていて 5.5 km/sec の層が 9.9 km の厚さを持つていることが知られている．またこの地域の一般的な傾向として，すでに前に

7) R. Yoshiyama, *Bull. Earthq. Res. Inst.*, **35** (1957), 627-640.

もふれたように 5.5 km/sec の第1層は御母衣に近い所では極めて薄いかまたは所によつては全然ない位であるが南に下るに従つて次第に厚くなつているようである．八幡も長良川の川筋に当つているのでここに 5.5 km/sec の層が適当な厚さで存在していると考えることは無理な推察ではないと考えられるであろう．

今八幡において一様な厚さ H をもつ第1層があるとき，ほぼ同じ位の深さの所で起つた地震を観測した場合を考えてみよう．この時のp波の走時を T_p とすれば T_p は次のようにかくことが出来る．

$$T_p=\Delta/V_{p2}+D_{vp1,vp2} \tag{1}$$

ここに

Δ: 震央距離

V_{p1}: 第1層のp波速度

V_{p2}: 第2層のp波速度

$D_{vp1,vp2}$: H なる厚さで V_{p1} の速度をもつ平行層が V_{p2} なる層の上に存在していることに基くp波による delay time.

同様にs波についての走時を T_s とすれば上のp波の記号をsで置きかへたと考へれば T_s は次のようにかくことが出来る．

$$T_s=\Delta/V_{s2}+D_{vs1,vs2} \tag{2}$$

八幡におけるp-s時を τ とおけば (1), (2) を組合はせることによつて

$$\tau-(D_{vs1,vs2}-D_{vp1,vp2})=\Delta/k \tag{3}$$

すなわち

$$\tau-H\cdot\cos i(1/V_{p1}-1/V_{p2})=\Delta/k$$

ここに

$$\sin i=V_{p1}/V_{p2}=V_{s1}/V_{s2}$$

$$k=1/(1/V_{p2}-1/V_{p2})$$

(3) の左辺括弧の中は，第 1,2 層の p, s の速度及び層の厚さ H により定まる常数である．V_{p2}, V_{s2} に対してはすでにのべた 6.0, 3.6 km/sec の値を用いることとし，第1層のs の速度 V_{s1} に対しては，$V_{p1}=5.5$ km/sec, $V_{p1}/V_{s1}=1.67$ によりきまる値を用いるとすれば，$V_{s1}=3.3$ km/sec を得る．H としてどのような値を採用するのが最も適当であるかについてはわれわれは何等の資料をもつていない．いずれ八幡観測点の解析が宮村研究室において行われるであろうから，converted wave の計測またはその他の方法で第1層の厚さについて何等かの根拠ある推論が得られることを期待するものであるが，現在の所は八幡から約 40 km 南々西にある岐阜で第1層の厚さ 9.5 km ということが知られているだけにすぎないので，ここには仮りにその半分の厚さ $H=5$ km と仮定して (3) 式の括弧の中の数値を計算することとした．このようにして補正量として求められた値は

$$(D_{vs1,vs2}-D_{vp1,vp2})=0.25 \text{ sec}$$

となつた．

すなわち八幡観測点で得られている p-s 時については上に述べたような仮定を許す限りにおいては，観測値から 0.25 sec を差引くことにより表面層の影響を取除いて考えてよいこととなつた訳である．

上の計算を行うに当つては，八幡の地下構造として第1層が水平成層であること，震源の深さが第1層の厚さと殆ど同じ位であることを仮定している．実際の場合においては，上の仮定が正確に充たされている訳ではないであろうが，第1層と第2層との境界面が多少の傾斜をなしている程度ではこの補正量に大きな影響をあたえることはない．又この境界面の傾斜が特に急であると推定される理由は全くないので今の場合水平成層を仮定しても差支えないであろう．震源の深さについては，後にのべるように，今回の余震では震源の深いものでも 15 km 位であるので余震域からほぼ 50 km 位距つている八幡観測点の補正量をもとめる場合には震源の深さが変化しても補正量はほとんど影響をうけないと考えてよいであろう．従つて全ての余震について八幡の p-s 時には上にのべた補正量を加えることとした．この補正を加えたものに k を乗じたものが第1表に八幡の震源距離として示されている．

5. 震 源 分 布

このようにして第1表に各観測点毎に求められている震源距離に基いて，作図的に求められた震央が第8図に示されている．第8図において震央を示す印の肩の所にある数字はその余震の震源の深さを示すものである．三角の印は正確には3つの円が交わらなかつたものであり震央位置の誤差も丸印のものに較べ大きいと考えられると同時に震源も非常に浅いと考えなくてはならない．第1表最後の欄震源の深さを示す所で深さ 0 km と記されているのは多くはこの種の地震である．

×印は勝原，蛭ケ野，八幡から求められた震央，＋印は石徹白の記象を参照して求められた震央である．石徹白の観測は別の観測を主目的としたものであつたので紙送り速度も 2 mm/sec であり倍率も他に較べて低かつたため p-s 時の精度も幾分劣ると考えねばならないであろうから，他のものと区別するため＋印で示されている．本震の震央は大きい×印で示されている

これらの震央分布図を見て気付かれる主な点を次に列記することとする．ただし3点観測を行い得た期間が短かかつたので第8図に見られるものが余震全体の傾向を示すか否かについては疑問がある．特に余震域の問題を考える際にこれだけで充分な資料であるとはいい得ない恨みがある．しかし大体の傾向はこの図にあらわれていると考えられるので主な点を以下に考察することとしよう．

i) 余震の震央は北西は打波川，北東は小池，石徹白を結ぶ線，南は勝原，石徹白の線で囲まれる地域の中にほとんど集つている．この地域は本震による震害が最も大きかつた地域に当つている．しかし本震による被害の著るしかつた地域は更に北にのびて白山南麓もその中に含まれていたようであるが，われわれの観測からは白山南麓には余震は起つてい

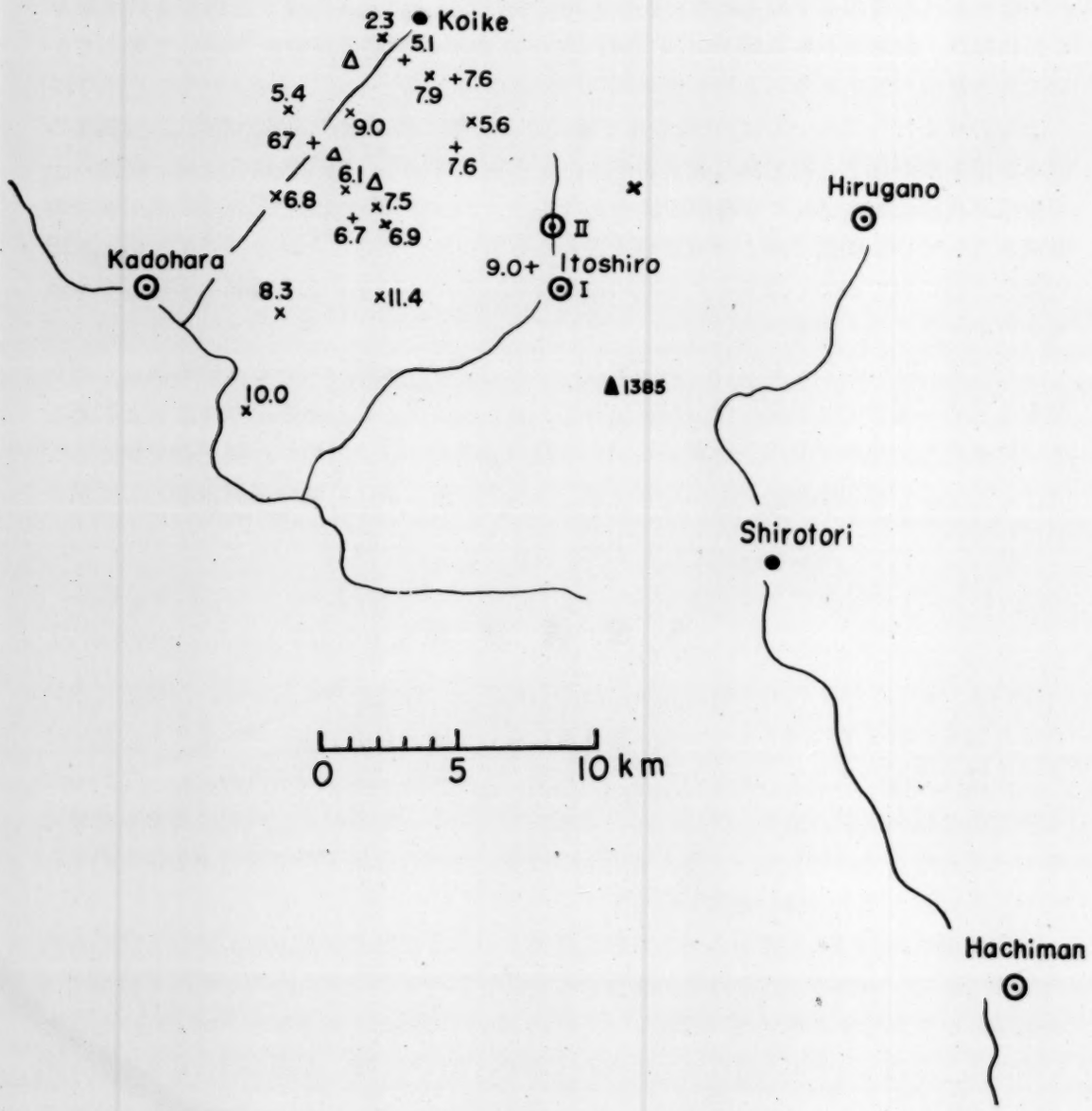

Fig. 8. Epicentres of aftershocks
× Epicentres determined from the stations Kadohara, Hirugano, Hachiman.
+ Epicentres determined from the stations Kadohara, Hachiman and Itoshiro.
Thick cross represents the epicentre of the main shock.
Figures attached to the marks indicate the focal depth in km.

るのが見られなかつた.

ii) 次に注目されることはこの余震域が著るしく狭いことである. 先きにものべたようにここに得られている地域が余震域の全域を尽くしているとはいい得ないが大体の傾向はあらわすものと考えられるとするならば, JMA 発表による本震の magnitude 7.2 と考えあわせてこの余震域が著るしく小さいことは注目に値する.

iii) 震源の深さについては，深い所に起つたものが見られなかつたことも特徴の一つである．本震の深さは 40 km と発表せられているが，われわれの観測した余震では 15 km 以上の深いものは見られなかつた．

iv) この余震分布で特に注目せられることは深さ数粁またはそれより浅いと考えられるような極めて浅い余震が多数発生していると考えられる点である．しかもこの浅い余震は余震域の中の北部すなわち小池—石徹白をむすぶ線に近い地域に多く南に行くに従つて浅い地震は発生しなくなるようである．なお北部には浅い地震と同時にやや深い余震も同時に発生していることも附言しておかなくてはならないであろう．

v) これらの余震の発震機構については別の機会にゆずりたいと思うが，勝原の記録については引波で始まつているものが多いことが気付かれた．

謝　　辞

これらの観測を行うにあたつて種々便宜を与へられた福井県大野市，岐阜県大野郡高鷲村の当局の各位に厚く御礼を申し上げる．余震回数の資料を引用することを許された福井地方気象台三宅台長に御礼を申し上げる．HES の設置について御配慮をいただいた萩原教授に，余震震央をきめるために観測資料を提供して下さつた宮村摂三，安芸敬一氏を始め八幡観測点の観測員各位，並びに石徹白の観測結果を使用することを許された金井清，長田甲斐男両氏に，厚く御礼を申し上げる．蛭ケ野観測点設置に協力された神沼克伊氏，記録の読み取りに協力された前田良弘氏にも厚く感謝する．

34. Aftershocks of the Kita Mino Earthquake of August 19, 1961.

—Observations at the Kadohara and the Hirugano stations—

By Syun'itiro OMOTE, Ikuo KARAKAMA, Naoyoshi NAKAJIMA,
Sadao SAITO,
Earthquake Research Institute,
and Ichiro KAYANO,
Graduate School, The University of Tokyo.

For the purpose of carrying out the observations for the aftershocks of the Kita-Mino earthquake of August 19, 1961, we set up two temporary stations at Kadohara and Hirugano. In cooperation with the Hachiman station which was also installed temporarily for the observation of the aftershocks by Miyamura et al, a net for the observation of the aftershocks began its operation on 25th August and closed its activity on 20th September. The ocations of these stations will be seen in Fig. 1. Frequency diagrams of the p-s duration times for the shocks observed at these stations are shown in Figs. 4, 5 and 6. Maximum frequencies of the p-s duration times are 1.0, 1.2 and 4 sec for Kadohara, Hirugano and Hachiman respectively.

As there are only three stations that give the p-s duration times for each shock, difference

time methods are used for determining the focus of each shock. Now, the distance Δ between a station and the focus can be expressed by a simple formula $\Delta=kt$, where t represents the p-s duration time, k a constant value, which is usually named as the Omori constant. It is necessary to give the assumed numericals for the k, in order that we obtain the location of hypocentres from the observed times at three stations. Fortunately, the area of our seismic net was traversed by a line of observation stations for the large explosion at Miboro, so that the crustal structure of the area covered by our seismic net was partly known and the velocity of the P waves was given as 6.0 km/sec, whereas that of the S waves was not reported. While, the ratio of the P velocity V_p to the S velocity V_s is studied by Yoshiyama basing his studies on the observations of natural earthquakes that occurred in the central part of Japan. Referring to his paper, we assumed V_p/V_s would be 1.67, then it is apparent that the k is given as $k=8.9$. It may be seen that this value is somewhat largar compared with the values assessed in other earthquakes that occurred in the regions not far from the Kita Mino area. Smaller values of k, however, would give greater difficulty in providing explanations for the observed data shown in Table 1, especially for the lines of the earthquakes Nos. 16 and 17.

It was also necessary to make some estimations on the structure of the uppermost layer under the Hachiman station by which we may get reasonable locations for the epicentres. The p-s duration time observed at the Hachiman station is reduced by 0.25 sec in order that the effect of the surface layer be eliminated, and this reduced figure is multiplied by the k.

Under these reasonable assumptions, 25 shocks are located and the distribution of the foci is seen in Fig. 8. The period in which all the three stations operated at the same time was so short that it may be going too far to say that the epicentres in Fig. 8 cover the whole area in which the aftershocks has taken place, it would, however, be safe to say that the epicentres in Fig. 8 would represent the general trend on the distributions of the foci of the aftershocks that accompanied the Kita Mino earthquake. One of the most remarkable points to be noticed from this figure is that the area covered by the epicentres is limited in such a small area that it seems that the aftershock area of the Kita Mino earthquake will give a notable exception for application of the formula that defines the area of epicentres of aftershocks from the magnitude of the main shock. Another point to be noticed is that the depth of the foci of these aftershocks are so shallow and no shock seems to be located below the level of 15 km from the surface of the earth.

地震研究所彙報
第39号 (1961) 895-908頁

35. 北美濃地震余震観測

——岐阜県八幡町における観測——

地震研究所 宮村摂三 堀実一 安芸敬一 松本英照 安藤誠一

(昭和36年9月26日発表—昭和36年10月31日受理)

1961年8月19日岐阜，福井，石川3県境界付近に発生した北美濃地震にともなう余震群を，本震震央南南西30 kmの岐阜県郡上郡八幡町において8月27日より約1ケ月間磁気テープ記録による多成分観測装置によつて観測した．辺長1 kmにちかい3点観測によつて初動の到来方向，みかけの速度をもとめ余震群の分布を現地でただちに推定することができたが，それによると余震域は本震震央の西方にひろがるごくせまい面積をしめ，深度は0～25kmの地殻内にかぎられることがわかつた．余震域の面積A(km^2)は本震の規模(M=7.2)から宇津・関の公式 $\log A = M-4$ で推定されるものにくらべいちぢるしくせまい．なお余震群以外の局地的小地震が観測されたことも注目にあたいする結果である．

1. 序　　言

1961年8月19日14時33分，岐阜，福井，石川3県境界付近に発生した**北美濃地震**にともなう余震活動は，ほぼ同程度の規模とおもわれる三河地震 (1945. 1. 13) のものなどにくらべ，かなり不活溌のようであつた．したがつて**余震観測**は当然高感度地震計によりおこなわれなくては有効でないとおもわれた．しかも種々の事情で震源位置の決定をおこなうにたる多数の観測班を出動させることも不可能であつた．

このようなばあい，比較的せまい範囲におかれた多数の地震計の(Seismometer array)集中記録をおこない，各点の地震動の対比により波動の到来方向，みかけの速度，振動面など各種の情報をもとめる，いわゆる**波動相関法観測***を利用すれば，一観測班でもある程度余震群の活動状況を推定できる．筆者ら[1,2,3]はすでにこの方法を無線地震計と磁気テープ記録装置とをもちいて常時微動および地震動の研究に利用してきたが，その後これらの装

* 3点観測法 Tripartite Observation Method はこのもつとも簡単な例であり，ソ連でおこなわれている КМИЗ (Корреляционные Методы Изучения Землетрясений)，米国におけるあたらしい観測所 (Wichita Mountains Seismological Observatory) のものなどはその模範的な例である．

1) K. Aki, M. Tsujiura, M. Hori, and K. Goto, *Bull. Earthq. Res. Inst.*, **36** (1958), 71～98.
2) S. Miyamura and M. Tsujiura, *Bull. Earthq. Res. Inst.*, **37** (1959), 359～374.
3) K. Aki and M. Tsujiura, *Bull. Earthq. Res. Inst.*, **37** (1959), 207～232.

置に種々改良をくわえ，トランジスター化した無線地震計用端局装置とあたらしい無終端磁気テープ利用のひきがね式磁気テープ記録装置を試作した[4]．これらの装置は余震観測のような野外臨時観測のために軽量可搬型につくられたものではなかつたが，無線部分をのぞいて，送受信端局装置を直結し，あたらしい磁気テープ記録装置とともにもちいて，観測に出動，波動相関法による余震観測をこころみることにした．

2. 観 測 場 所

観測場所の選定は波動相関法観測においては従来の余震観測のばあいとちがいその観測点を余震域内にえらぶことは有利でない．というのは，そうすると，ちかい，ちいさい地

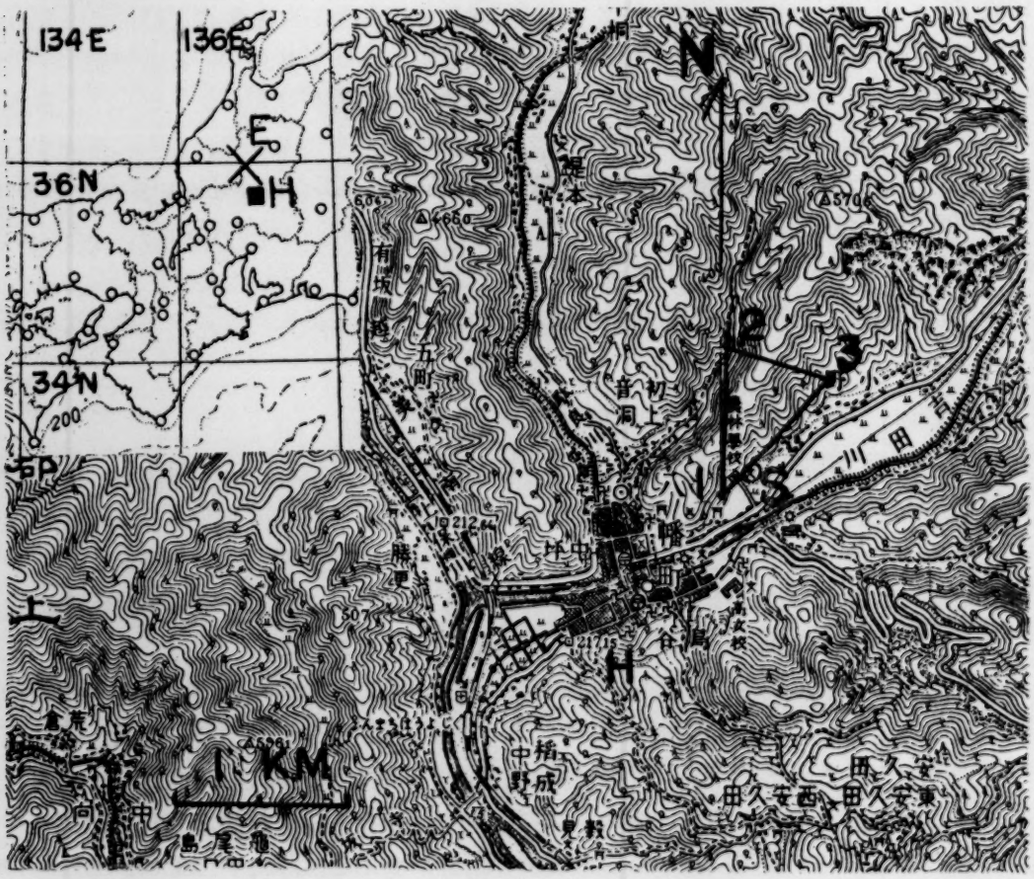

Fig. 1. Location map of the tripartite stations for the observation of aftershocks accompanying the Kita Mino (North Mino) Earthquake, Aug. 19, 1961, at Hachiman, Gifu Prefecture, Central Japan. E: Epicenter of the main shock. H: Hachiman. S: Recording room at Gujo High School. 1, 2, 3: Tripartite seismometer stations. 1～2=830 m, 2～3=626 m, 3～1=914 m. Azimuth of 1→2: N02°03′E.

Foundation. No. 1: Paleozoic chert. No. 2: Rhyolite dyke through Paleozoic formation. No. 3: Paleozoic greywacke sandstone.

4) M. TSUJIURA and H. MATUMOTO, *Bull. Earthq. Res. Inst.*, **40** (1962), (in press).

震ばかりとりすぎるおそれがあり余震域全体について一様な観測ができないことになる．また観測点の直下付近でおこる地震がおおくなり，これらに対しては多点観測による方位決定などの精度も非常にわるくなる．地震計の感度は相当たかいのであるからこの点もちかくで観測する必要はない．しかし無論あまり遠方では到来する初動は P_n, P^* のような屈折波となり，その観測からは地殻内地震の震源深度を決定することができなくなるし，もちろん記録できる地震数も非常にへつてしまう．したがつて，予想される余震群の発生深度とみあつた適当な距離だけ余震域からはなれた位置をえらぶ必要がある．

高感度地震計による観測においてはまた当然堅固な岩盤上のできるだけ常時的雑微動水準のひくいしづかな場所に地震計を設置する必要のあることはいうまでもない．しかし一方観測装置のために安定した交流電源を供給すること，観測装置をある期間設置する観測室をみつけること，観測員の滞在勤務の便，輸送交通の便などおおくの条件も考慮して観測場所は撰定しなくてはならない．

これらの諸点を綜合的に判断してわれわれは観測地を岐阜県郡上郡の中心地八幡町付近にもとめることにした．同地は気象庁発表の本震震央から南南西 30 km，岐阜市のほぼ北北東 50 km にあたり，国鉄越美南線にそい，長良川に吉田川，小駄良川の合流する付近に位置する．地質は大体秩父古生層の分布する地域で，地形は山がせまり，谷はせまいので，かたい岩盤も発見しやすいとおもわれた（第1図参照）．

観測室は八幡町小野の県立郡上高等学校体育館の配電室を利用することができた．つぎに地震計（換振器）を設置する**観測点**には第1図にしめした No. 1～3 の位置をえらび，新鮮な岩盤をほりだし，コンクリートをうつて地震計台をつくつた基礎の岩石は第1観測点では秩父古生層硅岩 (Paleozoic Chert)，第2観測点では秩父古生層をつらぬく流紋岩岩脈 (Rhyolite Dyke)，第3観測点では秩父古生層硬質砂岩 (Paleozoic Greywacke Sandstone) であつた．**観測点の位置**は簡単な測量によつて ±5 m の精度でもとめた．

3. 観 測 装 置

観測装置の系統図は第2図にしめすとおりであるが，その主要部分はすでにのべたように無線地震計* RTS-I および RTS-II の送信および受信部端局装置および記録装置としてつくられたものであり，これについては別にくわしく報告される予定[5]であるので，ここでは今回の観測における使用状態についてのみ簡単にしるすこととしたい．

地震計（換振器）は No. 1～3 の各観測点に上下動1台づつ，第1観測点には東西動・南北動の2台の水平動地震計も併置した．上下動・水平動とも本所技術部製の動線輪動電換振器で，自己周期 $T_0=1$ sec，減衰 $h=2$ にそろえた．地震計の出力は遮蔽ビニール線により観測室にみちびかれてそれぞれの回線の増巾器にはいる．

無終端磁気テープのながさは録音再生間の遅延時間が約 30 sec になるようにえらばれ

* RTS: Radio Telerecording Seismograph.

5) *loc. cit.* 4).

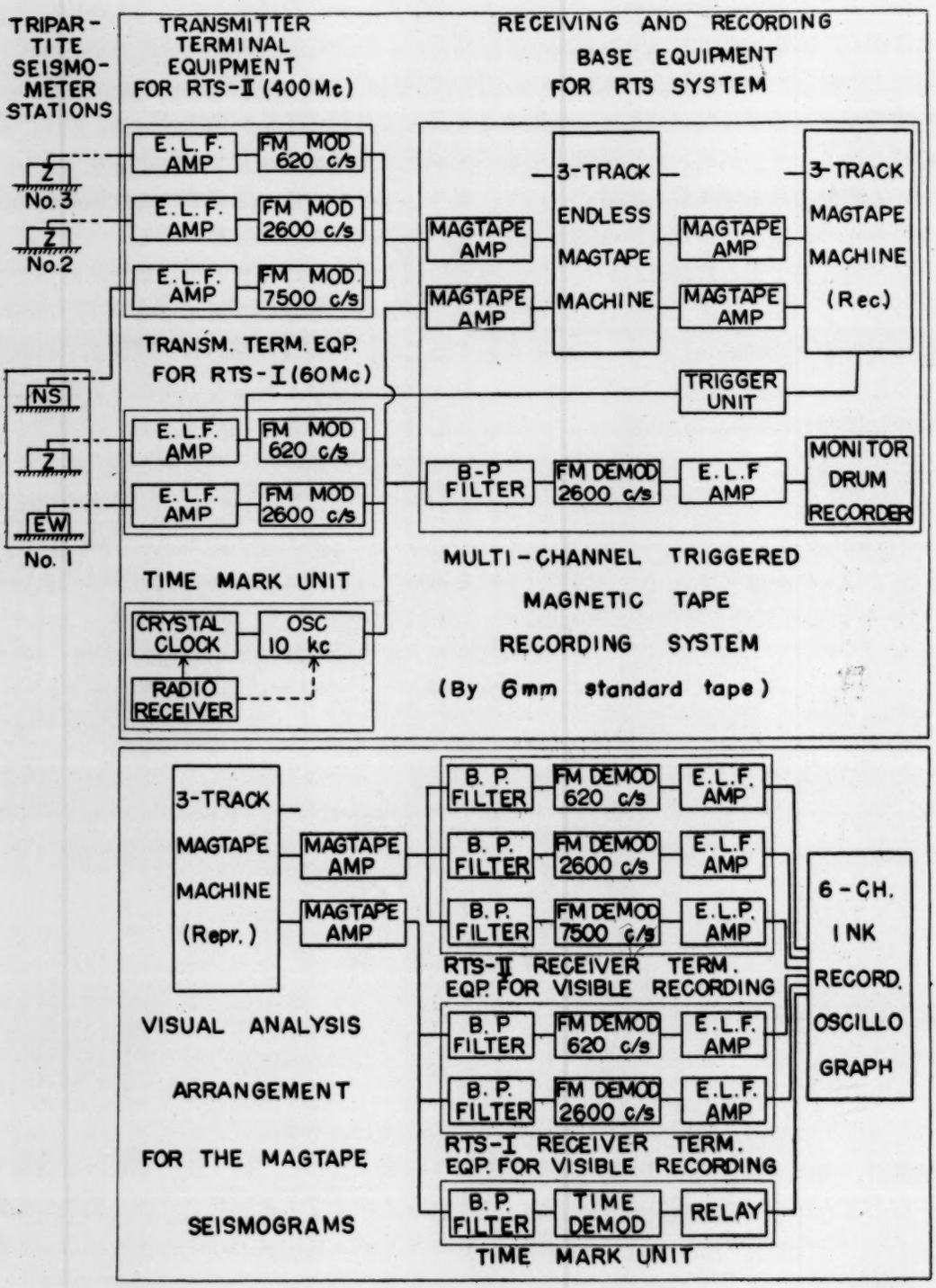

Fig. 2. Schematic diagram of the instrumentation. (E. L. F.: Extremely low frequency, i. e. 3~30 c/s. MOD: Modulator. DEMOD: Demodulator. OSC: Oscillator. MAGTAPE: Magnetic tape recorder. B. P. FILTER: Band pass filter.)

た．これは保存用磁気録音機がひきがね装置により地震の S 波が主要動で起動したとしても S-P<30 sec のものが初動から記録されるというようにしたことになる．**ひきがね装置**は数サイクル以上はやい振動が入力換算電圧 50 μV 以上で 0.3 sec 以上つづくと保存用磁気録音機のモーターを起動し，録音を開始させ，約 90 sec のちに自動的に停止させるようにした．磁気テープ記録には**水晶時計**からみちびかれた分秒時がいれられているが，90 sec のうちにはかならず分刻時があるので，これから記録上の秒はわかるが，分を同定することはできない．このためには別に 1 成分だけを**モニター記録**として大型記録円筒にインクがき検流計で連続記録し，それにいれられた時分刻時を利用する．この連続記録紙速度約 4 mm/sec，1 行 1 mm おくりで，1 日 1 回の記録紙とりかえをおこなう．ここにはひきがね装置を起動させないような小地震やのろい振動の遠方の他震（普通の近地地震）も記録されている．

観測装置全体の**綜合倍率特性**は第 3 図曲線 B にしめすようなものであり，各成分できるだけ特性はそろえるようにした．第 1～3 の各観測点においた上下動地震計を第 1 観測点にあつめ，ならべてとつた地震動の再生記録の一例を第 4 図にしめしたが，検流計のふれが飽和して振巾のちいさくなつている第 3 回線の初動付近の一部分をのぞけば，すべての波形が，振巾までほとんど一致した記録をしめしていることがわかる．水平動の 2 台についても，同一方向にならべてとつた記録はよく一致した記録をしめした．

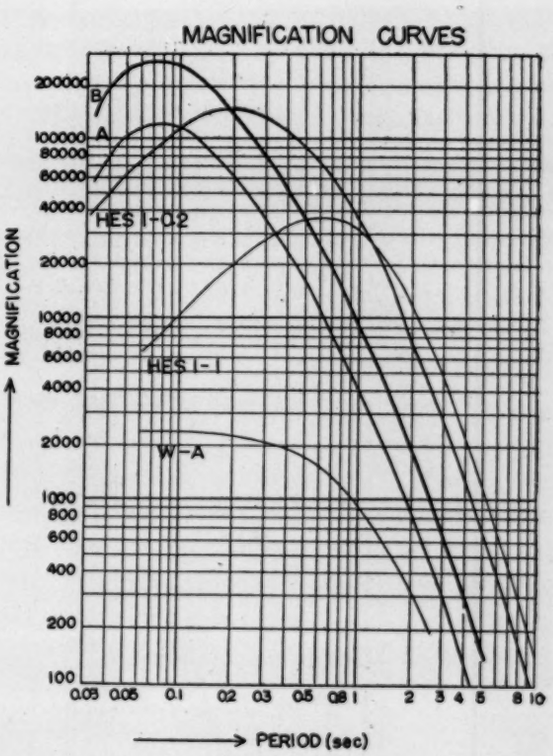

Fig. 3. Magnification curve of the seismograph system used at Hachiman, 1961. Aug.-Sept. (B). Magnification curves of the seismographs at Tsukuba Station, HES 1-0.2, HES 1-1 and W-A are shown for comparison's sake. HES 1-0.2: Hagiwara electromagnetic seismograph of Tp=1 sec, Tg=0.2 sec with film reader enlargement. HES 1-1: The same of Tp=1 sec, Tg=1 sec. W-A: Wood-Anderson torsion seismograph.

4. 観 測 実 施

観測期間は本震後約 1 週間をへた 8 月 27 日より 9 月 20 日までであり，途中停電その他の事故による中断をのぞいて連続的観測をおこなつた．保存用磁録音機に録音された地震は毎日 1 回インクがきオツシログラフに 6 mm/sec と 36 mm/sec の記録紙速度で再生して解析に利用する．第 2 図において解析の磁気録音機とモニター記録のためのフィル

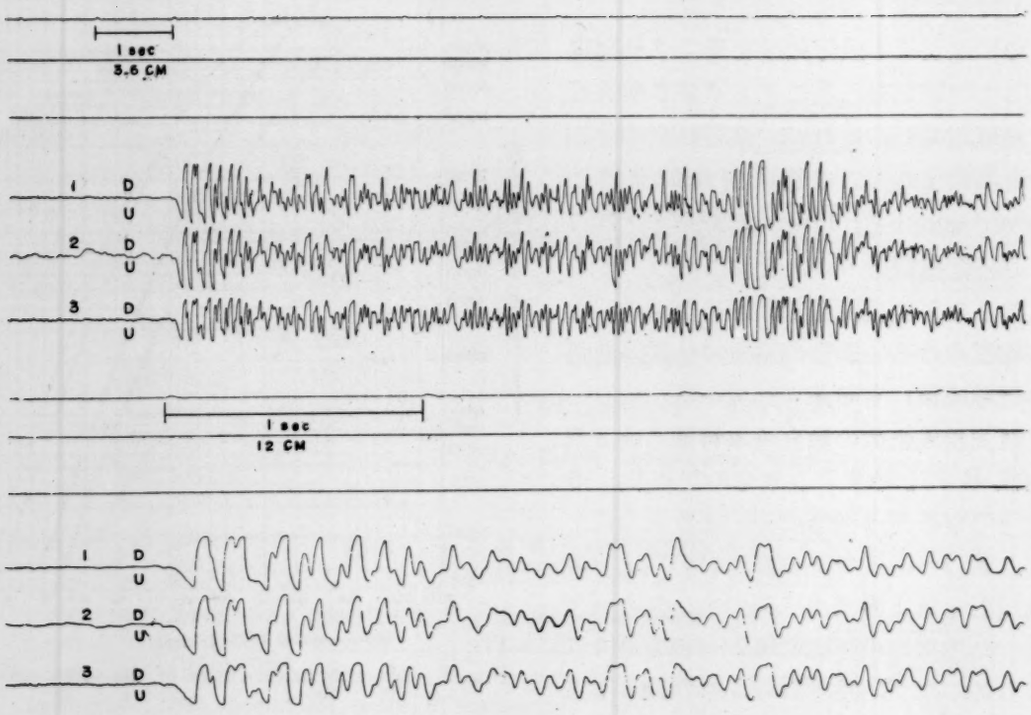

Fig. 4. Reproduced magnetic records of an earthquake by three vertical component seismographs installed at No. 1 station. The seismometers or transducers of the three seismographs 1-3 had been installed at No. 1, 2, and 3 respectively.

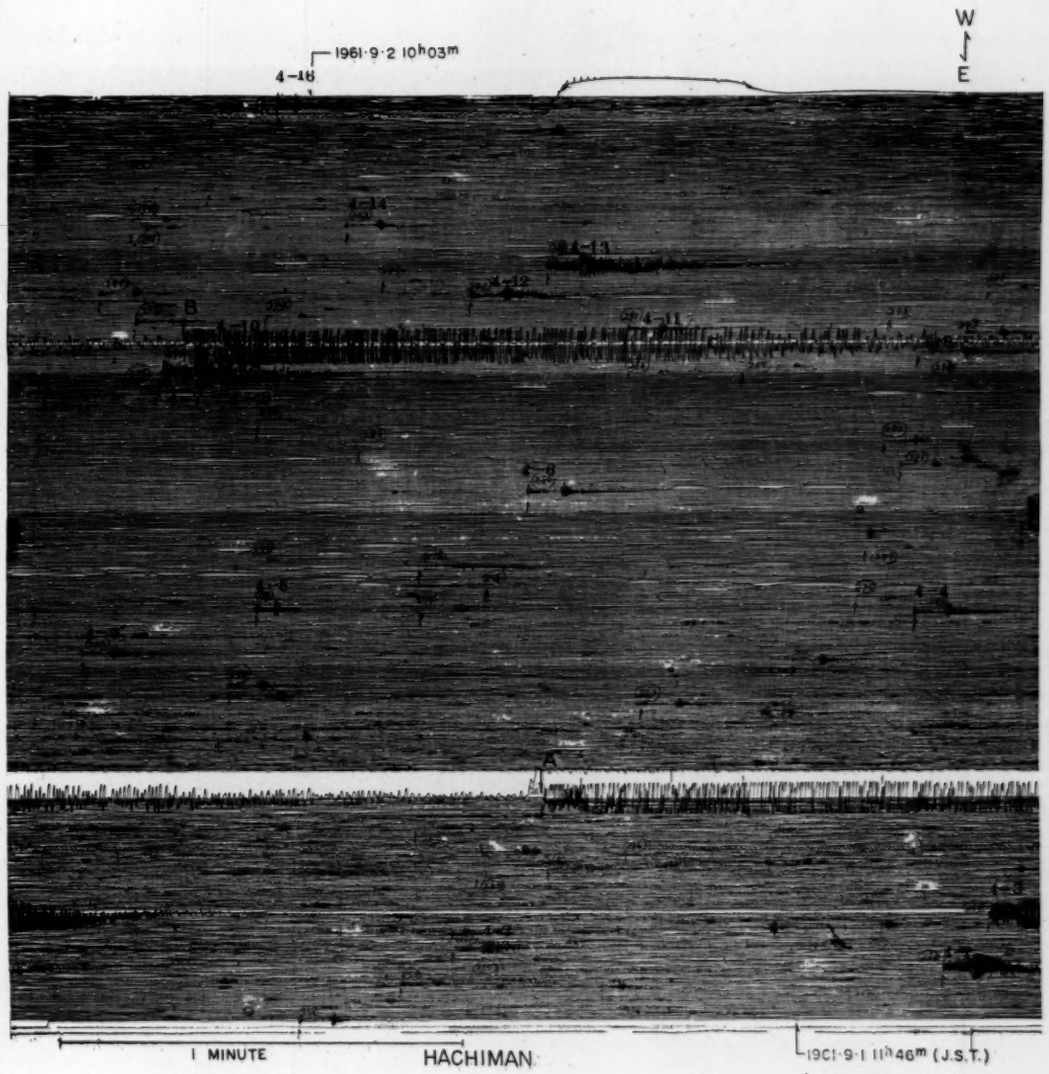

Fig. 5. An example of the monitor drum record for one day. Numbers 4–13 etc. are given for the earthquakes recorded by the magnetic tape recorder. A: Origin Time, 17 h 21 m. Epicenter (Kii Strait, Central Japan. 33.9°N, 135.0°E. Depth: 10 km) B: Origin Time. 03 h 59 m. Epicenter (Western part of Kanagawa Pref., Central Japan. 35°.4N, 139°.0E. Depth: 15 km)

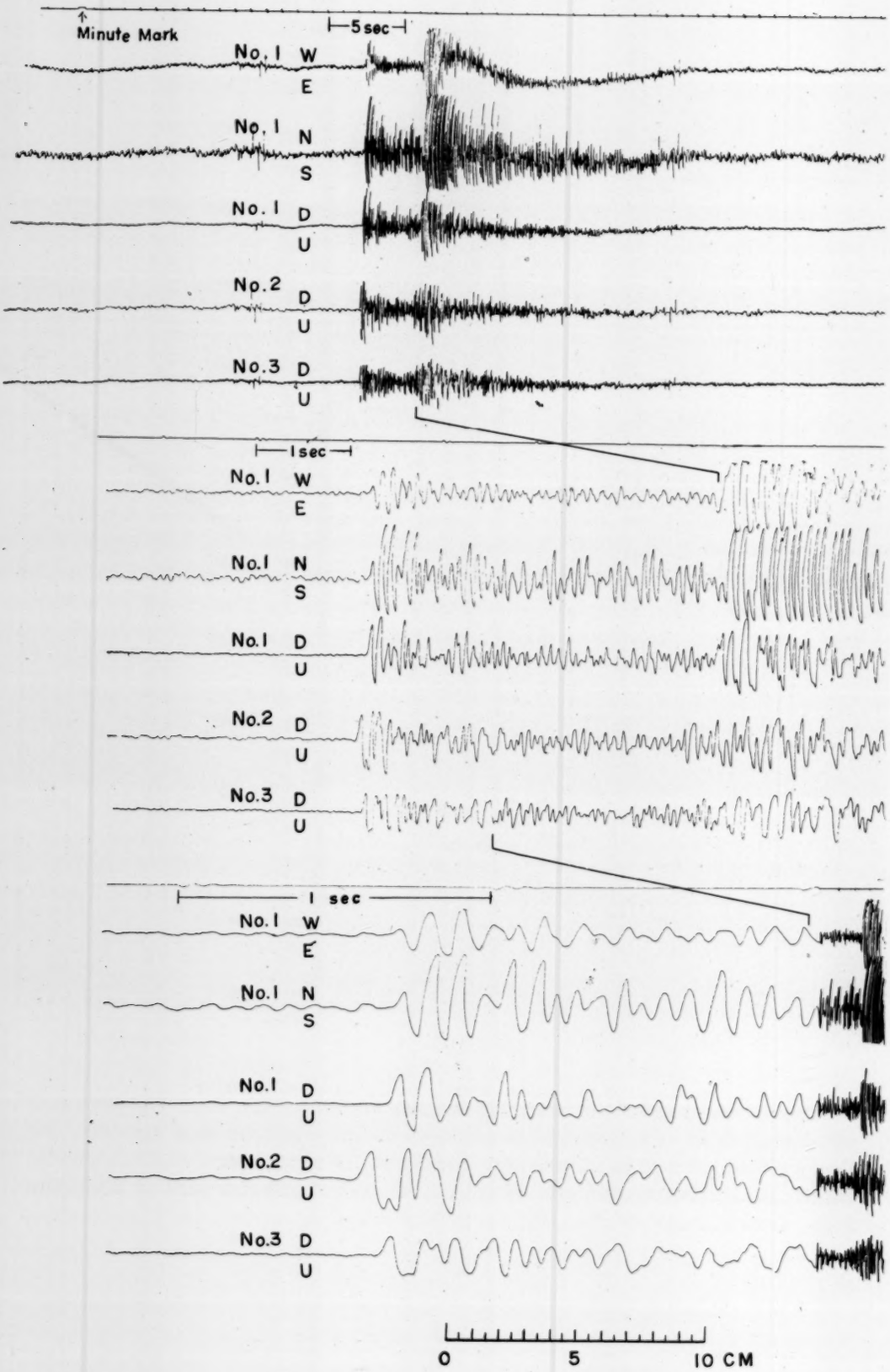

Fig. 6. An example of the magnetic records of an after-shock reproduced by three different paper speeds.

ター，検波器，等は実際には専用のものがなく，それぞれ観測用のもの，解析用のものを利用していたので，解析用の再生記録をとるときには観測の方は中止しなければならなかつた．つまり毎日1回記録紙とりかえの際 30～60 分観測を中断したことになる．しかしこれによつて毎日前日の地震の解析をすませてゆくことができた．モニター記録の検測も毎日おこなつた．

モニター記録の第一例を第5図に，**解析用再生記録**の一例を第6図にかかげた．第5図で 4-13 etc. とかいてある地震はひきがね装置が作動して磁気テープ記録のえられたもので，4 はリール番号，13 はそのリールのなかでの地震番号である．

5. 観 測 結 果

観測結果の詳細の解析については別に報告される予定[6]であるから，ここには暫定的に現地でまとめられた結果だけを簡単に報告する．

モニター用連続観測の検測によれば全期間の有効観測時間 611.2 時間に記録された地震数は 753 回，うち余震 616回，余震以外の局地地震 63回，遠方の地震(近地地震)74回である．ただし磁気テープ保存記録のとれなかつた小地震は一応 S-P=3～6 sec のものを余震とした．余震外の局地地震とは S-P<10 sec で磁気テープ記録の解析から余震域外にあると推定されたもの 18 個と磁気テープ記録がなくて震央の推定できない小地震のうち，S-P<3 sec および S-P>6 sec の範囲のものをとつた．磁気テープ記録された地震 149 個のうち余震とおなじ S-P をもちながら方位がちがい余震でないことのあきらかなものは6個にすぎないから，上記余震数 616 回にふくまれるかもしれない余震外局地地震数は $(616-149)\times(6/149)\fallingdotseq 19$ 個，約 3% 程度にすぎないとみてよかろう．

このような意味での余震をとつてその毎日1時間あたりの**余震数の消長**をしめしたものが第7図である．余震数は比較的順調に減少し，われわれの観測期間においては，他の大地震の余震群中にしばしばみられるような，本震の規模 M に対し M-1～M-2 程度の規模をもつような**おおきな余震**はみられなかつた．9月19日の余震数はややおおいが，これらはす

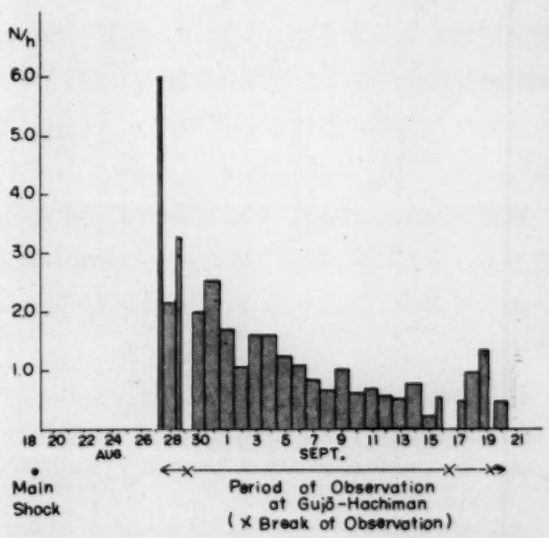

Fig. 7. Average Number of after-shocks per hour observed at Hachiman, Gifu Prefecture, Central Japan, after the Kita Mino (North Mino) Earthquake, Aug. 19. 1961.

6) K. Aki, *Bull. Earthq. Res. Inst.* **40** (1962), (in press).

べてちいさい地震であつて，特別におおきい余震があつて余震活動がふえたというのではなかつた．

記録されたすべての地震の**初期微動継続時間S-Pの頻度分布**をとると第8図のようになり，余震群は S-P=4～5.5 sec，特に S-P=4.5～5.0 sec のあいだに集中しており，観測点八幡から震源距離 D=25～50 km のせまい範囲におこつていると推定された．

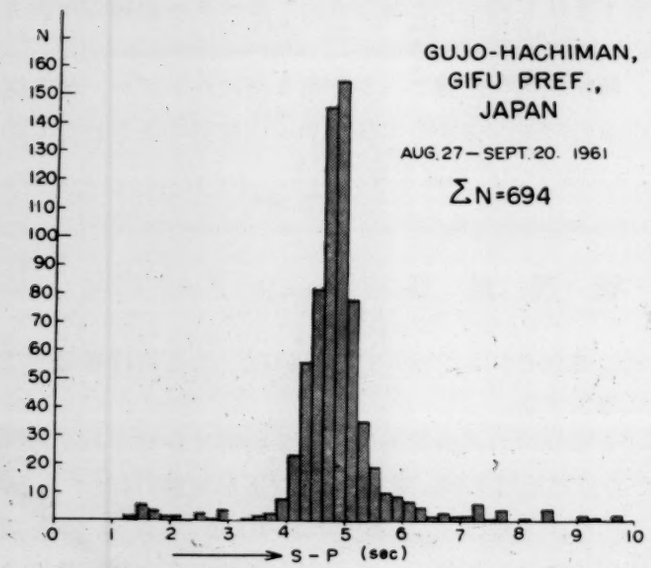

Fig. 8. Frequency distribution of S-P times of local earthquakes observed at Hachiman, Gifu Prefecture, Central Japan, after the Kita Mino (North Mino) Earthquake Aug. 19., 1961.

磁気テープ記録として保存された地震は全部で 149 個あり，それらの再生記録によつて，第1～3 観測点に到達した初動のたちあがりの時刻差から，初動の到来方位とみかけの速度を計算することができた．第9図は初動の到来方位と S-P 時間とから推定された震央位置を，初動のおし・ひきを区別して記入したものである．S-P 時間から震源距離をもとめるには，御母衣爆破実験[7]からえられたこの付近の P 波の速度 V_p=6.0 km/sec とポアツソン比 σ=0.25 を仮定して，大森常数を $k=V_{S-P}$=8.2 km/sec としてもとめた．本震の位置が余震域の一端に偏していることは従来しられている事実と一致する[8]．

初動のみかけの速度 V_{ap} を震央の方位別に余震群についてだけ記入したものが第10図である．みかけの速度は V_{ap}=6～8 km/sec に分布し，特に 7 km/sec 前後のものがおおいようである．おし・ひきもみかけの速度も方位的にはつきりした特徴はしめしてないようである．

御母衣爆破実験の結果からこの付近の地殻構造断面を推定し，これにみかけの速度 V_a=6～8 km/sec で入射する震波線と等 S-P 時間線とを記入したものが第11図であつて，これによつて余震群の位置は深度 0～25 km にあることが推定される．

余震域の面積 A と本震の規模 M とのあいだには**宇津・関の公式** $\log A=M-4$ (A in km²) の成立することがしられている．気象庁の公表した本震の規模は M=7.2, Pasadena

7) T. MIKUMO *et al.*, *Bull. Earthq. Res. Inst.*, **39** (1961) 327～349.
8) T. MATUZAWA, *Bull. Earthq. Res. Inst.*, **14**, 38～67.
9) T. UTSU and SEKI, *Zisin* (*Journ. Seism. Soc., Japan*), [ii]. **7** (1955), No. 7, 233～240.

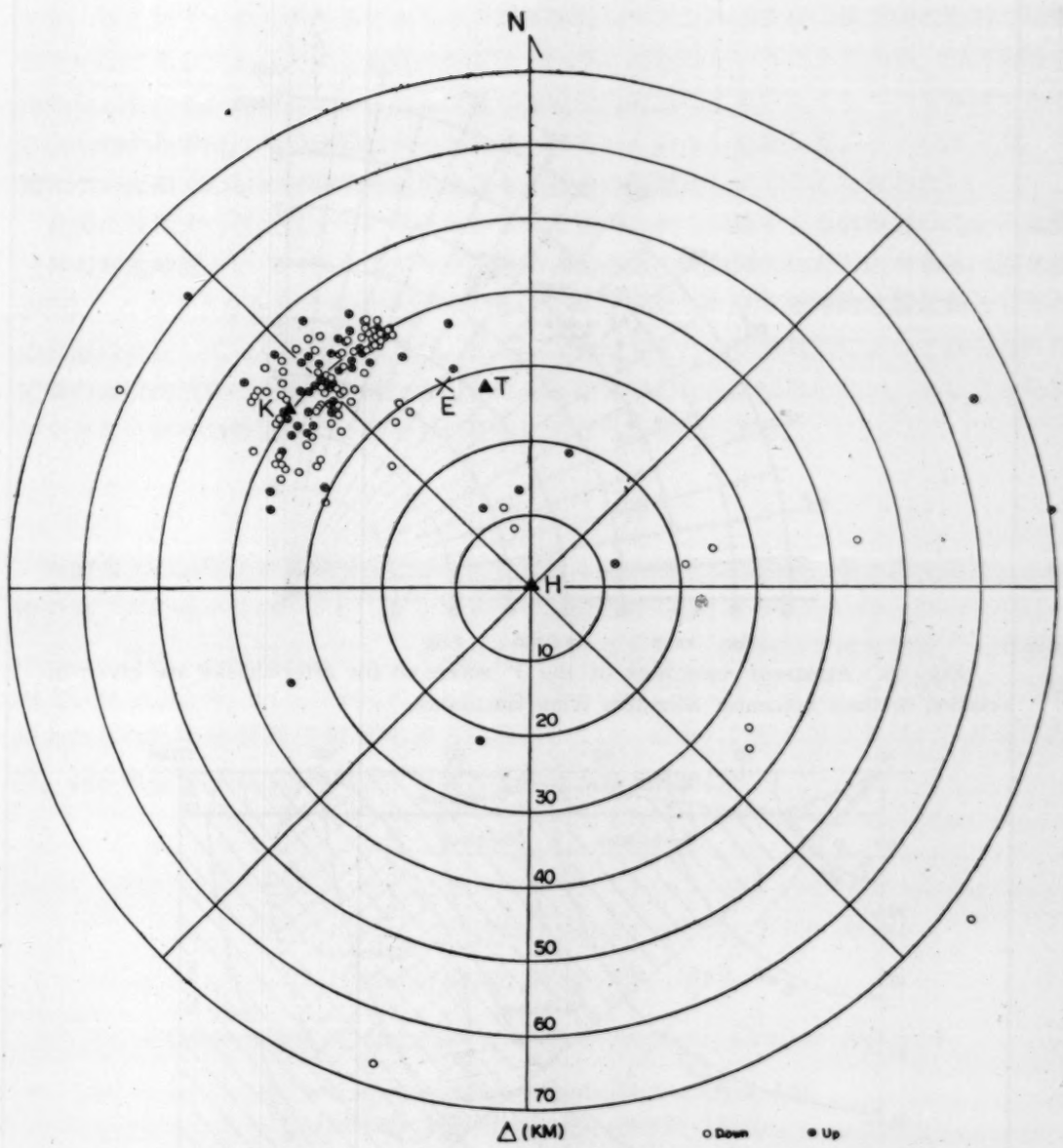

Fig. 9. Epicenters located by a correlational method applied to the tripartite observations at Hachiman, Gifu Prefecture, Central Japan, after the Kita Mino (North Mino) Earthquake, Aug. 19, 1961. H: Hachiman (Gujo County, Gifu Prefecture). K: Kadohara (Ōno City, Fukui Prefecture). T: (Hirugano, Takasu Village, Gujo County, Gifu Prefecture). Epicenter of the Kita Mino Earthquake. Epicentral distances are calculated by the assumption of Omori constant k or the velocity of fictitious S-P waves being 8.25 km/sec.

の発表によれば $M=7.5$ ということである．上記公式をあてはめると余震域の面積は $A=1590$ または 3170 km² となる．一方われわれの観測からえられた第 9 図をみて余震域をかんがえると $A=20\,\text{km}\times 30\,\text{km}^2$ 以上にはかんがえられない．これから逆に M をだ

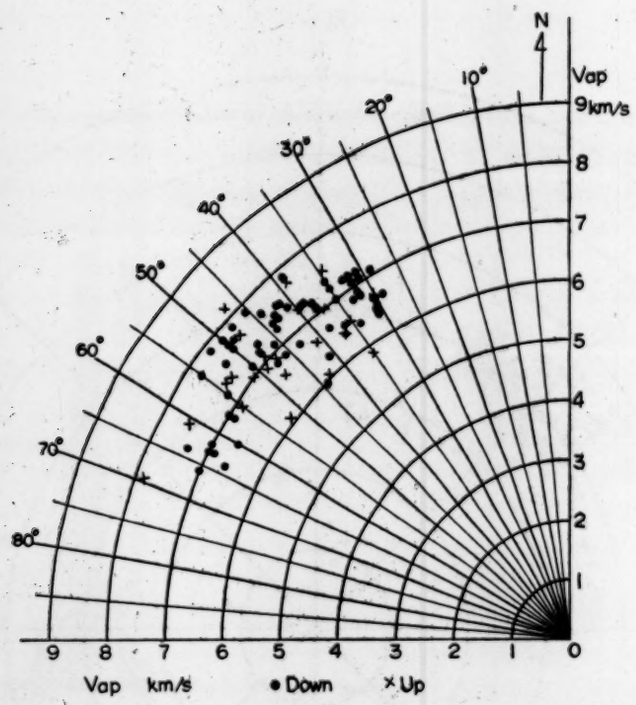

Fig. 10. Apparent velocities of the P waves of the after-shocks are given in relation to their epicenter azimuths from Hachiman.

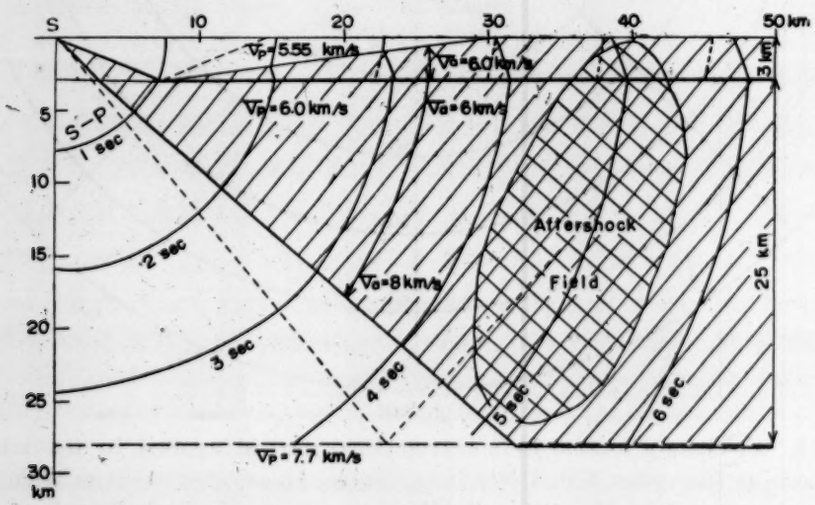

Fig. 11. Vertical section of the Earth's crust in the epicentral region of the Kita Mino Earthquake and aftershock field inferred from the S-P times and apparent velocities of P waves. S: Station, i. e. Hachiman.

せば M=6.8 になる. M の精度からみてこの差を問題にする必要はないかもしれないが, 一応これは (i) われわれのとつた余震域が従来の研究対象とされた地震の余震群よりもせまい意味の余震をとつているのか, (ii) 実際にこの地震の余震活動が従来のものにくらべ特にせまい範囲に集中しているのか, あるいは (iii) また本震の規模推定に問題がある

のか，をしめすものといえるであろう．萩原尊礼ら[10]によれば筑波山観測所の記録で同観測所に関する公式からだすと本震の規模は $M=6.5$ になるということである．一方余震の消長などをかんがえあわせると余震活動が従来の大地震のばあいにくらべ大変単純であることもわかるので，その空間的分布がかぎられていることも想像しやすいといえよう．本震についてのくわしい計測学的検討とともに将来の問題としてのこしておきたい．

最後に注意すべき点はすでにのべたように本震のちかくに集中する余震群のほかに**余震以外の局地地震**というべきものがわづかであるが各方位に観測されたことである（第9図参照）．このような局地地震の活動が今回の北美濃地震とは別に**常時的地震活動**としてこの付近に存在しているものであるか，あるいはこれもまた北美濃地震によつて誘発された**広義の余震的活動**であるのかはいまのところ不明といわなければならない．もしできれば将来さらに同様の観測をくりかえして研究してみたいものである．

6. 謝　辞

本観測については現地において岐阜県土木部，同八幡土木出張所，県立郡上高校，八幡町役場，その他の後援をえた．ここにあつく感謝の意を表したい．

また，今回の出張観測に関し，本所所長代理河角教授，余震観測班担当萩原，表両教授および技術部長実川技官のあたえられた御後援について謝意を表する，また観測点の測量にあたられた技術部岡田教官の協力に感謝したい．最後に計器の撤収輸送には技術部大貫，鈴木両技官の協力をえたので併記して感謝する．

---

35. Observation of Aftershocks of the Kita Mino Earthquake, Aug. 19, 1961.

—Observation at Hachiman, Gifu Prefecture, Central Japan.—

By Setumi MIYAMURA, Minoru HORI, Keiiti AKI,
Hideteru MATUMOTO and Seiichi ANDO,
Earthquake Research Institute.

After the Kita Mino (North Mino) Earthquake of August 19th, 1961, we hurried to Hachiman, Gujo County, Gifu Prefecture, Central Japan, about 30 kms south-east of the epicenter to observe its aftershock activity for several weeks. Tripartite stations were occupied, as shown in the map of Fig. 1, near the temporary observation room at Gujo High School and from Aug. 27th to Sept. 20th the observation were executed almost continuously.

A block diagram of the instrumentation used is given in Fig. 2. Five seismograph channels, i. e. three vertical components at the tripartite stations No. 1～3 and two horizontal components at No. 1 station, were adjusted to have the same magnification character as that

10) T. HAGIWARA and I. KAYANO, *Monthly Meeting of the Earthq. Res. Inst.*, Sept., 26, 1961.

given in Fig. 3. Fig. 4 shows an example of the seismograms indicating the identity of of three vertical component channels used at the tripartite stations. An example of the monitor record is given in Fig. 5. Fig. 6 shows an example of the magnetic seismograms reproduced by an ink-writing oscillograph with three different paper speeds.

The daily average numbers of the aftershocks recorded by the monitor per hour, diminished gradually with a slight rise and fall during the observation period as seen in Fig. 7. It seems to decrease quite smoothly and we had no remarkable aftershock of a magnitude 1 or 2 grades less than the main shock which often used to occur in the aftershock sequences of big earthquakes. The frequency distribution of S-P times is illustrated in Fig. 8, which clearly shows a sharp mode between 4 and 5.5 sec, characterizing a narrow space concentration of the aftershock activity.

From the magnetically recorded seismograms, the tripartite stations method allowed us to determine the azimuths of epicenters and the apparent velocities of the P waves. If we calculated the velocity of a fictitious S-P wave, Vs-p, or Omori's constant k, from the P wave velocity of 6.0 km/s obtained by the Miboro explosion experiments, we got Vs-p=8.2 km/s, assuming the Poissn's ratio $\sigma=1/4$. Using this value of k we can obtain the epicentral distance of each shock by its S-P time. Thus the distribution of earthquake epicenters was obtained as in Fig. 9, the azimuths and distances from the station having been calculated as stated above. Apparent velocities of P waves for the aftershocks are plotted according to their epicentral azimuths from the station in Fig. 10, together with the directions of the initial motions. As the apparent velocities of the P waves of the aftershocks lie between 6 and 8 km/s, the seismological profile of the Earth's crust obtained by the explosion seismic experiments tells us that the aftershock field is distributed in the crust at a depth of 0~25 km as illustrated in Fig. 11.

When we apply the Utsu-Seki's formula, connecting the aftershock area A in km^2 and the magnitude of the main shock as $\log A=M-4$, the aftershock area of the Kita Mino Earthquake becomes $A=1590$ km^2 or 3170 km^2, for the magnitude of the shock was published as $M=7.2$ or 7.5, by J. M. A. or Pasadena respectively. However, the real aftershock area cannot be estimated from Fig. 9 as having larger than $A=20\,\text{km}\times 30\,\text{km}=600\,\text{km}^2$, which gives the value $M\leq 6.8$. On the other hand T. Hagiwara and I. Kayano reported that the data at Tsukuba Station gave $M=6.5$. It seems to suggest that the main shock had a special character making it worth while to proceed with further investigations in the future.

Finally we must notice that several small local shocks were observed in different azimuths other than the aftershock area and it will be necessary to execute a same kind of observation in future in order to investigate whether such local shock activity means an ordinary back ground seismicity of this region or some kind of aftershock activity in a broader sense of the word.

地震研究所彙報
第39号(1961) 909-934頁

36. 北美濃地方の地質構造に関する2,3の問題

地震研究所 村井勇
津屋弘達

(昭和26年9月26日発表—昭和26年9月30日受理)

I. まえがき

昭和36年8月19日，美濃山地北部に著しい地震が発生した．震央は岐阜県郡上郡白鳥町北部の大日岳付近と報告された．震央が山地内にあつたため，被害は少なかつたが，根尾断層を生じた濃尾地震（明治24年，1891年），及び根尾断層の延長上に発生したと解釈される福井地震(昭和23年,1948年)に近い位置に発生した地震として注目された．その位置はまた，日本島弧の地体構造上最も基本的な構造の1つである“内帯中央線”あるいは“飛騨構造帯”に接近しており，構造地質学上極めて興味あるものと考えられた．筆者等は，この地震による地変の調査と，あわせて北美濃地方及びその周辺地域の地質構造についての予察的調査を行うため，約2週間にわたつて現地踏査を行つた．以下にその結果を報告して，今回の北美濃地震と地質構造との関係について検討するための資料に供したいと思う．

現地踏査にあたつて，多くの人々の協力を得たが，特に電源開発株式会社御母衣出張所からは種々の便宜を賜わつた．ここに記して謝意を表したい．また，美濃，飛騨山地の地質構造について,及び飛騨構造帯に関する色々な問題について種々御教示いただいた,東京大学理学部地質学教室の佐藤正助教授，および信州大学文理学部地学教室の亀井節夫講師に感謝する．なお，この報告中の図の作製と浄書は地震研究所小諸支所の細谷与七氏の助力によるものである．

II. 地震による被害と地変

震央が美濃山地の奥部にあつたため，地震による家屋や人命の損害は少なかつた．震央付近では，道路のひびわれ，沈下,落石,崖崩れ，山崩れ等が各所で発生した．道路の被害は，急峻な山地内の急斜面に切り開かれた部分や，河川の流路に接する部分に集中しており，そのほどんどが，谷寄りの道路肩の崩壊や沈下と，それに伴なうひびわれ，および山がわの切り割り上に露出する岩塊の落石や崩壊によるものであつた．道路の被害の著しかつたのは，岐阜県下では，郡上郡白鳥町長滝より大野郡白川村御母衣に至る国道，特に白鳥町，歩岐島一西洞の間,歩岐島より石徹白に至る道路,御母衣より大白川温泉に至るダム工事道路，福井県下では，大野市鳩ケ湯より小池に至る道路，葛原付近の国道，朝日より石徹白に至る道路，石川県下では，石川郡白峯村市ノ瀬より白山山頂に至る登山道路であつた．

山崩れ，落石は，白山より別山を経て大日岳に至る尾根にそつて，およびその周囲に著しく発生した．すなわち，市ノ瀬一別当出合の間，甚之助谷，大崩れ，別山尾根，打波川上流，石徹白川上流，および大白川上流等に著しく，特に小池部落と大白川ダム工事現場では大きな被害を受けた．大白川の山崩れは，ダム工事のため露出した岩石が崩壊しやすくなつていたことが，特に大きな被害を出す原因となつたと考えられる．白山の尾根ぞいに生じた山崩れと落石は，手取層群の上に分布する白山火山の噴出物（火砕物質と熔岩流，1部に火砕流堆積物）の崩壊によるものである．大日岳の周囲に生じた山崩れ，落石は，節理の顕著な発達を見せる安山岩の熔岩流と流紋岩質火砕流堆積物（熔結凝灰岩）が崩壊して発生したものが多い．

地震断層と認められるようなものは，今回の地震では発見されなかつた．小池，石徹白，歩岐島，長滝等の各地で，地面の小規模のひびわれや沈下が生じたが，断層運動と関係があると認められるものはなかつた．別山の尾根上に，尾根の方向を横断して NNW-SSE 方向の著しいひびわれが生じ，地震断層の疑がもたれたが，しかしその積極的な証拠はない．ただし，その方向は，手取層群中に発達する断層系の1つの方向にほぼ一致している．この地方の地質構造は非常に複雑で，数多くの断層が発達するが，それらの断層で地震の際の運動したと認められたものはない．

白鳥町大中南方の長良川の川中で，地震後天然ガスの烈しい噴出が続いた．これは，手取層群中の断層（走向 N80°E および N80°W）より微かに噴出していたものが，地震の際に急にその量を増したものである．大白川温泉では，湧出口が山崩れによつてふさがれ，別の湧出口より多量に出るようになつた．また，白峰村白峰の発電所で温泉の湧出が報告されている．

以上に記したように，今回の地震によつて発生した地変は，いずれも表層部に起つた現象で，地震断層と認められるものは発見されなかつた．ただし，被害や地表の分布状態を見ると，白峰村市ノ瀬より白鳥町長滝に至る NNW-SSE 方向の帯上に集中しているようにも思われ，これは，郡上郡八幡町より長良川にそつて NNW へ延びる断層系の延長上にあり，また，福井平野より根尾谷に至る根尾断層北半の NNW-SSE の方向とも平行しており，注目に価する．

III. 地 質 の 概 略

この地方および周囲の地域の地質については，古くから調査が進められて，地質図も数多く作製されている．すなわち，大石三郎 (1933)，井尻正二 (1936)，嵐 由之(1940)，鈴木好一(1943) 等の主として中生層の手取層群の研究があり[1]，最近は，前田四郎(1950, etc.)，藤 則雄 (1958)等の主として手取層群の研究[2]，亀井節夫 (1949, etc.)，石岡孝吉

1) 大石三郎 地質学雑誌 **40** (1933), 481-482.
井尻正二 地質学雑誌 **43** (1936), 479-481.
嵐 由之 地質学雑誌 **47** (1940), 499.
鈴木好一 資源科学研究所彙報 **3** (1943), 75-84.

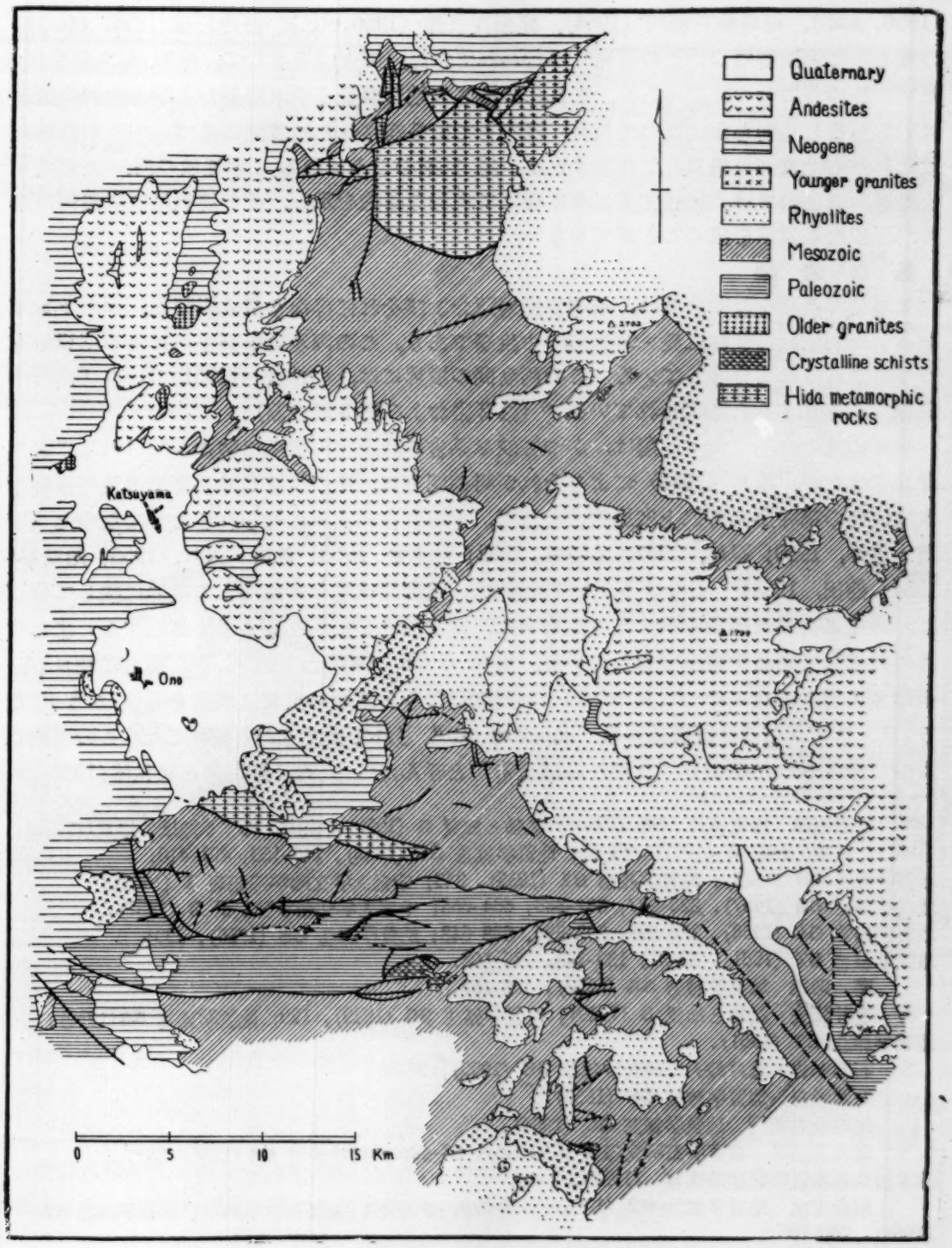

第1図　九頭竜川・手取川上流地域の地質図
前田 (1952, 57, 61), 河合 (1956, 59)等より編纂

(1950, etc.), 尾崎金右衞門 (1954), 鹿沼茂三郎 (1956, etc.), 河合正虎 (1956, etc.) 等の主として古生層についての研究[3] が行われてきた. 調査は主として, 手取川, 九頭竜川, 足羽川等の谷にそつて進められ, これらの地区の地質構造と手取層群および古生層の層序はいちぢるしく明らかになつてきた. 現在までに公表された地質図に基づいて, 本地域全般にわたる地質図を編集して作製すれば, 第 1 図のようになる. 本地域の内, 九頭竜川上流域および南域は, 後述するように極めて複雑な構造を示し, その解釈には異論があつて, 正確な地質図を描くことができない.

基 盤 岩 類

本地域の基盤をなす岩層は, 飛騨変成岩類およびそれに伴なう深成岩類と, ゴトランド紀 (シルル紀) および二畳・石炭紀の古生層であり, この両者はほぼ東西に走る境界をもつて南北に分れて分布している. この両者間の境界には, 小林貞一(1951)のいう "内帯中央線" が存在すると考えられている.[4] (第 2 図および第 5 図参照)

飛騨山地のゴトランド紀層は, かつて岐阜県吉城郡上宝村稲地で神津淑祐(1911)により発見されたが, 亀井 (1949) によりそれが再確認され, その後岐阜県大野郡清見村楢谷や本地域内の福井県大野郡上穴馬村の各所で, その存在が次々に知られるようになつた (石岡・亀井, 1950; 尾崎, 1952; 亀井等, 1952; 藤本等, 1953; 前田・浜口, 1955; 尾崎等, 1954; 前田, 1958). このゴトランド紀層は, 飛騨変成岩と古生層との境界に接して分布し, 非常に複雑な構造を呈する古生層中に, 薄岩層として挟みこまれて存在する. またそれに接近して結晶片岩が分布している, 亀井 (1955, 1957) はこのような構造に注目し, 飛騨変成岩の外縁にそつて起つた烈しい運動により古生層は複雑な構造をもつようになり, ゴトランド紀層は基底部から "squeeze out" されて出てきたと解釈して, この運動によつて擾乱された地帯を "ひだ外縁構造帯" と呼んだ[5]. 一方, 野沢保と礒見博(1956)は,

---

2) 前田四郎 地質雑誌 **56** (1950); 鉱物と地質 **3** (1950); 白山をめぐる地域の地質(石川県) (1951); 鉱物と地質 **4** (1951), 53-55; 地質学雑誌 **58** (1952), 145-153, 401-410; 地質学雑誌 **59** (1953); 地質学雑誌 **61** (1955), 343; 千葉大学文理学部紀要 **1** (1955); 地質学雑誌 **63** (1957), 225-237, 357-365, 664-668; 千葉大学文理学部紀要 **2** (1957); 地質学雑誌 **64** (1958), 388-398, 583-594, 638-643; 地質学雑誌 **65** (1959), 290; 地質学雑誌 **67** (1961), 23-31, 133-142, 189-198.

藤 則雄 地質学雑誌 **64** (1958), 157-158.

3) 亀井節夫 鉱物と地質 **3** (1949); 地質学雑誌 **55** (1949), 120; 地質学雑誌 **56** (1950); 地質学雑誌 **57** (1951).

石岡孝吉・亀井節夫 地質学雑誌 **56** (1950), 57-58.

石岡孝吉 地質学雑誌 **56** (1950).

尾崎金右衞門 地質学雑誌 **60** (1954).

鹿沼茂三郎 東京学芸研究報告 **7** (1956), 37-42; 地質学雑誌 **62** (1956), 361; 藤本治義教授還暦記念論文集 (1958), 1-48.

河合正虎 地質学雑誌 **62** (1956), 559-573; 5 万分 1「荒島岳」(1957); 地質学雑誌 **62** (1959), 760-765.

4) 小林貞一 「白山をめぐる地域の地質, 特に手取統について」石川県土木計画課 (1951).

5) 亀井節夫「"ひだ外縁構造帯" について」ひだ山地の地質研究会連絡紙 No. 7 (1955).

亀井節夫・猪郷久義「ひだ外縁構造帯の地質」地質学雑誌 **63** (1957), 413.

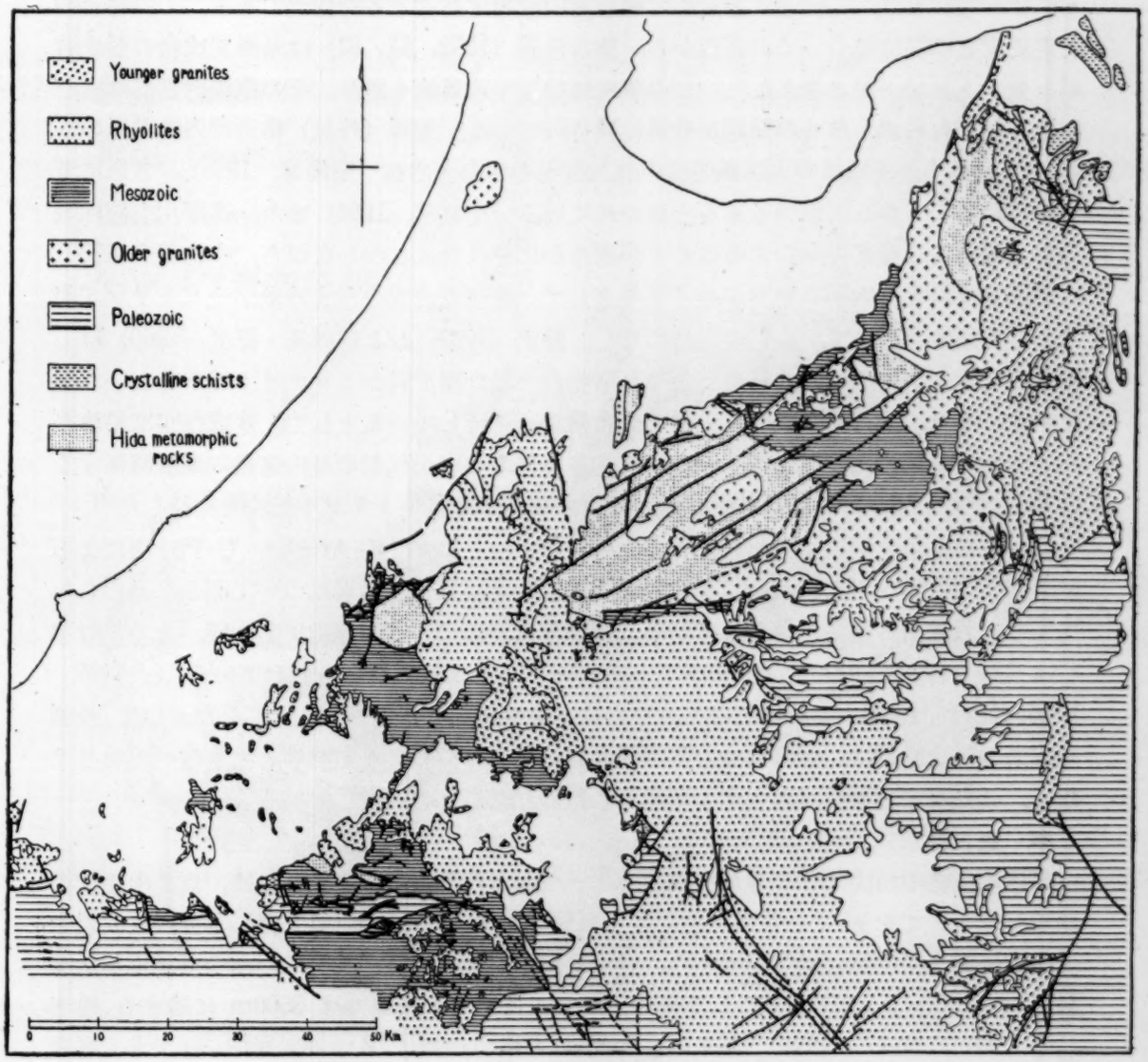

第2図　飛騨・越前・美濃山地の地質概略図

飛騨山地中央部の船津付近の研究に基づき，飛騨変成岩・船津花崗岩・古生層の分布と主要構造方向がほぼ平行していること等から，飛騨変成岩の形成が船津花崗岩の迸入と密接な関係を有すること，および船津花崗岩の迸入の晩期に著しい変位運動が起り，古生層との境界に沿つてミロナイトをつくつたことを推論して，飛騨変成岩および船津花崗岩の南縁帯とそれに接する古生層の擾乱帯を“ひだ構造帯”と呼んだ[6]

前述したように，飛騨（外縁）構造帯においては，結晶片岩とゴトランド紀層の帯状分

6)　野沢　保・磯見　博「船津付近で見られるひだ変成岩と，船津花崗閃緑岩と古生層との関係」地質学雑誌　**62** (1956), 104–113.

布が認められるが，これらに接近して礫岩層の分布することも特徴的である．この礫岩層と変成岩との関係についての研究から，藤本治義（1952，53，57）は飛騨変成岩の形成時期を先ゴトランド紀と考えた[7]．この解釈に対しては異論もあり，その積極的証拠はまだ確認されておらず，多くの問題が今後に残されている．飛騨（外縁）構造帯内の礫岩のうち，九頭竜川上流地域の大谷礫岩は中部二畳紀のものとされ（尾崎等，1953），さらに若い時代のものである可能性もあると説かれている（小林学，1954）．また，高原川上流地域の村上礫岩も二畳紀のものであることが明らかにされた．しかしながら，小林英夫(1958)は飛騨変成岩と古生層の構造が全く異るとして，飛騨変成岩の形成時期が先ゴトランド紀である可能性を話いている[8]．これに対し，野沢（1959）および礒見・野沢（1960）は，藤本の先ゴトランド紀説の根拠となつた楢谷の一梨含礫片岩がミロナイトであるという疑を示し，また，飛騨変成岩と古生層の分布構造は平行しているとして，変成作用は船津花崗岩の深成作用と同時に進行したもので，古生代末～中生代初の造山運動に直接関係すると考えた[9]．一方，加納博（1961）は，礫岩の研究から先ゴトランド紀説を支持した[10]．

これらの論争を解決するための有力な手段の1つとして，K-Ar 法や U-Pb 法による絶対年代の測定が考えられる．現在飛騨変成岩および船津花崗岩について測定が進められており，興味ある結果が得られている．飛騨変成岩についての測定によれば，その絶対年代は 180×10^6 年前後であり，船津花崗岩の時代も，これにほぼ一致している（久野等，1960；斎藤等，1961）．これは三畳紀末またはジュラ紀初期に相当する[11]．したがつて，飛騨変成岩の形成時期は，中国地方の三群変成岩の形成時期の三畳紀前半と大きなへだたりはなく，この両者の形成が秋吉造山運動期に行われたことを示唆している．

中 生 界

手取川上流の白山周囲の地域や九頭竜川上流およびその南部の地域には，広く中生代の地層が分布してをり，それらは一括して手取層群と呼ばれている（第3図）．基盤の変成岩および古生層上に不整合にのつており，ジュラ紀中期より白亜紀後期にわたつて堆積した地層で，その厚さは，白山地域では 2000～2500m，九頭竜川南域では 3500m に達する．前田(1950, etc.) は手取層群を下部より，九頭竜・石徹白・赤岩の3つの亜層群に区分し，河合

7) 藤本治義・鹿沼茂三郎「岐阜県清見村の新発見の後島系と麦島片麻岩との関係」東京文理大地質学古生物学教室談話会記事，**3** (1952)，3.
藤本治義・鹿沼茂三郎・緑川洋一「岐阜県清見村のゴトランド系」東京教育大研究報告，第2号 (1953).
藤本治義「飛騨山地の地質研究」地質学雑誌 **63** (1957)，388-396.

8) 小林英夫「飛騨変成帯」鈴木醇教授還暦記念論文集，(1958)，123-140.

9) 野沢 保「ひだ構造帯の 2，3，の礫状岩について」地質学雑誌 **65** (1959)，272-279.
野沢 保「ひだ変成岩の時代について（予報）」地質学雑誌 **65** (1959)，463-469.
礒見 博・野沢 保「ひだ変成岩の構造」地球科学，第 48 号(1960)，11-20.

10) 加納 博「Maturity からみた大谷礫岩と沢渡礫岩—含花崗岩質礫岩の研究（その10)—」地質学雑誌 **67** (1961)，350-359.

11) H. Kuno, H. Baadigraard, S. Goldich, and K. Shiobara, "Potassium-argon dating of the Hida metamorphic complex, Japan", *Japan. Jour. Geol. Geogr.*, **31** (1960)，273-278.
斎藤信房 他2名「カリウムアルゴン法による岩石の年令決定」地質学雑誌 **67** (1961), 425-426.

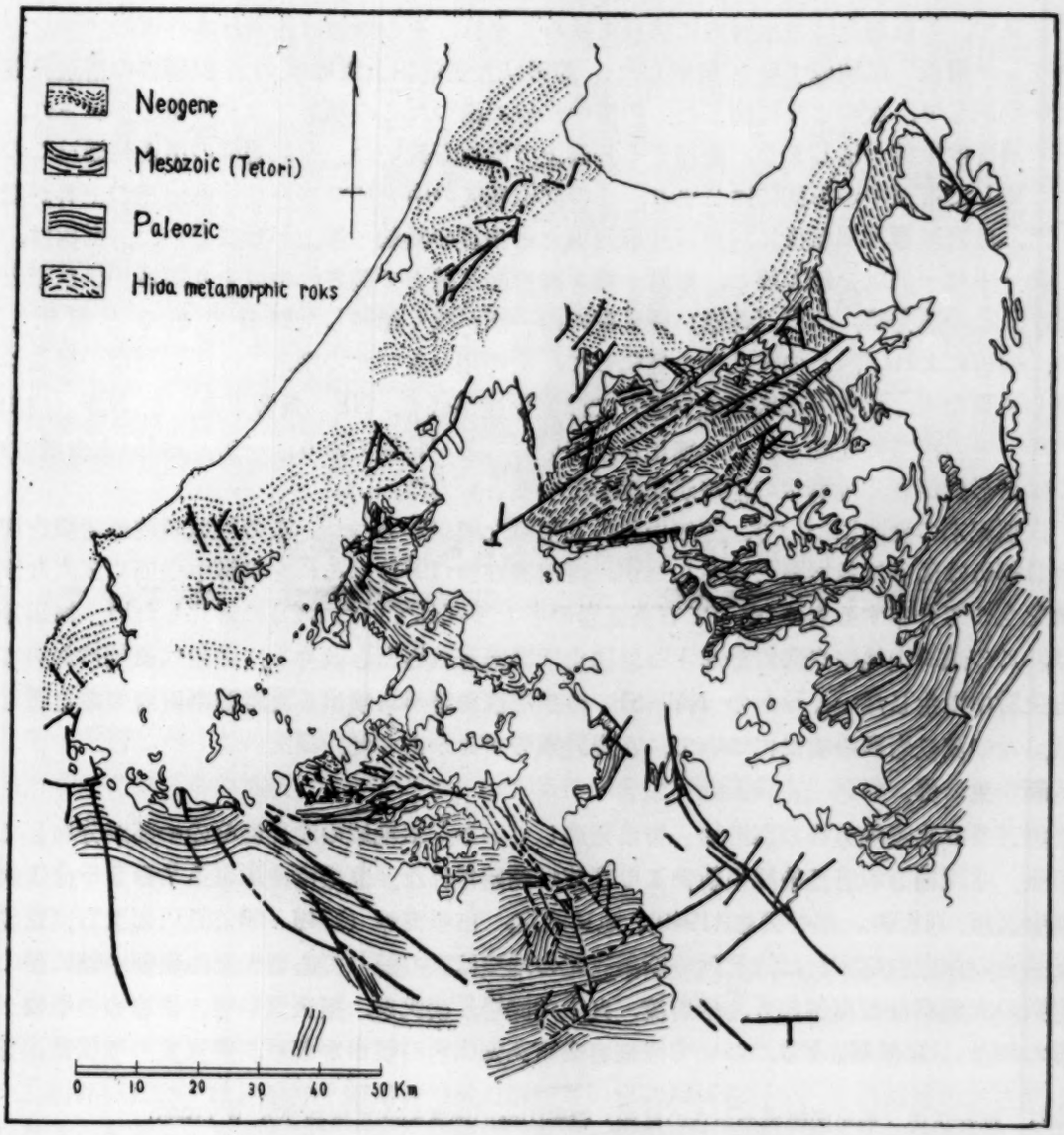

第3図　飛騨・越前・美濃山地の地質構造図

頭竜・石徹白の2層群に区分した.

白山地域の手取層群は E～W ないし ESE～WNW の褶曲軸をもつ緩い褶曲構造を示すが, 九頭竜川上流地域では, いちぢるしい変形作用をうけて, 基盤の飛騨変成岩. 古生層と共に複雑な断層構造を示している. 河合 (1955, 56, 59) は, この地域では大規模なデッケン構造が発達すると解釈し, これが越前・美濃山地において広範囲に拡がつているとして表日本衝上系と呼んだ. この衝上系に対し, 北側の区域では飛騨変成岩と深成岩類の複合体が手取層群・面谷流紋岩類と古生層の上に衝上しており, これを裏日本衝上系と呼んだ. これらの衝上系は中生代後期に徐々に完成したもので, その変動を中部日本変動

と呼んだ[12]。一方，前田 (1961) は，基盤岩類はデッケン構造を形成するとは認められないと見て，手取層群は古生層内に挟長に挟みこまれ，その構造は西南日本外帯の“サンドウイッチ構造”に類似すると解釈した．前田は九頭竜川上流地域の手取層群の構造発達史を解析して，次のように論じた．内帯中央線に沿つたこの地域では沈降帯が形成され，手取層群の堆積がはじまり，動揺する基盤上で堆積が続いた．手取層群の構造発達はこのようにして堆積中から既にはじまり，この間堆積区の中央部で谷戸口片麻岩塊の上昇が続いた．赤岩亜層群堆積後に谷戸口片麻岩塊と古生層の隆起・衝上が形成された．前田は，中島一中竜一油坂を結ぶ線と，巣原一箱ケ瀬を結ぶ線とで劃され地域を九頭竜川擾乱帯と呼び，この部分は，ひだ (外縁) 擾乱帯内の一部が強く錯雑した部分であると解釈した．前田によれば，この擾乱帯を境にして，その南および北の地区では手取層群の構造は著しく異なり，北部 (飛騨変成岩区) では変形度が低く，NE (飛騨方向) と NW (白山方向，との構造に支配されて地塊化されていることが特徴であり，一方，南部(古生層区) では変形度が高く地溝状の構造が発達しているという[13]．

白亜紀末の変動についで，流紋岩類の大規模な噴出があつた．この地域の流紋岩類を河合(1956)は面谷流紋岩類と命名したが，河田清雄等(1961)はこれを飛騨中央部に広大な面積をもつて分布する岩体(かつて石英斑岩の名で呼ばれていたもの)に対比した[14]．河田等は，この飛騨山地中央部に分布する岩体を“濃飛流紋岩”と改称し，中生代後期において古生層中に生じたいくつかの NW-SE の断層破砕帯から噴出した熔結凝灰岩であるとした．この流紋岩類の噴出についで，花崗岩類の貫入があつた．

新 生 界

第三系は北陸地方日本海沿岸一帯に発達している．本地域の北部にその一部が分布している．北陸地方の第三系は中新世より堆積が開始された．薗部竜一による7万5千分1大聖寺図幅 (1939)，福井図幅 (1940)；池辺展生，市原実等 (1949，50，51) による調査の結果その他を参照すれば，北陸の新第三紀の地史は次の通りである[15]，中新世中期に安山岩類の大規模な噴出が起り，熔岩流，火山角礫岩，凝灰岩，凝灰質砂岩，泥岩等の堆積が行われた (岩稲層，F_2)，ついで流紋岩や石英安山岩の噴出が起り，凝灰質の堆積物，特

12) 河合正虎「根尾図幅調査からの略報」飛騨山地の地質研究連絡紙 No. 9 (1955)．
河合正虎「飛騨山地西部における後期中生代の地殻変動，第1報 (荒島岳南方山地の地質学的研究)」地質学雑誌 **62** (1956)，559-573．
河合正虎「飛騨高原西郎における後期中生代の地殻変動，第2報(越前・美濃山地の地質学的研究)」地質学雑誌 **65** (1959)，760～765．

13) 前田四郎「福井県九頭竜川南域における手取層群の構造発達史の一解釈」地質学雑誌 **67** (1961)，189-198．

14) 河田清雄他5名「中央アルプスとその西域の地質，その2；濃飛流紋岩類」地球科学 第54号 (1961)，20-31．

15) 池辺展生「富山県西部及石川県東部の第三紀層」地学，**1** (1949)，14-26．
市原実 他4名「富山県及石川県の地質学的研究(其の2)」地学 **2** (1950)，17-27．
池辺展生 他4名「富山県及石川県の地質学的研究(其の3)」地学 **3** (1951)，7-16．
市川 渡・細野義夫 他「石川県の地質」日本地質学会関西支部北陸部会 (1955)．
坂本 亨 他4名「富山積成盆地南縁部の新生界」地質調査所月報 **10** (1959)，75-82．

に緑色凝灰岩層が形成された(山中累層，医王山火山岩層，F_3)．このような烈しい火山活動につづいて，中新世後期より鮮新世前期にかけて海浸が進行し，厚い海成層が堆積した(余川層群，厚さ 3000 m，F_3～H_1)．鮮新世中後期には海退期に入り，いくぶん縮少した海域に砂質の海成層が堆積した(氷見層群，大桑層，H_2)．その後鮮新世より更新世にかけては，海退後の湖や河口に陸成層の堆積があつた(卯辰山層，I)．第四紀には山地内部で火山活動が盛んとなり，白山，大日岳等の地域で安山岩類の噴出が起つた．大野盆地等では河成段丘の発達が著しい．

北陸地方の第三系は，第三紀末の地殻変動により変形作用をうけ，緩い褶曲および撓曲を示し，また断層によつて切られている．構造の主軸は ENE-WSW ないし NE-SW の方向をもち，基盤の地塊運動を反映しているような状態を示す．この変動は，現在に至るまで影響をおよぼしているものと考えられ，越前・美濃・飛騨山地の地形，特に河成段丘や切峰面の高度分布から，最近における断層運動を知ることができる．

IV. 北美濃地方およびその周辺地域に発達する fracture system

本地域では，前述のように，三畳紀，白亜紀末，第三紀末に地殻変動があつた．既に詳しく記したように，三畳紀と白亜紀末の変動は内帯中央線或いは飛騨（外縁）構造帯を中心にして進行した．この変動の影響はさらに新生代にもおよんでいると考えられる．すなわち，北陸の第三系の堆積盆地の形成も，これにつづく造構造運動も，飛騨構造帯を中心として起つた基盤の運動に強く支配されているようである．恐らくこの地域に発達する構造線のあるものは長い運動の歴史をもち，第四紀に入つてなお活動したと考えられる．大野盆地では河成段丘を切る断層の存在が，段丘面の高度のくいちがいから示唆されるし，飛騨山地，越前・美濃山地では，基盤岩類中に発達する断層にそつて顕著な断層地形が認められ，そのうちのあるものは，最近の運動を暗示している．筆者の 1 人の津屋(1937)は，かつて，根尾断層が古生層中に発達する既存の断層と密接な関係をもつことを明らかにした[16]．また，村井 (1955) は，福井平野周辺地域の第三系の構造解析を行い，この地域の第三系は特徴的な節理系の発達を示し，それが越前岬付近の海岸にそつて地層の方位の廻転と並行して急廻転していることに注目して，そのような構造の廻転は敦賀湾―琵琶湖―伊勢湾にわたる構造帯の活動と関係あるものと解釈した．すなわち，この構造帯を境にして，西側が南方に水平に変位するような運動を行い，この運動にひきずられて第三系は現在見られるような構造を示すに至つたと考えた[17]．この地帯は，日本島弧を横断する重要な構造帯と考えられ，深発地震の集中する地帯でもある（第 12 図参照）．第四紀に入つてもなお活動を続けており，それは桑名付近の第四系に顕著な断層や撓曲構造が見られることからも明らかに知れる．根尾断層はこの構造帯に平行している．同様の NNW-SSE 方向をもつ

16) 津屋弘達「水鳥の地震断層と付近の地質」地震 **9** (1937), 398-410.
17) 村井　勇「福井平野周辺地域の地質構造解析」地震研究彙報 **33** (1955), 122-151.

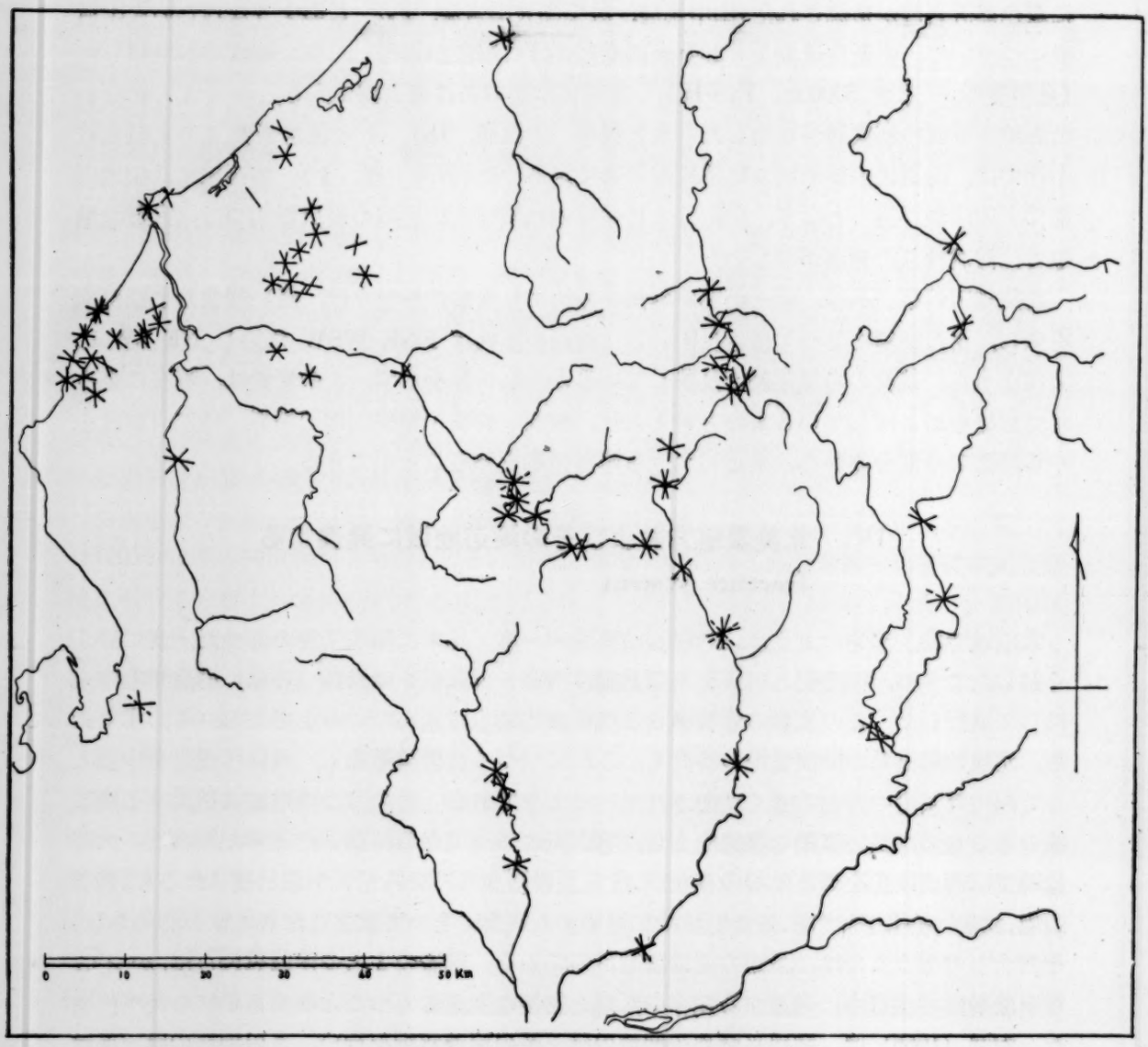

第4図 facture system の分布図

断層は，飛騨·越前·美濃山地一帯に発達しているものと考えられる．このことは，地形的にも NNW-SSE ないし NW-SE の方向をもつた直線状の谷が，これらの山地一帯に見られることからも知れる．そのような断層のうちのあるものは，ごく近い時代に活動している．すなわち，これらの山地では，切峰面を描くと，重要な断層谷を境としてその高度がいちぢるしいくいちがいを示す場合があり，最近における断層の活動を物語つている．岡山俊雄(1931)は，美濃・越前山地の断層地形についてこの事実を示している[18]．また，河田等(1961)は，濃飛流紋岩の噴出にあたつて支配的な役割を果した NNW-SSE 方向の断層のうちの最も大きなものである阿寺断層が，比較的新しい時期に活動したと述べている．この

18) 岡山俊雄「美濃越前地内の断層地形」地理学評論 **7** (1931), 920-942, 1035-1062.

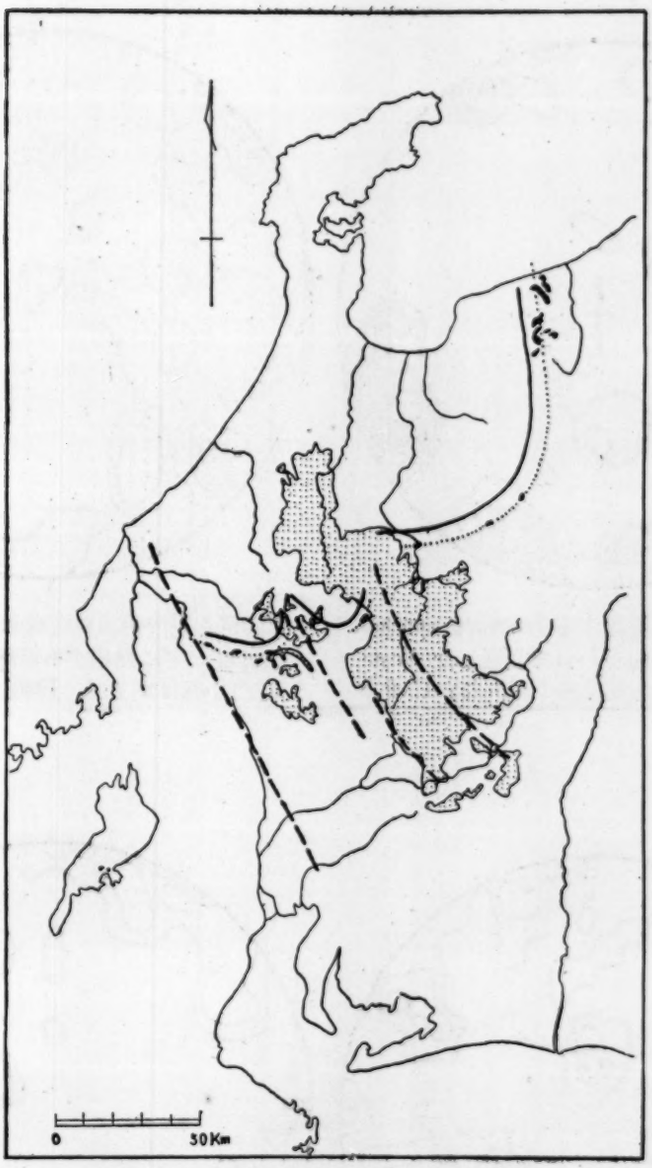

第5図 飛騨構造帯の概念図

実線は飛騨変成岩と古生層との境界，点線は古生層の結晶片岩の分布する地帯を示す．破線は飛騨変成岩および古生層の弧状分布を切る構造線．中央に分布する岩体は濃飛流紋岩．

ように，本地域においては，NNW-SSE 方向の断層系はきわめて重要な構造となつており，その活動は現在まで続いていると考えられる．

礒見と野沢 (1960) は，飛騨変成岩帯とこれをとりまく褶曲した古生層の外縁帯とを一括して“ひだ深成変成帯”と呼び，その構造について説明して，変成岩全体の弧状分布に対して主要構造がほぼ法線と切線の関係にある方向を示すことを指摘した．事実，この2つの構造の階段状組合せは，飛騨深成変成岩帯の全般にわたつて認められ，更に南方の非

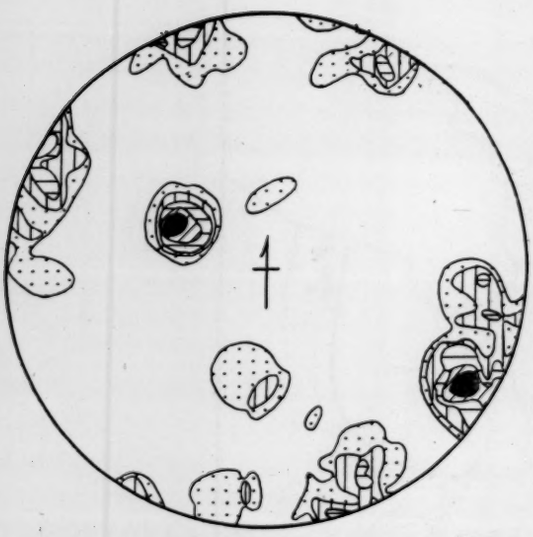

谷戸口片麻岩中に発達する fracture system. 福井県大野郡和泉村谷戸口で測定した fracture の極46個の2%図型. (15-13)-11-8.5-6.5-4.5-0%.

富山県八尾町南方の花崗岩体（微斜長石斑状花崗岩）中に発達する節理系. (4)-3-2-1-0%. (小林ほか7名, 1956)

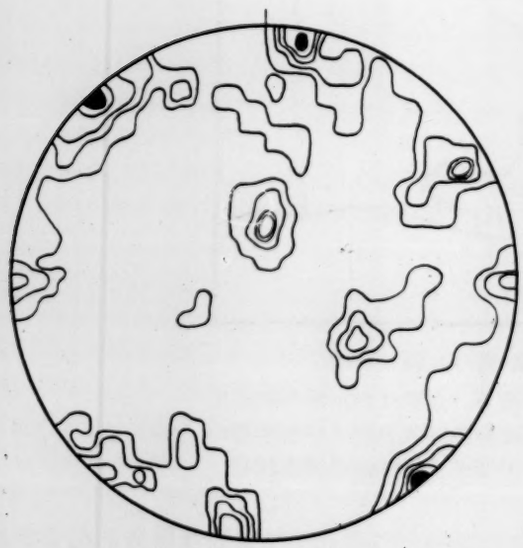

飛騨北部の長棟川花崗岩の節理系. (12-10)-8-6-4-2-0%. (春日井・山田・青木, 1956)

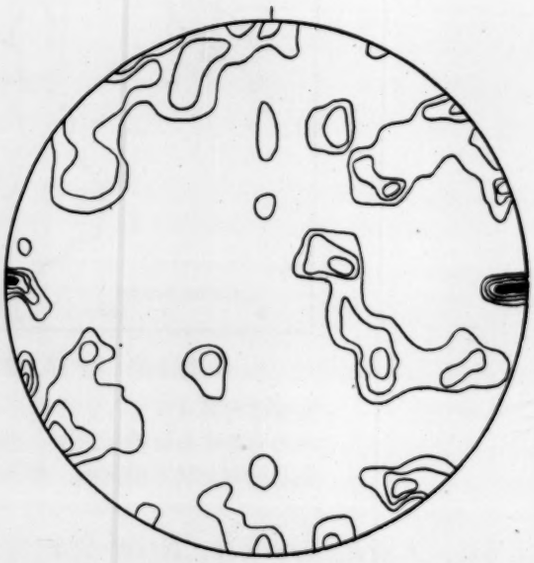

飛騨北部の小口川花崗岩の節理系. (12-10)-8-6-4-2-0%. (春日井・山田・青木, 1956)

第6図 飛騨変成岩および花崗岩類中の fracture system.

岐阜県本巣郡根尾村水鳥付近で測定した fracture の極 53 個の 2％図型. (15–11.5) –7.5–5.5–4–0%.

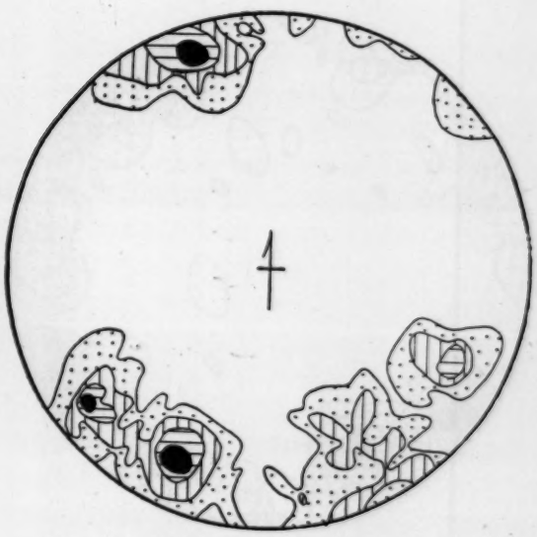

岐阜県本巣郡根尾村平野付近で測定した fracture の極 33 個の 3％図型. (15–12)–9–6–0 %.

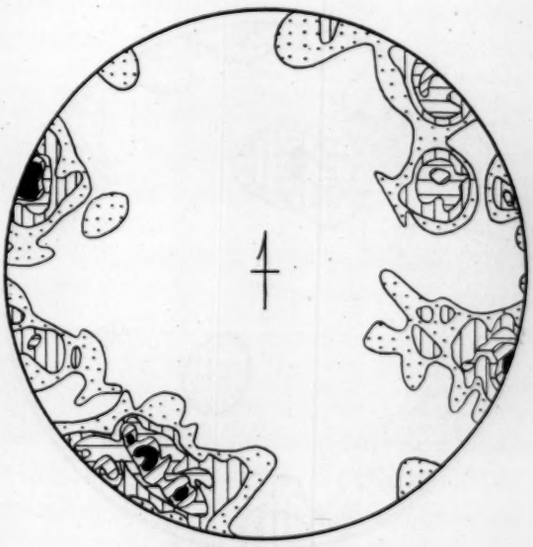

岐阜県本巣郡根尾村平野—本巣村日当間で測定した fracture の極57個の 2％図型. (12.5–10.5)–9–7–5.5–2.5–0%.

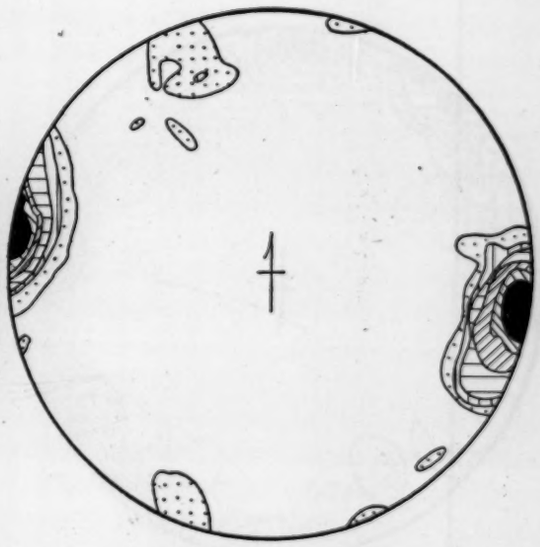

岐阜県本巣郡本巣村赤石および揖斐郡谷汲村長瀬付近で測定した fracture の極28個の 3％図型. (39–35.5)–28.5–21.5–14.5–10.5–7–0%.

第 7 図a　古生層中の fracture system.

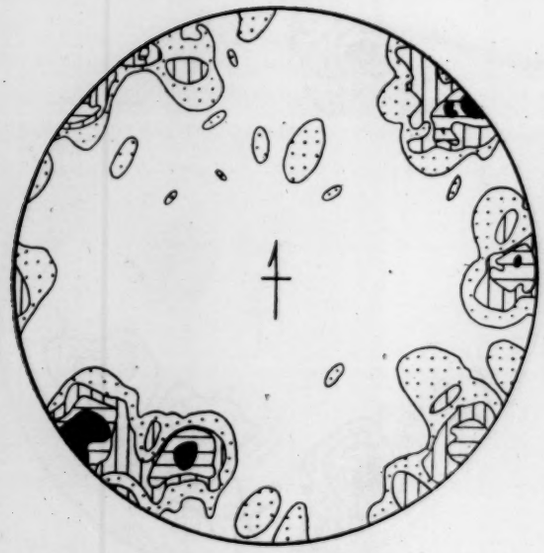

岐阜県郡上郡美並村半在一根村間で測定した fracture の極 59 個の2％図型. (13.5-10)-7-5-3.5-0%.

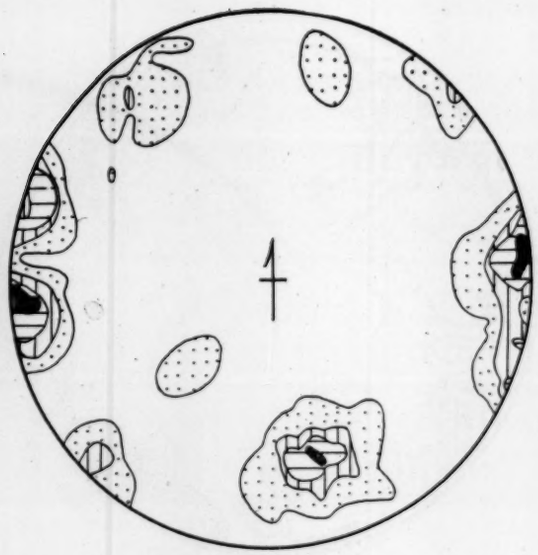

岐阜県郡上郡八幡町小瀬子で測定した fracture の極 31 個の3％ 図型. (19.5-16)-13-9.5-6.5-0%.

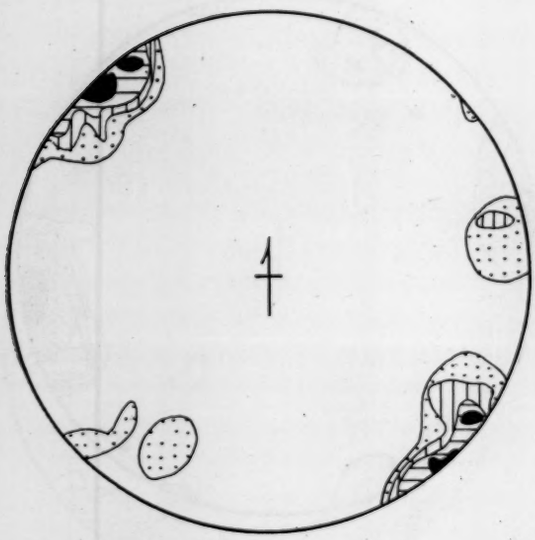

岐阜県郡上郡大和村万堰で測定した fracture の極 20 個の3％図型. (35-25)-20-15-10-0%.

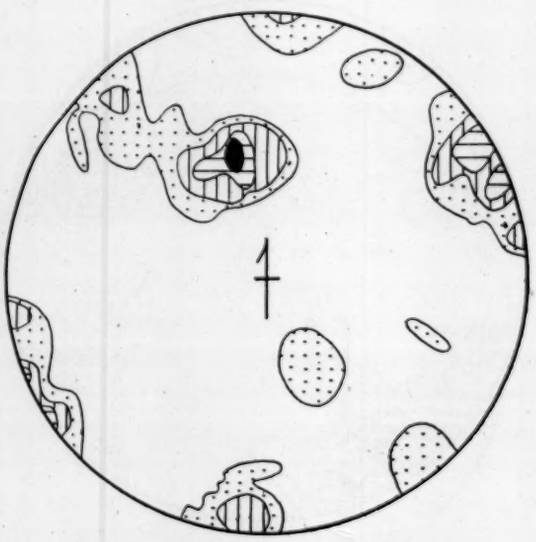

福井県大野郡和泉村大谷で測定した fracture の極31個の3％図型. (16-13)-9.5-6.5-0%.

第7図b 古生層中の fracture system.

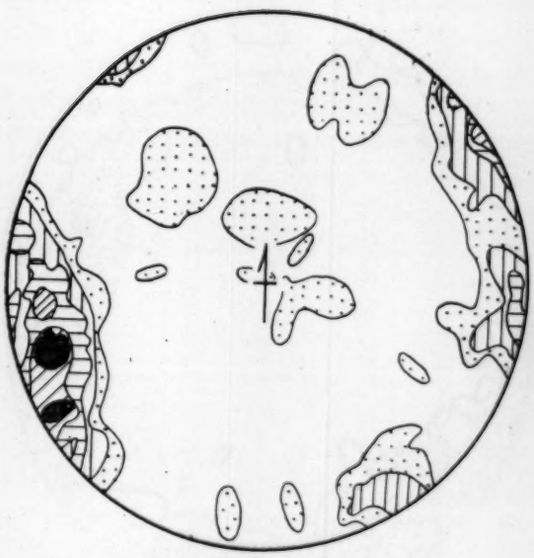

岐阜県武儀郡金山町地蔵堂で測定した fracture の極 39 個の 3% 図型. (24-18)-13-10.5-7.5-5-0%.

岐阜市日野坂で測定した fracture の極41個の3%図型. (17-14.5)-12-10-7.5-7-0%.

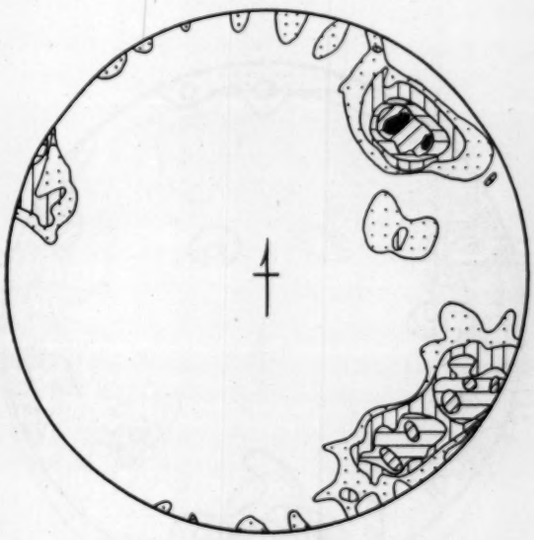

岐阜県吉城郡国府村上広瀬で測定した fracture の極 45 個の2%図型. (20-18)-13.5-9-6.5-4.5-0%.

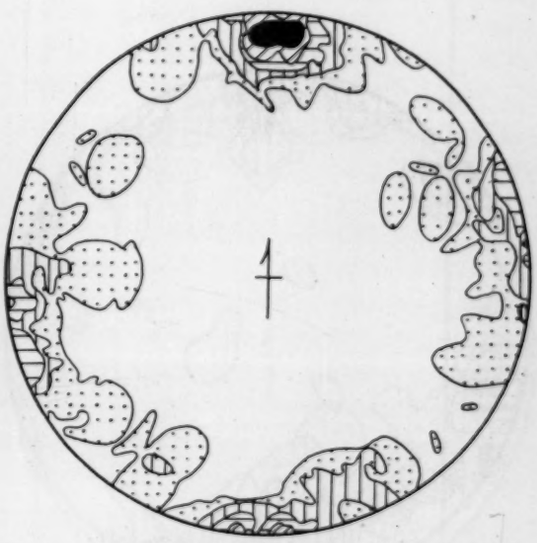

敦賀市新保で測定した fracture の極 74 個の2%図型. (19-13.5)-11-8-5.5-2.5-0%.

第7図c　古生層中の fracture system.

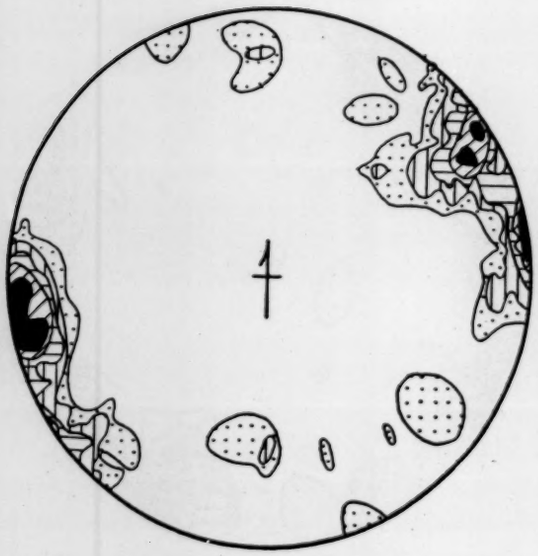

米原市米原駅北方で測定した fracture の極46個の2％図型. (19.5-13)-11-8.5-6.5-4.5-0%.

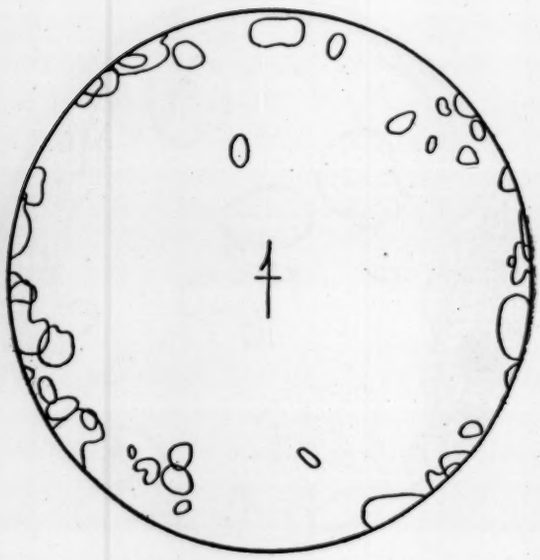

極大区の複合図型.

第7図d 古生層中の fracture system.

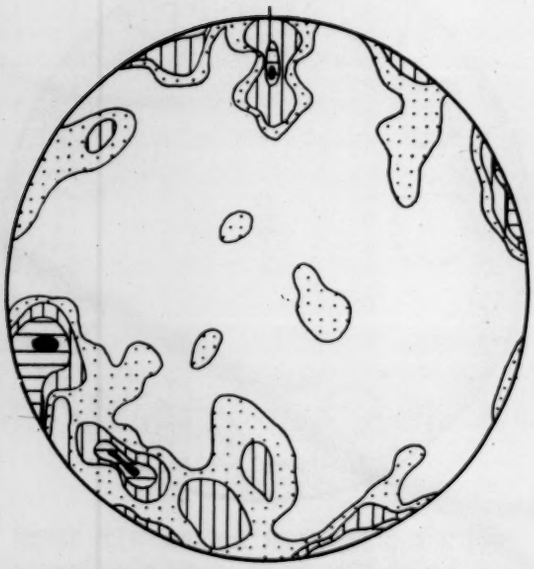

福井県大野郡和泉村荷暮付近の節理系，荷暮砂岩層. (10)-8-6-4-2-0%. (前田，1957)

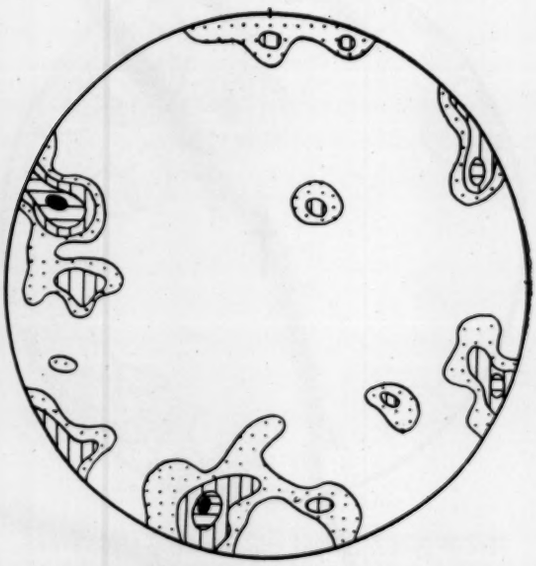

荒城川沿いの地区の節理系，栃尾頁岩砂岩層. (12.5-10)-7.5-5-2.5-0%. (前田，1958)

第8図a 手取層群中の fracture system.

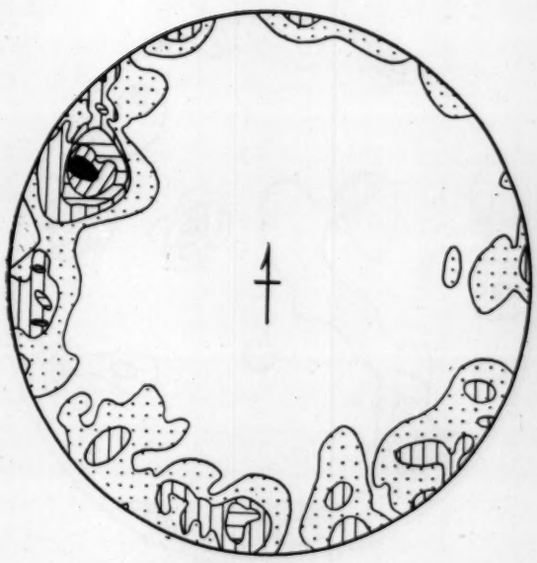

岐阜県大野郡荘川村牧戸—野々俣間で測定した fructure の極 60 個の 2％図型．(18.5-16.5)-13.5-10-6.5-3.5-0％．

岐阜県・福井県境油坂峠付近で測定した fracture の極 79 個の 2％図型．(11.5-10)-7.5-5-2.5-0％．

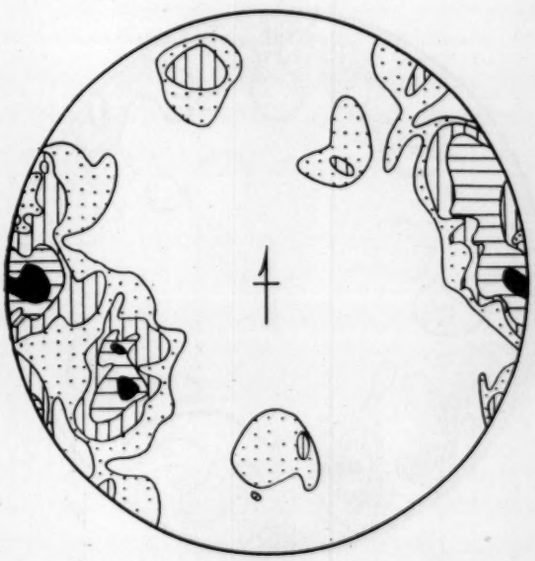

福井県大野郡和泉村持穴で測定した fracture の極 42 個の 3％図型．(16.5-14.5)-9.5-7-5-0％．

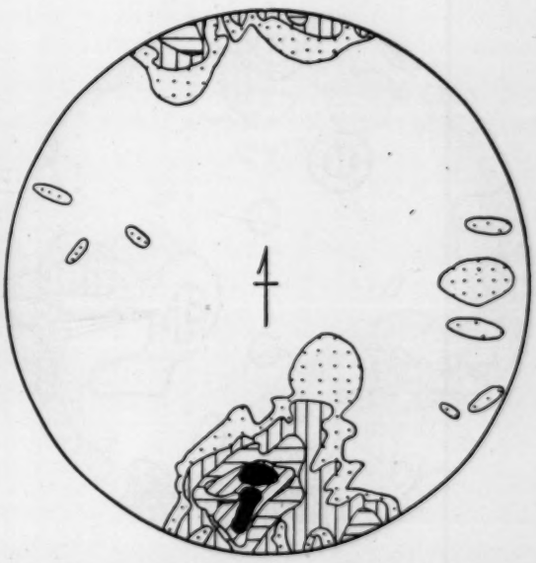

福井県大野郡和泉村朝日で測定した fracture の極 32 個の 3％図型．(20-19)-15.5-12.5-9.5-6.5-0％．

第 8 図 b　手取層群中の fracture system.

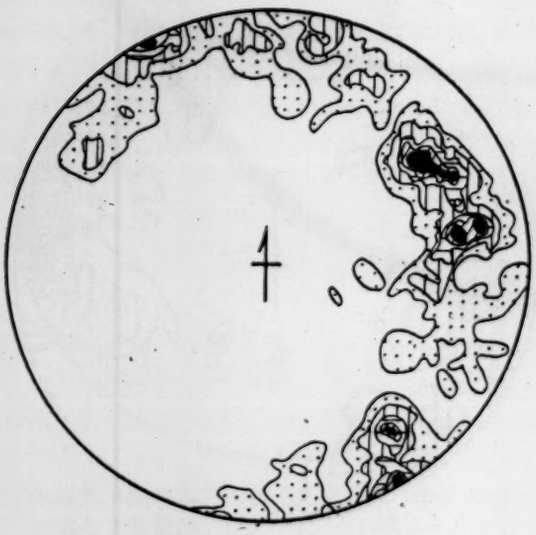

福井県大野郡和泉村下山付近で測定した fracture の極 119 個の1％図型. (9-6.5)-6-5-3.5-1.5-0%.

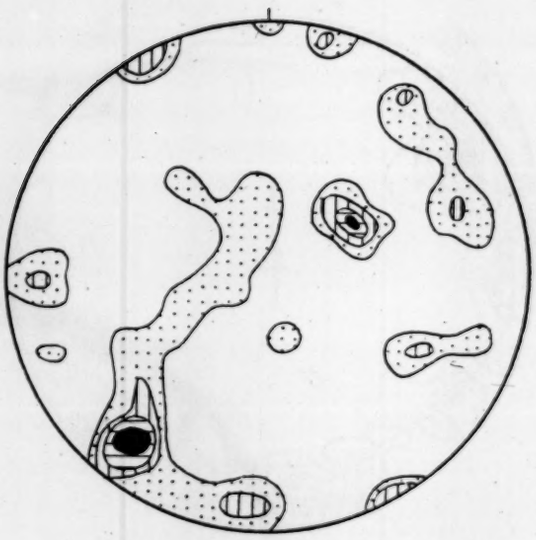

九頭竜川上流の大納川ぞいに発達す節理系, 下若生子砂岩頁岩互層. (12.5-10)-7.5-5-2.5-0%. (前田, 1961)

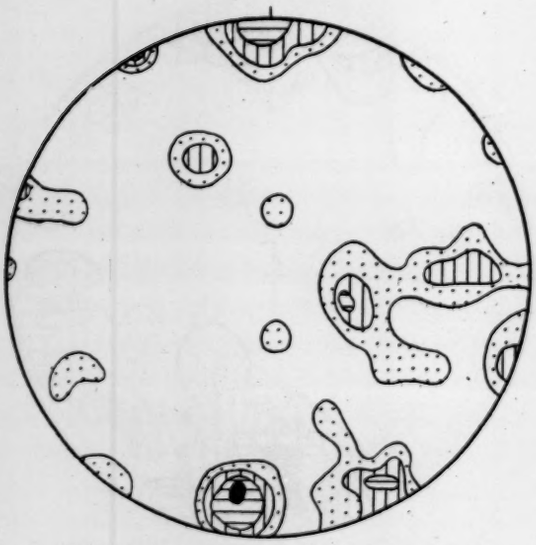

九頭竜川上流の大納川ぞいに発達する節理系, 道斉礫岩砂岩層. (12.5-10)-7.5-5-2.5-0%. (前田, 1961)

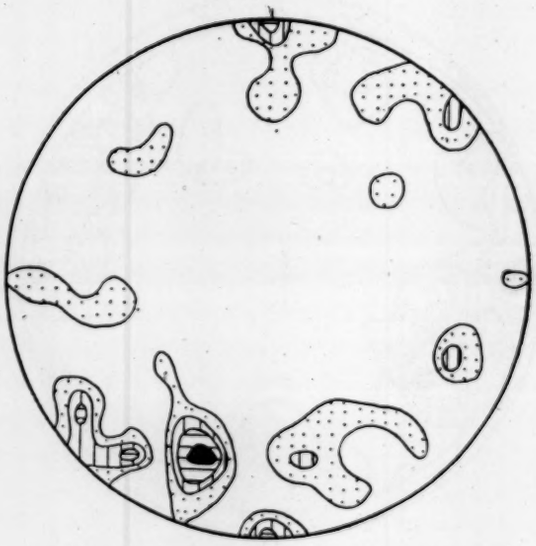

九頭竜川上流の大納川ぞいに発達する節理系, 貝皿頁岩層. (12.5-10)-7.5-5-2.5-0%. (前田, 1961)

第8図c 手取層群中の fracture system.

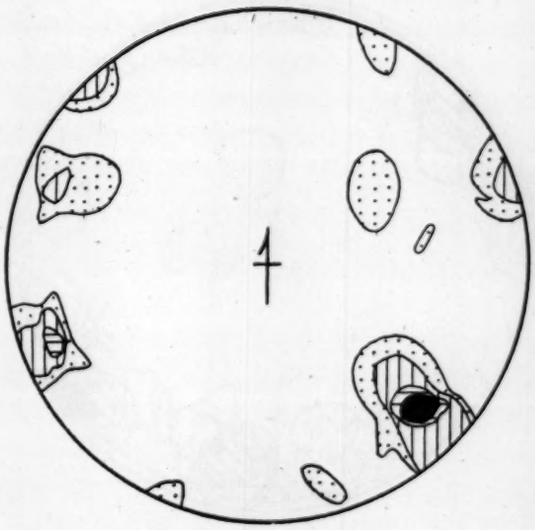

岐阜県大野郡荘川村牧戸付近で測定した fracture の極 21 個の3％図型. (28.5-24)-19-14.5-9.5-0％.

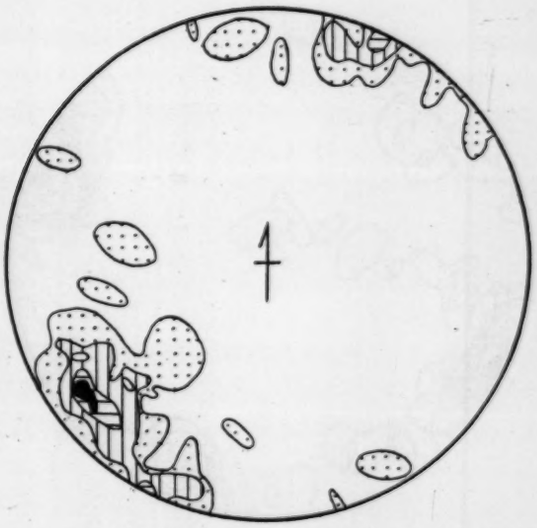

岐阜県大野郡荘川村岩瀬で測定した fracture の極 27 個の3％図型. (18.5)-15-11-7.5-0％.

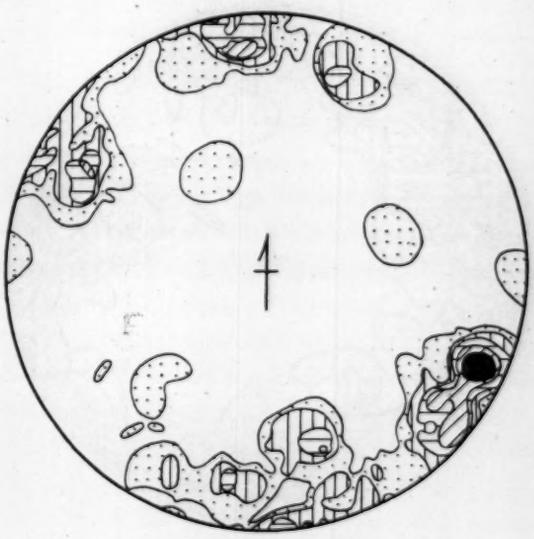

岐阜県大野郡白川村尾神で測定した fracture の極 56 個の2％図型. (12.5-10.5)-9-7-5.5-3.5-0％.

岐阜県大野郡白川村福島で測定した fracture の極 78 個の2％図型. (11.5-9)-7.5-5-4-2.5-0％.

第9図 a　濃飛流紋岩類中の fracture system.

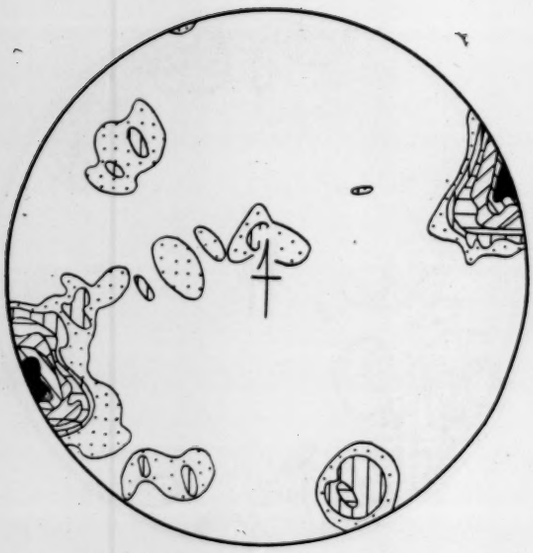

岐阜県武儀金山町で測定した fracture の極 44 個の2％図型．(27-25.5)-20.5-15.5-9-7-4.5-0%．

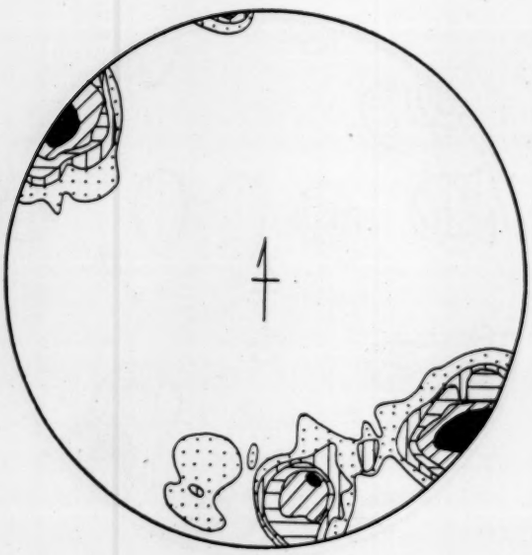

岐阜県益田郡下呂町で測定した fracture の極 25 個の3％図型．(36-28)-20-16-12-8-0%．

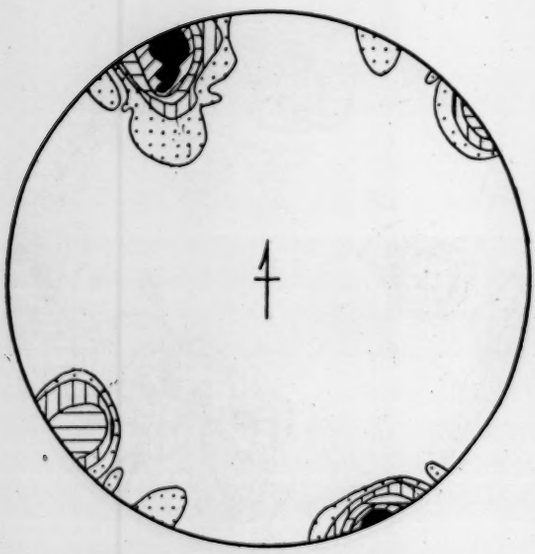

岐阜県益田郡萩原町上呂で測定した fracture の極 22 個の3％図型．(45.5-41)-32-22.5-13.5-9-0%．

岐阜県高山市飯山付近で測定した fracture の極 97 個の2％図型．(10.5-8)-6-4-3-2-0%．

第9図b 濃飛流紋岩類中の fracture system.

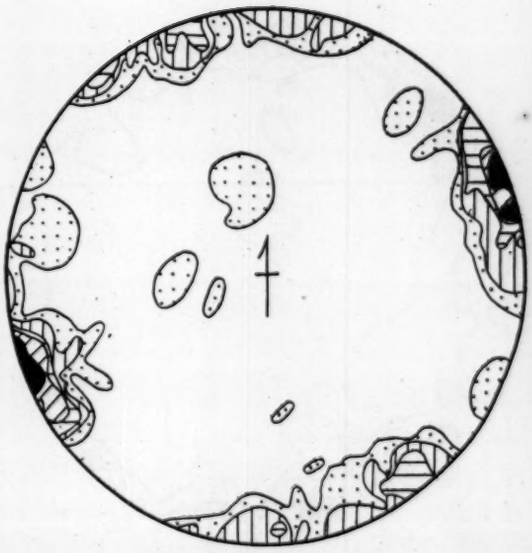

岐阜県郡上郡白鳥町神道で測定した面谷流紋岩中の fracture の極 56 の 2％図型. (18-14.5)-10.5-7-5.5-3.5-0%.

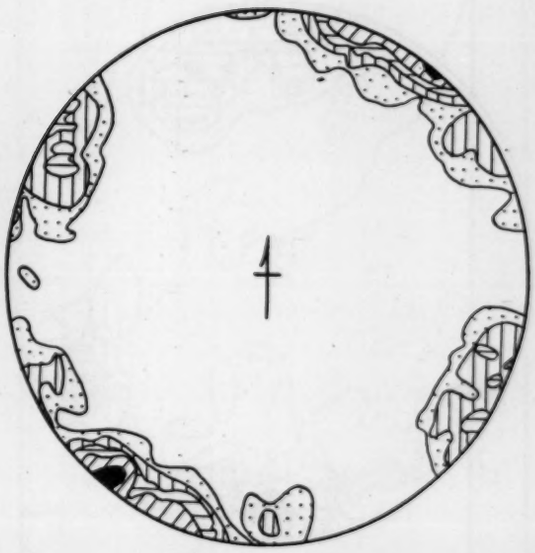

岐阜県郡上郡白鳥町釜ヶ洞で測定した安山岩中の fracture の極 53 個の 2％図型. (21-17)-13-9.5-5.5-4-0%.

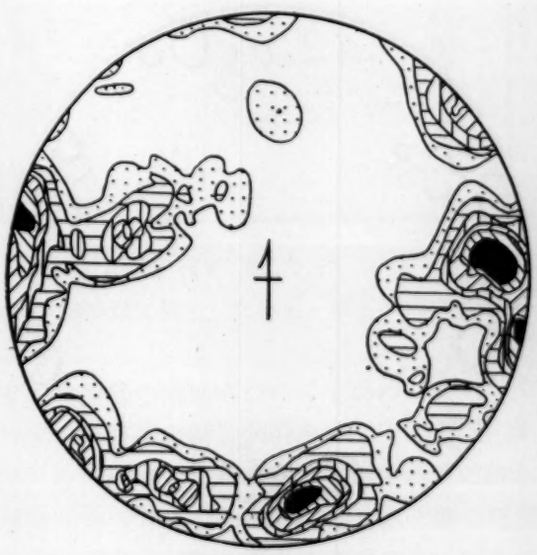

岐阜県郡上郡白鳥町中将で測定した安山岩中の fracture の極 85 個の 2％図型. (13-10.5)-8-6-4.5-3.5-2-0%.

福井県大野市葛原で測定した安山岩中の fracture の極 85 個の 3％図型. (9.5-8)-6-3.5-2.5-0%.

第 10 図　面谷流紋岩，および安山岩類中の fracture system.

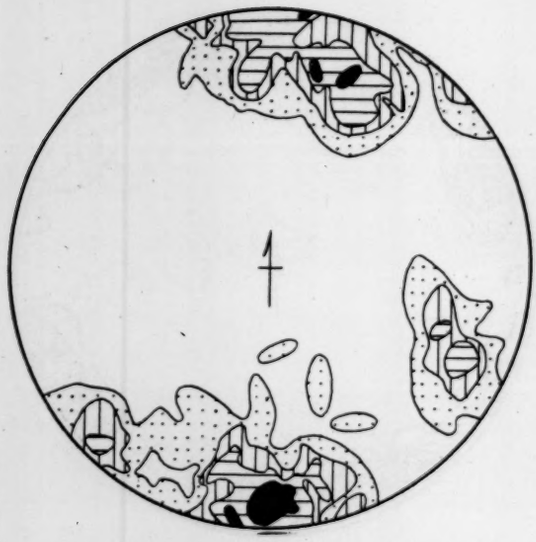

石川県能美郡鶴来町で測定した緑色凝灰岩層中の fracture の極 41 個の 3％図型．(19.5-14.5)-10-7.5-5-0％．

福井県鯖江市西鯖江で測定した緑色凝灰岩層中の fracture の極 78 個の 2％図型．(16.5-13)-10-7.5-5-2.5-0％．

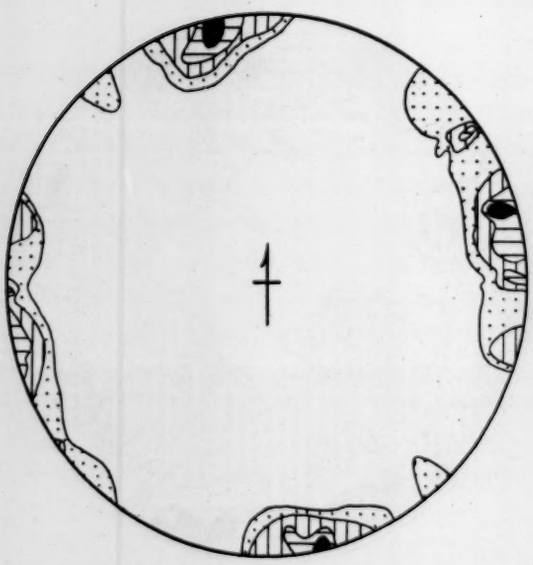

約阜県大野郡荘川村岩瀬で測定した段丘堆積層中のひびわれの極 20 個の 3％図型．(30-25)-20-15-10-0％．

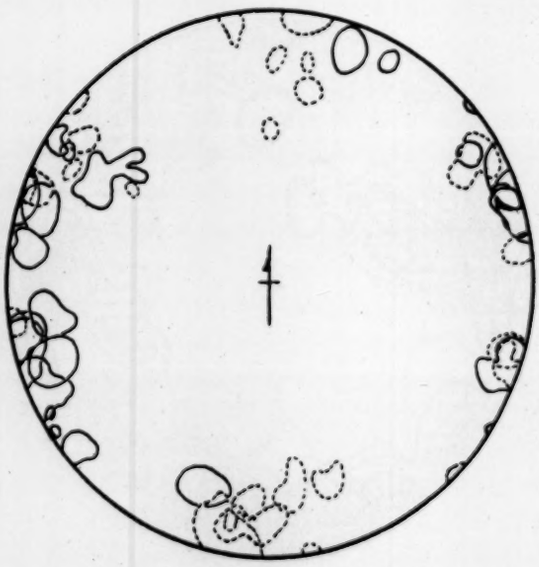

福井県平野東方山地の第三系中に発達する fracture system の極大区，副極大区の複合図型．(村井，1955)

第 11 図　第三系および第四系中の fracture system.

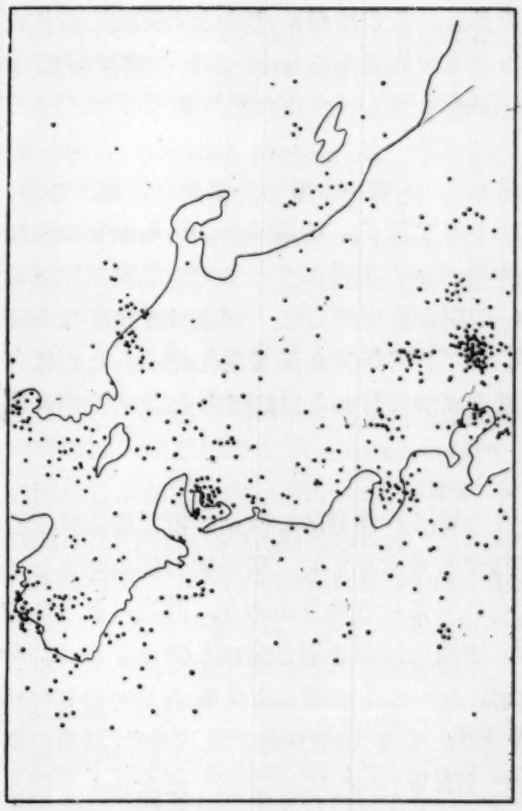

第 12 図a 震 央 分 布 図
1926-1956 間に発生した地震，深さ 109km 以浅.

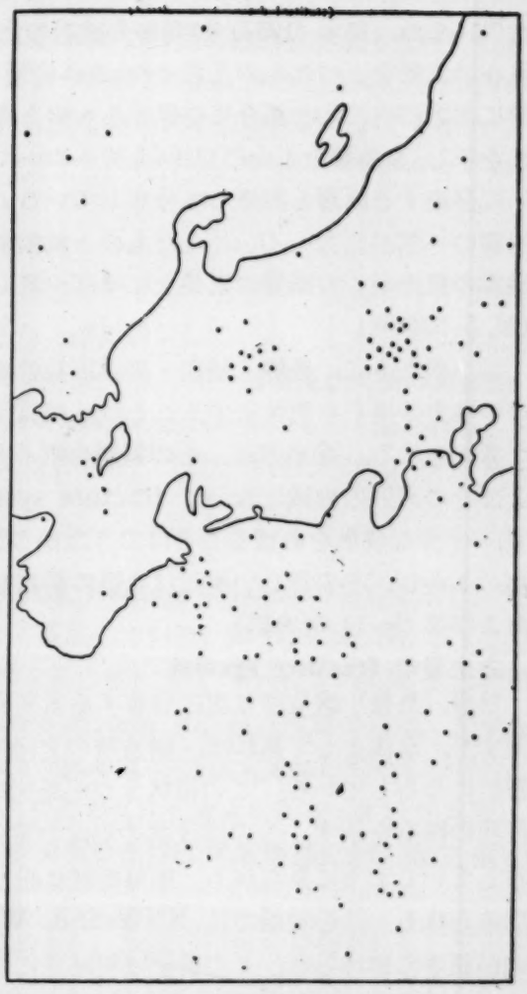

第 12 図b 震 央 分 布 図
1926-1956 間に発生した地震，深さ100km以深.

変成古生層の地域についても認めることができる．さらに北陸の第三系も，これにほぼ平行する階段状の構造配列を示している．美濃・越前山地における NNW-SSE 方向の断層系は，この法線方向の構造に相当する．これらの深成変成岩帯の主要構造および古生層の主要構造は，三畳紀の秋吉造山運動の際に完成されたものと考えられるが，中生代末において再び活動してその特性を明確化し，新生代においても著しい影響を残しているものと解釈される．法線方向の構造は，とくに中生代末以降の地殻変動の際に重要な役割をもつたと考えられ，飛騨変成岩帯の弧状分布を胴切りにして，水平方向に著しいくちがいを生ぜしめたように見られる．特に濃飛流紋岩の分布を境にして，西側が東側に対して10数 km 程南に向つて変位しているような構造を示していることは注目に価する．飛騨変成岩の分布する地帯内の唯一の古生層と考えられている石徹白の古生層については多くの議論があ

り，小林貞一 (1951) および小西健二 (1954) は，飛騨変成岩の "Dach" であると説明した[19]．また，藤本 (1957) は飛騨変成岩の上に不整合にのつていたものが断層運動の結果現在の位置をとつたものと考えた．これに対し，礒見・野沢 (1960) は，飛騨外縁帯が局部的に北方にへこんだ部分に位置するものと考えた．その南部に分布する古生層は構造の乱れを示し，古生層の走向の変化(北方へのへこみ)が，郡上八幡から白鳥にかけての長良川ぞいに発達する断層と関係して分布しているようであり，この断層にそう水平変位により古生層の一部が北方へくいこんだものと解釈することも可能である．そして，今回の北美濃地震の震央がこの断層の延長上にほぼ位置していることも，はなはだ興味ある事実である(第 5 図参照)．

以上のように，飛騨・越前・美濃山地の地質構造については，極めて重要な問題があり，この地方の構造を明確にすることは，地質学上ばかりでなく，地震学上からも重要な課題と考えられる．筆者等は，その課題を解くための手がかりを得ようとして，北美濃地域およびその周囲の地域において fracture system の調査を実施した．調査は予察的なもので，十分な成果をあげることはできなかつたが，2，3 の興味ある資料を得ることができた．しかし，その詳しい検討は今後の綿密な調査をまつて行わなければならない (第 4 図および第 6～11 図参照)．

古生層の fracture system

飛騨 (外縁) 構造帯以南に分布する未変成の古生層は，部分的には小規模な褶曲構造を示すが，全体として見れば，構造帯の方向に平行する走向をもち，高角度の傾斜をなして帯状に分布している．この帯状分布が局部的な乱れを見せる場合があり，前述のような階段状の構造を示す．この階段状の走向の変化は，法線方向の断層と密接な関係をもつて分布しているように見られる．根尾断層に沿う地域においても同様な古生層の走向の変化が認められる．この地域では，NNW-SSE，WNW-ESE の 2 方向(法線方向)の割れ目系の発達が顕著に認められ，この構造は根尾谷にそつて NNW へ延び，南部では水鳥より関へ向つて ESE へ延びている．根尾断層がこのような fracture system の発達状態と密接な関係を有することは明白である．長良川上流においては，前述のように古生層の走向の変化が認められるが，この地域では NNW-SSE，NW-SE の 2 方向 (法線方向) の割れ目系の発達が顕著で，この構造は長良川にそつて NNW へ延びている．古生層が均質な帯状分布を示し，階段状の走向の変化を示さない地域では，単純な様相をもつた fracture system の均質な発達が見られる．このような地域では切線方向と法線方向の顕著な節理系の発達が認められる．飛騨 (外縁) 構造帯に接する地域では，切線方向の割れ目系の発達が著しく，これは高角衝上断層系を代表するものと解釈される．デッケン構造を示唆するような低角の割れ目系は認めることができなかつた (第 7 図参照)．

手取層群の fracture system

本地域の手取層群はほぼ W-E 方向の軸をもつ緩かな褶曲構造を示している．白山地区では NE-SW，NW-SE の 2 方向の構造による地塊化が特徴的で，九頭竜地区では W-E 方

19) 小西健二「福井県石徹白村の古生層」地質学雑誌 **60** (1954)，7-17.

向の衝上断層系で切られて地溝状の構造を示す．九頭竜川擾乱帯内の手取層群の fracture system はいく分不規則な発達を示し，衝上断層系の影響が強く表われている．白山地区の手取層群の fracture system では，E-W, NE, NW の 3 組の割れ目系よりなつている．後の 2 つの割れ目系は，前田 (1956, etc.) のいう飛騨方向および白山方向にそれぞれ相当する．このような割れ目系の発達は，九頭竜川擾乱帯内の手取層群についても認められるが，著して擾乱を受けたため，構造の乱れが目立ち，特に衝上断層系の影響を強く示している (第 8 図参照)．

流紋岩類の fracture system

濃飛流紋岩類は顕著な節理系の発達を示し，断層系の発達も目立つ．白鳥町付近の面谷流紋岩の fracture system は，手取層群のそれとほぼ類似している．しかし庄川流域の地区では，やや異つた様相を示し，かつ変化が大きい．この部分は濃流紋岩類の西縁部の断層系の集中する部分に相当するものと考えられ，構造の乱れが多いものと思われる．流紋岩体の中央部では，fracture system は，比較的単純，均質な発達を示すようである (第 9 図参照)．

新生界の fracture system

福井平野の東方地域に分布する第三系は，均質な fracture system の発達を示し，その特徴は，手取層群の fracture system によく類似している．E-W, NW, NE の 3 方向の割れ目が認められ，これらの内 NW, NE の 2 組の割れ目は wrench fault 状の断層構造を反映するものと考えられる．この fracture system の方位は地層の走向，傾斜と密接な関係にあり，その変化につれて fracture system の方位も変化している (村井, 1955)．これらの構造は，基盤の飛騨変成岩帯の構造の反映と考えられる (第 11 図参照)．

安山岩類も顕著な節理系の発達を示し，その大体の傾向は手取層群および第三系の fracture system に類似する (第 10 図参照)．

段丘堆積層中にしばしば著しいひびわれが認められ，断層の存在も期待される．庄川流域において調査した 1 例について見れば，そのひびわれ系は，第三系のそれに共通の特徴を示すようにも見うけられる．この点については今後綿密な調査を行う必要がある．

V. むすび

北美濃地震は，飛騨構造帯および九頭竜擾乱帯に近い位置に起り，かつ濃尾地震，福井地震の震央にも近かつたので，構造地質学上大きな興味がもれた．しかし地震断層と認確できるものは発見されなかつた．ただし，震央付近の根尾断層の北半の方向 (NNW-SSE) に平行する帯上の地区に被害・地変が集中したようにも見うけられたのは注目してよい．この帯はまた，長良川に沿う NNW-SSE 方向の断層系の延長にあたる．震央が飛騨構造帯の北側の変成岩区内にあるか，あるいは南側古成層区にあるかは明らかでない．震央と報告された大日岳付近では，火山噴出物によつて基盤岩類がおおわれてしまつている．石徹白に分布する古生層の構造から，この地区では構造帯の外縁が北方にくい込んでいるとも考えられる．fracture system の調査はこの地域の構造の解明に十分役つものと期待される．

36. *Some Notes on the Geologic Structure of the Kita Mino District.*

By Isamu MURAI and Hiromichi TSUYA,
Earthquake Research Institute.

On August 19, 1961, a local but destructive earthquake occurred in the mountains of the Kita Mino district on the borders of Gifu, Fukui and Ishikawa prefectures, Central Japan. The writers carried out a field survey on the damage and topographic changes caused by the earthquake, and at the same time made a reconnaissance on the geologic structure of the district to see its effect, if any, on the earthquake features.

The damage to buildings was rather slight, and no trace of new earthquake-fault could be found anywhere in the epicentral area. But rock falls, land slides, and cracks in the ground occurred on the steep mountain slopes as well as on the road cuttings in many places in the area. Most of these ground disturbances were distributed within a zone extending in the NNW.-SSE. direction from Ichinose in Ishikawa pref. to Shiratori in Gifu pref. and running parallel to the trend of the north wing of the Neo (Midori) fault formed at the time of the great Mino-Owari earthquake of 1891.

The epicentre of the present earthquarke was located near the tectonic line (or zone) called the Median Line of the Inner Zone of Southwest Japan, or the Hida Tectonic Zone. It represents the border zone between the Hida metamorphic rocks and the adjoining Paleozoic formations. The main structural framework of the metamorphic formations and the Paleozoic formations near the tectonic zone is a "stepped" combination of two structural trends, tangential and normal to the arc of their distribution. The tangential trend represents the thrust system that predominates in the tectonic zone, while the normal trend represents the fault system having a trend of NNW.-SSE. or NW.-SE. The structural framework is such that the thrust structure and even the arc of the tectonic zone itself have been displaced more or less horizontally by the fault system. The Neo fault represents a fault belonging to this fault system. The zone most severely disturbed by the present earthquake is situated close to the Hida Tectonic Zone and seems to follow the trend of the same fault system, lying on the extension of the NNW.-SSE. faults in the upper course of the river Nagara in Gifu pref.

地震研究所彙報
第39号(1961)935-942頁

37. 北美濃地震被害地の地質
第1報　福井県打波川上流～岐阜県石徹白川上流地域

地震研究所　森本良平
松田時彦

(昭和36年9月26日発表—昭和36年10月30日受理)

まえがき

1961年8月19日の北美濃地震は，白山の南西麓を中心に若干の被害を与えた．筆者らは震央付近の地質および地震断層の存否を知るのを目的として，同年8月下旬から10月下旬まで，数回にわたつて被害地の踏査および資料の収集を行った。本稿はその調査結果

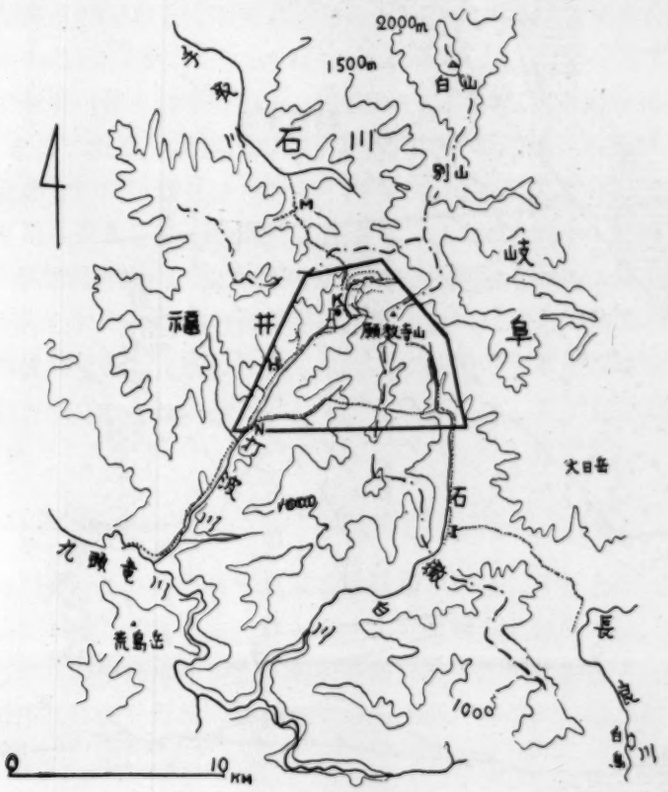

第1図　調査地域
点線は踏査ルート　H: 鳩ヶ湯; I: 石徹白; K: 小池; M: 三谷; N: 中村

の1部である．主な踏査ルート(第1図)は，九頭竜川支流の打波川上流沿い，石徹白川上流沿い，および両川間の山地横断である．

なお，打波川沿いの地質については，前田四郎[1] の地質調査がある．

1) 前田四郎「福井県打波川および石徹白川流域の手取層群の層序と構造」地質雑 63 (1957), 357-365.

地 質 の 概 略

この地域の中央，願教寺山とその南につづく山嶺部は広く新生代の安山岩に被われ，中生代およびそれ以前の岩石は，主に打波川および石徹白川の谷沿いに露出する．その主な岩石は，飛騨片麻岩類(古生代?)，手取層群(中生代後期)，流紋岩質凝灰岩とそれを貫く流紋岩（中生代末期）および，これらを被う新旧の安山岩類(第三紀後期～第四紀)である(第2図地質図参照)．このほか，調査地域の南西隣（上打波桜久保）には，軽微な変成作用を受けた古生代層と思われる，黒色泥質岩・石灰岩・凝灰岩からなる地層が小範囲に露出す

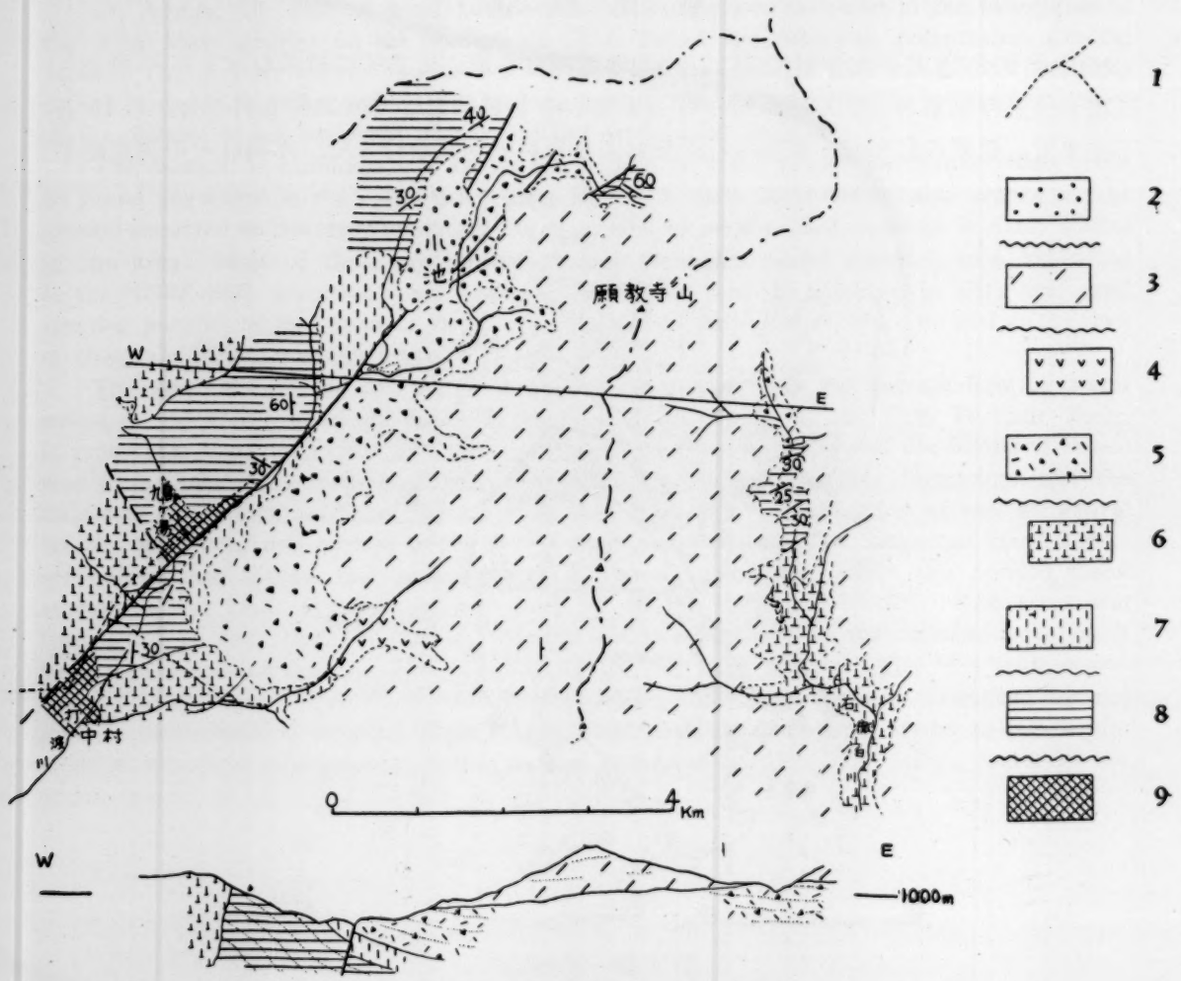

第 2 図　願教寺山付近の地質図

1　発電用水路(隧道)
2　地辷り堆積物
3　新期安山岩類
4　玢岩
5　古期安山岩類
6　流紋岩(一部迸入岩)
7　流紋岩質凝灰岩
8　手取層群
9　飛騨片麻岩類

る．また，安山岩～玢岩の岩脈があるが，地質図では大部分省略した．

中生代の地層は飛騨片麻岩類の上に不整合にのり，一般に 30°～50° 傾き，打波川沿岸では，小池奥平部落の西を中心とする不完全な盆状構造を示す．顕著な断層（鳩ケ湯―小池断層と呼ぶ）が打波川沿いにあり，各時代の地層分布がこれを境にして喰い違つている．

次に主な地層を古い順に簡単に記載する．

1)　飛騨片麻岩類

打波川沿いに，鳩ケ湯―小池断層に分断されて，鳩ケ湯付近と中村付近に露出する．両地域とも主に黒雲母角閃石片麻岩からなる．比較的有色鉱物が多く，その配列方向の明瞭なものと，片状構造のあまり明瞭でない石英閃緑岩様のものとが野外で区別できるが，両者は密接に相伴つて産する．中村地域にはこれらの岩石に伴つて結晶質石灰岩がある．

2)　手取層群

打波川の谷で飛騨片麻岩の上に不整合にのる．石徹白川では背斜をなして露出する．広い分布地域は打波川北西山地で，そこでは海抜 1300 m 以上まで分布する．主に石英質礫ないし花崗岩質の砂岩（多くは中粒ないし粗粒）で，しばしばその中に 0.5～5 cm の円礫（珪質岩が多い）をまじえる．新鮮面では淡青灰色で一般に褐色を帯びて風化する．しばしば炭質黒色頁岩あるいは炭層をはさむ．これらのいずれにも炭化した植物破片をみる．鳩ケ湯北東方発電用水取入口付近の黒色頁岩中に *Cladophlebis* sp. (*C. denticulata* (Brongniart)?) が見出された．また同地付近転石中から *Corbicula tetoriensis* Kobayashi & Suzuki が得られた．この地域の手取層群からは海成を示す資料は得られず，大部分あるいは全部陸成層であると思われる．なお，本地域の手取層群は前田四郎により赤岩砂岩層（手取層群上部）とされ，時代はジュラ紀後期ないし白亜紀初期と推定されている．厚さ約1000 m.

3)　流紋岩類

流紋岩類には，凝灰岩と迸入岩がある．

3a) 流紋岩質凝灰岩　これは打波川流域の手取層群の上にそれとほぼ平行に重なり共通の地質構造を示している．すなわち，鳩ケ湯―小池断層の北西側では，手取層群とともに盆状構造に参加してその中央部を満し，同断層南東側では手取層群とともに北東にゆるく傾斜している．層序的には平行状の不整合であろうが，構造的には調和している点は注意すべきである．

凝灰岩は，塊状緻密のため山腹においてやや丸味を帯びた白い壁をつくることが多い．大部分は淡灰色で，時に褐色のレンズ状小斑点をもつた珪長質の凝灰岩で，一部は熔結凝灰岩である．鏡下で少量の石英斑晶の小破片は認められるが．石英の斑晶を欠き斑晶の斜長石は大部分炭酸塩鉱物で置換され，一般に変質が著しい．有色鉱物は認め難い．この凝灰岩の下位に帯褐色塊状，節理の発達した熔岩 (?) を伴うことがある（小池西方桧谷）．厚さ 100 m 以上．また，中村東方ミノ又谷には，著しく変質硬化した凝灰角礫岩，石英斑晶の目立つ流紋岩質凝灰角礫岩，および軽石凝灰岩の小露出がある．

3b)　その他の流紋岩　打波川流域で，飛騨片麻岩・手取層群および上記の凝灰岩を不調

和に貫く流紋岩体がある．これは新鮮面で灰色，風化面で褐色を呈し，斜長石斑晶のほか多量の石英が目立つ．流理構造や角礫状部分はなく比較的均質である．少量の黒雲母斑晶をもつものがある．

石徹白川沿いの流紋岩は石英斑晶を普通にもつが，所によりゆるいまたは垂直に近い流理構造を示す．しばしば柱状節理が発達する．迸入岩か噴出岩か明らかでないが，まれに豆灰石 (pisolite) をふくむ凝灰岩が発見される(転石で)ので，少くとも一部は噴出したものであろう．

これら流紋岩は，この地域の南方で記載されている面谷流紋岩[2] あるいは濃飛流紋岩[3] に相当するものであろう．

4) 安山岩類

不整合で接する新旧2つのグループに分けられる．

4a) 古期安山岩類 願教寺山の西～北西および南西の谷沿いによく露出する．いずれも露頭は海抜約 1100 m までで，それより高い所は新期安山岩類が不整合に被う．願教寺山北西，打波川上流部では東または北にゆるく傾斜し(局部的には 60° 以上の急傾斜)，石徹白川上流部では南に 20°～30° 傾く．本層の分布の西縁で鳩ヶ湯一小池断層に切られる．

打波川流域では，下部は凝灰角礫岩，上部は軽石凝灰岩からなる．石徹白川流域では後者だけが露出する[4]．

下部の凝灰角礫岩は，普通輝石紫蘇輝石安山岩(*Vd* 型)の大小の類質岩塊からなり，不明瞭で大まかな層理が認められる．砂岩などの異質礫をふくむ火山円礫岩に移化することがある．

上部の軽石質凝灰岩には，淘汰がよく火山礫や炭質物をふくみ層理を示し時には乱堆積を示す部分(風成一水成堆積物)と，塊状で淘汰不良でほとんどすべてが軽石片・ガラス片からなる部分(軽石流様堆積物)とがある．両者とも願教寺沢の底によく露出し，両者が上下に数回繰り返し重なつているのがみられる．厚さ 100 m 以上．一般に露頭で黄色を帯び，ゆるく膠結している．軽石は斜長石・紫蘇輝石・角閃石(少量)の斑晶をもち安山岩質である．

これら古期安山岩類は，現在の地形と無関係に新期安山岩類の下に不整合に横たわり，断層によつて転位し，また岩石が多少変質している（紫蘇輝石斑晶は粘土鉱物・炭酸塩鉱物などで置き換えられていることがある）ことなどの点から，第三紀後期(鮮新世後期?)のものと考えられる．

4b) 新期安山岩類 新期安山岩類は，願教寺山およびその南につづく 1600 m 級の山嶺部を構成し，安山岩の熔岩および泥流堆積物が繰り返し重なつたものである．石徹白川

2) 河合正虎・平山 健・山田直利 五万分之一地質図幅説明書「荒島岳」 地質調査所 (1957).

3) 河田清雄・山田直利・礒見 博 村山正郎・片田正人「中央アルプスとその西域の地質，その 2: 濃飛流紋岩類」 地球科学 54 号 (1961), 20-31.

4) なお，このほかに，この地域の東南方，上在所北方の石徹白川左岸に，新期安山岩熔岩に被われて軽石流堆積物が小範囲露出する．詳細な層位関係は未詳である．

沿いでは海抜約 900 m(南部)ないし 1100 m(上流部)にその下底があり,比較的平坦な面をもつて前述の軽石凝灰岩・手取層群・流紋岩類を被う. 厚さ約 600 m. 福井県側(山腹の西斜面) では東へゆるく傾き下つているのが観察されたが一般に水平に近い. 熔岩はしばしば滝をつくり, 泥流堆積物はいくつかのやや平坦な堆積面を残している. 願教寺山北西の海抜 1200 m の平坦面(原の平)は, 軽石凝灰岩 (古期安山岩類) を被う約 50 m の厚さの熔岩がつくるものである (第 3 図). 熔岩の一部は打波川沿いに小池奥平入口まで流下し

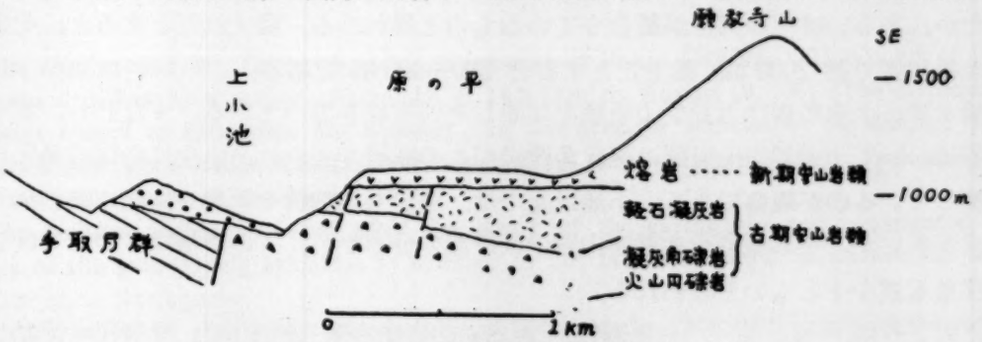

第 3 図　小池付近の地質断面図

凝灰角礫岩 (古期安山岩類下部) を不整合に被つている.

新期安山岩類の岩石は, 紫蘇輝石普通輝石安山岩 (*Vd* 型), 角閃石紫蘇輝石普通輝石安山岩などである. 多量の角閃石斑晶をもつ安山岩は上位に比較的多い.

この新期安山岩類の時代は, その地形との密接な関係からみて, 第四紀であろう.

なお, ミノ又谷には単斜輝石をふくむ角閃玢岩のやや大きな迸入岩体があるが, 周囲の安山岩類との関係は明かでない.

5)　地辷り堆積物

小池部落のある丘陵は地辷り地形を示し, その厚い堆積物からなる. 下小池西方桧谷に面した小沢では, 厚さ約 100 m(海抜 900 m から 1000 m 以上まで)に達する. 褐色土壌または葉理のある砂をマトリックスとしてその中に手取層群の砂岩泥岩および安山岩の大小の岩塊がふくまれている. 現在は樹木に被われ, 安定しているものと思われる.

断層と北美濃地震

この地域で最も顕著な地質断層は, 打波川沿いに北東一南西方向に走る鳩ケ湯一小池断層 (新称)である. このほか, 1～2 の推定断層と断層粘土を伴つた *N* 20°W の 2 本の断層および玢岩を破砕する東西方向の断層がいずれもミノ又谷で観察されたが, その意義は明らかでない.

北美濃地震との関係は, 結論を先に言えば, この地域でもつとも著しく若い断層である鳩ケ湯一小池断層が今回の地震で活動した証拠は得られなかつた. また, その他に確実に地震断層と思われるものは発見できなかつた.

6)　鳩ケ湯一小池断層

中村西方から北東へ鳩ケ湯を経て小池北方に達する, 長さ 10 km 以上の断層である.

小池南西での観察では，断層面は垂直ないし西に急傾斜している．手取層群を切る部分ではとくに巾 10 m 以上の粘土を伴う破砕帯を形成し，その断層粘土は山腹崩壊の一原因になつている．鳩ヶ湯の鉱泉の泉源は，ほぼこの断層上に位置する．

この断層は，飛騨片麻岩類から古期安山岩類までの各地層を切断し，両側の地層の露出をやや規則的に移動させている(地質図参照)．地層の分布のずれから推定すると，この断層に沿う変位は北西側の地盤がこの断層を境にして北東方へずれ動いたか南東側へのし上げたか，あるいはその両方が組合つているものと思われる．横ずれだとすると，その量は鳩ヶ湯付近で約 2000 m，衝上だとすると 200～400 m である．

鳩ヶ湯一小池断層は古期安山岩類を切断しその東縁を限つている．すなわち，奥平西方桧谷において，古期安山岩類の凝灰角礫岩がこの断層で切られ，中生代の熔結凝灰岩に直接接しているのが観察できる．小池以北では，地辷り堆積物や新期安山岩に被われて不明の点が多いが，手取層群や古期安山岩の破砕部の分布から，この断層は3つに分岐して，変位量も減少するものと思われる．

このように，鳩ヶ湯一小池断層は，古期安山岩類（第三紀末期?）堆積後も活動したことはたしかであるが，新期安山岩類を変位させているか否かは今後の精査にまたねばならない．

7) 北美濃地震との関係

調査地区およびその周辺では，家屋・道路の破壊，石垣・墓石の倒壊などの被害のほかに，山腹の崩落・尾根上の亀裂が各所に見られた．尾根上の亀裂の方向は，尾根ののびの方向にほぼ一致し，その他に一般的な方向性は認められなかつた．これらの被害程度は調査地域内で一様ではないが，概して願教寺山の周辺で著しい．

鳩ヶ湯一小池断層は上述のように，第三紀末以後も活動した新しい顕著な断層であるが，今回の地震でそれが活動した証拠は得られなかつた．この断層は，発電用導水隧道を3ヶ所で，林道を4ヶ所で横断する．それらの地点における隧道壁（コンクリート巻き）および道路上には喰い違い等の異常は認められなかつた．隧道内には地震直後多数の亀裂を生じたが，それは主に導水隧道が山腹沿いの浅所を通過している部分に多く，まれには，その山側の壁が数 mm 程度押し出した．断層通過推定地点でとくに亀裂の密集あるいは壁の移動はなかつた（導水路の位置を第1図に示した）．

そのほかの地域でも地震断層の生成を思わせる地形的な変位は，野外で観察されなかつた．

謝　　辞

上記の調査については福井県森広大野市長，岐阜県郡上郡野田白鳥町長および町役場の各位，その他現地の多数の方々にお世話になつた．ここに厚くお礼申し上げる．また，化石について御教示下さつた木村達明博士および速水格博士，発電用水路の被害について御教示下さつた北陸電力上打波発電所の方々に，感謝する．

なお，この調査費用の一部は文部省綜合研究費を使用した．

37. Geology of the Area Damaged by the Kita Mino Earthquake. Part I. The Upper Reaches of the Uchinami River and the Itoshiro River, Fukui and Gifu Prefectures, Japan.

By Ryohei MORIMOTO and Tokihiko MATSUDA,
Earthquake Research Institute.

The area around Mt. Gankyoji-yama, 45 km east of Fukui City and 70 km north of Gifu Gity, was attacked by a severe earthquake at 14 h 33 m on August 19, 1961 (The earthquake was later named as Kita Mino Earthquake). In this area, in addition to the damage done to houses and stone walls, fissures were opened on narrow ridges. Many rock fall and earth fall took places on the steep cliffs.

The writers visited the area after the shock of the earthquake and investigated the geology of the area paying attention to whether or not faults occurred in connection with the Kita Mino Earthquake.

As shown below, the highly metamorphosed rocks of the Paleozoic (?) age are the oldest rocks in this area. Overlying them, younger Mesozoic sedimentary rocks and rhyolitic tuff are developed, which are not metamorphosed but gently folded or tilted. These rocks are covered widely by the older and younger andesite groups of the late Cenozoic age.

Quaternary	Landslide deposits	Sand, mud and gravel.
	Younger andesite group	Lava flows and mud-flows (hyp-aug-andesite and hornb-hyp-aug-andesite).
Late Pliocene ?	Older andesite group	Tuff breccia in the lower and pumice tuff in the upper.
Upper Cretaceous	(Rhyolite intrusion)	
	Rhyolite tuff	Welded tuff, tuff breccia (and lava flows ?).
	?	
Lower Cretaceous~ Upper Jurassic	Tetori group	Arkose sandstone, conglomerate and coaly shale (non-marine).
Paleozoic ?	Hida gneiss complex	Biotite-amphibole gneiss.

A remarkable fault (Hatogayu-Koike fault) is found, running in a southwest to northeast direction along the Uchinami River and dipping steeply northwestward. The outcrops of each terrain on both sides of the fault are separated and displaced, suggesting that the fault is a right-lateral strike-slip fault or a thrust which lifted the northwest side. If it is a strike-slip fault, displacement of about 2000 m explains the discontinuity of outcrops on both sides of the fault line. If it is a thrust, the amount of displacement is estimated as 200–400 m. The age of faulting is considered to be young, because the fault cuts all the terrains lying beneath the younger andesite group, although it is uncertain whether or not the younger andesite group is disturbed by this fault.

During their field observation the writers found no topographic features indicating the activity of this fault in the Kita Mino earthquake. The strikes of fissures opened on ridges show no regional orientation, but they depend upon the local topography. The fissures run generally parallel to the elongation of the ridges. Fissures on the road surface are also orientated parallel to the shoulder of the road. Waterway tunnels stretching from a power plant were examined immediately after the quake. Many cracks were found running on the concrete wall of the tunnels. The fault line of the Hatogayu-Koike fault crosses the tunnels at three localities. Any particular features indicating the relative movements along the fault, however, were not observed at these points.

In all other parts of the area, the writer could find no evidence of the occurrence of the earthquake fault relating to the Kita Mino earthquake.

Bulletin of the Earthquake
Research Institute
Vol. 39 (1961), pp. 943-951

38. *Seismic Characteristics in Ground of Mountainous Formation. (Observation of the After Shocks of the Kita Mino Earthquake.)*

By Kiyoshi KANAI and Kaio OSADA,

Earthquake Research Institute.

(Read Oct. 24, 1961.—Received Oct. 31, 1961.)

1. Introduction

It is well known that earthquake motions depend greatly on the seismic characteristics of ground and damage to buildings and other constructions caused by earthquakes have a considerably close relation to the ground formations on which they are built.[1] Almost all of the past investigations which had been carried out from the present standpoints were made by the phenomena in plain lands.

The Kita Mino earthquake of August 19, 1961 occurred in land of mountaineous formation. A general description of it is presented by other researchers in the present Bulletin.

In order to investigate the relation among the earthquake motions, the seismic characteristics of ground in land of mountaineous formation and damage to various kinds of construction, we made an observation of the after shocks of the present earthquake in the epicentral area during the period from August 26 to August 29.

2. Observation of the after shocks

The observation of the after shocks was made by two seismographs of the inverted pendulum type with a smoked paper recording system. The characteristic curves of the two seismographs are shown in Fig. 2. The positions of the four temporary seismograph stations located on various types of ground are represented in Fig. 3. The standard station is represented by No. 1 in Fig. 3 and the simultaneous observations of

1) K. KANAI, "Semi-empirical Formula for the Seismic Characteristics of the Ground," *Bull. Earthq. Res. Inst.*, **35** (1957), 309, foot-note 1)-4).

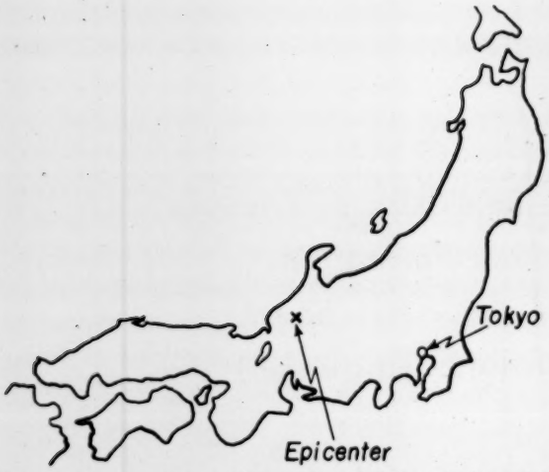

Fig. 1. Epicenter of the Kita Mino earthquake.

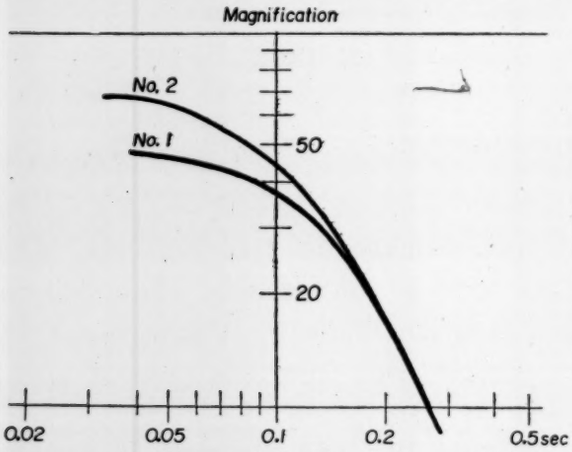

Fig. 2. The characteristic curves of the two seismographs.

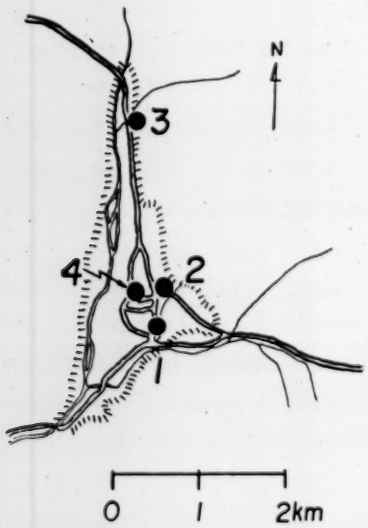

Fig. 3. The positions of the four temporary seismograph stations.

(1): Hakusankan, Shimozaisho, Itoshiro, Shiratori-machi;
(2): Taniya-ryokan, Nakazaisho, Itoshiro, Shiratori-machi;
(3): H. Itoshiro, Kamizaisho, Itoshiro, Shiratori-machi;
(4): J. Uemura, Nakazaisho, Itoshiro, Shiratori-machi;

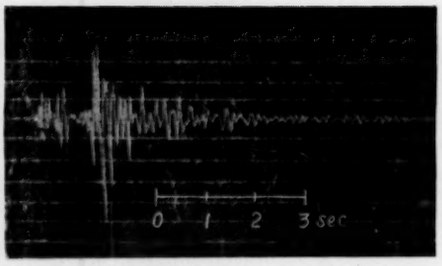

Fig. 4. Representative record of the after-shock observed at the station, No. 4, Aug. 27, 1961. Original×4.5.

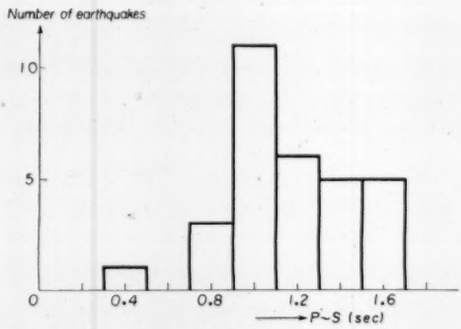

Fig. 5. Relation between the duration of preliminary tremors, so-called P-S time, and number of earthquakes observed at the standard station.

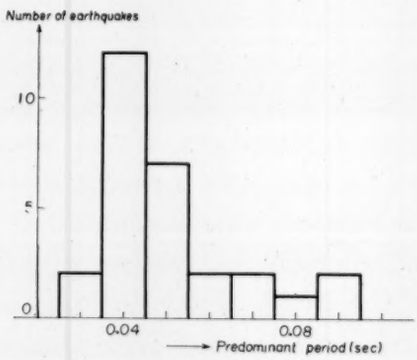

Fig. 6-1. Relation between the predominant periods of the preliminary tremors of after shocks and number of them observed at the standard station.

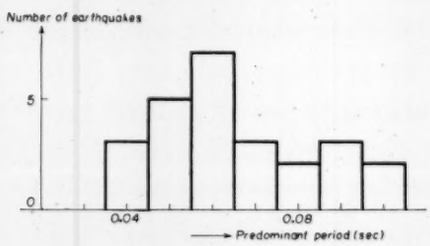

Fig. 6-2. Relation between the predominant periods of the main shocks of after shocks and number of them observed at the standard station.

Table 1. The results of observations of after-shocks of the Kita Mino earthquake.

Date	Time	Station	P-S time (sec)	Predominant period (sec)		Max. displ. (μ)	Max. accel. (gal)
				P	S		
8.25	15.29	1	1.2	0.044	0.052		
	15.37	〃	1.1	0.043	0.064		
	17.21	〃	1.1	0.050	0.059		
	19.06	〃	1.1	0.044	0.074		
8.26	7.22	1	—	0.071	0.039		
	9.43	〃	1.2	0.070	0.15		
	10.19	〃	0.92	0.081	0.093		
	12.00	〃	0.90	0.040	0.056		
	13.47	〃	1.6	0.053	0.073		
	15.59	〃	1.6	0.029	0.042		
	21.22	〃	1.4	0.13	0.12		
	22.34	〃	1.5	0.053	0.12		
	23.41	〃	1.6	0.055	0.062		
8.27	0.13	1	1.0	0.051	0.15		
	4.56	〃	1.5	0.053	0.11		
	13.05	〃	1.6	0.048	0.084	20	37
	〃	4	1.3	0.070	0.14	21	10
	14.21	1	—	0.042	0.088	3.9	3.9
	〃	4	1.2	0.088	0.11	3.5	2.1
	14.22	1	1.4	0.042	0.088	11	10
	〃	4	1.4	0.11	0.11	10	4.2
	14.37	1	1.0	0.042	0.074	6.0	2.5
	〃	4	1.1	0.088	0.13	21	6.5
	16.05	1	1.2	0.090	0.10	36	13
	〃	4	1.1	0.090	0.15	58	15
	19.26	1	0.97	0.042	0.050	—	—
	〃	2	2.3	—	—	—	—
8.28	2.32	1	0.46	0.025	0.048	—	—
	〃	2	0.53	—	—	—	—
	2.52	1	1.3	0.043	0.12	39	12
	〃	2	1.4	0.088	0.13	31	5.9
	11.32	1	1.7	0.050	0.097	29	9.0
	〃	2	1.6	0.070	0.10	12	8.7
	16.17	1	0.88	0.045	0.094	13	85
	〃	2	0.84	0.090	0.14	14	21
	16.22	1	0.84	0.092	0.11	63	15
	〃	2	0.88	0.092	0.16	49	6.9
	20.22	1	1.1	0.062	0.059	26	13
	〃	3	0.97	0.067	0.10	20	17
	21.31	1	1.0	—	0.044	3.5	—
	〃	3	1.1	0.079	0.10	—	—
8.29	0.49	1	1.2	0.046	0.046	6.8	13
	〃	3	1.0	0.10	0.14	15	15
	2.13	1	1.3	—	—	2.4	5.2
	〃	3	1.3	0.084	0.10	8.4	6.8
	9.31	1	1.1	0.044	0.052	4.0	8.5
	〃	3	—	0.084	0.10	6.0	8.4
	9.34	1	0.97	0.041	0.059	—	—
	〃	3	0.97	0.070	0.14	—	—

the after shocks were made between the standard station, No. 1, and each of the other three stations, Nos. 2, 3, 4, successively.

During 5 days, we observed 32 after-shocks and the data concerning them are listed in Table 1. The representative record obtained on the mountaineous formation of the ground is illustrated in Fig. 4.

Fig. 5 shows the relation between the duration of preliminary tremors, so-called P-S time, and the number of earthquakes observed at the standard station. From Fig. 5, it will be concluded that the after shocks observed originated several km away from the temporary seismograph stations because the P-S times of the after shocks ranged from 1 to 1.5 seconds.

The relations between the predominant periods of the preliminary tremors as well as the main shocks and the number of after shocks observed at the standard station are shown in Fig. 6. It will be seen from Fig. 6 that the predominant periods of the preliminary tremors and the main shocks of earthquakes take about 0.4 sec and 0.6 sec, respectively. Consequently, it may be concluded that the predominant periods of about 0.4 sec and 0.6 sec mean the natural periods of the ground, on which the standard station is located, caused by dilatational waves and distortional waves, respectively, because it may be considered that the the ratio of the two predominant periods mentioned above is approximately equal to the ratio of the velocities of the dilatational waves and distortional waves in the ground.

The relations between the maximum displacements as well as the maximum accelerations and the predominant periods of the after shocks observed at the four temporary seismograph stations are shown in Fig. 7.

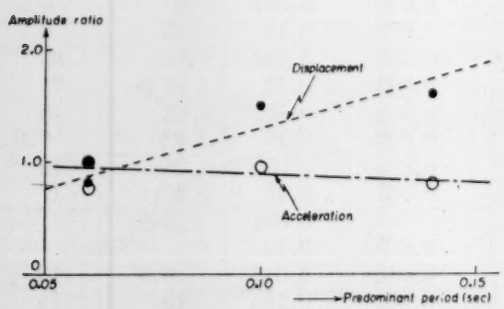

Fig. 7. Relations between the maximum displacements and the maximum accelerations and the predominant periods of the after shocks observed at the four temporary seismograph stations.

At any rate, it is ascertained from Fig. 7 that the larger the predominant period of the mountaineous formation of ground is (the softer or thicker the ground is), the larger the displacement of the earthquake motions is, on the contrary, the sense of acceleration is rather the reverse.

3. Application of an empirical formula for the strong earthquake-motions spectrum.

The acceleration spectrum of earthquake motions on bed rock may be adopted as a schematic view as shown in Fig. 8 which is estimated from the so numerous data of more than fifteen years observations at a 300 meter depth in the Hitachi Mine, Japan.

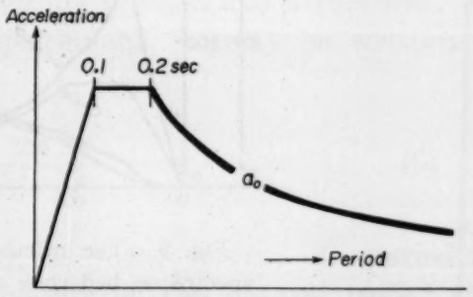

Fig. 8. Schematic view of the acceleration spectrum of earthquake motions on bed rock.

The empirical formula concerning the acceleration spectrum on bed rock represented by a_0 in Fig. 8 and that on ground surface, a, may be written as follows[2]:

$$a_0=\frac{10^{0.61M-1.73\log R+0.13}}{T}, \tag{1}$$

$$a=a_0\left[1+\frac{1}{\sqrt{\left[\frac{1+\alpha}{1-\alpha}\left\{1-\left(\frac{T}{T_0}\right)^2\right\}\right]^2+\left[\frac{0.3}{\sqrt{T_0}}\left(\frac{T}{T_0}\right)\right]^2}}\right], \tag{2}$$

in which, M=magnitude, R=hypocentral distance, α=impedance ratio of ground to bed rock, T=period of waves, T_0=predominant period of ground. From (1) and (2), the displacement spectra of earthquake motions on bed rock and ground surface can be written as follows:

$$\text{bed rock}; \quad u_0=a_0\left(\frac{T}{2\pi}\right)^2, \tag{3}$$

$$\text{ground surface}; \quad u=a\left(\frac{T}{2\pi}\right)^2. \tag{4}$$

As the first step of the present investigation, we assume $M=7$ and $R=50$ km and adopt $T_0=0.1$ sec which is the average value of the predominant periods of ground in the epicentral area of the Kita Mino earthquake; substituting these values in (1)-(4), we obtained four kinds of spectra, that is; accelerations and displacements on bed rock and ground surface, as shown in Fig. 9.

2) K. KANAI, "An Empirical Formula for the Spectrum of Strong Earthquake Motions," *Bull. Earthq. Res. Inst.*, **39** (1961), 88.

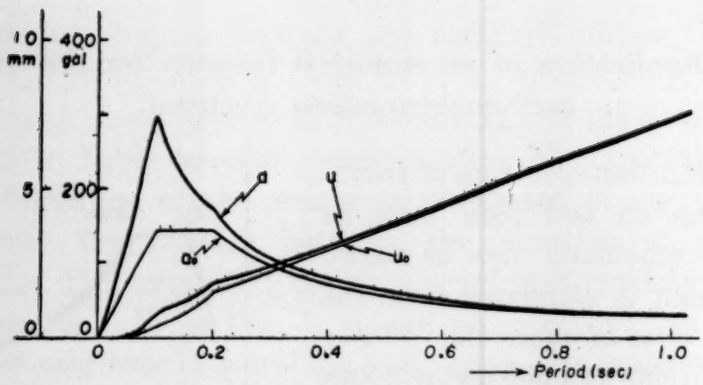

Fig. 9. The calculated acceleration and displacement spectra on bed rock and on ground surface.

Next, the calculated results of behaviour of simplified structures to earthquake motions having the characteristics shown in Fig. 9 will be compared with the effects of the Kita Mino earthquake on various kinds of actural structures.

(i) The case of the deflection of old-Japenese-style wooden houses.

The inclination, θ, of the one mass system of the fraction of critical damping, h, and of the height of the centre of gravity, H, under the condition of resonance with earthquake motions, u, may be expressed as follows:

$$\theta=\frac{u}{2hH} \tag{5}$$

The results of numerical calculations using (5) and Fig. 9 in the cases where $H=500$ cm and $h=0.05$, 0.1 for respective values of u corresponding to the natural periods of the houses, $T_0=0.1$, 0.3, 0.6 and 1 sec, are shown in Table 2. In general, the old-Japanese-style wooden house shall be partially damaged with about 1/30 radian inclination and collapses completely with about 1/15.

Table 2. The calculated values of inclination in wooden houses.

h	T_0			
	0.1	0.3	0.6	1.0
0.05	1/670	1/210	1/110	1/70
0.10	1/1300	1/420	1/220	1/140

The fact in which there was scarcely any damage to wooden dwellings except that caused by earth flows or land slides, at the time of the

present earthquake[3] agrees with the result of the present investigation in which all of the values in Table 2 are less than 1/30.

(ii) The case of shearing vibration in solid-like structures.

The displacement of shearing vibrations in solid-like structures, U, caused by earthquake motions of displacement, u, may be written as follows:

$$|U|=\frac{|u|\cos kz}{\sqrt{P^2+Q^2}} \tag{6}$$

where, z=axis, $k=2\pi/VT$, V=velocity of shear waves, T=period of waves, P and Q are terms depending mainly on the natural period and the damping factor of the structure, respectively. Accordingly, the maximum strain in a solid-like structure under the condition of resonance caused by earthquake motions of displacement, u, can be written as follows:

$$\frac{\partial U}{\partial Z}=\frac{2\pi u}{2h'VT_0} \tag{7}$$

in which, h' and T represent the apparent damping coefficient and the natural period of structure, respectively. The results of the numerical calculations using (7) and Fig. 9 in the cases, where V=2 km/sec and h'=0.05, 0.1 for respective values of u corresponded to T_0=0.1, 0.3, 0.6, 1.0 sec, respectively, are shown in Table 3.

The fact that the damage to good and rough construction works of concrete structures caused by the present earthquake was scarce and slight[4], respectively, can be interpreted by the present results in which

Table 3. The calculated values of the strain on rigid constructions.

h'	T_0			
	0.1	0.3	0.6	1.0
0.05	2×10^{-4}	2× 〃	2× 〃	2× 〃
0.10	1×10^{-4}	1× 〃	1× 〃	1× 〃

3) Y. OSAWA, "On the Damage to Buildings during the Kita Mino Earthquake of August 19, 1961," *Bull. Earthq. Res. Inst.*, **39** (1961), 869-872.

4) T. OKUBO, "Damage to Public Works Structures caused by the Kita Mino Earthquake", *The Annual Meeting on Earthq. Engg.*, Japan Soc. Civil Engineers, Oct. 18, 1961.

the values in Table 3 correspond approximately to the strength of weak concrete.

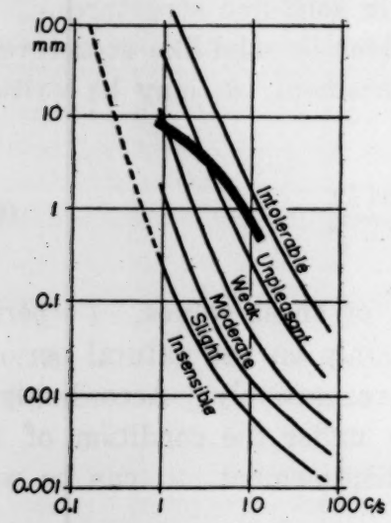

Fig. 10. Relation among the amplitude, the frequency of harmonic vibrations and human susceptibility.

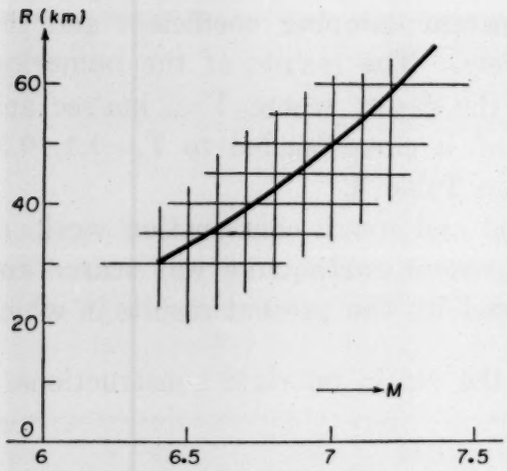

Fig. 11. The values of magnitude (M) and hypoceutral distance (R) on the curve satisfy the actual phenomena caused by Kita Mino earthquake.

(iii) Human senses.

A graph[5] of the relation among the amplitude, the frequency of the harmonic vibrations and human susceptibility is reproduced in Fig. 10. The fat line in Fig. 10 represents the amplitude of the earthquake motion at the ground surface as shown in Fig. 9. The fat line in Fig. 10 tells us that the result obtained by the empirical formula, (4), agrees with the human experience at the time of the Kita Mino earthquake[6] when the consideration that the human susceptibility to shocks is lower than to harmonic motions[7] is taken into account.

(iv) Partial conclusion.

From the present investigations, it can be said that the facts of the effects to the actual structures as well as to humans caused by the Kita Mino earthquake were thoroughly interpreted by the results of the numerical calculations by using the empirical formula concerned with strong earthquake-motion spectrum.

As a further consideration, though it has been outlined in the above discussions utilizing the

5) M. ŌSHIMA, "Vibration and the Human Being", *Rep. Steel Labour Health*, Vol. 2, No. **3-4** (1953), 30, (in Japanese).

6) F. KISHINOUYE and I. ONDA, "On the Kita Mino earthquake", *Bull. Earthq. Res. Inst.*, **39** (1961), 857-868.

7) F. KISHINOUYE, "Human Susceptibility to Shock Vibrations of the Ground", *Bull. Earthq. Res. Inst.*, **33** (1955), 207-210.

results of numerical calculations under the assumptions of $M=7$ and $R-50$ km, the same results will be obtained when the values on the curve in Fig. 11, calculated from (1) are used. In other words, the interpretations carried out in this section agree rather closely with every case using the values of M and R as shown in Fig. 11, furthermore, in the present stage of investigations concerning the magnitude as well as the hypocenter of the Kita Mino earthquake, the values of M and R, ranging in Fig. 11 may be considered as plausible.

4. Conclusion

From the present investigations, it is ascertained that the predominant period of the short period of earthquake motions in ground of mountaineous formation corresponds to the natural period of a thin weathered layer of it.

Furthermore, from the present investigations, it is still further verified that the empirical formula for the spectrum of strong earthquake motions is applicable to destructive earthquakes[8]. In conclusion, the authors are much obliged to Miss S. Yoshizawa who has assisted them in preparing this paper.

---

38. 山地地盤の振動性状

(北美濃地震の余震観測)

地震研究所 金井　清
長田甲斐男

北美濃地震(1961年8月19日14時33分)の余震の2カ所3組における同時比較観測の結果，山地においても，また，卓越周期の長い地盤ほど，最大変位は明かに大きく，逆に，最大加速度はやや小さいことがわかつた．そして，山地における地震動の短周期の卓越振動は，薄い風化層の増巾作用によるものと考えられる．

本地震で，(i)木造家屋には，直接，地震動による被害はなく，(ii)コンクリート構造物のうち古くなつたりして粗雑なものには多少の被害があり，(iii)人体には強く感じた，などの事実は，本地震のマグニチュードと震源距離が第11図の曲線の中に含まれる値であれば，強震動のスペクトラムに関する実験式を使つた計算で一応の説明がついた．言い換えると，前述の実験式は北美濃地震の地震動にもあてはまることになつた．

---

8) K. KANAI, "An Empirical Formula for the Spectrum of Strong Earthquake Motions", *Proc. II World Conf. Earthq. Engg.*, (1960), 1541.

I. MURAMATU and T. YABASHI, "The Seismic Intensity at a Certain Dam Site", *ditto*, 1593.

北美濃地震調査報告あとがき

昭和36年8月19日福井，石川，岐阜の三県下に被害をおよぼした規模7の地震が起つた．従来地震研究所は大地震の度毎に各般の調査を行い，地震の本性と，震災の予防並びに対策の研究に資すると共に，その記録を後世に伝えることを業務として来た．それでこの地震は震央が山地にあり被害は幸に軽微であつたが，かなりの大地震でもあり，地震地理学的にも興味ある地域に起つたので，東京大学本部および文部省の援助を得て，直ちに現地に各種の調査班を送り，或は広域に通信調査を行い，地震，地質現象，或は地震工学的に被害および地盤を調査し，また余震観測，水準測量等を行つた．中央並びに現地官民各位の御協力によつて，ほぼ所期の調査を遂行することができた．

それら調査の中一応のまとまりを見たものが本報告であり，残る部分も，また本調査に基づく進んだ研究結果も順次本誌に発表される予定である．

以上の諸調査の費用調達に際し示された東京大学事務局；文部省大学学術局学術課，研究助成課，会計課ほか関係当局の方々の御好意に対しここに厚く感謝の意を表したい．

また本所調査班に対し三県所属の諸機関並びに現地の方々の供与された並々ならぬ御便宜，御協力に対しては深甚の感謝と敬意を表する．

また気象庁，並びにその管下諸地方気象台；及び国土地理院が貴重な観測資料と幾多の便宜を与えられ御協力を惜しまれなかつたことに対してもここに銘記して心からの感謝を捧げる次第である．

昭和36年9月

地震研究所長事務代理

河　角　　廣

―所　　報―

◎談話会記事

第390回談話会 (昭和36年7月25日)

1. 地磁気永年変化第1報　　行武毅
   （1） 地磁気永年変化の時間特性
   （2） 非双曲子磁場の西方移動
2. 地磁気変化と地球自転速度　　行武毅
   （1） 外部磁場の変化と自転速度
   （2） 地球磁場の 11 年変化によつて期待される自転速度変化
3. 不均質な媒質内を伝わる弾性波の安定性について （第2報）　　吉山良一・音田功
4. 強震記象を耐震構造の研究に使う場合の一試案　　金井清

第391回談話会 (昭和36年9月26日)

1. 表面波が同じ分散性を示す領域を求める試み （第2報）　　三東哲夫
2. コロンビア型地震計による表面波の観測 （第8報）
   ラブ波の分散 （第2報）　　三東哲夫
3. 表面波と層構造 （1） Lg および Rg について　　山口林造
4. 表面波と層構造 （2） 海洋構造を伝わる表面波　　山口林造・木沢綏・佐藤泰夫
5. 不均質媒質における表面波の分散について　　高橋健人
6. 地球熱学 第8報の1
   日本海溝附近の地殻熱流量測定結果　　上田誠也・宝来帰一・安井正・赤松英雄
7. 地球熱学 第9報
   日本における地殻熱流量分布 序報　　上田誠也・宝来帰一
8. 内部力源による半無限媒質の破壊に関する実験 （その1）　　茂木清夫
9. 浅間火山に発生する地震と噴火の関係 （続報）　　水上武郎・平賀士雄・内堀貞務・宮崎紀也・行田也
10. 強震動の周期特性 （第2報） 補遺　　金井清
11. 日本海溝附近の地磁気全磁力測定結果　　上田誠也・藪内夫・宝来帰一・安井正
12. 昭和 36 年8月 19 日北美濃地震の踏査報告
    地震踏査概報　　岸上冬彦・音田功
    地変および地質概報　　森本良平・松田時彦

家屋被害の報告　大沢胖

13. 北美濃地方の地質構造に関する二三の問題　村井勇・津屋弘達

14. 昭和 36 年8月 19 日の地震調査概報（白山付近）　吉山良一

15. 北美濃地震およびその余震について　萩原尊礼・茅野一郎

16. 北美濃地震余震観測報告（速報）

（1） 概説　萩原尊礼

（2） 福井県勝原および岐阜県蛭ケ野における観測　表俊一郎・中島直吉・斎藤貞夫・唐鎌郁夫・茅野一郎・神沼克伊

（3） 岐阜県八幡町における観測　宮村摂三・安芸敬一・堀実照・松本英一・安藤誠

17. 台湾のサイスミシテイー　徐明同（萩原所員紹介）

第 392 回談話会（昭和 36 年 10 月 24 日）

1. 磁気制振器について　力武常次

2. 地球磁場の西方移動速度ならびに地球回転速度の変動　力武常次

3. 地殻変動における 2, 3 の特性について　岡田惇

4. 台湾のサイスミシテイー（補遺）　徐明同（萩原所員紹介）

5. 北美濃地震余震観測
勝原および蛭ケ野における観測（続報）　地震研究所余震観測班

6. 山地地盤の振動性状（北美濃地震余震）　金井清・長田甲斐男

追加　北美濃地震地域の踏査報告　森本良平

第 393 回談話会（昭和 36 年 11 月 28 日）

1. 地球磁場の西方移動と永年変化　行武毅

2. 地中地震計について　嶋悦三

3. 蓼の海における氷震観測 I　表俊一郎・山崎良雄・小牧昭三吉・中島直昭・上野昭穂保・大工原貞二

4. 長岡地震の被害地域における常時微動測定結果　田中貞二

5. 長岡地方の家屋の振動実験結果　金井清・森下利三

第 394 回談話会 (昭和 36 年 12 月 19 日)

1. 表面波から発震機構を求める方法の精度について　安芸敬一
2. 近地地震波のみかけの速度・方向とそのかたよりの解釈
   第 1 報　北美濃余震の場合　安芸敬一
3. 地球振動と地球の静的変形　竹内均・斎藤正憲・小林直太 (萩原所員紹介)
4. 振動する楕円浪源によつて発生する水波の方向性について　桃井高夫
5. 振動する正方形の浪源によつて発生する波について　桃井高夫
6. 地震の時に起つた湖水の振動について　岸上冬彦

Index to Vol. 39.

Page

AIDA, I. and TAKAHASI, R., (17) Studies on the Spectrum of Tsunami. (in Japanese) 523

AIDA, I.; TAKAHASI, R.; HIRANO, K.; HATORI, T. and SHIMIZU, S., (16) Observations at Miyagi-Enoshima Tsunami Observatory during the IGY Period. (in English) 491

AKAMATU, K., (2) On Microseisms in Frequency Range from 1 c/s to 200 c/s. (in English) 23

AKI, K., (8) Crustal Structure in Japan from the Phase Velocity of Rayleigh Waves. Part 1. Use of the network of seismological stations operated by the Japan Meteorological Agency. (in English) 255

AKI, K.; MIYAMURA, S.; HORI, M.; MATUMOTO, H. and ANDO, S., (35) Observation of Aftershocks of the Kita Mino Earthquake, Aug. 19, 1961. —Observation at Hachiman, Gifu Prefecture, Central Japan.— (in Japanese) 895

ANDO, S.; MIYAMURA, S.; HORI, M.; AKI, K. and MATUMOTO, H., (35) Observation of Aftershocks of the Kita Mino Earthquake, Aug. 19, 1961. —Observation at Hachiman, Gifu Prefecture, Central Japan.— (in Japanese) 895

ASANO, S., (13) Reflection and Refraction of Elastic Waves at a Corrugated Boundary Surface. Part II. (in English) 367

FUTI, H.; UYEDA, S.; TOMODA, Y., HÔRAI, K. and KANAMORI, H., (6) Studies of the Thermal State of the Earth. The Seventh Paper: A Sea Bottom Thermogradmeter. (in English) 115

HAGIWARA, T. and KAYANO, I., (33) Seismological Observations of the Kita Mino Earthquake, August 19, 1961 and its Aftershocks. (in Japanese) 873

HATORI, T. and TAKAHASI, R., (11) Wind Wave Observation off Omaezaki, Shizuoka Prefecture, Japan. (in Japanese) 351

HATORI, T. and TAKAHASI, R., (20) On the Tsunami which accompanied the Hiuganada Earthquake of Feb. 27, 1961. (in Japanese) 561

HATORI, T.; TAKAHASI, R.; HIRANO, K.; AIDA, I. and SHIMIZU, S., (16) Observations at Miyagi-Enoshima Tsunami Observatory during the IGY Period. (in English) 491

HIRANO, K.; TAKAHASI, R.; AIDA, I.; HATORI, T. and SHIMIZU, S., (16) Observations at Miyagi-Enoshima Tsunami Observatory

during the IGY Period. (in English) 491
HÔRAI, K.; UYEDA, S.; TOMODA, Y.; KANAMORI, H. and FUTI, H., (6) Studies of the Thermal State of the Earth. The Seventh Paper: A Sea Bottom Thermogradmeter. (in English) 115
HORI, M.; MIYAMURA, S.; AKI, K.; MATUMOTO, H. and ANDO, S., (35) Observation of Aftershocks of the Kita Mino Earthquake, Aug. 19, 1961. —Observation at Hachiman, Gifu Prefecture, Central Japan.— (in Japanese) 895
HSU, M. T., (29) Seismicity of Taiwan (Formosa). (in English) 831
KANAI, K., (4) An Empirical Formula for the Spectrum of Strong Earthquake Motions. (in English) 85
KANAI, K., (12) A New Problem Concerning Surface Waves. Preliminary Notes). (in English) 359
KANAI, K. and OSADA, K., (38) Seismic Characteristics in Ground of Mountainous Formation. (Observation of the After Shocks of the Kita Mino Earthquake.) (in English) 943
KANAI, K. and TANAKA, T., (5) On Microtremors. VIII. (in English).. 97
KANAI, K. and YOSHIZAWA, S., (15) On the Period and the Damping of Vibration in Actual Buildings. (in English) 477
KANAMORI, H.; UYEDA, S.; TOMODA, Y.; HORAI, K. and FUTI, H., (6) Studies of the Thermal State of the Earth. The Seventh Paper: A Sea Bottom Thermogradmeter. (in English) 115
KARAKAMA, I.; OMOTE, S.; NAKAJIMA, N.; SAITO, S. and KAYANO, I., (34) Aftershocks of the Kita Mino Earthquake of August 19, 1961. —Observations at the Kadohara and the Hirugano stations— (in Japanese) 881
KAYANO, I. and HAGIWARA, T., (33) Seismological Observations of the Kita Mino Earthquake, August 19, 1961 and its Aftershocks. (in Japanese) 873
KAYANO, I.; OMOTE, S.; KARAKAMA, I.; NAKAJIMA, N. and SAITO, S., (34) Aftershocks of the Kita Mino Earthquake of August 19, 1961. —Observations at the Kadohara and the Hirugano stations— (in Japanese) 881
KISHINOUYE, F., (3) Further Studies of Microseisms by Observation. (in English) 77
KISHINOUYE, F. and ONDA, I., (31) Field Studies of the Kita Mino Earthquake on August 19, 1961. (in English) 857
KIZAWA, T. and YAMAGUCHI, R., (26) Surface Waves and Layered Structures. Part 2. Theoretical dispersion curves for suboceanic surface waves. (in English) 669

MATSUDA, T. and MORIMOTO, R., (37) Geology of the Area Damaged by the Kita Mino Earthquake. Part I. The Upper Reaches of the Uchinami River and the Itoshiro River, Fukui and Gifu Prefectures, Japan. (in Japanese) 935

MATUMOTO, H.; MIYAMURA, S.; HORI, M.; AKI, K. and ANDO, S., (35) Observation of Aftershocks of the Kita Mino Earthquake, Aug. 19, 1961. —Observation at Hachiman, Gifu Prefecture, Central Japan.— (in Japanese) 895

MIKUMO, T., ÔTSUKA, M., UTSU, T., TERASHIMA, T. and OKADA, A., (10) Crustal Structure in Central Japan as Derived from the Miboro Explosion-Seismic Observations. Part 2. On the Crustal Structure. (in English) 327

MIYAMURA, S.; HORI, M.; AKI, K.; MATUMOTO, H. and ANDO, S., (35) Observation of Aftershocks of the Kita Mino Earthquake, Aug. 19, 1961. —Observation at Hachiman, Gifu Prefecture, Central Japan.— (in Japanese) 895

MORIMOTO, R. and MATSUDA, T., (37) Geology of the Area Damaged by the Kita Mino Earthquake. Part I. The Upper Reaches of the Uchinami River and the Itoshiro River, Fukui and Gifu Prefectures, Japan. (in Japanese) 935

MURAI, I., (7) A Study of the Textural Characteristics of Pyroclastic Flow Deposits in Japan. (in English) 133

MURAI, I. and TSUYA, H., (36) Some Notes on the Geologic Structure of the Kita Mino District. (in Japanese) 909

NAKAJIMA, N.; OMOTE, S.; KARAKAMA, I.; SAITO, S. and KAYANO, I., (34) Aftershocks of the Kita Mino Earthquake of August 19, 1961. —Observations at the Kadohara and the Hirugano stations— (in Japanese) 881

OKADA, A., (18) Land Deformation accompanying with Nagaoka Earthquake, Feb. 2nd, 1961. (in Japanese) 537

OKADA, A.; MIKUMO, T.; ÔTSUKA, M.; UTSU, T. and TERASHIMA, T., (10) Crustal Structure in Central Japan as Derived from the Miboro Explosion-Seismic Observations. Part 2. On the Crustal Structure. (in English) 327

OMOTE, S.; KARAKAMA, I.; NAKAJIMA, N.; SAITO, S. and KAYANO, I., (34) Aftershocks of the Kita Mino Earthquake of August 19, 1961. —Observations at the Kadohara and the Hirugano stations— (in Japanese) 881

ONDA, I. and KISHINOUYE, F., (31) Field Studies of the Kita Mino Earthquake on August 19, 1961. (in English) 857
OSADA, K. and KANAI, K., (38) Seismic Characteristics in Ground of Mountainous Formation. (Observation of the After Shocks of the Kita Mino Earthquake.) (in English)..... 943
OSAWA, Y., (32) On the Damage to Buildings during the Kita Mino Earthquake of August 19, 1961. (in Japanese) 869
OSAWA, Y. and YAMAMOTO, M., (19) On the Damage to Buildings during the Nagaoka Earthquake of February 2, 1961. (in Japanese) 549
ÔTSUKA, M.; MIKUMO, T.; UTSU, T.; TERASHIMA, T. and OKADA, A., (10) Crustal Structure in Central Japan as Derived from the Miboro Explosion-Seismic Observations. Part 2. On the Crustal Structure. (in English) 327
SAITO, S.; OMOTE, S.; KARAKAMA, I.; NAKAJIMA, N. and KAYANO, I., (34) Aftershocks of the Kita Mino Earthquake of August 19, 1961. —Observations at the Kadohara and the Hirugano stations— (in Japanese)..... 881
SANTÔ, T. A., (1) Rayleigh Wave Dispersions across the Oceanic Basin around Japan (Part III). —On the Crust of the South-Western Pacific Ocean— (in English)..... 1
SANTÔ, T. A., (23) Division of the South-Western Pacific Area into Several Regions in each of which Rayleigh Waves Have the Same Dispersion Characters. (in English)..... 603
SANTÔ, T. A., (24) Dispersion of Love Waves along Various Paths to Japan (Part 1). (in English)..... 631
SHIMIZU, S.; TAKAHASI, R.; HIRANO, K.; AIDA, I. and HATORI, T., (16) Observations at Miyagi-Enoshima Tsunami Observatory during the IGY Period. (in English)..... 491
TAKAHASHI, T., (27) The Dispersion of Love Waves in Heterogeneous Half Space overlain by a Homogeneous Layer. (in English) ... 811
TAKAHASHI, T., (28) Dispersion Curves for the Higher Modes of Surface Waves in Heterogeneous Media. (in English)..... 823
TAKAHASI, R. and HATORI, T., (11) Wind Wave Observation off Omaezaki, Shizuoka Prefecture, Japan. (in Japanese)..... 351
TAKAHASI, R. and AIDA, I. (17) Studies on the Spectrum of Tsunami. (in Japanese) 523
TAKAHASI, R. and HATORI, T., (20) On the Tsunami which accompanied the Hiuganada Earthquake of Feb. 27, 1961. (in

Japanese) 561
TAKAHASI, R., HIRANO, K., AIDA, I., HATORI, T. and SHIMIZU, S., (16) Observations at Miyagi-Enoshima Tsunami Observatory during the IGY Period. (in English) 491
TANAKA, T. and KANAI, K., (5) On Microtremors. VIII. (in English) .. 97
TERASHIMA, T.; MIKUMO, T.; ÔTSUKA, M.; UTSU, T. and OKADA, A., (10) Crustal Structure in Central Japan as Derived from the Miboro Explosion-Seismic Observations. Part 2. On the Crustal Structure. (in English) 327
TOMODA, Y.; UYEDA, S.; HÔRAI, K.; KANAMORI, H. and FUTI, H., (6) Studies of the Thermal State of the Earth. The Seventh Paper: A Sea Bottom Thermogradmeter. (in English) 115
TSUYA, H. and MURAI, I., (36) Some Notes on the Geologic Structure of the Kita Mino District. (in Japanese) 909
UTSU, T.; MIKUMO, T.; ÔTSUKA, M.; TERASHIMA, T. and OKADA, A., (10) Crustal Structure in Central Japan as Derived from the Miboro Explosion-Seismic Observations. Part 2. On the Crustal Structure. (in English) 327
UYEDA, S., (21) An Interpretation of the Transient Geomagnetic Variations Accompanying the Volcanic Activities at Volcano Mihara, Oshima Island, Japan. (in English) 579
UYEDA, S. and YABU, T., (22) Some Experiments on Thermal Shock Fracture of Rocks. (in English) 593
UYEDA, S., TOMODA, Y., HÔRAI, K., KANAMORI, H. and FUTI, H., (6) Studies of the Thermal State of the Earth. The Seventh Paper: A Sea Bottom Thermogradmeter. (in English) 115
YABU, T. and UYEDA, S., (22) Some Experiments on Thermal Shock Fracture of Rocks. (in English) 593
YAMAGUCHI, R., (25) Surface Waves and Layered Structures. Part 1. Influence of a low velocity layer and some study on Lg and Rg waves. (in English) 653
YAMAGUCHI, R. and KIZAWA, T., (26) Surface Waves and Layered Structures. Part 2. Theoretical dispersion curves for sub-oceanic surface waves. (in English) 669
YAMAMOTO, M. and OSAWA, Y., (19) On the Damage to Buildings during the Nagaoka Earthquake of February 2, 1961. (in Japanese) 549
YOSHIYAMA, R., (30) Earthquake near the National Park Hakusan on August 19th, 1961. (in Japanese) 849

YOSHIZAWA, S. and KANAI, K., (15) On the Period and the Damping of Vibration in Actual Buildings. (in English) 477
YUKUTAKE, T., (14) Archaeomagnetic Study on Volcanic Rocks in Oshima Island, Japan. (in English) 467
The Research Group for Explosion Seismology, (9) Crustal Structure in Central Japan as Derived from the Miboro Explosion-Seismic Observations. Part 1. Explosions and Seismic Observations. (in English) 285

索 引 第 39 号

頁

相田　勇・高橋竜太郎 (17) 津波スペククトルの研究 1. ウエーブアナライザーの製作 2. 江の島津波観測所で観測された津波及び常時長波の周期分析 3. 日本各地で観測さたチリ津波の周期分析 (邦文) 523

相田　勇・高橋竜太郎・平能金太郎・羽鳥徳太郎・清水静子 (16) 江の島津波観測所における IGY 期間中の観測 (英文)..... 491

赤松　敬 (2) 微動について (英文)..... 23

安芸敬一 (8) レーリー波位相速度法による日本の地下構造の研究 第1報 (英文) 255

安芸敬一・宮村摂三・堀　実・松本英照・安藤誠一 (35) 北美濃地震余震観測——岐阜県八幡町における観測—— (邦文)..... 895

安藤誠一・宮村摂三・堀　実・安芸敬一・松本英照 (35) 北美濃地震余震観測——岐阜県八幡町における観測—— (邦文)..... 895

浅野周三 (13) 波型の境界面における弾性波の反射，屈折 第2報 (英文)..... 367

淵　秀隆・上田誠也・友田好文・宝来帰一・金森博雄 (6) 地球熱学 (第7報) 海底地温勾配測定装置 (英文)..... 115

荻原尊礼・茅野一郎 (33) 1961年8月19日北美濃地震とその余震観測概説 (邦文) 873

羽鳥徳太郎・高橋竜太郎 (11) 静岡県御前崎沖 (御前岩) における波浪観測 (序報) (邦文) 351

羽鳥徳太郎・高橋竜太郎 (20) 1961年2月27日 日向灘地震に伴なった津波について (邦文)..... 561

羽鳥徳太郎・高橋竜太郎・平能金太郎・相田　勇・清水静子 (16) 江の島津波観測所における IGY 期間中の観測 (英文)..... 491

平能金太郎・高橋竜太郎・相田　勇・羽鳥徳太郎・清水静子 (16) 江の島津波観測所における IGY 期間中の観測 (英文)..... 491

宝来帰一・上田誠也・友田好文・金森博雄・淵　秀隆 (6) 地球熱学 (第7報) 海底地温勾配測定装置 (英文)..... 115

堀　実・宮村摂三・安芸敬一・松本英照・安藤誠一 (35) 北美濃地震余震観測 ——岐阜県八幡町における観測—— (邦文)..... 895

徐　明同 (29) 台湾の地震活動 (英文) 831

金井　清 (4) 強震動スペクトルに関する実験式 (英文)..... 85

金井　清 (12) 表面波に関する一つの問題 (序報) (英文)..... 359

金井　清・長田甲斐男 (38) 山地地盤の振動性状 (北美濃地震の余震観測) (英文) 943

金井　清・田中貞二　(5)　常時微動について 第8報 (英文) 97
金井　清・吉沢静代　(15)　実在建物の周期と減衰 (英文) 477
金森博雄・上田誠也・友田好文・宝来帰一・淵　秀雄　(6)　地球熱学 (第7報) 海底地温勾配測定装置 (英文) 115
唐鎌郁夫・表俊一郎・中島直吉・斎藤貞夫・茅野一郎　(34)　北美濃地震余震観測——勝原及び蛭ケ野における観測 (邦文) 881
茅野一郎・萩原尊礼　(33)　1961年8月19日北美濃地震とその余震観測概説 (邦文) 873
茅野一郎・表俊一郎・唐鎌郁夫・中島直吉・斎藤貞夫　(34)　北美濃地震余震観測——勝原及び蛭ケ野における観測 (邦文) 881
岸上冬彦　(3)　観測による土地の脈動の研究 続報 (英文) 77
岸上冬彦・音田　功　(31)　1961年8月19日北美濃地震踏査概報 (英文) 857
木沢　綏・山口林造　(26)　表面波と層構造 (2) 海洋構造を伝わる表面波の理論的分散曲線 (英文) 669
松田時彦・森本良平　(37)　北美濃地震被害地の地質 第1報 福井県打波川上流～岐阜県石徹白川上流地域 (邦文) 935
松本英照・宮村摂三・堀　実・安芸敬一・安藤誠一　(35)　北美濃地震余震観測——岐阜県八幡町における観測—— (邦文) 895
三雲　健・大塚道男・宇津徳治・寺島　敦・岡田　惇　(10)　御母衣爆破地震動観測による日本中部の地殻構造　第2部　地殻構造について (英文) 327
宮村摂三・堀　実・安芸敬一・松本英照・安藤誠一　(35)　北美濃地震余震観測——岐阜県八幡町における観測—— (邦文) 895
森本良平・松田時彦　(37)　北美濃地震被害地の地質　第1報　福井県打波川上流～岐阜県石徹白川上流地域 (邦文) 935
村井　勇　(7)　火砕流堆積物の組織的性質 (英文) 133
村井　勇・津屋弘達　(36)　北美濃地方の地質構造に関する 2, 3 の問題 (邦文) 909
中島直吉・表俊一郎・唐鎌郁夫・斎藤貞夫・茅野一郎　(34)　北美濃地震余震観測——勝原及び蛭ケ野における観測 (邦文) 881
岡田　惇　(18)　長岡地震による地盤変動 (邦文) 537
岡田　惇・三雲　健・大塚道男・宇津徳治・寺島　敦　(10)　御母衣爆破地震動観測による日本中部の地殻構造　第2部　地殻構造について (英文) 327
表俊一郎・唐鎌郁夫・中島直吉・斎藤貞夫・茅野一郎　(34)　北美濃地震余震観測——勝原及び蛭ケ野における観測 (邦文) 881
音田　功・岸上冬彦　(31)　1961年8月19日北美濃地震踏査概報 (英文) 857
長田甲斐男・金井　清　(38)　山地地盤の振動性状 (北美濃地震の余震観測) (英文) 943

大沢　胖　(32)　北美濃地震における家屋の被害について（邦文）..... 869
大沢　胖・山本正勝　(19)　昭和36年2月2日長岡地震の家屋被害について（邦文）..... 549
大塚道男・三雲　健・宇津徳治・寺島　敦・岡田　惇　(10)　御母衣爆破地震動観測による日本中部の地殻構造　第2部　地殻構造について（英文）..... 327
斎藤貞夫・表俊一郎・唐鎌郁夫・中島直吉・茅野一郎　(34)　北美濃地震余震観測――勝原及び蛭ケ野における観測（邦文）..... 881
三東哲夫　(1)　日本周辺の海洋底をつたわるレーリー波の分散（第三報）――東南太平洋の地殻構造――（英文）..... 1
三東哲夫　(23)　西南太平洋海域を，夫々の内部でレーリー波が同一の群速度を示す様ないくつかの地区に分けること（英文）..... 603
三東哲夫　(24)　日本周辺を伝わるラブ波の分散について（英文）..... 631
清水静子・高橋竜太郎・平能金太郎・相田　勇・羽鳥徳太郎　(16)　江の島津波観測所における IGY 期間中の観測（英文）..... 491
高橋健人　(27)　均質な表面層のある不均質な半平面における Love 波の分散（英文）..... 811
高橋健人　(28)　不均質な媒質における表面波の Higher Modes の分散曲線（英文）..... 823
高橋竜太郎・羽鳥徳太郎　(11)　静岡県御前崎沖（御前岩）における波浪観測（序報）（邦文）..... 351
高橋竜太郎・相田　勇　(17)　津波スペクトルの研究　1. ウエーブアナライザーの製作　2. 江の島津波観測所で観測された津波及び常時長波の周期分析　3. 日本各地で観測されたチリ津波の周期分析（邦文）..... 523
高橋竜太郎・羽鳥徳太郎　(20)　1961年2月27日　日向灘地震に伴なった津波について（邦文）..... 561
高橋竜太郎・平能金太郎・相田　勇・羽鳥徳太郎・清水静子　(16)　江の島津波観測所における IGY 期間中の観測（英文）..... 491
田中貞二・金井　清　(5)　常時微動について　第8報（英文）..... 97
寺島　敦・三雲　健・大塚道男・宇津徳治・岡田　惇　(10)　御母衣爆破地震動観測による日本中部の地殻構造　第2部　地殻構造について（英文）..... 327
友田好文・上田誠也・宝来帰一・金森博雄・淵　秀隆　(6)　地球熱学（第7報）海底地温勾配測定装置（英文）..... 115
津屋弘達・村井　勇　(36)　北美濃地方の地質構造に関する 2, 3 の問題（邦文）..... 909
宇津徳治・三雲　健・大塚道男・寺島　敦・岡田　惇　(10)　御母衣爆破地震動観測による日本中部の地殻構造　第2部　地殻構造について（英文）..... 327

上田誠也 (21) 伊豆大島における火山活動と地磁気変化についての一解釈 (英文) 579
上田誠也・薮 武夫 (22) 岩石の熱衝撃破壊について (英文) 593
上田誠也・友田好文・宝来帰一・金森博雄・淵 秀隆 (6) 地球熱学 (第7報) 海底地温勾配測定装置 (英文) 115
薮 武夫・上田誠也 (22) 岩石の熱衝撃破壊について (英文) 593
山口林造 (25) 表面波と層構造 (1) 低速層の影響および Lg と Rg について (英文) 653
山口林造・木沢 綏 (26) 表面波と層構造 (2) 海洋構造を伝わる表面波の理論的分散曲線 (英文) 669
山本正勝・大沢 胖 (19) 昭和36年2月2日 長岡地震の家屋被害について (邦文) 549
吉山良一 (30) 昭和36年8月19日 白山国定公園附近に発生した地震の調査概報 (邦文) 849
吉沢静代・金井 清 (15) 実在建物の周期と減衰 (英文) 477
行武 毅 (14) 伊豆大島熔岩による古地磁気学 (英文) 467
爆破地震動研究グループ (9) 御母衣爆破地震動観測による日本中部の地殻構造 第1部 御母衣爆破地震動の観測 (英文) 285

BULLETIN

OF THE

EARTHQUAKE RESEARCH INSTITUTE

UNIVERSITY OF TOKYO

VOL. 39

1961

東京大学

地震研究所彙報

第 39 號

昭和 36 年

CONTENTS.

Vol. 39.

Part 1. March, 1961.

Papers and Reports.

Page

1. T. A. SANTÔ, Rayleigh Wave Dispersions across the Oceanic Basin around Japan (Part III).—On the Crust of the South-Western Pacific Ocean—(in English) 1
2. K. AKAMATU, On Microseisms in Frequency Range from 1 c/s to 200 c/s. (in English)..... 23
3. F. KISHINOUYE, Further Studies of Microseisms by Observation. (in English) 77
4. K. KANAI, An Empirical Formula for the Spectrum of Strong Earthquake Motions. (in English)..... 85
5. K. KANAI and T. TANAKA, On Microtremors. VIII. (in English).. 97

Part 2. June, 1961.

6. S. UYEDA, Y. TOMODA, K. HÔRAI, H. KANAMORI and H. FUTI, Studies of the Thermal State of the Earth. The Seventh Paper: A Sea Bottom Thermogradmeter. (in English) 115
7. I. MURAI, A Study of the Textural Characteristics of Pyroclastic Flow Deposits in Japan. (in English) 133
8. K. AKI, Crustal Structure in Japan from the Phase Velocity of Rayleigh Waves. Part 1. Use of the network of seismological stations operated by the Japan Meteorological Agency. (in English) 255
9. The Research Group for Explosion Seismology, Crustal Structure in Central Japan as Derived from the Miboro Explosion-Seismic Observations. Part 1. Explosions and Seismic Observations. (in English)..... 285
10. T. MIKUMO, M. ÔTSUKA, T. UTSU, T. TERASHIMA and A. ÔKADA, Crustal Structure in Central Japan as Derived from the Miboro Explosion-Seismic Observations. Part 2. On the Crustal Structure. (in English) 327

11. R. TAKAHASI and T. HATORI, Wind Wave Observation off Omaezaki, Shizuoka Prefecture, Japan. (in Japanese) 351

Part 3. September, 1961.

12. K. KANAI, A New Problem Concerning Surface Waves. (Preliminary Notes). (in English) 359
13. S. ASANO, Reflection and Refraction of Elastic Waves at a Corrugated Boundary Surface. Part II. (in English) 367
14. T. YUKUTAKE, Archaeomagnetic Study on Volcanic Rocks in Oshima Island, Japan. (in English) 467
15. K. KANAI and S. YOSHIZAWA, On the Period and the Damping of Vibration in Actual Buildings. (in English) 477
16. R. TAKAHASI, K. HIRANO, I. AIDA, T. HATORI and S. SHIMIZU, Observations at Miyagi-Enoshima Tsunami Observatory during the IGY Period. (in English) 491
17. R. TAKAHASI and I. AIDA, Studies on the Spectrum of Tsunami. (in Japanese) 523
18. A. OKADA, Land Deformation accompanying with Nagaoka Earthquake, Feb. 2nd, 1961. (in Japanese) 537
19. Y. OSAWA and M. YAMAMOTO, On the Damage to Buildings during the Nagaoka Earthquake of February 2, 1961. (in Japanese) 549
20. R. TAKAHASI and T. HATORI, On the Tsunami which accompanied the Hiuganada Earthquake of Feb. 27, 1961. (in Japanese) 561

Part 4. December, 1961.

21. S. UYEDA, An Interpretation of the Transient Geomagnetic Variations Accompanying the Volcanic Activities at Volcano Mihara, Oshima Island, Japan. (in English) 579
22. S. UYEDA and T. YABU, Some Experiments on Thermal Shock Fracture of Rocks. (in English) 539
23. T. A. SANTÔ, Division of the South-western Pacific Area into Several Regions in each of which Rayleigh Waves Have the Same Dispersion Characters. (in English) 603
24. T. A. SANTÔ, Dispersion of Love Waves along Various Paths to Japan (Part 1). (in English) 631
25. R. YAMAGUCHI, Surface Waves and Layered Structures. Part 1.

Influence of a low velocity layer and some study on Lg and Rg waves. (in English) 653
26. R. YAMAGUCHI and T. KIZAWA, Surface Waves and Layered Structures. Part 2. Theoretical dispersion curves for sub-oceanic surface waves. (in English) 669
27. T. TAKAHASHI, The Dispersion of Love Waves in Heterogeneous Half Space overlain by a Homogeneous Layer. (in English).. 811
28. T. TAKAHASHI, Dispersion Curves for the Higher Modes of Surface Waves in Heterogeneous Media. (in English)..... 823
29. M. T. HSU, Seismicity of Taiwan (Formosa). (in English)..... 831

Papers and Reports on the Kita Mino Earthquake

30. R. YOSHIYAMA, Earthquake near the National Park Hakusan on August 19th, 1961. (in Japanese)..... 849
31. F. KISHINOUYE and I. ONDA, Field Studies of the Kita Mino Earthquake on August 19, 1961. (in English) 857
32. Y. OSAWA, On the Damage to Buildings during the Kita Mino Earthquake of August 19, 1961. (in Japanese) 869
33. T. HAGIWARA and I. KAYANO, Seismological Observations of the Kita Mino Earthquake, August 19, 1961 and its After-shocks. (in Japanese) 873
34. S. OMOTE, I. KARAKAMA, N. NAKAJIMA, S. SAITO and I. KAYANO, Aftershocks of the Kita Mino Earthquake of August 19, 1961. —Observations at the Kadohara and the Hirugano stations— (in Japanese) 881
35. S. MIYAMURA, M. HORI, K. AKI, H. MATUMOTO and S. ANDO, Observation of Aftershocks of the Kita Mino Earthquake, Aug. 19, 1961. —Observation at Hachiman, Gifu Prefecture, Central Japan.— (in Japanese) 895
36. I. MURAI and H. TSUYA, Some Notes on the Geologic Structure of the Kita Mino District. (in Japanese) 909
37. R. MORIMOTO and T. MATSUDA, Geology of the Area Damaged by the Kita Mino Earthquake. Part I. The Upper Reaches of the Uchinami River and the Itoshiro River, Fukui and Gifu Prefectures, Japan. (in Japanese) 935
38. K. KANAI and K. OSADA, Seismic Characteristics in Ground of Mountainous Formation. (Observation of the After Shocks of the Kita Mino Earthquake.) (in English)..... 943

Postscript on the Reports of the Kita Mino Earthquake, by H. KAWASUMI 953

目　次

第 39 号

第 1 冊　昭和 36 年 3 月

論文及報告

頁

1. 日本周辺の海洋底をつたわるレーリー波の分散（第三報）
——東南太平洋の地殻構造——（英文）……三東哲夫 1
2. 微動について（英文）……赤松敬 23
3. 観測による土地の脈動の研究 続報（英文）……岸上冬彦 77
4. 強震動スペクトルに関する実験式（英文）……金井清 85
5. 常時微動について 第8報（英文）……金井清・田中貞二 97

第 2 冊　昭和 36 年 6 月

6. 地球熱学（第7報）海底地温勾配測定装置（英文）……上田誠也・友田好文・宝来帰一・金森博雄・淵秀隆 115
7. 火砕流堆積物の組織的性質（英文）……村井勇 133
8. レーリー波位相速度法による日本の地下構造の研究 第1報（英文）……安芸敬一 255
9. 御母衣爆破地震動観測による日本中部の地殻構造 第1部 御母衣爆破地震動の観測（英文）……爆破地震動研究グループ 285
10. 御母衣爆破地震動観測による日本中部の地殻構造 第2部 地殻構造について（英文）……三雲健・大塚道男・宇津徳治・寺島敦惇・岡田悖 327
11. 静岡県御前崎沖(御前岩)における波浪観測（序報）（邦文）……高橋竜太郎・羽鳥徳太郎 351

第 3 冊　昭和 36 年 9 月

12. 表面波に関する一つの問題（序報）（英文）……金井清 359
13. 波型の境界面における弾性波の反射，屈折 第2報（英文）……浅野周三 367
14. 伊豆大島熔岩による古地磁気学（英文）……行武毅 467
15. 実在建物の周期と減衰（英文）……金井清・吉沢静代 477

16. 江の島津波観測所における IGY 期間中の観測（英文）……高橋竜太郎・平能金太郎・相田勇・羽鳥徳太郎・清水静子 491

17. 津波スペクトルの研究
1. ウェーブアナライザーの製作
2. 江の島津波観測所で観測された津波及び常時長波の周期分析
3. 日本各地で観測されたチリ津波の周期分析（邦文）……高橋竜太郎・相田勇 523

18. 長岡地震による地盤変動（邦文）……岡田惇 537

19. 昭和36年2月2日 長岡地震の家屋被害について（邦文）……大沢胖・山本正勝 549

20. 1961年2月27日 日向灘地震に伴なつた津波について（邦文）……高橋竜太郎・羽鳥徳太郎 561

第 4 冊　昭和 36 年 12 月

21. 伊豆大島における火山活動と地磁気変化についての一解釈（英文）……上田誠也 579

22. 岩石の熱衝撃破壊について（英文）……上田誠也・藪武夫 593

23. 西南太平洋海域を，夫々の内部でレーリー波が同一の群速度を示す様ないくつかの地区に分けること（英文）……三東哲夫 603

24. 日本周辺を伝わるラブ波の分散について（英文）……三東哲夫 631

25. 表面波と層構造 (1) 低速層の影響および Lg と Rg について（英文）……山口林造 653

26. 表面波と層構造 (2) 海洋構造を伝わる表面波の理論的分散曲線（英文）……山口林造・木沢綏 669

27. 均質な表面層のある不均質な半平面における Love 波の分散（英文）……高橋健人 811

28. 不均質な媒質における表面波の Higher Modes の分散曲線（英文）……高橋健人 823

29. 台湾の地震活動（英文）……徐明同 831

北美濃地震調査報告

30. 昭和36年8月19日白山国定公園附近に発生した地震の調査概報（邦文）……吉山良一 849

31. 1961年8月19日北美濃地震踏査概報（英文）……岸上冬彦・音田功 857

32. 北美濃地震における家屋の被害について（邦文）……大沢胖 869

33. 1961年8月19日北美濃地震とその余震観測概説（邦文）……萩原尊礼・茅野一郎 873

34. 北美濃地震余震観測
——勝原及び蛭ケ野における観測——（邦文）……表俊一郎・唐鎌郁夫・中島直吉・斎藤貞夫・茅野一郎 881

35. 北美濃地震余震観測
——岐阜県八幡町における観測——（邦文）……宮村摂三・堀実一・安芸敬一・松本英照・安藤誠一 895

36. 北美濃地方の地質構造に関する 2, 3 の問題（邦文）……村井勇・津屋弘達 909

37. 北美濃地震被害地の地質 第1報 福井県打波川上流～岐阜県石徹白川上流地域（邦文）……森本良平・松田時彦 935

38. 山地地盤の振動性状（北美濃地震の余震観測）（英文）……金井清・長田甲斐男 943

北美濃地震調査報告あとがき……河角広 953

昭和37年3月10日 印刷
昭和37年3月15日 発行

東京都文京区本富士町一番地
東京大学構内
編纂兼
発行者 東京大学地震研究所

東京都新宿区山吹町一八四番地
印刷者 笠井康頼

東京都新宿区山吹町一八四番地
印刷所 株式会社 国際文献印刷社

売捌所
東京都中央区日本橋通二丁目六番地
丸善株式会社

Sold by Maruzen Co., Ltd., Nihonbashi-dôri, Chûô-ku, Tôkyô.
Price of this copy: 1,313 Yen. (Postage exclusive.)

BULLETIN OF

THE EARTHQUAKE RESEARCH INSTITUTE

UNIVERSITY OF TOKYO

Vol. 39, Part 4. December, 1961.

Contents.

Papers and Reports.

Page

21. S. UYEDA, An Interpretation of the Transient Geomagnetic Variations Accompanying the Volcanic Activities at Volcano Mihara, Oshima Island, Japan. (in English) 579
22. S. UYEDA and T. YABU, Some Experiments on Thermal Shock Fracture of Rocks. (in English) 593
23. T. A. SANTÔ, Division of the South-western Pacific Area into Several Regions in each of which Rayleigh Waves Have the Same Dispersion Characters. (in English) 603
24. T. A. SANTÔ, Dispersion of Love Waves along Various Paths to Japan (Part 1). (in English) 631
25. R. YAMAGUCHI, Surface Waves and Layered Structures. Part 1. Influence of a low velocity layer and some study on Lg and Rg waves. (in English) 653
26. R. YAMAGUCHI and T. KIZAWA, Surface Waves and Layered Structures. Part 2. Theoretical dispersion curves for suboceanic surface waves. (in English) 669
27. T. TAKAHASHI, The Dispersion of Love Waves in Heterogeneous Half Space overlain by a Homogeneous Layer. (in English) 811
28. T. TAKAHASHI, Dispersion Curves for the Higher Modes of Surface Waves in Heterogeneous Media. (in English) 823
29. M. T. HSU, Seismicity of Taiwan (Formosa). (in English) 831

Papers and Reports on the Kita Mino Earthquake

30. R. YOSHIYAMA, Earthquake near the National Park Hakusan on August 19th, 1961. (in Japanese) 849
31. F. KISHINOUYE and I. ONDA, Field Studies of the Kita Mino Earthquake on August 19, 1961. (in English) 857
32. Y. OSAWA, On the Damage to Buildings during the Kita Mino Earthquake of August 19, 1961. (in Japanese) 869
33. T. HAGIWARA and I. KAYANO, Seismological Observations of the Kita Mino Earthquake, August 19, 1961 and its Aftershocks. (in Japanese) 873
34. S. OMOTE, I. KARAKAMA, N. NAKAJIMA, S. SAITO and I. KAYANO, Aftershocks of the Kita Mino Earthquake of August 19, 1961. —Observations at the Kadohara and the Hirugano stations— (in Japanese) 881
35. S. MIYAMURA, M. HORI, K. AKI, H. MATUMOTO and S. ANDO, Observation of Aftershocks of the Kita Mino Earthquake, Aug. 19, 1961. —Observation at Hachiman, Gifu Prefecture, Central Japan.— (in Japanese) 895
36. I. MURAI and H. TSUYA, Some Notes on the Geologic Structure of the Kita Mino District. (in Japanese) 909
37. R. MORIMOTO and T. MATSUDA, Geology of the Area Damaged by the Kita Mino Earthquake. Part I. The Upper Reaches of the Uchinami River and the Itoshiro River, Fukui and Gifu Prefectures, Japan. (in Japanese) 935
38. K. KANAI and K. OSADA, Seismic Characteristics in Ground of Mountainous Formation. (Observation of the After Shocks of the Kita Mino Earthquake.) (in English) 943

Postscript on the Reports of the Kita Mino Earthquake, by H. KAWASUMI 953

Institute Notes.

Index.

(For the papers written in Japanese or in occidental languages, the abstracts are given in occidental languages or in Japanese respectively.)